Glaciers, Climate and the "8.2ka Event" in Iceland

Lindsay Sugden

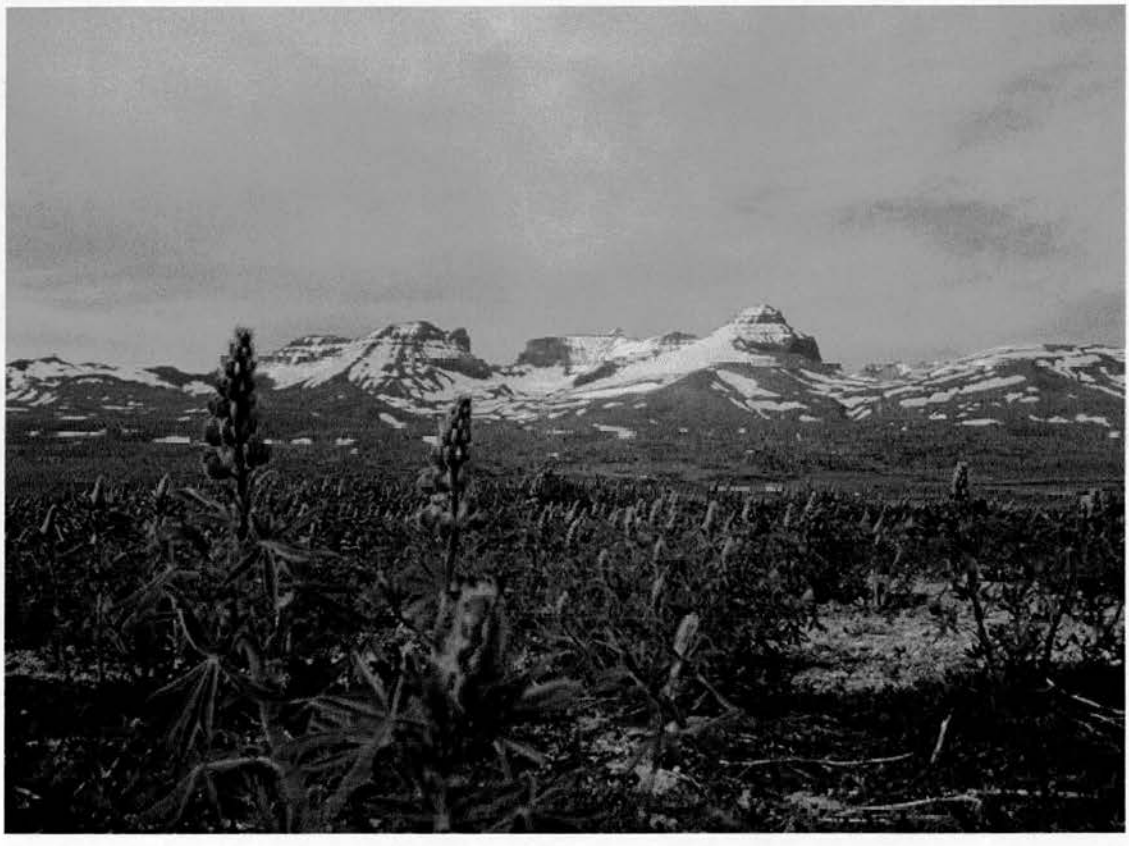

Doctor of Philosophy
School of GeoSciences
University of Edinburgh
2006

ABSTRACT

The aim of this thesis is to use the geomorphic record of NE Iceland to assess the consequences of the "8.2ka event", the largest recorded climatic reversal in the Holocene. Iceland is a sensitive and strategic location in which to study the impact of the event, given the evidence that it was triggered by a North Atlantic fresh water anomaly. The research combines new high resolution empirical evidence with ice sheet modelling to assess the extent and nature of glacial activity at 8.2ka. New geomorphic evidence is presented for the Early Holocene in the Borgarfjörður Eystri region of northeast Iceland. In total, thirteen landform 'suites' are identified which are indicative primarily of glacial activity, but also contain evidence for mass-movement events. Landform suites are backed by cliffs or scree slopes, and consist, in the upper parts, of high-relief ridges and terraces interpreted as landslide deposits. The middle and lower parts are made up of longitudinal ridges and hummocky terrain, with clear terminal and lateral moraines defining former glacier margins. Phases of glacial and mass-movement activity which generated these landforms are Holocene in age, dated to between 7600-4000 Cal. Yrs. B.P. It is suggested that glacial advances represent the primary response to the 8.2ka cooling event, while the mass-movement events which occurred later were a result of paraglacial slope instabilities, and thus can be seen as a secondary response. Ice sheet modelling experiments suggest that extreme climatic conditions, involving a temperature drop of as much as 7°C, would have been necessary to initiate glaciers in the locations where Holocene activity has been observed. It is suggested that abundant debris supplies generated from the friable exposures of rhyolitic bedrock, would have inhibited the ablation of glacier ice, so that cooling may not have had to be as much as 7°C to promote and preserve the recorded glacial activity. This study presents evidence for a time-transgressive glacial and geomorphic response to the 8.2ka event in Iceland, providing a site-specific example of regional environmental response to climate change. The record can be correlated with environmental changes at this time in the North Atlantic and beyond, promoting understanding of potential response mechanisms to future rapid climate change events.

Declaration

In accordance with the University of Edinburgh regulations, I declare this thesis is my own work except where stated.

Lindsay Sugden
June 2006

Acknowledgements

Firstly this research could not have been carried out without the financial support of the Carnegie Trust for the Universities of Scotland.

Thanks must go to my supervisors *Nick Hulton* and *Andy Dugmore* for their continued support and encouragement throughout the PhD. In addition, I am very grateful to everyone at *S.U.E.R.C* (particularly *Gordon Cook*) for the help with attaining radiocarbon dates.

Various other staff in the department have also helped me see sense at one time or another, including *Anthony Newton* and *Pete Hill* (on the microprobe), *Mike Kaplan*, *David Sugden,* and *Chris Place* (with endless computer problems). I would also like to thank the people of *Borgarfjörður Eystri* who let me loose on their land, and the Tourist Board of northeast Iceland.

My fieldwork would have been impossible or incredibly depressing without the help and friendship of *Colin Goldblatt, Fraser Sugden, Kate Smith, Nick Pike, Mark Naylor* and *Andy Casely*, who all helped me dig some holes, put up with me and stopped me from going mad. I could also not forget to mention *Ed* the Landrover who was a reliable fieldwork companion for two seasons.

Lynne and Chris Sugden have been a continued support throughout, for which I am eternally grateful, and thanks also go to all my as-yet-unmentioned friends, family and fellow-musicians, for without them I would not have made it this far.

Contents

Table of Figures

Chapter 1

Chapter 2

Chapter 3

Chapter 4

Chapter 5

Chapter 6

Chapter 7

Table of Tables

1 Introduction and Background

1.1. Introduction

The aim of this research is to understand the mechanisms and characteristics of environmental response in Iceland to the largest recorded climatic reversal in the Holocene, the "8.2ka event". The results presented here help to determine the nature of the "8.2ka event" in a region where an environmental response is highly likely to have occurred. Recorded evidence of specific response to this 'event' in such a sensitive and strategically placed location improves knowledge about potential response mechanisms to future rapid climate change events. The research is pursued by a fieldwork- and modelling-based study of putative geomorphic response to the "8.2ka event" in Iceland.

The "8.2ka event" (Alley et al. 1997) was the biggest climatic fluctuation in the Holocene. It was more significant and of a higher magnitude than the Little Ice Age, yet was a fraction of the magnitude and duration of a full glacial/interglacial cycle. Understanding climate events of this intermediate scale is invaluable on human timescales. This study presents a new onshore record of environmental change in the early Holocene, in an area close to the putative core of the 8.2ka event, the North Atlantic. This record is assessed here as a means to learn more about the environmental history of Iceland, a particularly sensitive environmental system. Iceland maintains a detailed and dateable environmental record since deglaciation from the Last Glacial Maximum, and is thus an ideal site in which to study the effects of such a rapid climate perturbation. Understanding the nature of response to a climate event of this scale has significant implications, as it is suggested that any future climate change induced by the effects of global warming could be analogous to the "8.2ka event".

1.2. Objectives

In pursuit of the overall aim, the project tests the hypothesis that there was a geomorphic response mechanism to the 8.2ka cooling event in Iceland, with the following specific objectives:

- Quantify the magnitude and mechanisms of environmental response to the 8.2ka event in Iceland, by studying the potential causal connection between this Early Holocene cooling event and glacial activity occurring at this time.
- Determine the specific glacial processes involved in manifesting response to the 8.2ka event.
- Assess the extent to which non-glacial geomorphic activity in the field area at this time was triggered or intensified (directly or indirectly) by the 8.2ka event.
- Determine the value of geomorphic evidence for reconstructing past environmental changes in response to rapid climate fluctuations.
- Provide a case-study of specific response mechanisms to an extreme climate event, and assess the implications of these results for predicting the potential effects of future climate changes of comparable magnitude.

1.3. Approach

To achieve the above aims, the research assesses the Icelandic glacial record, and its links with climate change. Other potential climate proxies for this time period, such as the biostratigraphic record, are problematic because the event is so short-lived, and Iceland does not maintain a good record. The glacial record is a good palaeoclimatic indicator as it is extensive in Iceland, it provides field evidence, and it can be modelled. A fieldwork and modelling approach is thus used to investigate putative response mechanisms to the "8.2ka event" in the Borgarfjorður region of northeast Iceland, as a means of assessing the impact of the event. Three key lines of evidence are addressed, namely the landform record (derived from geomorphic

mapping), a dated chronology (based on tephrostratigraphy and radiocarbon dating) and modelling experiments (constrained by field data). The study will focus on understanding the complexities of environmental response to climate forcing. Specifically, the research investigates the extent to which the glacial and climate records are coupled. Geomorphic events which occurred in the field area during the early to mid Holocene are studied, and the extent to which these events may represent potential response mechanisms to the "8.2ka event" is assessed. Through investigations into spatial and temporal variations in geomorphic evidence, conclusions can be drawn about the nature and complexity of process-response mechanisms, and the multitude of ways in which response might occur to future climate events.

The approach combines empirical data and modelling in combination because it allows assessment of the evidence at a variety of spatial and temporal scales. This in turn can present information ranging from single landform genesis processes, to landscape-wide processes responsible for development of numerous suites of landforms. Initially the research is data orientated, focusing on evidence presented in the geomorphic maps, the value of which is maximised by conceptual modelling of preservation potential and topographic control on landform development. As the research develops, the emphasis shifts more towards numerical modelling which is constrained by the geomorphic data gathered in the field.

1.3.1. Field-based evidence

Detailed geomorphic mapping of the field area in northeast Iceland (Figure 1.3-a) enables a reconstruction of geomorphic events during the Holocene. Dating control on the reconstructed chronology is achieved using tephrostratigraphy and radiocarbon dating, which allows correlation with events in the North Atlantic and further afield. Through this well-constrained chronology, specific geomorphic response mechanisms which could be related to the "8.2ka event" are detected. The field data provides high resolution evidence at a range of scales from single landform elements, through suites of landforms, to landscapes. Through this highly detailed

evidence, information can be resolved about small-scale but significant processes which have implications for understanding the specific mechanisms of response to the "8.2ka event".

Figure 1.3-a: Location of the field area, Borgarfjörður Eystri, in Iceland

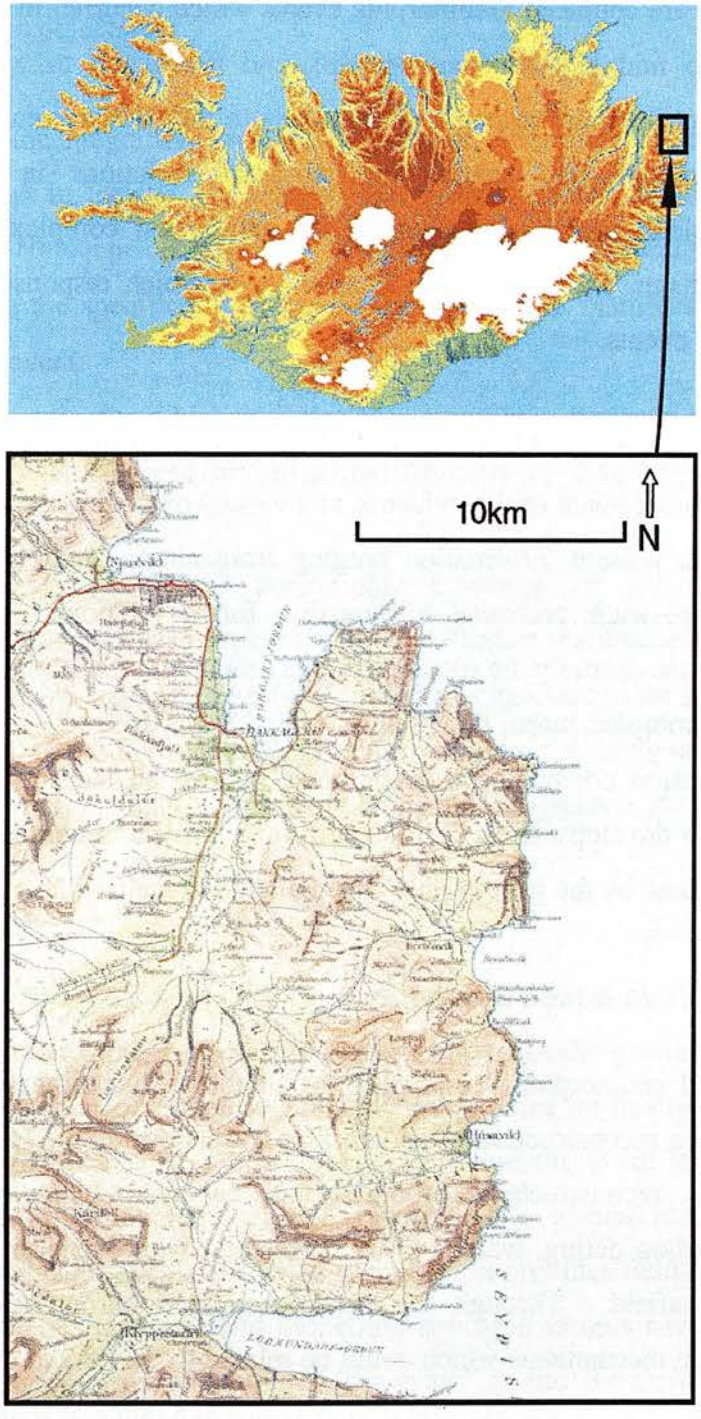

1.3.2. Modelling evidence

Modelling (both conceptual and numerical) extends the value of this small-scale detailed field evidence presented in the geomorphic maps, enabling investigations to be carried out into universal processes at landscape scales. Conceptual modelling focuses on understanding the influence of topographic and lithologic controls on landform preservation potential and morphological characteristics, by developing general rules applicable across the whole landscape universally. Numerical modelling does not have the spatial resolution of field data, but allows experiments to be run at a landscape scale, investigating the effects of changing climatic input conditions on specific geomorphic processes, and on the subsequent landform record. Geomorphic processes are seen as active responses to climatic and other forcing mechanisms, responding differently according to initial conditions and the magnitude and type of forcing mechanism. Modelling enables controlled experiments to be carried out to test the nature of process response to different input conditions and forcings, such as those representing the 8.2ka climatic fluctuation.

1.4. Background: The "8.2ka event"

The Holocene has contained several climatic oscillations (Haas et al. 1998; Korhola et al. 2000; Matthews et al. 2000; Nesje et al. 2000), of which the "8.2ka event" was the most prominent, representing the largest and most rapid shift in global climate during this time (Alley et al. 1997). Following the Younger Dryas, warming is thought to have been interrupted by this short-lived but widespread cooling, which peaked on the Greenland ice sheet at around 8,200 cal years B.P (Alley et al. 1997). It has been widely suggested that the event led to environmental responses globally, at least in the Northern Hemisphere, but the magnitude, spatial expression and mechanisms of this response are not well understood. In comparison to other climatic fluctuations in the late-glacial and early Holocene, such as the Younger Dryas and the Little Ice Age, which were both longer-lasting and more complex in structure, the "8.2ka event" was unusual, exhibiting characteristics of an event which was simple in structure, but difficult to explain in terms of simple cause-and-effect

relationships. The event attracts a degree of interest because it serves as a potential model for the influence of global warming trends on North Atlantic circulation, the hypothesis being that increased melt from Greenland and other Arctic ice caps may lead to short term freshening of ocean surface waters, and a weakening, slowing down, or cessation of the North Atlantic deepwater circulation.

The aim in this section is to provide a critical review of the size, causes, spatial extent and expression of environmental response to the "8.2ka event" in a key range of proxies across the globe. Understanding the impact of this event can give significant insight into the sensitivity of the global environmental system. This review will provide global context for the new evidence presented in this thesis, which addresses the glacial and geomorphic effects of the "8.2ka event" in Iceland.

1.4.1. Triggering Mechanisms of the "8.2ka event"

It has been suggested that the "8.2ka event" was induced by the final melting of the Laurentide Ice Sheet, and associated peak in freshwater input to the North Atlantic. This in turn could have caused a weakening of the North Atlantic thermohaline circulation and a related regional cooling episode which may have had global implications (Klitgaard-Kristensen et al. 1998; Barber et al. 1999; Nesje and Dahl 2001a; Renssen et al. 2001). This freshwater outflow event has been dated to 8,470 cal. yr BP (Barber et al. 1999), around 270 years before the peak in cold conditions in Greenland. While some disagree with this proposed mechanism for the "8.2ka event" (Hu et al. 1999; Snowball et al. 2002), it is likely that changes in ocean circulation patterns were a key factor.

There are a number of possible explanations as to how a salinity anomaly in the North Atlantic resulting from fresh-water input could promote significant changes in the global ocean-atmosphere system (Zahn 2003). 'Switching off' the North Atlantic conveyor would dramatically alter patterns of heat transport, which in turn could affect sea surface temperatures in a wider area. This forces changes in precipitation and wind trajectories towards Asia, and influence patterns of monsoon activity. If

the event was triggered in the North Atlantic, the spatial patterns of response to it may reflect this.

1.4.2. Approaches:

Definition of the "8.2ka event"

The term "8.2ka event", as defined by Alley et al. (1997) relates to the dating for an event in the Greenland ice core records. The problem with naming this event as such in a wider context is that it is suggestive of a synchronous event of well-constrained age. It prejudices the possibility of understanding the event as globally time-transgressive, Furthermore, it does not take into account the duration of the build up and decay of the event, and that it may not have had a single 'peak'. 8.2ka was one moment in an event which may have lasted several centuries. The name of the event also disregards the potential for the Southern Hemisphere records to be out of phase with their Northern Hemisphere counterparts. Consequently, climatic events related to the "8.2ka event" may have occurred in time-periods which do not specifically include the date 8.2ka BP.

Study Methods

For disparate records to be comparable, and cross-correlated, a number of methodological issues must be addressed. There are significant assumptions involved in so-called 'wiggle-matching', where peaks or troughs in one record are linked to similar variations in a different record with no necessary causal link between the two. It is not necessarily the case that the more pieces of evidence found for an event, the more certain its existence becomes, and it is vital to consider what conclusions may be drawn from records which show no evidence for an event.

Recorded "evidence" for the "8.2ka event" in proxies implies that the exact duration and magnitude of the event is unclear, and a single 'peak' date for the event is not common to all records. However, the characteristics of the recorded response do not necessarily reflect variations in actual response mechanisms. As a result, in order to assess the expression of the event in terms of environmental characteristics,

magnitude and duration of response, recorded environmental changes at 8.2ka are assessed with respect to the following factors:

- Geographical position
- Resolution of the record (deemed to be a measure of dating precision and accuracy).
- The environmental system from which the record is derived

From this it will be possible to assess whether various fluctuations in disparate environmental records reflect a wide-spread synchronous or time-transgressive climate event, or a series of unrelated regional oscillations.

Proxy Record Selection

Figure 1.4-a: Summary of locations from which proxy records discussed in this study originate

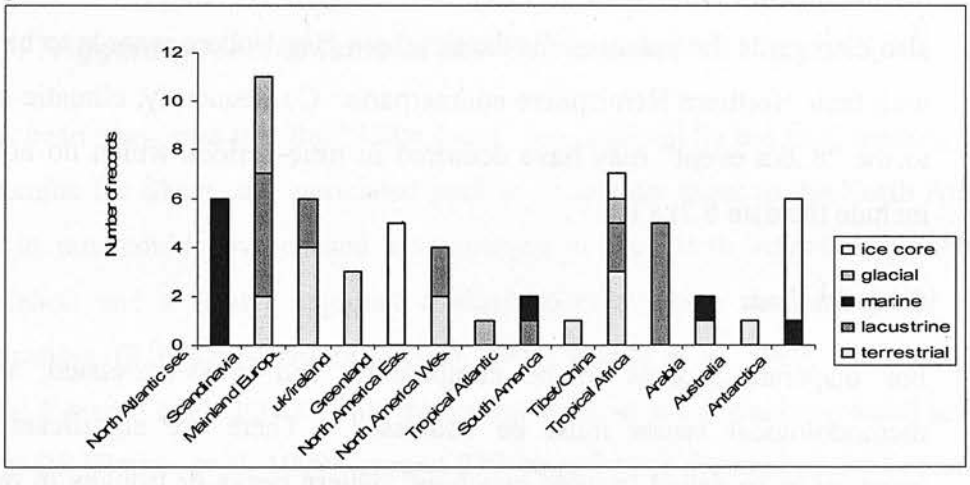

We aim to characterise the nature of system response to the "8.2ka event" through time and space, based on published evidence. An analysis of available environmental records, selected to be representative of the key regions of the globe, should help indicate the nature of response mechanisms to such an event globally. Figure 1.4-a summarises the various records used, and their origins. We utilise records of both high and low resolution, and from multiple environmental systems. On the basis of currently available records, using only high resolution records restricts the geographical area which it is possible to cover and makes it more difficult to develop a characterisation of global response to the event. Restricting the

search to records from only one specific type of proxy would again restrict the geographical area, and indicate the response of only one type of system.

Chronology

To evaluate spatial and temporal variations in the recorded effects of the "8.2ka event", chronologies must be calibrated onto a common time-scale. Unless otherwise stated, dates henceforth are in calendar years Before Present (cal. yr. BP). Calibration of non-calendar year dates is carried out using the methods outlined in Table 1.4-a. Figure 1.4-a shows the timing of all recorded 'evidence' for the event. Records are grouped by region and arranged in order of relative distance from the North Atlantic. It may be possible to test the North Atlantic trigger hypotheses by assessing whether the timing of potential response varies with distance from the triggering point. Records of highest resolution (annual or seasonal) are highlighted to show the best-constrained dated environmental changes which may have occurred in response to the event. Where dating error margins are known, they are included to show the possible spread of dates. Where dating errors are not known, or only minimum dates are recorded, dotted lines indicate an uncertainty margin.

1.4.3. Spatial Variations

The following section outlines the varying putative response to a climatic event around 8.2k cal. yr BP with geographical position, as recorded in the proxy records (see Figure 1.4-b and Figure 1.4-c). Appendix I summarises the details of the records used which indicate a possible response to the event. We highlight considerable spatial variation globally, in the magnitude and environmental characteristics of the response, and in the timing and length of the response time.

Timing and putative responses

Leads and lags in the timing of environmental perturbations between regions, as illustrated in Figure 1.4-b, provide an indication of the way in which the global environmental system may have responded to and propagated the "8.2ka event" through space. This has implications for understanding the global teleconnection

mechanisms responsible for promoting an event occurring in one region into a globally significant climatic and environmental oscillation.

A general trend is evident in Figure 1.4-b, where dates of environmental change vary increasingly before or after 8.2ka the further away they are from the North Atlantic area. The approximate date for the initiation of the North Atlantic salinity anomaly (8.47ka) is included in Figure 1.4-b, in order to assess whether spatial variations in timing of environmental change supports the North Atlantic trigger hypothesis. Allowing for errors in the dating of the freshwater outflow, if this event was the trigger, all recorded environmental change should post-date 8.47ka. In most regions, with the exception of the Tibet/China area, and tropical Africa, environmental changes do post-date this time so they are consistent with global propagation of a North Atlantic cooling.

Putative responses in the North Atlantic, Scandinavia, Greenland, Eastern North America, mainland Europe and the British Isles lie mostly between 8.5 and 8ka. Dates from the tropical Atlantic appear to generally lag those from the North Atlantic region, as do those from Antarctica. However, it would still be possible within the large dating error margins, for the Antarctic environmental changes to precede the North Atlantic. The same problem is evident in the Australian record, with large error margins making identification and exact timing of the putative response hard to quantify. Dates from Asia and Africa are variable, some preceding the North Atlantic area in their start dates, but extending as far as 7.5ka. The African records which show a shorter event do generally occur synchronously with the North Atlantic area. Asian records showing shorter possible response times do significantly precede 8.47ka however (Figure 1.4-b). Dates from Arabia are well-constrained and show a short event of 400 years which associates well with other records.

Figure 1.4-b: Timing of environmental change putatively associated with the 8.2ka event

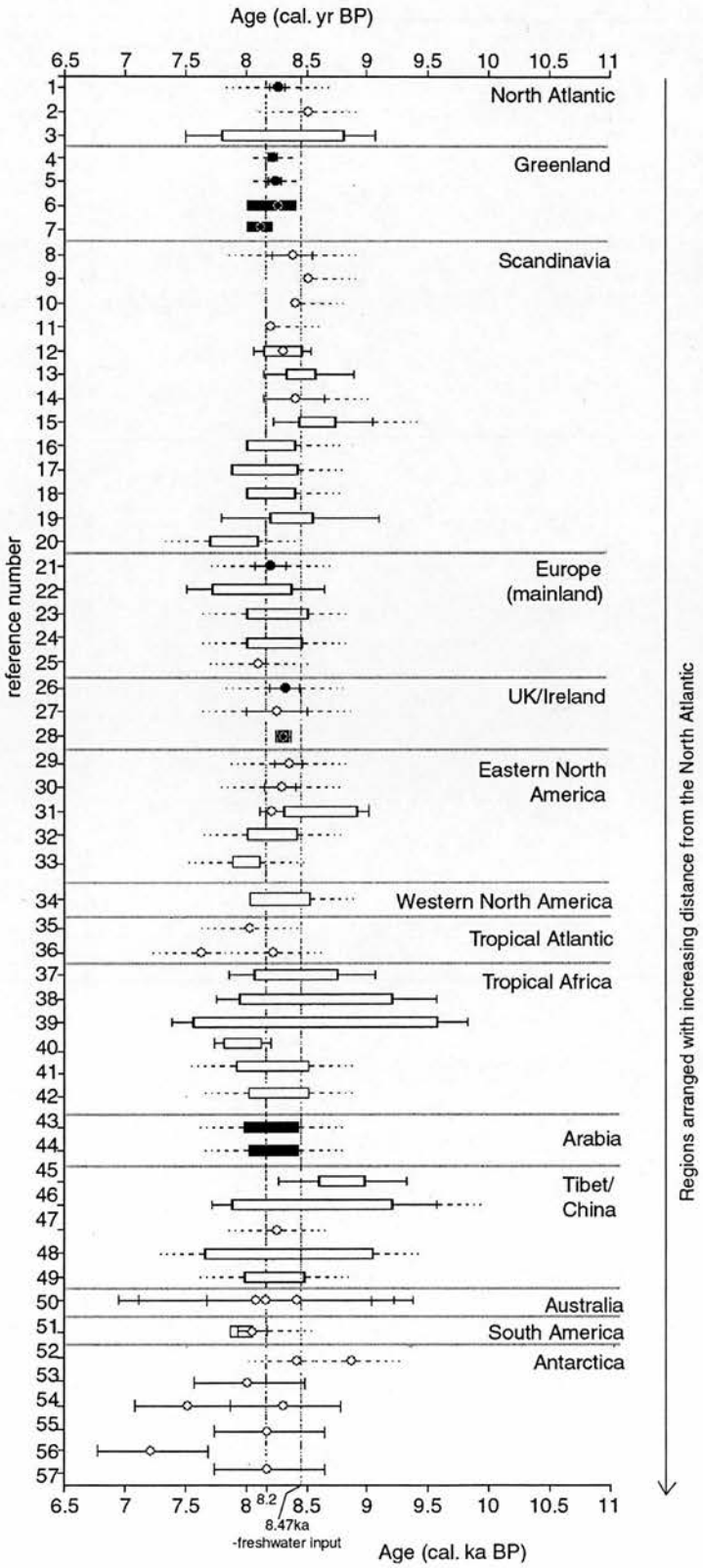

Figure 1.4-b illustrates the timing of the "8.2ka event", as suggested by the proxy records discussed in this section. See Table 1.4-a for reference information.
Records are organised by geographical region and calibrated onto a common time-scale.

Circles indicate peak dates, solid rectangles show recorded duration of change, solid lines show error margins, and dotted lines indicate where error margins are unknown.

Table 1.4-a: Calibration and Reference Information and key for Figure 1.4-b

Region	Number	Reference	Original dating method	Calibration Method
North Atlantic	1	(Klitgaard-Kristensen et al. 1998)	C^{14}	(Stuiver and Reimer 1993)
	2	(Andruleit and Baumann 1998)	C^{14}	(Winn et al. 1991)
	3	(Bianchi and McCave 1999)	C^{14}	?
Greenland	4	(Johnsen 1992)	ice core	n/a
	5	*Dansgaard, 1987*	ice core	n/a
	6	(Alley et al. 1997)	ice core	n/a
	7	(Johnsen et al. 2001)	ice core	n/a
Scandinavia	8	(Barnett et al. 2001)	C^{14}	(Stuiver et al. 1993)
	9	(Nesje et al. 2000)	C^{14}	(Stuiver et al. 1993)
	10	(Nesje et al. 2000)	C^{14}	(Stuiver et al. 1993)
	11	(Nesje et al. 2000)	C^{14}	(Stuiver et al. 1993)
	12	(Korhola et al. 2000)	C^{14}	(Stuiver et al. 1993)
	13	(Karlén 1976)	C^{14}	OxCal
	14	(Dahl and Nesje 1994)	C^{14}	OxCal
	15	(Dahl and Nesje 1996)	C^{14}	OxCal
	16	(Nesje et al. 2001a)	C^{14}	(Stuiver et al. 1998)
	17	(Seierstad et al. 2002)	C^{14}	(Stuiver et al. 1998)
	18	(Matthews et al. 2000)	C^{14}	(Stuiver et al. 1993; Stuiver et al. 1998)
	19	(Hammarlund et al. 2003)	C^{14}	(Stuiver et al. 1993)
	20	(Snowball et al. 2002)	unclear	?
Europe	21	(Von Grafenstein et al. 1998)	C^{14}	?
	22	(Haas et al. 1998)	C^{14}	OxCal
	23	(Rousseau et al. 1993; Rousseau et al. 1994)	C^{14}	(Stuiver et al. 1993)
	24	(Wagner et al. 2002)	C^{14}	?
	25	(Magri and Parra 2002)	C^{14}	(Stuiver et al. 1998)

UK/Ireland	26	(McDermott et al. 2001)	U-Th	?
	27	(Rousseau et al. 1998)	C^{14}	OxCal
	28	(Baldini et al. 2002)	U-Th	?
Eastern N.	29	(Kneller and Peteet 1999)	C^{14}	OxCal
America	30	(Laird et al. 1998)	C^{14}	(Stuiver et al. 1993)
	31	(Hu et al. 1999)	C^{14}	(Stuiver et al. 1993)
	32	(Kurek et al. 2004)	C^{14}	(Stuiver et al. 1993; Stuiver et al. 1998)
Central N.	33	(Seppä et al. 2003)	C^{14}	
America				
Western N.	34	(Menounos et al. 2004)	C^{14}	(Stuiver et al. 1998)
tropical Atlantic	35	Street-Perrott & Perrot, 1990	C^{14}	OxCal
	36	Hughen et al, 1996	C^{14}	(Stuiver et al. 1993)
tropical Africa	37	(Street-Perrot and Perrott 1990)	C^{14}	OxCal
	38	(Street-Perrot et al. 1990)	C^{14}	OxCal
	39	(Street-Perrot et al. 1990)	C^{14}	OxCal
	40	(Stager et al. 2003)	C^{14}	(Stuiver et al. 1993)
	41	(Gasse 2000)	C^{14}	(Stuiver et al. 1993)
	42	(Gasse 2000)	C^{14}	(Stuiver et al. 1993)
Arabia	43	(Neff et al. 2001)	U-Th	(Stuiver et al. 1998)
	44	(Gupta et al. 2003)	C^{14}	(Stuiver et al. 1993)
Tibet/China	45	(Van Campo and Gasse 1993) (Van Campo et al. 1996) (Gasse et al. 1996)	C^{14}	OxCal
	46	(Lehmkuhl 1997)	C^{14}	OxCal
	47	(Thompson et al. 1997)	Ice core	n/a
	48	(Yi et al. 2003)	C^{14}	(Stuiver et al. 1998)
	49	(Zhang et al. 2000)	C^{14}	(Stuiver et al. 1993)
Australia	50	(Nott et al. 1999)	Thermo-luminescense	

South America	51	(Pendall et al. 2001)	C^{14}	(Stuiver et al. 1993)
Antarctica	52	(Taylor et al. 2001)	C^{14}	(Stuiver et al. 1993)
	53	(Masson et al. 2000) VOSTOK	Ice core	n/a
	54	(Masson et al. 2000) KOMOSOMOLKAIA	Ice core	n/a
	55	(Masson et al. 2000) BYRD	Ice core	n/a
	56	(Masson et al. 2000) LAW	Ice core	n/a
	57	(Masson et al. 2000) TAYLOR	Ice core	n/a

Environmental characteristics and magnitude of environmental changes at 8.2ka

There is great disparity in both the timing of the event globally, and in the way it manifests itself. While in Scandinavia and some parts of mainland Europe, the change at 8.2ka is thought to have been cold and wet, in Greenland, the Mediterranean, Eastern North America, tropical Atlantic, central Asia, Africa, and Antarctica, records have shown changes that produce distinctly dryer and colder climates (see synthesis in Figure 1.4-c).

The magnitude and length of putative response to the event varies significantly with different records. In order to compare the relative magnitudes of response, the size of 8.2ka fluctuation in the record relative to a surrounding mean was measured. All the records collected were compared and placed within a suitable magnitude bracket (Figure 1.4-d and Figure 1.4-e). A measurement was made of the observed duration of the fluctuation in the record, and it was placed within a suitable bracket. Figure 1.4-c shows the relative magnitudes and length of putative response times through space. The greatest magnitude of environmental change was evident in Greenland ice cores, where records indicate a possible response which is half the amplitude of the Younger Dryas (Alley et al. 1997), but very short lived (Barber et al. 1999; Renssen et al. 2001). This short-lived and high magnitude event in Greenland had contrasting

correlatives elsewhere. While in Europe and Eastern North America the fluctuation was of a similar structure to Greenland, in tropical Africa, Asia, and Antarctica, the environmental change was lower magnitude but longer-lasting.

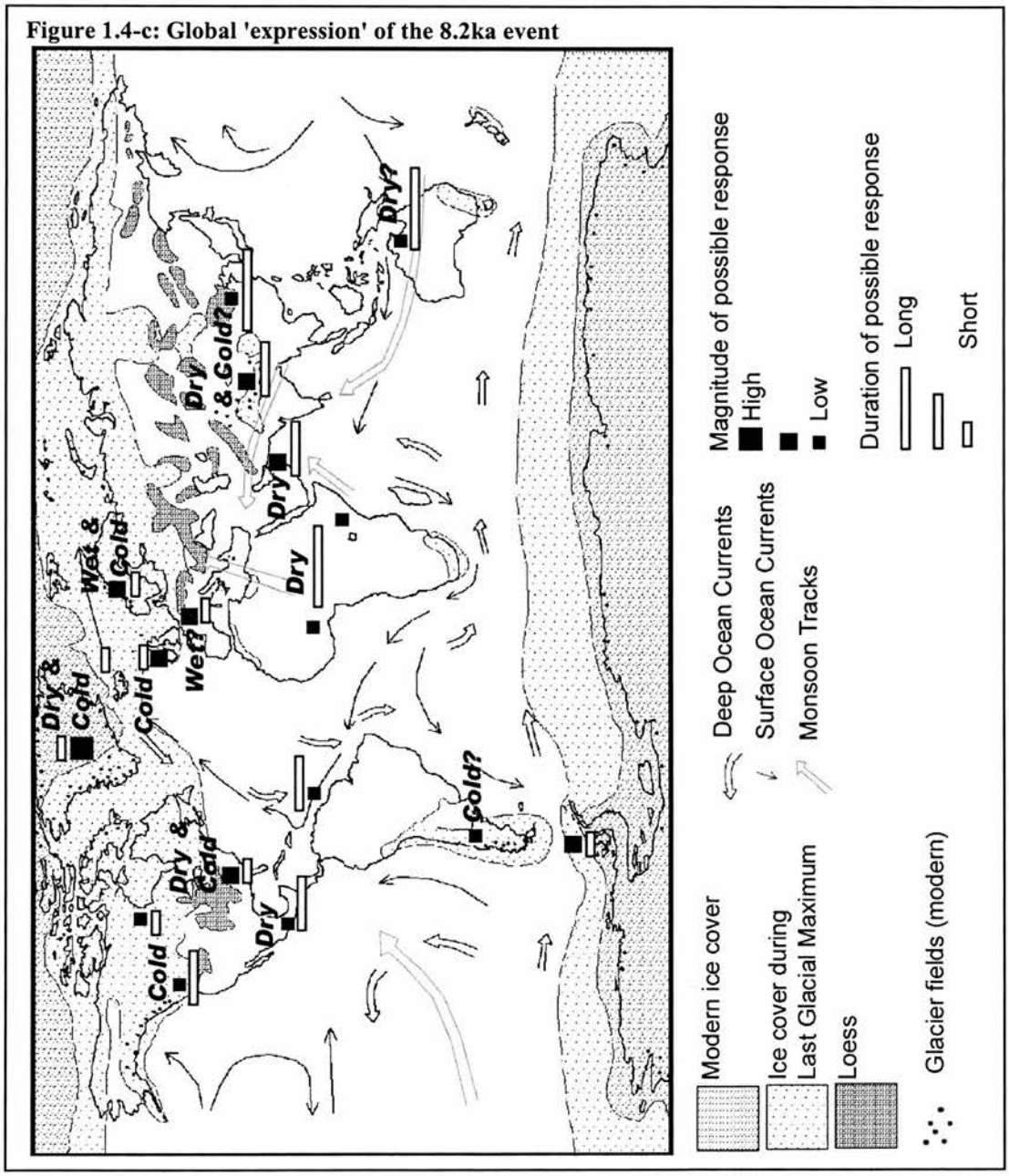

1.4.4. Variations due to recording techniques & inherent system characteristics

A key question to address is whether the observed differences in magnitude and timing of environmental change are proportional to the differences in magnitude and

length of climatic influence through space, or determined by dating and recording techniques and inherent properties of different types of environmental system. Further, it is important to ascertain whether the different timings and expressions in the environmental records described above, represent variations in the inherent properties of the 'event', or regional variations as a result of regional conditions.

Record Resolution

This section aims to outline how the expression of environmental change varies in the proxies as a function of the resolution of the record. Figure 1.4-d shows the records with a discrete phase of change, and how the duration of the event varies with the resolution of the record. It can be seen that low magnitude and longer putative response times (more than 1000 years) tend to be exhibited in low resolution records.

Figure 1.4-d: Association between record resolution and recorded "response" duration

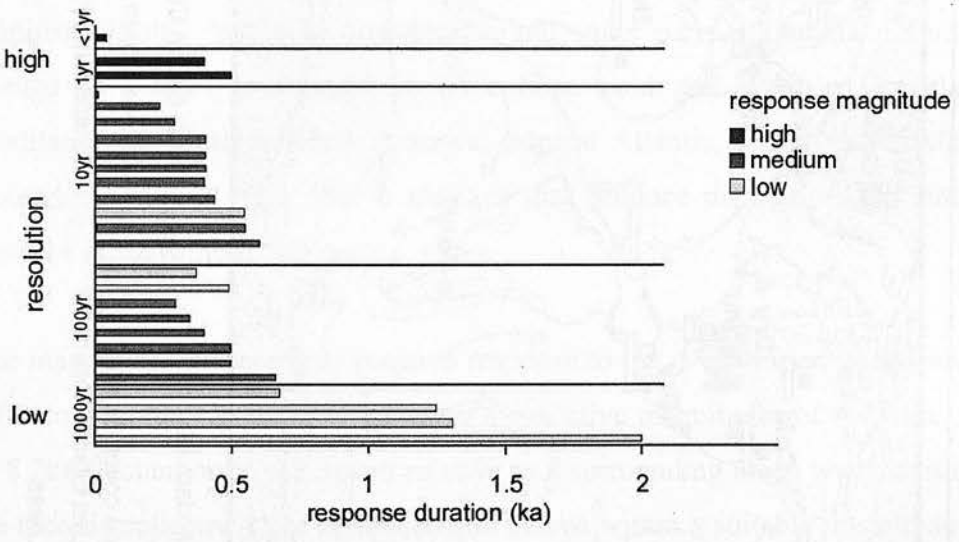

The records showing the highest magnitude changes are of high (annual) resolution. In the record which identifies seasonal variations, the duration of recorded change is very short. Though the records of medium magnitude vary in resolution from decadal to centennial, there is correlation between variables in the extremes (longest and shortest duration of environmental change; highest and lowest magnitude).

It is concluded that, although not the only defining factor in the way the event is expressed in proxies, record resolution does have an influence and therefore must be considered in any direct comparison between disparate proxies. This point is illustrated well by three separate speleothem records of different resolutions taken from the same cave in Ireland (McDermott et al. 1999; McDermott et al. 2001; Baldini et al. 2002). The highest resolution record shows a distinct cold and dry spell with two peaks, lasting for a total of 37.5 years (Baldini et al. 2002). The resolution is sufficient to show seasonal variations in temperature and precipitation. An earlier record from the same speleothem but of coarser resolution displayed a single peak at 8.32ka with error margins of 120 years (McDermott et al. 2001). The first speleothem record from this location showed centennial variations, and documented no evidence of change associated with the "8.2ka event" (McDermott et al. 1999). In lower resolution records, because dates are less precise, any fluctuation appears to be either longer lasting or completely absent from the record.

Issues of resolution are again evident in records from Western North America. Only one record from this area (Menounos et al. 2004) recorded evidence for a possible response to the "8.2ka event". This was in the form of a glacial advance in British Columbia, Western Canada, dated to between 8.63 and 8.02ka BP. Other records from Western North America (Mann and Hamilton 1995; Hansen and Engstrom 1996; Pellatt et al. 2001; Palmer et al. 2002; Barron et al. 2004) show no significant environmental change in temperature records, vegetation patterns or in other proxies to a cooling event around 8.2ka. In fact temperatures are thought to have been warmer than at present (Palmer et al. 2002). Menounos et al. (2004) suggest that the lack of evidence in other proxies from the region is due to the low resolution of such records, and a subsequent inability to record a short-lived cooling of the climate. A 15,000 year marine record from the Gulf of California is presented by Barron et al. (2004), which shows no evidence of a specific change at or near 8.2ka. However, sampling was taken only once every 40-100 years, so it is possible that any response to a climatic fluctuation which may have lasted less than 40 years (Baldini et al. 2002) would not show up in this record. It is significant that the environmental change recorded by Menounos et al. (2004) is of a low magnitude. The recorded

glacial advance which may have occurred in response to the "8.2ka event" is considerably less extensive than the advance recorded in response to the more recent Little Ice Age, a climatic cooling of a lower magnitude than that at 8.2ka. In Eastern North America, records show environmental change at the time of the "8.2ka event" as greater in magnitude than response to the Little Ice Age. This highlights a real spatial variation in responses to a global Holocene climate change.

African and Asian records used in this study seem to show a long-lasting event, which may in fact correspond to the lower resolution dating rather than the actual length of response time. A period of increased dune formation due to increased aridity was recorded in northern Australia (Nott et al. 1999), with dates for individual dune formation centring around 8.2ka and 6ka. However, the recorded dates contain potential errors stretching almost 2000 years around each date, which means it is difficult to differentiate between what may be two shorter phases of aridity and a single longer arid spell. It is significant that the aridity indicated by the low resolution Australian record is comparable with dry periods in the Asian and African records.

At present, the record resolution from these regions is low, which makes realistic correlations error-prone. However, the existence of a recorded precipitation reduction between 8.4 and 8ka in two high resolution records from the Arabian peninsula (Neff et al. 2001) and the Arabian sea (Gupta et al. 2003), indicate a change in the monsoon system. As the monsoon system is a major environmental control on environmental conditions in tropical Africa and Asia (Street-Perrot et al. 1990), it is possible that the long dry spells recorded in the lower resolution African and Asian records may be related to the monsoon weakening recorded in the Arabian records.

There is a relative dearth of climate and environmental records spanning the Holocene in areas such as tropical South America (Argollo and Mourguiart 2000). The absence of evidence for change at 8.2ka and afterwards in South America may be due to the lack of sufficient high resolution records. Numerous ice cores have

been extracted from tropical South America (Thompson et al. 1998; Thompson et al. 2000; Ramirez et al. 2003) but resolution is poor in comparison to ice core records from the polar regions, often showing only 100 to 200 year variations.

The Antarctic records, representing 5 different ice cores, show peak dates varying by over a thousand years (Masson et al. 2000). This may be a result of low resolution and poorly-constrained dates for the Early Holocene parts of the ice cores, and makes the characterisation of regional change in Antarctica difficult, as we cannot ascertain whether the changes in the Antarctic are in phase with the northern Hemisphere at this time.

Inherent system characteristics

The type of proxy environmental record used greatly influences the recorded magnitude and duration of climatic change, and Figure 1.4-e illustrates this. Certain systems (such as glacial) are likely to respond quicker and to a greater extent to climate forcing than other systems (e.g. marine). Marine systems, therefore may never fully respond to a short-lived climate change. This means that although, as shown in Figure 1.4-e, marine environments like the North Atlantic Ocean indicate a relatively low magnitude climatic forcing in terms of the proxy record generated, the 'real' climatic fluctuation is likely to have been of a greater magnitude. This is highlighted by the fact that the Greenland ice core record, a reliable indicator of climatic variations, shows a climatic 'event' of a much greater magnitude.

Similarly, in Figure 1.4-e, pollen records generally exhibit longer putative response times than other proxies. Rather than indicating real spatial variations in the characteristics of the event, this may be indicative of sampling resolution or the fact that these vegetation communities are slow to respond to this type of change. Many records show no environmental change at or around the time of the event. However, absence of evidence is not necessarily evidence of absence. Nott et al. (1999) hypothesise that the lack of evidence for their early Holocene Australian arid phase in pollen cores is due to the abrupt and short-lived nature of the climatic fluctuation.

Figure 1.4-e: Influence of system type on recorded "response" magnitude

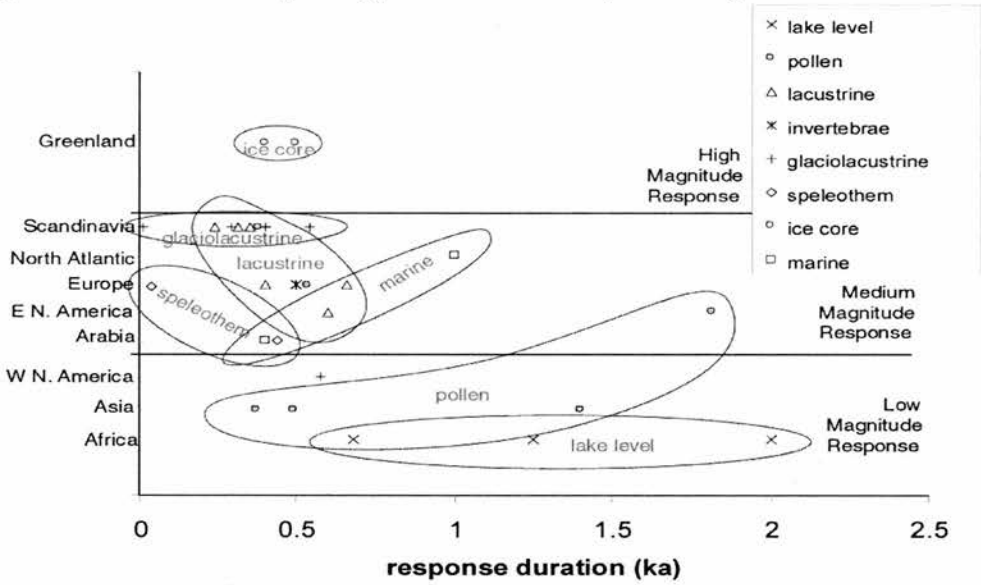

1.4.5. No Response?

Evidence of environmental change in Australia, Western North America and South America that could be part of a response to the "8.2ka event" are limited to a single record in each area, while many records for tropical South America show no specific evidence of a cooling event at this time (Thompson et al. 1998; Argollo et al. 2000; Thompson et al. 2000; Baker et al. 2001; Cross et al. 2001; Abbott et al. 2003; Ramirez et al. 2003). In southern South America, numerous environmental proxies are available (Markgraf 1993; Heusser 1995; Glasser and Hambrey 2002; Markgraf et al. 2002; Markgraf et al. 2003; Glasser et al. 2004; Moreno 2004), but none show environmental changes at 8.2ka. These dates cover the northern and southern parts of South America, and include ice core, lake level, lacustrine, glacial and palynological records of varying resolution. High resolution (decadal) ice core records from tropical South America, which were sufficient to record a response to the Little Ice Age cooling event, did not record environmental change at the time of the "8.2ka event" (Thompson et al. 2000).

Overall there is a lack of evidence for any significant response to the "8.2ka event", even in high resolution records from South America, as noted by Glasser et al. (2004). However, it cannot be ruled out that the Patagonian peat record (Pendall et al. 2001) may be indicative of a small response to the "8.2ka event". Dating uncertainty from radiocarbon at this point in the record is around +/- 110years, which would allow a possible connection with 8.2ka, with a peak response slightly lagging the Greenland record.

1.4.6. Causal Mechanisms and Global Teleconnections

To understand how events in disparate regions are related, the existence of an underlying cause, or chain of events, which resulted in the observed pattern of environmental change globally must be investigated. Co-incidence and/or correlation of events may indicate a temporal but not causal relationship. The ocean and atmosphere constitute the main mechanisms of global energy transport, which influence climatic conditions and create teleconnections between different regions (Mikolajewicz et al. 1997; Clark et al. 2002). Correlations have been made between climatic events in Africa and Europe (Magri et al. 2002), Africa and Asia (Street-Perrot et al. 1990; Lamb et al. 1995; Gasse et al. 1996), Australia and Asia/Africa (Nott et al. 1999), the North Atlantic and Asia (Gasse 2000; Gupta et al. 2003), the North Atlantic/Greenland and Antarctica (Grootes et al. 2001), and between the North Atlantic and North Pacific (Mikolajewicz et al. 1997), supporting the hypothesis that forcing of a climatic event in one region can have distinct climatic effects over a wider area. It is therefore possible that a trigger for the "8.2ka event" in one region would have global effects.

Figure 1.4-c shows the major routes of oceanic and atmospheric energy transport, through which a forcing mechanism in one part of the globe may induce abrupt climatic changes elsewhere. From Figure 1.4-c, North Atlantic circulation can be seen to link North America, Greenland and Europe by the North Atlantic Conveyer. It is less clear how climatic perturbations in this region may relate to those in Africa and Asia. Monsoon systems in tropical Africa and Asia are thought to be an

important mechanism in global energy re-distribution and climate forcing (Porter and Zhisheng 1995; Gasse et al. 1996; Porter 2001; Huang et al. 2002; Gupta et al. 2003; Zahn 2003).

A weakening of the monsoon system is recorded in high resolution Arabian proxies between 8.4 and 8ka (Neff et al. 2001; Gupta et al. 2003). This weakened monsoon is evident in characteristics of response throughout Africa and Asia, showing distinctly dry conditions at this time. This is supported by work suggesting a synchronicity between the African and Asian records characterised by a weakening of the monsoon, leading to arid conditions (Van Campo et al. 1996). Dry conditions are also recorded in Australia at this time (Nott et al. 1999), which would also be linked through the monsoon.

It is not yet possible to clarify whether the distinct weakening in the monsoon could be a direct effect of the North Atlantic salinity anomaly, or whether it represents an independent climatic event occurring at a similar time. It is significant that the regions which show the initiation of a response pre-dating the freshwater input to the North Atlantic, are those in areas affected by monsoon variations (Asia and Africa). This suggests that the monsoon changes may pre-date the salinity anomaly, so it could not be an effect of the "8.2ka event". With increased high-resolution records such as the Arabian records, it will be possible to date the onset of environmental change in Asia and Africa with more accuracy. It is conceivable that, given the apparently synchronous environmental changes in disparate regions, the effects of a weakened monsoon served to help transfer and propagate the effects of the North Atlantic salinity anomaly to a wider area beyond the immediate North Atlantic.

Environmental changes have been recorded in Antarctica (Masson et al. 2000), and in Antarctic peninsula marine records (Taylor et al. 2001), which might be explained as a result of ocean currents flowing between the North and South Atlantic regions. However, better environmental data is needed in order to assess the existence of a bipolar seesaw and inter-hemispheric linkages in this case. If the Antarctic records indicate a true response to the same 8.2ka triggering event as that in Greenland and

the North Atlantic, one would expect to find a response in southern South America, as their climate is strongly coupled with the Antarctic climate through the Antarctic circumpolar current (Grootes et al. 2001). The non-existence of the event in tropical South America but potential response in the southern region corresponds with a possible relationship between the hemispheres.

Summary – global expression of the 8.2ka event

A high magnitude, short-lived cooling event found in the Greenland ice core records at 8.2ka is also strongly evident in Eastern North America, the Tropical Atlantic, the North Atlantic and Europe. In Tropical Africa, Arabia and Asia, contemporaneous environmental changes are represented by more subdued but longer lasting events related to changing monsoon patterns. Limited and less well-constrained evidence indicates possible related environmental change in Western North America, South America, Australia and Antarctica. Environmental change globally has been characterised by colder, wetter or dryer climates.

Data on environmental changes in the Early Holocene is often unreliable due to the resolution of the record, and the inherent properties of the different systems, some of which respond more quickly and to a greater extent than others. It is suggested that although some records show a climatic change lasting for as long as one thousand years, the event was shorter-lived than that, and in some areas the duration of these episodes may have been exaggerated by comparatively low resolution records. Further research and improved dating is required before specific leads and lags between different regions can be identified with certainty. However, by including low resolution records in the review, it has been possible to get a broad idea of the global expression of the "8.2ka event", and to highlight areas in which further study would be particularly useful. It is important that increased interest in the event, does not result in its characterisation as a climatic fluctuation of a higher magnitude or higher global significance than evidence suggests. Awareness of this event and the recovery of higher resolution records for the relevant time period in other parts of the globe may help indicate the potential environmental changes induced by any future weakening of the North Atlantic.

1.5. Background: Potential Icelandic response to the "8.2ka event"

If the "8.2ka event" manifested itself as a cooling event in Iceland, there is a multitude of ways in which the environment may have responded. The potential expression of the "8.2ka event" in Iceland can be best hypothesised when viewed in its spatial and temporal context. Initially, the "8.2ka event" in Iceland is viewed relative to the environmental effects of the event in the surrounding North Atlantic region. Secondly, the extent of Icelandic environmental (mainly glacial) response to other known climatic fluctuations through time is discussed, with reference to the relative magnitudes and duration of the cold spell. An important focus of this study is to resolve the glacial history of Iceland just prior to 8.2ka. The nature of environmental 'response' to such a short-lived, extreme cooling event will be defined to a large extent by the initial climatic and environmental conditions at the time of onset.

It is acknowledged that the existence of similar fluctuations in different records does not imply a causal relationship, nor does the fact that a system has responded in a certain way to one event mean that it will respond in the same way to a similar event at another point in time. However, knowledge of the way in which disparate environments have responded to specific climatic fluctuations, and the way in which a specific environment has responded to temporally distinct climate events, is valuable. It gives an insight into the sensitivity of the system to change and the synchronicities between different systems, and therefore can provide invaluable information on the ways in which a system might have responded to a less well documented 'event' such as the "8.2ka event".

1.5.1. Spatial context: The North Atlantic and surrounding land masses

Environmental changes thought to be related to the "8.2ka event" have been detected in Greenland, Scandinavia, North America, Europe and the North Atlantic, as highlighted in 1.4. When attempting to determine environmental change in Iceland

at this time, and its relation to the "8.2ka event", one must consider how Icelandic climate is linked to that of these surrounding regions. The North Atlantic acts as a conveyor of climatic events through its circulation patterns (illustrated in Figure 1.5-a), allowing synchronous events on surrounding land masses to be attributed to a unified cause. The influence of the North Atlantic is outlined, which is of particular significance given the evidence for a North Atlantic trigger for the "8.2ka event".

Figure 1.5-a: Ocean circulation patterns around Iceland

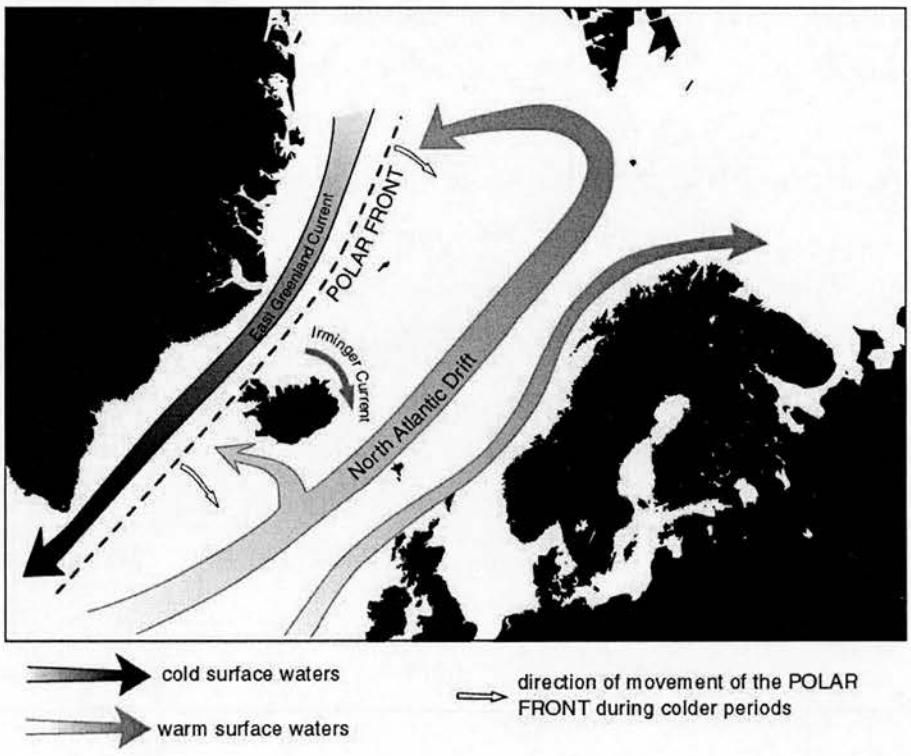

Figure 1.5-a shows the current location of Iceland relative to the North Atlantic Polar Front, which is formed where cold waters from the Arctic meet warm waters from the tropics. Movement in the position of this front warms or cools Iceland's climate. The ocean circulation patterns are derived from the literature (Bauch and Weinelt 1997; Birks and Koç 2002).

The climate and environmental history of the North Atlantic region is tied to shifts in the North Atlantic Polar Front, shown in Figure 1.5-a. The Greenland ice core records and Scandinavian records are roughly in phase with records of variations in this front, which is driven by the ocean thermohaline circulation (Sveinbjörnsdóttir and Johnsen 1990; Ingólfsson et al. 1997). Because of Iceland's proximity to the polar front, the island is sensitive to minor fluctuations in its position (Norðdahl et al. 2001). The front need not move far in a south and eastwards direction, to causes

cold waters to surround Iceland, with dramatic climatic implications. Therefore Iceland has the potential to offer a high resolution record of system response to climate change (Ingólfsson et al. 1997; Knudsen and Eiriksson 2002). Dramatic changes in Iceland's climate through time, which induce changes in environment such as ice cover and vegetation, have been shown to correlate well with records of changes in ocean and atmospheric circulation in the North Atlantic region (Eiríksson et al. 2000; Norðdahl et al. 2001; Knudsen et al. 2002). This indicates that changes in circulation patterns associated with the "8.2ka event" are highly likely to have influenced the Icelandic environment in a comparable way.

Variation in freshwater influx to the North Atlantic disrupts normal patterns of circulation, with a direct influence on climate (Ingólfsson et al. 1997). As previously discussed, the catastrophic drainage of two Laurentide glacial lakes during the ice sheet's final stages of deglaciation is considered to be a possible cause of the "8.2ka event" climate oscillation (Klitgaard-Kristensen et al. 1998; Barber et al. 1999; Nesje et al. 2001a; Renssen et al. 2001). In addition, the importance of the final melting of the Scandinavian ice sheet into the North Atlantic, which occurred at a similar time, can not be ignored (Bauch et al. 1997; Birks et al. 2002). Deglaciation of both these ice sheets would have released considerable freshwater into the system from the east and the west in early Holocene times. A fluctuation at 8.2ka is evident in a number of marine records, indicating cooler surface waters, changes in salinity associated with meltwater influx, and disrupted circulation patterns (Andruleit et al. 1998; Klitgaard-Kristensen et al. 1998; Eiríksson et al. 2000; Birks et al. 2002). This would have had a major influence on the location of the polar front, and thus the climate in the North Atlantic and Iceland.

Based on proxy records from a large number of other studies, evidence for climatic and environmental change in the North Atlantic region at 8.2ka cal. yr BP is considerable, on and offshore (e.g. (Alley et al. 1997; Andruleit et al. 1998; Klitgaard-Kristensen et al. 1998; Von Grafenstein et al. 1998; Barber et al. 1999; Bianchi et al. 1999; Nesje et al. 2001a; Baldini et al. 2002; Wagner et al. 2002; Alley and Agustsdottir 2005). Strong evidence for a glacial advance in Scandinavia

correlated with the "8.2ka event" is named the "Finse event", dated to between 8420 and 7880 yrs BP, (Dahl et al. 1996; Matthews et al. 2000; Nesje et al. 2000; Nesje et al. 2001b; Seierstad et al. 2002). A climate fluctuation at this time has been recorded on the North Icelandic shelf (Eiríksson et al. 2000), but there is no recorded evidence of this event in Icelandic glacial records to date. Given the overwhelming evidence for a significant climatic change in the North Atlantic region at 8.2ka, and the causal link between Iceland's climate and North Atlantic Ocean circulation patterns, it is highly likely that Iceland was subject to a climatic oscillation at this time. Deriving the magnitude and mechanisms of this climate event in Iceland, and the extent (if any) of environmental "response" to it, is a principle aim of this research.

1.5.2. Temporal context: Iceland's response to previous climate fluctuations

At present, there is little information regarding the effects of the "8.2ka event" on the Icelandic environment, although valuable geomorphic evidence for climate change in Iceland is provided by its glacial history. Extensive literature exists addressing the deglaciation history of Iceland (Norðdahl 1990; Norðdahl and Hjort 1993; Ingólfsson and Norðdahl 1994; Gudmundsson 1997; Ingólfsson et al. 1997; Kirkbride and Dugmore 2001; Norðdahl et al. 2001; Caseldine et al. 2003), providing information on Icelandic glacial response mechanisms to specific climatic fluctuations, notably the Younger Dryas (YD) and Preboreal (PB) oscillations. It has been suggested that the YD and PB climate fluctuations were associated with cooling induced by freshwater input to the North Atlantic from North American ice (Fisher et al. 2002; Teller and Leverington 2003), an event which has significant impact on thermohaline circulation patterns and associated climate conditions (Clark et al. 2002). As has been discussed, strong evidence exists for such a triggering mechanism for the 8.2ka event (Alley et al. 1997; Barber et al. 1999; Fisher et al. 2002; Teller et al. 2003; Alley et al. 2005). Therefore, although the older events had variable magnitudes and durations, recorded glacial response to the better-known Preboreal and Younger Dryas oscillations (reviewed in the following section), may have implications for the

potential existence, magnitude and mechanisms of an Icelandic response to the "8.2ka event".

In addition to studies of glacial limits, the link between ice cover and relative sea level has received much attention (Norðdahl 1990; Norðdahl et al. 1993; Norðdahl et al. 2001). Retreating ice (and the subsequent glacial unloading) induces isostatic rebound and associated lowering of relative sea level, allowing for the genesis of progressively lower raised shorelines (Ingólfsson et al. 1995). This relationship between ice cover and sea level is accentuated by the characteristics of the Icelandic landscape. The ocean crust is relatively thin in Iceland and therefore highly deformable, resulting in a quick reaction to overburden such as ice cover (Norðdahl 1990). The relative sea level changes associated with other cooling periods may give an indication of the likelihood that some raised shorelines relate to the "8.2ka event". Major climatic stages since the Last Glacial Maximum (L.G.M.), and the nature of Icelandic glacial response to them, are outlined below:

1) Retreat from the Last Glacial Maximum (L.G.M.)

During the Last Glacial Maximum, at around 20,000^{14}C yrs BP, ice probably reached well beyond the present coastline, with some high altitude mountainous areas being ice-free or containing corrie glaciers. Termination of the last inland ice sheet began at around 13,000^{14}C yrs BP (Haflidason et al. 1995; Eiríksson et al. 2000), which calibrates to ~16 cal. ke BP using OxCal, resulting in the retreat of ice to within the present coastline (Ingólfsson et al. 1994), leaving considerable amounts of coastal eastern Iceland ice-free. The field area relevant to this thesis may have become ice free at this time.

2) Younger Dryas

The Younger Dryas cooling began at around 12,900 cal. yrs BP, lasting until an abrupt termination which is dated to 11,500-11,600 cal. yrs. BP in Norway (Gulliksen et al. 1998) and 11,450-11,390 cal. yrs BP in the Greenland (GRIP) ice core (Björck et al. 1996). The Younger Dryas represented a re-advance of the

Icelandic Ice Sheet to cover all but a few peripheral areas (Figure 1.5-b (i)). The extent of Younger Dryas ice in the field area has not been studied in detail, but mapping has been carried out in Eastern Iceland, immediately south of the field area (Norðdahl 1990; Norðdahl et al. 2001), the results of which are shown in Figure 1.5-b (ii). This study is thought to provide a good indication of Younger Dryas ice extent in the Borgarfjörður Eystri region, due to its proximity to the region. Two levels of raised beach, associated with glacial moraines, have been identified by Norðdahl et al. (2001), which are dated to Younger Dryas and Preboreal times by radiocarbon dating of shell samples. The locations of these shore-lines, are illustrated in Figure 1.5-b (ii).

3) Preboreal

The so-called Preboreal period was a short-lived climatic deterioration occurring shortly after the termination of the YD, dating to 11,300-11,150 cal. yrs. BP in the (Björck et al. 1997), and 11,200-11,050 cal. yrs BP in GRIP (Björck et al. 1996; Fisher et al. 2002; Teller et al. 2003). The Preboreal is thought to have induced glacial advance or still-stand in Iceland (e.g. Hjartarson et al. 1988; Norðdahl 1990; Ingólfsson et al. 1994; Norðdahl et al. 2001). The early Preboreal in Iceland consisted of an inland ice sheet from which a considerable amount of the present day land-cover protruded, though much of it was under water, due to the glacial loading of the land. In Eastern Iceland, a re-advance named the *Berufjörður stage* by Norðdahl (1990) was correlated with the Preboreal cold spell. A further study (Norðdahl et al. 2001) mapped in detail the positions of the associated Preboreal-age fossil coastlines in Eastern Iceland, illustrated in Figure 1.5-b (ii) (Norðdahl et al. 2001). In South Iceland, the age of the much-documented Búði moraines is disputed (Norðdahl 1990), though they may also be related to a Preboreal advance (Hjartarson and Ingólfsson 1988).

If the fossil coastlines recorded by Norðdahl et al. (2001), and illustrated in Figure 1.5-b (ii), are indicative of the ice limits during the Preboreal, a significant amount of mountainous coastal land was ice free. The field area for the current study,

Borgarfjörður Eystri, is in close proximity to the coast, and has a generally relatively low altitude, therefore the Preboreal re-advance is likely to be of limited extent here.

Figure 1.5-b: The Younger Dryas in Iceland

(i) *Ice extent over Iceland during the Younger Dryas*

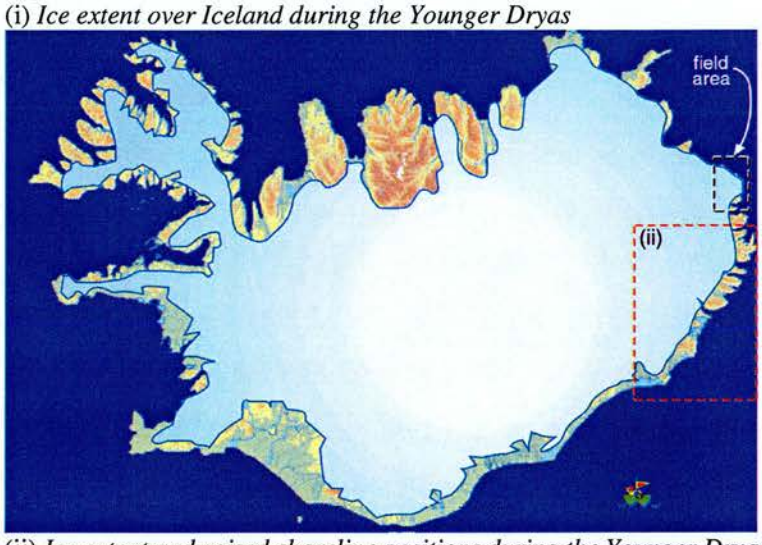

Figure 1.5-b (i) shows the estimated extent of the Icelandic ice sheet during the Younger Dryas. Figure 1.5-b (ii) (Norðdahl and Einarsson 2001) shows detail of Younger Dryas ice cover in eastern Iceland, with associated raised shorelines. It also shows the recorded positions of raised shorelines thought to relate the Preboreal glacial advance / still-stand.

(ii) *Ice extent and raised shoreline positions during the Younger Dryas and Preboreal periods*

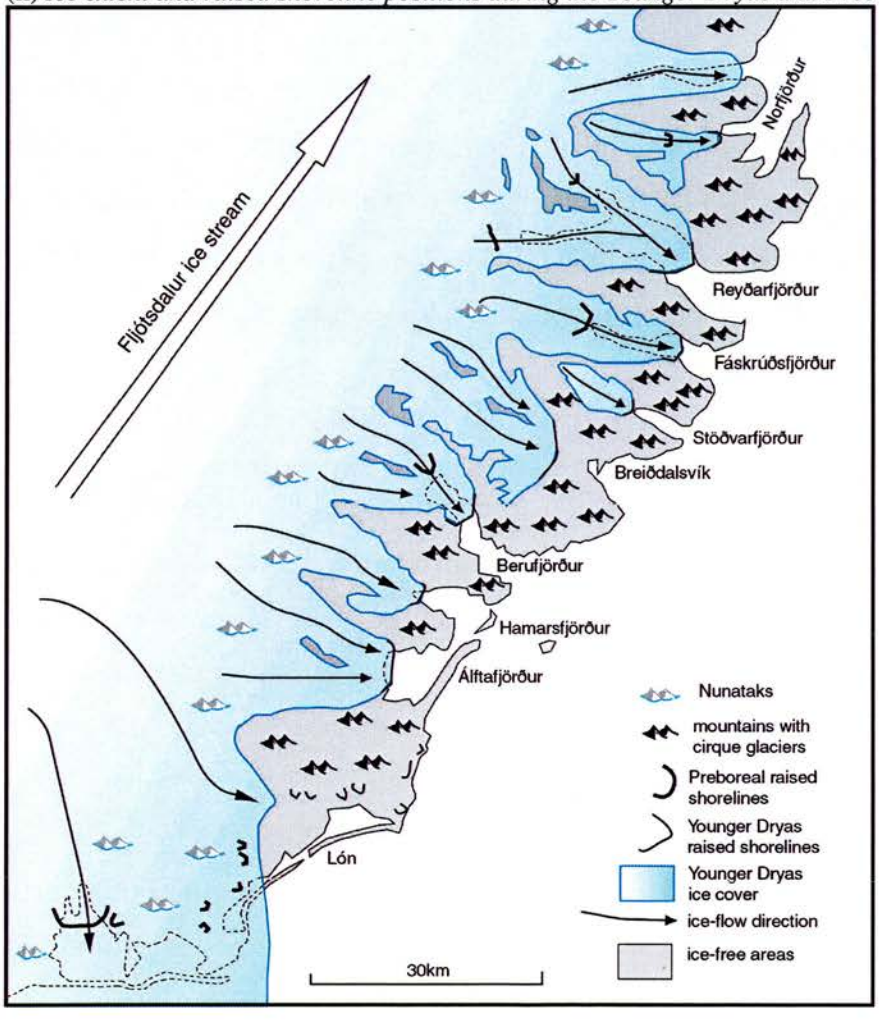

The Younger Dryas and Preboreal oscillations recorded in surrounding regions

The Preboreal and Younger Dryas glacier advances in Iceland, described above, correspond with fluctuations recorded in many proxy records from the North Atlantic and surrounding land masses (Sveinbjörnsdóttir et al. 1990). Greenland ice cores have recorded distinct drops in temperature relating to the Younger Dryas, and Preboreal climate events (Sveinbjörnsdóttir et al. 1990; Blunier et al. 1995; Grönvold et al. 1995; Johnsen et al. 2001; Muscheler et al. 2004), and North Atlantic marine records have found evidence for oceanic cooling and re-organisation of ocean circulation patterns associated with the Younger Dryas (Bauch et al. 1997). In Scandinavia, extensive research on the final stages of deglaciation from the LGM shows evidence for a Younger Dryas advance (Dahl et al. 1994; 1996; Dahl et al. 2002; Seierstad et al. 2002). A further glacial re-advance in Scandinavia termed the "Erdalen event" (Dahl et al. 2002), may relate to the Icelandic Preboreal advance. These records also show climatic deteriorations at 8.2ka, which are relatively of a lesser magnitude than the Younger Dryas or Preboreal, but of greater magnitude than any subsequent Holocene climatic fluctuation. This suggests that a further advance in Iceland is likely, though of a lesser magnitude than the Preboreal advance.

1.5.3. Conditions in Iceland at the time of initiation of the 8.2ka event

The extent of possible Icelandic response to the "8.2ka event" is defined by the environmental (and glacial) conditions at the time of the initiation of the cold spell. From environmental proxies, the timing of the onset of a warmer climate following the Preboreal is not well-defined (Gudmundsson 1997), making it is difficult to resolve the climatic conditions at the onset of the 8.2ka event. Knowledge of early Holocene glacial activity post-dating the Younger Dryas is limited. It is suggested that the main Icelandic ice sheet began retreating following deposition of the Buði moraines in the Preboreal (Kaldal and Vikingsson 1991). The culmination area of the Icelandic ice sheet, now reduced to an inland ice sheet in the Central Highlands, moved southwards towards the location of present ice centres as deglaciation progressed. A series of ice limits in the Central Highlands, within the Preboreal moraines, are recorded by Kaldal et al. (1991). These are undated due to the lack of

dateable organic material, but are thought to represent stages in this retreat of the central Icelandic ice sheet.

Conditions in the North Atlantic region immediately preceding the "8.2ka event", as recorded in the proxies discussed in 1.4, suggest a climate comparable to today, if not slightly warmer (e.g. Alley et al., 1997). Based on the available evidence, it is likely that the field area was completely free of any outlet lobes of the Icelandic ice sheet by the onset of the 8.2ka event. The climatic conditions would therefore be comparable to modern day. In the Central Highlands, ice cover is likely to have been more extensive than it is under present conditions, due to the remnants of the decaying Icelandic ice sheet. It is possible that some of the stand-still limits recorded by Kaldal et al. (1991) may relate to an 8.2ka climate deterioration.

1.6. Summary

Given the strong evidence for environmental change in Iceland in response to the Younger Dryas and Preboreal climate fluctuations, it is highly probable that Iceland was subject to the impact of the "8.2ka event". The results of this study, determining Icelandic response to the 8.2 ka event, are key to understanding the nature and the impact of the event. The next stage of the research is to study the nature of the evidence for environmental changes in Iceland at this time, and to assess the extent to which these changes are related to climate. Glacial records are the best method of climatic reconstruction in Iceland, given the extensive history of glaciation and the glaciers' sensitivity to climate change. Therefore the research primarily focuses on clarifying the extent and nature of glacial activity at the time of the "8.2ka cooling event", in a region of Iceland which maintains a good early Holocene geomorphic and stratigraphic record. Evidence of non-glacial geomorphic activity in the field area is also utilised as a means of gaining further insight into the possible wider environmental implications of the "8.2ka event". The variety of scales considered in this study, from individual landform elements, through landform suites, to landscapes as a whole, provide evidence about specific process at a range of scales.

This spatially varying process information provides evidence for the nature of specific response mechanisms to climate change.

2 Methodology

2.1. Introduction

Given the current state of knowledge on the "8.2ka event", and it global significance, there is still much work to be done developing good understanding of its mechanisms and manifestations. In the light of this background, the utility of the evidence presented here for understanding the "8.2ka event" is assessed. In essence the project aims to assess the existence and value of geomorphic evidence for a response to the "8.2ka event" maintained in the landscape record, and the extent to which this record indicates past glacial activity and climate-environment interactions. Evidence is derived primarily from field data, which serves as a constraint for modelling preservation potential and ice flow. The specific aim of the field-based research is two-fold. The landform record is assessed as an indicator of geomorphic activity. From this information, hypotheses are generated as to the processes responsible for landform genesis and modification, with particular interest in glacial process, which is a key climate indicator. Secondly, field data aims to put the geomorphic evidence in the context of a dated chronology of geomorphic events, enabling comparison with the climate record. Fieldwork results highlight the unique nature of palaeoclimatic and palaeoenvironmental information held in the landform record, but also emphasise the complexities of the geomorphic system as a climatic indicator.

2.1.1. Methodological Motivations

The work is motivated by the aim to provide a much-needed terrestrial record of the putative response to the "8.2ka event" in a region which is highly likely to have responded to the climate fluctuation (as outlined in Chapter 1). Glaciers are climatically sensitive and thus ideal tools for environmental reconstruction in Iceland. The research methodology is designed to assess the nature of glacial response to the 8.2ka event through integration of high resolution spatial data

(geomorphic evidence) with lower resolution ice sheet modelling data, in the context of a specific field area.

A field-based (and thus regional) study is a valuable means of achieving the research aims, because it can retrieve the high resolution data representing specific geomorphic processes which is unattainable with larger-scale studies. Geomorphic evidence from fieldwork can help develop information on small-scale glacier fluctuations and processes, such as the exact position of past ice margins. Such knowledge of process is necessary for any study of climate-glacier interactions.

Modelling further promotes the research aim by enabling development of knowledge on interactions between glacial process and climate from a larger-scale perspective. The modelling approach is one focused on uncovering landscape-scale universal rules which govern glacier-climate interactions, rather than being concerned with details of individual landform-genesis processes. Modelling aims to reveal the underlying processes and mechanisms which connect disparate landform-genesis events. It achieves this through a series of controlled experiments investigating the glacial impact of changing input (climate) conditions. The geomorphic record forms the real-world constraint on which modelling is based, and the hypotheses developed from the field evidence are testable through these modelling experiments.

The research utilises a combination of high-resolution geomorphic information from field data, and landscape-scale laws governing glacial response mechanisms derived from modelling, for a multi-scaled approach to the research aims. The modelling can draw together the disparate, but highly detailed process-oriented geomorphic evidence, and aid understanding of the way in which a region as a whole responds to climatic events such as the 8.2ka event.

2.2. Field Site Selection

Iceland is an ideal study area for assessing the effects of climate change, given its sensitivity to small fluctuations in the position of the North Atlantic Polar Front (discussed in Chapter 1). Within Iceland, choice of a specific field site for the purposes of this research depends on the region's potential to hold a good geomorphic and sediment record of glacial (and other) activity for the early Holocene time period. For a sedimentary and geomorphic record of glacial activity to have been maintained until the present day, any subsequent glacial activity must necessarily have been less extensive than the one of interest. Each subsequent glaciation removes or re-works deposits from previous glaciations through erosion and deposition. As outlined in Chapter 1, Iceland has been subject to a series of shorter-lived returns to glacial conditions since the onset of deglaciation from the Last Glacial Maximum. As the research aims to locate a surviving record of an early Holocene glacier advance (at around 8.2ka cal. yr. BP), any more recent glaciations in the region would have to be of a lesser magnitude than the 8.2ka advance.

Areas of Iceland which contain currently active glaciers, mostly outlet lobes of the main ice sheets, are expected to have been active in early Holocene times when climates were comparable to the modern day. It is therefore highly likely that expansion of these glaciers occurred in response to the climatic cooling at 8.2ka recorded in the proxies. However, the problem inherent to these regions for reconstructing Early Holocene glacial limits is their extensive glacial history. The main ice sheets have remained throughout the Holocene, and recent climate fluctuations such as the Little Ice Age cold period have resulted in sizeable re-advances of the outlet glaciers. The effect is that evidence of previous glacial advances is removed by the more recent activity.

The climatic threshold beyond which a glacial advance is instigated is dependent on the initial conditions. The climatic conditions necessary to initiate the growth of a new glacier are more extreme than those necessary to induce re-advance of an

existing glacier. Therefore a cold spell may pass which causes glaciers feeding off ice sheets to expand, but which is not sufficient to force growth of new glaciers in unglaciated valleys. A more intense cold spell may occur which causes both expansion of existing glaciers and initiation of new ones. The choice of a field area must consider the magnitude of the 8.2ka event in comparison to climate events which post-date it. A site needs to be selected which is likely to have endured a glacial advance in response to the 8.2ka event to a greater extent than to any later event. In the literature it is evident that currently glaciated areas of Iceland were subject to extensive Little Ice Age glacier advances, so the potential for an early Holocene record being preserved is low (Kirkbride and Dugmore 2001).

The Borgarfjörður Eystri region in the northern part of the Eastern Fjords is an ideal location for studying Early Holocene environmental change in response to climate. The area contains only 2 or 3 currently active glaciers (or permanent ice patches), and probably supported a limited Little Ice Age re-advance constrained to high corries (Gudmundsson 1997). This small-scale Holocene glacial history, combined with the minimal effect of people on the landscape, results in the preservation of a good geomorphic and sediment record of past glacial activity. Reconnaissance by Dr Andy Dugmore and Dr Nick Hulton in summer 2002 indicated that sites lying between 100 and 400m in this region were likely to contain good records of glacial re-advance and geomorphic activity in the early Holocene period.

Based on the recorded deglacial history of Iceland (Ingólfsson et al. 1997; Norðdahl and Einarsson 2001), the Eastern Fjords are thought to have been mostly ice free by the end of the Preboreal (Chapter 1), comparable to today. Given the current existence of some permanent ice patches and small glaciers in corries lying above 900m, the area appears to be very near the threshold of full glaciation, and may need only a small change in climatic conditions to trigger more extensive regional glacial activity. This hypothesis is strengthened by some early ice sheet modelling experiments. The growth and decay of the last Icelandic ice sheet over the LGM and Younger Dryas time period is simulated using GLIMMER (described below). Following the modelled LGM, temperatures are increased in an attempt to deglaciate

Iceland until it reaches its modern day equivalent ice cover. However, the Eastern Fjords were difficult to deglaciate, and ice lingered in many areas when temperatures were returned to modern conditions. Although this is an experimental model run, it may be indicative of an inherent topographic characteristic which is favourable to ice growth, and is naturally close to the threshold of larger scale glaciation (Gyte 2005).

Potential field sites were selected following detailed analysis and initial geomorphic mapping from aerial photographs of the Borgarfjörður area, and from other parts of the Eastern Fjords and Southeast which lay in similar altitudinal ranges. Initially, field reconnaissance was used in conjunction with the preparatory mapping to identify the best sites. Regions were identified which appeared to maintain a good landscape record, and particularly showed preservation of landforms pertaining to past glacial limits. In addition, sites were chosen which demonstrated the potential for tephrochronological dating, maintaining good Holocene sediment records.

2.3. The role of geomorphological analysis

Geomorphological analysis is a method for extracting information about past geomorphic events from the landscape using morphological data. It is an important tool for this study because it can reveal information on the extent and nature of glacial (and other) events which may have occurred in response to climatic change, particularly the 8.2ka cold event. Information provided by geomorphic evidence is two-fold. On a larger scale, it provides data on spatial extent and limits of glaciers or other systems. For example, detailed reconstructions of past ice margin positions at high spatial resolution can reveal the extent of glacial response to a climatic fluctuation. On a smaller scale, the characteristics of individual landforms can reveal information on specific processes responsible for landform genesis, which may be an indicator of the mechanisms by which a system (for example, a glacier) has responded to changing climatic conditions.

As previously stated, glaciers are an important climatic indicator, so to assess the impact of the 8.2ka event, particular attention is paid to uncovering the glacial history of the field area. However, any inference made on the past existence of glaciers is dependent on the interpretation of specific landforms as being indicative of glacial process. The research also aims to assess the existence of non-glacial geomorphic activity in the field area, as this can provide further information on climate and preservation potential. A key methodological issue, therefore, is to develop a consistent approach to interpretation of process from geomorphic evidence. Following the results from the first field season, key types of landform suites and associated landform elements were identified as significant, due to their regular occurrence in the field, and thus their potential for representing regional geomorphic change in response to a climatic or other forcing. Multiple working hypotheses were developed to explain processes of landform genesis and evolution responsible for creating these distinctive landforms mapped in the field area. Further air photograph analysis following the first field season enabled identification of new areas of interest, which appeared to contain similar features. Geomorphic work in the second field season covered a wider geographical area than the first season, but focussed specifically on the identified key suites of landforms, and associated landform elements. Field observations were motivated by the aim to test the developed hypotheses.

2.3.1. Hypotheses

The research aims specifically to test the following Hypotheses:

- All suites of features were formed by the same processes of landform genesis, *or* they were formed by different processes.
- These landform genesis processes occurred at the same time, so each suite of features is the same age *or* landform genesis occurred at different times and features are of different ages.
- The landforms signify:
  - a specific response mechanism to the 8.2ka cooling event.

- a synchronous response mechanism to a regional climatic or environmental change though not at 8.2k.
- multiple small-scale response mechanisms to changes in local environmental conditions (slope stability, micro-climate, snow accumulation, debris production).

The first hypothesis is testable through geomorphic evidence, and is tackled in Chapter 4. The second requires the development of a dated chronology, based on tephrostratigraphy and radiocarbon dates, which is presented in Chapter 5. The third hypothesis relies on interpretation of the results of the first two hypotheses (Chapter 6) combined with correlation with climate proxies, and modelling experiments (Chapter 7).

2.3.2. Geomorphic mapping

Geomorphic information was gathered using a combination of field observations and air photograph analysis, using geomorphic mapping. Initial mapping was based on aerial photograph interpretation, and subsequent mapping was completed from field observations recorded directly onto air photograph copies.

A non-genetic mapping scheme is developed by the author in order to record detailed geomorphic evidence while maintaining objectivity prior to assessment of landform-process correlations. There are significant dangers in assigning genetic terms to landforms in mapping, as they define the processes involves in landform genesis before all the evidence has been fully assessed, and may result in the disregarding of lines of evidence which do not fit the pre-defined hypothesis. Morphologically descriptive mapping terms allows for the existence of multiple working hypotheses.

Development of a mapping scheme requires a basic level of landform interpretation as parallels must be drawn between spatially distinct landforms based on morphological characteristics. This is necessary for any differentiation between landforms to take place. The morphological categories set out in the following

section, and summarised in Figure 2.3-a, are designed as so because they are thought to best distinguish the main landform types observed in the field area. Given the nature of the real world, there is always a continuum in landform morphology, and clear categories do not necessarily exist. The consistency of landform characteristics within a defined category will be outlined in the Chapter 3 when geomorphology results are discussed in full. The mapping scheme is developed for use in the Borgarfjörður region, in order to achieve the research aims of this project. Although the main categories of the scheme may not be the most appropriate to describe geomorphology of other regions, the methodological principles of the scheme are transferable to any other region.

The mapping scheme describes the landscape with reference to *landform elements*, *landform units* and *landform suites*. This hierarchical structure is utilised following reconnaissance of the field area, as it is appropriate and necessary to represent characteristics of spatially distinct groups of landforms exhibiting clear margins (suites), as well as defining features of individual landforms (elements) and landform groups (units). The distinction between landform suites and landform elements helps to symbolise the multi-scale approach to the research. At a landscape-scale, it assesses the factors affecting the distribution of landform suites, whilst at the scale of individual landform elements it focuses on interpreting small-scale landform-genesis processes.

Figure 2.3-a: Geomorphic mapping methodology

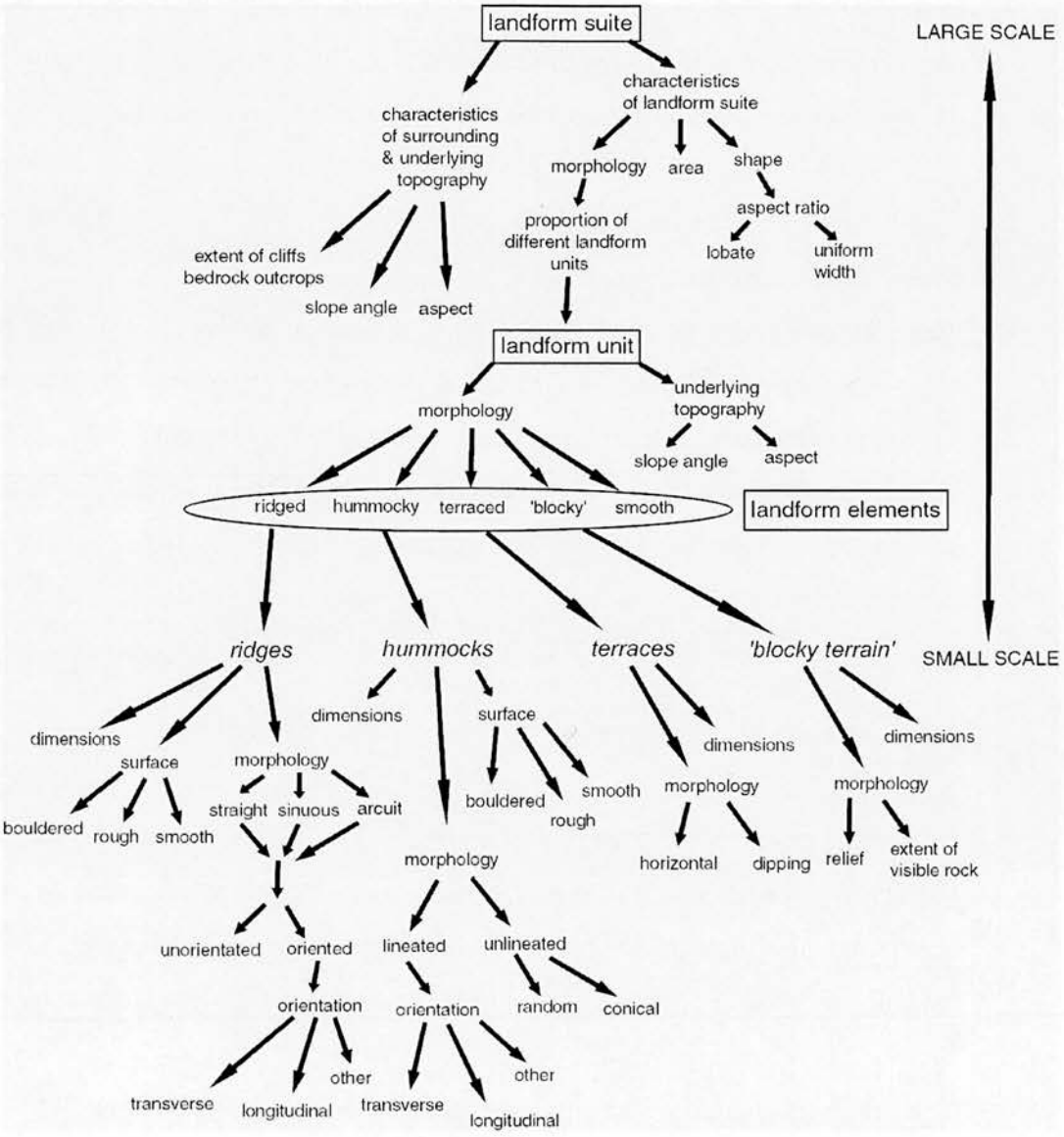

Figure 2.3-a presents the methodology behind collection of geomorphic data information and associated mapping techniques. As can be seen it is carried out on a variety of scales, from landform suites at the top, through landform units, to landform elements at the bottom.

Landform Suites

Landform suites are groups of associated landform elements. The location, spatial context and margin positions of landform suites are indicative of the type of system responsible for suite genesis, and the interaction between this system and the surrounding topography. Defined suites provide the framework within which to

address characteristics of landform element units. Suites are classified initially by observing the land from a distance (from aerial photographs or direct field observation), to detect groups of landform elements with distinct margins. Mapping of landform suites involves recording information on three main aspects:

1. Area and shape
2. Slope angle and aspect
3. General Morphology

The *area and shape* of the landform suite is defined by the position of the margins. From this, aspect ratio can be derived, and comments made as to the specific shape i.e. lobate. Secondly, the *slope angle* and *aspect*, or group of slope angles and aspects associated with the area within the margins of the suite are recorded.

Landform Units

To record the general morphology of a landform suite, a number of descriptive terms are used to differentiate between areas of grouped landform elements ("landform units") which share morphological characteristics. These are "smooth", "hummocky", "ridged", "terraced" and "blocky". These categories are developed based on observation of the main landform element groups occurring in the field. A landform suite may be assigned one term, but most likely a number of terms are assigned to different aerial units within the same suite, and comments are made as to the regularity and consistency of the landform elements as a whole within each unit. For example, an area of hummocky terrain with well-defined terminal ridges will be mapped initially by its margins. Slope angles of the underlying topography are recorded and the area is assigned a general morphology, which in this example would be largely 'hummocky', with a smaller unit assigned 'ridged'.

Landform Elements

The landscape is assessed at a smaller scale, by mapping characteristics of individual *landform elements*. The morphology of these individual landforms can provide important information on process of genesis that cannot be resolved only by assessing the landform suite as a whole. This more detailed analysis may be carried

out in a basic form from aerial photography, but direct field observations are necessary to collect morphological information. Initially the following landform elements are mapped based on the categorisation set out above for units of landforms, but to define each individual landform element in the group:

1. Ridges
2. Hummocks
3. Blocky deposits
4. Terraces

In addition to basic classification of landforms using the above terms, the mapping includes information on landform *dimensions*, specific *morphology*, and *surface features*. "Dimensions" simply describe factors pertaining to size, including height, length, width and area. "Morphology" details the shape of the landform, in terms of factors such as sinuosity, linearity, orientation and dip. Data on "surface features" is concerned with the nature of the surface and is sub-divided into "smooth", "rough" and "bouldered". Within the latter sub-division further descriptions of the type and exact position of surficial debris would be recorded. For example, a "ridge" may be assigned as "arcuit" in morphology, with an orientation across the slope, and some boulders on the ridge crest. Thus it would be defined as a transverse, arcuit, boulder-crested ridge.

Classification of Ambiguous Landform Elements

Consistent classification strategies must be adopted for identifying and recording all landform elements and attributes. There are methodological considerations involved in defining some landform attributes, given the aim here to provide non-genetic geomorphological descriptions. The classifications made here are simply descriptions of the current appearance of the landforms, and make no claims as to origins.

Defining a landform as bedrock as opposed to as a depositional form of different origin can be ambiguous, given high rates of weathering which can reduce large bedrock masses to loose rock and scree deposits, of unknown origin. There is a

continuum in attributes for ridges, hummocks and terraces, from "bedrock" through "blocky" to "bouldered", and finally no attribute is added, classified as simply "ridge", "hummock" or "terrace". Definitions of landform elements as "bedrock" are reserved for the cases in which intact continuous bedrock is clearly evident. "Blocky" is defined as 'containing intact bedrock blocks', though not as a continuous mass, and potentially lying at varying angles of repose. Areas labelled as "bouldered" are defined as those with a fairly continuous scattering of boulders which appear to be superimposed on the landform elements as opposed to being a significant intact part of them. It is acknowledged that, due to the existence of both basaltic and rhyolitic geology in the field area, and related variation in weathering rates, recorded data on existence of bedrock blocks associated with landform elements may be skewed towards the more resistant basalts. Given the potential for significant weathering to have taken place, classifications of "blocky" and "bouldered" is not definitive in terms of the origin of the boulders or blocks, and does not preclude later classification as "heavily weathered bedrock". Where landform elements are defined with unspecified material make-up, the classification does not necessarily rule out that some of these may be bedrock in origin, but states that no intact bedrock is observed. These possibilities will be assessed and clarified in the interpretation section to follow.

A second classification which may be ambiguous is the distinction between a "scree" slope and a "scar face". A scar face is defined as a steep slope containing no significant morphology and being made up of scoured bedrock. Scree, in contrast, is made up of loose unstable rock fragments, and can be found on steep and gentle slopes.

2.3.3. Associations of Geomorphic evidence with lithological and topographic information

The mapping scheme outlined above provides a framework on different scales for making associations with lithological and topographic units. Making such associations is necessary when it comes to interpretation of process, because the

topographic and lithological context of landform suites and elements can influence landform development. The research is concerned with the interactions between climate and geomorphic activity, but topography and lithology are also controlling factors on the extent and characteristics of this activity. Recording topographic and lithological attributes helps to define the extent of this non-climatic influence when interpreting the geomorphic evidence.

On the scale of landform suites, each landform suite is maintained in the context of a slope area or individual drainage basin, which has specific characteristics relating to topography (slope angles, concavity, aspect, altitudinal range) and lithology (geology, erodibility, stability). This information can be recorded in association with landform suite data. Similarly, smaller scale topographic and lithological characteristics can be associated with individual or groups of landform elements.

Use of Digital Elevation Model

The process of gathering the attribute data necessary to make topographic associations is aided by the development of a high resolution (7m x 7m) Digital Elevation Model of the field area. The DEM has been generated using photogrammetric interpolation of air photographs. Air photos contain an element of aerial distortion and skew due to the flight angle, but this distortion is rectified with geo-referenced control points gathered in the field using a Global Positioning System, and a series of automatically generated tie-points. Following DEM generation, the 8 aerial photographs which cover the field area are re-calibrated and merged together to provide a geographically correct base upon which the geomorphological data can be mapped.

The development of this DEM means that topographic and lithological attributes can easily be attributed to mapped geomorphological data. A series of layers can be overlaid on the DEM topography in ArcView, namely geology and geomorphology. In addition, elevation, slope angle and slope aspect information can be extracted

from the DEM and overlaid. This enables the analysis of geomorphic data carried out in Chapter 4.

2.4. Chronology

In order to link geomorphic events with climate events, it is necessary to fit the geomorphic evidence described in 2.3 into an events chronology. An initial relative chronology is based on landforms' relative locations. The stratigraphic record better constrains this relative chronology based on the principle of superimposition, where younger materials overlay older materials. The use of age-equivalent horizons (tephra layers) allows the development of an extensive high resolution stratigraphy for the field area, which can be used to date associated landforms. To constrain absolute dates for these age equivalent horizons, radiometric dating is used on peat deposits within the stratigraphy. The development of this well-constrained dated chronology of geomorphic events allows comparison and correlation with other proxy records. In the following sections, the tephrochronological method is outlined, and the history of its application in Iceland and further afield is briefly reviewed.

2.4.1. Tephrochronology

Tephrochronology is an incremental dating method recording deposition of tephra layers, which are volcanic ash layers produced during explosive volcanic eruptions (Thórarinsson 1944; 1979; 1981). Sediment accumulation is a continuous process through time, and tephra layers are preserved within the stratigraphy as time-marker horizons representing the date of their associated volcanic eruption. When sedimentary profiles are excavated, the volcanic source of tephra layers can be identified based on physical and geochemical data, enabling genetic links to be made between layers found in different places. In this way, a regional tephrostratigraphy can be constructed.

Volcanic source areas

The main volcanic zones in Iceland are concentrated along the Mid-Atlantic ridge region, which runs in a roughly southwest to northeast direction through Iceland's interior (see Figure 2.4-a). Each system has its own unique petrography and geochemical signature (Haflidason et al. 2000). Some systems produce tephra of identical geochemical compositions, making it difficult to differentiate between them (Haflidason et al. 2000). However, data on physical properties, combined with geochemical analysis of a tephra layers using an Electron Microprobe, can go a long way to revealing its volcanic origin.

Figure 2.4-a: Iceland's volcanic zones and systems

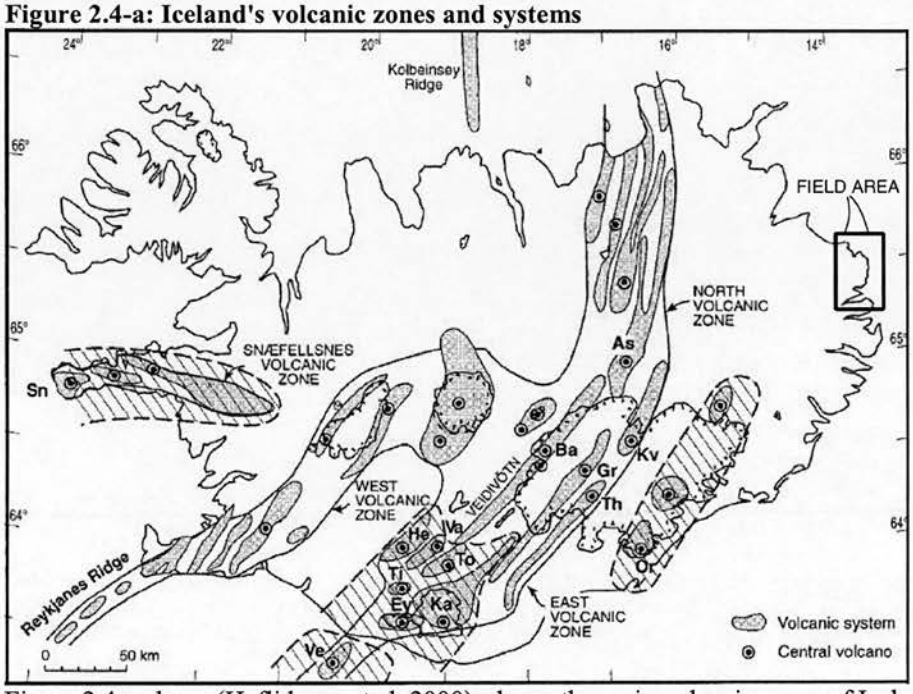

Figure 2.4-a above (Haflidason et al. 2000), shows the main volcanic zones of Iceland, and thus the potential source areas for tephras observed and recorded in the field. Volcanic system names are abbreviated as follows: As, Askja; Sn, Snaefellsjökull; Ba, Bárdarbunga; Kv, Kverkfjöll; Gr, Grímsvötn; Th, Thordarhyrna; He, Hekla; Va, Vatnafjöll; To, Torfadalsvatm; Ör, Öraefajökull; Ti, Tindarfjallajökull; Ka, Katla; Ey, Eyjafjallajökull; Ve, Vestmannaeyjar.

Identification of tephra layers

1) In the field

Tephra layers are classified in the field based on colour and grain size, which allows initial distinctions between layers to be made.

Colour: Tephra layers range in colour and are classified from white, through olive, brown, grey and blues, to black. Colour is logged as seen in the context of the sedimentary section, so there is a certain level of subjectivity depending on availability of light source, and the colour of proximal sediments.

Grain Size: In the field, the grain size of tephra shards can be identified by observation and feel. They are classified into the following categories: "very fine", "fine", "medium" and "course", where "very fine" is clay-like in its feel, and "coarse" is greater than ~2mm in diameter. Grain sizes encountered within the study area are relatively small compared with other regions of Iceland due to the site's distance from the main volcanic systems.

Schematic representations of each section are drawn up following logging based on colour and grain-size observations recorded in the field. This allows cross-correlation and development of an initial tephrostratigraphic record, which identifies key 'marker' layers evident in most of the profiles. Initial correlations can be drawn with known Icelandic tephrostratigraphic records. This is discussed in further detail below.

2) Laboratory Analysis

Further analysis of tephra layers can be carried out following field work, to extract information on grain shape and geochemistry. Collection of this further information serves to confirm or refute correlations between tephra layers based on grain size and colour. It is not possible to analyse every tephra layer further, as this is time-consuming and costly, so layers are selected for analysis following initial correlations based on their likelihood to provide key correlative evidence. The acid digestion method is employed to clean tephra and remove organic matter prior to geochemical analysis. Tephra is then mounted on slides and filed to a given thickness to be used in the Electron Microprobe (Cambridge Instruments Microscan V), at the University of Edinburgh.

Initial suggestions of grain shape can be made through direct observation in the field for larger grain sizes. However, shape analysis is mostly carried out through microscope analysis. Shape or morphology of tephra grains may give indications of the depositional history of the grain (Haflidason et al. 2000). When analysed through a microscope, tephra shards vary greatly in appearance. Some have sharp edges and a "fresh" appearance, while others appear with "chewed" edges. The "chewed" shards are likely to represent tephra re-worked through erosion and transportation via glaciers, rivers or other geomorphic processes, and re-incorporated in the sediment profile at a later date. The "fresher" shards represent air-fall tephra which can be used as a direct time-marker horizon.

Geochemical data is derived from microprobe analysis of the tephra layer, which reveals its chemical make-up as proportions of different oxides (Silica, Iron, Titanium, Magnesium, Manganese, Aluminium, Calcium, Phosphorous, Potassium and Sodium). In the case of well-known Icelandic tephras, which go back to the mid Holocene, visible observations combined with geochemical data can provide good correlative evidence. For tephra layers pre-dating the known stratigraphy, layers can be linked to each other and key Early Holocene tephras can be identified.

Limitations on tephrostratigraphic dating

Identification of tephras, and correlations made between layers must be undertaken with consideration of the limitations to the dating method. The resolution and quality of a tephrochronological framework depends on the availability and accessibility of tephra profiles, and the preservation of a sufficient number of tephra layers. Erosive processes such as small-scale slope process, or larger scale glacial or fluvial activity, may remove sediments and tephra layers, leaving gaps in the recorded stratigraphic record.

There are further limitations relating to the interpretation of chronological information from the stratigraphy. Tephra layers are recorded as stratigraphic time-markers relating to airfall ash from a volcanic eruption. However, tephra layers may

be maintained in the stratigraphy which do not originate directly from airfall, but which have been re-worked through processes of erosion and transportation, and have been re-deposited. Although the geochemical composition of such layers can reveal the volcanic origin, their application as a time-marker horizon is restricted. Tephras can be re-deposited a significant time after the initial volcanic eruption, and may be re-deposited on top of the original airfall layer, resulting in complex stratigraphy. Tephra can be held within glaciers for a significant period of time, (Grönvold et al. 1995; Larsen et al. 1998) before melting out and being incorporated in sedimentary records. As a consequence, dates for such a tephra layer derived from radiocarbon dating of associated sedimentary layers, represent the date of re-deposition rather than the date of airfall. In recording tephra sequences with the intention of using them as time-markers, identification of reworked tephra is important. Tephra grain shape, observable by microscope analysis, can be suggestive of re-working in that it can appear "chewed".

A further limitation stems from the extent of post-depositional modification of tephra grains through weathering or diagenesis (Dugmore et al. 1992). The extent of such activity is related to the climatic and environmental setting of the tephra layer. It is suggested (Dugmore et al. 1992) that a more complete tephra layer may be preserved in peat than in loessial soil, following an experiment which showed that only the most silicic (and more stable) tephra shards of a known layer were present in the loess. This may be due to the increased time required to stabilise loess, and the increased likelihood of weathering in this stratigraphic environment.

These problems can be limited (though not completely solved) through careful site selection, and detailed assessment of all the evidence. Excavation of profiles can be avoided in geomorphic settings favourable to high levels of erosive activity, or which show evidence of sediment transportation processes which may have removed and/or re-deposited tephra layers. Recording of sedimentological characteristics can reveal information on materials removed by erosion from elsewhere, and subsequently redeposited, and should be noted within the stratigraphy.

Tephrostratigraphy for dating specific landforms

Once a regional tephrostratigraphic framework is developed, profiles can be selected which enable dating of mapped landforms. By excavating tephra profiles within and outwith the margins of geomorphic features, bracketing ages for genesis can be defined. Figure 2.4-b shows this method of dating landforms using tephrostratigraphy.

Figure 2.4-b: Dating Landforms with Tephrostratigraphy

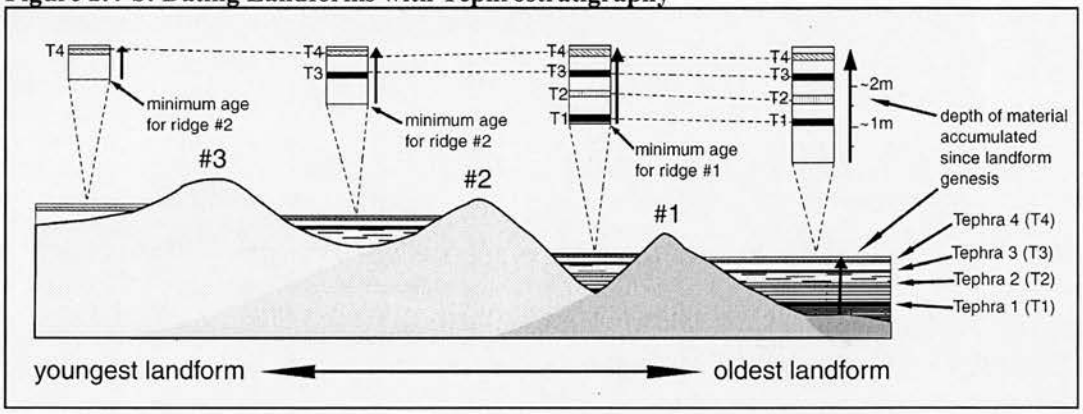

Three landforms are represented in Figure 2.4-b, which were deposited in three phases of geomorphic activity, which created the three ridges lines, #1, #2 and #3. The depth of sediment accumulation the surface of the landform (in available sediment traps) represents accumulation rates since the time the surface was last stable and ice free. Tephra layers provide time-marker horizons in this sedimentary record which enable specific layers to be dated and matched with occurrences of the same layer in different profiles. When geomorphic activity, such as a glacial advance, occurs, processes of erosion and debris transport remove or re-work the sediments which have previously accumulated, so that once the resultant landforms stabilise, sediment accumulation begins again from zero. Sediment traps located beyond the limits of a landform suite generated by such activity will maintain a continuing sedimentary record of accumulation from before the initiation of the geomorphic event, throughout its activity, and since its stabilisation. Meanwhile, sediment traps within the margins of the landforms will record accumulation since geomorphic activity ceased. If, when this sedimentary record is exposed, an age can be associated with the lower-most layer (through a known or dateable tephra layer, or

a radiocarbon dated layer), this age will represent a minimum age for the cessation of the geomorphic activity. In this way a dated chronology can be developed to date specific landforms.

History of Icelandic tephrochronology

In order to make correlations between tephra layers found in the field, and specific dated eruptions, the extensive body of literature on Icelandic volcanism and associated tephra deposition must be drawn upon. Tephrochronology was first used as a dating method by Thórarinsson (1944). and has subsequently been used as a tool in environmental reconstruction by many authors in Iceland (Thórarinsson 1979; 1981; Larsen et al. 1998; Larsen et al. 1999; Larsen et al. 2001; Wastegård 2002; Caseldine et al. 2003). Tephra is primarily air-borne, and can thus travel significant distances depending on prevailing winds, so its application is not restricted to Iceland, and inter-correlations are possible between palaeoenvironmental records from a wide region. Icelandic tephra has been found in Greenland Ice Core records (Grönvold et al. 1995), the North Atlantic (Lacasse et al. 1998; Haflidason et al. 2000) Scandinavia (Birks et al. 1996; Zillen et al. 2002; Davies et al. 2003; Bergman et al. 2004) and the UK and Ireland, (Dugmore et al. 1995; Pilcher et al. 1996; Lowe and Turney 1997; Davies et al. 2002; Chambers et al. 2004), enabling correlations between disparate regions to be made with the identification and inter-correlation of tephras (Wastegård et al. 2001; van den Bogaard and Schmincke 2002; Boygle 2004). Icelandic tephrostratigraphy is well-constrained for the Historic period, where documentary evidence is detailed, but the pre-historic record is relatively sparse, as explained below.

Historic Record

The historic record of Icelandic volcanism is well-constrained, with over 200 documented explosive Icelandic eruptions in the past 1100 years (Larsen 2000). Much of this information is obtained through written documentation of eruptions, often resolving to the day of the eruption. The oldest eruption documented in such records is the source of the so-called "settlement layer", Landnam, which occurred

~870-930AD (Thórarinsson 1981). The Vatnajökull ice record also provides an excellent correlative tool for dating, given the preservation of tephras within the ice (Larsen et al. 1998). Due to Iceland's high accumulation rate for peat and soil, tephra layers deposited a matter of years apart may be distinguishable from each other (Thórarinsson 1981).

Pre-historic Record

Given the scope of this research, aiming to date Early Holocene geomorphic activity, we must appeal to the pre-historic tephrostratigraphic record. The documented eruptive history of Iceland from pre-historic times is lower resolution than the historic record, because there are no written records. Pre-historic tephra layers can be dated using ^{14}C analysis of organic matter immediately above and below them. Where exact dating is not possible, estimations can be made based on accumulation rates constrained by some known ages. The use of tephrochronology for dating has been restricted until recently to dates younger than the Hekla 5 tephra, which is dated to 6100 ^{14}C yr BP (Haflidason et al. 2000). This is because the biogenic record only extends back to the early Holocene. A further limitation on tephrochronological dating is Iceland's extensive history of glaciation, (discussed in Chapter 1). Much of the country was ice covered until around 9700yr BP (Hjartarson and Ingólfsson 1988; Norðdahl 1991), meaning that airfall tephra layers could not be preserved in the sedimentary record. The tephra record for the late glacial/early Holocene period has been extended by the discovery of tephra deposits in lake sediments on the Skagi peninsula (Rundgren et al. 1997), which is thought to have been ice free for a longer period than much of the rest of Iceland, making it an ideal location for extending tephrostratigraphy. The association of terrestrial tephras with those found in marine and ice core records further extends the time period for which tephrochronology can be applied.

2.4.2. Radiometric Dating

The relative correlative dating framework provided by the tephrostratigraphy is constrained into an absolute chronology through independent radiocarbon dating of

tephra layers recovered from peat deposits. This establishes dating control for many unknown early Holocene tephras, enabling accurate dating of landforms connected with the 8.2ka event. It also extends and builds on the Icelandic tephrostratigraphy for the Early Holocene, and for northeast Iceland, which has not received much attention. Radiocarbon samples are chosen to provide an age-depth profile which will better constrain soil accumulation rates and correlative ages for the mid to early Holocene. To allow accurate dating of tephras, the thin layers of peat immediately above and below each tephra layer are used. Accelerated Mass Spectrometry is utilised to date these small samples, a process which was carried out at the Scottish Universities Environmental Research Council laboratory in East Kilbride.

The tephrostratigraphic information gathered in the field and in the laboratory, combined with radiocarbon dated peat layers, allows for the development of a high-resolution dated stratigraphic framework within which to base the chronology of geomorphic events. This enables comparisons and initial correlations to be made between the geomorphic record and climate proxies.

2.5. Use of Models

Modelling is a spatially integrative tool by which disparate lines of evidence can be drawn together. Conceptual and numerical modelling is utilised in combination with field evidence, as a means of uncovering the underlying connections between landforms and landform suites.

2.5.1. Conceptual Models

Conceptual modelling is designed to determine the value of the mapped field evidence. It is concerned initially with preservation potential of landforms, and then with extent of modification. It cannot be assumed that the landscape is static and landform elements are observable now as they were at the time of initial genesis. Landforms may go through stages of modification by processes of erosion, re-distribution and deposition. The extent of this modification varies depending on

individual landform characteristics, and may result in the total removal of a landform. Modelling of landform preservation potential attempts to explain the observed distribution of landforms in relation to the topographic context of each element. Slope angle is used as a proxy for the extent of post-genesis modification, using the rule that steeper gradients are subject to more intense erosional (and thus modificational) activity. Modelling preservation potential in this way places a set of rules across the field area at a landscape scale, which allows some explanations to be made for the spatial distribution of different landforms at the scale of individual elements.

2.5.2. Numerical Models

Numerical modelling is a further means of placing a set of rules on the landscape to test response to set climate input conditions, by creating an experimental framework within which controlled experiments can be carried out. The motivation for the modelling is to tests hypotheses regarding the relationship between glaciers and climate. Hypotheses are developed for the field area based on the geomorphic and chronological evidence. The evidence which has survived to the present day is of sufficiently high resolution to provide useful information on the nature of the glacial activity which occurred, in terms of the number of stand-stills or re-advances, and some erosional and depositional characteristics.

The study uses the ice sheet model GLIMMER to simulate ice growth and decay in response to climatic change on a 250m-resolution Digital Elevation Model representing the Borgarfjörður Eystri region. Glacial response to variations in the magnitude and duration of a hypothesised climate fluctuation can be modelled, by changing the input temperature and precipitation, and running the model for varying numbers of model years.

The research is primarily a study of specific regional response to a particular climate fluctuation. This data collected in the field describes the land at the scale of individual landform elements, landform units, and at a larger scale of landform

suites, as a means of explaining processes and system interaction with the surrounding topography and lithology. The high resolution of this data is not consistent across the field area because it focuses on key suites of landforms. Numerical modelling, in contrast, maintains a constant data resolution across the field area, though the resolution is a great deal lower. When high-resolution regional field data is combined with modelling experiments, the results become a tool in understanding the potential manifestations and mechanisms of geomorphic response to extreme climate events on a wider scale (Hulton et al. 2003).

3 Geomorphology Results

3.1. Introduction

This section presents the results of geomorphological mapping. Primarily, detailed information is presented on the small-scale geomorphology of each valley in the field area. Based on this data, the geomorphology of the whole field area is assessed on a large scale, identifying key landform types and the relationships between landform elements, landform suites, and the general topography. The evidence for currently active geomorphic processes is also discussed here to highlight the possibility of post-genesis modification of landforms.

Topographic and Geological characteristics of the Borgarfjörður region

Figure 3.1 a: Geological setting

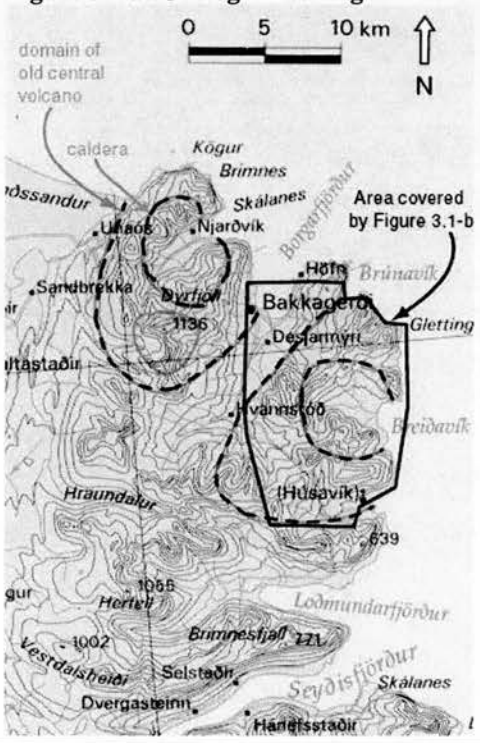

The Borgarfjörður region lies within Iceland's eastern Tertiary Basalts, and is Iceland's second largest rhyolite area. The rhyolite, which creates a relatively smooth topography due to its higher susceptibility to weathering, is interspersed with basaltic intrusions which form the rugged peaks and knolls. The old central volcanoes dominate the topography and geology of the Borgarfjörður region. The calderas of two old volcanoes are centred around the bays of Njarðvík and Breiðavík, as shown in Figure 3.1-a.

Presenting Results of Geomorphology

For the purposes of mapping, the field area is split into 9 main regions of roughly equal areas, the locations of which are shown on the site map, Figure 3.1-b, and each area is represented by a detailed geomorphic map in 3.2. These regions (1-9) are Borgarfjörður, Brúnavík, Kjólsvík, Svínavík/Breiðavík, Leirfjall/Breiðavík, Víkurá-East, Víkurá-Central, Víkurá-West/Mosdalur, and Hrafná.

Figure 3.1-b: Topographic Map of the Borgarfjörður region, showing location of landform suites mapped in detail in section 3.2.

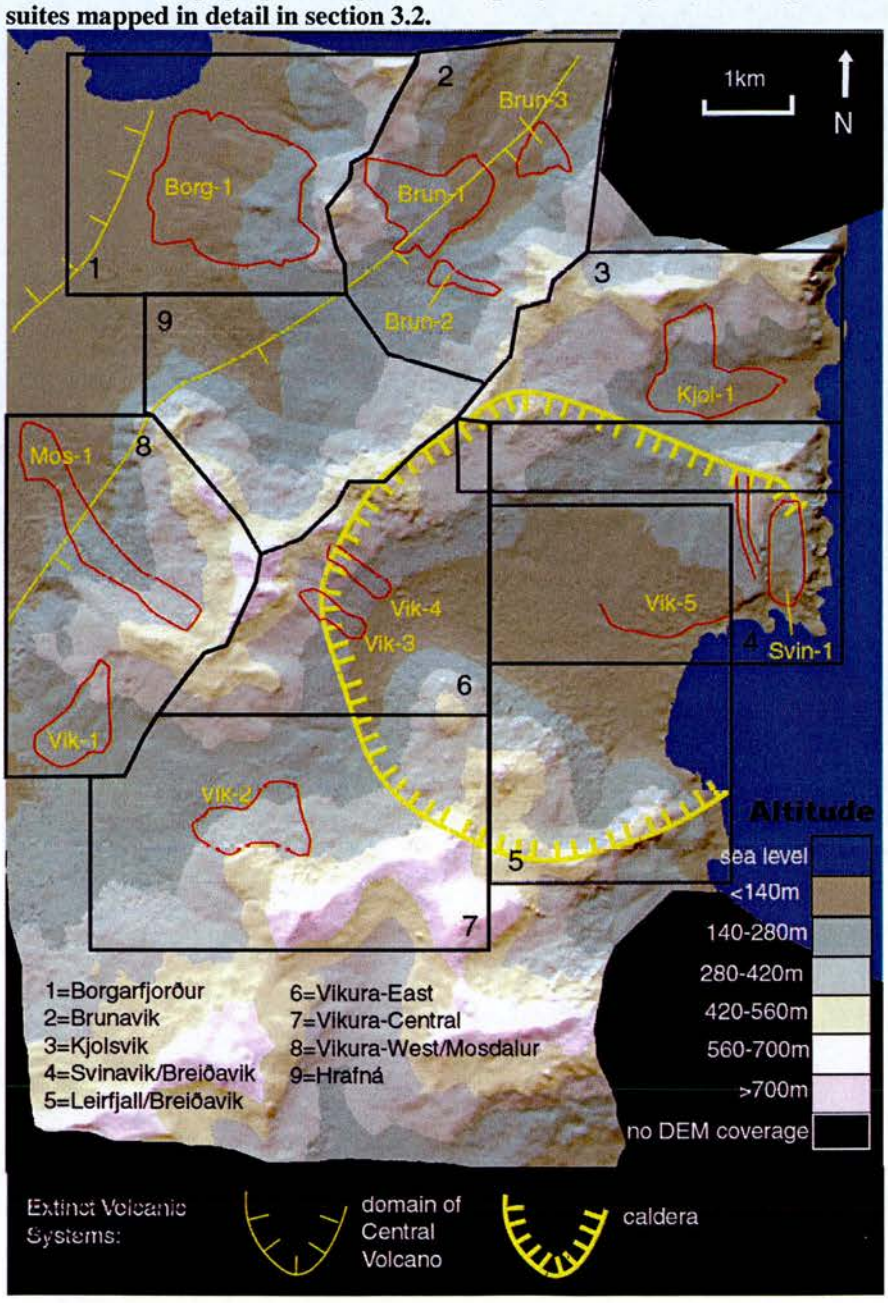

Figure 3.1-b shows the topography of the main field area (derived from a Digital Elevation Model developed by the author). The red lines indicate the margins of so-called "landform suites" identified as significant geomorphic features. The black boxes represent the areas covered by the more detailed geomorphic maps presented in 3.2.

3.2. Detailed geomorphology results

Each of the nine regions of the field area highlighted in Figure 3.1-b is assessed in turn, and geomorphological characteristics described in this section and displayed in the associated geomorphic maps. Annotated photographs and diagrams are used to illustrate characteristic landform types, and the geomorphic maps contain arrows (in green) indicating the direction from which an associated annotated photographs have been taken.

Figure 3.2-a: Geomorphic Mapping Symbols

ridge (crest position)		bedrock ridge (large)	
rigde crest & margin		bedrock cliff	
boulder-crested ridge		bedrock ridge (small)	
bouldered area		scree	
hummock (lineated)		area of smooth bedrock hummocks (small)	
hummock (unlineated)		smooth bedrock hummock (large)	
hummock (conical)		exposed scar slope	
hummocky area		'blocky' terrace/ridge (with intact bedrock)	
terrace (sediment)		terrace (bedrock)	
terracettes (soil/turf)		shallow gully	
small-scale ridges & furrows (soil & turf)		deep gully	
lake		very narrow gully	
river		recently active river channel	

The symbols illustrated in Figure 3.2-a are developed following initial analysis of the field data, and are thought to provide a regionally specific characterisation of the landscape of the Borgarfjörður Eystri area. They are employed in the detailed mapping presented in the following section.

3.2.1. Borgarfjörður

Figure 3.2-b: Geomorphic Map of the Borgarfjörður landform suite

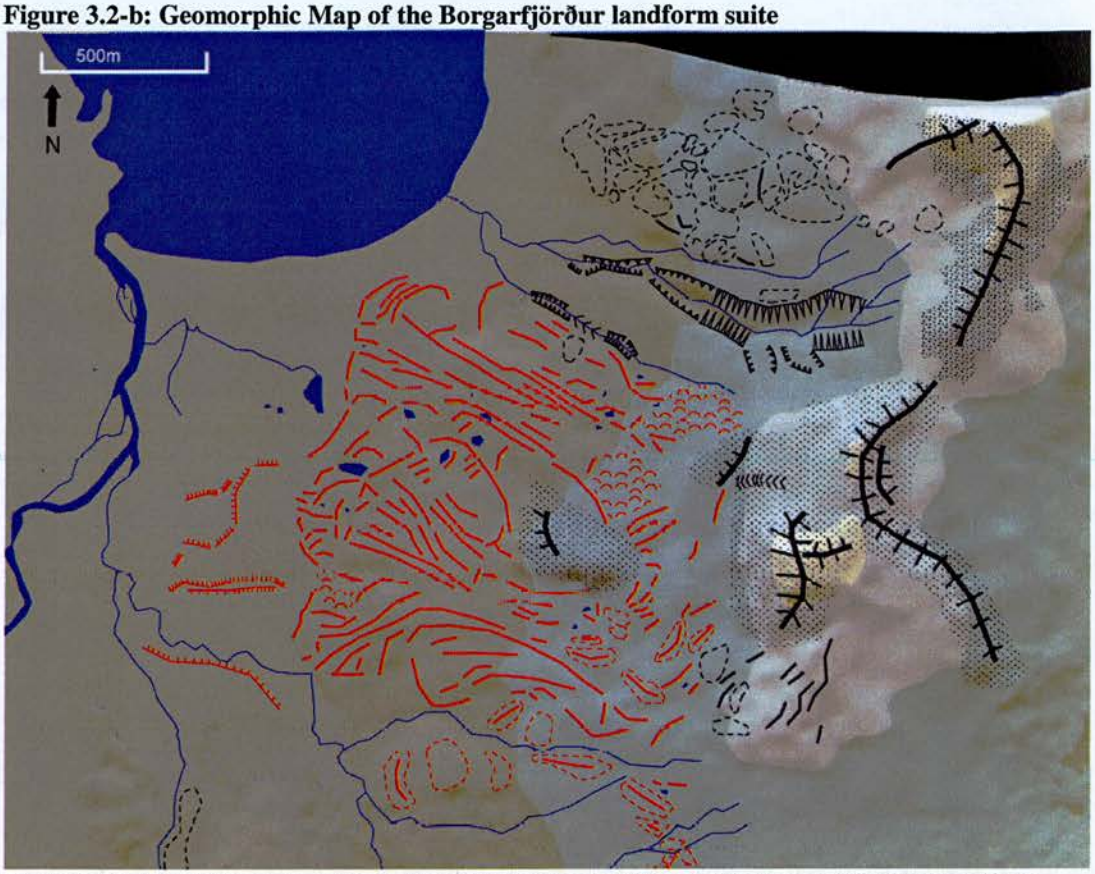

Figure 3.2 b shows the main geomorphological features of the so-called Borgarfjörður Landform Suite. Clear ridge-lines can be seen to extend down-slope from the hill tops to near sea level, and clear terminal ridges delineate the lower margin of the suite.

The Borgarfjörður valley is a wide and flat-floored north-south oriented valley opening onto the sea in the north, shown in Figure 3.2 b. The west-facing valley side is dominated by a group of landforms situated between an upper altitude of 320m, and a lower margin at around 9m, named here as the "Borgarfjörður landform suite". This suite, mostly consisting of transverse and longitudinal ridges, covers an area roughly westwards from the foot of the steep summit of Svartafell (illustrated in Figure 3.2-c (i)), a mountain consisting of a bedrock (rhyolite and basalt) plug surrounded by scree slopes. The lateral and terminal margins of the landform suite are well-defined by steep-sided ridges. The overall lobate, flow-like shape is striking on observation from aerial views (Figure 3.2-b and Figure 3.2-c (i)), and from the opposite valley side (see Figure 3.2-c (viii)).

Figure 3.2-c: The Borgarfjörður landform suite and associated illustrations

(i)

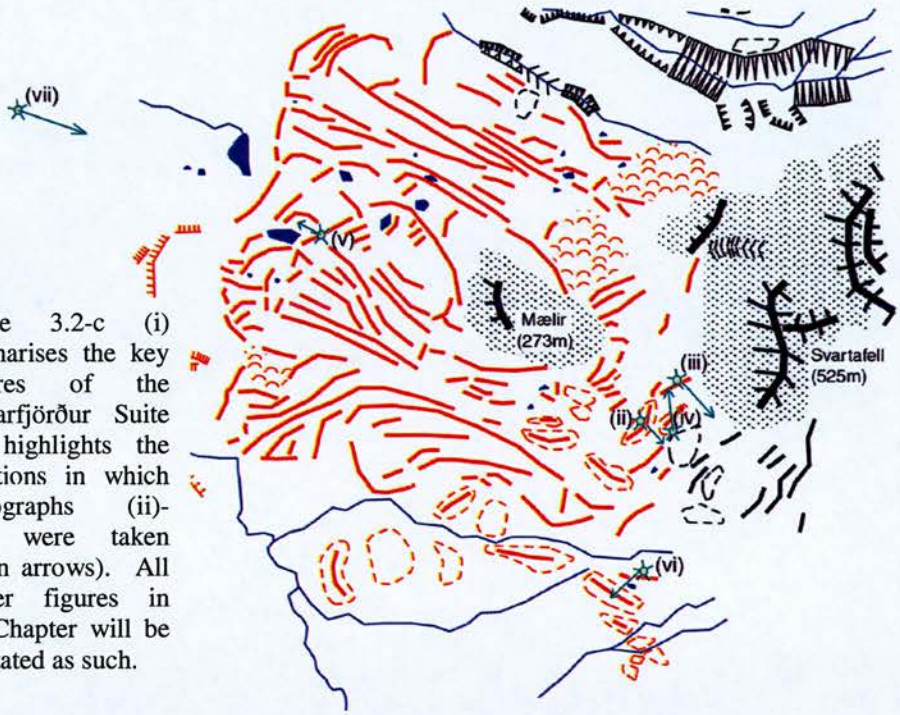

Figure 3.2-c (i) summarises the key features of the Borgarfjörður Suite and highlights the directions in which photographs (ii)-(vii) were taken (green arrows). All further figures in this Chapter will be annotated as such.

(ii)

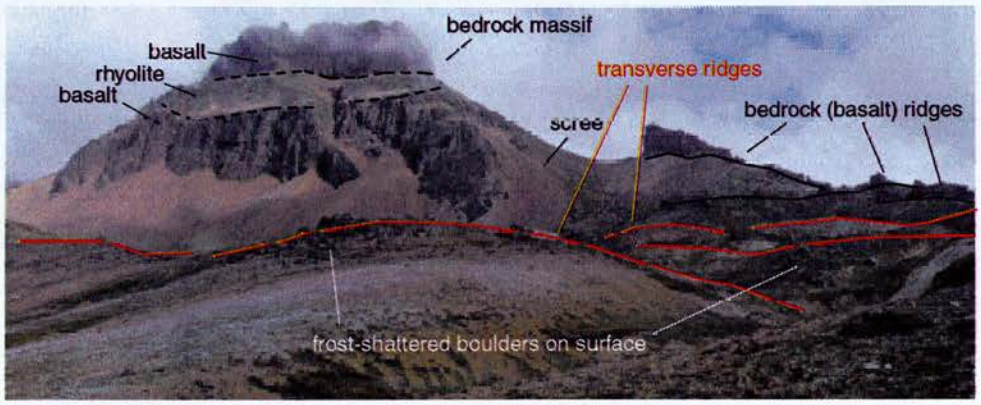

(iii)

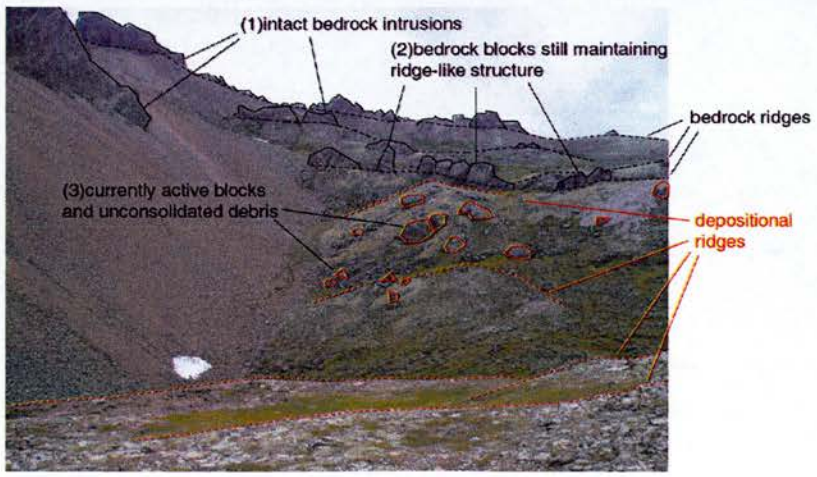

Figure 3.2-c: continued

(iv)

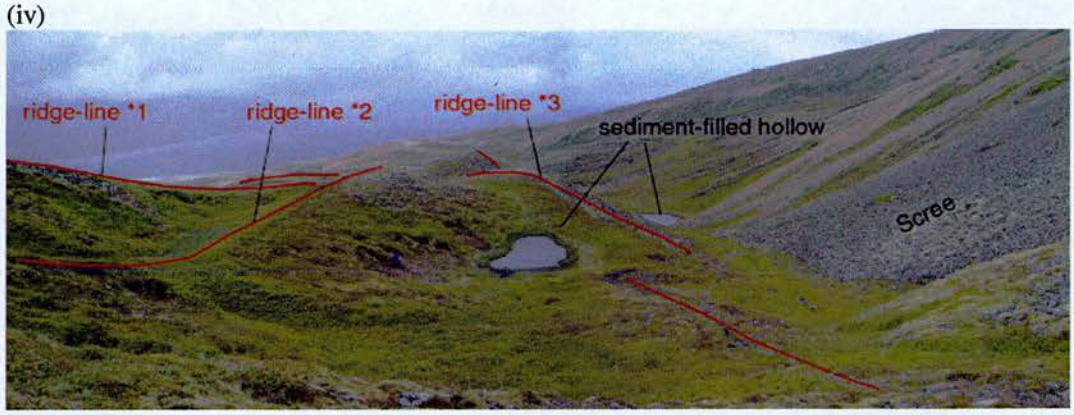

(v)

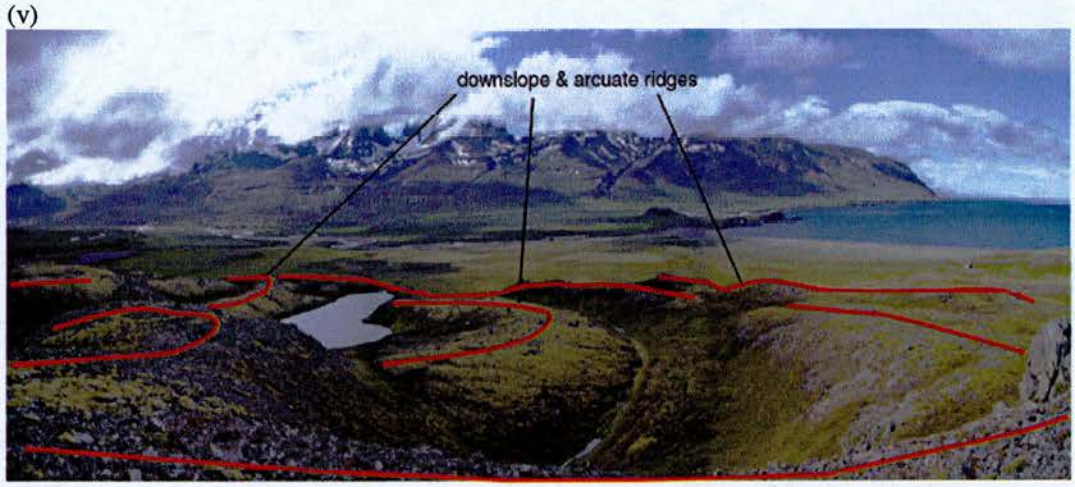

(vi)

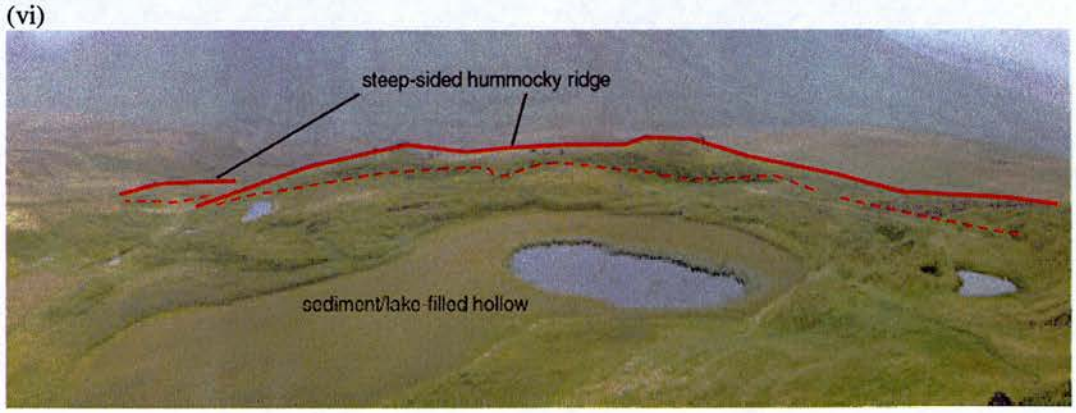

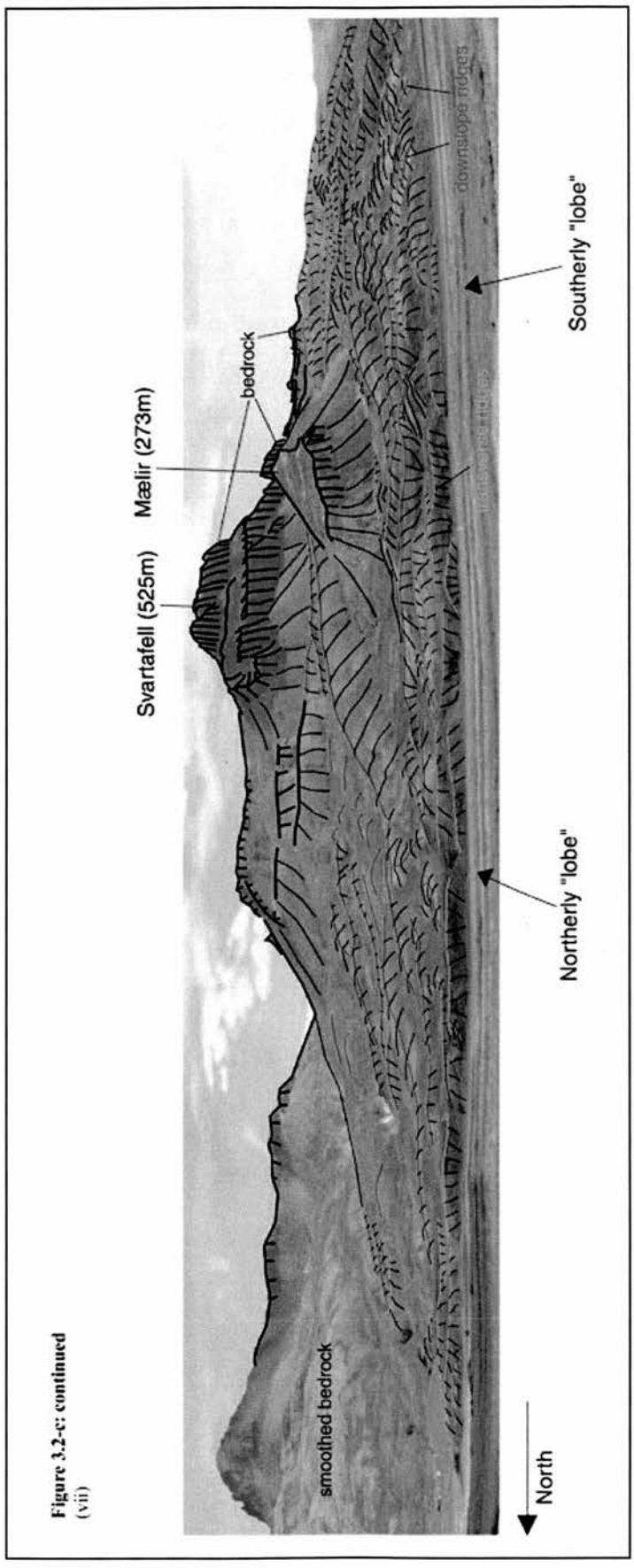

Figure 3.2-c: continued (vii)

Upper Borgarfjörður Suite

The upper part of the landform suite, as far down as the protruding bedrock knoll, Mælir, is characterised by multiple levels of transverse ridges. The first set of ridges immediately to the south of Svartafell (ridge line 1 in Figure 3.2-c (iii)) are bedrock ridges, being made up of extensive continuous and intact bedrock (basalt) blocks and columns reaching heights of 20 metres, and clearly following bedrock orientations visible in the mountain summit. Further down-slope the transverse ridges change character, becoming more rounded and lower. This transition from bedrock to non-bedrock ridges is shown in Figure 3.2-c (ii) and (iii). The second level of ridges (ridge line 2 in Figure 3.2-c (iii)) contain large basalt blocks, still maintaining a ridge-like structure, but less continuous than level 1, and with more evidence of instability. The third level of ridges is very different and the transition is abrupt. There is no evidence of bedrock, and the ridges have more subdued relief, being made up of frost-shattered detritus in a silt/clay matrix, with occasional scattered boulders, as illustrated in (iii).

Immediately to the West (down-slope) of Svartafell, the first visible ridge is steep backed and rises 15 metres from the foot of the scree slope behind, as illustrated in Figure 3.2-c (iv). The front of this ridge forms a series of terrace-like levels made up of progressively lower transverse ridges, with sediment built up behind them and a series of small lakes, as shown in Figure 3.2-c (iv). This area of transverse ridges completes the upper part of the landform suite.

Lower Borgarfjorður Suite

The bedrock knoll, Mælir, marks a transition in the character of the landform elements. Beyond this knoll, the suite is defined by a series of longitudinal and arcuate ridges, with smooth, rounded surfaces. These ridges form two 'lobes' on either side of the Mælir knoll (the northerly and southerly lobes highlighted in Figure 3.2-c (vii)), defined by distinct marginal ridges. Longitudinal ridges characterise the main body of these two 'lobes', extending down-slope towards the margins, often continuously for almost a kilometre. The lobes are juxtaposed and merge together in the lowest part of the suite, below Mælir, forming a distinct transverse terminal ridge

rising approximately 7 metres from the valley floor (which lies at an altitude of between 6 and 9 metres above sea level). Up-slope of the terminal ridge, at least three further transverse and arcuate ridge-lines are distinct in both the lobes, sometimes connected to longitudinal ridges from up-slope. The down-slope face of these transverse ridges is generally steep and high (up to 10 metres drop from crest to base), whilst the up-slope face is of a gentler slope angle, and the ridge-crest rises only around 3 metres from the base. An example of these characteristic ridges is shown in Figure 3.2-c (v). In this way, the general surface altitude of the landform suite drops step-like towards sea-level as the transverse ridges get closed to the terminal ridge.

The outer-most lateral margin of the suite, immediately to the south of the main ridged area, is defined by less continuous ridges and hummocks, which have rough boulder-crested surfaces, as shown in Figure 3.2-c (vi). These ridges share more morphological characteristics with the transverse ridges at the top of the deposits behind Mælir than with the longitudinal ridges of the lower suite.

3.2.2. Brúnavík

Figure 3.2-d: Geomorphic Map of Brúnavík valley

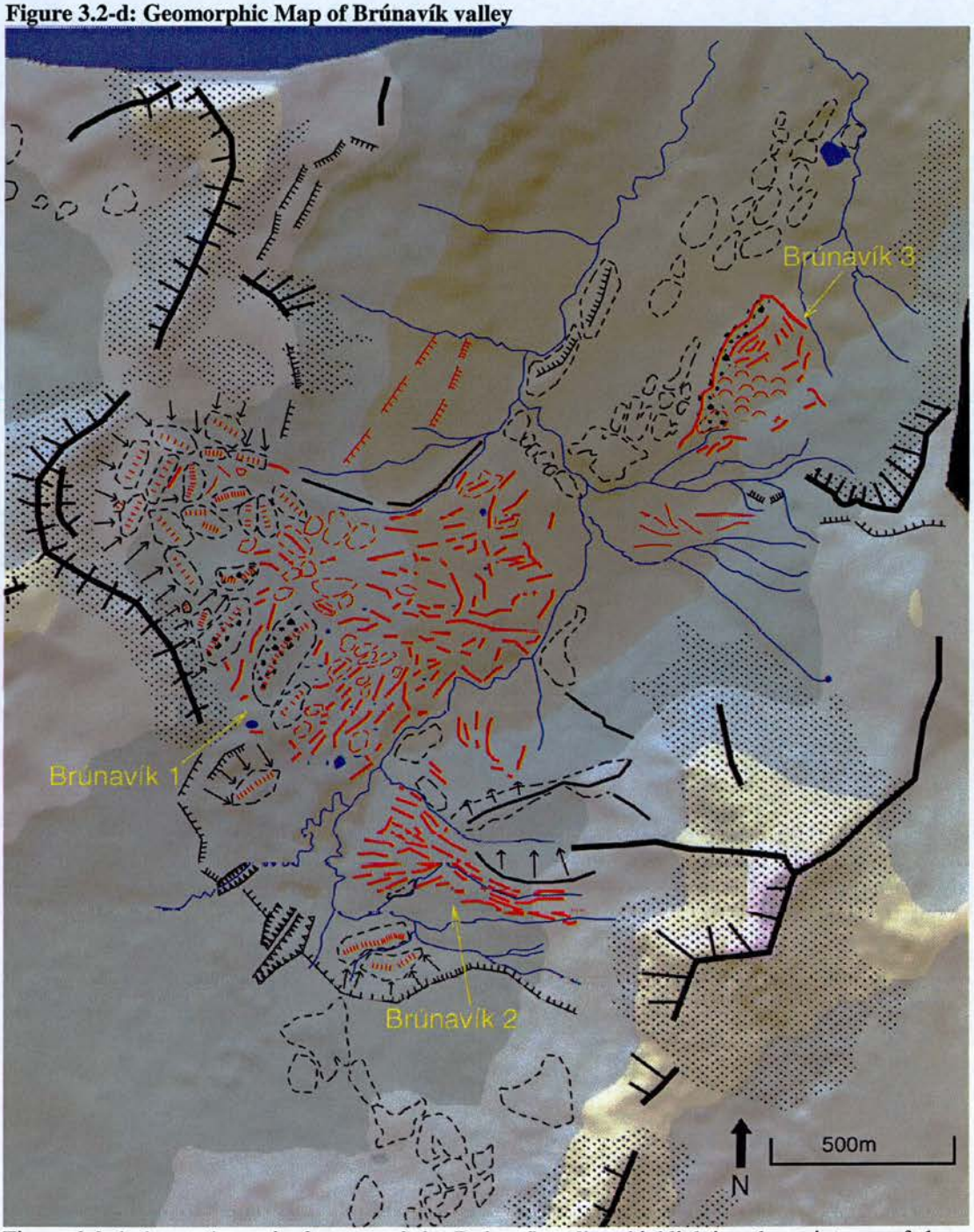

Figure 3.2-d shows the main features of the Brúnavík valley, highlighting the existence of three landform suites, Brúnavík 1, 2 and 3, which all exhibit a lobate shape. The three suites have different characteristics in terms of the landform elements which make them up, as will be discussed.

The Brúnavík valley, shown in Figure 3.2-d, is confined on the southeast and northwest by steep-sided northeast-southwest oriented bedrock ridges, mostly

fronted by cliff faces, with scree slopes at the base. The drainage divide marking the upper limit of the Brúnavík basin lies parallel to, and just to the south-west of a bedrock terrace, oriented in a northwest-southeast direction (seen at the south-west edge of Figure 3.2-d). The basin drains directly to the sea, which is just beyond the northeast edge of the area covered by Figure 3.2-d. Three suites of landforms are observed which are worthy of discussion, Brúnavík 1, Brúnavík 2 and Brúnavík 3, highlighted in Figure 3.2-d.

Brúnavík 1

The most obvious topographic feature in the Brúnavík valley is a large suite of ridges and hummocks, defined by clear margins, which is constrained by high cliff faces to the south and west, and by a steep hill slope to the north. This suite of landforms is named here as the "Brúnavík 1 Suite". The area of ridges and hummocks extends from the scree slopes at the cliff-foot, to the base of the Brúnavík valley at the main river, where it opens into a wide fan shape on the valley floor. The suite exhibits a lobate shape as seen in Figure 3.2-e (i) and (ii). It is divided into three areas, A, B and C, the locations of which are highlighted in Figure 3.2-e (i) and (ii), and which are described in detail below.

Figure 3.2-e: Brúnavík 1 suite and associated illustrations

(i)

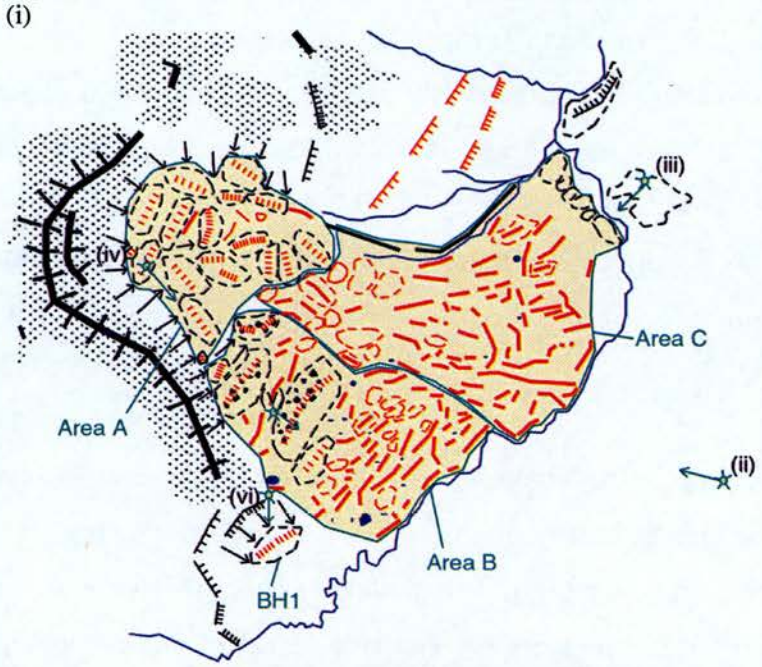

(ii)

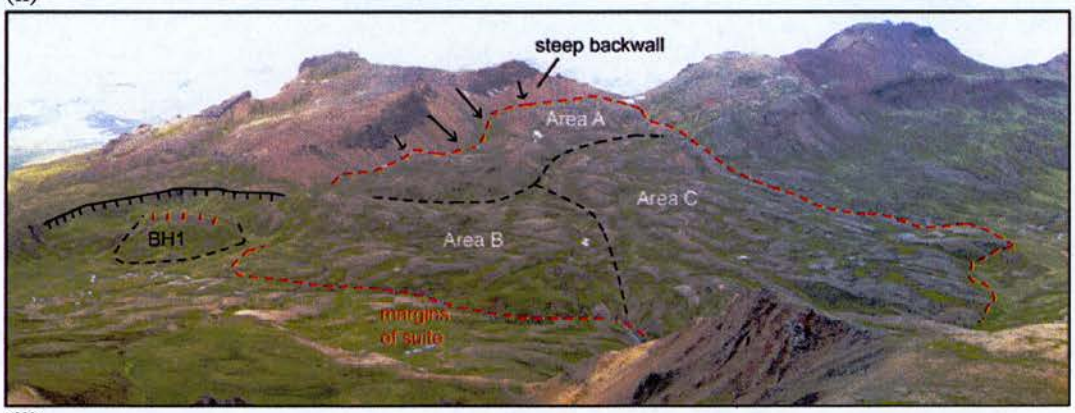

(iii)

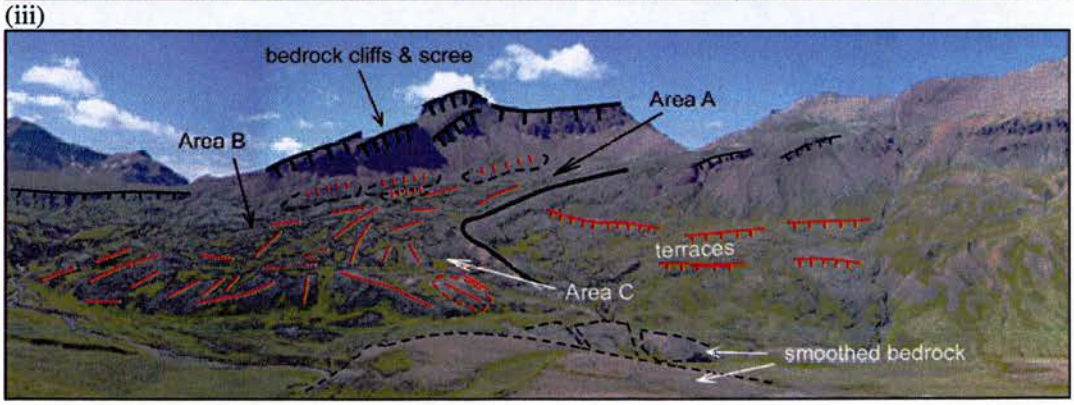

Figure 3.2-e : continued

(iv)

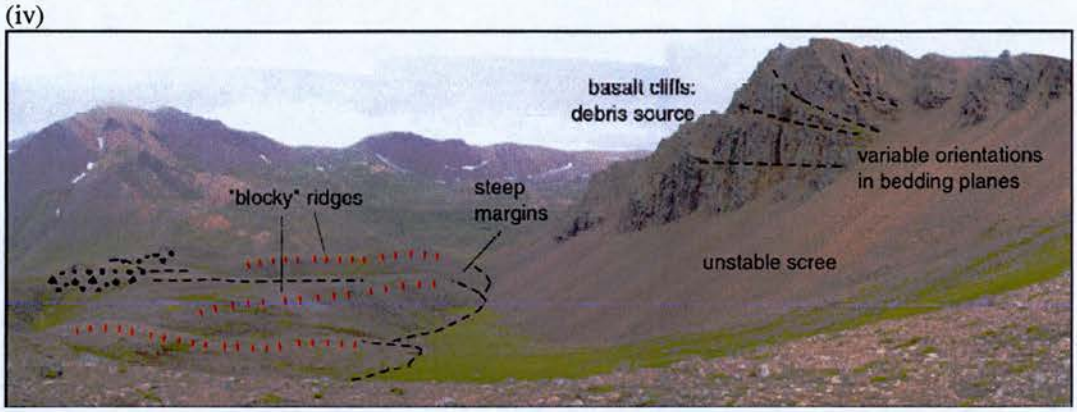

(v)

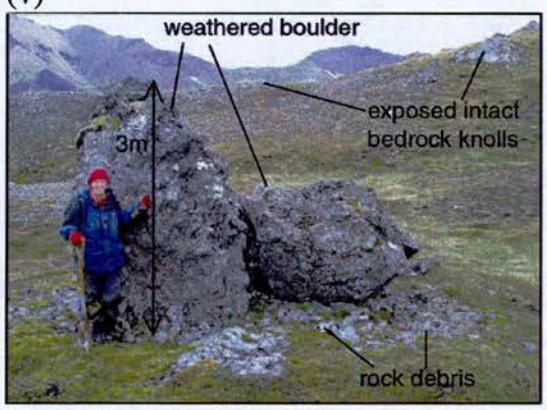

(vi)

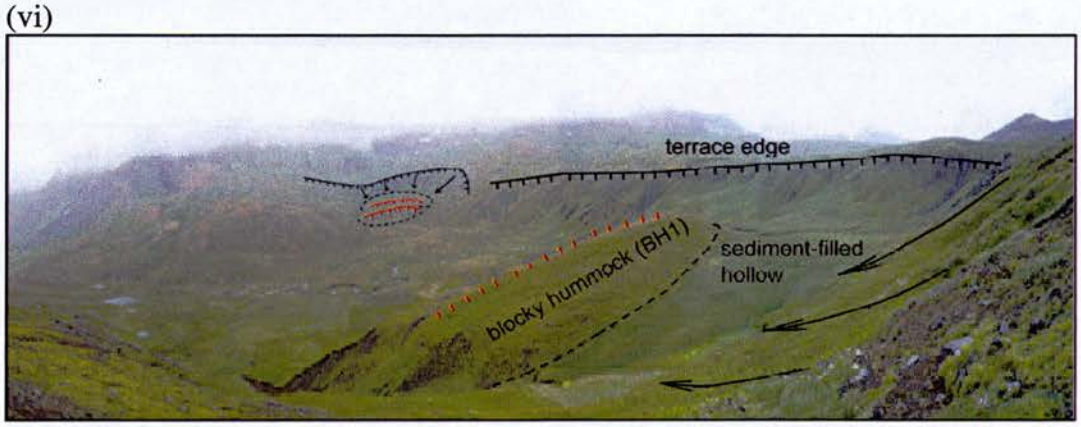

Area A

The upper region of the Brúnavík 1 suite immediately below the cliff faces, Area A, is distinctive, being made up of large-scale blocky hummocks. Figure 3.2-e (iv) illustrates the characteristic large hummocks, found at the foot of the cliff and scree

slopes. They largely have orientations matching the orientation of the juxtaposed cliffs, and contain large proportions of intact bedrock, evident in the basalt blocks protruding from the smoother surface. Tests were carried out to compare the orientation of rock jointing between the blocks and the cliffs above, which showed no correlation between rock blocks and potential source. However, the jointing structure of the cliffs varies significantly and is not straight, but curved, making this orientation test problematic (see Figure 3.2-e (iv)). There is a transition from 'blocky' hummocks containing intact bedrock, towards hummocks with large boulders scattered on the surface, with increased distance from the cliff face.

Area B

The lower part of this landform suite is divided into Area B and Area C due to the characteristic differences in morphology, shown in Figure 3.2-e (i) and (ii). The upper area is dominated by large hummocks containing large blocks of rock and scattered boulders (Figure 3.2-e (v)). The lower part contains a series of transverse ridges interspersed with a significant number of small lake-filled hollows. The southern edge of Area B (and the lateral margin of the entire landform suite) is poorly defined with no distinct marginal ridge. A large blocky hummock (BH 1, shown in Figure 3.2-e (vi)), containing intact bedrock, is found immediately below a clear terrace level with a scar face on its flanks. This shares characteristics with the blocky hummocks in the upper part of the Brúnavík 1 suite.

Area C

Area C contains many ridges and hummocks which are not clearly defined, but some indication of orientation can be observed. Many long, sinuous ridges follow a longitudinal orientation to the valley floor. These are interspersed with three vaguely defined transverse ridge levels. The northern lateral margin is clearly delimited by a bedrock ridge, shown in Figure 3.2-e (iii), which follows a down-slope orientation. North of this margin, two terrace levels are observed on the southeast-facing valley slope, gently dipping to the North, which can also be seen in Figure 3.2-e (iii). There is no visible evidence of bedrock exposures in these terraces.

Brúnavík 2

Figure 3.2-f: Brúnavík 2 suite and associated illustrations

(i)

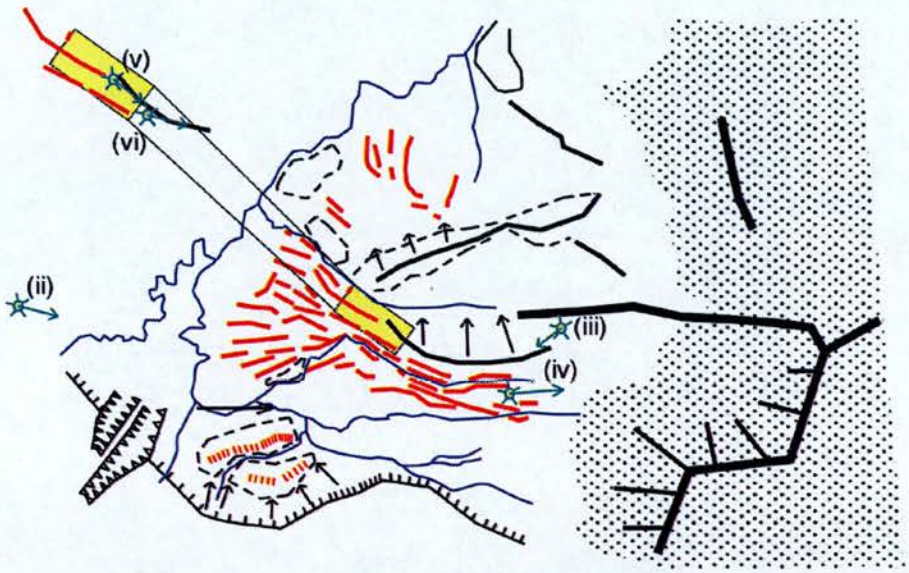

(ii)

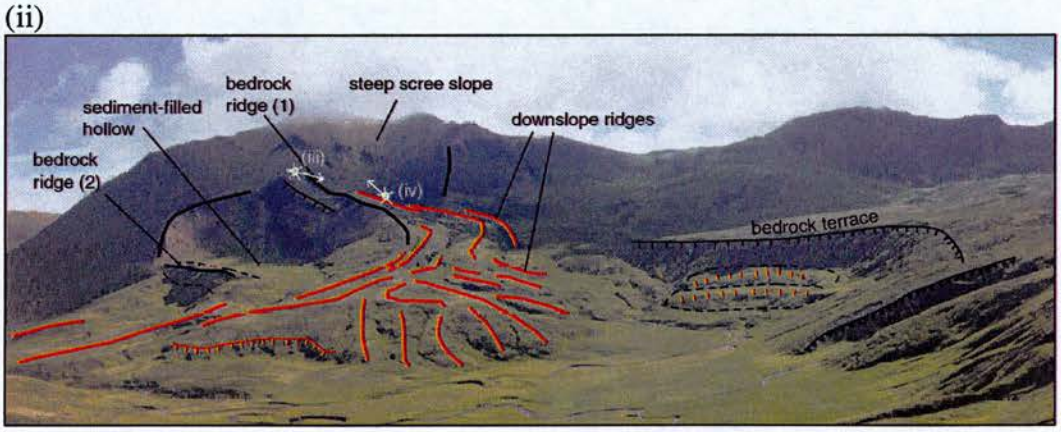

(iii)

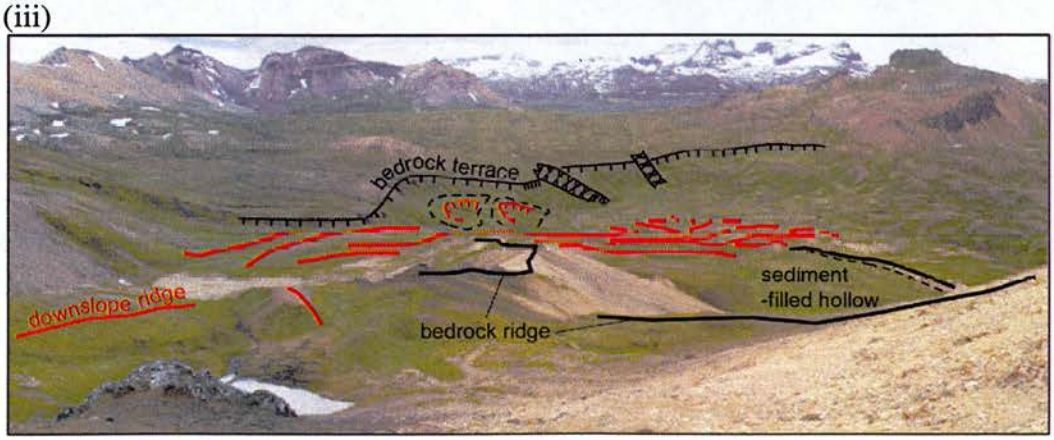

Figure 3.2-f: continued
(iv)

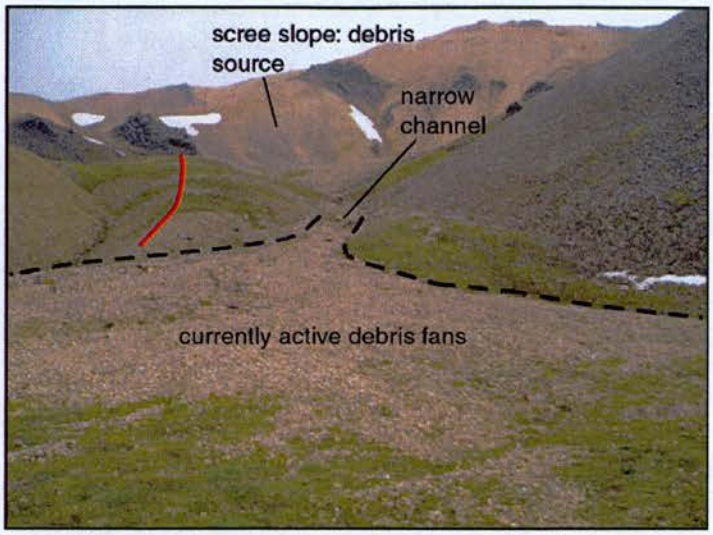

(v)

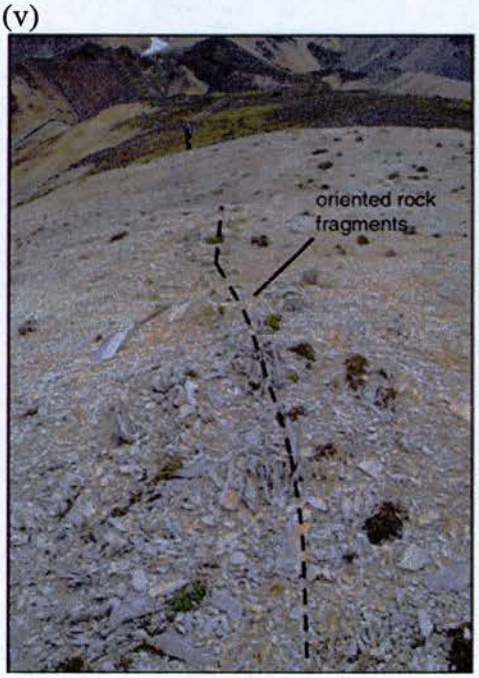

(vi)

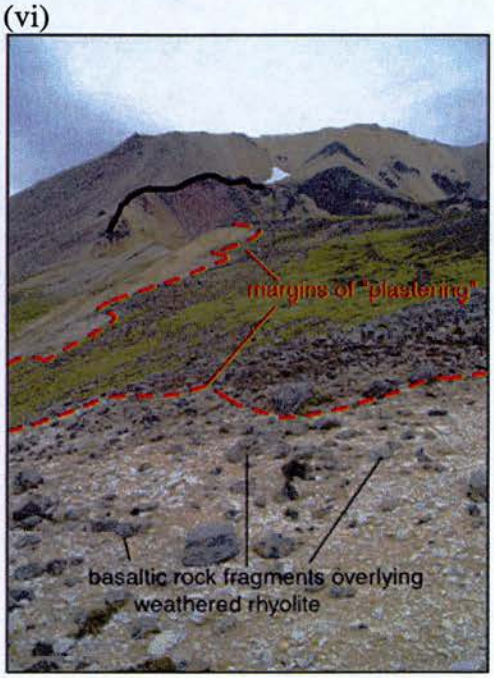

Significantly smaller in area than Brúnavík 1, is a suite of clearly lineated ridges extending from a small west-facing cliff-backed depression in the hillside, named the Brúnavík 2 suite. The suite is made up almost entirely of longitudinal linear rides, which terminate abruptly in a steep terrace-like edge, with a transverse terminal ridge in one part. The suite of ridges forms a lobate shape, widening beyond the visible end of a bedrock ridge which extends from the main ridge top behind in an east-west direction (see Bedrock Ridge (1) in Figure 3.2-f (ii)). A bedrock hummock, oriented

southeast-northwest, forms an outer margin for the northern edge of the suite (shown in Figure 3.2-f (v) & (vi)). Close observation reveals the existence of a layer of sediment superimposed on the bedrock hummock at its southern and western edges, which forms a continuous layer with the adjoining longitudinal ridge. Above the suite are a series of debris fans extending from scree slopes to cover the upper part of the ridges. In the narrow upper area, ridges follow the orientation of the bedrock ridge, and orientations spread outwards in a fan in the lower part. A second bedrock ridge (Ridge (2) in Figure 3.2-f (ii)) is evident at a lower altitude, to the north of Bedrock Ridge (1), oriented east-northeast to east-southeast. A flat sediment-filled area is contained between these ridges. Beneath Bedrock Ridge 2, some further lineated longitudinal ridges are evident which share morphological characteristics with the main body of the Brúnavík 2 suite.

As outlined in the methodology section, ambiguities arise from classifying features as bedrock and non-bedrock. Rhyolitic areas are particularly difficult to classify as rhyolite weathers more easily than basalt and will retain less of its original form. In the Brúnavík 2 landform suite there are significant ridges defined as bedrock, and some are juxtaposed with non-bedrock ridges. Here we explain how the classifications were derived. As can be seen in Figure 3.2-f (i), the northern-most longitudinal ridge which defines the lateral margins of the Brúnavík 2 suite is bedrock, and a ridge which continues down-slope, following the same orientation, is defined as non-bedrock. Figure 3.2-f (v) shows the surface of the "bedrock" (rhyolite) ridge. As can be seen, the protruding rocks on the ridge crest, while being heavily weathered, retain a clear orientation which extends the length of the ridge. This indicates the existence of a continuous bedrock mass, which is likely to be linked to the bedrock ridge upslope. It is clear however, that all the longitudinal ridges within this suite are not bedrock. Figure 3.2-f (vi) shows where deposited material, made up of basaltic rock fragments in a soil matrix, overlie a ridge made up of weathered rhyolite.

Immediately to the south of Brúnavík 2, is a bedrock terrace level adjoining both east and west flanks of the Brúnavík valley. A number of gullies are cut into the edge of

this terrace. Two blocky hummocks containing intact bedrock, immediately to the south of the Brúnavík 2 suite, are positioned immediately below the bedrock terrace, forming two further terrace levels.

Brúnavík 3

Figure 3.2 g: Brúnavík 3 suite and associated illustrations

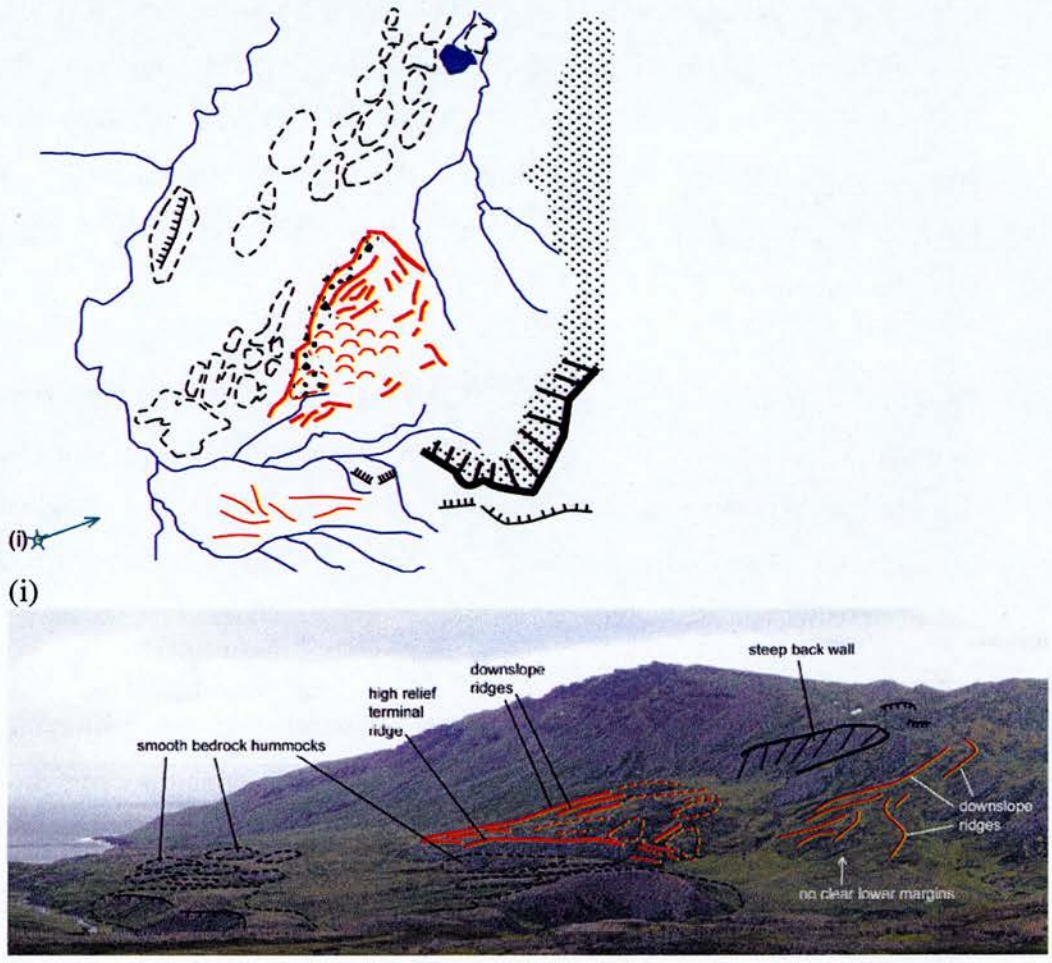

To the north of Brúnavík 2 is a further suite of ridges and hummocks, with a clear lower margin, named as Brúnavík 3, shown in Figure 3.2 g. The upper margin of the suite is not clear, being made up of a generally hummocky area which gradually reduces in relief up-slope. Above the suite is a steep cliff-face, which faces north and west forming a well-constrained, sheltered depression in the hillside. A large debris fan spreads from the cliff face to the top of the hummocky area. The lower margin is a clear terminal transverse ridge, which is boulder crested and high, with

five further transverse ridges stacked behind it. Lateral margins are clear on the northern edge, defined by an area of longitudinal ridges, but the southern edge is mostly made up of hummocky terrain which has no clear orientation or clear lateral margin. Unlike the Brúnavík 1 and 2 suites, Brúnavík 3 does not reach the base of the valley but terminates at an altitude of 100 m. Below Brúnavík 3 and on the wide flat valley floor are a series of bedrock hummocks which are oriented parallel to the direction of the river flow, northeast-southwest. These are very smooth rhyolite hummocks, mostly in an oblong shape.

3.2.3. Kjólsvík

Figure 3.2-h: Geomorphic map of Kjólsvík basin

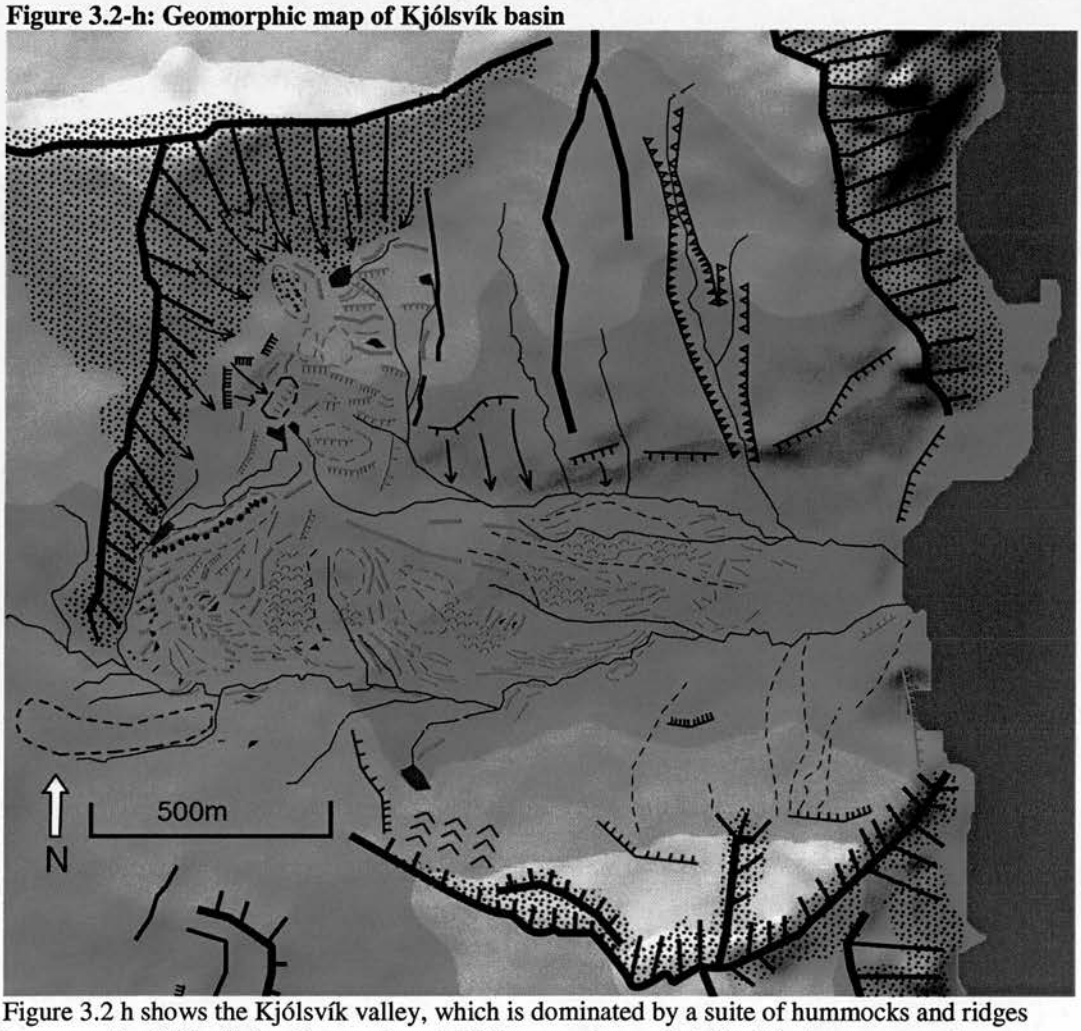

Figure 3.2 h shows the Kjólsvík valley, which is dominated by a suite of hummocks and ridges known as the Kjólsvík landform suite, which has margins well-defined by transverse and longitudinal ridge lines.

The Kjólsvík valley, shown in Figure 3.2-h, is oriented in an east-west direction and

flanked by cliffs or steep slopes on the North, West and South, opening out to the sea at the eastern edge. The main ridge line to the north lies from west to east, and a sub-valley cuts back into the slope, constrained by high basalt cliffs to the north and west, and, in the upper part, to the west by a bedrock ridge extending south from the main ridge. Where the valley reaches the coast, the land drops abruptly in a cliff edge into the sea.

Kjólsvík Suite

The most significant geomorphic features fill the floor of the sub-valley and much of the northern part of the main valley, forming the "Kjólsvík suite", which will be described here in detail. It has three morphologically distinctive areas, split here into the upper, middle and lower parts, the margins of which are illustrated in Figure 3.2-i (ii).

Figure 3.2-i: Kjólsvík landform suite and associated illustrations

(i)

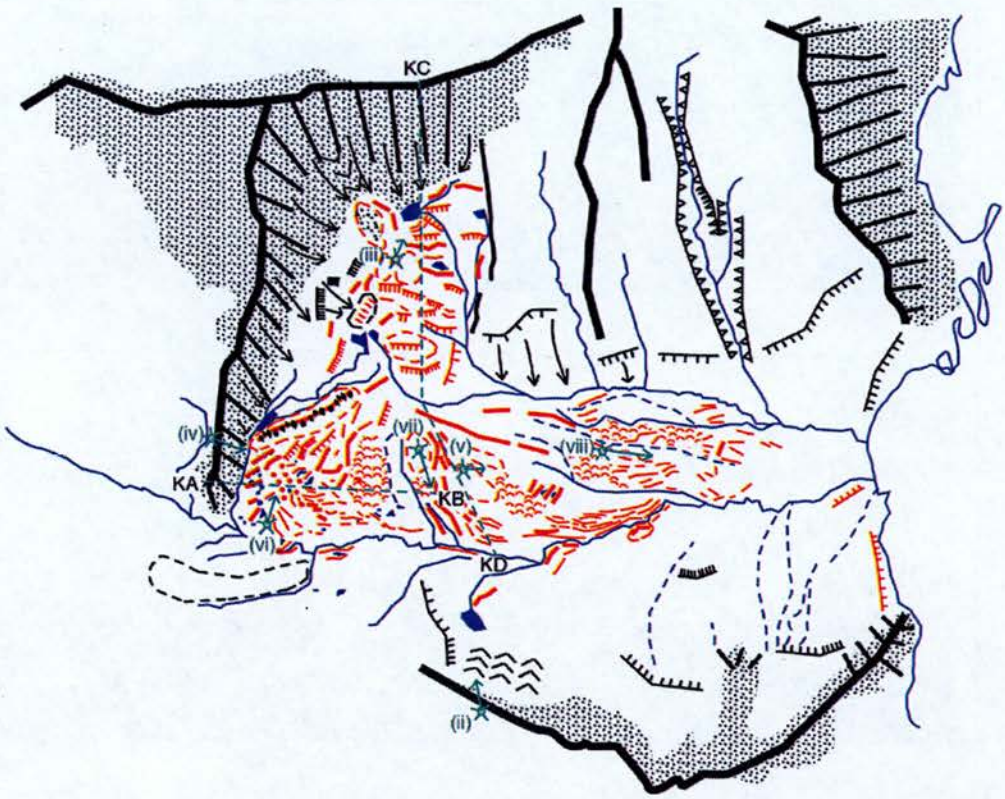

(ii)

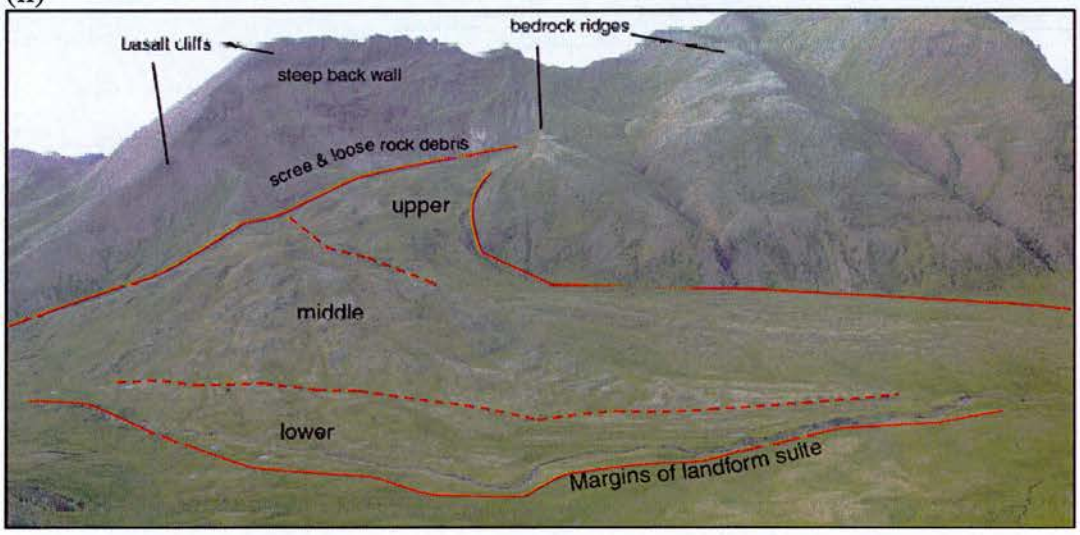

Figure 3.2-i: continued

(iii)

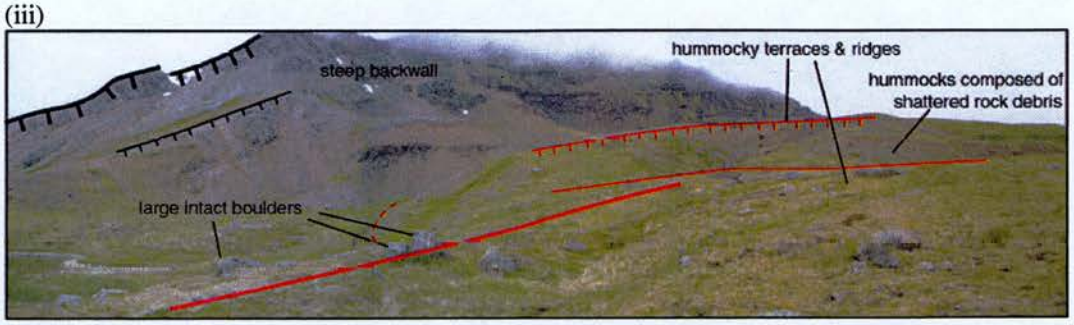

(iv)

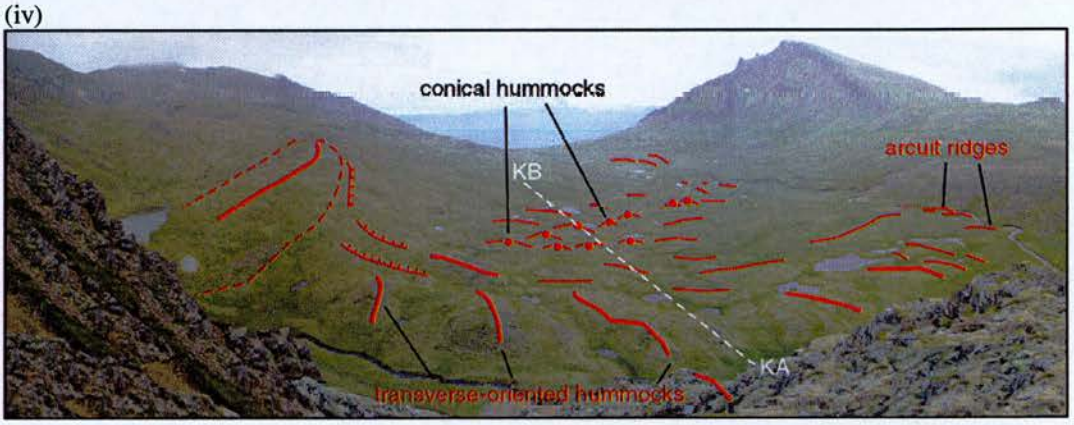

(v)

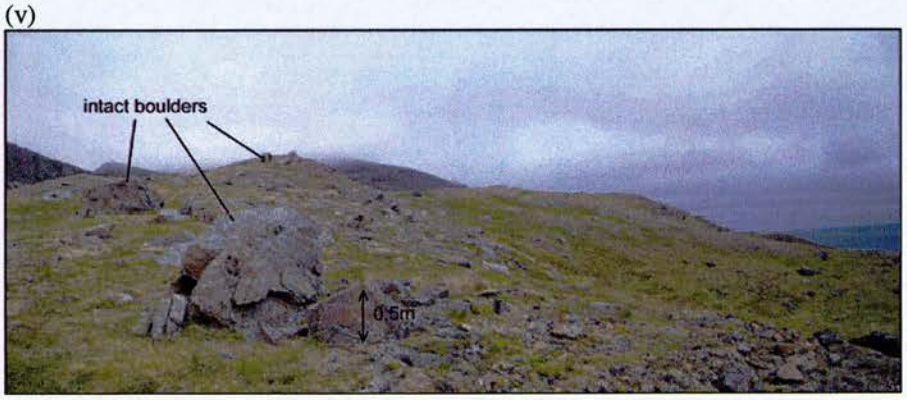

(vi)

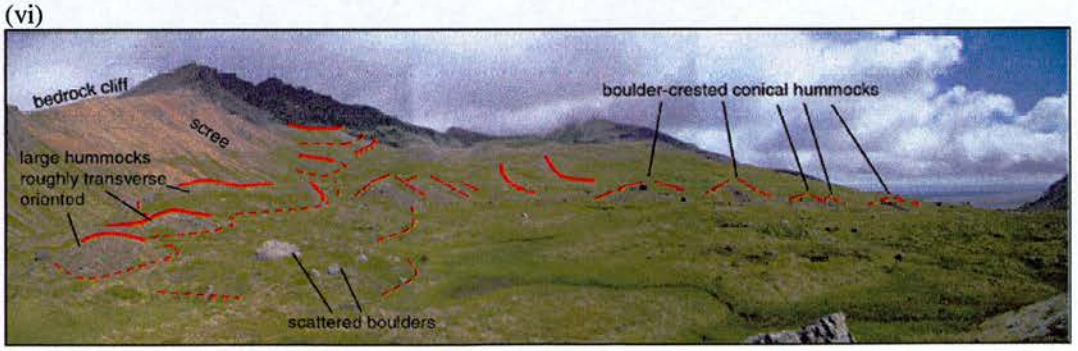

Figure 3.2-i: continued

(vii)

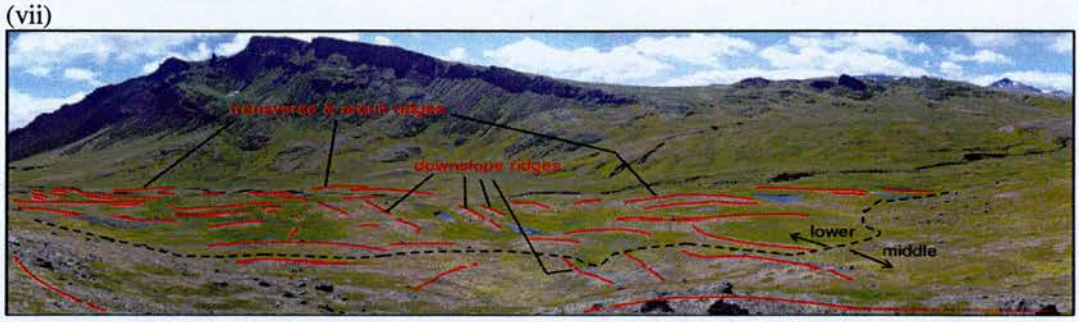

(viii)

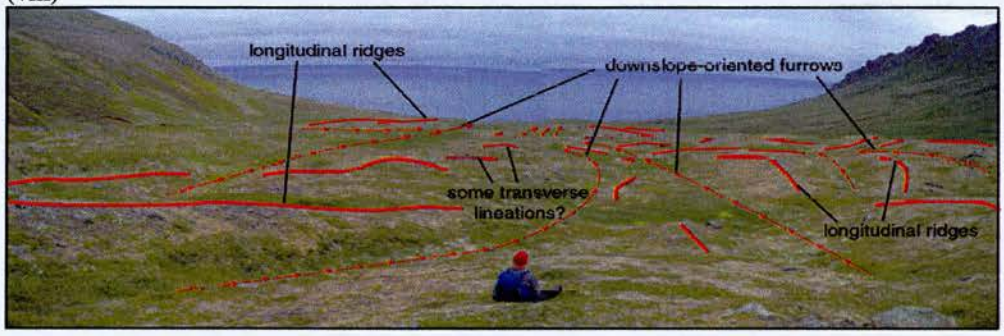

(iix) Cross-section between locations KA – KB (illustrated in Figure 3.2-i (i) and (iv))

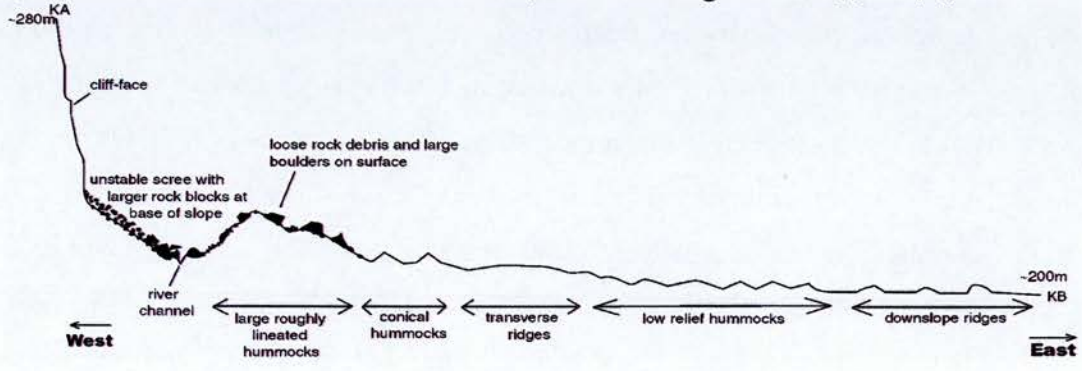

(ix) Cross-section between locations KB – KC (illustrated in Figure 3.2-i (i))

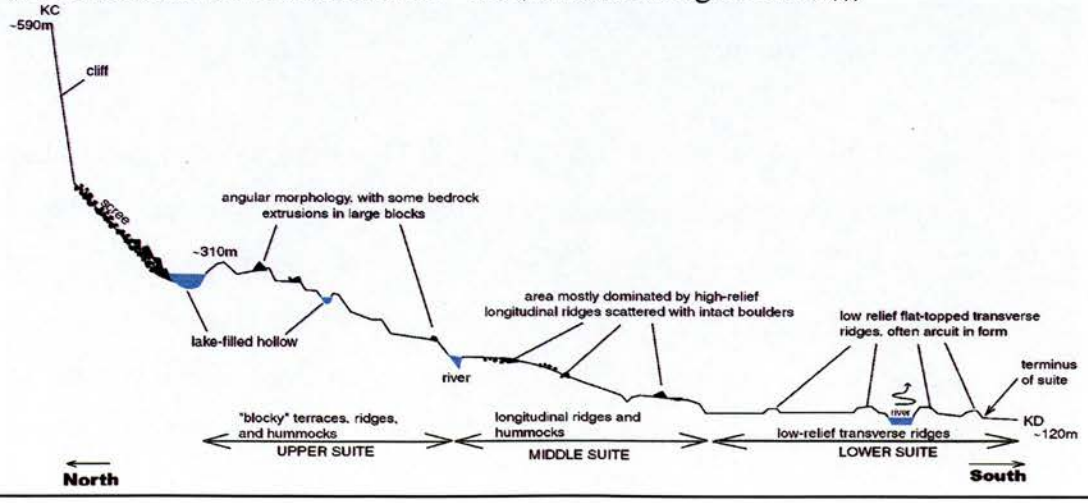

Upper suite

The upper part of the sub-valley, part of which is shown in Figure 3.2-i (iii), contains a series of terrace levels combined with hummocks of varying orientation. The hummocks contain some visible blocks of intact bedrock, while the terrace levels are not well-connected but rather a number of separate short terraces with different dip angles. Five lake-filled hollows are found in the upper part, and are in some cases fronted by transverse ridges. The upper part of the suite drops in altitude rapidly at the point where the sub-valley meets the main valley and opens out.

Middle Suite

The middle section of the suite lies on a shallower slope angle than the upper part, and begins at the break of slope where the upper section abruptly drops in altitude. Working from west to east across the middle, there is a transition in landform element morphology, illustrated in Figure 3.2-i (iv) and (iix). At the foot of the western cliffs, a lake-filled hollow and an outflow river separates the scree slopes from a series of parallel, steep-sided, and mostly boulder-crested hummocky ridges. These ridges are all roughly oriented in a northeast-southwest direction. Many small lakes are positioned in this area, indicating the existence of hollows. Eastwards from this unit of hummocky ridges is an area of cone-shaped hummocks, arranged in two parallel lines in a northwest to southeast direction. Further east is a unit of transverse parallel ridges (at least ten), often separated by small lakes. The next adjoining landform unit is made up of generally hummocky terrain, with small un-orientated mounds. This area merges into a series of longitudinal ridges and another hummocky area.

Beyond the area shown in cross-section in Figure 3.2-i (iix), much of the rest of the middle Kjólsvík suite appears to be generally small hummocks, becoming more ridge-like in the far eastern region. Figure 3.2-i (viii) shown this ridged area. A related orientation is not clear but river channels appear to take eastwards routes through long down-slope oriented ridges and furrows. There is some evidence for super-imposed ridges oriented perpendicular to the main west-east pattern, shown in Figure 3.2-i (viii). The furthest east part of this unit does not have clear margins,

with ridges still oriented east-west. The ridges are less distinct the further east they lie, gradually disappearing with no clearly definable terminus.

Lower Suite

The lower part of the suite begins at another break-of-slope (highlighted in Figure 3.2-i (vii), where the underlying topography becomes essentially flat. The key difference between the upper and middle suite, and the lower suite, is that the lower section appears to contain a number of separate landform elements superimposed on a relatively flat and subdued underlying topography, while in the upper and middle sections, topography is created entirely by connected landform elements, and has a generally rough appearance. The main landform elements visible in the lower suite are east-west oriented arcuit and transverse ridges, which form distinct margins, with several distinct levels behind (up to seven in places). The lower section ridges are generally flat-topped and less than a metre in height, rising from flat ground dotted with lake-hollows, shown clearly in Figure 3.2-i (vii).

Eastern end of south-facing Kjólsvík valley

The main morphological feature of the eastern end of the northern Kjólsvík valley is the bedrock terrace which runs at an altitude of between 40 and 80 m, and has a steep scar face beneath it running to the valley floor. This terrace level is broken by a gully to the east. It is notable that this terrace level ends where the eastern margin of the upper Kjólsvík landform suite begins.

North-facing side of Kjólsvík valley

The north facing valley side is backed by cliffs like the south-face, but the slopes are in general much steeper than on the opposite side. From east to west, the high cliff edge becomes a lower bedrock terrace beyond the summit of Grenmór, and then becomes a low col between the Kjólsvík valley and the lower Víkurá valley. The main morphological feature of the north-facing valley side is the bedrock terraces at the eastern end, and the gullies and loose scree slopes covering much of the slopes.

3.2.4. Svínavík/ Breiðavík

Figure 3.2-j:Geomorphic Map for Svínavík/Breiðavík region

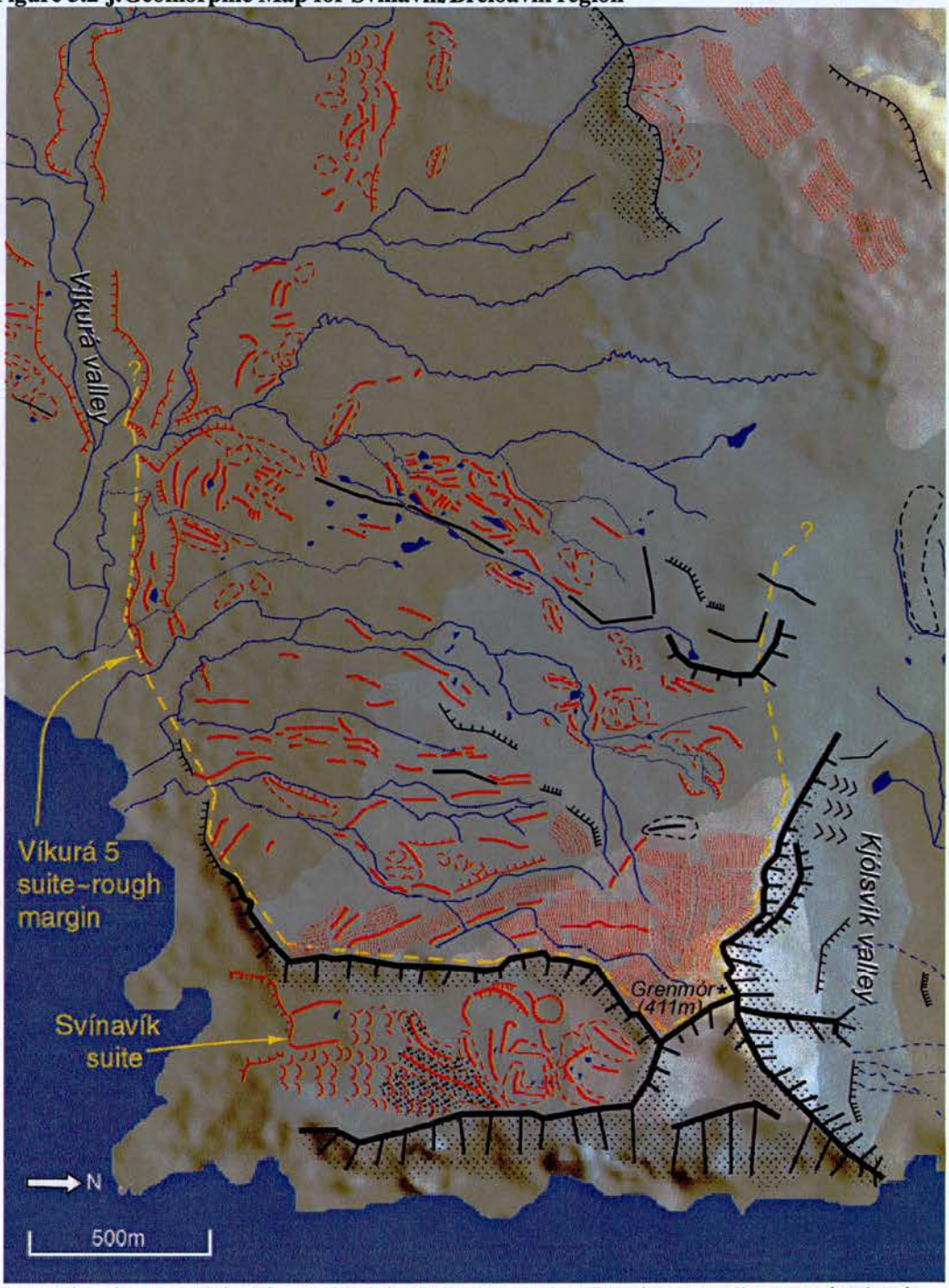

The region illustrated in Figure 3.2-j includes the Svínavík suite, a well constrained suite of hummocky ridges backed by steep cliffs, and the Víkurá 5 suite, which has less clear margins and consists of a series of ridges, mostly longitudinal, which cover the Grenmór hillslope almost to sea level.

Víkurá 5

The suite of landforms named "Víkurá 5", shown in Figure 3.2 j, consists mostly of clearly oriented ridges and some hummocky areas. The suite cover the hillside from Grenmór summit to the Víkurá valley floor, with topography dipping both from east to west in the upper-eastern part and from north to south in the upper-western part. The lower region displays a clear margin, where transverse ridges meet a terrace level. The eastern margin is defined by a series of north-south orientated ridges, which begin near the edges of the cliffs (which delimit the Svínavík basin), and lie, parallel, at progressively lower altitudes. A clear lateral margin for the whole suite at the western edge is less clear. The upper limits of the landform suite lie at the drainage divide between the Víkurá and Kjólsvík basins. At the eastern edge of the divide, steep cliffs drop northwards to Kjólsvík, but moving further west the divide becomes a low col with smooth topography.

Figure 3.2-k: Víkurá 5 Suite and associated illustrations

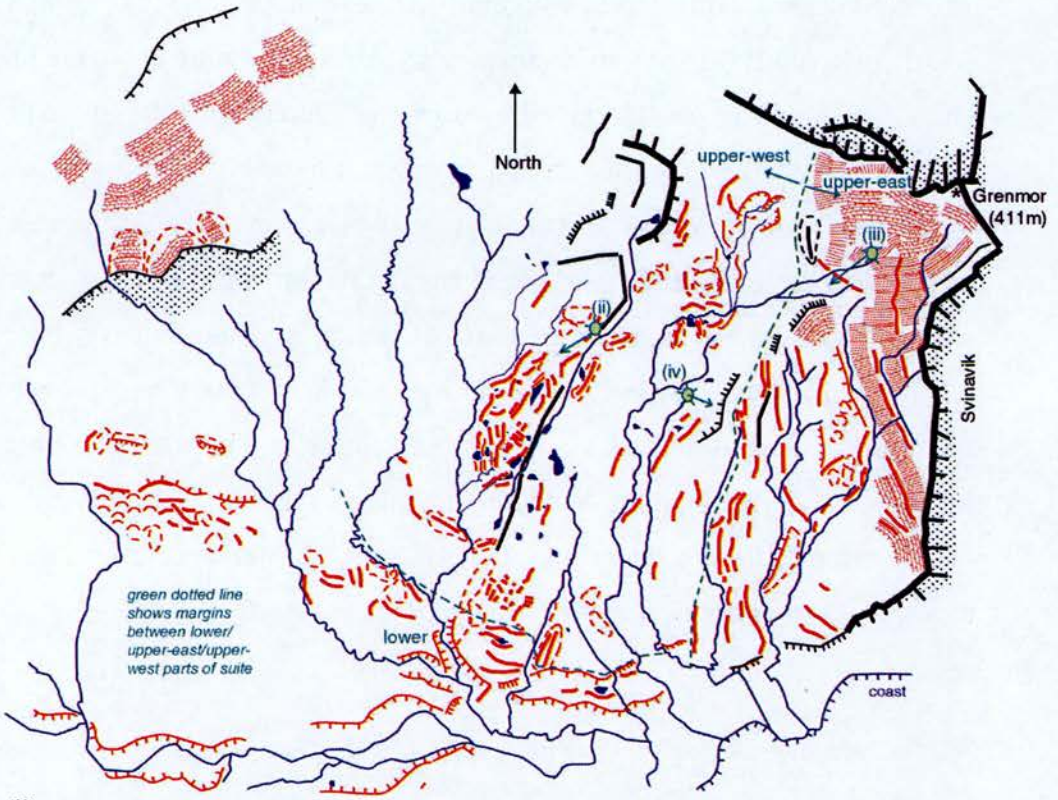

(ii)

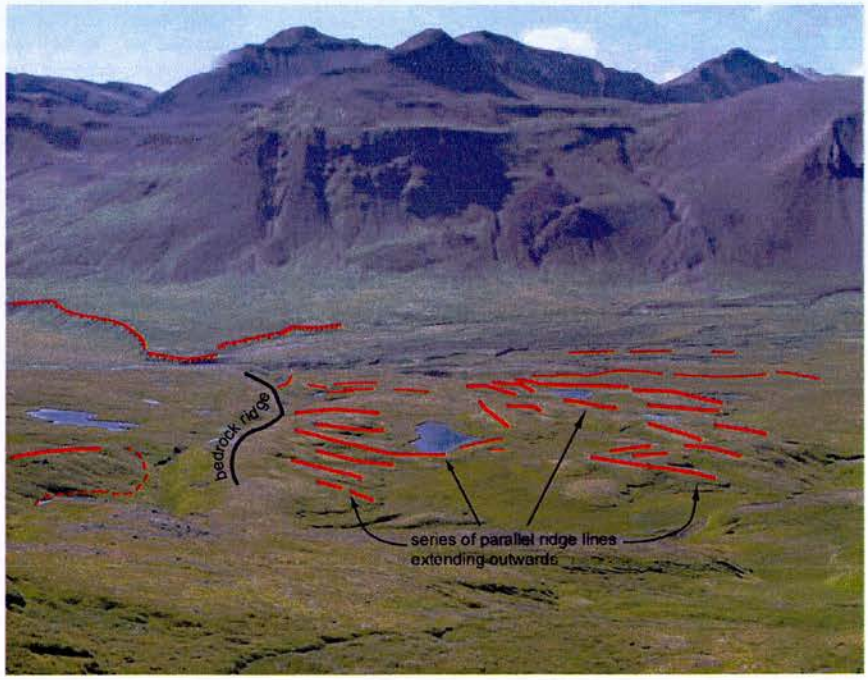

Figure 3.2-k (continued)
(iii)

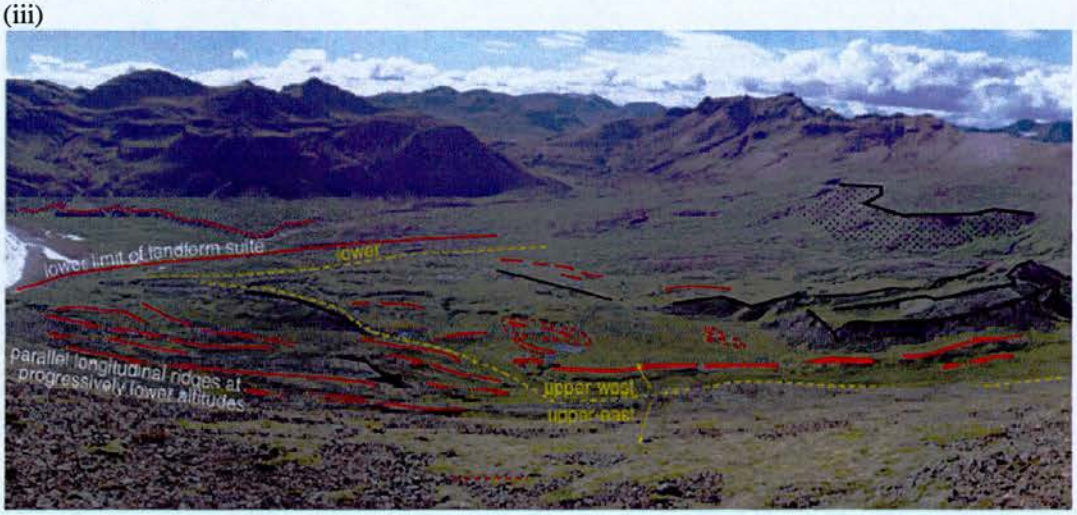

(iv)

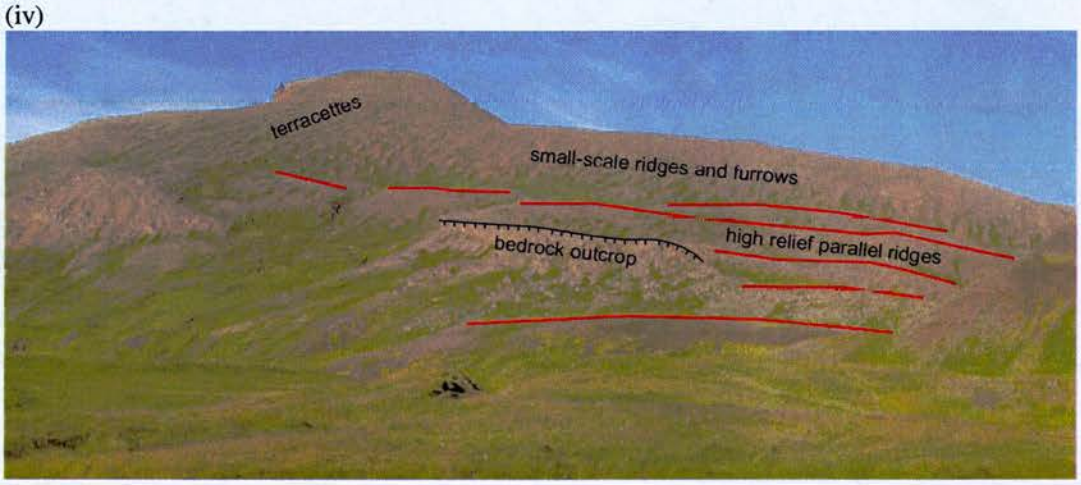

Upper-eastern part of Víkurá 5

A main feature of the upper eastern slope extending from Grenmór is the series of long, straight, parallel ridges, shown clearly in Figure 3.2-k (iii) and (iv), which lie between altitudes of ~350 m and ~50 m. The river network on this slope emphasises the morphology, with rivers draining north to south, essentially across the slope as forced by the orientation of the ridges. The rivers cut through to flow down-slope at some points in a roughly east to west direction and then flow north to south again when they meet the next ridge. The pattern is accentuated by the existence of some bedrock ridges and terraces oriented in a north-south direction. In the highest altitude areas, superimposed on this pattern of parallel ridges, are areas of miniature terraces, which are oriented across the slope, and small-scale ridge and furrow terrain, oriented down-slope, as seen in Figure 3.2-k (iv).

Upper-western part of Víkurá 5

At the base of the upper-eastern area the slope gets gentler and is south-facing. The upper part is dominated by a long bedrock ridge which extends almost the whole length of the slope in a north-north-east to south-south-west direction (see Figure 3.2-k (ii) and (iii)). The remaining upper-western area of the suite is made up of mostly longitudinal ridges super-imposed on a relatively smooth gently sloping surface. Further sets of bedrock intrusions create small sub-basins near the drainage divide in this region. An area of small lake-filled hollows interspersed with arcuate ridges, extend from such a bedrock basin, (clearly visible Figure 3.2-k (ii), a photograph taken looking down-slope from within the basin). These ridge-lines form a series of lateral and terminal limits to the landform suite, though they are not connected to the lowest margin of the whole suite.

Lower part of Víkurá 5

The generally north-south oriented ridges of the upper Víkurá 5 suite terminate near the valley bottom and transverse ridges form a margin, seen in Figure 3.2-k (iii). Two lakes fill hollows between transverse ridges, which are steep-backed and boulder-crested. The Lower part of the Víkurá 5 suite is connected to a raised terrace level, which is traceable to the opposite valley side, further explained in 3.2.5 (Leirfjall/Breiðavík).

Svínavík

The Svínavík basin, as seen in Figure 3.2-l, is an isolated drainage basin which is separated from the rest of the field area by steep cliffs on the North and West, with further cliffs dropping to the sea at the South and East.

Figure 3.2-l: Svínavík suite and associated illustrations

(i)

(ii)

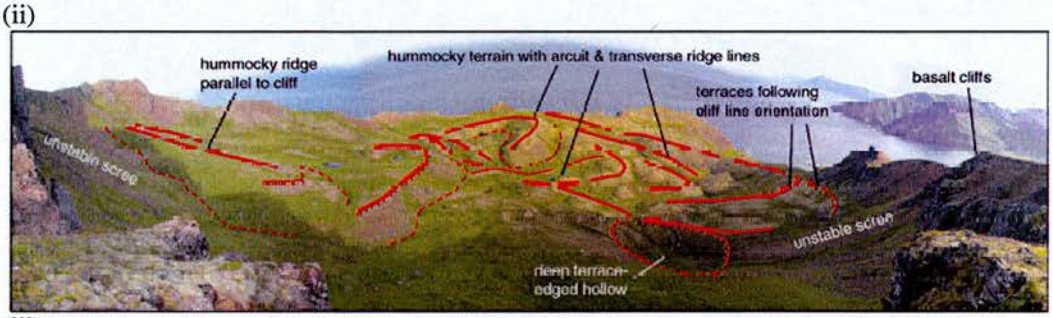

(iii)

Figure 3.2-l: continued

(iv)

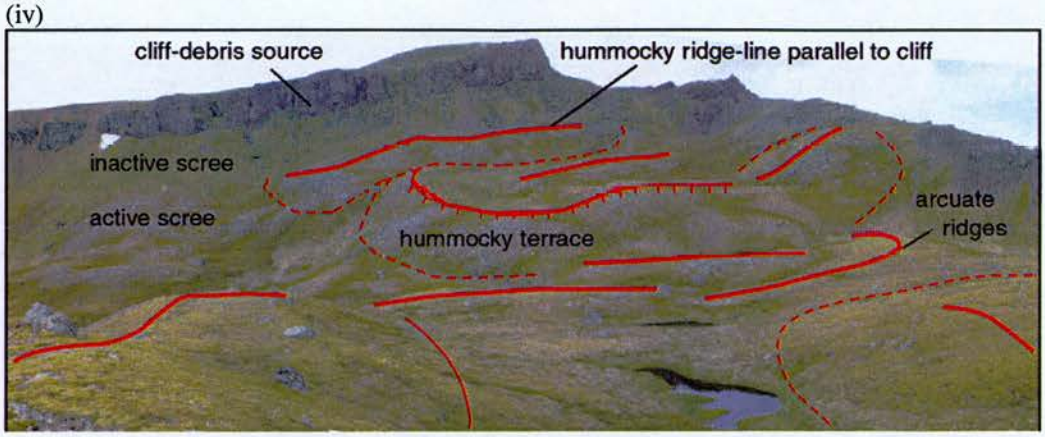

(v)

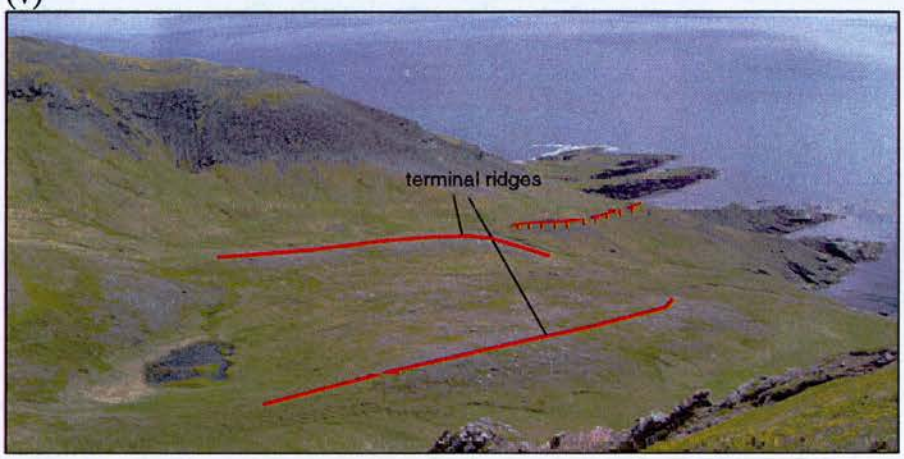

The upper area of the basin is made up of large-scale hummocky terraces and ridges, with heights upwards of ten metres, which begin at the foot of mostly active scree slopes (see Figure 3.2-l (ii) and (iv)). The surface of these hummocks contains a small number of scattered boulders and angular rock fragments. The visible ridge lines are mostly oriented transverse to the slope, although around the cliff-edges they are found to follow a more down-slope orientation parallel to the cliff faces. Superimposed on this general pattern a number of small ridge features are found which are more arcuit in form, and rise only a metre or two from the surface.

A sharp transition is found between this upper area and a second area of hummocky terrain, where the surface is characterized by continuous angular basalt rocks of between 0.5 m and 2 m in diameter (see Figure 3.2-l (iii)). These ridges generally follow a down-slope orientation. The lower margins of the Svínavík suite are less

well-defined than in other suites, with a terrace edge which drops straight to the sea signifying the lower margin, unlike in other suites where a steep-sided transverse or arcuit ridge forms the margin. Two longitudinal ridges just above the terrace edge define a lateral margin (see Figure 3.2-l (v)).

3.2.5. Leirfjall/Breiðavík

Figure 3.2-m: Geomorphic map of the Leirfjall/Breiðavík region

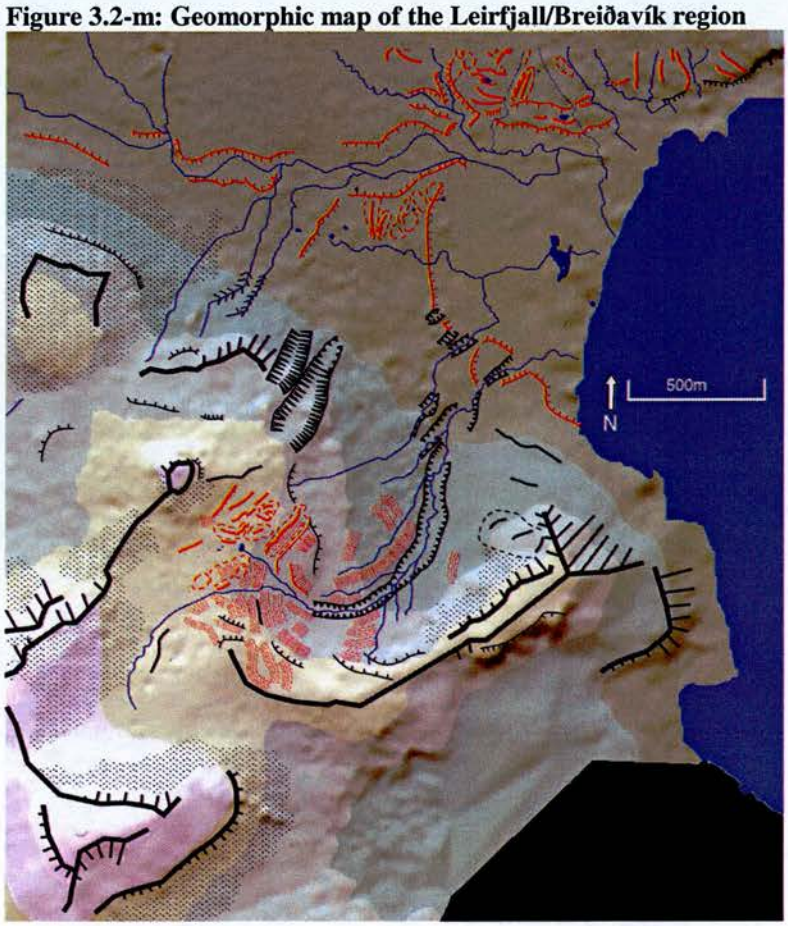

The Leirfjall basin, shown in Figure 3.2-m, is a sub-valley of the main Víkurá valley, which drains eastwards and northwards towards the sea. It does not contain significant large-scale geomorphology.

The Leirfjall basin is well-constrained, steep sided and surrounded by cliffs and scree slopes. It consists of a steep northeast-southwest oriented valley, which opens out into a wide basin at the foot of Hákarlshaus (557m) and Leirfjall (775m).

Figure 3.2-n: Leirfjall basin and associated illustrations

(i)

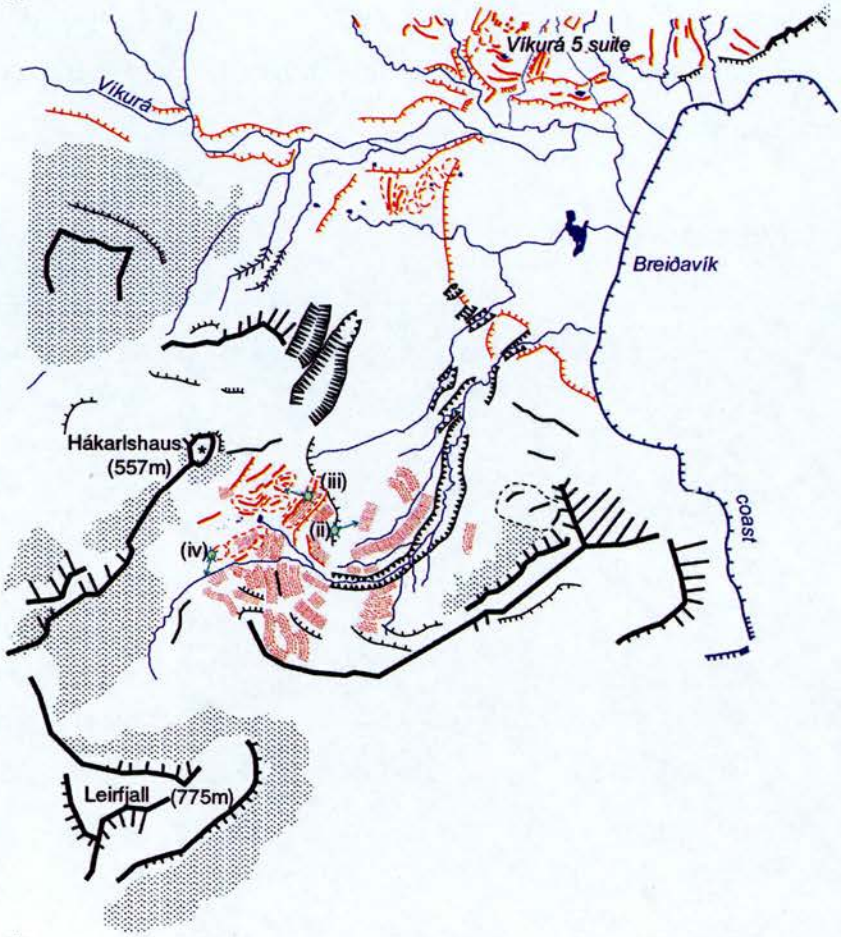

(ii)

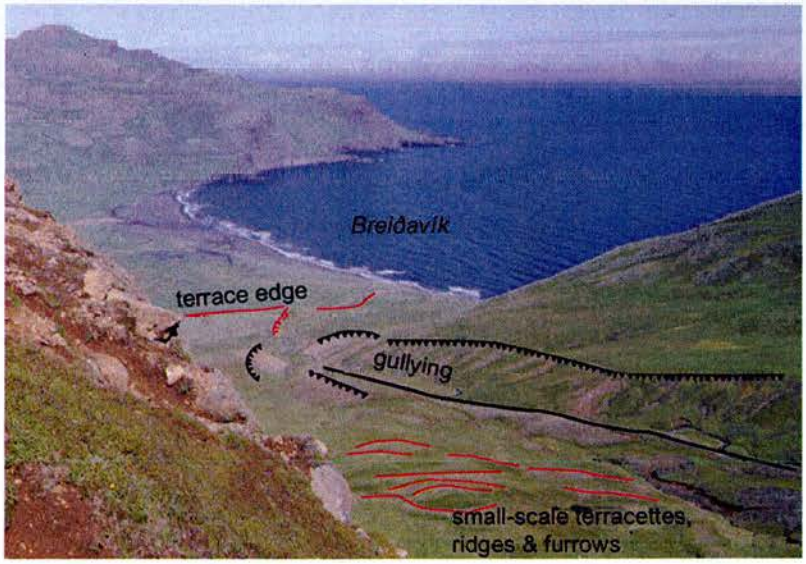

Figure 3.2-n: continued

(iii)

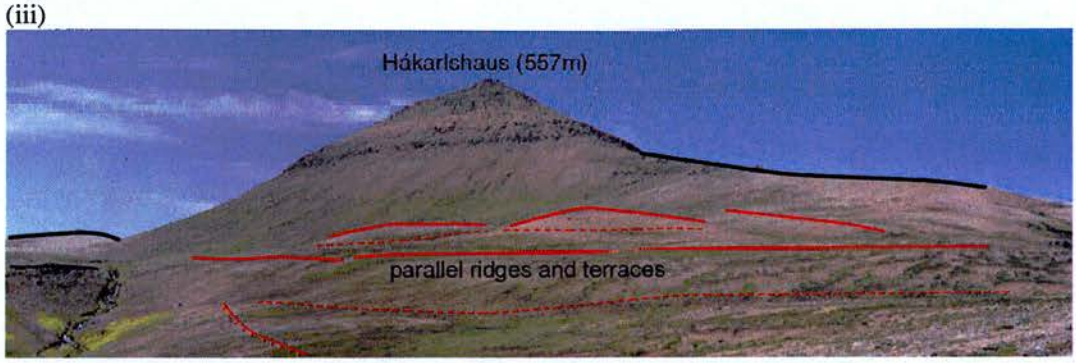

(iv)

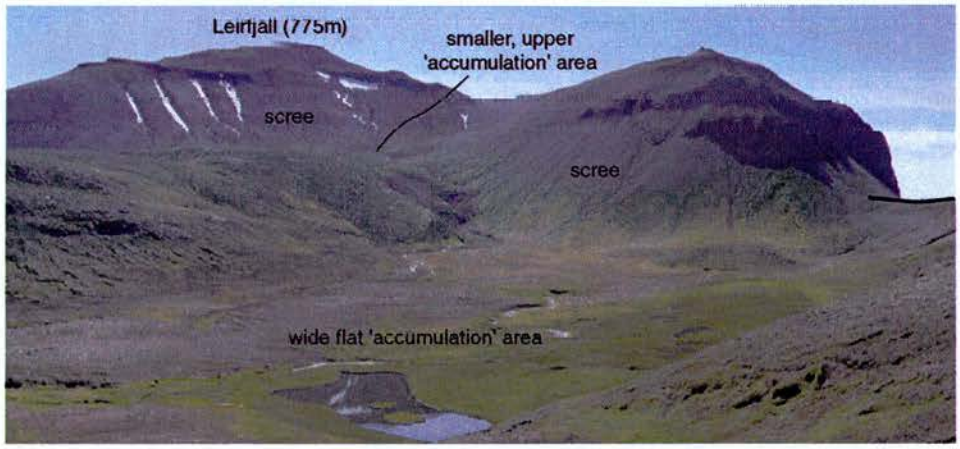

Much of the basin's surface in the steep lower region is made up of a series of small-scale terracettes, ridges and furrows, illustrated in Figure 3.2-n (ii). Transverse terraces are on the steeper slopes and ridge-and-furrow terrain on gentler slopes, oriented down-slope. The surface of the valley floor is dissected with numerous gullies which run the full length of the valley. The rivers draining out of this basin flow directly to the sea, cutting through a raised terrace level at the base of the slope (shown in Figure 3.2-n (i), which sits between 25 and 50 metres above sea level, and is traceable on north and south-facing sides of the main Víkurá valley.

The upper part of the Leirfjall basin opens out into a wide flat basin, shown in Figure 3.2-n (iv), which is dominated by series of bedrock terraces around the edges, but contains no significant relief on its floor. An area of parallel ridges, hummocks and terraces around the summit of Hákarlshaus (557m), shown in Figure 3.2-n (iii), define the extent of large-scale geomorphic feature of this basin.

3.2.6. Víkurá –East

Figure 3.2-o: Geomorphic Map of Víkurá-East region

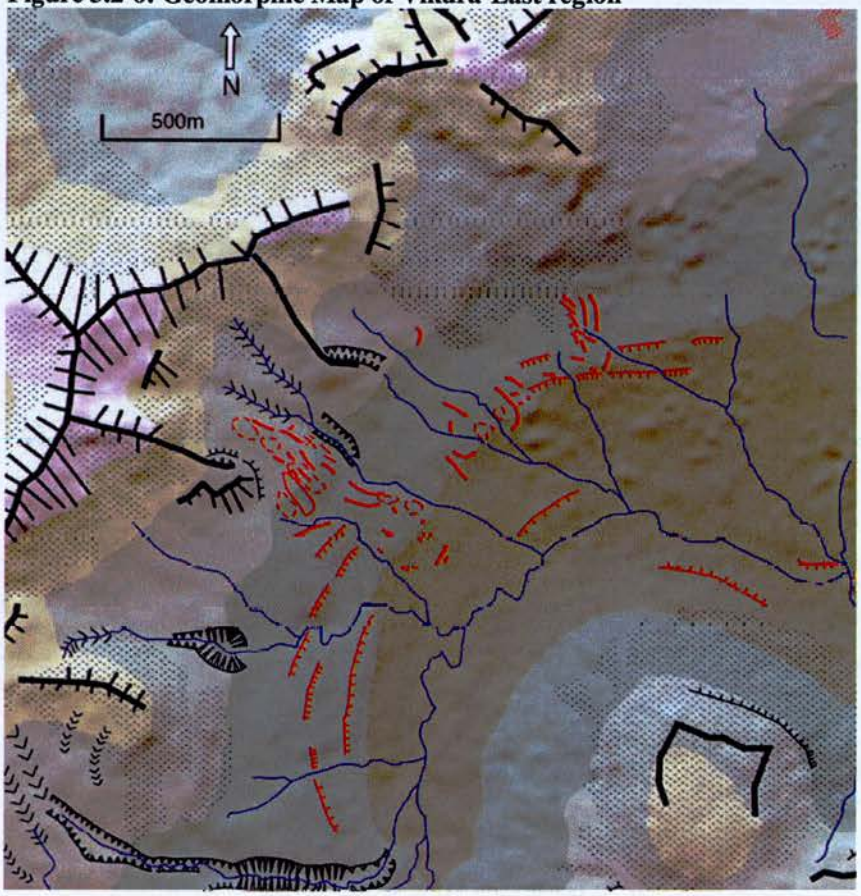

The eastern Víkurá valley is dominated by a series of parallel terraces, as illustrated in Figure 3.2-o. In two main places these terrace levels are dissected by units of longitudinal ridges and lineated hummocks, which make up the Víkurá 3 and 4 suites. The exact locations of these 'suites', which are less well-defined than other suites in the area, is shown in Figure 3.2-p.

Víkurá 3 & 4

As shown in Figure 3.2 o, two, and in places three, terrace levels are traceable (though sometimes discontinuously) the full length of the east-draining Víkurá valley (up to the Víkurá 5 suite), on the east- to south-facing valley side. The terrace levels dip gradually towards the sea, and although not continuous, the dip is a constant angle through all the terraces. On the opposite valley side, there is a further terrace dipping in the same direction and at an altitude comparable with the lowest terrace level of the other side. There are two areas on the east- to south-facing valley side in which the terraces are not visible. These are in the locations of the Víkurá 3 and 4 landform suites, shown in Figure 3.2-p (i). The lower margins of these suites fall below the terrace levels. The lower margins of these landform suites are not as

distinct as those of other suites. Víkurá 3 has a short terminal transverse ridge, and contains a small number of longitudinal ridges in its middle section. At the upper part of Víkurá 3 the morphology is more one of large hummocks, largely oriented in a longitudinal direction. Víkurá 4, highlighted in Figure 3.2-p (ii) maintains two distinct high arcuit ridges, which curve from longitudinal to transverse orientation. Up-slope of these ridges are a number of mainly longitudinal ridges, although no clear margins at the sides. At other places on this valley side, the terrace level is dissected by river channels or series of poorly defined ridges and hummocks similar to the Víkurá 3 and 4 landform suites named here.

Figure 3.2 p: Víkurá 3 & 4 landform suites and associated illustrations

(i)

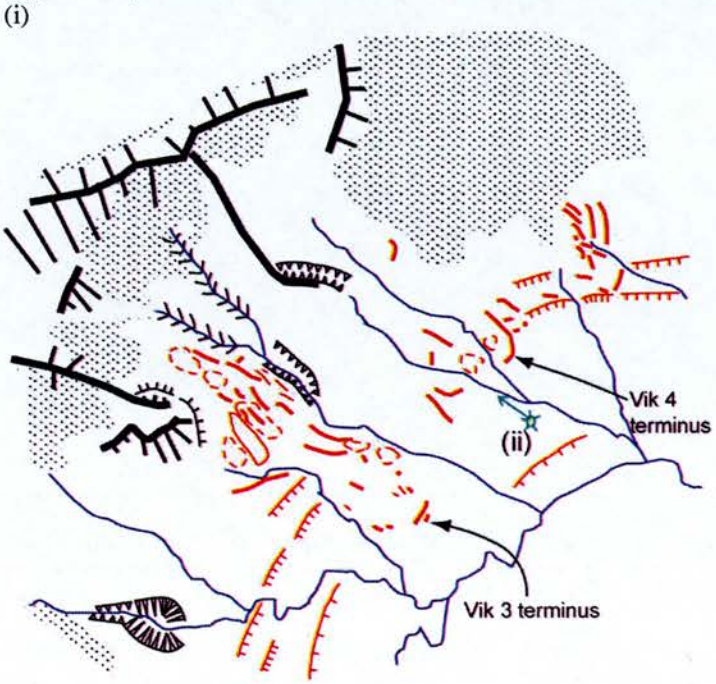

(ii) Víkurá 4

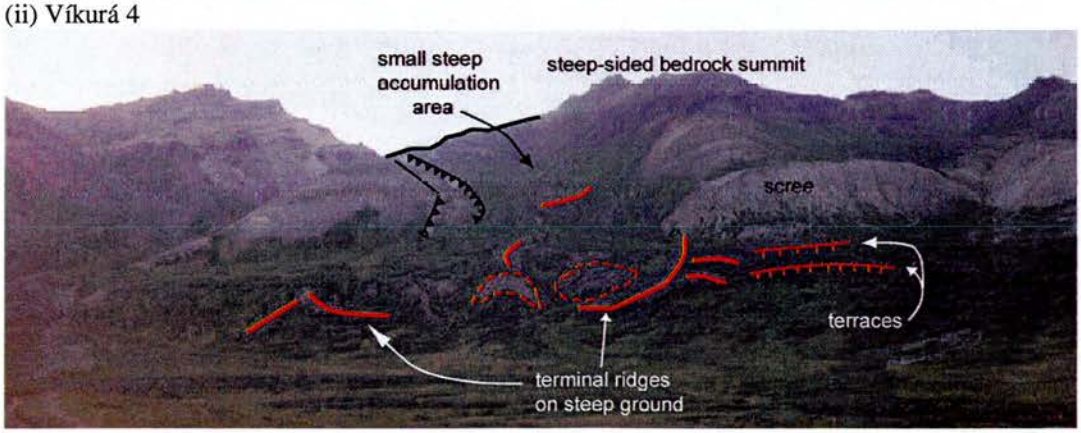

3.2.7. Víkurá –Central

Figure 3.2-q: Geomorphic map of the Víkurá-Central region

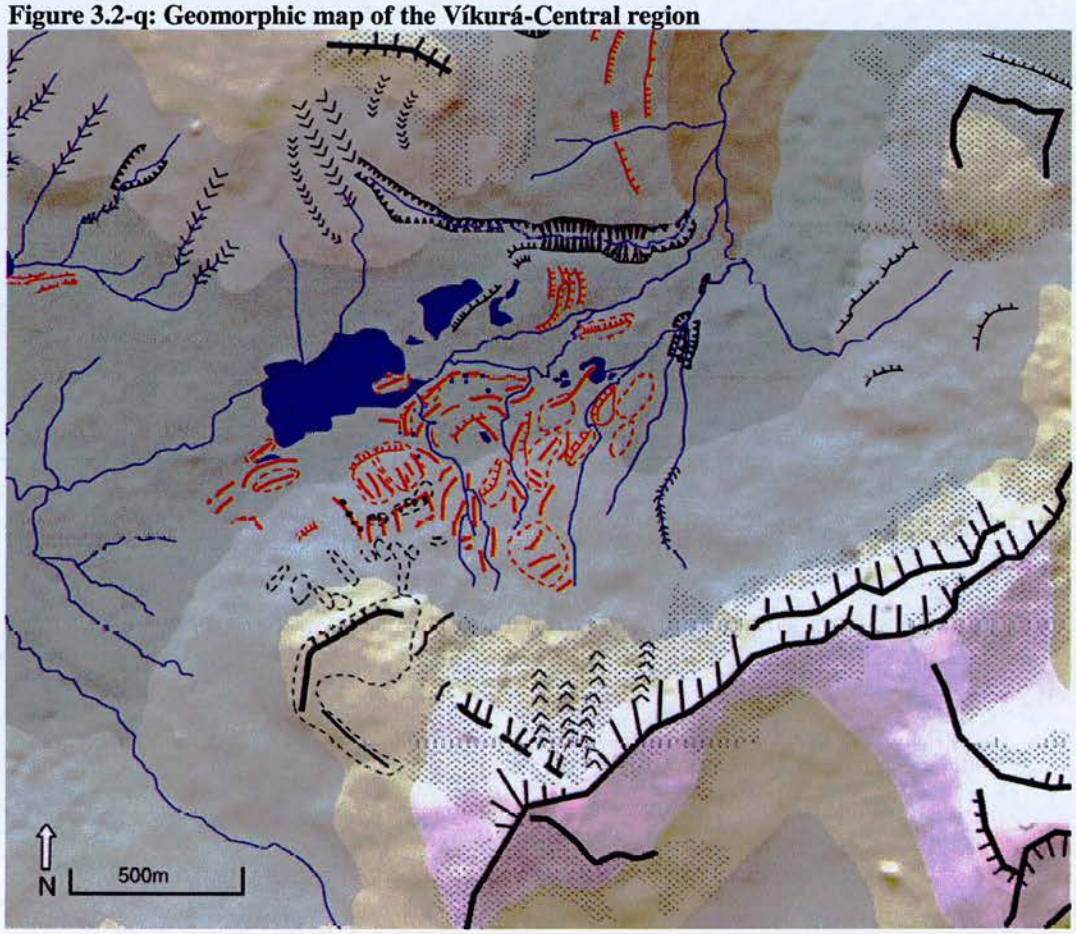

Figure 3.2-q shows the main feature of the middle part of the Víkurá valley. To the top of the map, the terraces described above are visible. Moving south-west up the Víkurá valley, there are a series of lakes, the largest and most westerly of which marks the drainage divide between east and west-draining areas. An area made up of ridges and hummocks meets these lakes on the north-facing valley side, with a clear lower margin defined by arcuate ridges. This suite of landforms is named as the "Víkurá 2 Suite".

Víkurá 2

Figure 3.2-r: Víkurá 2 landform suite and associated illustrations

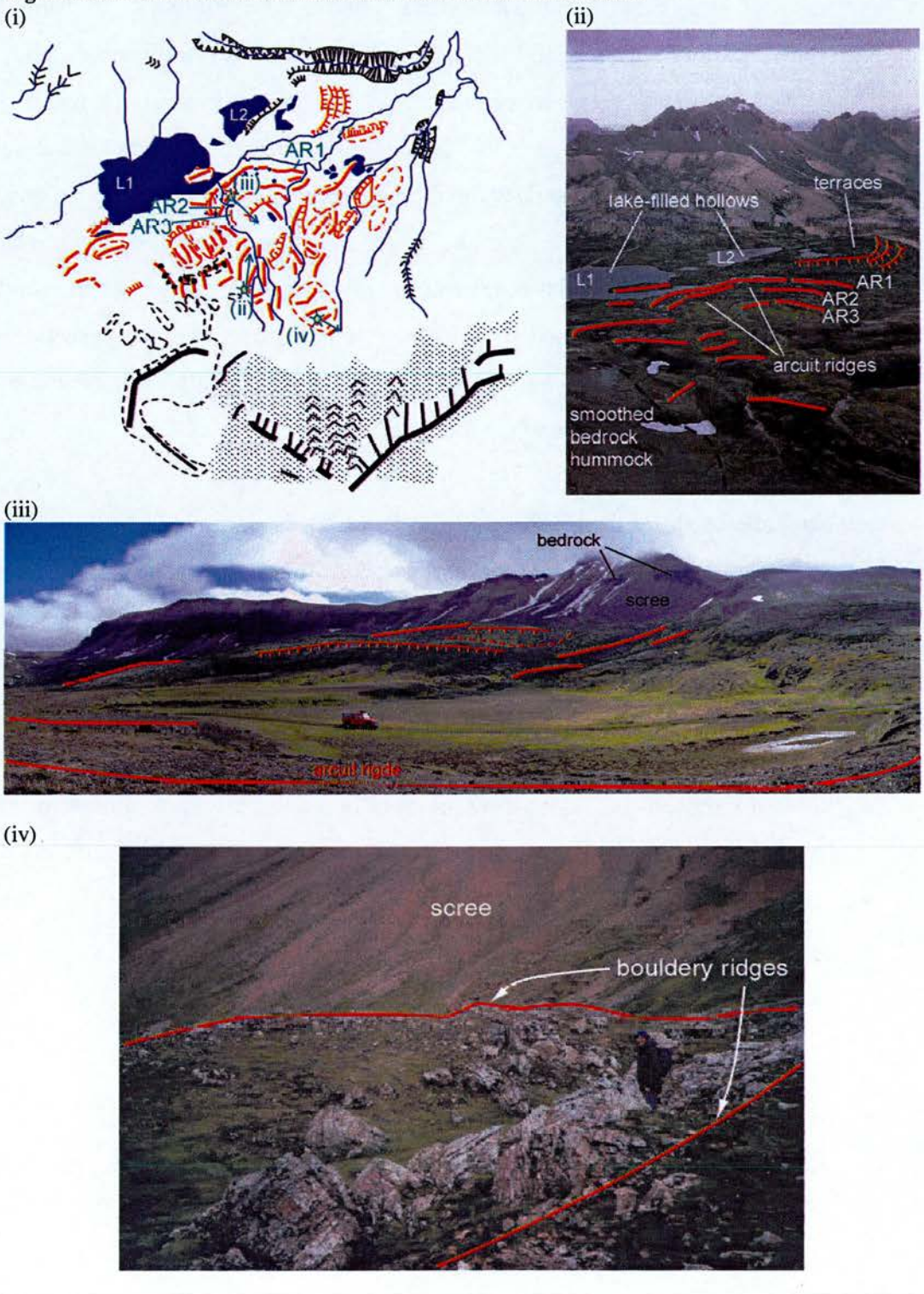

At the south-eastern edge of lake (L1), as illustrated in Figure 3.2-r (i), a series of clear arcuit ridges meet the water's edge, and behind them (upslope) is a further series of ridges and hummocks which make up the Víkurá 2 landform suite. As shown in Figure 3.2-r (i) and (ii), three arcuit ridge levels are visible (AR1, AR2 and AR3), with small lakes between them. Figure 3.2-r (iii) is a photograph taken from the western edge of ridge AR2, and demonstrates the low relief nature of these ridges, which lie on flat and subdued topography. They are flat-topped and, rise only around one metre from the surrounding ground, with the exception of the lake-side of the outermost ridge, which drops four metres to the lake edge. At the south-western edge of AR1, a flat-topped straight ridge extends in a westerly direction and stops abruptly. At the south-western edge of Lake L1, another set of arcuit ridges is visible, though less distinct than the others.

Up-slope of this lower part of the suite which is dominated by low relief arcuate ridges, and where the slope breaks upwards from the flat valley floor, the upper suite becomes more continuously hummocky and rough. Immediately up-slope of the ridges, two transverse terraces, visible in Figure 3.2-r (iii), form the edge of large hummocks, which are juxtaposed with longitudinal linear ridges. Further up-slope from here, the area is characterised by boulder-crested ridges and hummocks, often lineated transversely, which contain large bedrock blocks, as shown in Figure 3.2-r (iv).

3.2.8. Víkurá-West/Mosdalur

Figure 3.2-s: Geomorphic map of Víkurá-West and Mosdalur region

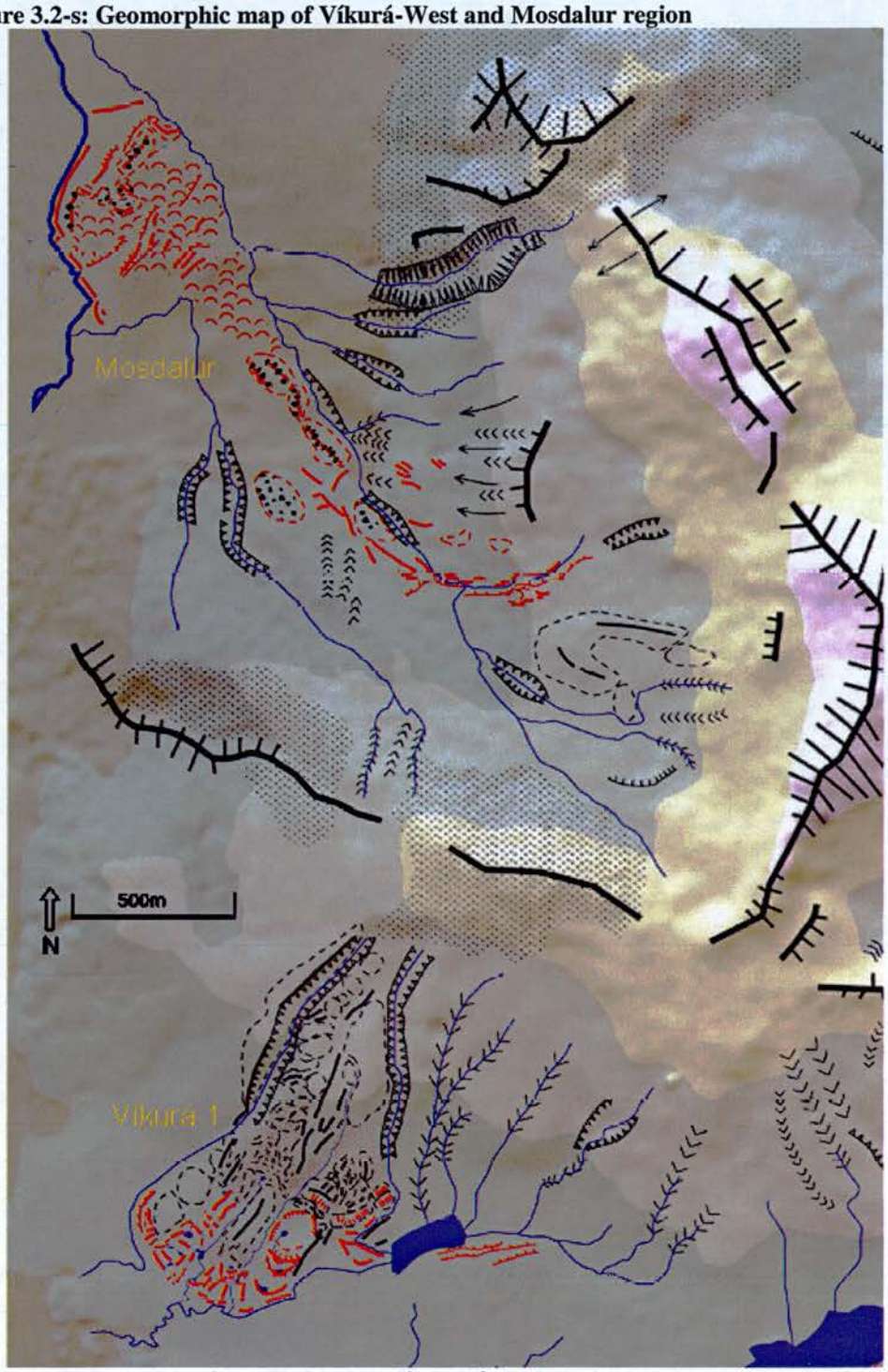

Figure 3.2-s shows the existence of two landform suites, Víkurá 1 and Mosdalur, both of which exhibit clear lower margins.

Víkurá 1

Figure 3.2-t illustrates the Víkurá 1 suite, which drops from northeast to southwest from the summit of a round-topped rhyolite hill, and is flanked by deep lateral gullies. There are two key areas of this suite, the upper of which is predominantly a set of bedrock features, and the lower part, which contains a series of mostly transverse and arcuit ridges.

Figure 3.2-t: Víkurá 1 landform suite and associated illustrations

(i)

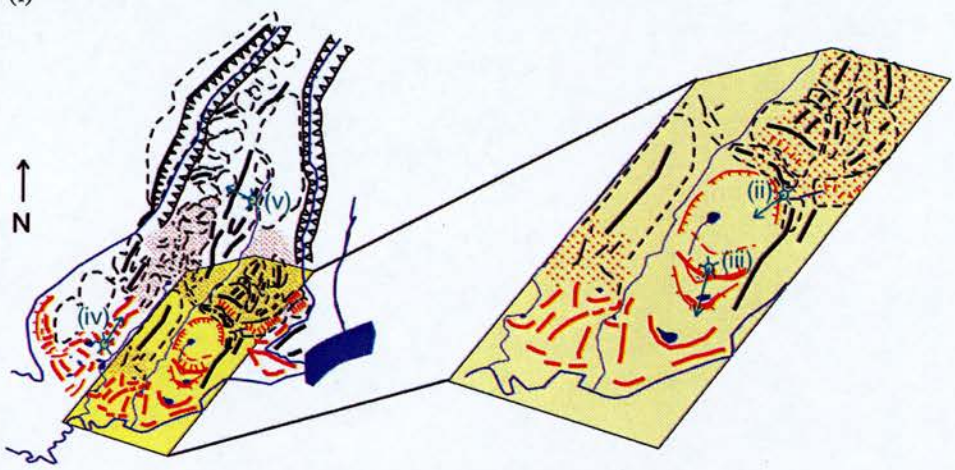

(ii)

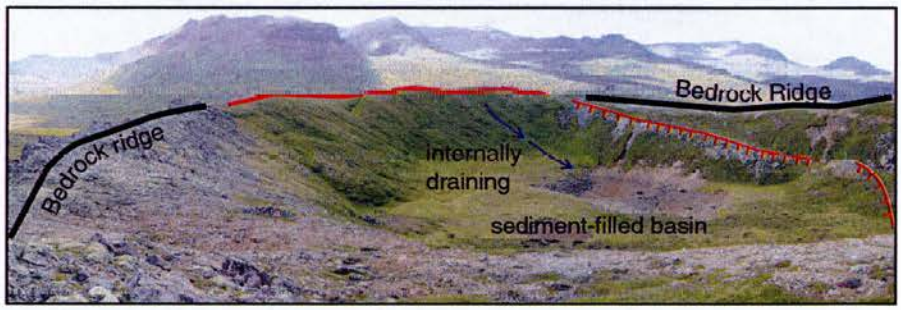

(iii)

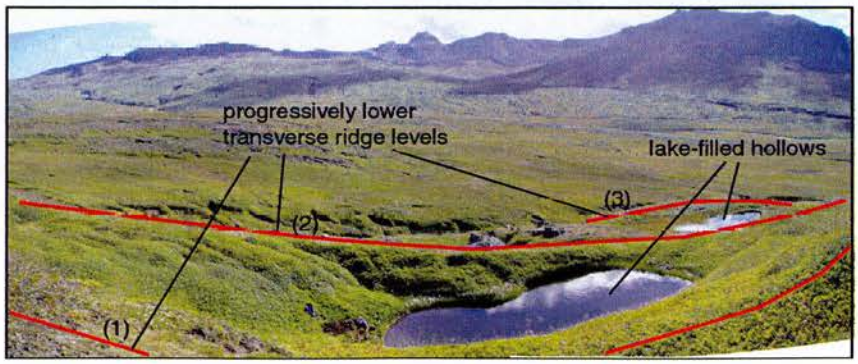

Figure 3.2-t: continued

(iv)

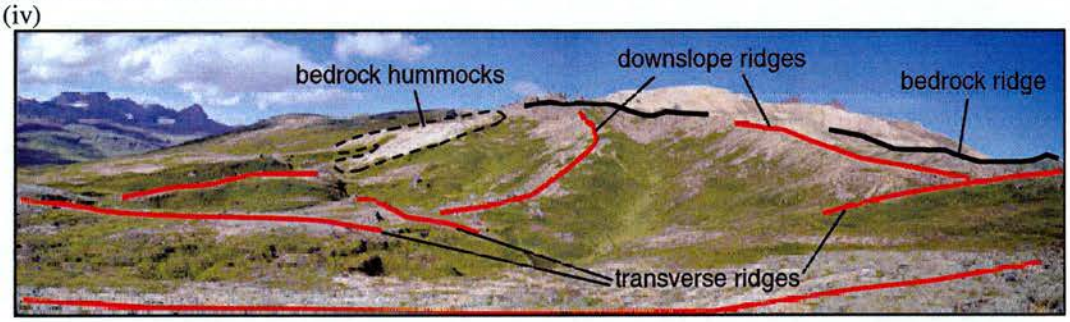

(v)

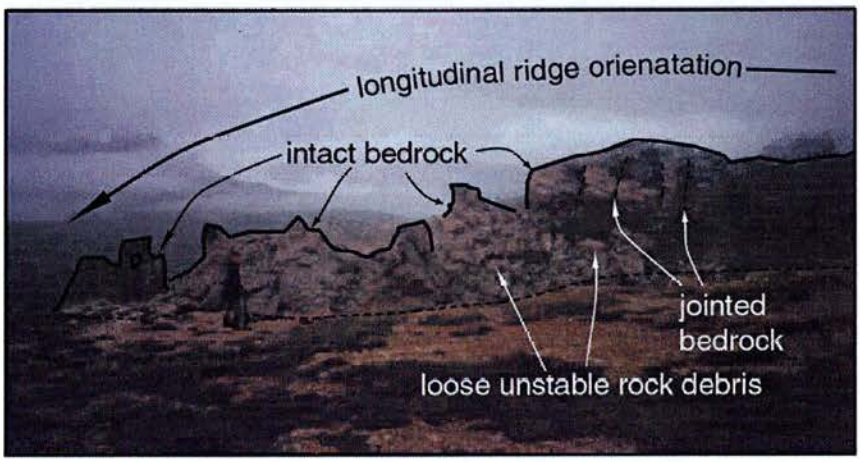

Upper Víkurá 1 Suite

The upper part of the Víkurá 1 suite is made up of a series of bedrock hummocks and ridges with a thick but discontinuous covering of large angular rock debris. The lateral margins of the suite are clearly marked by discontinuous, steep-sided longitudinal bedrock ridges and lineated hummocks, which widen towards the base to form a fan shape. The landforms in much of the upper area have little clear orientation, but some major longitudinal ridge lines are visible in places, especially on the eastern side, as illustrated in Figure 3.2-t (v). Discontinuous bedrock blocks appear to maintain a constant orientation, separated by piles of unstable rock debris. The western side is made up of generally hummocky terrain but with significant protruding bedrock blocks. Amongst this chaotic bedrock, as we move downslope, various smooth mounds become visible, which have no clear evidence of bedrock extrusions, but which are heavily connected to the bedrock patterns.

Lower Víkurá 1 Suite

The lower section has a different character. While some bedrock features mark the lateral margins of the suite, the lower margins are defined by a clear row of arcuit ridges. A notable set of landform elements in the lower part is highlighted in Figure 3.2-t (i) and photographed in Figure 3.2-t (ii). An internally-draining hollow, backed by a bedrock ridge and terraces, is constrained by two parallel ten-metre high bedrock ridges on the west and east, and fronted by a steep transverse ridge with very different character to the lateral bedrock ridges. It can be seen that the lateral ridges contain large amounts of protruding intact (though often heavily broken down) bedrock, while the transverse front ridge has no rocky extrusion. This front ridge also contains, a 2 m diameter and ~2 m deep hollow on the ridge crest (it may have been deeper as on excavation of this hole a base was not reached). The front ridge is steep on the inside, but on the outside, as shown in Figure 3.2-t (iii), it drops in a series of three terrace-like steps, each of which has an arcuit ridge at the front with a small lake-filled hollow behind.

To the west of this set of features, further arcuit ridges form the lower limits of an area of longitudinal ridges, following the same orientation as the bedrock ridges higher up, but showing no evidence of bedrock extrusions. These ridges are illustrated in Figure 3.2-t (iv). A number of lakes cover this area, indicating the existence of sediment-filled hollows. The lower section to the west is dominated by two high, steep-sided bedrock ridges, and on the western edge, a large bedrock hummock.

Mosdalur

Figure 3.2-u: Mosdalur suite and associated illustrations

(i)

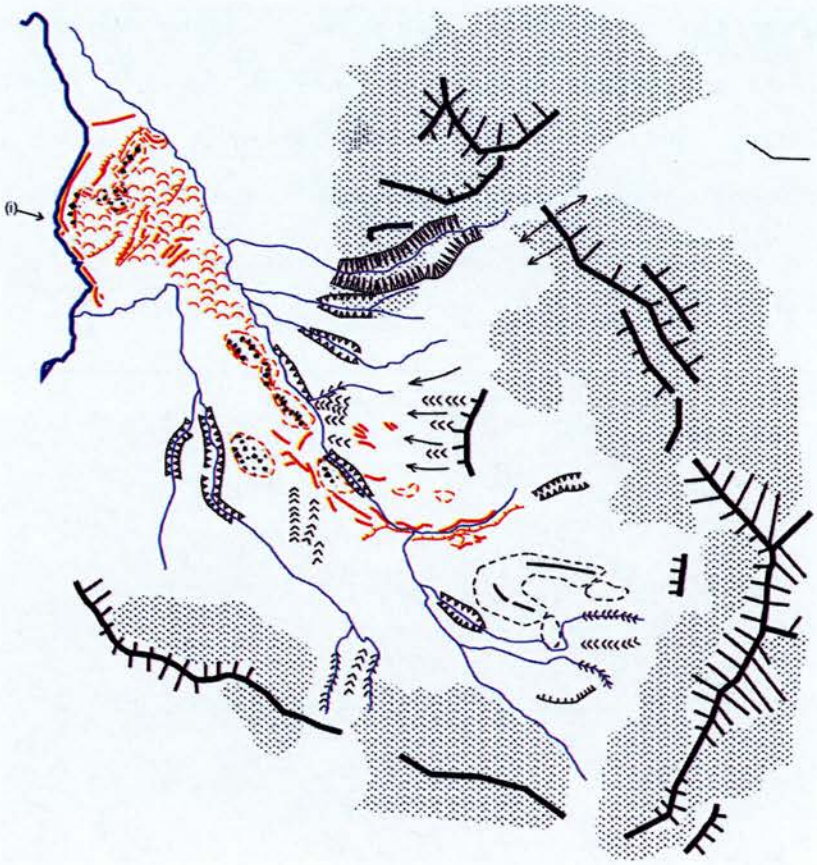

(ii)

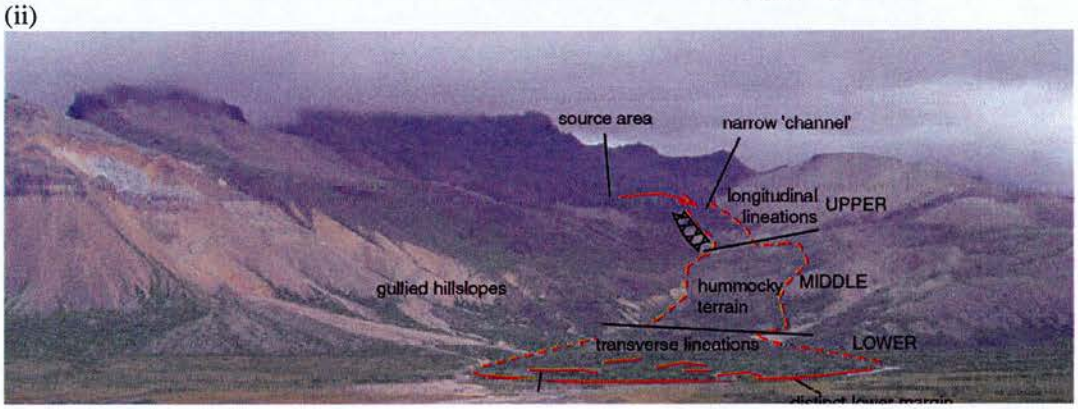

The so-called Mosdalur landform suite occupies its own basin, constrained by cliffs and steep, gullied slopes to the northeast, east and south. It has three main areas of distinctive morphology, the upper, middle and lower. The upper area originates in a wide gently-sloping basin backed by scree slopes. Landform elements become visible at the point where the basin narrows and drops down-slope rapidly.

Longitudinal ridges extend alongside steep-sided gullies to characterise the upper part of the landform suite, shown in Figure 3.2-u (ii). The middle area is wider and on gentler slopes. It is defined by generally hummocky terrain with some interspersed longitudinal ridges, with rough boulder-crested surfaces. In the lower part the suite widens significantly as it meets the valley floor, as shown in Figure 3.2-u (ii). This region contains hummocky terrain with a series of transverse ridges, the lowest of which defines a clear, steep-fronted, lower margin.

3.2.9. Hrafná

Figure 3.2-v: Geomorphic map of Hrafná basin

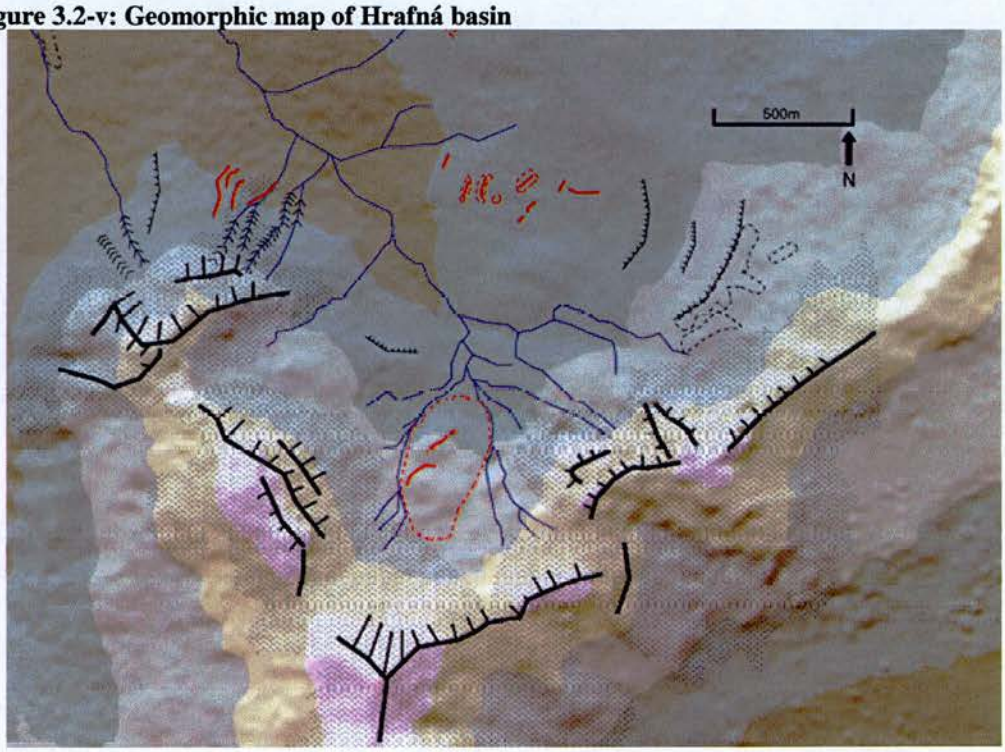

The Hrafná basin is a subsidiary of the main Borgarfjörður valley, and contains one distinctive landform type which is not observed anywhere else in the field. It is large, elongated hummock, is made up of loose rock debris, and is covered by very little vegetation, unlike the rest of the field area. Its geographical location is shown in Figure 3.2-v, and its distinct appearance is evident from Figure 3.2-w (ii). It is situated at the foot of two mountain peaks containing bedrock cliffs and exposures,

whose slopes are made up almost entirely of loose scree. The surface of the hummock is rough, with some indication of indistinct ridge lines.

Figure 3.2-w: Hrafná basin

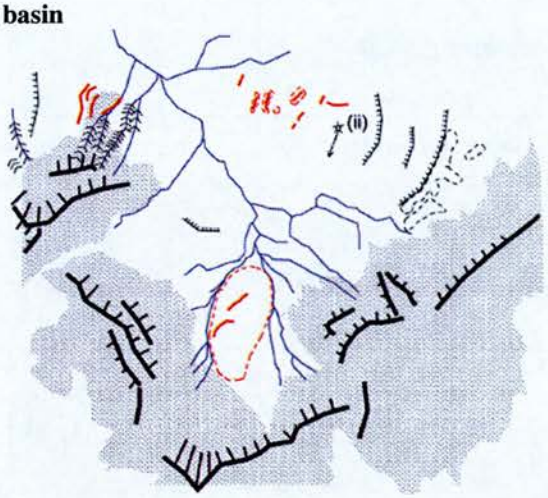

(ii)

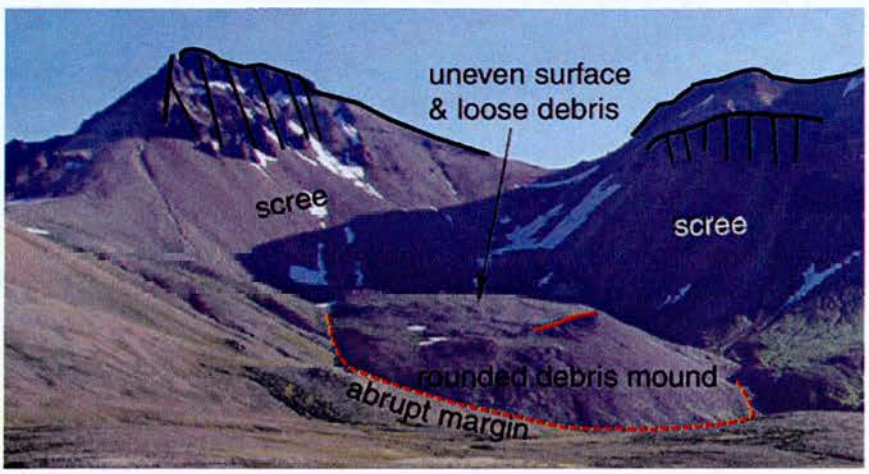

3.3. Beyond immediate field area limits

Due to time constraints, the geographical area studied and mapped in detail had to be limited. The mapping described in 3.2 included the collection of G.P.S ground control points to enable development of a high resolution Digital Elevation Model of the area (see Chapter 2 for details). Various adjoining regions were assessed in order to broaden knowledge of the variable geomorphology of the area, and to look for any further examples of debris-transport activity. The area mapped and presented in 3.2 lies fully within the domain of an old central volcano, which gives it a distinctive

rhyolitic geology. By assessing some regions outwith this rhyolite area, any variations in geomorphic characteristics relating to geology can be addressed.

3.3.1. Loðmundarfjörður

Figure 3.3-a: Loðmundarfjörður

(i)

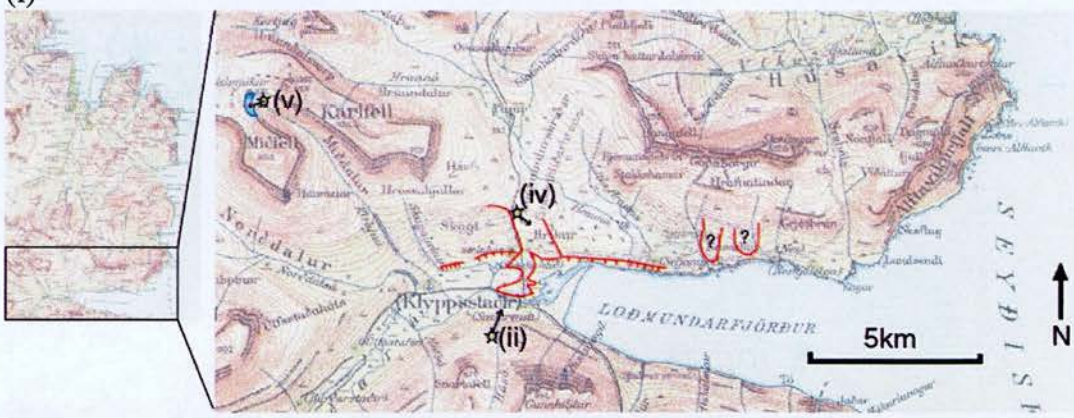

Figure 3.3-a (i) above shows the topography of the Loðmundarfjörður basin. Red lines indicate the margins of landforms of interest. The blue patch represents the location of permanent ice cover. The locations from which photographs were taken are highlighted in this figure, with the exception of Figure 3.3-a (iii), the location of which is shown within Figure 3.3-a (ii) below.

(ii) Loðmundarfjörður Landform Suite

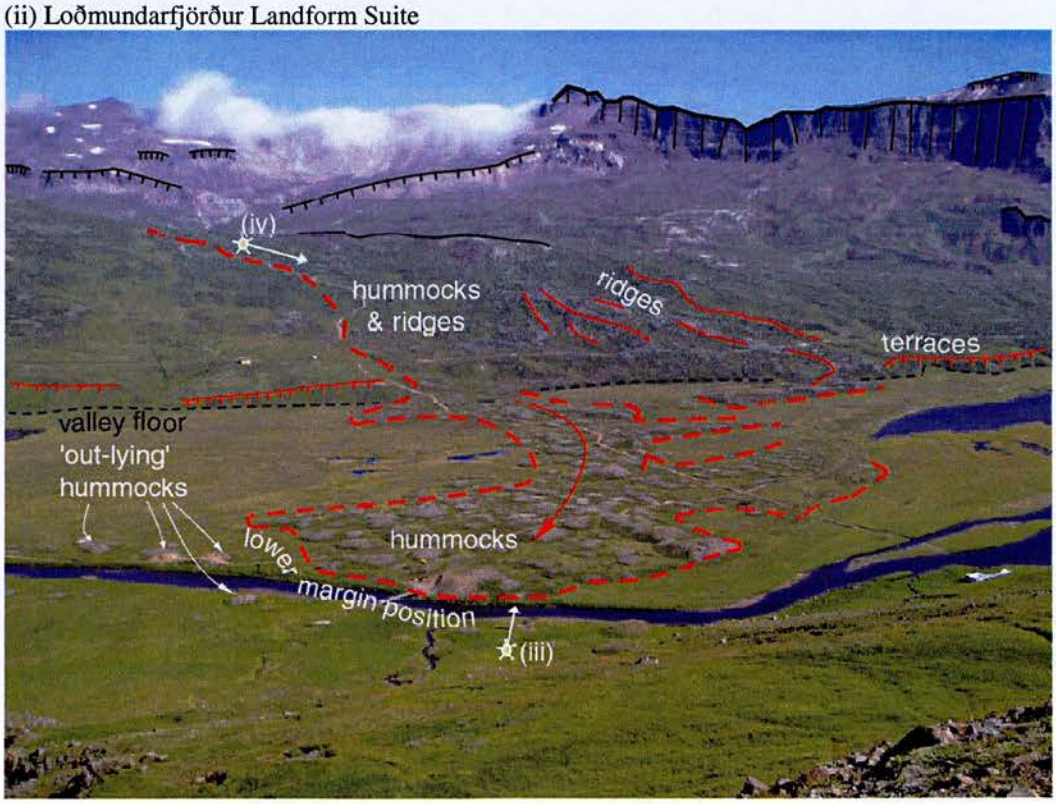

Figure 3.3-a (continued)

(iii)

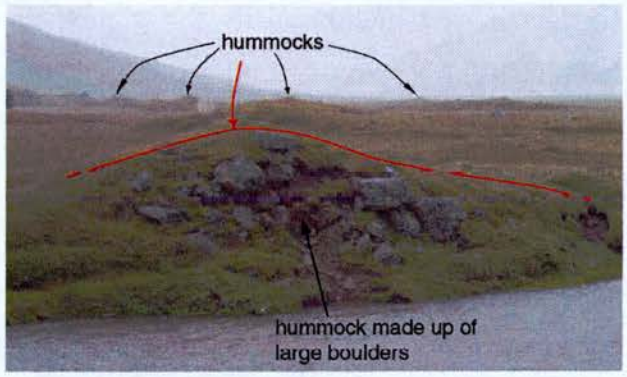

(iv)

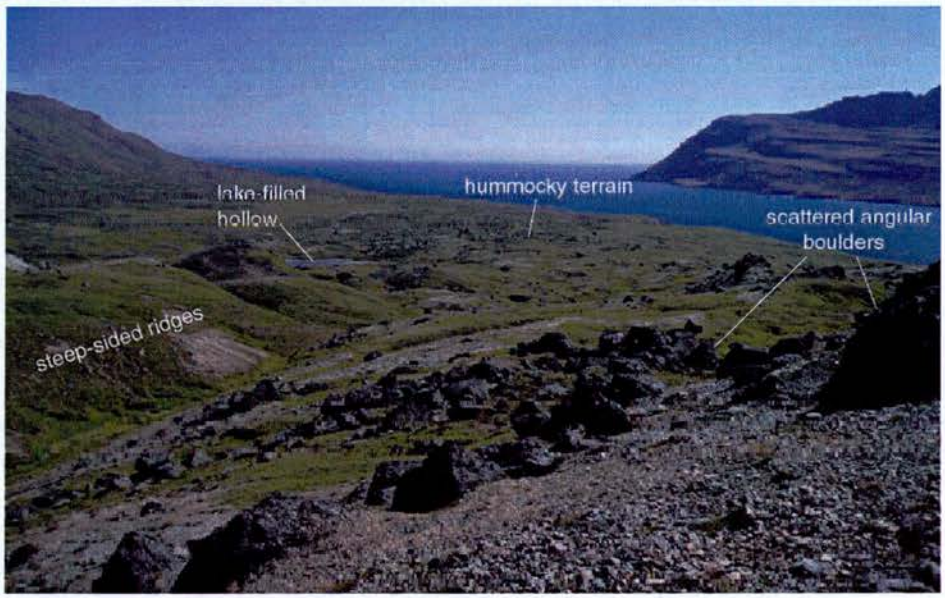

(v)

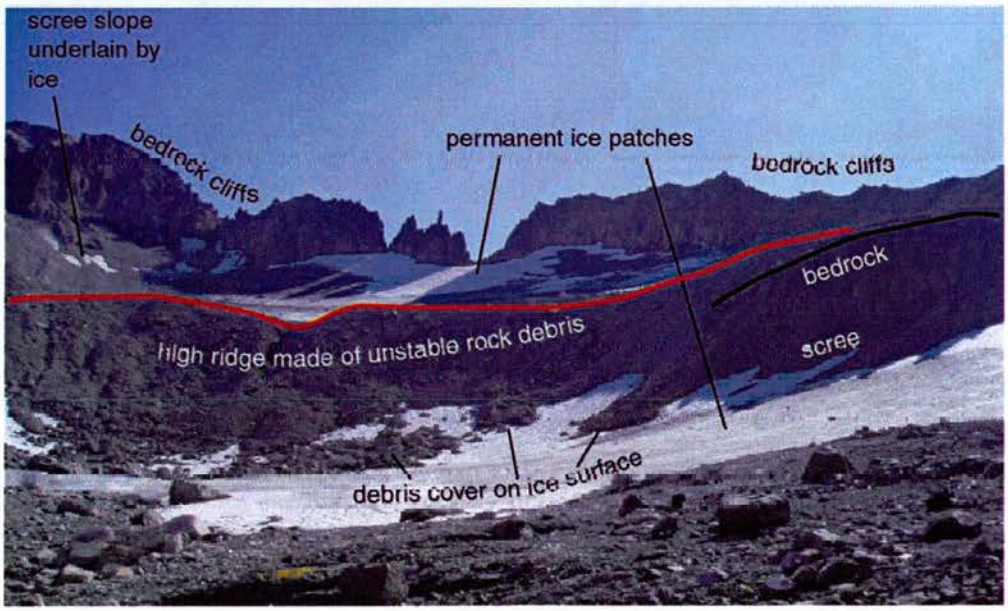

Loðmundarfjörður Landform Suite

A previously documented landform suite, thought to be a rock-slide deposit (**refs**), is found in Loðmundarfjörður, to the south of the field area. This set of landforms is shown in Figure 3.3-a (ii), and it can be seen that the overall shape of the suite, with a lobate snout and narrow upper, shares some morphological characteristics with other landform suites mapped in this project. However, the Loðmundarfjörður suite varies in some key ways. The most striking difference is in the material make-up and surface features of landform elements. These ridges and hummocks are composed of very large boulders, as shown in Figure 3.3-a (iii). It can be seen in Figure 3.3-a (iv) that the rock debris covers the surface of most of the landforms in the suite, a trait which is usually reserved for selected landform elements in the upper regions of other landform suites.

In terms of the morphology, the hummocky terrain that makes up the majority of the area of the suite displays less organized lineations or patterns than other suites. Lateral margins are not defined by longitudinal ridges. A greater proportion of the Loðmundarfjörður suite lies on the valley floor, beyond the break of slope, than on the valley side (shown in Figure 3.3-a (ii)), so that the terminus of the landform suite extends further across the valley floor than the terminus of other mapped suites.

Other parts of the Loðmundarfjörður valley

It can be seen from Figure 3.3-a (i), that the existence of two other sets of landforms is highlighted further east from the Loðmundarfjörður suite. These landform suites extend from the valley side, southwards towards the sea, where they terminate abruptly in terraces. They are made up of ridges and hummocks exhibiting more orientation than the Loðmundarfjörður suite.

To the west of the Loðmundarfjörður suite, the valleys of Miðdalur and Norðdalur are investigated. They were found to contain little geomorphology, with the steep valley sides largely dominated by continuous bedrock steps and terraces. However, near the summit of Miðfell (1024 m), an area containing permanent ice patches is

observed (the location of which is shown in Figure 3.3-a (i). These ice patches lie in a sheltered basin on the east- and north-facing sides of the Miðfell massif, and are shown in Figure 3.3-a (v). It can be seen that they occupy a debris-rich basin, with a high debris supply provided by the surrounding cliffs. Much of the ice is covered in loose debris which appears to have originated from scree slopes and debris ridges immediately above the ice. Similar ice patches are discovered around the Dyrfjöll massif, described below in 3.3.2.

3.3.2. Dyrfjöll/Jökuldalur

Figure 3.3-b: The location of the Dyrfjöll glaciers

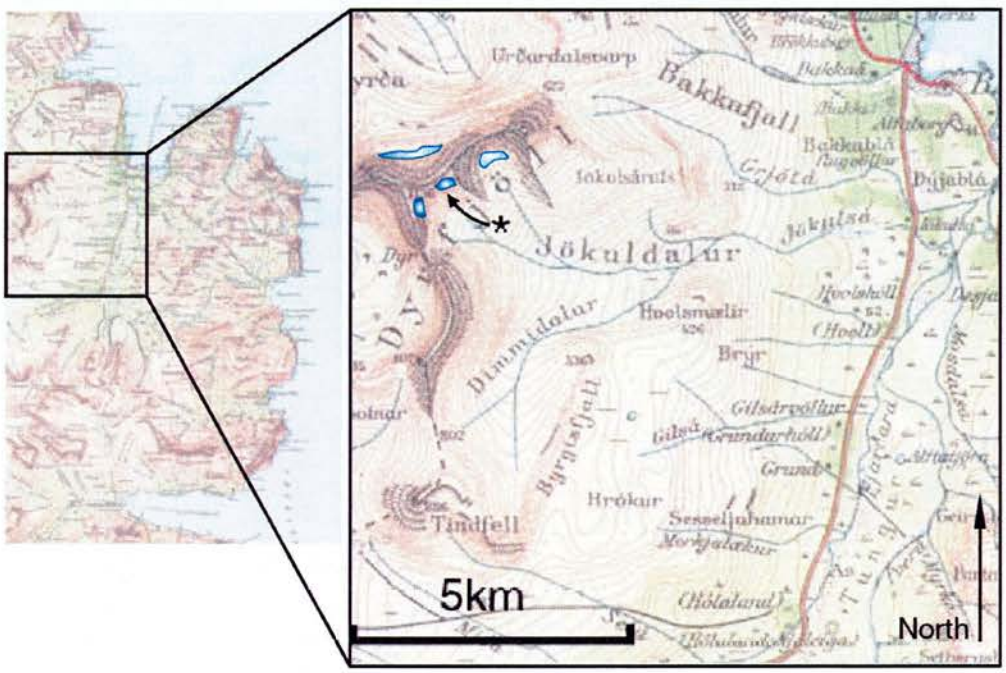

The blue patches represent approximate locations of currently active small glaciers/permanent ice patches, photographed in Figure 3.3-c (north-facing) and Figure 3.3-d (East-facing). One of these small glaciers is investigated in detail (highlighted by a "*").

The Dyrfjöll massif, one of the highest in the northern part of the eastern fjörds, is found immediately to the west of the main field area, and is made up of several peaks reaching up to 1136 m. Dyrfjöll supports some of the region's very few currently active (though limited) glacial systems, which consist of small ice patches in north and east-facing cliff-backed corries.

Figure 3.3-c: North-facing slopes of Dyrfjöll massif

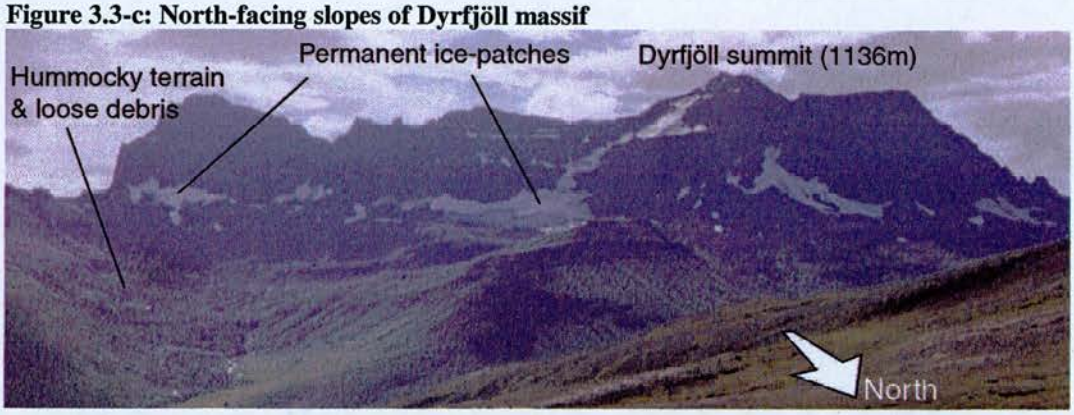

Figure 3.3-d: East facing slopes of Dyrfjöll massif in (i) mid-June, and (ii) late August

(i)

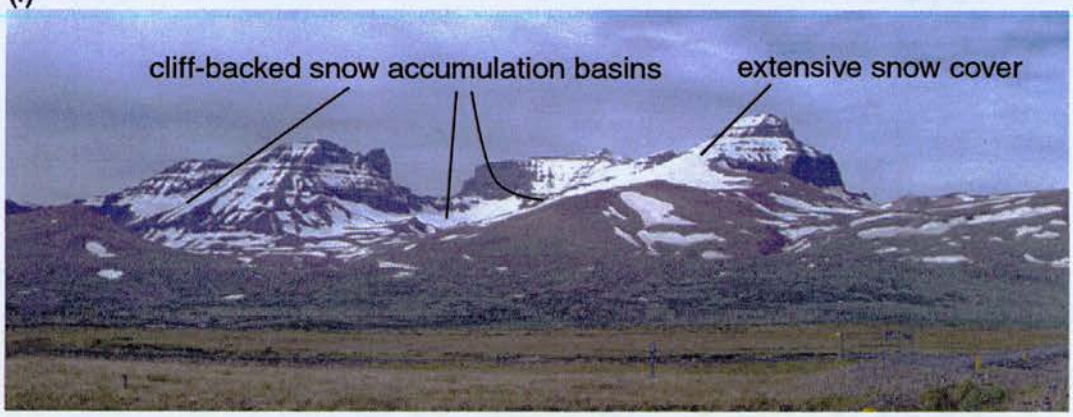

(ii)

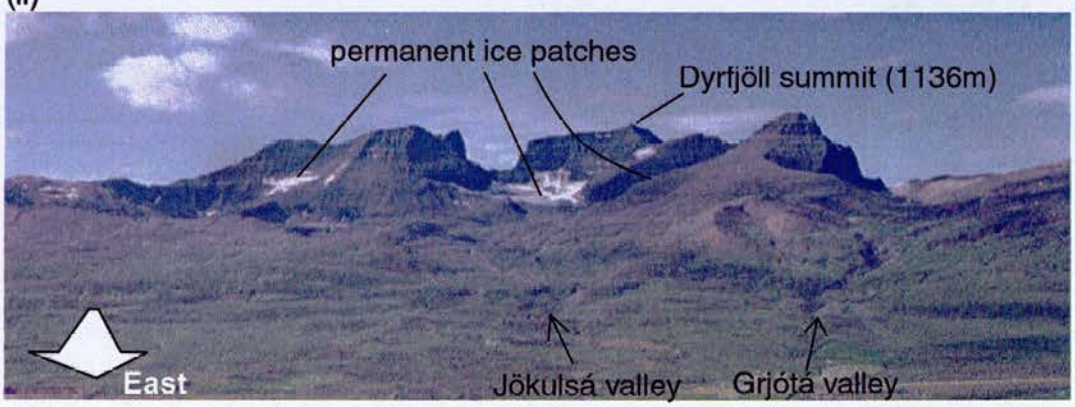

Figure 3.3-c and Figure 3.3-d illustrate the extent of permanent ice on the Dyrfjöll massif, the main areas of which are marked on the map in Figure 3.3-a. Identification of ice which is permanent all year round is undertaken by observing its extent in late August, when the melt from the previous winter will have completed, and the accumulation of new snow has not yet occurred. In both field seasons of 2003 and 2004, visible ice cover on the Dyrfjöll massif was observed throughout the

summer. The differences between early and late summer snow and ice cover is clearly shown in the observable variations between Figure 3.3-d (i) and (ii), which show the massif in June and August respectively.

Figure 3.3-e: Example of one of the small Dyrfjöll glaciers (in late-August)

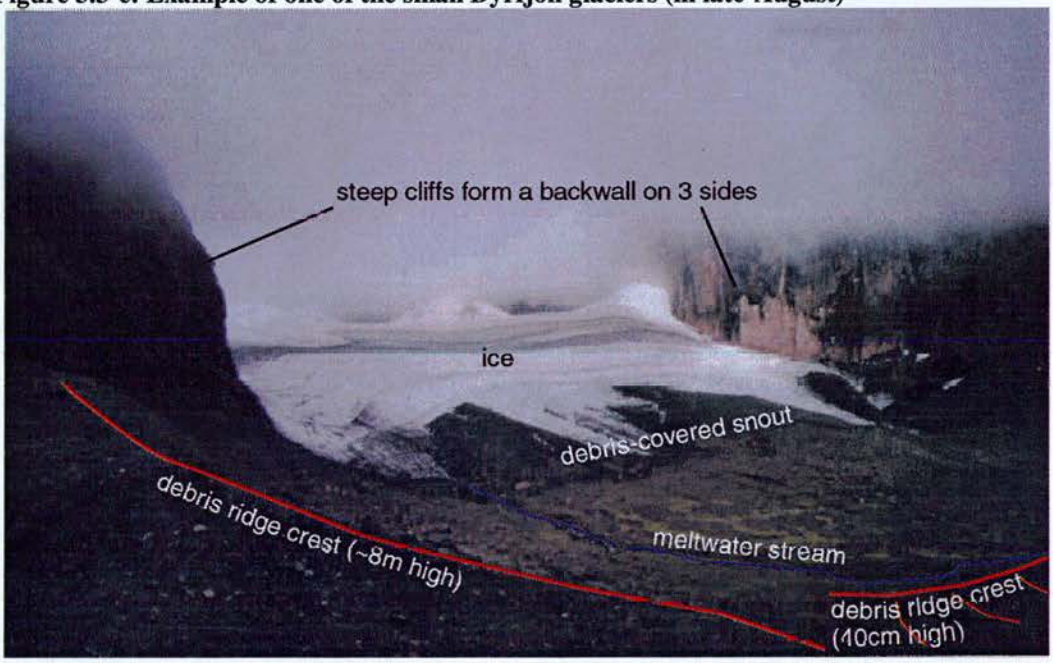

Figure 3.3-e shows the ice in late-August, prior to new snow accumulation. The ice is approximately 400m wide. The exact longitudinal length is less clear because the snout is debris-covered, and there is a gradual transistion from clean ice to debris-covered ice, which becomes ice-cored debris mounds. The clean ice extends about 200m from the cliffs behind.

One of the permanent ice patches is assessed in detail, and is shown in Figure 3.3-e above. As can be seen, it is situated in a well-constrained cliff-backed corrie (high cliffs surround the ice at the back, though this is obscured by cloud in Figure 3.3-e). Beyond the snout of the ice, a series of arcuate ridges are found, two of which are illustrated in Figure 3.3-e. The first is a low ridge rising only around 0.4 m, made of loose debris. The second is a much higher ridge with steep sides, also made of loose debris. At least five other clear ridge levels are visible running roughly parallel to these two, the stability of which increases with increased distance from the ice. Further down the Jökuldalur (the valley of the Jökulsá river, the location of which is highlighted in Figure 3.3-d (ii)), the ridges associated with this ice patch merge with another set of ridges which extend up-slope to the ice patch in the adjoining corrie.

Figure 3.3-f: The lower Jökuldalur valley

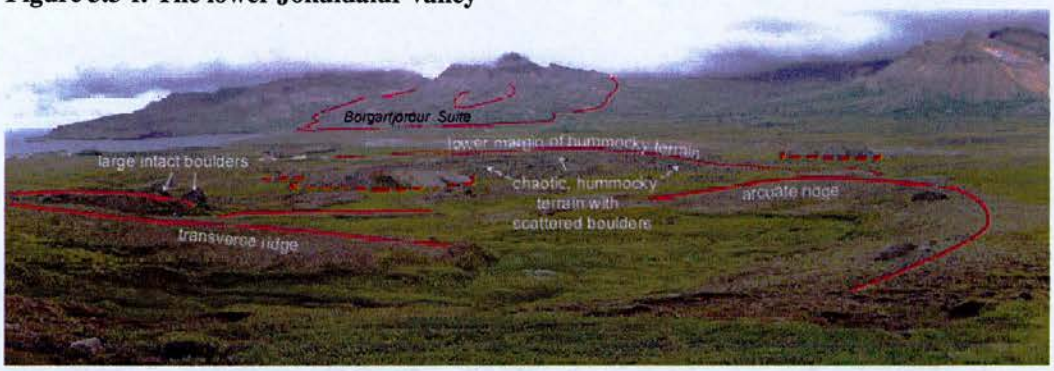

Figure 3.3-g: Jökuldalur geomorphology

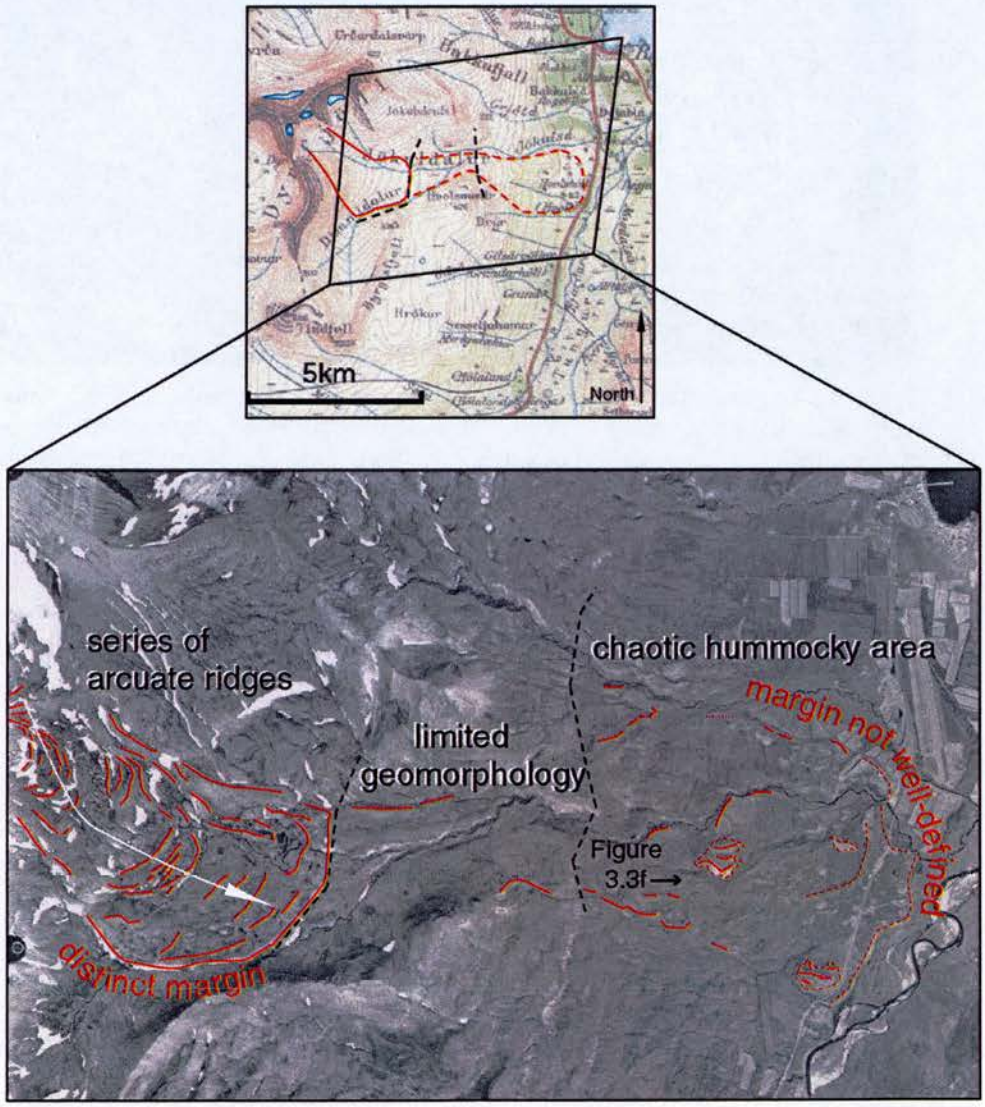

A series of roughly parallel arcuate and transverse ridges are found to continue all the way down Jökuldalur to an altitude of around 420m, where a clear terminal ridge is visible (see Figure 3.3-g). Beyond this point, towards the foot of the valley where Jökuldalur meets the main Borgarfjörður valley, landforms are sparser, and the valley floor is narrow between two bedrock hills. Beyond these bedrock constraints, more landforms are visible widening towards the base. Figure 3.3-f shows a view looking eastwards from this point on the lower slopes of Jökuldalur (the Borgarfjörður Suite is visible on the opposite valley side). Some arcuate and transverse ridges are found on these lower slopes, as shown in Figure 3.3-f, but the area is mostly dominated by chaotic hummocky terrain, with a continuous coverage of large scattered boulders. This chaotic hummocky terrain is clearly visible in Figure 3.3-g, and its lower margins are not clearly defined by a terminal ridge.

The geomorphology of the Dyrfjöll massif and Jökuldalur is characteristically different from landform suites mapped in 3.2. Primarily this is because of the existence of limited but currently active glaciation in the high corries of Dyrfjöll. The suite of arcuate ridges which descend from these high corries share a generally lobate shape with the previously mapped landform suites, but since this Jökuldalur suite is made up almost entirely of arcuate ridges, it is distinct. Below the clear margin of this 'primary' suite is a further suite of landforms covering a roughly lobate-shaped area, though exhibiting no clear marginal ridge. Its chaotic debris-covered surface and overall shape is similar to that of the Loðmundarfjörður suite described in 3.3.1.

3.4. Key Landform Types and Characteristics

Field observations of the geomorphology of the Borgarfjörður region of northeast Iceland reveal the existence of a number of distinctive landform suites sharing morphological characteristics. An idealised landform suite is presented in Figure 3.4-a, to summarize the morphology and topographic setting of the main landform units observed in the field.

Figure 3.4-a: Idealised landform suite

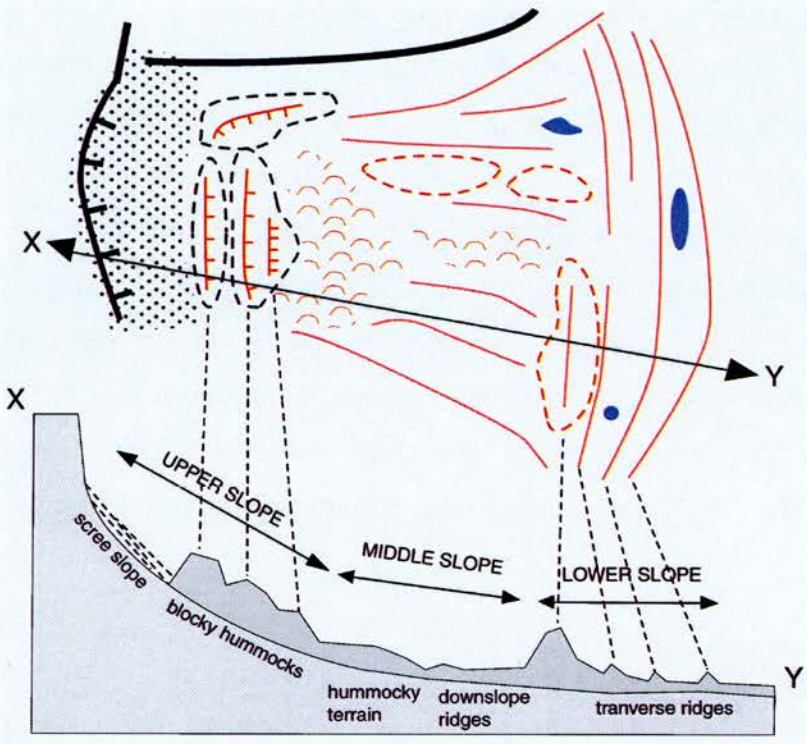

Figure 3.4-a represents an idealised landform suite which is developed based on the observed characteristics of the landform suites mapped and described in 3.2.

The landform suites are all generally lobate in overall form, originating on relatively steep slopes, and widening towards the base as the slope gets gentler. The suites are generally backed by cliffs and/or steep scree slopes originating from bedrock peaks. The upper parts of the suite are often skirted laterally by bedrock ridges extending from the main ridge tops behind. Lower margins are well-defined by either transverse and arcuit ridges, or a terrace edge in arcuit form. The main body of the suites contain units of characteristic landform elements, generally associated with the progressively gentler upper, middle and lower slopes, highlighted in Figure 3.4-a.

Within each landform suite there is geomorphic diversity, determined by the aerial extent of each landform unit, and by the relationship between the landforms and the locally specific underlying and surrounding topography and geology. In general, the upper slopes are characterized by *blocky hummocks* and *terraces*. Middle slopes represent a transition from *hummocky terrain* to *longitudinal (downslope) ridges.*

Transverse and *arcuit ridges* are generally found on the lower slopes. Observations are made here on the characteristics of these four main landform units, in terms of their consistency across the landscape, their morphology, and their topographic and lithological associations. Records of material composition rely on partial information limited by the existence and accessibility of exposed sections, and inferences made based on surface features such as rock outcrops, and general morphology. The composition of landform elements is seen to vary more with local geological factors than according to the type of landform. Where surrounding bedrock is mostly rhyolitic, the landforms tend to be composed of small angular rock fragments, which create a smooth appearance. Conversely, where the source area is basaltic, landforms exhibit a rougher surface, containing more intact boulders and large rocks.

3.4.1. 'Blocky' hummocks/terraces

Surrounding Topography

'Blocky' landform elements are generally found in groups at the uppermost part of the landform suites, backed by either cliffs or very steep scree slopes, often with a clear 'scar' surface. For example, Kjólsvík and Brúnavík 1 display this well. The overall slope angle underlying these elements tends to be relatively steep. Such deposits are not found to extend beyond the base of a slope, but terminate at the valley floor, if not before.

Morphology

The upper part of the blocky landform unit is typically made up of a series of ridges and terraces mostly oriented across the slope, or in line with the angle of the surrounding scar faces and scree slopes. The upper ridge closest to the scar-slope has a very steep back, and is found to be up to 30 metres in height. Due to the unstable nature of the slip-slopes, the hollow formed between the uppermost ridge and the slip slope becomes filled with frost-shattered debris and fallen boulders. Therefore the back ridges may in fact be of greater height than is observed. Subsequent lower ridges are steep on the down-slope side but less so on the up-slope

side, often forming terrace-like steps down the slope. Lower in the deposit, the ridges become more chaotic in their orientation patterns, and the surface is often more characterised by hummocky rather than ridge-like terrain. Ridges and hummocks reach heights of around 20 metres. Longitudinal ridges are common in the lower part. A clear margin can be seen where this type of deposit ceases, as there is a steep drop and often a distinct cross-slope oriented ridge or terrace.

There are also a number of smaller-scale 'blocky' units consisting of a single terrace-like hummock containing intact bedrock, and backed by a bedrock terrace and short scar-slope behind. These small units are found in Brúnavík valley surrounding the long bedrock terrace which joins opposite valley sides at the western end.

Composition

These landforms tend to contain very large blocks of heavily frost-shattered but intact bedrock of sizes ranging from 5-15 metres. These blocks are from the basaltic bedrock, and appear deeply imbedded in the ridges, subject to current frost-action resulting in *in situ* fracturing. Aside from these boulders, ridges are made up of angular and sub-angular rhyolitic and basaltic rock fragments (<30 cm) in a silt or clay matrix. Due to the intensity of frost activity, it is hard to tell if the whole deposit has this composition, or if this only represents a very thick covering of frost-shattered detritus which hides the original nature of the materials.

3.4.2. Hummocks

Surrounding topography

Hummocky terrain is generally found on the middle slopes, often associated with units of longitudinal ridge.

Morphology

Hummocky terrain is the most spatially variable landform type identified in the field, in terms of the size of individual hummocks, their relief, their orientation and their surface features. The characteristics of hummocky terrain depend on the location it

is found within the landform suite. When it is found in the upper reaches of a landform suite, it tends to consist of high relief, steep-sided landform elements, which may have some lineations. These landforms have much debris cover, such as is exhibited in the ridges in the upper part of the Svínavík landform suite, shown in Figure 3.2-1 (ii). In lower parts of landform suites the hummocks tend to be of lower relief, with less continuous debris cover, and a smoother surface.

Composition

The composition of the hummocky terrain is indicated by the surface debris cover and morphology. Where a significant amount of the surface is debris-covered and rough, the hummocks are likely to contain large rock fragments. Smoother, lower relief hummocks contain, on investigation, small angular rock fragments.

3.4.3. Longitudinal ridges

Surrounding Topography

Long ridges oriented longitudinally occur in groups, mostly in the upper to middle part of the landform suites, and often make up much of the body of the suite (Brúnavík 2, Borgarfjörður 1). When the ridges occur individually or in small groups, they tend to occur on steep slopes, but in large groups they are found on shallower gradients.

Morphology

These ridges tend to lineate outwards down-slope in a fan shape, mostly following the orientation of adjoining bedrock ridges. Within the suite the ridges usually rise up to about two metres in height, and have subdued morphology. However, the outer ridges which form the lateral margins of the suites usually drop around ten metres steeply on the outside edge. Where the longitudinal ridges form the terminal margin of the suite, they drop steeply forming an arcuit-shaped terrace. The longitudinal ridges often adjoin a transverse ridge in a smooth curve. There are some small-scale examples of this type of morphological unit, which lie on steep slopes, but these are not steep-fronted or with marginal ridges. Their morphology is less well-defined.

Composition

Ridge tops often maintain scattered boulders and rocks. Some of the ridges which form the margins of the deposits are bedrock ridges. The composition of ridges within the suite is a mixture of matrix-supported rhyolitic and basaltic rocks. The matrix often has a high proportion of clay in the upper layers. Rock fragments are generally very angular.

3.4.4. Transverse and arcuit ridges

Surrounding topography

Transverse ridges occur mostly in the lower parts of the deposits, on the relatively flat land beyond the base of the slope. They generally form the terminal margins of landform suites.

Morphology

There are two types of transverse ridge, one with subdued relief, rising up to two metres from the surrounding topography to wide flat tops. In the low-lying areas they take an arcuit form and several (usually dissected) ridges lie parallel to each other moving up-slope (e.g. Kjólsvík 1, and Víkurá 2). Lake-filled hollows are found between most of these ridge lines. The arcuit transverse ridges often link into longitudinal ridges, forming clear edges (Borgarfjörður 1). The other type of transverse ridge is more steep-sided, higher, and with a clearer ridge crest. These tend to occur on the steeper slopes above the valley floor and are more associated with longitudinal ridges and hummocks (e.g. lower Víkurá 1, upper Borgarfjörður 1). Again the ridges form parallel stacks upslope, often taking on the appearance of a series of terrace levels. Small hollows are found between these ridge levels but also on the crests of them.

Composition

The composition of these ridges is much the same as that of the longitudinal ridges, with some scattered boulders on the ridge tops and *in situ* shattered rock.

3.5. Summary

It has been seen that the Borgarfjörður region contains a series of landform suites which share characteristics related to the shape and topographic setting of the suites as a whole, and the morphology and relative location of distinct landform units. Characteristic landform units can be identified throughout the field area, with each landform unit appearing to have a preferred topographic setting. Whilst general associations can be drawn between distinct landform suites based on morphological similarity, the possibility of genetic links between these landform suites cannot be proved without further investigation, given the disparities between suites when observed in detail. These disparities relate to the variable proportion of different landform types within each suite, and the characteristics of the landform suite as a whole. Suites vary a great deal in overall area, and whilst the shape of the suites is generally lobate, the extent of this is spatially variable. In some cases, such as the Kjólsvík suite, the width of the suite is much greater than the length. In contrast, suites such as the Mosdalur suite are significantly longer than they are wide. The size of the source areas in which the suites originate can vary from a well-constrained basin (e.g. Brúnavík 1), to a steep scree slope with no obvious accumulation zone (e.g. Víkurá 2).

The morphological information presented in Chapter 3 is further developed in Chapter 4, which assesses the value of this geomorphic evidence in relation to local topographic and lithological characteristics, as a means of explaining the observed variations between landform suites.

4 Value of Geomorphic Evidence and significance of its spatial distribution

4.1. Introduction

As stated in Chapter 2, the research aims to use geomorphic evidence as an indicator of past geomorphic (particularly glacial) activity, to reconstruct the nature of response to the 8.2ka cooling event. Chapter 3 identified the existence of thirteen landform suites indicative of geomorphic activity, which constitute the "geomorphic evidence" referred to in the remaining chapter. Chapter 4 aims to determine the value of this geomorphic evidence for climatic reconstruction. "Geomorphic activity" is defined here as some process of debris transport involving re-distribution of debris. This debris re-distribution may have been enabled or enhanced by water, ice or gravity, and the specific transportation processes may have involved a variety of mass-movement activities. The research aims necessitate defining the way that climate controls such processes. However, both climatic and non-climatic factors influence the extent and nature of geomorphic activity, resulting in a geomorphic record which is potentially de-coupled from climate. While the existence of ice, and to a lesser extent water, is inextricably associated with climate, the way these mediums behave and interact with debris is influenced by topographic and lithological factors.

The amount of non-climatic influence on geomorphic evidence must therefore be quantified, before a climate signal can be derived. Through detailed assessment of the extent of topographic and lithological control on landform development, the potential for reconstructing climatic conditions based on the available geomorphic evidence is evaluated in this chapter. From this discussion, it will be possible to draw conclusions regarding the nature and extent of regional geomorphic response mechanisms to climatic change, and thus inform modelling work.

Hypotheses Testing

The purpose of the research is to test the Key Hypotheses, highlighted in Figure 4.1 a, that:

The observed landform suites represent geomorphic (debris transport) processes which were triggered by the 8.2ka climatic cooling event.

It has been seen in Chapter 3, that evidence for such geomorphic activity does not occur in all drainage basins, and there are characteristic variations in the morphology and size of indicator landform suites. The key question to address is whether these disparities indicate that different types of systems (i.e. glacier/debris flow/landslide) created the landforms, and if so whether this is still compatible with the Key Hypothesis. If all landforms were formed by the same type of system, the reasons for the diversity in characteristics must be assessed, and the compatibility with the Key Hypothesis addressed. With this in mind, a series of 'secondary' hypotheses are developed (illustrated in Figure 4.1-a) to explain the spatial variation in geomorphic evidence. All these hypotheses have distinct implications with regards to testing the key hypothesis set out above. The premise forming the basis of these secondary hypotheses, is that if the mapped suites of landforms do indicate regional geomorphic response to a single climate forcing (the 8.2ka event), then variations in morphology and preservation must be explainable by the influence of non-climatic factors (i.e. topographic and lithological control). If disparities in the nature of geomorphic evidence cannot be explained by such non-climatic factors, then the landform suites cannot represent a regional response to a single climate event. The following chapter attempts to evaluate the Secondary Hypotheses shown in Figure 4.1-a, that is, to test which is the most compatible with the geomorphic evidence, and therefore gives the best indication of the validity of the Key Hypothesis.

Figure 4.1-a: Explaining variations in landform characteristics

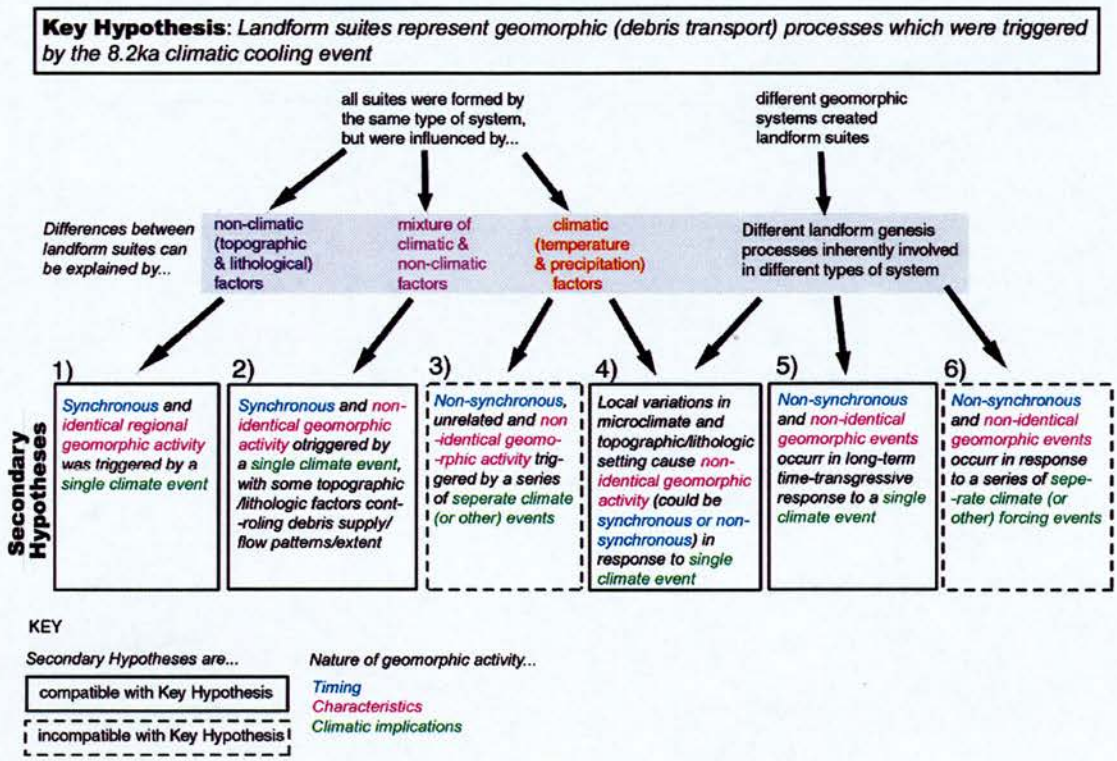

Figure 4.1-a first presents the "Key Hypothesis" to be tested, which is designed to address the principle aim of the research by assessing the geomorphic evidence for the 8.2ka event. The "Secondary Hypotheses" at the bottom of the Figure offer a series of possible events (which vary in their synchrony, their geomorphic characteristics, and their associated climatic implications), all of which could theoretically result in the formation of the observed landform suites with their spatially variable characteristics. Not all of these Secondary Hypotheses are compatible with the Key Hypothesis, so testing them will promote interpretation of the validity of the Key Hypothesis.

To test the Secondary Hypotheses, it is necessary to define what factors are responsible for creating the observed spatial distribution and characteristics of the geomorphic evidence. Figure 4.1-a summarises the types of factors which may influence the character of the geomorphic evidence (grey box), and highlights which secondary Hypotheses are compatible with each.

If all landform suites were generated by the same type of system, such as glaciers, other influencing factors must be responsible for the disparities between suite characteristics. These factors could be climatic or non-climatic. If climatic factors are shown to be the main influence on geomorphic characteristics, then the geomorphology displays a clear climatic signal, and multiple landform suites with different characteristics must represent multiple climate triggering events. Therefore, variations between landform suite extent and characteristics are not compatible with there being a regional response to a single climate event at 8.2ka. If non-climatic factors are shown to be the main influence on geomorphology, then this allows for the existence of de-coupling between process and climate, which allows for characteristic variations in the geomorphic signature of a single climate event. Though the existence of de-coupling does not prove categorically that the landforms *do* share a common trigger, it means that the observed spatially variable landforms are theoretically compatible with the Key Hypothesis as they could be related to a single climatic event. Alternatively it is possible that the landform suites have variable characteristics because they were formed by different types of debris transport system.

Figure 4.1-b: Explaining spatial variation in nature of geomorphic evidence

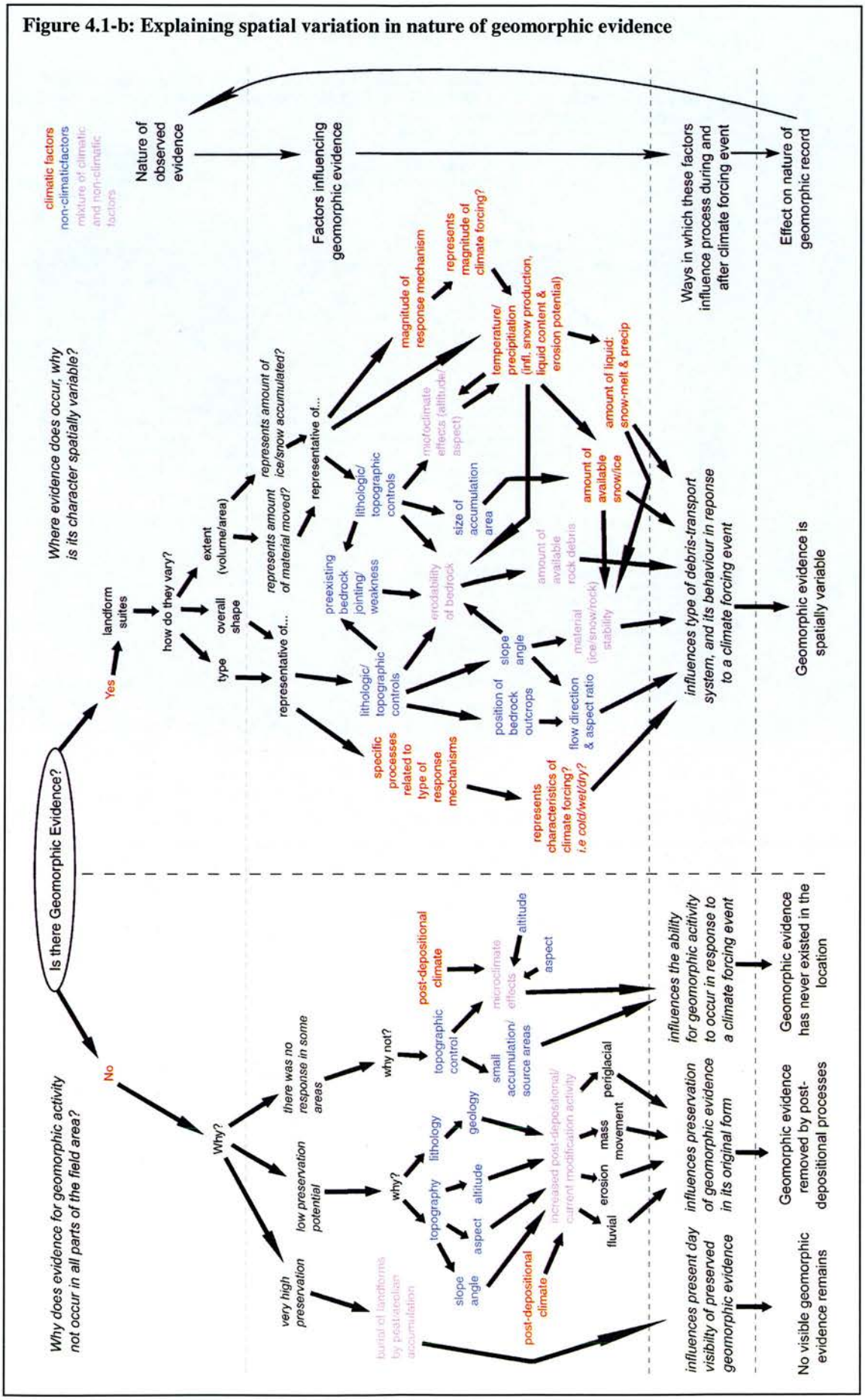

In Figure 4.1-b, the climatic and non-climatic influencing factors mentioned in Figure 4.1-a are discussed in detail. An attempt is made to outline the factors which influence the nature of geomorphic activity and the existence and nature of geomorphic evidence, with a view to testing the Secondary Hypotheses set out in Figure 4.1-a. Figure 4.1-b is set out in two parts, to tackle two key questions relating to the uniformity of geomorphic evidence across the field area. These questions are outlined below:

- Why does evidence for geomorphic activity not occur in all parts of the field area?
- Where evidence does occur, why is its character spatially variable?

The first question is addressed on the left-hand side of Figure 4.1-b, where conflicting hypotheses are presented for why geomorphic evidence does not occur in some areas (explained in 4.2). The second question addresses why landform morphology and size varies spatially (right hand side of Figure 4.1-b), and presents a summary of possible explanations for these characteristic differences (explained in 4.3). The influencing factors considered in Figure 4.1-b are colour-coded to differentiate between factors related to climate and those non-climatic. Through this analysis, an understanding is gained of the extent that lithology and topography influence the geomorphic record, and thus "distort" the climate signal. This will inform hypotheses testing.

4.2. Explaining the existence and non-existence of geomorphic evidence: Preservation Potential

This section discusses the first key question tackled by Figure 4.1-b in more detail, in an attempt to explain the lack of geomorphic evidence (i.e. the lack of landforms indicative of significant debris-transport activity) in certain parts of the field area. If the lack of evidence for geomorphic activity in certain basins represent a real lack of "response", this requires explanation relating to the individual characteristics of each basin. Alternatively, the lack of evidence may represent the extent of post-depositional removal, reworking, or burial of geomorphic evidence by later processes

in certain areas, which needs to be quantified in terms of individual basin preservation potential.

Through detailed analysis of basin characteristics, we aim to test two hypotheses (based on those shown in Figure 4.1-b) explaining the distribution of landform suites in the field area:

- The current existence and distribution of observable geomorphic evidence is a true representation of the areas in which response did and did not occur.
- The current existence of observable geomorphic evidence is directly related to the preservation potential of drainage basins on which landforms were originally created, and thus does not indicate all the basins in which response actually occurred.

Defining "Preservation Potential"

To test the conflicting hypotheses set out above, the study assesses the ability of a basin and related slopes to *preserve* intact landforms since genesis. Landform preservation is defined as a measure of the extent to which landforms are "visible" at present, in their original form. Landforms may be visibly and actually removed by erosion, or accumulation may cause the original landform to be well-preserved beneath layers of depositional materials, thus being visibly (but not actually) removed.

Figure 4.2-a: Preservation and Burial of Landforms

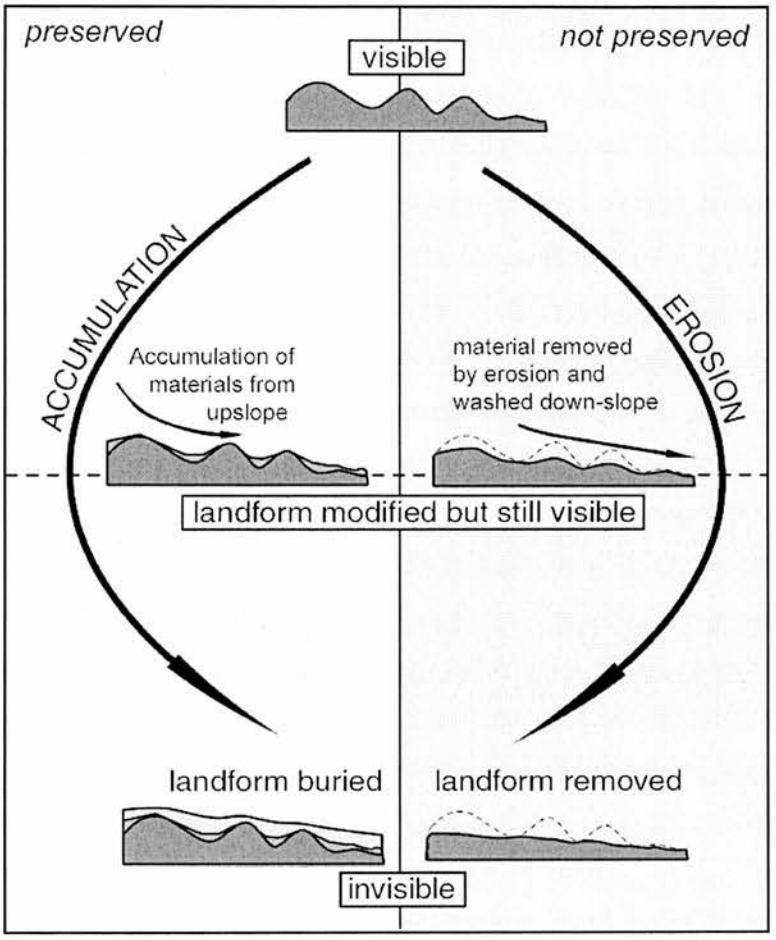

Figure 4.2-a illustrates the contrasting processes by which geomorphic evidence may be effectively "erased" from the landscape. On the left, the original landform is well preserved, but accumulation of materials such as peat and aeolian soil reduces the relief of the landform, gradually rendering it invisible to empirical observation. This accumulation may be a result of erosion, transportation and deposition of materials from up-slope. On the right, the landform is subject to erosion and thus the original form is modified and eventually removed, leaving observable morphology much like that formed by accumulation. Materials are re-worked and transported down-slope by various slope processes, eventually being re-deposited elsewhere.

The processes illustrated in Figure 4.2-a happen in combination, with a single set of landforms being subject to phases of erosion and deposition, often simultaneously. Given the nature of slope processes, erosion, modification and removal of landforms is most likely to occur on the steeper upper slopes of a landscape, where more active erosion can take place. Preservation but burial of landforms is most likely on the lower slopes and valley floors, as a result of the afore-mentioned erosive processes, or other more catastrophic mass-movement processes such as landslides, occurring up-slope, transporting materials down-slope to accumulate on top of the lower landforms. These processes of erosion, transportation and deposition are directly influenced by slope angle.

To test the extent of landform burial, a proxy for accumulation rates is available as part of a tephrochronological analysis (explained fully in Chapter 5), which provides time-transgressive marker horizons by which to date accumulated layers of material. By calculating the depth of material above a tephra layer of known age it is possible to estimate the accumulation rates in the time elapsing since tephra deposition. Using this method, it is revealed that accumulation rates in the field area are very low, with the highest rates at around three metres of accumulation in the last 10,000 years. It is therefore concluded, that the lack of visible geomorphic evidence in certain areas is most likely a result of erosion processes rather than burial. With such low accumulation rates, it is unlikely that whole landforms would be covered and become undetectable. "Preservation potential" is thus defined for this study as the likelihood for a landform to remain visible for observation to the present day.

Defining Geomorphic "Evidence"

Geomorphic "evidence" is used from this point on as a term to describe all visible occurrences of landforms which are associated with the landform suites mapped and explained in Chapter 3. The landform suites indicate the debris transport systems which may have been active in response to the 8.2ka event, and which therefore form the key evidence required for this research.

4.2.1. Topographic controls on preservation at a landscape scale

This section estimates preservation potential of the field area as a whole based on the potential for erosive processes to occur which may have removed visible geomorphic evidence. Slope angle is utilized as a proxy for this type of preservation potential because the amount of landform- and slope-modification work done by geomorphic systems such as fluvial, periglacial, paraglacial and mass movement is closely linked to potential energy input to the system, and thus slope gradient. The topographic characteristics of the field area are categorized into three types of slope. This categorisation was chosen because when the field area was split into these slope angle units, it best represented key slope areas: valley floor; lower slopes; upper slopes; steep scree/cliffs; and mountain tops.

1. Gentle slopes (<14°)

These areas are likely to contain the best-preserved landforms. Low relief results in subdued fluvial, periglacial, paraglacial and mass movement activity, which limits the extent of processes potentially modifying the landforms. Current river channels and associated flood plains are excluded as they are subject to current or recent erosive activity.

2. Steep slopes (14°-28°)

Increased slope angles and related increased relief encourages more active fluvial, periglacial, paraglacial and mass movement processes, which result in low preservation potential of landforms. Any remnants of landforms remaining are likely to be significantly modified and less well-defined than those on gentle slopes.

3. Extreme slopes (>28°)

Extreme slopes in the field area are either loose scree slopes which are continuously active or near-vertical cliffs and rock outcrops. Preservation potential is effectively zero.

Figure 4.2-b: Preservation Potential of Geomorphic record with slope angle

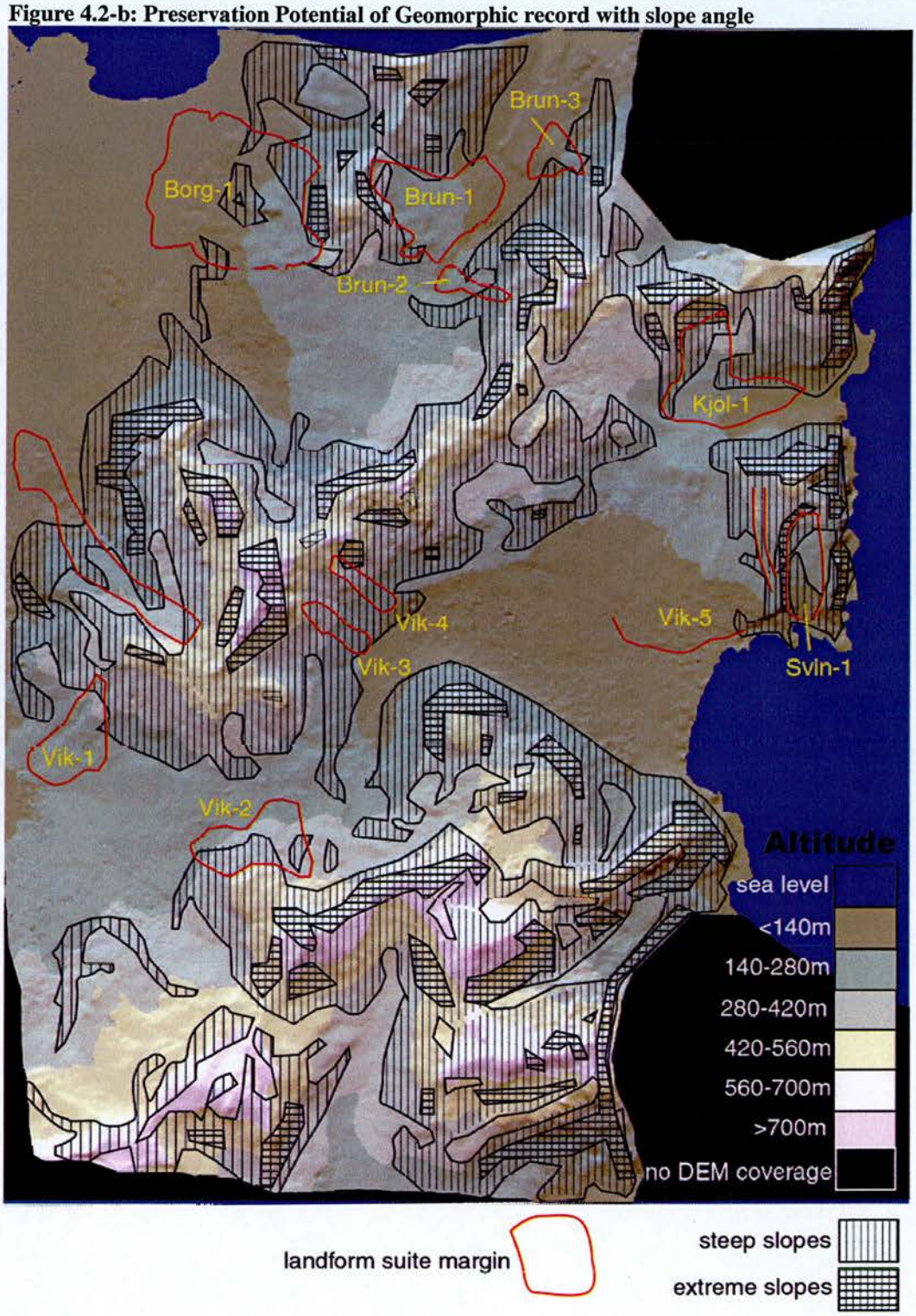

Figure 4.2-b shows the expected preservation potential of the field area based on slope angle, and shows the position of landform suites indicative of geomorphic activity and putative response to the 8.2ka event. It can be seen that most areas containing landform suites maintain slope angles of less than 14 degrees (gentle slopes with high preservation potential).

It is clearly evident from Figure 4.2 b that those drainage basins containing geomorphic evidence are those on the shallower slopes, indicating a relationship between slope angle and preservation potential. The source area of the deposits is often on steeper slopes (e.g. *Brun-2*, *Kjol-1, Vik-2*), but with the main body on gentler slopes. The only exceptions to this general pattern are the landform suites *Vik-3* and *Vik-4*, which appear to be fully on the steeper slope angle (14-28°). It is significant that, as discussed in Chapter 3 these particular landform suites are less well-defined than the other suites, containing a high proportion of land within their margins classified as containing "no significant relief". This leads to the suggestion that the slopes on which the landform suites *Vik-3* and *Vik-4* were deposited are of a gradient too steep to maintain all the original geomorphic evidence, as these slopes have a low preservation potential. Figure 4.3-j shows the slope angle make-up of each landform suite, and it can be seen that *Vik-3* and *Vik-4* do have a significantly higher proportion of surface on steeper slopes.

4.2.2. Topographic controls on preservation at drainage basin scale

The significance of the spatial distribution of landform suites in the field area is assessed in more detail by addressing the preservation potential for geomorphic evidence in each drainage basin, related to individual basin characteristics (slope angle, aspect and altitudinal range). The field area is split into basins, the locations of which are illustrated in Figure 4.2-b, which are analysed individually for comparison between those with geomorphic evidence and those without.

Slope Angle

Slope angle has been shown to be a significant factor in preservation at a landscape scale, and here we approach it in more detail.

Figure 4.2-c: Relationship between extent of geomorphic evidence in each drainage basin, and slope angle

(i)

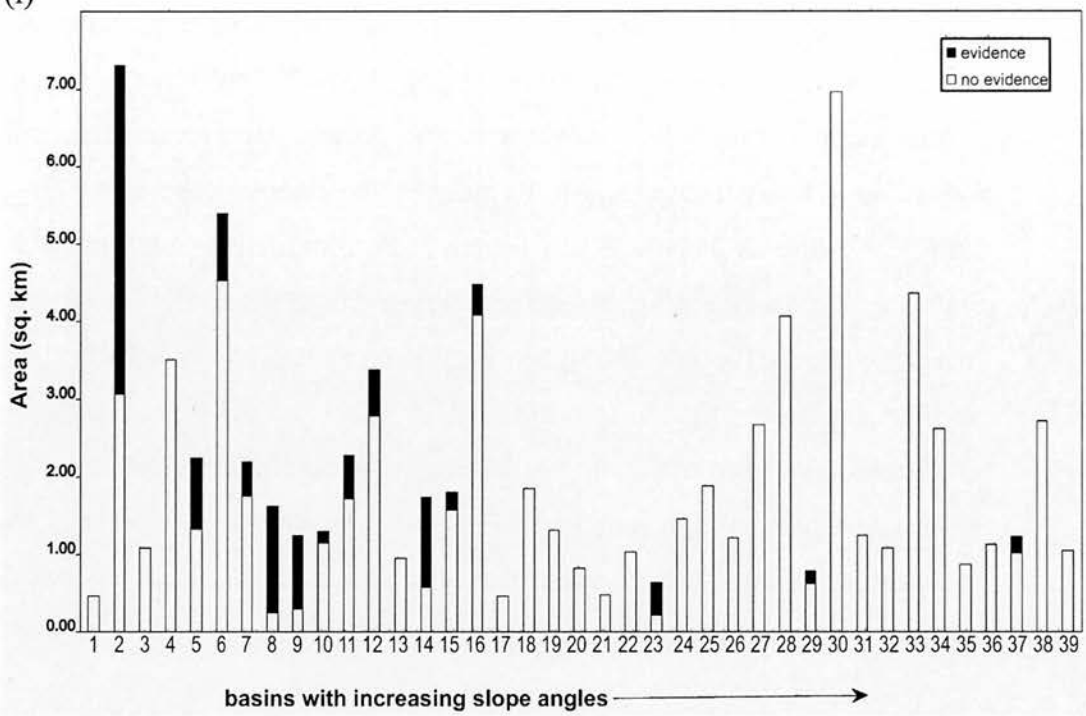

(ii)

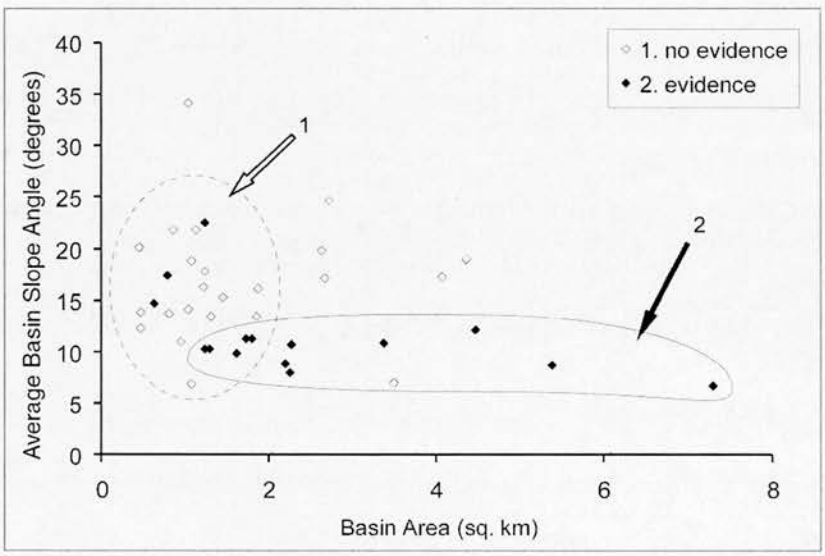

Figure 4.2-c (i) arranges drainage basins in order of increasing average slope angle, also displaying the plan area of each basin, and the proportion of this area which contains landforms associated with a mapped landform suite. Basins containing some evidence are largely restricted to gentler slope angles. Figure 4.2-c (ii) plots the average slope against the plan area of each drainage basin, differentiating between those basins which contain geomorphic evidence and those which do not. Two distinct groups are evident. Group (1) is a clustering of points representing basins with small areas, and slope angles which are generally steeper, and of which most contain no geomorphic evidence. Group (2) represents a group of basins with average slopes of around 10° and larger plan areas, most of which do contain geomorphic evidence.

Figure 4.2-c (i) and (ii) show the relationship between drainage basin average slope angle, and the existence of visible and preserved landforms, in order to more rigorously test the hypothesis that increased slope angle reduces preservation potential of geomorphic evidence. There is a distinct difference between basins of steeper and shallower gradients, with those containing geomorphic evidence mostly constrained to the shallower slopes at around 10° (as was also seen in Figure 4.2-b). This is clear evidence that slope angle is a decisive factor in preservation of landforms, probably due to its impact on erosional processes.

Drainage basin plan area

The above analysis shown in Figure 4.2-c also enables an assessment of the significance of basin area for maintaining geomorphic evidence. What is also evident from Figure 4.2-c is that evidence tends to occur in basins which range in size from less than 0.5 sq. km to over 7 sq. km. Basins containing no evidence tend to be smaller, on average. This suggests that basins which are larger, and therefore have larger accumulation areas and higher volumes of debris supply, are more prone to active debris-transport processes.

Aspect

Basin aspect is investigated as a possible controlling factor on the observed existence of geomorphic evidence. It is postulated that aspect may play an important role as North-facing basins may be subject to increased frost action, snow accumulation and associated weathering and erosion processes, and thus have a lower preservation potential. However, this may be counter-balanced by the fact that Northerly aspects may be more likely to accumulate snow and ice, and thus produce greater geomorphic response. Figure 4.2-d aims to test these assertions.

Figure 4.2-d: Aspect distribution of drainage basins

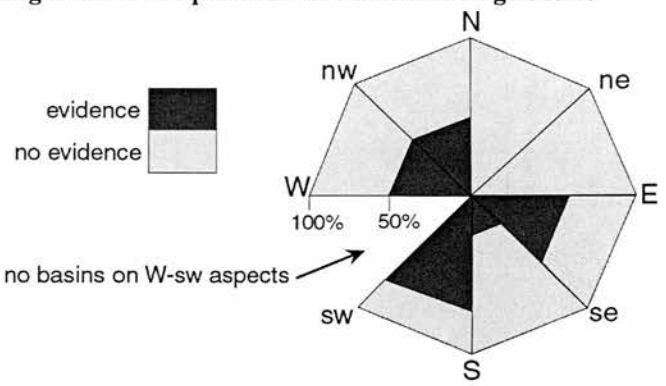

Figure 4.2-d adds the number of drainage basins found on each aspect, and distinguishes between those containing geomorphic evidence and those which do not. The number of drainage basins on each aspect containing evidence is represented here as a proportion of the total number of drainage basins on that aspect.

It is seen from Figure 4.2-d that there is no very clear distinction between aspects in terms of the distribution of geomorphic evidence. Northerly to Easterly aspects appear to contain no evidence, while the greatest proportion of evidence occurs on south to south-westerly aspects, which may be related to the increased weathering and erosion expected on north-facing slopes. Generally more westerly aspects seem more likely to hold evidence than easterly ones, which could be linked to the prevailing weather directions. A clear aspect influence on preservation is not clear however, so aspect is not suggested to be a key controlling factor.

Altitudinal Range

Figure 4.2-e: Basin altitudinal range ordered by summit altitude

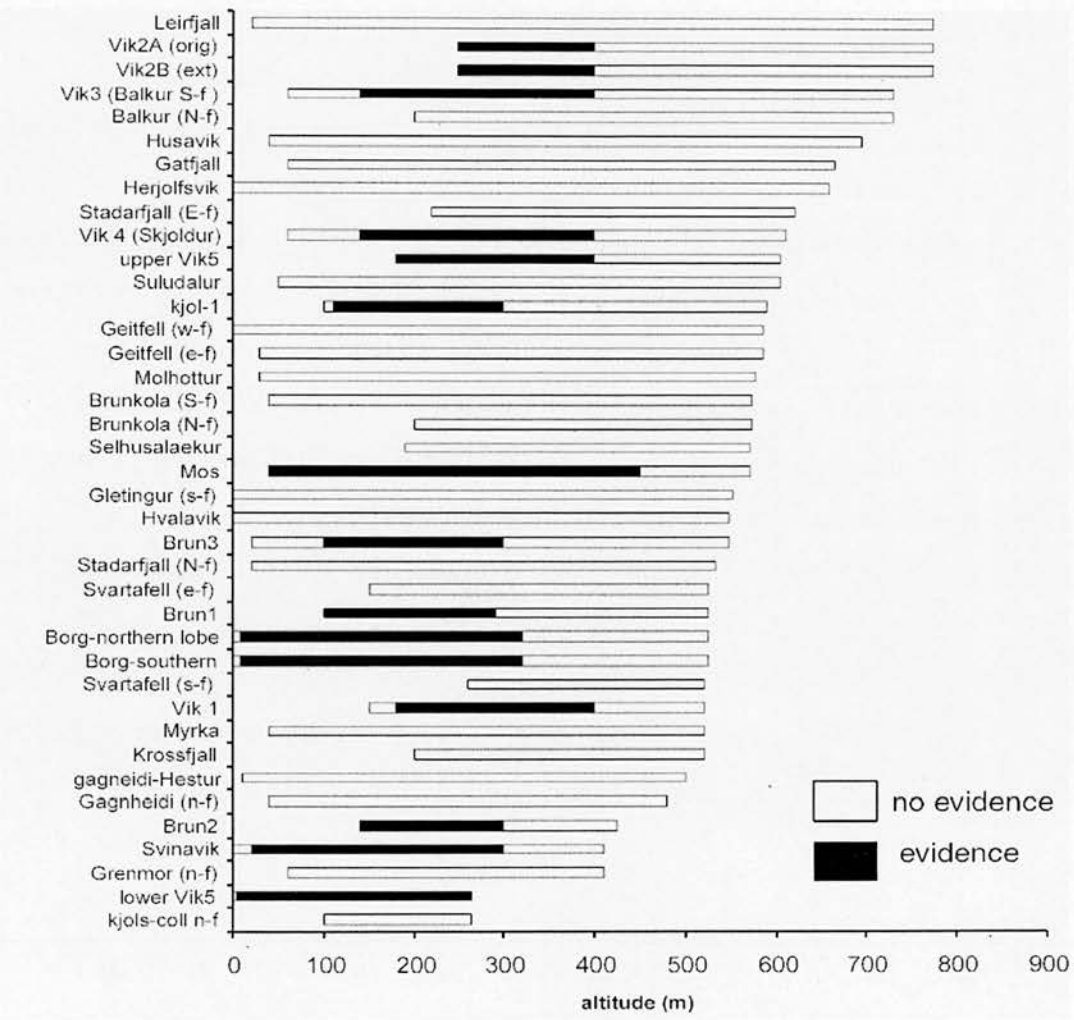

Figure 4.2 e shows the total altitudinal range of each drainage basin, with the upper altitude representing the highest peak, and the lower altitude representing the valley floor. The altitude range within which mapped landform suites occur in each basin is highlighted. Basins are arranged in order of increasing upper altitude.

Altitude and altitudinal range is also assessed as a possible controlling factor on the existence of geomorphic evidence, as shown in Figure 4.2 e. As is evident, the basins containing evidence of geomorphic activity do not uniformly occur only in basins with a certain upper altitude or range of altitudes. However, in the basins where evidence occurs, the upper altitudinal limit of surviving evidence is always between 280m and 400m, regardless of the altitude of the whole basin. This suggests

that upper basin altitude has no real effect on the existence of geomorphic evidence, but that there is a threshold upper altitude band, below which geomorphic activity is either more active, or more likely to be preserved.

Conclusions: Preservation Potential

It is concluded from this study of preservation potential, that the second hypothesis outlined above is true. This suggests that the observed distribution of geomorphic evidence is controlled by topographic factors, most significantly determined by slope angle, and to a lesser extent by basin area. The non-existence of evidence in certain basins is largely explained by the low preservation potential of these basins due to their steep slope angles. Referring back to Figure 4.1b, the second hypotheses is therefore true, that the lack of geomorphic evidence in some areas reflects poor preservation potential rather than absence of geomorphic activity. Therefore, it is still possible that regional geomorphic activity occurred in response to the 8.2ka event.

Should it have been evident that geomorphic activity only occurred in some areas, it would seem more likely that this activity represented separate and unrelated events, and Secondary Hypotheses 3 and 6 in Figure 4.1a would be the most likely.

4.3. Explaining variations in type & extent of evidence for geomorphic activity

If the Key Hypothesis shown in Figure 4.1a is true, and the landform suites do represent geomorphic activity occurring in response to the 8.2ka event, then given their common causal trigger, one might expect the same type of geomorphic activity to occur everywhere, and thus morphological continuity to exist in landform characteristics. It has been seen in Chapter 3 that this is true to an extent, but there are also significant differences in morphology and size of landform suites. This section addresses the second key question raised by Figure 4.1b (right-hand side), by

attempting to explain the observed disparities in morphology and size between landform suites which have survived.

It has been established in 4.2 that preservation potential, defined by topography and lithology, is a major control on the existence of geomorphic evidence. The extent of topographic and lithologic control on the nature of the geomorphic evidence which remains is now assessed. Figure 4.3 a illustrates the methodological motivations for this part of the study. It is argued that, where geomorphic evidence occurs, if all disparities in landform suite type and extent are explained by these spatially variable topographic or lithological controls, then all landforms suites can conceivably have been formed by the same system type at the same time. In effect, variations in landform type and extent are "cancelled out" by the effects of localised topographic and lithologic features, enabling all landform suites to be attributable to the same cause. However, if topography and lithology do not account for morphological differences in landform type and extent, then the landforms must represent a series of separate geomorphic events. These events may be "separate" temporally, in that they happened at different times, or spatially, in that they involved several different types of geomorphic system. This section aims to test this assertion by assessing the relationships between topography, lithology and the type and extent of geomorphic activity.

Figure 4.3-a: Methodological Motivations

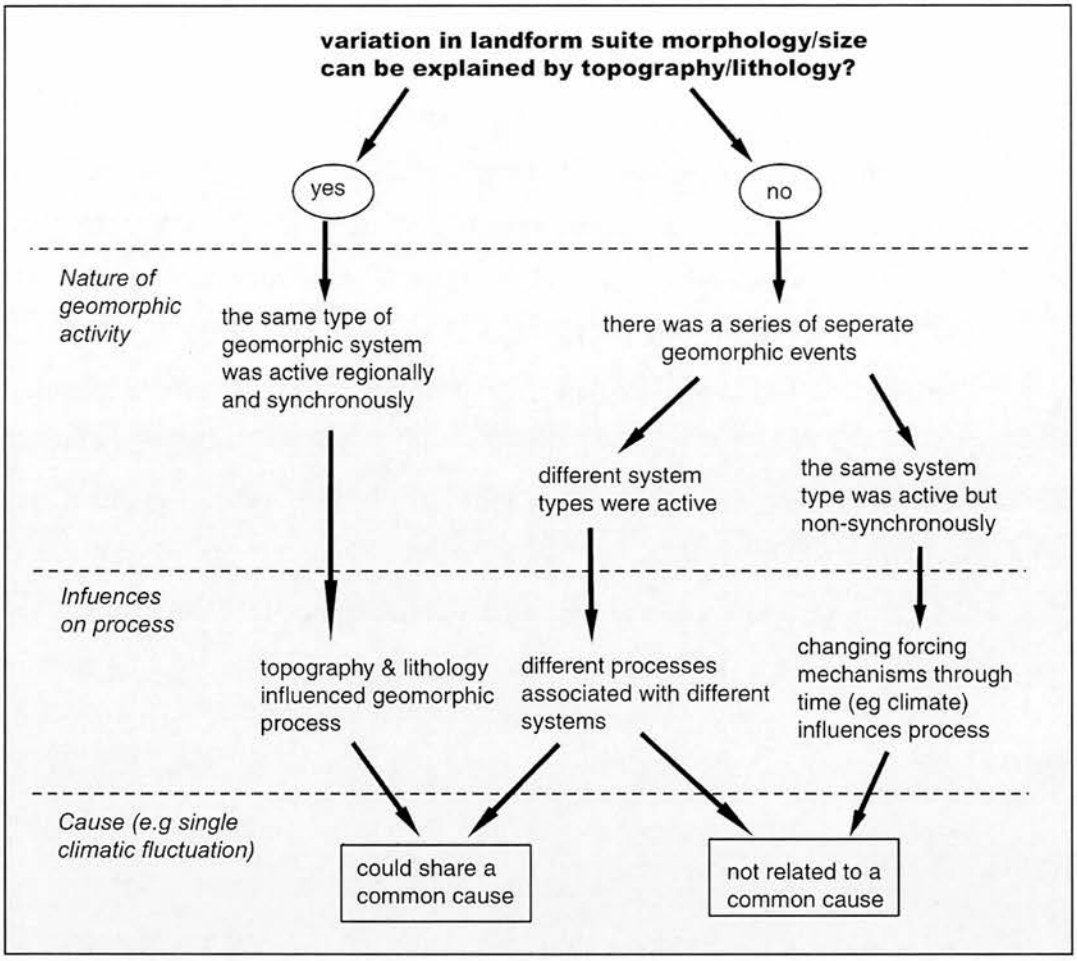

The problem is approached on two scales, looking at landform suites, and then at units of landform elements. Differences in the extent and shape of the landform suites, and variations in characteristics of landform elements and units, are addressed in relation to their topographic and lithologic context. Once the amount of topographic and lithologic control on landform suites can be quantified, the recorded extent of features might provide an insight into the relative strength of the forcing mechanism or mechanisms responsible for landform genesis. Characteristics of small-scale landform elements can provide an indication of the type of geomorphic system which was active, and the specific processes which generated the observed landforms.

4.3.1. Explaining topographic and lithologic controls on geomorphic activity

Each landform suite originates in a basin or small depression superimposed on a slope. Most of the landform suites form a continuous cover down-slope until reaching near the valley bottom. The characteristics of this underlying topography and associated lithology are a considerable influence on geomorphic processes of debris transport. In this section, the key non-climatic influences on the nature of geomorphic evidence, which were outlined in Figure 4.1-b, are described and explained. The main non-climatic influences are summarized as those associated with: slope angle; the size of potential accumulation area; altitude and aspect; and geology. Sections 4.3.2-4.3.4 go on to assess the relationship between these key topographic and lithologic factors, and the characteristics of the observed landform suites. The characteristics of the mapped suites are addressed in terms of their overall extent (4.2.2), their shape (4.3.3), and the distribution and nature of their associated landform elements (4.3.4).

Slope Angle

It has been shown that basin slope angle is arguably the most significant topographic control on preservation of landforms as a whole. It must now be ascertained whether slope angle is deterministic in defining process and thus morphology of individual landforms. Relief provides the energy input for geomorphic activity to occur, because it provides slopes with an associated gravitational pull. Slopes enable downwards movement of material (rock/sediment) by some form of mass-movement, and/or enhanced by water or ice. Increased slope angle may increase run-out speed and distance covered by a down-slope oriented debris-transport system. However, there is a threshold slope angle above which stability is detrimentally affected. On very gentle slopes, or flat ground, the energy input from high relief is not available, so geomorphic (debris-transport) activity is more restricted.

Size of Potential Accumulation Area

The underlying topography defines the size of the potential accumulation area for rock debris, ice and snow. Given a constant climate and consistent availability of material, the larger the accumulation area, the longer the run-out distance will be.

Altitude and Aspect

Altitude and aspect affect geomorphic activity indirectly through their effects on micro-climate (localised climate, 'superimposed' on the regional climatic regime). There is a lapse rate describing temperature drop with increased altitude, which involves a 1°C temperature drop for every 100m vertical ascent gained. In addition, solar insolation varies with slope aspect, and the prevailing wind direction will influence effective temperature and snow accumulation/ice growth on certain slopes (Saemundsson et al. 2003).

The implications of these micro-climatic effects on debris-transport processes (most likely involving ice, water and snow as well as debris) are two-fold. Firstly, reduced temperatures significantly aid snow and ice accumulation rates, and secondly, temperature and weather conditions influence rates of debris production through frost-shattering and weathering. Therefore, if all else is equal, the micro-climate regime caused by the topography effectively defines the ice/debris ratio of the geomorphic system which becomes active.

Increased retention of ice under cooler temperatures promotes glacial activity and increases subsequent run-out distance. The altitude of the source area defines the altitude at which initiation of activity occurs, and thus defines the type of activity which occurs in terms of the ice/debris ratio. The source area is the 'accumulation area', and its micro-climate influences the ability for snow and ice accumulation to occur. Regions which are colder due to being on an unfavourable aspect and at higher altitude will have high ice and snow content. At lower altitude, as temperature increases with the lapse rate, the lowest extent of a glacial system is related to the altitude-defined highest temperature at which ice can survive.

Debris production is likely to be enhanced by cooler temperatures which promote ice growth in bedrock joints and cracks, eventually resulting in the break down of rock into loose debris. This accentuation of rock joint weaknesses by ice results in the general instability of bedrock, and may enable large blocks to be separated from the parent rock. If the general climate is severe enough to enable glacial ice to accumulate, intensive periglacial activity (involving frost-shattering) is likely to occur on surrounding ice free surfaces.

Geology

Geology affects landform characteristics because it defines the strength of the bedrock, joint structures and resilience to erosion and weathering. These factors affect the volume of rock debris available, the shape and size of rock fragments, and the susceptibility to further weathering. The volume of produced debris and its geological characteristic have an impact on the type of geomorphic process occurring, because they define the type and amount of rock content. The geology of the field area is mostly rhyolitic, interspersed with basalt plugs and ridges. Basalt is more resilient to weathering than rhyolite, and often large rock blocks stay intact. Rhyolite breaks into much smaller shards, and breaks down more easily. The volume of debris supplied is an important controlling factor on process, due to its obvious influence on debris content of the system. The height and length of bedrock cliffs associated with each landform suite, combined with geological origin, are used as a proxy for debris supply in this study, and compared with the extent of landform suites. Any conclusions drawn as to the magnitude of energy input which induced debris-rich geomorphic activity must be balanced against an available debris supply proxy. The geomorphic processes generating, and subsequent morphology of landform suites will be affected by the type of debris which makes up the deposits, depending on whether large intact blocks or small shards are involved. Further, the geological make up of landforms will define post-depositional weathering rates, directly influencing observed morphology of landforms.

An additional geological influence on geomorphic process is the existence and distribution of bedrock ridges and plugs (usually of the more resistant basalt). An active debris transport system moving down-slope under the force of gravity may be restrained or directed by bedrock ridges it cannot over-ride. For example, bedrock ridges may 'channel' flow in a certain direction. Thus inter-comparisons of the shape (including aspect ratio) of landform suites should bear in mind the effects of such bedrock control.

4.3.2. Quantifying the effects of topographic/lithologic control on landform suite extent

Landform suite extent is an important aspect of the geomorphic evidence as it acts as a proxy for the necessary energy input to the system to induce geomorphic activity. This may represent the magnitude of climatic deterioration at the time of landform genesis. The "extent" of geomorphic activity can be defined by the amount of material moved (and how far it was moved), or by the position of the lowest margins. The contrasting definitions are applicable for different scenarios depending on the debris/ice/water ratio of the geomorphic system responsible for landform genesis. Where ice makes up a significant proportion of the volume of the system (such as a glacier), the distance travelled by debris, and the position of the lower margins defines the magnitude of the ice advance, and thus indicates the strength of the triggering mechanism. In systems where debris makes up the vast proportion of the total volume (such as a rockslide or landslide), the strength of the forcing mechanism is more likely to be represented by the volume of material moved. In this study, the physical size of the landform suites (complete area within visible margins) is used as a proxy for material moved. Estimates of the volume of material transported can be made based on the height of landform suite margins (e.g. terminal ridges), but given that landform height varies significantly in different parts of the landform suites, and that the definition of the position of the original land surface is based on subjective assumptions, it is concluded that such estimates are not meaningful in this study. The lower margin positions of the landform suites are used to derive 'run-out length'.

In order to define how much of the energy input responsible for triggering the geomorphic activity represents climatic forcing, variations in extent of the landform suites are analyzed with relation to topographic controls (slope angle, altitude, aspect and potential accumulation area) and with lithological controls (potential debris supply and geology).

Size of Accumulation Area

Figure 4.3-b: Run-out length of landform suites and size of potential associated accumulation area

(i)

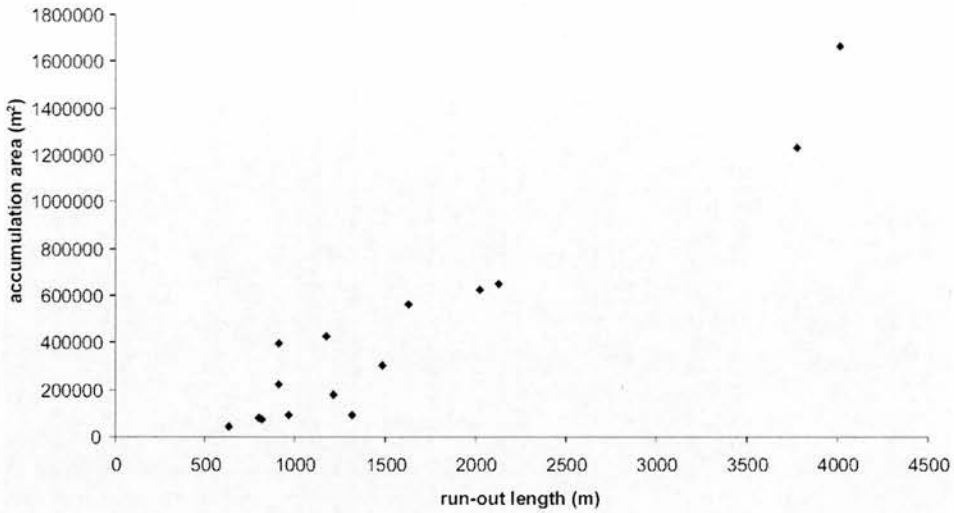

(ii)

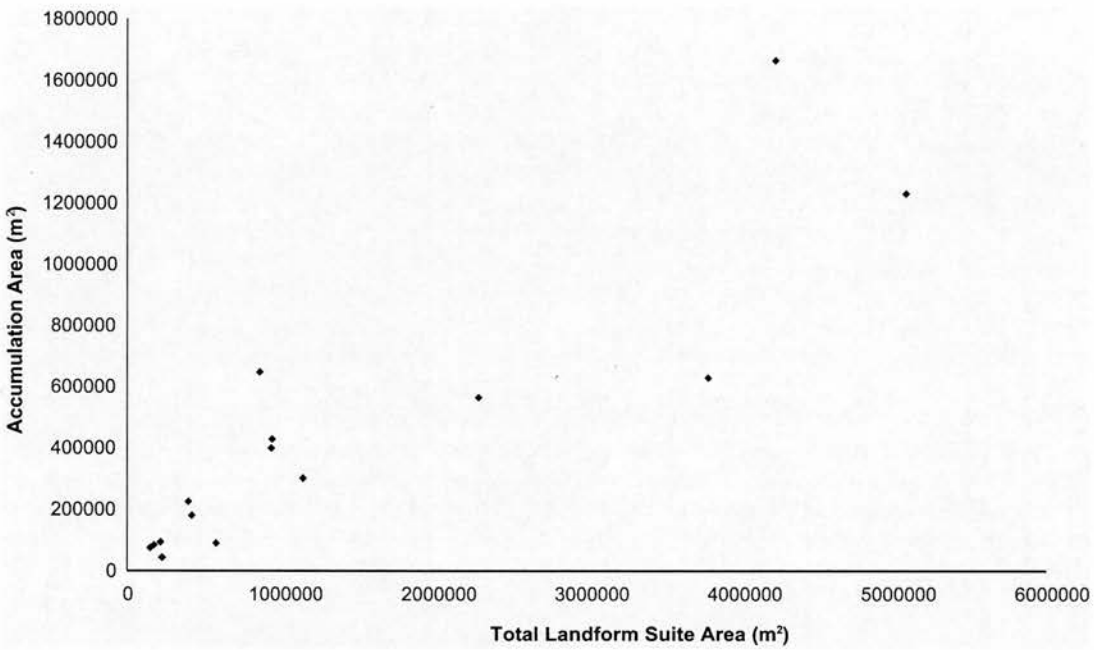

Potential accumulation area is mapped based on slope characteristics. Small basins or depressions are delimited by the cliff face behind, and where a break of slope or "lip" occurs at the front. In the cases where such a "lip" does not occur, the potential accumulation area is harder to define. An expected lower limit is suggested based on the relative position of surrounding cliffs and steep slopes. Despite its less definitive limit, the key point is that in some small basins, the accumulation area is evidently very small or near non-existent. Run-out length, shown in Figure 4.3-b (i), defines the direct length of each landform suite from the source to the lowest visible and preserved margin. Total landform suite area, shown in Figure 4.3-b (ii), refers to the area within mapped margins.

When potential accumulation area is graphed against run-out length and total landform suite area, a clear correlation if evident. From Figure 4.3-b, it can be seen that both run-out length and total area increase with increased accumulation area. This suggests that the position of the lower margin of a suite, and its overall area, is not directly influenced by forcing strength, but by size of accumulation area, which is in itself an artefact of the drainage basin topography.

Debris Supply and Geology

Figure 4.3-c: Variation in run-out length of landform suites with debris supply

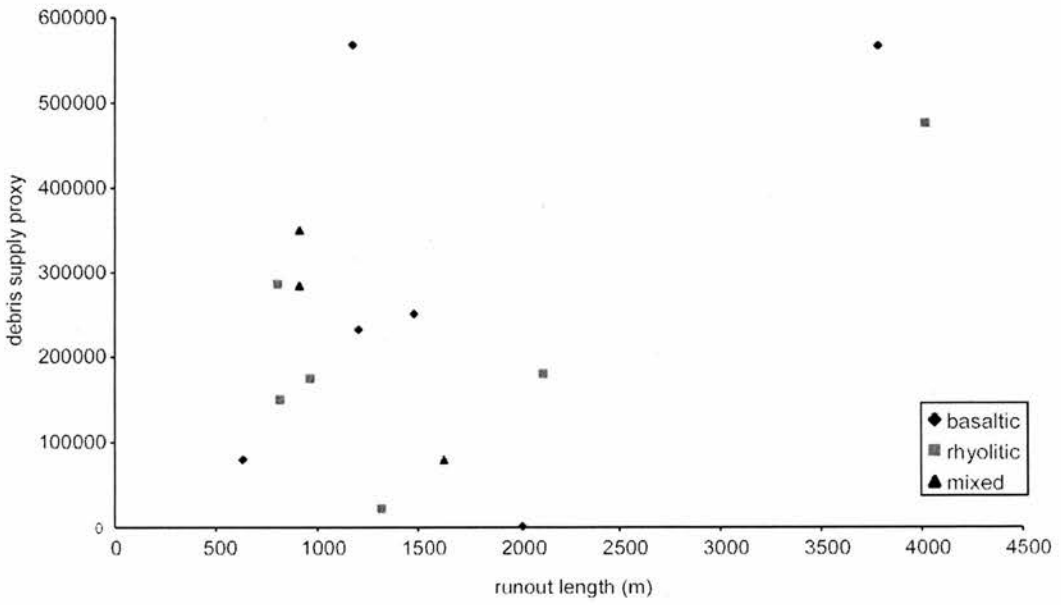

The debris supply proxy is based on the extent of bedrock cliff surrounding each landform suite, which is thought to be the main supplier of debris to any active debris-transport system on the valley floor. The debris supply proxy is defined by multiplying cliff perimeter by cliff height. This is a rough proxy and is not a definitive quantification of debris supply, but is expected to provide a rough indication of the potential rock debris supply, distinguishing between basins with large cliff source areas, and those without.

Figure 4.3-c compares run-out length with a debris supply proxy, defined by multiplying cliff perimeter and cliff height. There may be a slight tendency for those suites with very long run-out distances to have a higher debris supply, but for the other suites there is no real link between these variables. In order to assess the impact of geology on debris supply, basins are classified, according to the geology of

their source area, as basaltic, rhyolitic or mixed, and the debris supply proxy is again charted against run-out length (Figure 4.3-c). There appears to be no indication that certain geology produces more debris and thus longer run-out.

Slope Angle

Slope angle is another potential topographic control on landform suite extent, due to its inevitable effect on geomorphic process. Increased slope angle may promote geomorphic activity, due to the increased energy input to the system from increased relief. However, this increased slope angle may also affect the ability for landforms to maintain form due to post-genesis modification by slope processes. Figure 4.3-d shows the average slope angles of each drainage basin containing landform suites, and the suite run-out distance. It can be seen that there is a general trend for landform suites with shorter run-out distances to be in basins where average slope angles are relatively high. This trend only continues down to a slope angle of around 10°, where the graph is seen to level out, and run-out distances vary from ~600m to over 4km. This suggests the existence of a threshold slope angle for geomorphic activity.

Figure 4.3-d: variation in run-out distance with slope angle

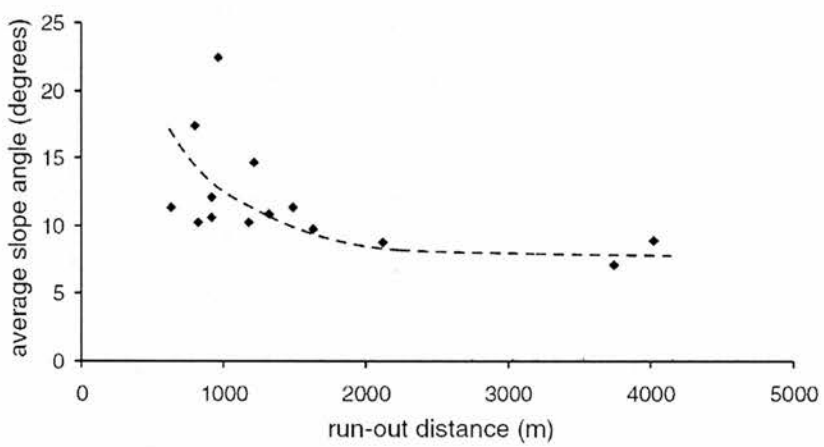

Altitude

To assess the effects of altitude on landform suite extent, we refer back to Figure 4.2-e, which highlights the altitudinal range of all the landform suites in the context of the range of their associated drainage basins. As discussed in 4.2, an upper

altitudinal band exists at which geomorphic evidence ceases to exist across all suites. This indicates an altitudinal control on initiation of geomorphic activity at the source, which is potentially related to temperature. There is no clear lower altitude representing a lower limit for geomorphic activity, or preservation of landforms. In basins where geomorphic evidence exists, landforms tend to occur down to the lowest altitudinal limit of the drainage basin as a whole, even when this is close to sea level. This indicates a degree of topographic control on the position of the lower margin, in that the debris transport activity responsible for landform genesis may only be stunted by reaching the foot of a slope. It does not appear to be restricted by reaching an altitude-defined temperature range where geomorphic activity becomes impossible.

Summary: Topographic and lithology influence on landform suite extent

This assessment has shown that landform suite extent has a strong correlation with size of potential accumulation area. In addition, slopes between angles of between 6 and 12° seem most favourable for producing long run-out distances. The impact of debris supply on landform suite extent is not clear from this analysis, and there is not a strong correlation between debris supply and run-out distance. There is a threshold upper altitude for landform suite source areas (between 280m and 400m), indicating a climate related control on initiation of geomorphic activity. However, run-out distance and landform suite area do not appear to be influenced by altitudinal controls. Most suites terminate at, or near the valley floor, with the exception of those with very small accumulation areas, or which lie on steeper slopes. This suggests that, should all slopes have reached sea level, landform suites with a large enough accumulation area and gentle enough slope angle would also be able to reach sea level. The main factors controlling landform suite extent are summarized in Figure 4.3-e. It can be seen that the landform suites which do not terminate at the valley floor have the shortest run-out distances, and the steepest slope angles. Those with the longest run-out distances have the shallowest slope angles. In conclusion, the pre-existing topography seems most important in defining the position of landform suite lower limits.

Figure 4.3-e: The main topographic controls on landform suite extent

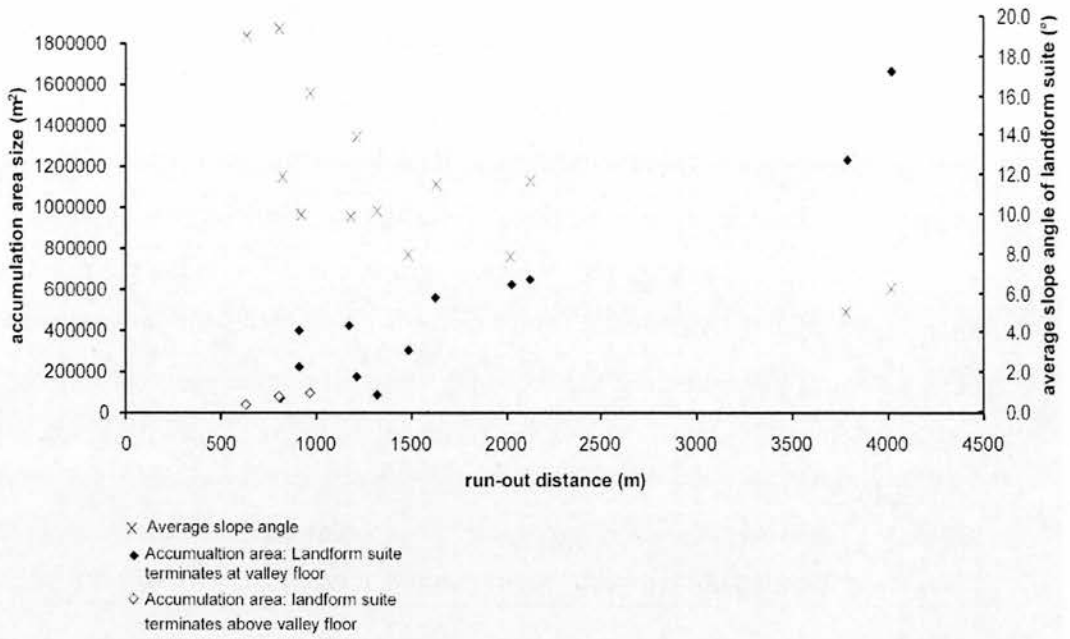

Figure 4.3-e plots run-out distance of all landform suites against the size of their accumulation area, and their slope angle. It differentiates between landform suites which terminate at the base of the slope, and those which terminate higher.

4.3.3. Quantifying the effects of topographic/lithologic control on landform suite shape

The shape of landform suites is valuable information because it may indicate the extent to which different systems are controlled by bedrock features. The hypothesis is tested that direction and shape of flow is influenced by and may be constrained by topography and lithology, in that bedrock ridges or massifs may force it in certain directions, or retard down-slope flow. The effects of such bedrock control on each landform suite must be quantified, or objective comparisons of lower margin positions may be problematic, representing local bedrock positions rather than the strength of forcing mechanisms on activity. Figure 4.3-f shows the position of the mapped landform suites relative to exposed bedrock features (ridges, cliffs and hummocks).

Bedrock control

Figure 4.3-f: Main geological features of the field area

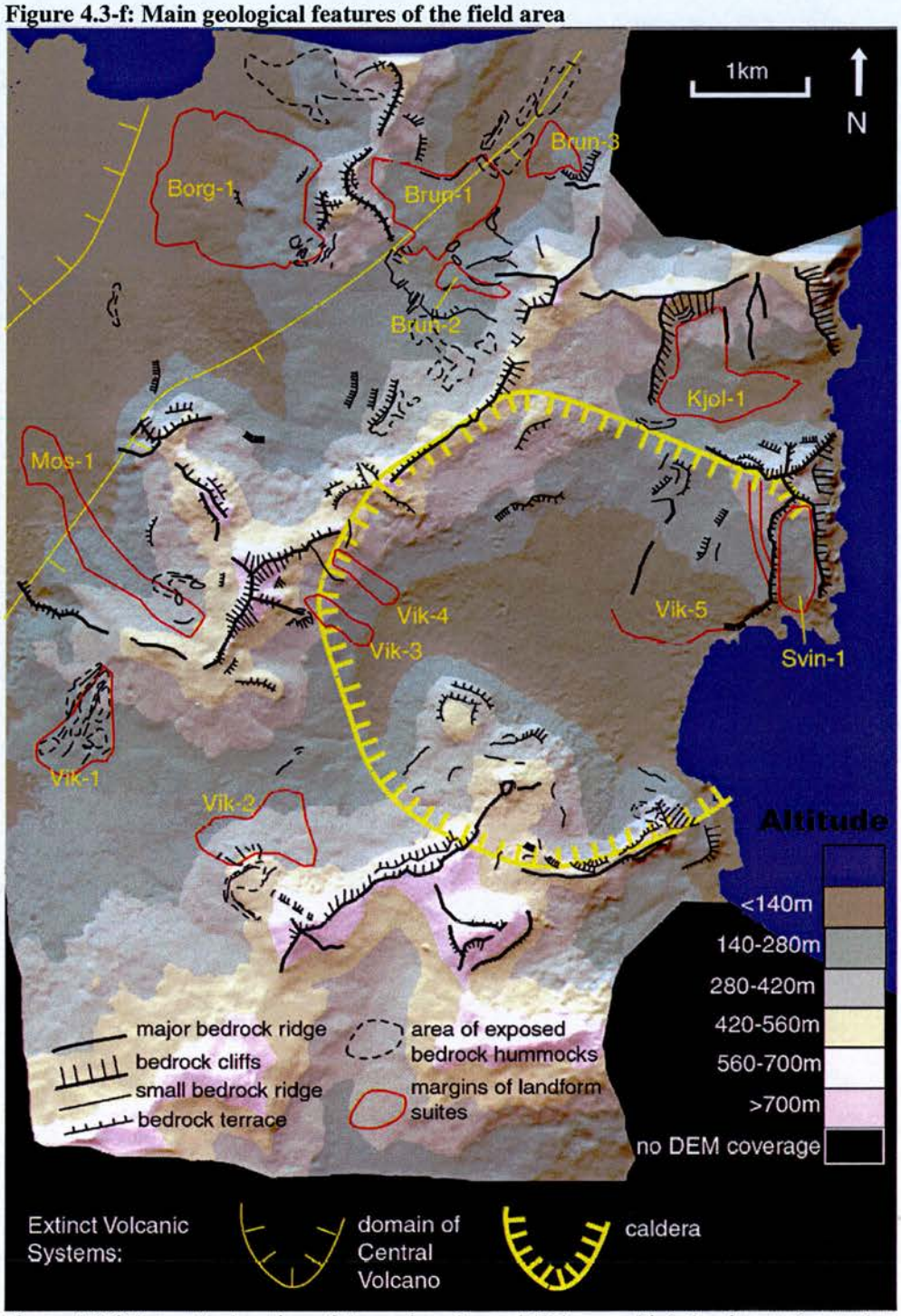

Figure 4.3-f shows the location of the extinct Central Volcano which dominates the geology of the area. Location is derived from the Geological Map of Iceland (Johannesson and Saemundsson). Also illustrated is the location of major exposed bedrock features, which are potential controls on the spatial distribution of geomorphic activity.

The exact extent of bedrock control on landform suite shape is hard to quantify, so a visual assessment is made to record bedrock influence on landform suite shape. This is based on observations made in the field recording the spatial distribution of bedrock exposures, which are mapped in Figure 4.3-f. The results are presented in Table 4.3-a, which summarizes the observed relationship between landform suites and bedrock features.

Table 4.3-a: Bedrock control on landform suite shape

Landform Suite	Bedrock exposure?	Description of bedrock features and their relationship with landform suite shape
Borg-1	Yes	Bedrock knoll in the middle of the landform suite appears to divert "flow" in two directions.
Brun-1	Yes	Constrained by bedrock cliffs to south and west, and a ridge to the north, extending the full length of the landform suite, forming the outer margin.
Brun-2	Yes	A series of ridges extending roughly westwards from source constrain this suite on its northern margin.
Brun-3	Yes	Bedrock cliffs to south and east of source area, and a series of ridges and lineated hummocks beyond the terminus.
Kjol-1	Yes	Bedrock cliffs to north and west, and a major ridge to the east constrain the upper part of the suite, and below this bedrock constraint, the suite expands in width dramatically.
Vik-5	Yes	A series of longitudinal bedrock ridges and terraces lie within the mapped margins of the suite.
Vik-4	No	
Vik-3	No	
Vik-2	Yes	Small area of smoothed bedrock hummocks define the upper margin of the western part of the suite.
Vik-1	Yes	Much of the area of this suite is made up of bedrock hummocks and ridges, so bedrock has a clear influence on the shape.
Mos-1	Yes	Upper suite 'channelled' by bedrock, and spreads outwards when it reaches the lower slopes.

It can be seen from Table 4.3-a and Figure 4.3-f, that most of the landform suites are juxtaposed with bedrock ridges and cliffs, at least in the upper reaches. It is evident that these bedrock features exert some control on the shape of the landform suite as a whole. The upper parts of the suites tend to be narrow, constrained by bedrock, but below the bedrock, the margins of the suites tend to expand outwards to form a lobate shape (this is exemplified in the Kjólsvík Suite).

Slope Angle

When the aspect ratio of landform suites is graphed against slope angle (Figure 4.3-g), a correlation is evident, where landform suites with higher aspect ratios (which are wider than they are long) are maintained on gentler slope angles, and those on steep slope angles have lower aspect ratios (being thin and long). This is what might be expected when considering the gravitational effect of slope angle. If a slope is steep, debris transported across it is likely to follow the quickest route downwards, and thus travel further downwards than outwards.

Figure 4.3-g: Aspect Ratio and slope angle

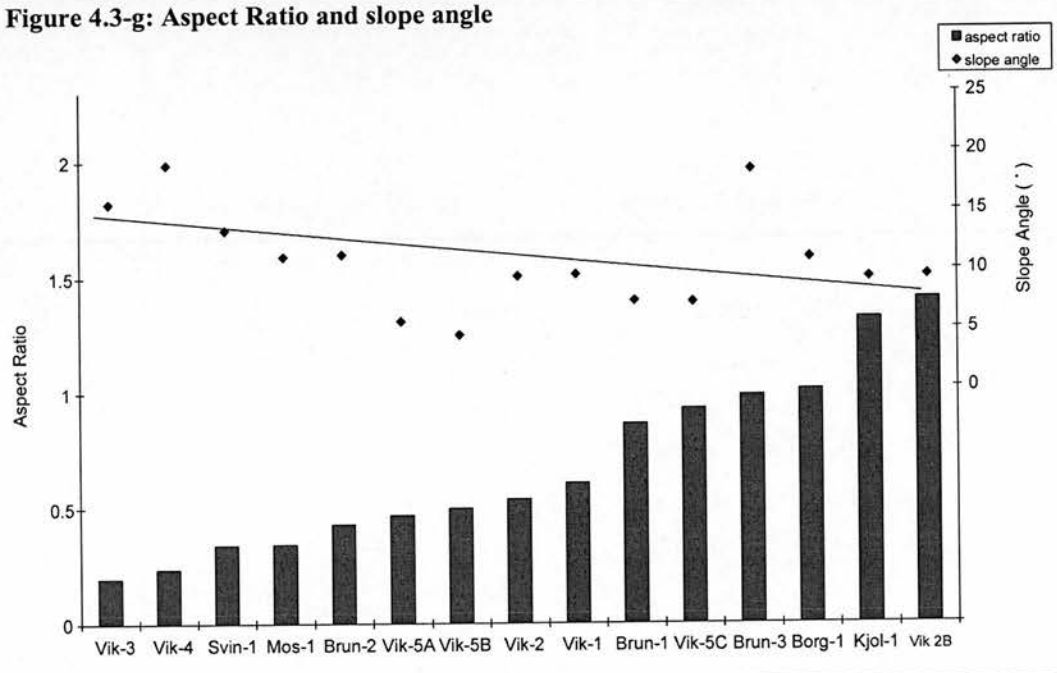

Aspect and Altitude

The effect of aspect and altitude on landform suite aspect ratio is summarized in Figure 4.3-h. As can be seen there is no significant correlation evident, showing that the micro-climate effects of aspect and altitude have little bearing on landform suite shape.

Figure 4.3-h: Relationship between aspect ratio, aspect and altitude

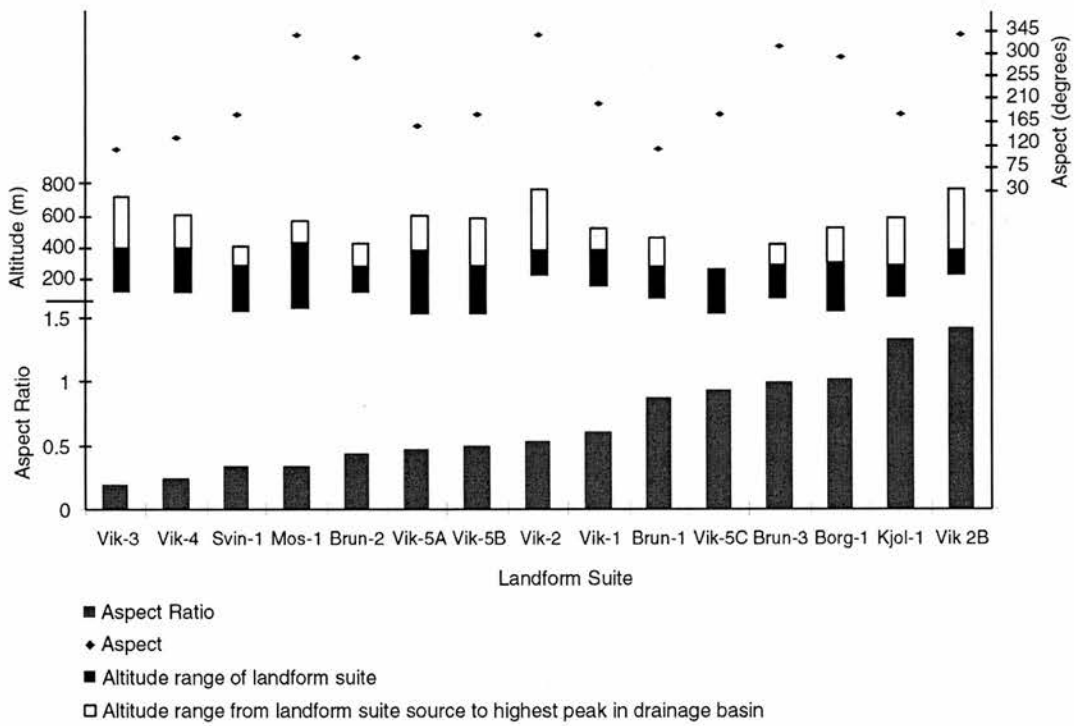

Summary: Topographic influence on landform suite shape

The key factor affecting landform suite shape appears to be the extent of bedrock control, and slope angle. This is largely an artefact of the specific geological background of the area. The region is made up of a series of old central volcanoes which have an associated structure of basalt ridges which extend from the volcanic plug. These ridges are likely to have constrained flow of material in certain directions. It is noted that landform suites with longer-thinner shapes are evident in areas with a high degree of bedrock control. This pattern is related to the distribution of bedrock ridges in the field area. It is hypothesised that landform area may be a

more reliable proxy for strength of forcing than the position of the lower margins, due to the significance of this topographic control on the shape.

4.3.4. Quantifying the effects of topographic/lithologic control on the characteristics of landform elements and landform units

It has been shown that topographic and lithological controls are important considerations when attempting to use landform suite extent as a proxy for strength of forcing mechanism. In particular, slope angle, and bedrock control appear to be most important in influencing landform suite shape, and the size of the potential accumulation area is a major influence on the overall size of the suite. In order to infer *process* from landforms, variations in the characteristics of individual landform elements are quantified. As revealed in Chapter 3, the landform suites tend to be composed of units of distinct landform elements, which have 'preferred' positions within the landform suite relative to each other. Figure 4.3-i shows the proportions of each landform element in each suite. The varying proportion of each unit in each suite creates a series of landform suites which, whilst sharing key characteristics, have distinctive differences. The aim here is to assess the extent to which this variation reflects different localised topographic and lithological controls, rather than being a reflection of the specific landform-genesis process. The main landform element groups are those discussed in Chapter 3: *transverse ridges*, *downslope/longitudinal ridges*, *hummocky terrain*, and *blocky hummocks*. The distribution and nature of each landform type is analysed in relation to potential topographic and lithological controls.

Figure 4.3-i: Variation in proportion of landform types with average slope angle

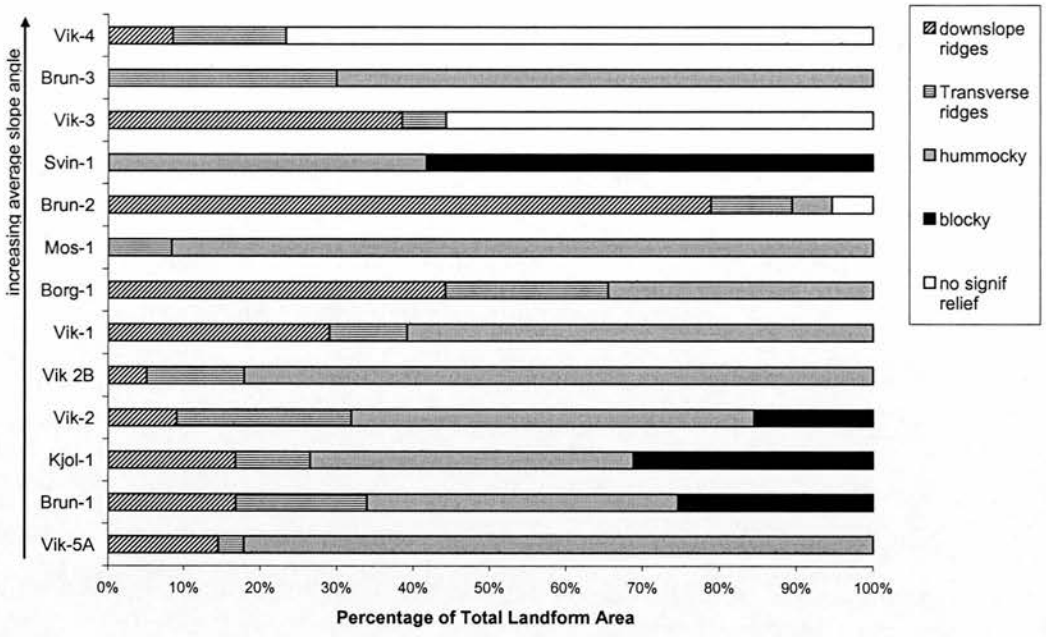

Figure 4.3-i shows the morphological make-up of each landform suite, by representing the proportion of the total area of the suite made up of the key landform types. Where land within the margins of a landform suite contains no visible landform features, it is classed as having "no significant relief". The landform suites are ordered by the average slope angle of the landform suite as a whole.
Downslope ridges: diagonal stripes, Transverse ridges: horizontal stripes, Hummocky Terrain: Grey, Blocky terrain: Black, No Significant Relief: White.

Slope Angle

It can be seen from Figure 4.3-i that the landform suites have variable characteristics related to the different proportions of landform types making them up. In ordering the landform suites by average slope angle, as in Figure 4.3-i, it can be seen that there is no clear relationship between the proportion of a certain landform type and slope angle. It is notable that the areas of land assigned "no significant relief" are generally on the steepest slope angles however. As discussed previously, this is related to the poor preservation potential of landforms on steeper slopes. The slope angle utilised in this figure, however, is an average angle for the whole landform suite. As was seen in Chapter 3, the upper, middle and lower slopes of all the landform suites tend to have characteristic slope angles, becoming gentler downslope. The use of average angles removes this detail from the study.

Therefore, Figure 4.3-j is developed, which presents the distribution of landform types on different slope angles.

Figure 4.3-j: Proportion of landform types found on different slope angles

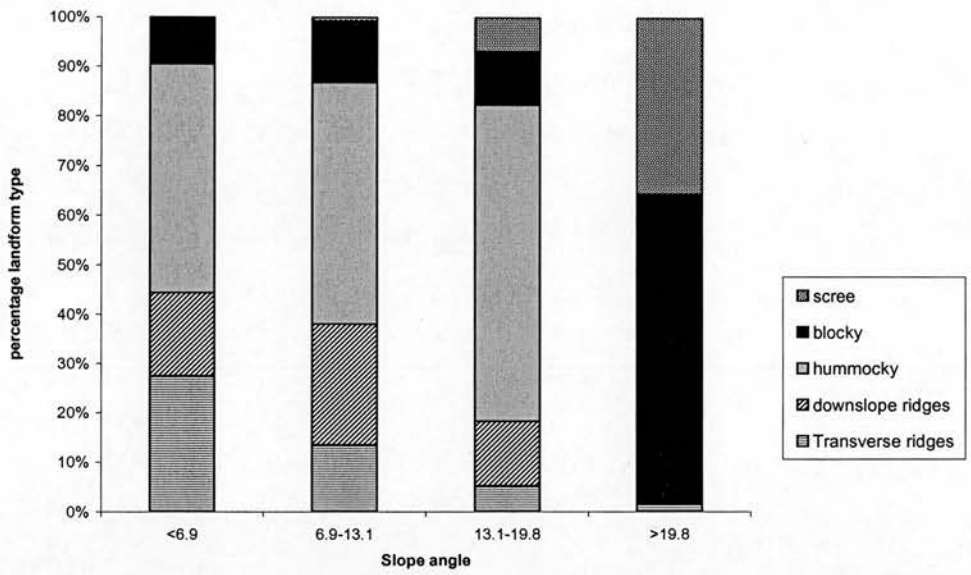

In Figure 4.3-j the slope angles on which key landform types were found within each suite are presented. The area covered by each landform type in all the landform suites is divided into four groups based on the slope angle. These slope angle 'brackets' are used because they provide a good representation of the main slope areas which make up the landform suites, when applied to all the suites uniformly.

It can be seen from Figure 4.3-j that there is some relation between slope angle and landform type. Transverse ridges are mostly found on the gentlest slopes. Down-slope oriented ridges are found in similar proportions over slopes of gentle and medium-steep angle, mostly occurring on slopes between 6.9 and 13.1°. Blocky hummocks are most common (by a significant amount) on the steepest slopes, over 19.8°, though these are also found in lesser proportions on gentle slopes. Scree and loose debris slopes are found, as would be expected, on the steepest slopes. Hummocky terrain is found across all but the steepest slope angles, mostly on slopes between 13.1 and 19.8°. It is evident from this study that slope angle is an important factor in determining landform types. This indicates a slope-related influence on geomorphic process.

Aspect and Altitude

There is no evidence of a variation in landform type with aspect. The effect of altitude is evident only in the tendency for different landform units to be found on upper, middle and lower slopes of landform suites, as described in Figure 3.4a, Chapter 3. The evidence presented in Figure 4.3-j shows a strong relationship between slope angle and landform type. Given the fact that the relative position of landform types within a suite is generally the same regardless of the altitudinal range of the basin, this tendency for certain landform types to be found on certain slope areas is attributed to slope angle rather than altitude.

Geology

The effects of geology on the shape of landform suites as a whole is outlined in Figure 4.3.3. The characteristics of individual landform elements and landform units are also influenced by geology. As previously explained, landforms made up of rhyolitic materials have a "smoother" and more rounded surface than those made up of more basaltic materials. This is exemplified in the difference between the Svínavík landform suite, which is made up of materials matching the surrounding basalt cliffs, and the Brúnavík 2 landform suite, which consists of rhyolitic rock fragments, originating from mainly rhyolite peaks. The Svínavík landform suite consists of large-scale blocky ridge and hummock features, with a significant amount of intact bedrock visible, and many scattered boulders, whilst the Brúnavík 2 suite is made up of low relief smooth ridges (See Chapter 3.2).

There appears to be a relationship between types of landforms making up a landform suite, and the surrounding geological setting. To quantify this relationship, the proportional variations in landform units are graphed against surrounding cliff extent, in Figure 4.3-k below.

Figure 4.3-k: Variation in proportion of landform type with cliff length

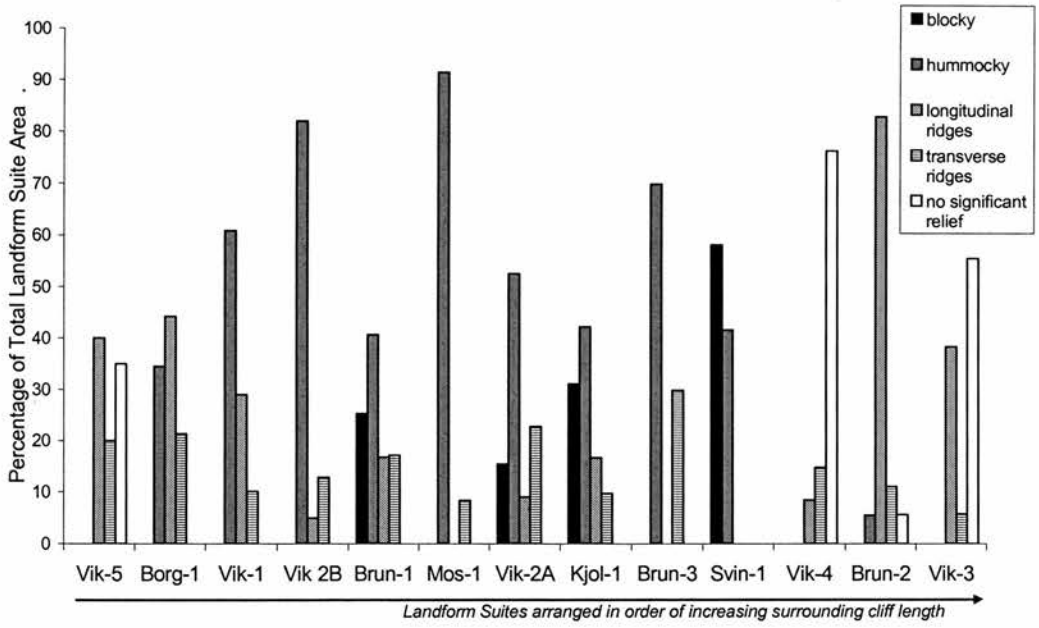

Figure 4.3-k shows the percentage of each landform suite total area, which is made up of each landform type, and orders landform suites with increasing surrounding cliff extent. The cliff extent is normalized according to the total area of the landform suite, to provide an indication of cliff length as a proportion of the total perimeter of the suite.

From Figure 4.3-k, it can be seen that there is a possible connection between the amount of "blocky" terrain, and the amount of surrounding cliff. Svínavík (Svin-1) has the highest proportion of blocky terrain, and has one of the highest surrounding cliff extents. The three landform suites which have a higher level of surrounding cliffs (Vik-3, Vik-4 and Brun-2) contain no 'blocky' landforms. Suites Víkurá 3 and Víkurá 4 appear high because they originate in basins surrounded by cliffs, but maintain only a small area of landforms, with a great deal of land which preserves little geomorphology, as discussed earlier in this Chapter. Brunavik 2 is an interesting suite because it covers a small area, despite originating in a large cliff-backed basin. However, the available rock is mostly the easily weathered rhyolite rather than the resistant basalt, which inevitably affects the eventual 'smoothness' of the landforms, and the visibility of any intact bedrock. Other landform types exhibit no clear relationship to cliff length from Figure 4.3-k.

This assessment is expanded to address the effects of bedrock features such as ridges and terraces, as well as cliffs, on landforms (Figure 4.3-l, 4.3-m, and 4.3-n). The fact

that there is an interaction between bedrock features and depositional landforms is displayed in the Víkurá 1 Suite, where depositional ridges are found constrained between bedrock ridges in the body of the suite. Three landform suites are assessed in detail, which are representative of all the main landform types. Two of these suites (Kjólsvík and Brúnavík 1) have extensive cliffs surrounding them, and the other (Borgarfjorður) is backed by bedrock knolls and extensive scree slopes. These suites all contain other bedrock features within or juxtaposed with their margins. This study assesses the potential links between the location and orientation of bedrock features and the variation in characteristics and orientation of landform elements with increased distance from bedrock.

Figure 4.3-l: Relationship between ridge type/orientation, and distance from potentially controlling bedrock features – Kjólsvík Suite

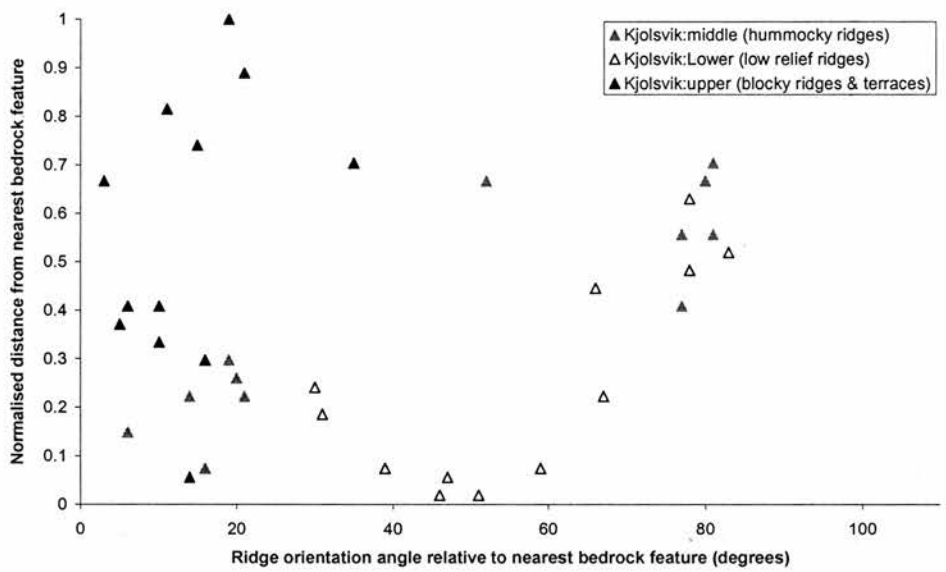

Figure 4.3-m: Relationship between ridge type/orientation, and distance from potentially controlling bedrock features – Borgarfjörður Suite

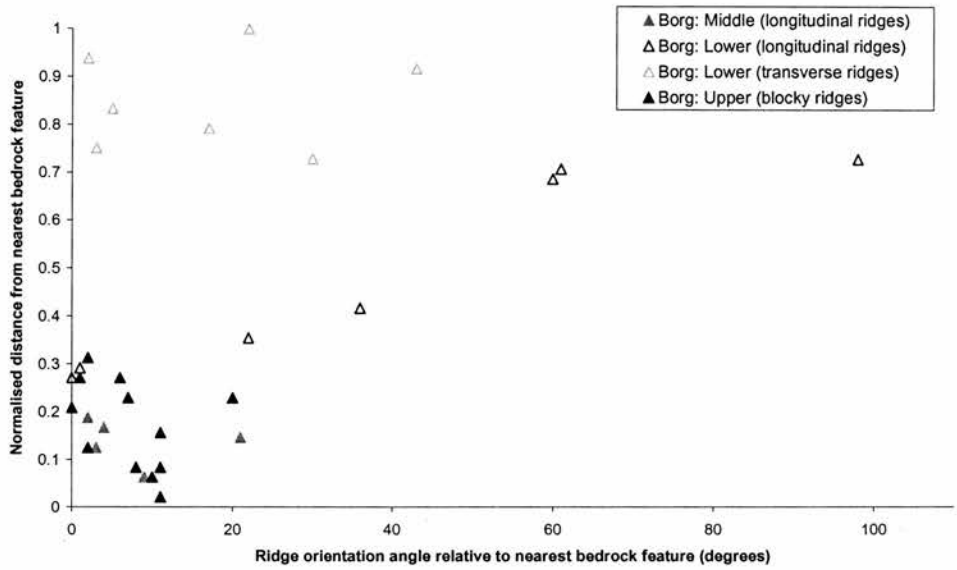

Figure 4.3-n: Relationship between ridge type/orientation, and distance from potentially controlling bedrock features – Brúnavík Suite

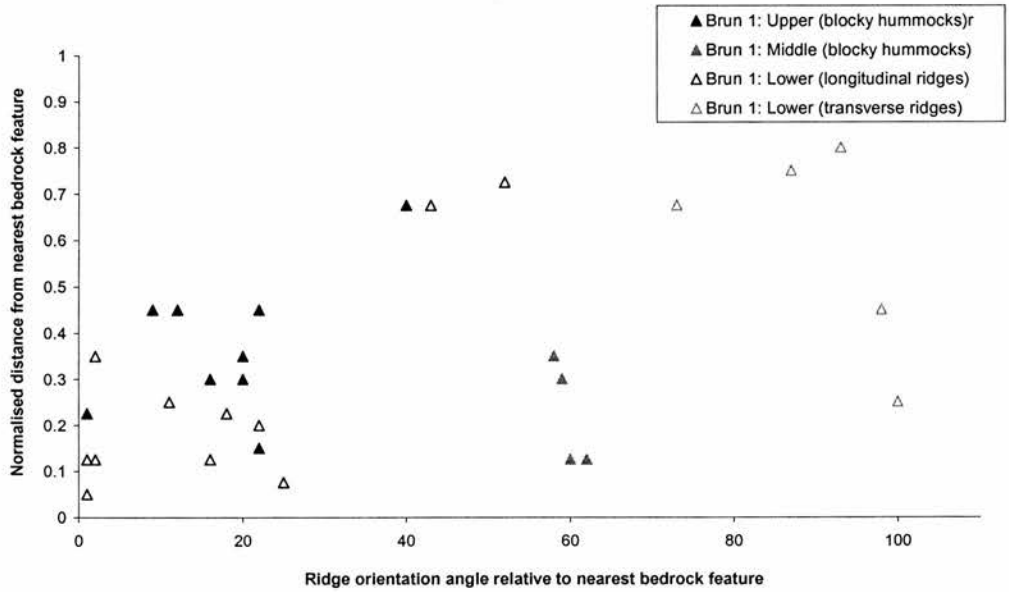

The upper suites are generally characterised by large scale blocky and hummocky ridges (and terraces), often with a lot of debris cover and intact rock blocks. It is evident that the orientations of these ridges are usually very close to the orientations of the nearest bedrock feature (in the case of these upper landform suites, that is, the

bedrock cliffs), and most lie with a 25° angle from the cliffs. This suggests a possible genetic link between the bedrock cliffs and the ridges below, and indicates that the type of geomorphic activity which moved debris into its current landform location did not move it a great distance.

This study reveals that where a bedrock feature such as a longitudinal ridge line is within the landform suite limits, or forms a margin, proximal landform elements tend to follow the orientation closely. For example, in Figure 4.3-n, the groups of points representing longitudinal ridges in the lower left hand-side of the figure, which have low angles of orientation are those which are close to the bedrock ridge which marks the outer (northern) margin of the Brúnavík 2 Suite (see Figure 4.3-f, which shows the main geological features of the field area). This provides evidence that the bedrock ridge orientation is potentially responsible for controlling landform element orientation, and therefore the geomorphic activity which formed them. A similar pattern is visible in the Víkurá 5 suite, where numerous longitudinal bedrock ridges are surrounded by depositional ridges of similar orientations.

In contrast, the ridges (usually transverse) which tend to mark the lowest margins of the landform suites, and which occur on the valley floor, show no real relationship with bedrock orientation. These low relief ridge lines are not often found in close proximity to bedrock features, and their orientation is highly variable, as shown in Figure 4.3-l, Figure 4.3-m, and Figure 4.3-n above.

Summary: Topographic and lithologic influence on landform type

It has been shown that slope angle is an important influence on the location of main landform types. Bedrock control is important in defining ridge orientation, and blocky terrain in the upper parts of a suite have a close relationship with the cliffs behind, in terms of their orientation and their rock content and debris cover. However, the juxtaposition of distinct landform units within the margins of each suite cannot be explained purely by claiming variable topographic and lithologic influence on a single system in different parts of the suite. Although landform elements appear to have "preferred" slope angles, it is not the case that a certain

landform type occurs everywhere (within landform suite limits) where the slope is at that angle. Further, although a connection is observed between surrounding cliffs and the ridges and hummocks which make up the upper parts of the landform suites, if this represented the characteristic geomorphic activity of a single system which created the whole landform suite, one would expect some link to be found between landform elements in the lower suite as well as in the upper.

It is suggested that a series of separate events is likely to have occurred to produce the observed spatial patterns of landform element units within each suite. When these observations of a single landform suite are viewed in the context of all the other suites in the field, common characteristics link spatially separate landform units. There are often more characteristic similarities between two spatially separate landform units (contained in disparate landform suites) than between two juxtaposed but characteristically different landform units within a single suite. For example, the transverse and arcuate ridges found at the lower margins of the Kjólsvík Suite share more similarities (morphologically and in their topographic setting) with the arcuate ridges at the base of the Vikura 2 suite, than with the hummocky and blocky terrain in the upper part of the Kjólsvík Suite. Such morphological connections may represent a genetic link between spatially separate landform units.

4.4. Summary

It is concluded from the above analysis, that the observed landform suites represent a series of geomorphic events which either (i) occurred time-transgressively, and/or (ii) which involved different types of geomorphic system. Neither of these scenarios rules out the possibility that the landforms represent a response to a single climate event, but rather suggest that (i) a non-synchronous response occurred, and/or (ii) this response involved more than one type of geomorphic activity. In Chapter 5, a dated chronology of geomorphic events in the field area is developed, based on tephrostratigraphic and radiometric dating of the observed landforms. This enables the testing of hypothesis (i), regarding the synchronicity of geomorphic activity.

Chapter 6 aims to classify the landforms based on genetic (process-based) interpretation. This clarification of the type(s) of geomorphic system(s) responsible for producing the observed geomorphic record enables testing of hypothesis (ii).

5 Chronology

5.1. Introduction

The aim of this chapter is to place the geomorphic evidence discussed in Chapters 3 and 4 within a temporal framework. This will enable the testing of hypotheses relating to the timing of geomorphic activity. The motivation behind this part of the study is to provide data which will, in combination with specific interpretation of the geomorphic evidence (Chapter 6), promote understanding of the causal connections between landforms in the field area. Ultimately, the provision of a dated chronology of geomorphic events will aid the assessment of the potential links between phases of geomorphic activity and climate fluctuations.

This chapter focuses on testing the hypothesis that geomorphic events in the area are asynchronous, by producing a well-constrained dated chronology for the field area. A relative chronology of geomorphic events is combined with tephrostratigraphic and radiometric dating to provide a high-resolution temporal framework within which the timing of geomorphic events is assessed at the scale of landform units and landform suites. The potential connections between separate geomorphic events and climate can then be addressed. The nature of causal connections implied by the relative timing of events is discussed in detail in Chapter 6.

5.1.1. Chronology and Causality

The relative timing of separate events is potentially indicative of the causal connections between them, in that for one event (A) to *cause* another event (B), event A must necessarily have been initiated before event B. The research requires chronological data in order to test the hypothesis that the "8.2ka event" is the overall causal trigger for generation of the observed landform suites. If this climate fluctuation is the primary *cause*, the geomorphic activity inferred from field evidence must necessarily have occurred *after* the initiation of the climate event. Because of

the complex nature of geomorphic activity and its relation with climate, the geomorphic activity may not necessarily have been regionally uniform (in character and in timing), as a regional and synchronous geomorphic event (the effect), initiated by a single climate fluctuation (the cause). It has been suggested in Chapter 4, based on geomorphic evidence, that a series of separate and non-uniform geomorphic events occurred in the field, and this section aims to test whether these events represent a time-transgressive response to a single climate forcing event. A time-transgressive response would imply that a series of discrete geomorphic events occurred over a period of time, all of which were, directly or indirectly, triggered by a single climate fluctuation (the primary cause). There may be asynchrony in the genesis time of landform suites as a whole, and/or non-synchronous and separate geomorphic events may have been responsible for the generation of the distinct landform units within each suite. Therefore knowledge of the relative timing of events will aid understanding of causal relationships. The ways in which knowledge of timing of events can provide initial indications of causal connections is illustrated in Figure 5.1-a below.

Figure 5.1-a: Cause and Effect relationships and relative timing of geomorphic activity and climate

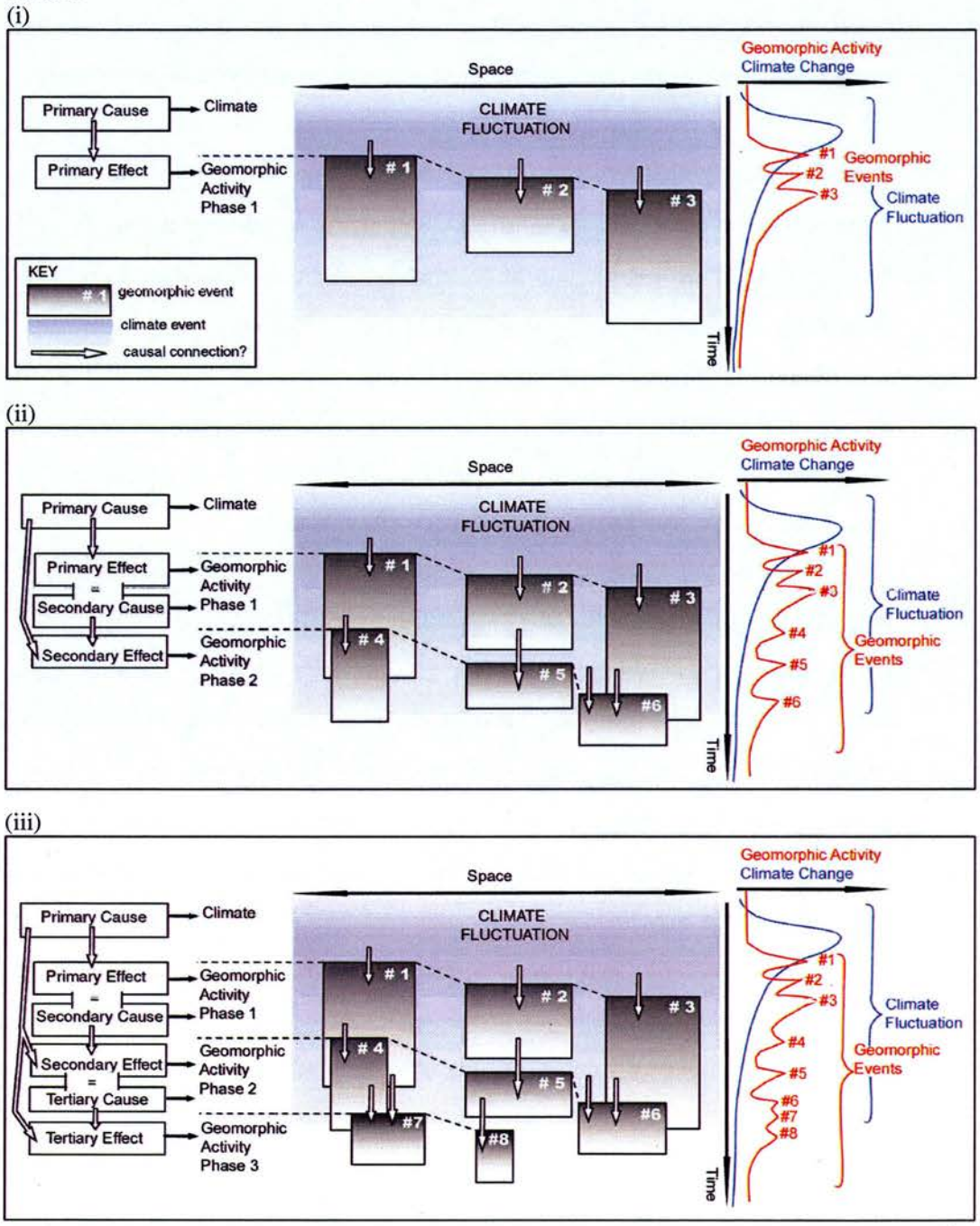

The climate fluctuations and geomorphic events illustrated in Figure 5.1-a represent *theoretical* events, though they may be analogous to events which occurred in response to the 8.2ka event.

Figure 5.1-a (i), (ii) and (iii) represent a stylised climate fluctuation and a series of theoretical geomorphic events occurring separately in space and time. For the purpose of explaining this figure, the spatial areas depicting geomorphic events are

imagined to be the areas in which the activity occurred, which may contain an identifiable landform record. In the context of this study, the climate fluctuation is assumed to be spatially uniform, because the field area is relatively small in size and spatial variation in strength of climate forcing is unlikely to be significant.

Figure 5.1-a (i) represents the initial geomorphic activity, which consists of three geomorphic events (#1, #2 and #3), occurring in different places following the climate fluctuation peak. The three events cover different spatial areas, are initiated at slightly different times, and do not last for a uniform period of time. They are hypothetically connected through space (this spatial connection will be discussed in 5.1.2), and collectively known as Phase 1 of geomorphic activity. The arrows represent the potential causal connection between climate (the primary cause) and geomorphic activity Phase 1 (the primary effect).

A further 3 geomorphic events (#4, #5 and #6, Phase 2) are represented in Figure 5.1-a (ii), which begin later than the initiation of Phase 1. These Phase 2 events occur in some of the same locations as Phase 1 events, and thus might be represented in the landform record as a unit of characteristic landform elements, morphologically distinct from the unit representing Phase 1. Event #4 is initiated while Event #1 is still active, and consists of geomorphic activity (and associated landform genesis) in ~2/3 of the area in which Event #1 occurred. Event #5 represents activity initiated after Event #2 has become inactive, promoting landform genesis over the whole land area occupied by the Event #2 geomorphic record. Event #6 occurs in part of the area in which Event #3 occurred, but also beyond its limits. Some of the Phase 2 activity may be causally related to the descending leg of the climate fluctuation. In addition, however, and perhaps most significantly, the altered condition of the landscape as a result of Phase 1 activity (Events #1, #2 and #3) may be the causal trigger (the secondary cause) for Phase 2 activity (the secondary effect). Phase 2 activity may consist of re-working of materials involved in Phase 1 activity, or represent the results of slope instabilities caused by Phase 1 activity.

Figure 5.1-a (iii) represents the occurrence of geomorphic events #7 and #8, which complete Phase 3, occurring in locations related to Events #4 and #5, post-dating Phase 2. Its occurrence in these locations is again indicative of a causal connection with Phase 2 activity.

Given the timings of Phase 1, 2 and 3 events relative to each other, and the location of all phases of geomorphic activity in roughly the same locations, a potential causal connection is evident between the separate phases of geomorphic activity. The *primary effects* of the climate fluctuation (which are directly influenced by climate) therefore become *secondary causes*, triggering *secondary effects* (which are indirectly caused by climate). These *secondary effects* can become *tertiary causes* which initiate *tertiary effects*. In this way it can be seen how combining spatial geomorphic evidence with knowledge of relative timing of events can aid the development of hypotheses regarding causal connections between climate and temporally separate geomorphic events.

5.1.2. Chronology and Spatial and Morphological Context

The chronology presented in this chapter has limitations based on the availability of dateable materials, visibility and consistency of tephra layers, choice of sample sites, and the inherent errors related to specific dating methods. The value of this chronology can be extended, when it is viewed in its spatial and morphological context. The causal links drawn in 5.1.1, between theoretical disparate geomorphic events which were not recorded as identical in timing, are related to the morphological similarity between landform units, which indicates a process connection. Figure 5.1-b builds on the theory presented in Figure 5.1-a, illustrating how geomorphic evidence can reveal information on process which enables causal links to be hypothesised between separate geomorphic events through space.

Figure 5.1-b: Connections between landform units and landform suites

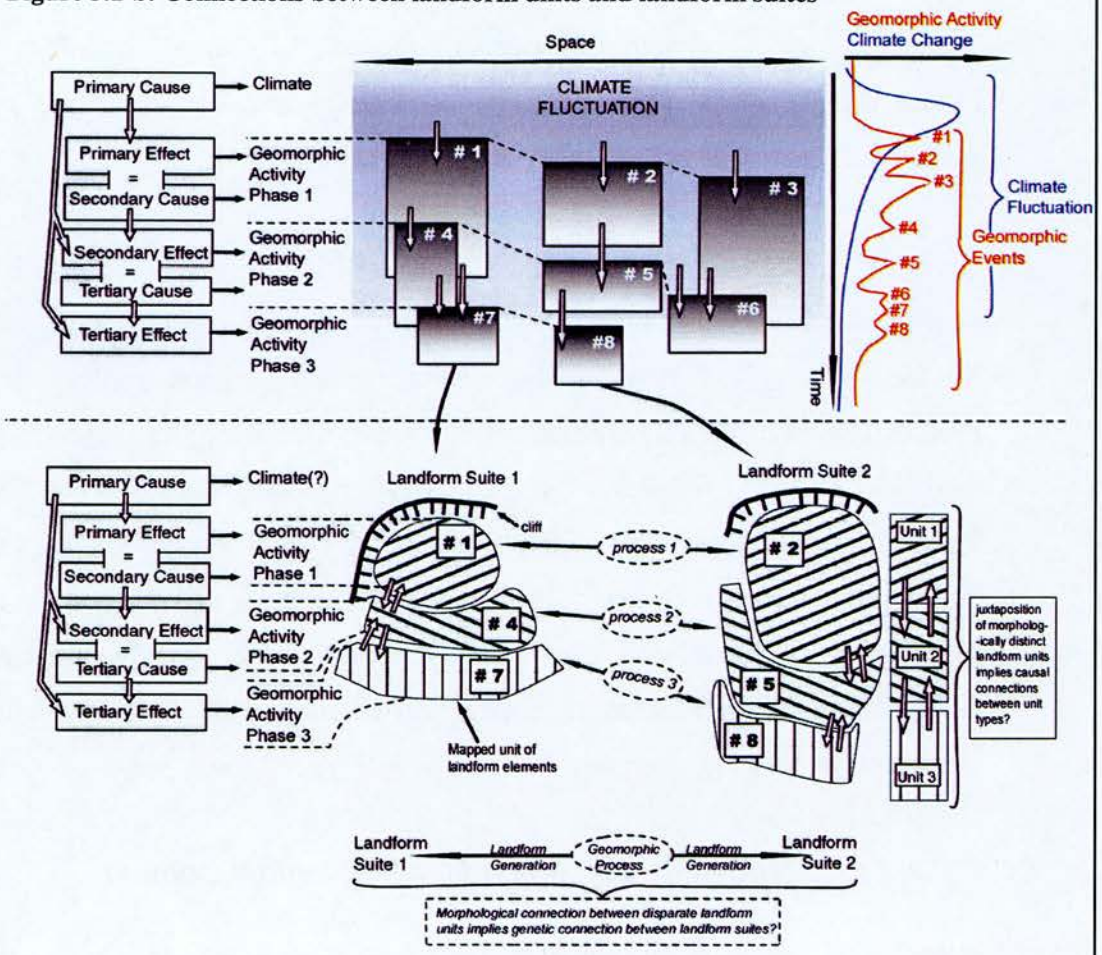

Figure 5.1-b repeats Figure 5.1-a (iii) at the top, and beneath, illustrates two theoretical landform suites made up of three distinct landform units, which share common characteristics in both suites. The link between spatially and temporally separate geomorphic events, and the geomorphic evidence is highlighted. The landforms represent the remaining observable evidence for phases of geomorphic activity, which are hypothetically linked to the phases of activity discussed in Figure 5.1-a. The numbers (#1…#8) shown within the landform units relate to the specific geomorphic event shown in the upper part of the Figure. In this case, Landform Unit 1 in both suites correlates to Phase 1 of geomorphic activity; Unit 2 correlates to Phase 2; and Unit 3 to Phase 3.

From Figure 5.1-b above, it can be seen how geomorphic evidence can be connected to specific geomorphic events and causal connections can be suggested. This study is of great value when it is considered that accurate dating of all landforms is not always possible in the real world. Through appeal to spatial and morphological context, causal connections can be suggested despite gaps in the dateable chronology. For example, it may be the case that Landform Suite 1 is dateable and has an age assigned to it, but Landform Suite 2 contains no suitable dateable material, so it is not possible to connect the two events based on their synchronous

timing. However, given their shared morphological characteristics, it is inferred that the three landform units in both suites were likely to be formed by three common processes, which indicates shared causal triggers. Therefore it is likely that the three landform units making up un-dateable Landform Suite 2 may have been formed at the same time as the equivalent units in Suite 1.

It was seen in Figure 5.1-a that knowledge of relative timing of separate geomorphic events occurring in the same location could indicate a cause and effect relationship between the event which occurred first and the event which followed it. Figure 5.1-b shows how the juxtaposition of different landform types in a suite can provide further information on the relative timing of events and causal connections. This information is useful when assessing landform suites which potentially represent multiple phases of geomorphic activity, where an old landform unit may be indicative of the process which became the causal trigger for the development of a younger landform unit. The nature of the morphological and stratigraphic link between these two units in the observable geomorphic evidence, and their locations relative to each other in the context of a slope or basin, can aid knowledge of relative timing and thus causal connections. For example, if Unit 1 in Figure 5.1-b overlies Unit 2, it must have occurred later, and thus Process 1 might have occurred in response to Process 2 ("Process 1" is equivalent to geomorphic activity Phase 1, and "Process 2" is equivalent to geomorphic activity Phase 2). It can be seen that by considering the spatial and morphological context, chronological data can be extended in value, and hypotheses can be developed regarding causal connections between separate landform suites, and between distinct landform units within a suite, or between different suites.

In the remaining part of the Chapter, a chronological framework for the field area is developed in order to determine the causal connections between landform genesis events and climate change.

5.2. Chronology: Results

In the context of the geomorphic evidence presented in Chapter 3, tephrochronology, constrained by radiocarbon dates, has been used to achieve dating control on the suites of mapped landforms. The tephrostratigraphic framework, developed based on the methods described in Chapter 2.4, is presented. Correlations are made with tephra layers described in other studies, and the relative chronology of geomorphic events recorded in the field is better constrained with absolute dates.

5.2.1. Stratigraphy

A series of tephra profiles were excavated in the field area, the locations of which are illustrated in Figure 5.2-a. A full list of G.P.S points for each profile is available in Appendix IV. The locations of tephra profiles were initially chosen based on the need to develop a tephrostratigraphy for the field area as a whole, which can be linked with tephrostratigraphic records from a wider region (Iceland, North Atlantic and possibly Greenland). Within this framework, profiles were selected which would enable dating of individual landforms. The aim of the tephrochronology is to provide bracketing ages for landform genesis, so tephra pits and sections are exposed within and outwith the margins of landform suites, suitably placed to determine maximum and minimum age brackets for genesis. In addition to this, the exact locations of exposures depended on finding an area which was an apparent sediment trap, allowing undisturbed accumulation over thousands of years. Further, currently active slopes or fluvial systems are avoided as recent activity will have distorted the record through erosion and reworking of sediments. Where possible, tephrostratigraphy is maintained within well-humified peat sections, which preserve tephra layers well.

Figure 5.2-a: Profile locations by group

Figure 5.2-a shows the locations of the main groups of tephra profiles presented in Figure 5.2-d. Names of groups relate to the names presented at the top of each figure section (i)-(x).

Abbreviations are as follows:
Borg = Borgarfjörður
Brun = Brúnavík
Kjol = Kjólsvík
Svin = Svínavík
Vik = Víkurá
Loð = Loðmundarfjörður

In addition to these groups, a number of reference profiles were collected outwith the immediate field area in the Lagarfljót region immediately to the west of the field area (profiles are named "Lagarfljot" in Figure

The red polygons indicate the locations of the identified landform suites. In 5.4.3, the locations of profiles used to date each landform suite are presented in the context of the detailed geomorphic maps.

Stratigraphic profiles

Data on stratigraphy and tephra characteristics were collected during excavation of around one-hundred-and-forty profiles in the 2003 and 2004 field seasons. Seventy-eight of the tephra profiles excavated in the field are illustrated in Figure 5.2-c. Whilst more profiles were excavated, those which showed evidence of poor tephra preservation, or contained little information, have not been presented here. Profiles are grouped by region, and their exact locations in relation to landform suites are shown in Figures 5.4-d to 5.4-p. The tephras shown in the illustrated profiles in the following section are characterised based on physical observations of colour and grain size recorded in the field (see stratigraphic key, Figure 5.2-b). Information on the type of materials which preserve the tephras and make up the remaining profiled depth is also recorded in detail. It is anticipated that, given the high resolution of the stratigraphic records presented here, if a tephra layer of greater than ~2mm is present in an excavated profile, it has been recorded as such, and is presented in the Figure

5.2-c. Tephra layers highlighted by a number and a "*" in Figure 5.2-c represent the layers which have been geochemically analysed, the results of which are discussed in 5.3.2.

Figure 5.2-b: Key for stratigraphic diagrams

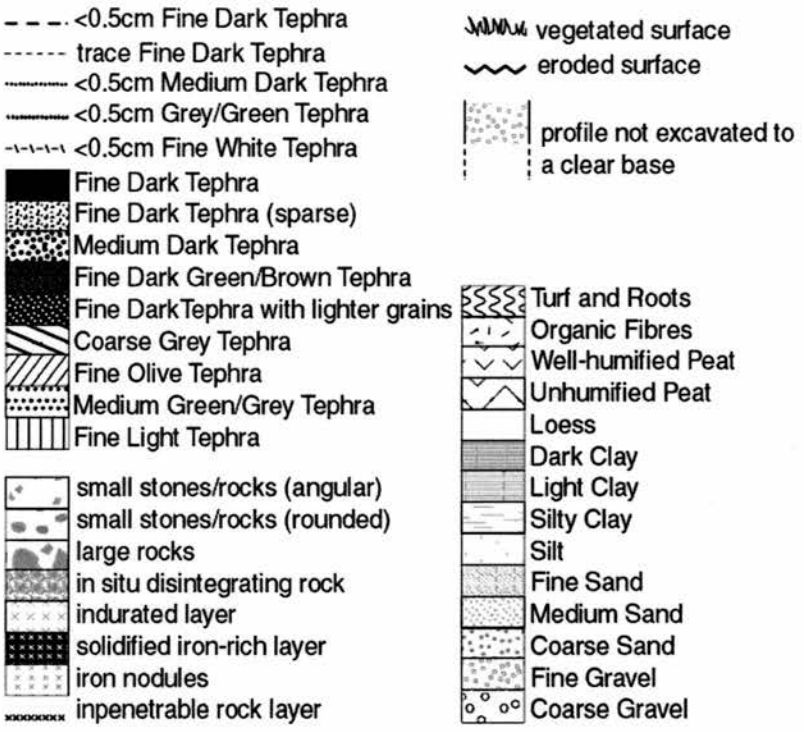

The classification of sediments used in the illustrated profiled in Figure 5.2-c are chosen with a view to best characterising the variety of sedimentary materials found in the field area. Grain size is measured on a relative scale based on feel, where coarse gravel has grains of >5mm, fine gravels >2mm, coarse sands ~1-2mm, medium sands ~0.5-1mm, fine sands <0.5mm. Silts have finer grain sizes than the finest sands, and in clays the grains are microscopic and more cohesive.

Figure 5.2-c (i): Stratigraphic profiles – Vikura I

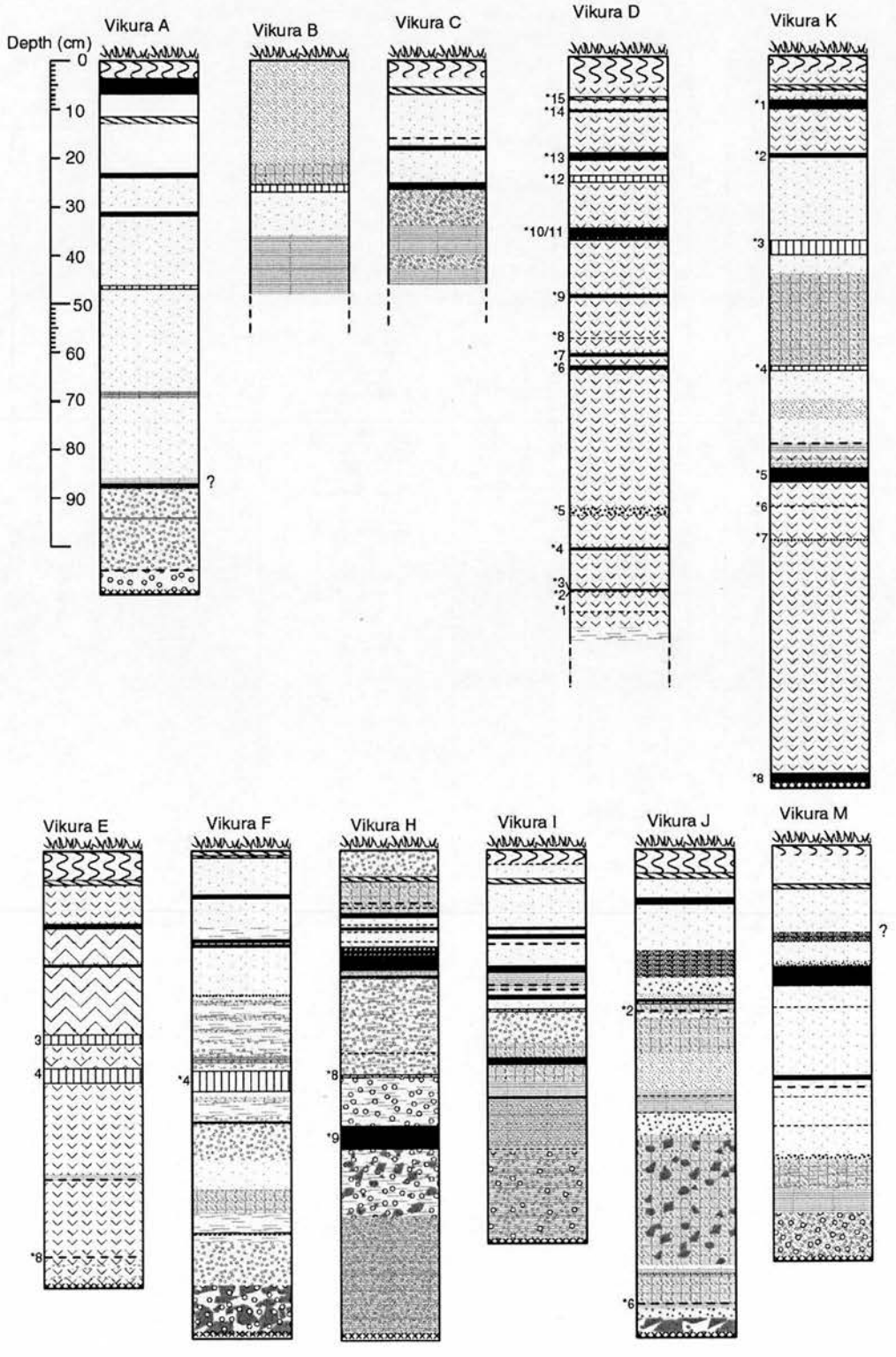

The depth scale shown above is utilised for all subsequent stratigraphic profiles

Figure 5.2-c (ii): Stratigraphic Profiles – Vikura I (continued)

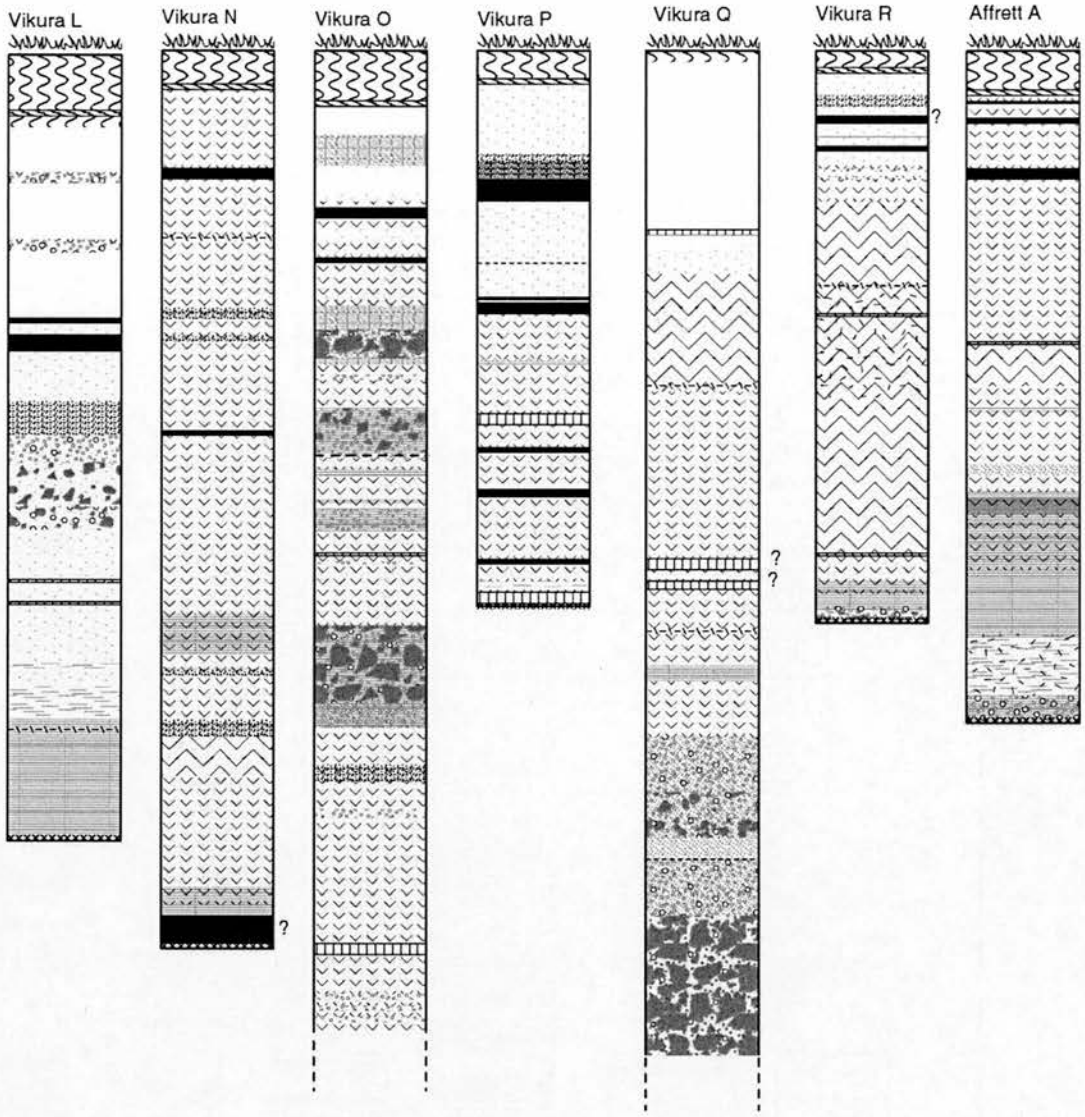

Figure 5.2-c (iii): Stratigraphic Profiles – Vikura II

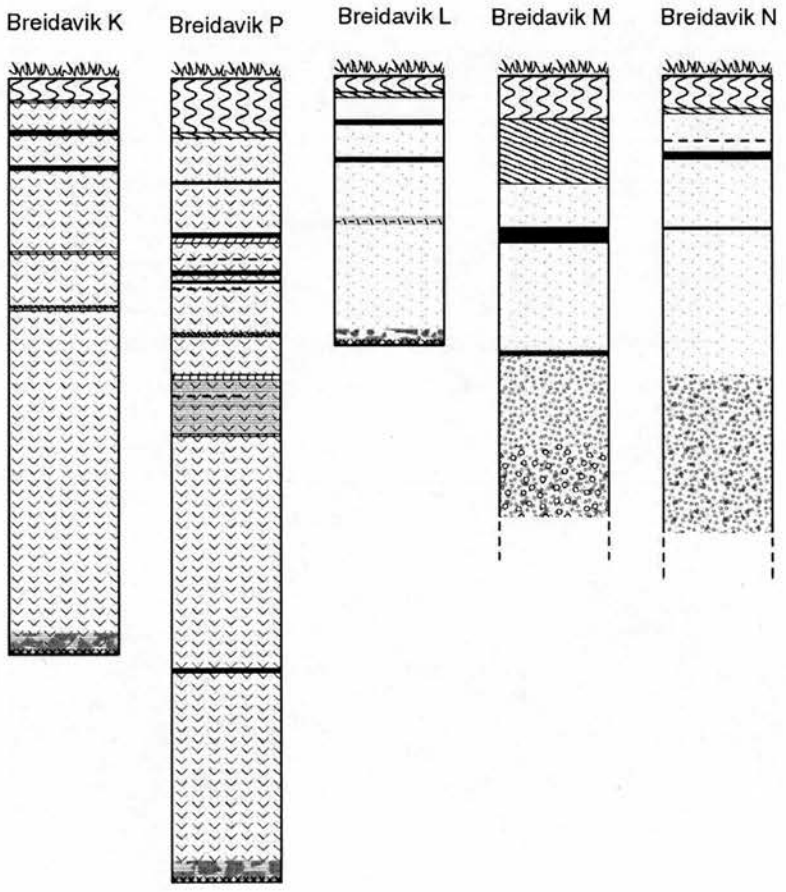

Figure 5.2-c (iv): Stratigraphic Profiles – Vikura III

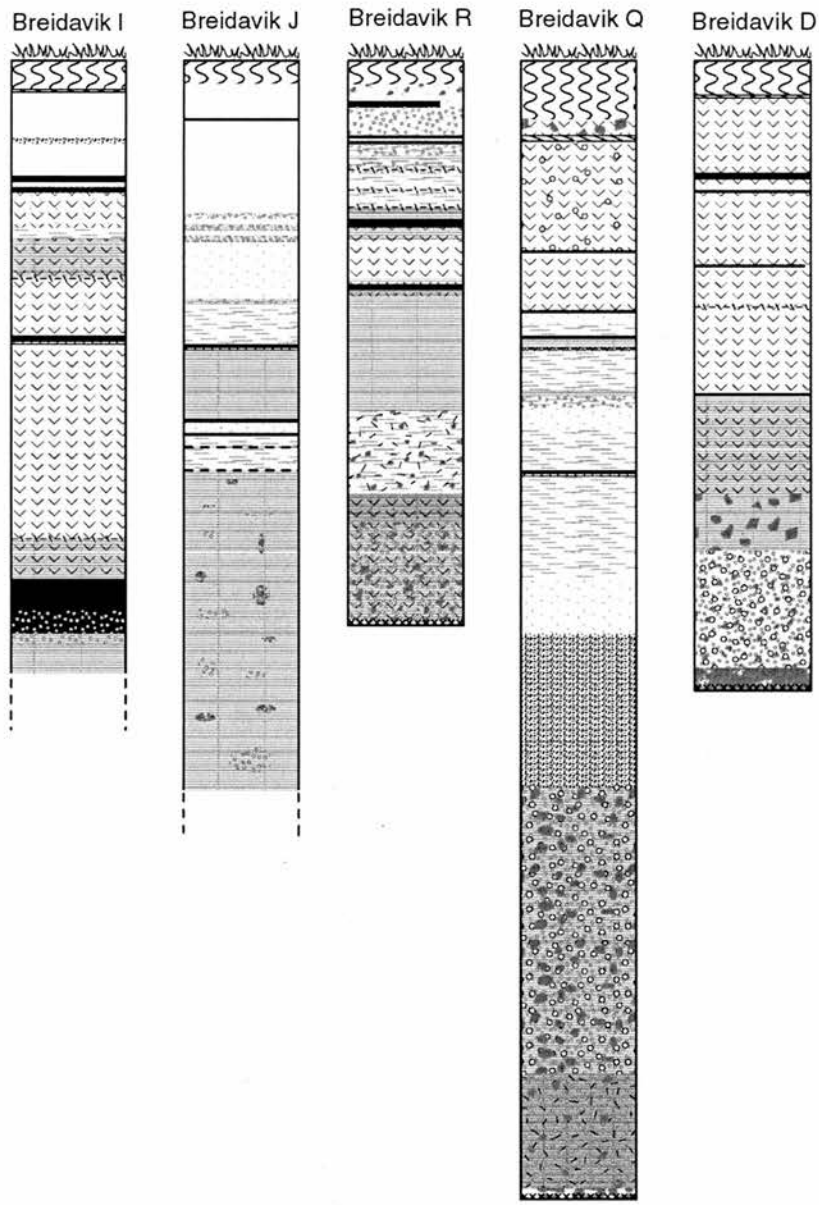

Figure 5.2-c (v): Stratigraphic profiles – Borgarfjörður

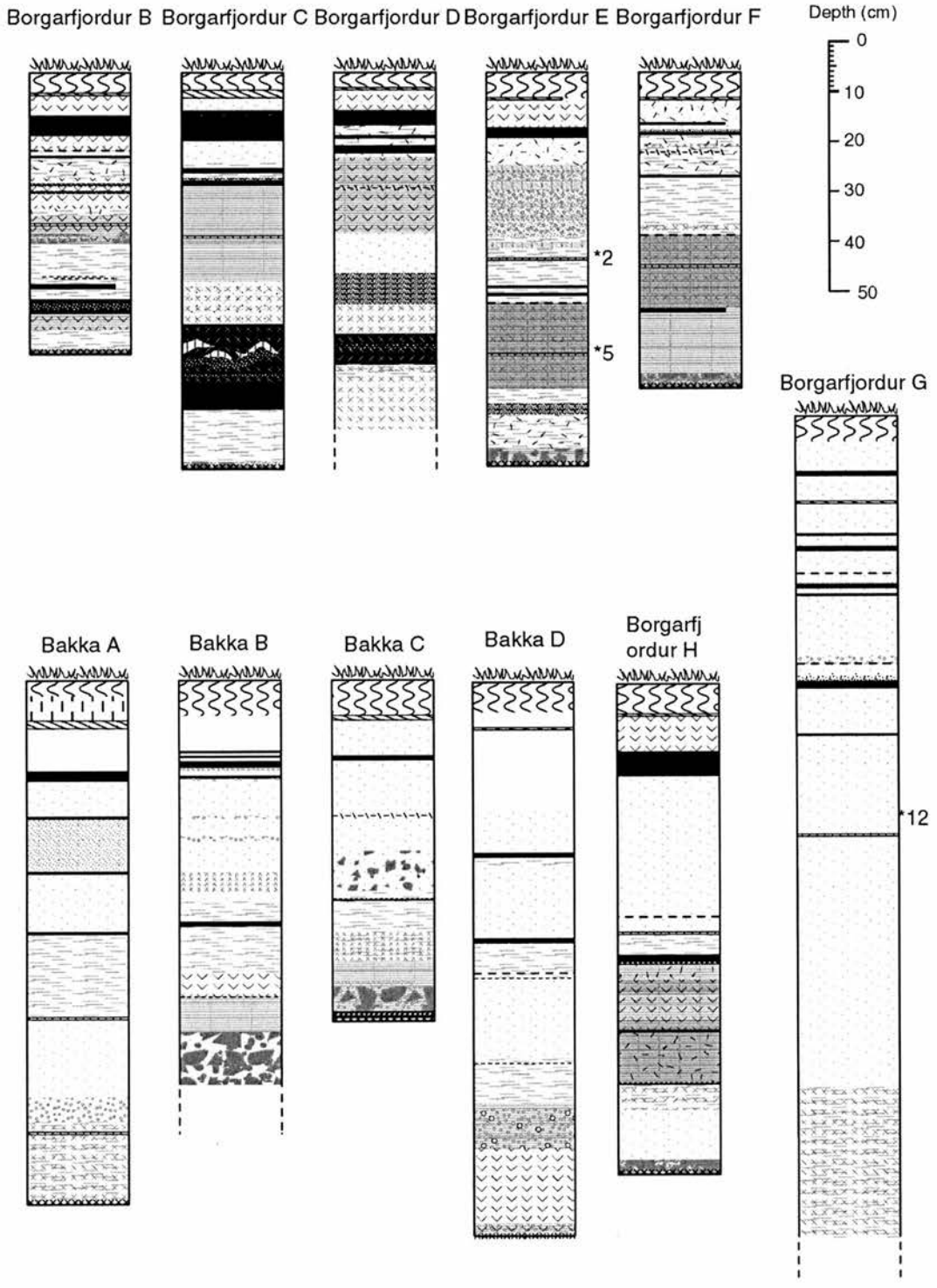

Figure 5.2-c (vi): Stratigraphic profiles – Borgarfjörður (continued)

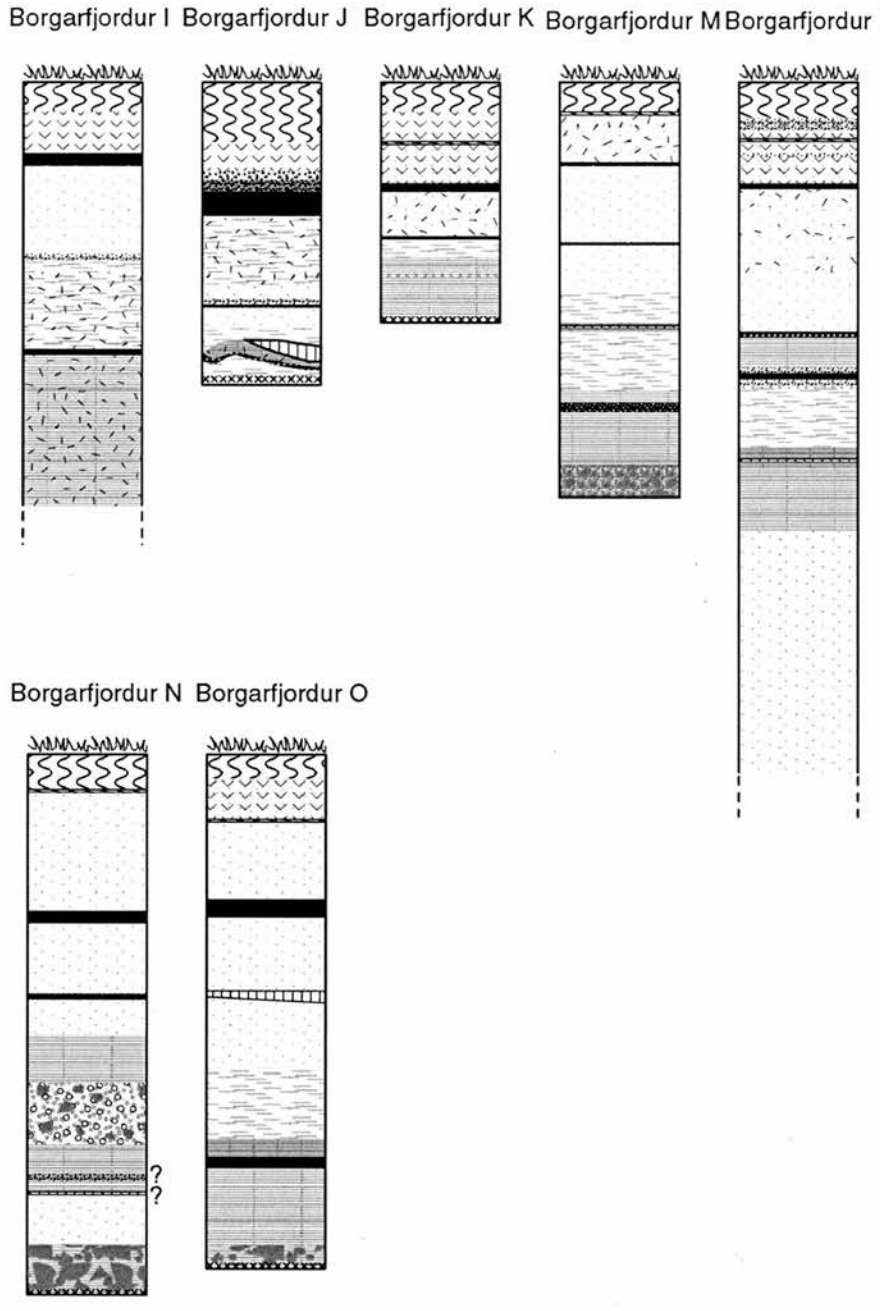

Figure 5.2-c (vii): Stratigraphic Profiles – Brúnavík

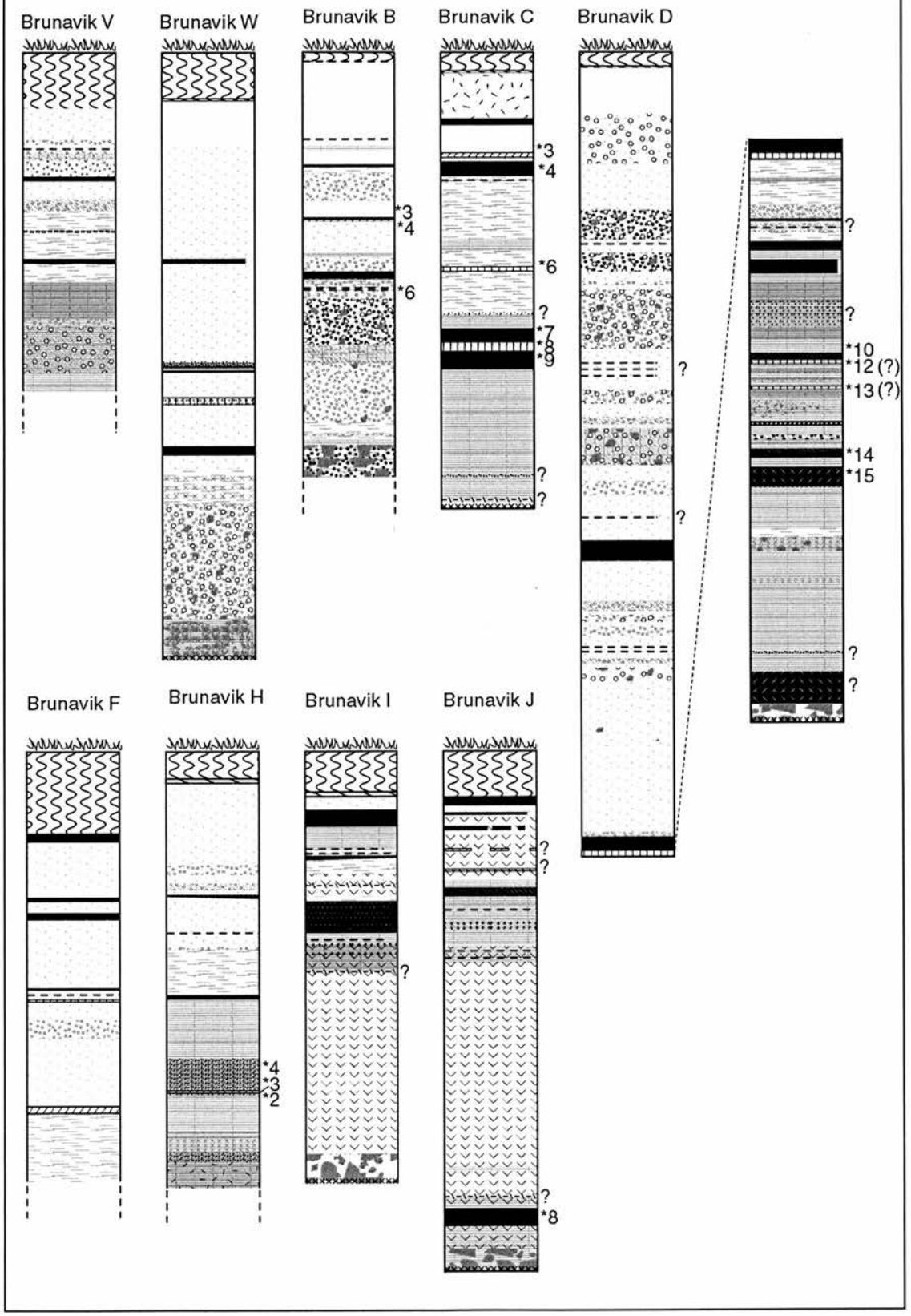

Figure 5.2-c (iix): Stratigraphic Profiles – Brúnavík (continued)

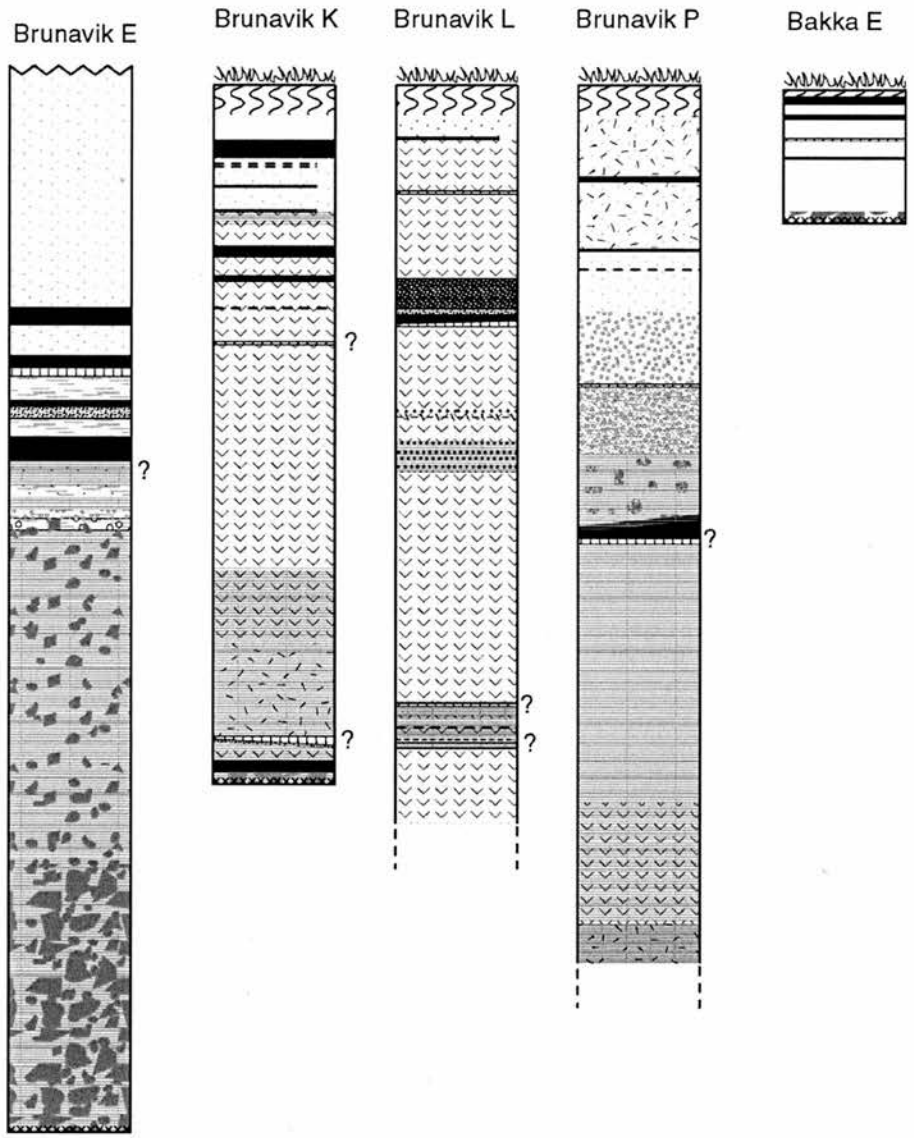

Figure 5.2-c (ix): Stratigraphic Profiles – Kjólsvík and Svínavík

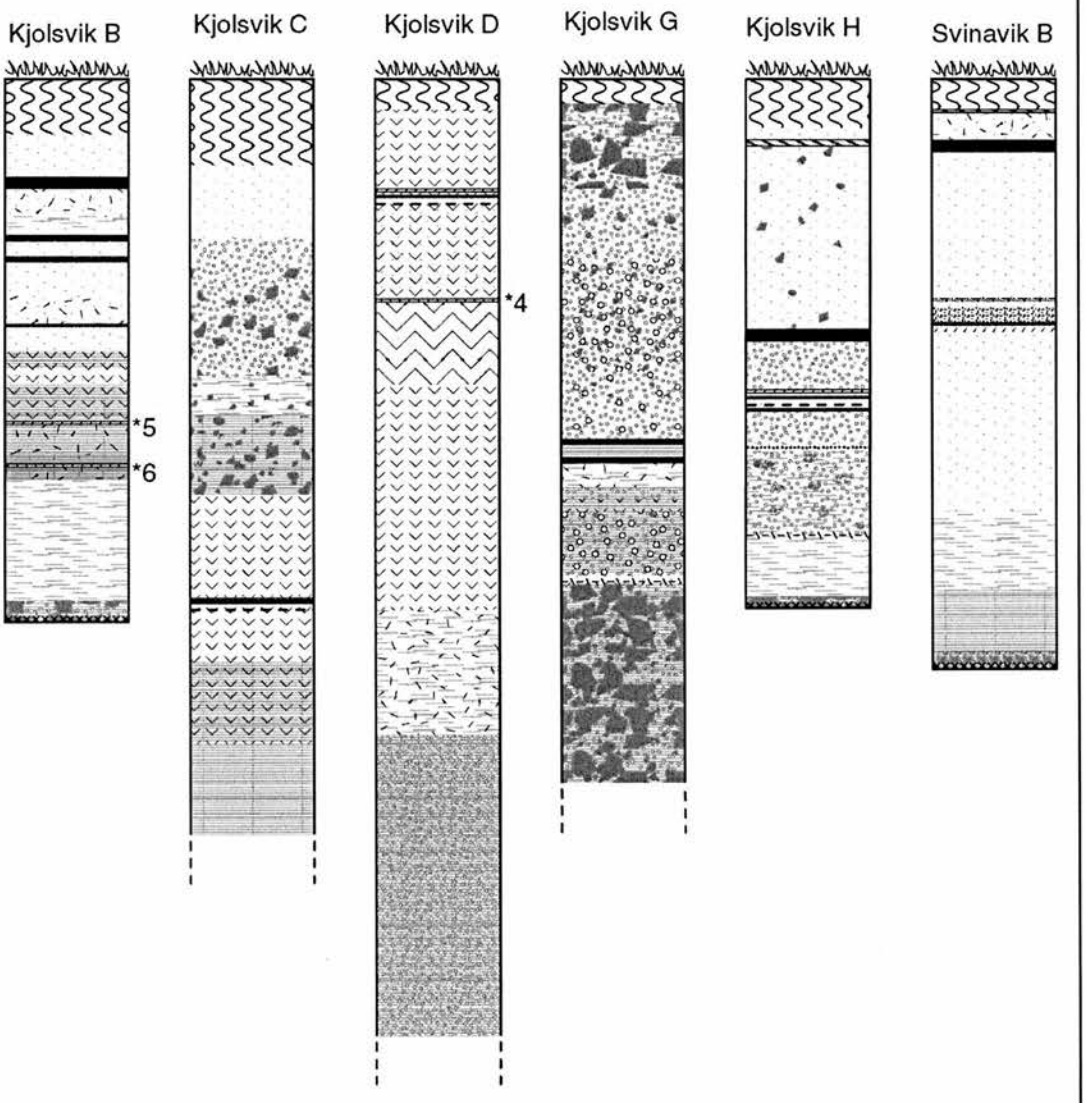

Figure 5.2-c (x): Stratigraphic Profiles – Lagarfljót, Húsavík, Jökulsá and Loðmundarfjörður

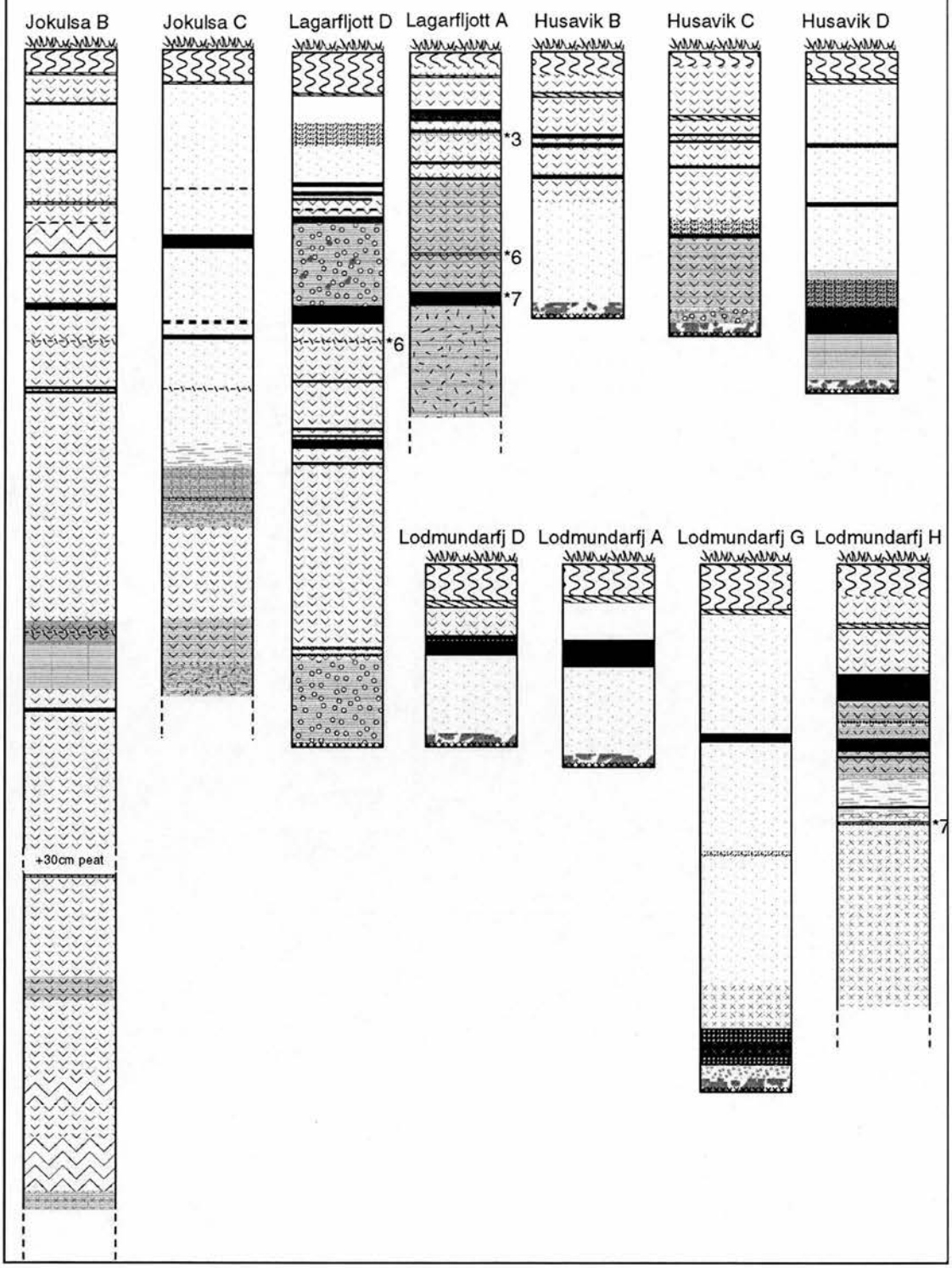

5.2.2. Geochemical data

Tephra samples were collected in the field, and selected for geochemical analysis following assessment of the initial stratigraphy. This selection of samples was motivated by a need to clarify putative links between certain tephra layers in disparate profiles, and to determine the origins of particular layers. Table 5.2-a presents average weight percentage values for each measured oxide in each analysed sample, and includes the standard deviation from the grains analysed in each sample (in *italics*). The full tables of geochemical data are found in Appendix II. The sample names of tephra layers characterised in the geochemical tables relate to those layers highlighted with a "*" in the stratigraphic diagrams in Figure 5.2-c.

Table 5.2-a: Summarised geochemical data from sampled tephras (weight % values)

Volcanic Origin	*Sample name*	*SiO2*	*TiO2*	*Al2O3*	*FeO*	*MnO*	*MgO*	*CaO*	*Na2O*	*K2O*	*Total*
Askja 1875	Vik D-15	72.63	0.77	12.25	3.31	0.09	0.65	2.34	3.50	2.39	98.10
	Vik D-15	*0.73*	*0.05*	*0.19*	*0.30*	*0.04*	*0.08*	*0.21*	*0.28*	*0.08*	*0.53*
Veiðivötn 1477	Vik D-14	49.50	1.99	13.50	12.91	0.23	6.47	11.15	2.41	0.25	98.70
	Vik D-14	*0.43*	*0.09*	*0.31*	*0.41*	*0.03*	*0.17*	*0.11*	*0.27*	*0.03*	*0.47*
Askja	Vik D-13	72.70	0.75	12.16	3.17	0.10	0.62	2.23	3.34	2.43	97.65
	Vik D-13	*0.64*	*0.04*	*0.14*	*0.18*	*0.02*	*0.05*	*0.17*	*0.29*	*0.08*	*0.81*
"Brúnavík B" (Grímsvötn)	Brun B-3	49.02	2.44	13.33	12.30	0.19	6.53	11.16	2.75	0.33	98.41
	Brun B-3	*0.28*	*0.14*	*0.17*	*0.48*	*0.06*	*0.30*	*0.36*	*0.09*	*0.06*	*0.40*
"Brúnavík A" Hekla (1158?)	Borg E-2	67.02	0.46	14.41	5.55	0.16	0.43	2.97	4.87	2.26	98.25
	Borg E-2	*1.40*	*0.04*	*0.48*	*0.40*	*0.03*	*0.03*	*0.23*	*0.37*	*0.12*	*2.50*
	Borg G-12	65.28	0.42	14.66	5.01	0.17	0.38	3.16	5.04	2.10	96.32
	Borg G-12	*2.22*	*0.03*	*0.91*	*0.60*	*0.05*	*0.06*	*0.33*	*0.37*	*0.24*	*3.02*
	La A-3	66.87	0.43	14.36	5.36	0.18	0.43	3.03	5.11	2.22	98.09
	La A-3	*1.14*	*0.04*	*0.64*	*0.36*	*0.05*	*0.04*	*0.19*	*0.34*	*0.13*	*1.39*
	Brun B-4	66.80	0.45	14.40	5.52	0.18	0.44	3.04	5.10	2.20	98.24
	Brun B-4	*0.50*	*0.03*	*0.17*	*0.12*	*0.03*	*0.02*	*0.05*	*0.12*	*0.12*	*0.66*
??	Brun B-6	49.06	2.05	13.75	11.17	0.20	7.27	11.96	2.58	0.31	98.66
	Brun B-6	*0.21*	*0.04*	*0.18*	*0.12*	*0.03*	*0.08*	*0.10*	*0.06*	*0.04*	*0.34*
Landnam	Brun C-3	50.10	1.75	13.81	12.18	0.23	6.61	11.42	2.42	0.20	99.02
	Brun C-3	*0.45*	*0.13*	*0.22*	*0.41*	*0.05*	*0.24*	*0.35*	*0.15*	*0.03*	*0.56*

??	Brun D-10	48.93	1.74	13.51	12.10	0.20	7.27	11.96	2.48	0.20	98.67
??	*Brun D-10*	*0.41*	*0.10*	*0.19*	*0.58*	*0.04*	*0.32*	*0.34*	*0.13*	*0.03*	*0.60*
Veiðivötn?	Brun C-4	49.52	1.95	13.37	13.11	0.25	6.06	11.05	2.52	0.24	98.35
	Brun C-4	*0.22*	*0.05*	*0.26*	*0.30*	*0.05*	*0.14*	*0.18*	*0.05*	*0.03*	*0.37*
??	Kjol B-5	45.36	2.61	15.10	12.88	0.19	7.31	10.76	2.85	0.40	97.84
	Kjol B-5	*0.35*	*0.10*	*0.45*	*0.29*	*0.05*	*0.22*	*0.19*	*0.11*	*0.03*	*0.50*
??	La-D6	48.19	1.98	13.33	12.05	0.24	6.75	11.32	2.63	0.25	97.05
	La-D6	*0.80*	*0.36*	*0.33*	*0.66*	*0.02*	*0.33*	*0.46*	*0.18*	*0.08*	*0.85*
Grímsvötn	Brun H-4	49.42	2.75	12.89	13.41	0.21	5.78	10.11	2.99	0.39	98.33
	Brun H-4	*0.27*	*0.15*	*0.38*	*0.37*	*0.06*	*0.50*	*0.43*	*0.17*	*0.06*	*0.38*
	Vik E-8	49.19	2.84	12.93	13.18	0.23	5.67	10.16	2.98	0.46	98.06
	Vik E-8	*0.91*	*0.19*	*0.31*	*0.65*	*0.02*	*0.48*	*0.60*	*0.15*	*0.12*	*0.33*
Hekla 3	Brun C-6	71.01	0.16	13.76	2.67	0.09	0.13	1.92	4.83	2.60	97.23
	Brun C-6	*1.80*	*0.04*	*0.76*	*0.58*	*0.04*	*0.03*	*0.54*	*0.41*	*0.54*	*2.41*
	Brun D-13	71.15	0.17	13.88	2.98	0.09	0.14	1.94	4.76	2.42	97.56
	Brun D-13	*0.97*	*0.02*	*0.32*	*0.11*	*0.04*	*0.01*	*0.07*	*0.69*	*0.07*	*1.86*
	Kjol B-6	70.67	0.24	13.90	3.04	0.13	0.19	2.18	5.16	2.45	98.00
	Kjol B-6	*1.23*	*0.19*	*0.96*	*0.25*	*0.04*	*0.16*	*0.44*	*0.36*	*0.24*	*0.99*
	Kjol D-4	70.48	0.17	14.01	2.85	0.08	0.14	2.05	5.19	2.47	97.48
	Kjol D-4	*0.93*	*0.03*	*0.66*	*0.25*	*0.06*	*0.02*	*0.23*	*0.34*	*0.21*	*1.65*
	Borg E-5	70.85	0.17	13.74	2.88	0.11	0.13	1.90	4.93	2.42	97.17
	Borg E-5	*1.34*	*0.02*	*0.37*	*0.12*	*0.04*	*0.02*	*0.06*	*0.14*	*0.08*	*1.86*
	Brun H-3	68.45	0.43	13.60	4.45	0.14	0.51	2.56	4.91	2.29	97.47
	Brun H-3	*4.22*	*0.53*	*0.82*	*2.67*	*0.06*	*0.74*	*1.14*	*0.44*	*0.40*	*1.11*
	Lo H-7	69.80	0.21	13.89	3.35	0.11	0.19	2.23	5.20	2.34	97.36
	Lo H-7	*2.39*	*0.10*	*0.59*	*0.95*	*0.04*	*0.15*	*0.74*	*0.12*	*0.30*	*1.45*
	La A-6	68.78	0.28	13.63	3.75	0.14	0.30	2.29	5.04	2.39	96.66
	La A-6	*3.15*	*0.25*	*0.49*	*1.70*	*0.03*	*0.36*	*0.85*	*0.26*	*0.27*	*1.02*
	Vik D-12	71.67	0.17	13.68	3.02	0.11	0.13	1.97	4.35	2.47	97.61
	Vik D-12	*0.39*	*0.01*	*0.17*	*0.12*	*0.02*	*0.02*	*0.03*	*0.41*	*0.08*	*0.53*
Veiðivötn	Brun H-2	48.90	1.82	13.51	11.72	0.20	7.19	11.99	2.45	0.22	98.30
	Brun H-2	*0.34*	*0.30*	*0.16*	*0.38*	*0.04*	*0.30*	*0.41*	*0.13*	*0.05*	*0.34*
Grímsvötn	Brun D-14	49.49	2.50	13.29	13.05	0.25	5.89	10.34	3.00	0.39	98.62
	Brun D-14	*1.00*	*0.14*	*0.31*	*0.59*	*0.05*	*0.82*	*0.90*	*0.16*	*0.12*	*0.63*
Vk 3&4	Vik K-4	72.70	0.05	11.64	1.01	0.04	0.03	0.50	3.72	4.31	94.03
	Vik K-4	*0.76*	*0.01*	*0.23*	*0.13*	*0.02*	*0.01*	*0.07*	*0.18*	*0.15*	*0.85*
	Vik K-3	72.40	0.09	11.95	1.33	0.05	0.07	0.65	3.92	4.26	94.72
	Vik K-3	*3.01*	*0.14*	*1.11*	*1.07*	*0.06*	*0.12*	*0.45*	*0.60*	*0.18*	*0.83*
	Vik H-8	73.66	0.04	11.67	1.07	0.03	0.04	0.59	3.71	4.58	95.39
	Vik H-8	*0.67*	*0.01*	*0.08*	*0.13*	*0.03*	*0.02*	*0.03*	*0.12*	*0.13*	*0.68*
	Vik F-4	73.46	0.05	11.61	1.05	0.05	0.03	0.54	3.62	4.54	94.94
	Vik F-4	*0.35*	*0.02*	*0.16*	*0.09*	*0.03*	*0.01*	*0.03*	*0.51*	*0.25*	*0.71*
	Vik J-2	73.24	0.05	11.63	1.05	0.04	0.03	0.57	3.96	4.40	94.96

	Vik J-2	*0.33*	*0.02*	*0.17*	*0.06*	*0.05*	*0.02*	*0.05*	*0.27*	*0.24*	*0.67*
	Vik J-6	72.46	0.07	11.52	1.24	0.06	0.04	0.59	3.97	3.90	93.87
	Vik J-6	*2.05*	*0.06*	*0.63*	*0.99*	*0.05*	*0.04*	*0.25*	*0.61*	*1.26*	*2.76*
Hekla 4	La A-7	60.55	0.88	14.20	8.43	0.26	1.10	4.35	4.76	1.68	96.60
	La A-7	*3.97*	*0.31*	*0.55*	*2.29*	*0.07*	*0.41*	*1.00*	*0.24*	*0.41*	*0.94*
	Brun C-7	62.48	0.77	14.63	7.97	0.23	0.93	4.21	4.29	1.77	*97.60*
	Brun C-7	*3.48*	*0.25*	*0.68*	*2.23*	*0.09*	*0.36*	*0.99*	*0.43*	*0.35*	*1.81*
	Brun C-8	69.09	0.33	13.47	4.26	0.16	0.33	2.40	4.75	2.43	97.33
	Brun C-8	*5.12*	*0.33*	*0.76*	*3.03*	*0.08*	*0.45*	*1.39*	*0.41*	*0.51*	*0.85*
	Brun C-9	64.68	0.48	14.48	5.10	0.16	0.61	3.57	4.72	1.99	96.02
	Brun C-9	*6.72*	*0.45*	*3.67*	*3.68*	*0.09*	*0.64*	*2.45*	*0.51*	*0.83*	*2.12*
	Vik D-10	69.65	0.37	13.34	4.09	0.15	0.48	2.44	4.69	2.40	97.77
	Vik D-10	*5.94*	*0.43*	*0.87*	*3.31*	*0.08*	*0.71*	*1.76*	*0.20*	*0.63*	*0.89*
	Vik D-11	61.03	0.92	14.31	8.58	0.25	1.18	4.46	4.34	1.59	97.09
	Vik D-11	*3.85*	*0.27*	*0.68*	*1.89*	*0.05*	*0.41*	*0.93*	*0.34*	*0.42*	*1.66*
	Vik K-5	64.80	0.66	13.91	6.22	0.19	0.91	3.38	4.27	2.31	96.96
	Vik-K-5	*6.87*	*0.51*	*1.03*	*4.07*	*0.11*	*0.79*	*1.82*	*0.70*	*0.99*	*1.10*
	Vik H-9	66.38	0.53	14.51	5.31	0.15	0.57	2.95	5.17	2.51	98.30
	Vik H-9	*6.49*	*0.52*	*1.94*	*4.23*	*0.09*	*0.61*	*2.03*	*1.18*	*1.27*	*1.54*
	Brun D-15	71.31	0.16	13.56	2.54	0.11	0.04	0.65	6.11	3.71	98.20
	Brun D-15	*2.14*	*0.09*	*1.66*	*1.20*	*0.04*	*0.03*	*0.35*	*0.97*	*0.52*	*1.24*
?	Vik D-9	49.56	3.15	12.89	14.32	0.26	4.90	9.09	3.07	0.67	98.43
	Vik D-9	*0.56*	*0.21*	*0.27*	*0.26*	*0.03*	*0.36*	*0.47*	*0.11*	*0.10*	*0.31*
	Vik K-7	47.92	3.18	12.76	14.38	0.26	5.07	9.29	3.10	0.64	97.08
	Vik K-7	*0.65*	*0.38*	*0.29*	*0.65*	*0.03*	*0.51*	*0.59*	*0.13*	*0.08*	*0.36*
?	Vik D-8	49.85	1.39	14.16	10.09	0.19	8.55	13.34	2.06	0.12	100.03
	Vik D-8	*0.33*	*0.06*	*0.28*	*0.83*	*0.01*	*0.56*	*0.52*	*0.11*	*0.04*	*0.62*
	Vik D-7										
?	Vik D-6	49.81	2.30	13.09	12.84	0.21	6.04	10.51	2.70	0.37	98.27
	Vik D-6	*0.80*	*0.21*	*0.24*	*0.39*	*0.04*	*0.53*	*0.74*	*0.22*	*0.11*	*0.64*
Grímsvötn	Vik K-8	48.29	1.96	13.25	12.34	0.21	6.89	11.32	2.58	0.32	97.48
	Vik K-8	*0.65*	*0.33*	*0.30*	*0.82*	*0.03*	*0.48*	*0.66*	*0.18*	*0.05*	*0.41*
?	Vik D-5a	73.71	0.08	11.68	1.66	0.05	0.02	0.56	3.43	4.27	95.45
	Vik D-5a	*0.32*	*0.08*	*0.30*	*0.88*	*0.03*	*0.01*	*0.17*	*0.73*	*0.53*	*0.53*
	Vik D-5b	49.53	2.23	12.18	12.56	0.23	6.59	11.32	2.36	0.32	97.67
	Vik D-5b	*1.00*	*0.40*	*3.31*	*1.05*	*0.02*	*1.52*	*2.88*	*0.75*	*0.16*	*2.50*
?	Vik D-4	49.29	2.47	13.32	13.12	0.23	6.33	10.59	2.79	0.34	98.84
	Vik D-4	*0.24*	*0.06*	*0.15*	*0.42*	*0.02*	*0.31*	*0.26*	*0.05*	*0.02*	*0.47*
?	Vik D-3	74.41	0.07	11.98	1.46	0.05	0.03	0.67	3.46	3.84	96.00
	Vik D-3	*1.67*	*0.06*	*0.48*	*0.58*	*0.04*	*0.03*	*0.33*	*0.53*	*0.79*	*1.60*
?	Vik D-2	75.05	0.04	12.01	1.13	0.04	0.03	0.50	3.17	4.11	96.09

	Vik D-2	*0.84*	*0.02*	*0.28*	*0.04*	*0.02*	*0.02*	*0.04*	*0.95*	*0.35*	*0.74*
Veiðivötn	Vik D-1a	48.72	1.84	13.96	10.95	0.19	7.83	12.32	2.41	0.22	98.71
	Vik D-1a	*0.26*	*0.03*	*0.15*	*0.16*	*0.02*	*0.15*	*0.05*	*0.05*	*0.03*	*0.46*
Grímsvötn	Vik D-1b	49.73	3.04	12.91	13.82	0.23	5.34	9.46	3.04	0.53	98.53
	Vik D-1b	*0.21*	*0.29*	*0.19*	*0.45*	*0.02*	*0.48*	*0.51*	*0.12*	*0.09*	*0.28*

Table 5.2-a presents AVERAGE values and *STANDARD DEVIATIONS* derived from all the grains analysed in each named sample. The "volcanic origin" column refers to the correlations which are developed in 5.3.2.

5.2.3. Radiometric Dating

The relative correlative dating framework provided by the tephrostratigraphy will be constrained into an absolute chronology through independent radiocarbon dating of pre-H4 (pre~4.2 cal. ka BP) tephra layers recovered from peat deposits. This will establish dating control for many unknown early Holocene tephras, and aid the development of a better constrained soil accumulation rate, enabling accurate dating of landforms which may be connected with the 8.2ka event. Radiocarbon dates for pre-H4 tephra layers will also extend and build on the Icelandic tephrostratigraphy for the Early Holocene, and for northeast Iceland, which has not received much attention.

Choosing the location of radiocarbon samples

The study was limited to ten radiocarbon dates. Therefore, geographic and stratigraphic locations of samples had to be chosen which would best serve to promote the research aims, that is, to date the observed landform suites discussed in Chapters 3 and 4, to assess their climatic significance.

As explained in Chapters 3 and 4, thirteen landform suites have been identified, and, given the provision of only ten dates, the best approach was to date well two profiles for which the tephrostratigraphy is well-resolved, and which are located respectively within and outwith one key landform suite. The locations of the radiocarbon-dated profiles are designed to provide minimum and maximum ages for a specific landform, and to act as reference profiles from which age-depth relationships can be

assessed, and pre-H4 tephra layers can be dated. It is then possible to deduce ages for other landform suites based on the improved tephrostratigraphy and the soil accumulation rates which the radiocarbon provides.

The other consideration in choosing samples is the availability of dateable material suitable for radiocarbon dating. Profiles which contain significant peat deposits were selected. Where possible, monoliths were excavated from such profiles whilst in the field, to enable controlled extraction of in situ peat back in the lab, providing high quality dateable samples.

Results

Two profiles, within and outwith landform suite *Víkurá-2* (see Chapter 3.2.7), were selected from which to retrieve radiocarbon samples. These profiles together bracket minimum and maximum ages for the arcuit moraine feature thought to represent a putative glacial advance at 8.2ka cal. yrs BP. Samples were taken in order to date key pre-H4 indicator tephras in each of two profiles which are respectively from within and outwith the margins of the mapped moraines (Víkurá K and Víkurá D). The basal peat was also dated.

The spread of samples through the profiles (the locations of which are illustrated in Figure 5.2-d) was chosen to provide an age-depth estimation which would better constrain soil accumulation rates and correlative ages for the mid to early Holocene. To allow accurate dating of tephras, the thin layer of peat immediately above and below each tephra layer (to provide minimum and maximum ages) was dated using Accelerator Mass Spectrometry (AMS) at the Scottish Universities Environmental Research Laboratory, East Kilbride (SUERC). Details of the procedures used are given in Appendix III. The radiocarbon ages derived for each sample are shown in Table 5.2-b, with tephra layers associated with each sample highlighted. Calibrated ages are derived from OxCal 3.9 (Bronk Ramsey 1995).

Table 5.2-b: Radiocarbon dates derived from AMS analysis

Associated Tephra	*Age*	*Lab No.*	*Sample*	*Fraction*	*δ13C*	Calibrated Age (BC/cal Ka BP)
VK-7	(min) 4400+/-35	GU-12842	Peat	Humic Acid	-28.4‰	3110-2910/ 5.11-4.92ka
VK-7	(max) 4480+/-35	GU-12841	Peat	Humic Acid	-28.1‰	3350-3080/ 5.35-5.08ka
VD-6	(min) 5100+/-35	GU-12838	Peat	Humic Acid	-26.7‰	3970-3790/ 5.97-5.79
VD-6	(max) 5150+/-35	GU-12839	Peat	Humic Acid	-26.5‰	3990-3940/ 5.99-5.94ka
VK-8	(min) 6565+/-40	GU-12840	Peat	Humic Acid	-28.5‰	5570-5470/ 7.57-7.47ka
VD-5	(max) 7810+/-40	GU-12837	Peat	Humic Acid	-29‰	6690-6570/ 8.69-8.57ka
VD-4	(max) 7910+/-35	GU-12836	Peat	Humic Acid	-28.2‰	6860-6640/ 8.86-8.64ka
VD-2	(max) 8345+/-40	GU-12835	Peat	Humic Acid	-30.1‰	7530-7310/ 9.53-9.31ka
VD-1	(max) 8450+/-35	GU-12833	Peat	Humic Acid	-29.7‰	7590-7380/ 9.59-9.38ka
Basal layer	8985+/-40	GU-12834	Peat	Humic Acid	-29.1‰	8280-8160/ 10.28-10.16ka

Figure 5.2-d: Location of radiocarbon samples within tephrostratigraphy

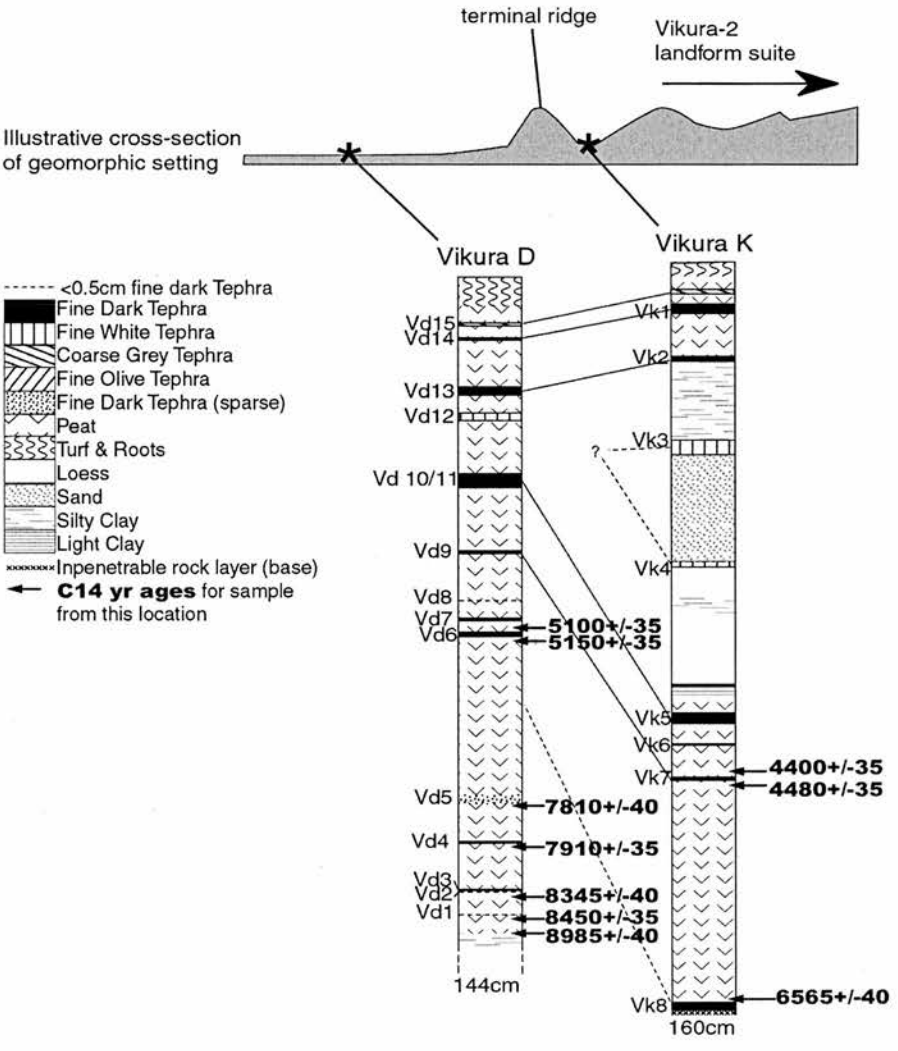

Radiocarbon dates are presented here in C14 years. Subsequent calibration of radiocarbon years to Calendar Years (cal. yr. BP) was undertaken using OxCal 3.9 (Bronk Ramsey 1995).

5.3. Development of a Tephrochronological framework

A new Holocene tephrostratigraphic record for the Borgarfjorður Eystri area of northeast Iceland is presented, which extends back to 8985+/-40 ^{14}C yrs BP (calibrated to 10.28-10.16 cal. ka BP using OxCal (Bronk Ramsey 1995), see Chapter 5.2.3). The use of geochemical data in addition to physical properties to correlate tephra layers in the field, and to link them with their genetic origin (in some cases the specific eruption), is explained in Chapter 2.4.1. Results are presented in

5.3.2. Where the existence of a tephra layer near the base cannot produce an age for the surface beneath, accumulation rates are used to derive ages (explained in 5.3.3). A dated stratigraphy is then produced, from which conclusions can be drawn as to the relative ages of mapped landforms.

5.3.1. Expected tephrostratigraphy

Before correlations are identified between tephras observed in the field, and those identified in the literature, it is useful to determine which layers are likely to exist in the field area. Tephra layers which provide the best time-marker horizons are a result of air-fall from volcanic eruptions. Therefore, the geographical extent of the tephra deposit is a result of the magnitude of the eruption, and the wind directions at the time of the eruption. Tephra will be deposited on the surface in the regions lying in the path of the wind, with the thickness of the tephra layer, and the coarseness of the grains, being linked to the distance from the eruption origin (Lacasse 2001). Isopach maps, which show the aerial spread and thickness of deposited tephra across Iceland, have been constructed for many of the well-documented eruptions (Haflidason et al. 2000). Through appeal to these it is possible to suggest which tephra layers one might expect to find in the field area. This serves as an informative backdrop against which to assess the observed stratigraphy, and when attempting to make correlations with known tephras based on geochemical data.

A summary of some of the main eruptions, whose tephra airfall directions suggest the possible existence of layers in the Borgarfjörður Eystri region, is shown in Figure 5.3-a. Layers noted here are Askja 1875, Hekla 1636, Veiðivötn 1477 (Benjamínsson 1980), Öræfajökull 1362 (Thorarinsson 1958), Hekla 1158, Vatnaöldur, Hekla 3 (Kirkbride et al. 2001) and Hekla 4 (Thórarinsson 1981; Kirkbride et al. 2001). In addition to these layers, the Saksunarvatn ash (9000 ^{14}C yr BP), is thought to have had a northerly and easterly distribution pattern from its Grímsvötn origin (Birks et al. 1996), making it a possible tephra layer to be found in excavated profiles in the field. Grímsvötn has the most frequent historic eruption

history of all volcanic systems in Iceland (Larsen 2000), making it a likely source of other tephra layers discovered in the field.

Figure 5.3-a: Tephra fallout which may have reached the field area, originating from well-documented eruptions.
(i) Isopach maps for known layers

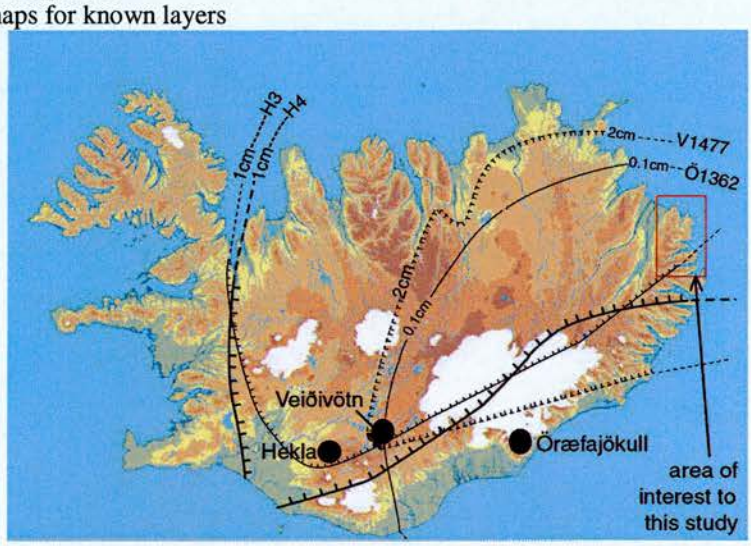

(ii) Other eruptions for which isopach maps were not found

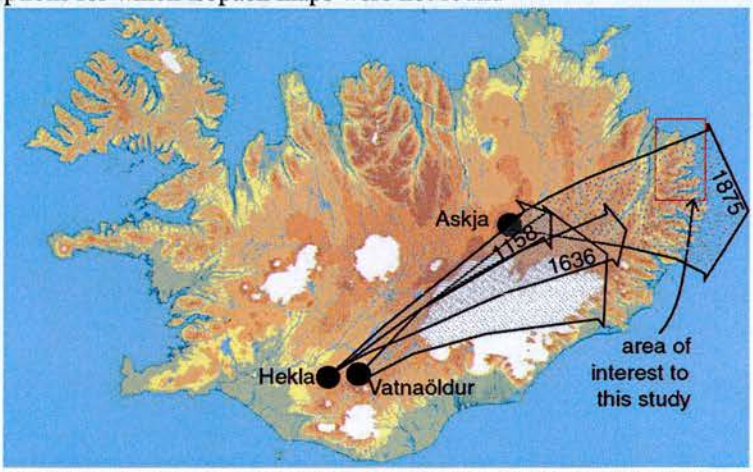

Figure 5.3 a represents the source areas of some well-known Icelandic tephras which one might expect to encounter in the Borgarfjörður Eystri region, as a result of wind patterns at the time of the eruption. Figure 5.3-a (i) presents a series of isopach maps of four key tephras. The contours representing Hekla 3 and Hekla 4 represent a 1cm thick tephra layer (Kirkbride and Dugmore 2001). The contour representing the 2cm Veiðivötn 1477 data was recorded in the literature to be an unknown "tephra a" (Benjamínsson 1980) which is now thought to relate to the V1477 eruption. The Öræfajökull data represents a layer of only 0.1cm in he field area (Thorarinsson 1958), so may be less easily identified in the field. Figure 5.3-a (ii) is adapted from Haflidason et al. (2000), and shows the main fallout directions of some other known tephras for which detailed ispoach maps were not found. There are likely to be many more tephra layers than those illustrated here, given the limited information available on pre-historic tephras

The location of the field site is both beneficial and limiting for tephrostratigraphy. It is relatively distant from the main volcanic regions, so the number of airfall tephra layers reaching the region, and the thickness of the layers, is low relative to more proximal areas. However, the Borgarfjörður region provides an excellent sedimentary record since the Younger Dryas due to the limited impact of the Little Ice Age (Gudmundsson 1997), which in many parts of Iceland has destroyed the Holocene sedimentary record (Kirkbride et al. 2001). The fact that Little Ice Age glacial activity was constrained to high corries, means that early Holocene sediments are preserved largely undisturbed. In addition, extensive well-humified peat deposits in the area enable good preservation of tephra layers. Therefore, if the tephra was deposited by airfall in the area, it is likely to be preserved in the stratigraphy, if only as a thin layer.

5.3.2. Correlations between tephra layers

Correlations can be made, to an extent, based on physically observable properties of the tephra (colour and grain-size), and the location of the tephra in a profile relative to other layers. However, given the fact that many layers are indistinguishable based on physical characteristics, and that every airfall tephra may not be visible or preserved in a profile, the geochemical "signature" of key tephra layer provides valuable correlative evidence. Volcanic systems can be distinguished between because of their often distinctive geochemical signature, which is reflected in their associated tephra. As seen in 5.2.2, nine major element oxides were measured from each tephra sample, to determine the geochemical signature, and where possible, the volcanic system of origin.

The visualisation of this geochemical signature makes the development of initial correlations easier. It is difficult to visualise all nine measure oxides in a single figure, so if the oxides can be identified which best explain the differences between tephra layers, identification of correlations is made easier. Those oxides which best explain differences, are those which are present in the most variable levels between volcanic origins. Variations in geochemical make-up between layers, defined by

weight percentage values of two or three key oxides plotted against each other, can then be graphed as a visualisation and correlation tool. Initial correlations can be tested by assessing the consistency of the full geochemical tables of each group of layers.

To assess which oxides are most significant, a number of triangular plots are developed which compare the levels of three oxides. Where variation in one oxide is large between volcanic origins, the points on the plot are more spread out, so that distinct groups of layers, which may be only subtly different, are more readily visible. Figure 5.3 b shows the geochemically characterised tephra layers in two triangular plots, each comparing variation in three oxides. When three oxides are compared against each other in such graphs, clustering of points occurs, indicating that the tephra layers represented by these points share geochemical characteristics in at least these three oxides. When such groups of points are consistently found to cluster in plots which investigate many different sets of three oxides, it strengthens the evidence for a common geochemistry between the layers, and thus strengthens the hypotheses for a shared volcanic origin.

It can be seen that the three oxides plotted in Figure 5.3 b (ii), show more variation than those in Figure 5.3 b (i). Clustering of points which occurs in Figure 5.3 b (i) is better defined in Figure 5.3 b (ii), indicating that the relationship between Silica, Iron and Titanium oxide is a key indicator of volcanic origin. For example, two points representing two layers which appear to correlate well with the Askja volcanic system, are visibly very separate from the other points in Figure 5.3 b (ii), whereas in Figure 5.3 b (i) they are in closer proximity to other points, and less easily distinguished. On investigation of the area of Figure 5.3 b (i) which represents the Katla system, it appears possible that some of the basaltic layers from this study may have an origin in Katla, as the points plot in the same region of the graph as the area representing Katla. However with reference to Figure 5.3 b (ii), it is clear that none of the tephras from this study correlate with Katla, as this volcanic region is distinct and distant from any of the points representing this study's tephras.

Figure 5.3-b: Major element composition of tephra layers sampled in the field, compared with composition of some well-documented Icelandic tephras

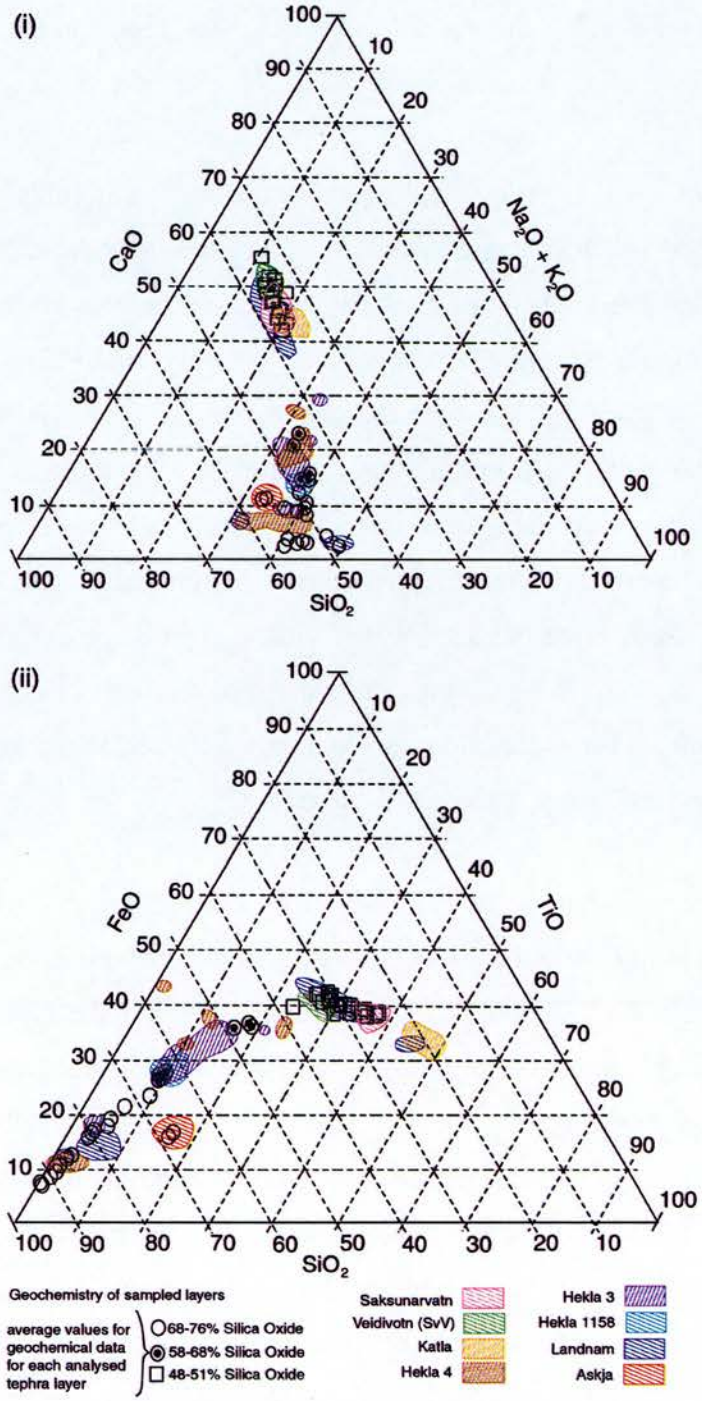

Geochemical data illustrated in these figures was derived from various references publishing Icelandic tephra geochemistry data (Boygle 1994; Dugmore et al. 1997; Hannon et al. 1998; Larsen et al. 1999; Wastegård et al. 2001; Hall and Pilcher 2002). The upper graph (i) plots Silica, Calcium and combined total alkalis (Potassium and Sodium Oxide), while the lower graph (ii) plots Silica, Titanium and Iron Oxide. Weight percentage values of various element oxides in all geochemically characterised tephra layers are normalized to 100%.

From Figure 5.3-b, possible correlations are identified between measured tephra layers, and a number of volcanic systems: Hekla, Askja, Veiðivötn, Torfajökull (origin of the Landnam ash) and Grímsvötn (origin of the Saksunarvatn ash). With reference to the relative position of tephra layers within the recorded stratigraphy, various dated Late and mid-Holocene tephras including Askja 1875, Veiðivötn 1477, Landnam, Hekla 3, 3295 +/-95 cal. yr BP (Zillen et al. 2002) and Hekla 4, 4390+/-107 cal. yr. BP (Zillen et al. 2002) are identified in the field area based on appearance, physical characteristics and geochemical composition, allowing provisional association with the existing Icelandic tephrostratigraphy. Information is presented here on each geochemically identified tephra layer, and where correlations are apparent with known Icelandic tephras, they are presented.

From Figure 5.3-b, the Titanium/Iron Oxide relationship is a key representative of geochemical variation between distinct tephras. The Titanium/Iron Oxide ratio, alongside ratios of Magnesium/Calcium Oxide, is commonly used in the literature as a visualisation tool for correlations (e.g. Dugmore et al. 1992b; 1995). Given their proven track-record as key indicators, in the following section, these are the main sets of oxides which are graphed to investigate correlations. It should be noted though, that identification of correlations are not based purely on this relationship, but on detailed assessment of all the geochemical data (Appendix II).

Geochemical data for known tephra layers in Figures 5.5-c to -n are derived from the following references (corresponding reference numbers are shown in the figure keys, alongside the name of each known tephra layer): 1 (Larsen et al. 1999), 2 (Boygle 1994), 3 (Wastegård et al. 2001), 4 (Hannon et al. 1998), 5 (Hall et al. 2002), 6 (Dugmore and Newton 1992a), 7 (Pilcher et al. 1996b) , 8 (Pilcher and Hall 1996a), 9 (Pilcher et al. 1995), 10 (Dugmore et al. 1995), 11 (Dugmore et al. 1992b), 12 (Dugmore et al. 1997) and 13 (Chambers et al. 2004).

Samples represented have names in the format "Abbreviated name, Letter, - Number", where the name refers to the general location of the profile (a sub-section of the field area), the letter refers to the specific profile in that region, and the

number refers to the sample analysed. For example "Vik D-4" represents Sample 4 taken from profile "D" in the Víkurá valley. In Table 5.3-a the abbreviations for different sub-sections of the field area are presented.

Table 5.3-a: Naming sub-sections of the field area

Sub-section of field area	Abbreviation
Víkurá	Vik
Brúnavík	Brun
Borgarfjörður	Borg
Kjólsvík	Kjol
Loðmundarfjörður	Lo
Lagarfljót	La

The geochemistry of all sampled and analysed tephra layers is illustrated below, using the geochemical data which is summarized in 5.2.2, and which is presented in full in Appendix II.

Figure 5.3-c: Correlations between tephra layers from this study, and "Landnam", Veiðivötn (Svv and 1477) and "Askja 1875"

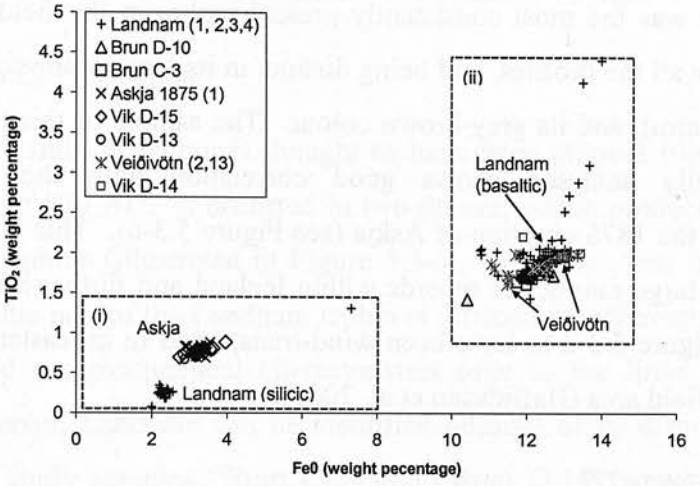

In Figure 5.3-c, key historic-age tephras are investigated. As can be seen, the Landnam ash has two distinct populations – basaltic and silicic. Tephras from the field area match the basaltic fraction but not the silicic. Askja ash is silicic and Veiðivötn ash is basaltic. In (i), correlations between sampled tephras and the silicic historic ashes are investigated, while in (ii) correlations with basaltic historic tephras are assessed.

(i) Landnam (silicic) and Askja

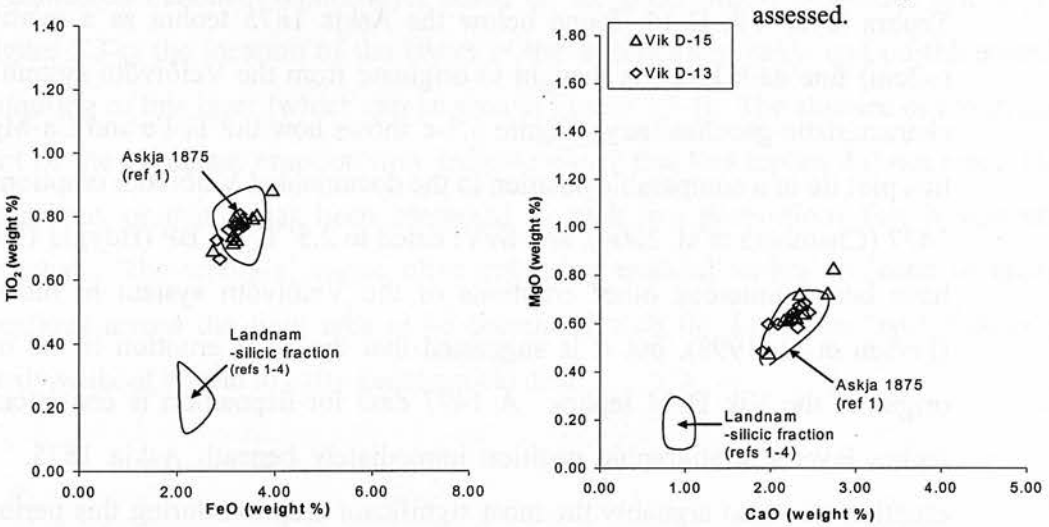

(ii) Landnam (basaltic) and Veiðivötn

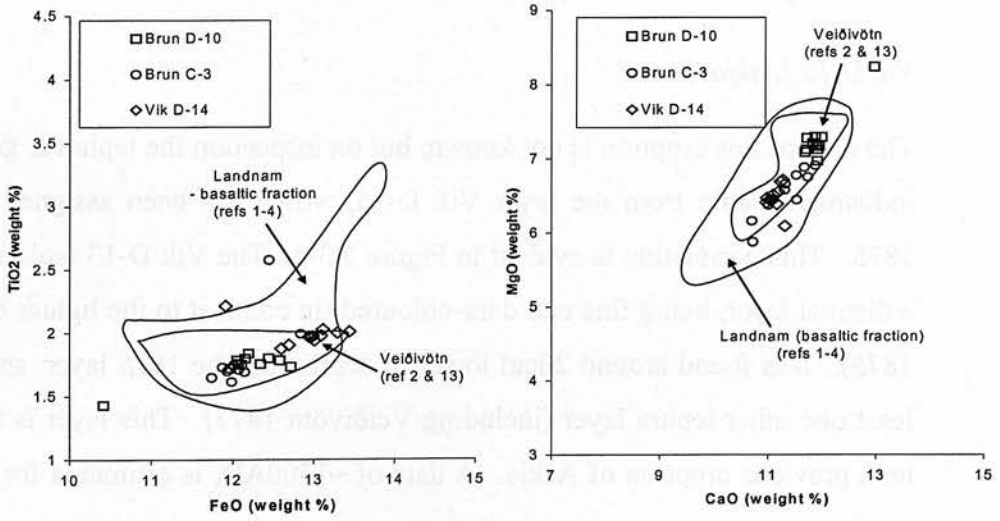

Vik D-15 [Askja 1875]

This tephra layer was the most consistently present tephra in the field area, being apparent in nearly all the profiles, and being distinct in its large grain-size relative to other tephras (>2mm), and its grey-brown colour. The sample of this tephra which was geochemically analysed shows good correlation with the documented geochemistry for the 1875 eruption of Askja (see Figure 5.3-c). This layer has been documented in a large number of records within Iceland and further afield, and has been shown in Figure 5.3-a to have been wind-transported in an easterly direction, directly over the field area (Haflidason et al. 2000).

Vik D-14 [Veiðivötn 1477]

Tephra layer Vik D-14, found below the Askja 1875 tephra as a relatively thick (~2cm) fine dark layer, is thought to originate from the Veiðivötn system due to its characteristic geochemistry. Figure 5.3-c shows how the Ti-Fe and Ca-Mg levels in this plot lie in a comparable position to the documented Veiðivötn eruption data from 1477 (Chambers et al. 2004), and SvV, dated to 2.5^{14}C yrs BP (Boygle 1994). There have been numerous other eruptions of the Veiðivötn system in historical time (Larsen et al. 1998), but it is suggested that the 1477 eruption is the most likely origin of the Vik D-14 tephra. A 1477 date for deposition is consistent with the tephra layer's stratigraphic position immediately beneath Askja 1875. The 1477 eruption was also arguably the most significant eruption during this period in terms of tephra production and deposition over mainland Iceland (Chambers et al. 2004).

Vik D-13 [Askja?]

The date of this eruption is not known, but on inspection the tephra is geochemically indistinguishable from the layer Vik D-15, which has been assigned to be Askja 1875. This correlation is evident in Figure 5.3-c. The Vik D-13 tephra is, however, a distinct layer, being fine and dark-coloured (in contrast to the lighter coarser Askja 1875). It is found around 20cm lower in depth than the 1875 layer, separated by at least one other tephra layer (including Veiðivötn 1477). This layer is considered to be a previous eruption of Askja. A date of ~1300AD, is estimated for this eruption

later in the chapter, based on relative stratigraphic location and accumulation rate, hence the name, for the purposes of this study, "A~1300".

Brun C-3 [Landnam]

The Landnam tephra is thought to have been erupted from the Torfajökull system around 870 AD. It occurred in two phases, which produced basaltic (B) and silicic (A) tephras (illustrated in Figure 5.3-c). It can be seen from Figure 5.3-c that the basaltic part of the Landnam tephra is difficult to differentiate from Veiðivötn tephra based on geochemical characteristics (due to the links between these systems). However, Landnam can be identified because of its distinctive olive-green colour. The study samples "Brun C-3" and "Brun D-10" were correlated with the well-documented Landnam tephra layer based on the geochemical properties evident in Figure 5.3-c, the location of the layers in the tephrostratigraphy, and on the unique colouring of this layer (which can be seen in Figure 5.3-l). The absence of the silicic part of the Landnam eruption may indicate either that this tephra did not reach the field area, or that it has been preserved in such low proportions that it was not detected. The tephra's unique olive colouring enabled tephra recorded in many locations across the field area to be correlated with the Landnam layer relatively easily without appeal to extra geochemical data.

Figure 5.3-d: Correlations between tephra layers from this study, and "Hekla 1158"

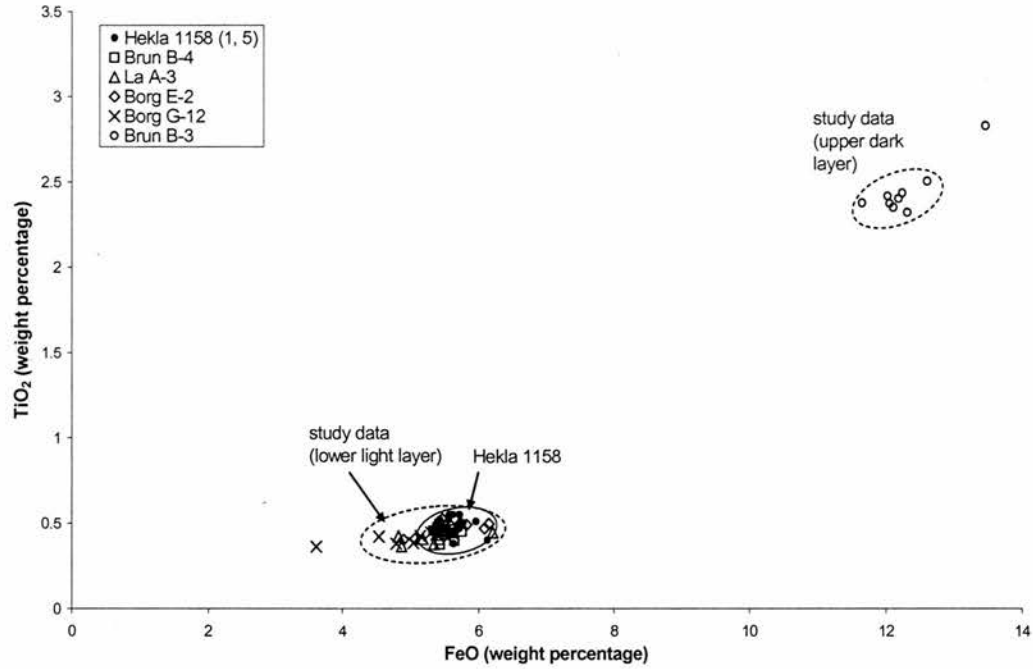

Figure 5.3-d illustrates the geochemical distinction between a pair of tephras found juxtaposed in many sections. The lower (lighter) tephra of the pair correlates with the Hekla 1158 tephra.

Brun B-3&4 [Hekla 1158 & an unknown basaltic layer]

Two layers, a fine dark tephra above (Brun B-4) and a fine light grey tephra below (Brun B-3), are commonly found juxtaposed in the field area (see illustrated photographs of profiles Brúnavík D and E in Figure 5.3-k). Their stratigraphic position shows them to be above Landnam, but below Veiðivötn 1477. The geochemistry of these layers is graphed in Figure 5.3-d. This distinctive double layer is traceable in some of the valleys in the field area, enabling correlations to be made, but the layers are not evident in all regions. Samples of light grey tephras, which were present in some profiles individually, are plotted in Figure 5.3-d. These tephras (Borg E-2, Borg G-12 and La A-3) are found to share geochemical characteristics with Brun B-3, the light part of the double-layer. This single light layer is never found in the same profile as the double layer, and the location in the profiles relative to other known tephra layers indicates a similar depositional age. It is concluded that these single light layers relate to the same eruption as the lower light layer Brun B-4.

When profile Brun D is investigated, it is seen that a thin and patchy later of silt is visible between the light and dark layers, showing that the deposition of these layers was temporally distinct, and probably a result of two separate eruptions. The lack of genetic link is backed up by the different geochemical properties of the light and dark tephras. The light tephra appears to share characteristics with the Hekla 1158 layer (see Figure 5.3-d). The Hekla 1158 tephra data plotted in Figure 5.3-d (Larsen et al. 1999; Hall et al. 2002), is better constrained in terms of the spread of data. However, the main body of the study data falls within this region, and is clearly a product of the Hekla system. On comparison with other Hekla eruption data, Figure 5.3-j shows the well-constrained cluster of data representing H1158, clearly distinct from other major Hekla eruptions. The Hekla 1158 eruption is thought to have taken a roughly easterly trajectory from the source (Figure 5.3-a), over the field area, so it is the most likely eruptive origin of the tephras Brun C-3, Borg E-2, Borg G-12 and La A-3.

The dark upper layer of the pair may have originated from the Grímsvötn system. The absence of this upper layer immediately above the light layer in some regions can then be explained in that the dark layer may be in existence, but separated by a thicker layer of sediment due to higher accumulation rates in some areas. Alternatively, the later eruption may have a less continuous cover due to the airfall patterns and weather conditions at the time of the eruption, combined with the topographic characteristics of the field area.

Figure 5.3-e: Other post-Hekla 3 basaltic tephras

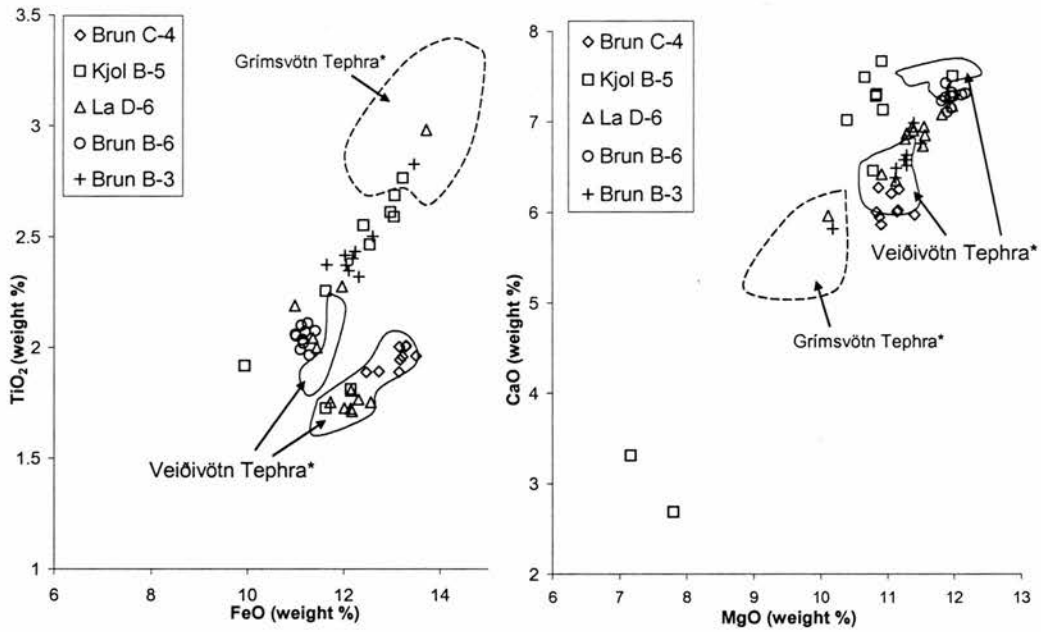

Figure 5.3-e represents the other basaltic tephras aged older than those discussed in Figure 5.3-d, but younger than Hekla 3. Clear relationships are observed between some sampled tephras and the Veiðivötn ash, but no sampled layers appear to correlate well with Grímsvötn ash. *Data for the Grímsvötn ash is derived from the Saksunarvatn eruption (Dugmore and Newton 1997; Wastegård et al. 2001). Veiðivötn data is for data for SvV and V1477 (Boygle 1994; Chambers et al. 2004).

Brun C-4 [Veiðivötn]

This layer is a fine dark tephra, with some greenish grains. It is assigned to be of Veiðivötn origin based on its geochemical properties. Figure 5.3-e shows the good correlation between Brun C-4 tephra shards, and Veiðivötn tephras. The layer is found immediately below the Landnam tephra, which would give it an age pre-dating ~870AD, thus not correlating with the well-documented V1477 eruption.

Kjol B-5, La D-6, Brun B-6 and Brun B-3 [unknown origin]

Four other basaltic tephras are analysed, which are found above the Hekla 3 tephra, for which geochemical data is presented in Figure 5.3-e. The best constrained of these layers is Brun B-6, which exhibits a strong clustering of points close to the area representing Veiðivötn. It is possible that this may represent a different Veiðivötn eruption. Many of the tephra grains from sample La D-6 also appear to correlate well with Veiðivötn. However, there are also a number of outliers of unclear origin,

so this correlation cannot be verified. Layer Kjol B-5 can be seen to have at least two main populations, one which may be of Veiðivötn origin, and one possibly of Grímsvötn origin, so its usefulness as a stratigraphic marker representing a clear airfall layer is questionable. Although Kjol B-6 and La D-6 were light coloured in appearance, their basaltic geochemistry shows that they may be mixed with light clays, not reflecting their true colours in their depositional environments. The layer Brun B-3 (the dark layer found immediately above Hekla 1158) is included in Figure 5.3-e, to show its possible connection to Grímsvötn. Based on its full geochemical data set, it does not resemble Veiðivötn in terms of its geochemistry.

Vik K-3 and Vik K-4 [unknown origin]

A pair of very fine pale tephra layers is found in profiles *Víkurá K* and *Víkurá E*, separated respectively by ~25cm of sand and ~5cm of peat. On inspection of the geochemical properties, the layers are found to have a characteristically low Titanium content (<0.1%). As can be seen from Figure 5.3-f, a number of other occurrences of tephras in the Víkurá valley (but nowhere else in the field area) share these geochemical properties, and can be ascribed the same volcanic origin. They are graphed in Figure 5.3-f, with the previously identified Askja tephras, and with the rhyolitic part of the Hekla 4 tephra (addressed later in this chapter), for comparison. The other occurrences of the unknown *Víkurá K* tephras are present as single layers, with the exception of two layers in the profile *Víkurá J*, which are separated by four other tephra layers and ~60cm of rocks and sand. The origin of these tephra layers could not be identified, but it is clear from the existence of multiple layers separated by other tephras, that at least two separate volcanic events are responsible for these tephras, and there may have been a significant time gap between them. As will be seen, further tephra layers sharing these unique, and tightly constrained geochemical properties, are found low down in profile Víkurá D, with two airfall layers dating to a minimum age of 8350+/-40 cal. yr. BP.

The study has been unable to trace the volcanic origin of these layers from the literature. It is a possibility that the layers may represent tephras of known origin which have been geochemically altered since deposition (such as described in

Dugmore et. al, 1992). However, if this were the case, more variation in the geochemistry of each tephra grain (and thus more spread in the data) might be expected, as processes inducing such modification are not likely to occur uniformly in each grain. In the light of available information, tephra layers exhibiting this distinct geochemical composition are described as being of unknown volcanic origin. For the purpose of this study this tephra will be referred to as the *Víkurá Tephra* (the Víkurá valley is the only location in the field area where this tephra has been identified). Samples Vik K-3 and Vik K-4 will be known as Tephras "Víkurá A" and "Víkurá B".

Determination of the stratigraphic position of layers Víkurá A and B relative to the key marker layer Hekla 3 has proved problematic. Occurrences of tephras matching this geochemistry, and in consistent stratigraphic locations relative to H4, A~1300 and V1477, have been identified in four profiles (Víkurá F, H, J and K), and a further two layers in profile Víkurá E are identified based on physical properties. However, none of these profiles also contain the layer Hekla 3, making determination of the relative stratigraphic location difficult. By way of temporal constraint it can be seen from the stratigraphic record in 5.2.1, that these layers post-date Hekla 4, and pre-date the Askja layer Vik D-13.

Figure 5.3-f.: Other post-Hekla 3 (?) silicic tephras

(i) Titanium/Iron

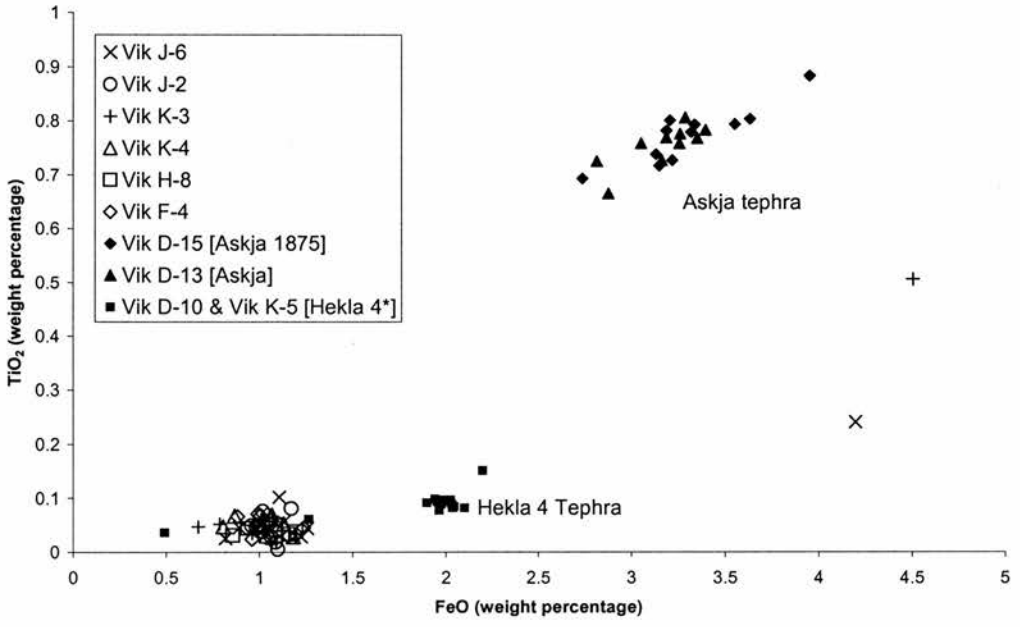

(ii) Calcium/Potassium

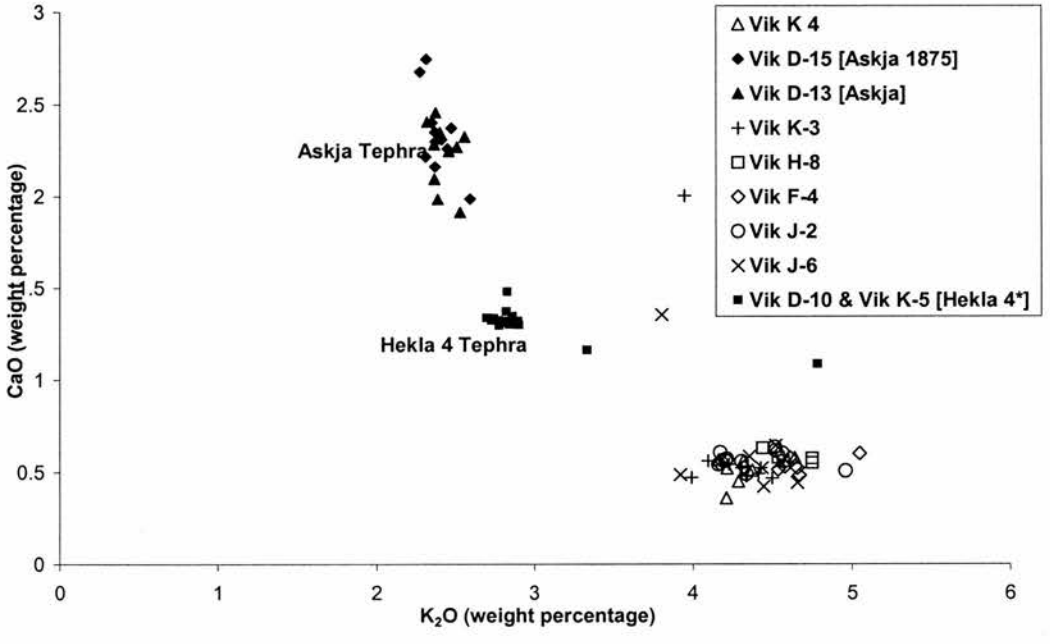

The Hekla 4 data here refers to only the highly silicic (rhyolitic) fraction of Hekla 4 tephra, from samples extracted in the field area. It can be seen that none of the sampled tephras have geochemical characteristics of Askja or silicic Hekla tephra, but have their own distinct characteristic.

Vik D-12 [Hekla 3]

Tephra layers with physical and geochemical characteristics compatible with the Hekla 3 tephra are found in most stratigraphic profiles excavated in the field. It is a very fine light yellow/white tephra, which is often found with very dark peaty clay, containing some fine dark tephra grains (see section on Brun H-2 and Brun H-4 below), immediately above and below it (see the illustrated example in profile Brúnavík D, Figure 5.3-k). Its distinctive sedimentary setting enables the layer to be traced across the field area, with geochemical analysis of samples from selected locations. Figure 5.3-g shows the spread of data found to represent Hekla 3 tephra. As can be seen, the tephras in the field area are found to match the small left hand cluster of Hekla 3 data very clearly (this region is highlighted in Figure 5.3-g (ii)), with only a few grains having similar characteristics to the right hand, less tightly packed cluster. There are a few outliers, highlighted in Figure 5.3-g (ii), which could be explained as anomalous grains which have (a) been washed into the Hekla 3 layer from above, (b) been a result of accidental contamination of the sample, or (c) represent a separate airfall tephra. Given the sparse nature of these outliers, the option (c) is unlikely, thus these grains can largely be ignored as non-representative.

Figure 5.3-g: Correlations between tephra layers from this study, and "Hekla 3"

i) All data

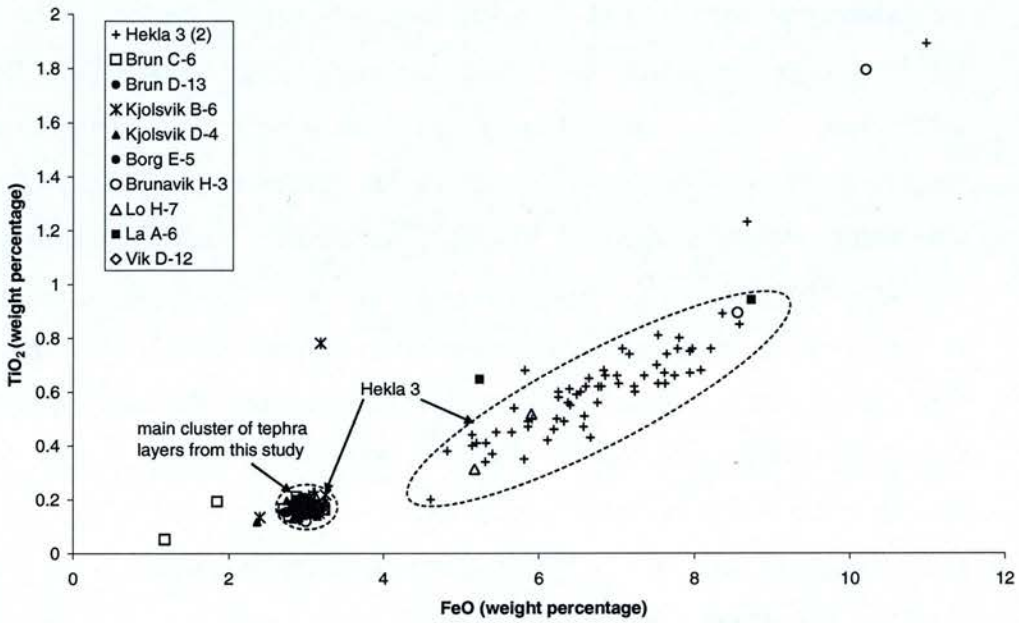

ii) Detailed view of main cluster of points from (i)

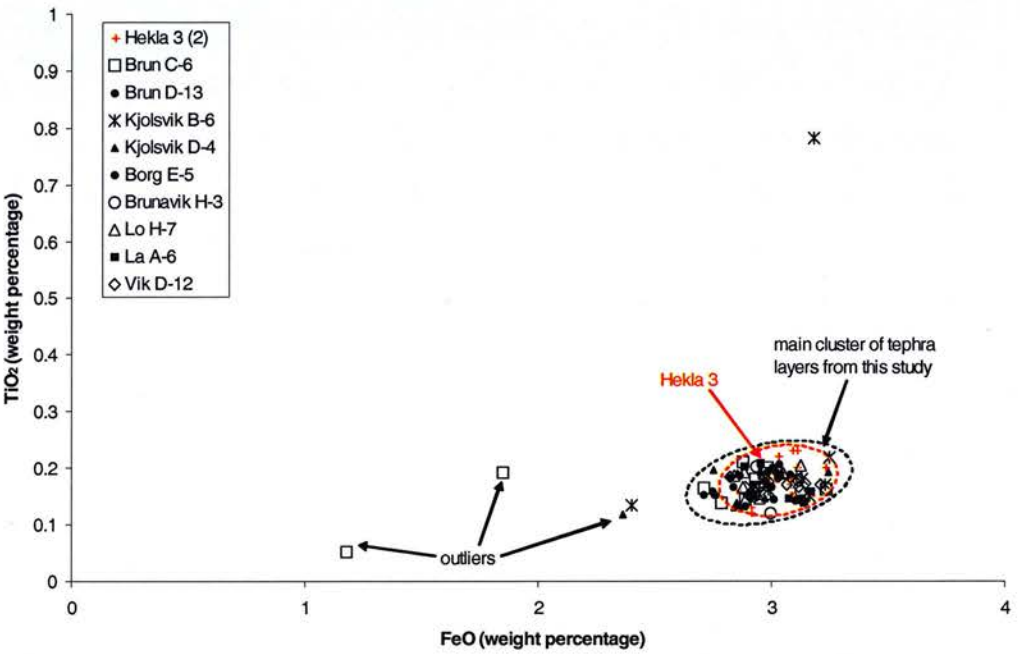

From (i) Hekla 3 is seen two have two main populations, one with FeO ~3% (group 1) and the other with FeO at ~4-9% (group 2). Tephras sampled in this research correlate well with the group 1 part of Hekla 3, though few grains correlate with group 2.

Brun H-2 and Brun H-4

These two fine dark basaltic tephras are found mixed with dark peaty clays immediately above (Brun H-4) and immediately below (Brun H-2) the fine white tephra thought to represent the Hekla 3 eruption. The two layers are distinct from each other, and are distinct from Hekla 3 in geochemistry, with characteristics suggestive of two separate volcanic origins; Grímsvötn and Veiðivötn (see the correlations evident in Figure 5.3-h). The sedimentary environments in which these tephras are found, mixed in peats and clays and not as a clear layer, is suggestive of re-worked, non-airfall tephra. However, most occurrences of the Hekla 3 tephra in the field area are also found between these two dark peat and clay layers, indicating that the tephras are in the correct place within the sedimentary sequence. In addition, some anomalous tephra grains found within the samples of Hekla 3 tephra, match the geochemistry of Brun H-2 (Veiðivötn), indicating that this tephra is likely to occur in close proximity to Hekla 3.

Brun D-14/Vik E-8

Tephra layer Brun D-14 is a ~2cm thick fine dark tephra found between layers identified as Hekla 3 and Hekla 4. It has been identified categorically in only one profile, Brúnavík D, making its use as a clear marker horizon problematic. From Figure 5.3-h, it can be seen that its geochemical range is well outside the limits of the main Hekla tephras, and it is likely to have a Grímsvötn origin, due to its proximity to the data representing Saksunarvatn. Layer Vik E-8 may relate to the same eruption, sharing geochemical characteristics, and being found just below a layer correlating to Vik K-3 and 4, described above, which occurred at around the time of Hekla 3.

Figure 5.3-h: Post-H4 basaltic tephra layers

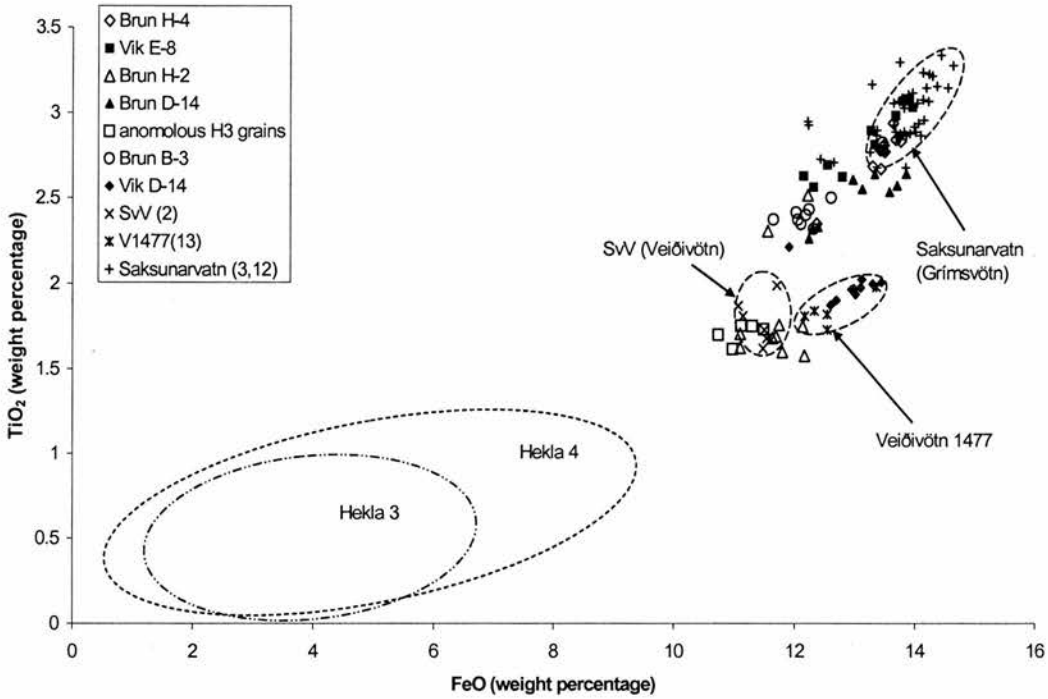

Post-H4 tephras sampled in the field are found to correlate with various Veiðivötn and Grímsvötn ashes, but not with Hekla basaltic tephras. The areas shown to represent H3 and H4 above are based on references 2-3 and 6-12.

Vik D-10/11 [Hekla 4]

The tephra layer found in the field area which is thought to represent the Hekla 4 tephra has both a light and dark component of fine tephra. The physical manifestation of the light and dark tephras varies from site to site. In some cases the light component is not visible (mostly where the layer is relatively thin), or in other cases it forms a lighter band of one to two centimetres, between the middle and the base of the dark layer (which can be found at a total thicknesses of up to six centimetres). The light component is highly silicic in geochemistry, whilst the dark component moves from dacitic (63-68% silica) to andecitic (52-63% silica), as can be seen in Figure 5.3-i. Figure 5.3-l shows photographic evidence of the dark-light-dark bands which characterise this layer.

The spread of Hekla 4 data from the references (Dugmore et al. 1992a; Dugmore et al. 1992b; Boygle 1994; Dugmore et al. 1995; Pilcher et al. 1995; Pilcher et al.

1996a; Pilcher et al. 1996b; Dugmore et al. 1997; Larsen et al. 1999), illustrated in Figure 5.3-i, shows a clear clustering of data points at an Iron Oxide level of ~2%, and Titanium Oxide level of ~0.01-0.2%. The precise location of this clustering renders this fraction of Hekla 4 grains distinct from the other silicic fractions of Hekla tephras from later eruptions (Hekla 3 and Hekla 1158, see Figure 5.3-j). The rest of the reference data is mostly dacite in nature, with a sparser distribution of points representing the andecite tephra. The study data also exhibits a clear clustering of the silicic (light) tephra in the same location as the reference data, clear evidence of a correlation with Hekla 4. It is notable, however, that the remaining field data is mostly andecite, with only a small number of dacite grains, in contrast to reference data. This may be suggestive of favourable transport of andecitic grains in an eastwards direction. It may be significant the highest levels of andecitic grains in the references were found in data from the Faroes (Dugmore et al. 1997; Wastegård et al. 2001), islands which lie in a roughly easterly trajectory from Iceland.

Figure 5.3-i: Correlations between tephra layers from this study, and "Hekla 4"

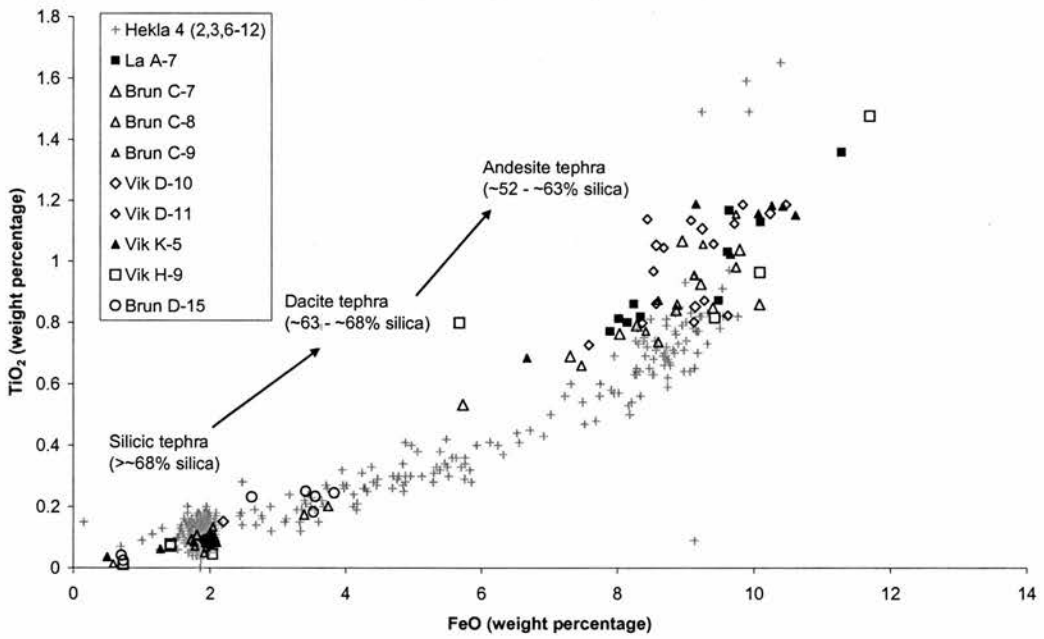

The tephras corresponding with H4 in the field have two distinct populations of silicic (rhyolitic) and andecitic tephras. The dacitic range of Hekla 4 ash derived from the literature is mostly missing in the field samples indicating selective transportation of different tephra fractions.

Figure 5.3-j: Variations in Calcium/Magnesium ratio with different Hekla tephras

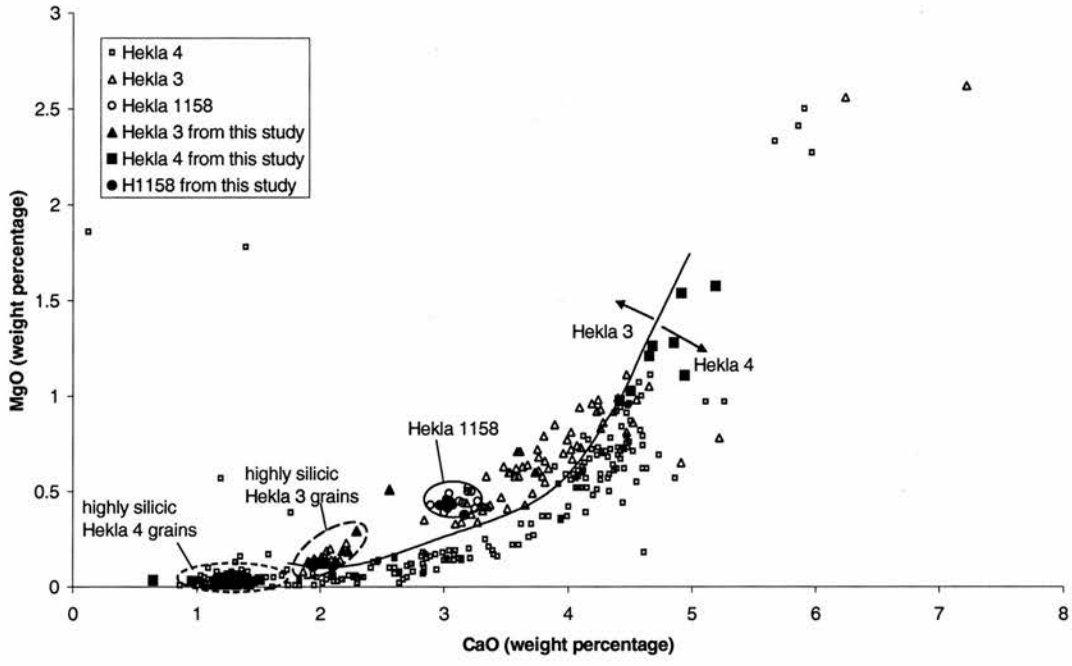

The MgO/CaO ratio clearly distinguish between the three key Hekla eruptions, H3, H4 and H1158. The points assigned to be "from this study" represent the average weight percentage from each type of tephra (silicic/andecite/dacite) found at each site, which has been named as one of the three Hekla layers. Other points refer to data taken from the literature (refs 2-3 and 6-12). The clear distinction between the 3 tephras within the study sample data is evident.

Figure 5.3-k: Photos and associated tephra logs showing Hekla 1158 and Hekla 3 in profiles Brúnavík D and E

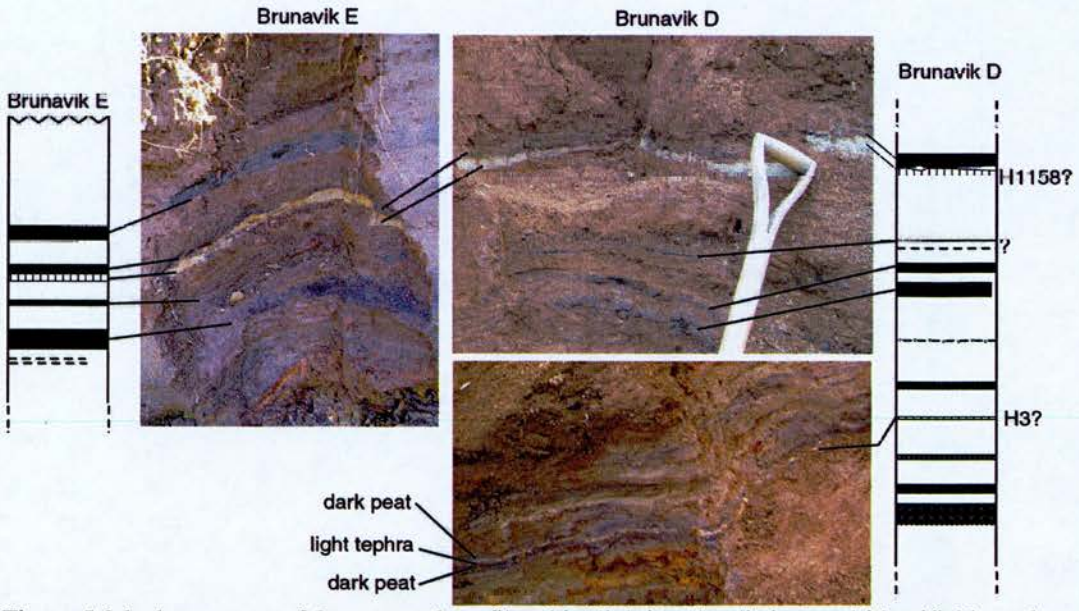

Figure 5.3-k shows parts of 2 excavated profiles, highlighting the distinct and identifiable tephras within the profiles. H1158 is particularly clear because of its juxtaposition with an upper dark tephra layer. Hekla 3 is often associated with layers of dark peaty clay above and below it, as seen.

Figure 5.3-l: Photos and associated tephra logs showing Askja 1875, Landnam, Hekla 3 and Hekla 4 in profile Brúnavík C

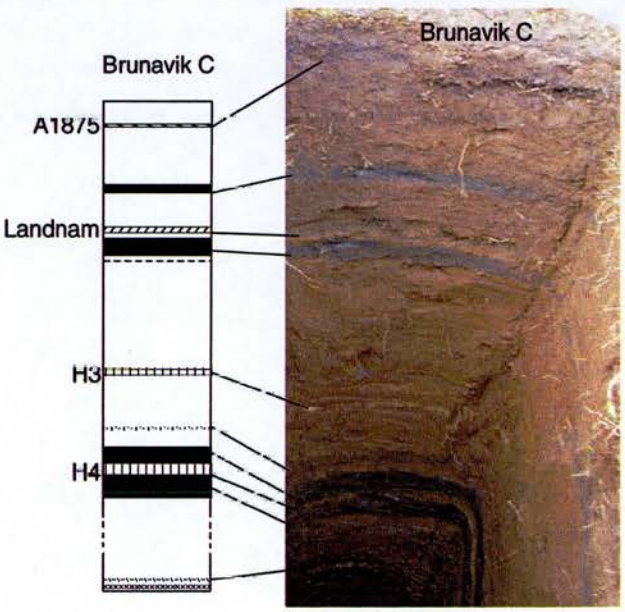

Figure 5.3-l shows a further example of an excavated profile. Of particular interest is the clear dark and light bands of the H4 tephra.

Pre-H4 Basaltic Tephras

All pre-Hekla 4 basaltic tephras which have been geochemically analysed, are presented in Figure 5.3-m, in comparison to other known basaltic tephras. Moving down the reference profile, Víkurá D, tephra Vik D-9 is the first to be found below H3. It is correlated with layer Vik K-7, based on stratigraphic location and geochemistry, shown in Figure 5.3-m. From this Figure, a Grímsvötn origin for this layer looks likely, due to its Titanium/Iron ratio, which is typical of Grímsvötn eruptions (such as Saksunarvatn, as illustrated). The dates for this tephra layer are constrained by radiocarbon dates, to between 5350 and 4290 cal. yrs. BP.

Layer Vik D-6 follows this Grímsvötn layer, and has geochemical characteristics inherent to Veiðivötn eruptions, as seen in Figure 5.3-m. It is dated to between 5790 and 5940 cal. yrs BP. Tephra layers Vik K-8 and Vik D-5 contain both silicic and basaltic grains, therefore do not represent airfall layers. From Figure 5.3-m, the basaltic part of Vik K-8 (Tephra A) has a Veiðivötn origin, and the basaltic part of Vik D-5 (Tephra B) is of Grímsvötn origin. Layer Vik D-4, beneath these layers, is a clear airfall layer, dating to 8.86-8.64 cal. ka BP, and also of Grímsvötn origin. The oldest layer identified in the field area is Vik D-1. However, it appears to have two main populations of tephra grains, correlating with Grímsvötn and Veiðivötn respectively. This layer dates to 9590-9380 cal. yrs BP.

Figure 5.3-m: Pre-H4 basaltic tephras

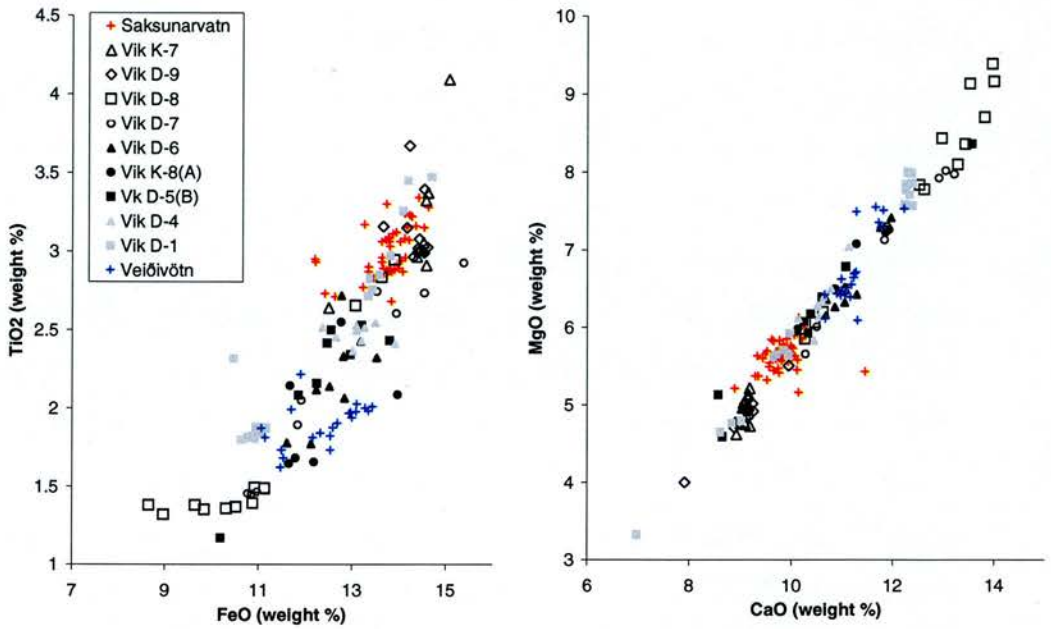

Figure 5.3-m highlights correlations between Grímsvötn (Saksunarvatn), Veiðivötn, and sampled tephras from this study.

Pre-H4 Silicic Tephras

Silicic tephras found below Hekla 4, are layers Vik D-2 and Vik D-3, which share distinct geochemical characteristics. The lowest layer (Vik D-2) dates to 9530-9310 cal. yrs BP. In addition, some of the analysed tephra shards from sampled Vik D-5 (tephra A) and Vik K-8 (tephra B) were silicic, and share the same distinctive characteristics as Vik D-2 and Vik D-3. Figure 5.3-n graphs these four tephra layers in comparison to other silicic tephras identified in the field. It can be seen from this figure that these four tephras all match the geochemical characteristics of tephras Vik K-3 and Vik K-4, of unknown volcanic origin. There is little spread in the data points representing these layers, highlighting a clear and well-constrained genetic connection.

Figure 5.3-n: Pre-H4 silicic tephras

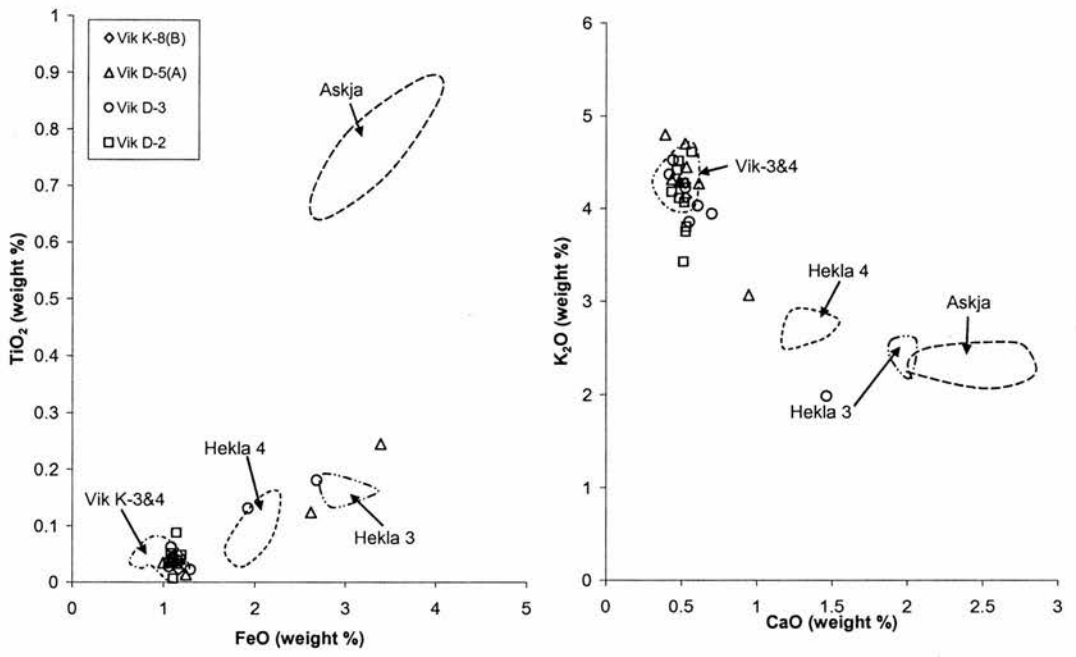

Figure 5.3-n shows the distinct clustering of data from samples Vik D-2 and Vik D-3 which correlates well with the younger layers Vik 3 & 4, of unknown origin. There are no correlations with the silicic H3, H4 or Askja tephras.

Summary

Correlations are evident between different tephra samples collected in the field, which enables the development of a tephrostratigraphy for the field area. In 5.3.3, we address the relationship between *depth* and *age* in stratigraphic profiles, as a means of estimating the ages of unknown tephra layers which have been characterised geochemically, and to estimate basal ages. In 5.3.4, the inter-correlated and dated tephrostratigraphy for the field area is presented, which ultimately enables dating of the mapped landform suites (in 5.4).

5.3.3. Developing an age-depth profile

In order to accurately constrain the dating of landforms which may be related to the 8.2ka event, minimum ages for landform genesis must be determined from stratigraphic profiles which lie within the limits of the landform suites. The oldest well-documented and dated tephra layer classified in the field area is Hekla 4. A

further 5 pre-H4 tephra layers have been dated with radiocarbon, as shown in 5.2.3. Where such pre-H4 tephra layers are sparse or unidentified, crude age estimates can be derived from soil accumulation rates. Initial observation shows that H4 is commonly found at around two thirds of the full profile depth, indicating Early to mid-Holocene ages for the lowest layers of most profiles, and thus Early to Mid Holocene ages for the landform suites. Soil accumulation rates cannot, however, be assumed to be uniform over time and space. Climatic conditions promoting or retarding erosion and accumulation may result in a variable rate over the Holocene period. The signal is further complicated when the different types of sediments recorded in the profiles are considered. Materials such as sands and gravels can accumulate to great depths in a single instantaneous depositional event, while peats accumulate more steadily over time. In addition, accumulation rates for soils and peat vary with altitude due to microclimatic effects, in that at higher altitudes, the rates are lower. Such variations are illustrated in Figure 5.3-o. Slope angle also affects net accumulation rates, as a result of preservation potential. Steeper slopes which are subject to more geomorphic activity will not preserve materials, and thus have a lower depth of accumulated materials.

Figure 5.3-o: Spatial variation in accumulation rates

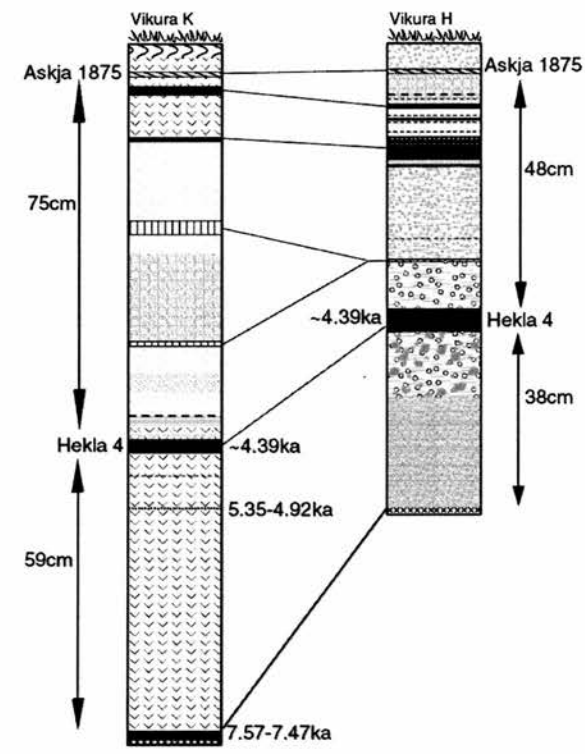

This figure shows profile Vikura K (excavated on a gently sloping valley floor at ~250m, just within the lower margins of the Víkurá 2 Suite), and Vikura H (excavated in the upper parts of Víkurá 2, at ~390m altitude). As can be seen, the marker horizons Askja 1875 and Hekla 4 are present in both profiles. The depths recorded between the Askja and Hekla tephras in the separate profiles are quite different due to the variable accumulation rates (possibly due to altitudinal variation). The depth of material below Hekla 4 in the Vikura H profile is comparable (relative to the proportional accumulation rate) to the depth of the equivalent pre-Hekla 4 section of the Vikura K profile, which is why it has been estimated to be a similar age. However, the materials in each profile are different, so such estimates must be made with care.

Due to the spatial variation in accumulation rates across all recorded tephra profiles, the development of a uniform age-depth profile applicable across the field area is difficult. However, an age-depth profile will improve these estimations of accumulation rates. The existence of known tephra markers and radiocarbon dates allows accumulation rates to be assessed over given time-periods, and in different depositional environments and sediment regimes, to assess the extent of temporal and spatial variations in rates. Figure 5.3-p represents the two best-constrained, radiocarbon-dated profiles, Víkurá K and Víkurá D. It highlights the effects of sediment type on net accumulation, with the silt/sand fraction of the Víkurá K profile maintaining a much higher accumulation rate than the peat fraction. Accumulation rates derived from Víkurá D are a useful guide as the profiles is made up entirely of peat, so is likely to show any variations through time clearly. Accumulation rates are shown to be reasonably low in Historic times remaining at around 0.05mm/yr. Rates appear to reach a maximum of 0.25mm/yr in the mid Holocene around 5000-6000 calendar years B.P., and then drop to a lower rate of around 0.18mm/yr in the early Holocene.

Figure 5.3-p: Accumulation rates for Vikura D and Vikura K

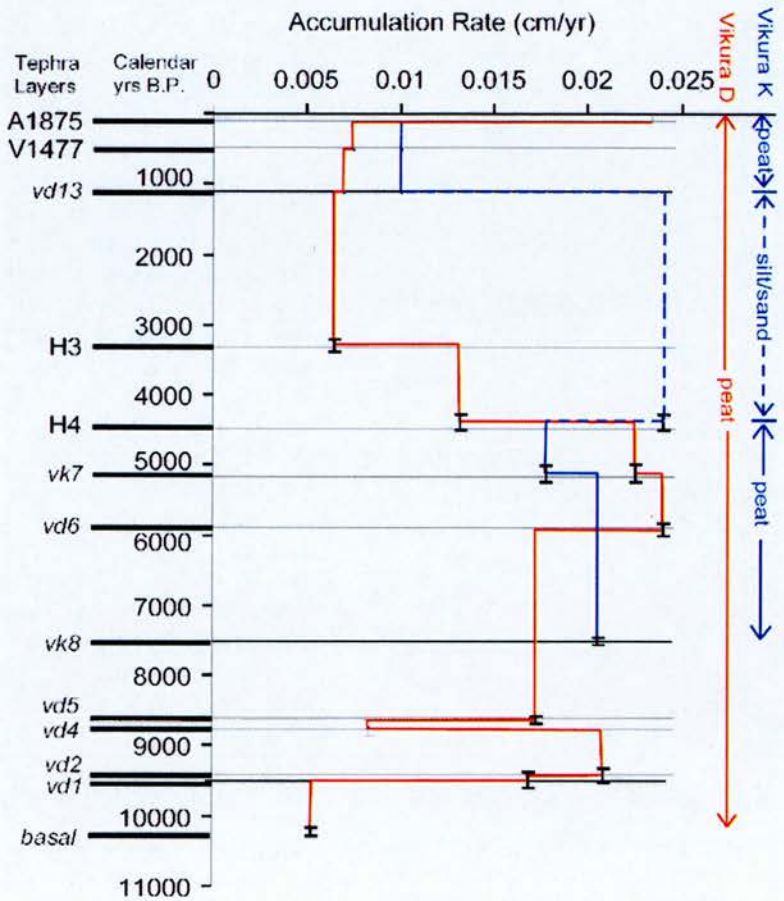

Figure 5.3-p shows accumulation rates of sediments in the two radiocarbon-dated profiles Vikura D and Vikura K. Average accumulation rates between each pair of known dates are calculated based on the depth of material accumulated over each known time period. Dates come from tephra layers or direct from radiocarbon dates. The profiles are largely made up of peat, except for the section covering tephra layer vd13 to H4 in the Vikura K profile. This section is made up of silt and sand and, as can be seen, displays a much higher accumulation rate than the peat.

The accumulation rates illustrated in Figure 5.3-p cannot be automatically transferred to any profile, given the spatial variations in rate described above. However, the relative variation in rate over time can be attributed to other profiles. The parts of profiles which are best constrained by tephra layers (usually the upper sections) are indicative of the general rate of accumulation in the particular topographic setting, and can indicate the relative variability in rate between any different material types found in a profile. This site-specific information combined with the data presented in Figure 5.3-p above, enable accumulation rates to be estimated for poorly constrained sections. A mid-Holocene maximum in accumulation rates, as shown here, may be applicable across the field area, and should thus be considered as significant when calculating basal ages for profiles based on accumulation rates alone.

5.3.4. Dated tephrostratigraphy

The correlations between tephra layers derived from the geochemical analysis (5.3.2), and physical characteristics, enable a tephrostratigraphic framework for the field area to be developed (Figure 5.3-q). The illustrated profiles initially presented in 5.2.1 are shown here without sedimentological data, only tephrostratigraphy, so that genetic links between tephra layers can be more easily recognized. Depths shown represent true depths of material, and demonstrate the variability in net accumulation between profiles. In 5.4, the profiles of key importance to landform dating will be assessed in more detail and scaled according to time rather than depth.

Tephras in the following stratigraphic diagrams have been labelled in **bold** where their origin has been identified as a well-known eruption, and in *italics* where a layer is traceable across the field area and has been named here for the purpose of this study. Table 5.3-b summarises the named layers and abbreviations included in the stratigraphic diagrams, their volcanic origin (derived from geochemical analysis, 5.3.2) and their age (based on the literature, radiocarbon dates, accumulation rates and relative location to other dated tephras). Where peat associated with tephra layers has been dated with radiocarbon, dates are included in red, calibrated to Calendar Years Before Present. Tephras sampled for geochemical analysis are numbered and highlighted with a "*". These numbers refer to the samples discussed in the geochemical analysis in 5.3.2. For example, sample *4 in profile Víkurá D, is the same as sample "Vik D-4" which has been geochemically analysed.

Table 5.3-b: Major Tephra Layers highlighted in the illustrated profiles below, and associated information

Abbreviation	Name	Volcanic Origin	Age (AD/cal. yrs BP)
A1875	Askja 1875	Askja	1875AD
V1477	Veiðivötn 1477	Veiðivötn	1477AD
A~1300	Askja ~1300	Askja	~1300AD (est.)
Bb	"Brúnavík B"	Grímsvötn	
Ba	"Brúnavík A"/Hekla1158	Hekla	1158AD
L	Landnam	Torfajökull	~870AD (Larsen et al. 1999)
Bc	"Brúnavík C"	Veiðivötn	~1000AD (est.)
Va & Vb	"Víkurá A" & "Víkurá B"	Unknown "Víkurá" Tephra	~4-3ka (est.)
H3	Hekla 3	Hekla	3.39-3.2ka (Zillen et al. 2002)
H4	Hekla 4	Hekla	4.283-4.497ka (Zillen et al. 2002)
*(Profile Víkurá K ***7**/ Víkurá D ***9**)*	tephra samples Vik K-7/Vik D-9	Grímsvötn	5.35-4.92 ka (calibrated C^{14} age)
*(Profile Víkurá D ***6**)*	tephra sample Vik D-6	Veiðivötn	5.99-5.79ka (calibrated C^{14} age)
*(Profile Víkurá K ***8**)*	tephra sample Vik K-8	1)Unknown "Víkurá" Tephra 2)Veiðivötn	7.57-7.47ka (min) (calibrated C^{14} age)
*(Profile Víkurá D ***5**)*	tephra sample Vik D-5	1)Unknown "Víkurá" Tephra 2)Grímsvötn	8.69-8.57 (max) (calibrated C^{14} age)
*(Profile Víkurá D ***4**)*	tephra sample Vik D-4	Grímsvötn	8.86-8.64 (max) (calibrated C^{14} age)
Ve & Vf	"Víkurá E" & "Víkurá F"	Unknown "Víkurá" Tephra	9.53-9.31ka (max) (calibrated C^{14} age)
*(Profile Víkurá D ***1**)*	tephra sample Vik D-1	1)Grímsvötn 2)Veiðivötn	9.59-9.38ka (max)

Figure 5.3-q: Dated Stratigraphy

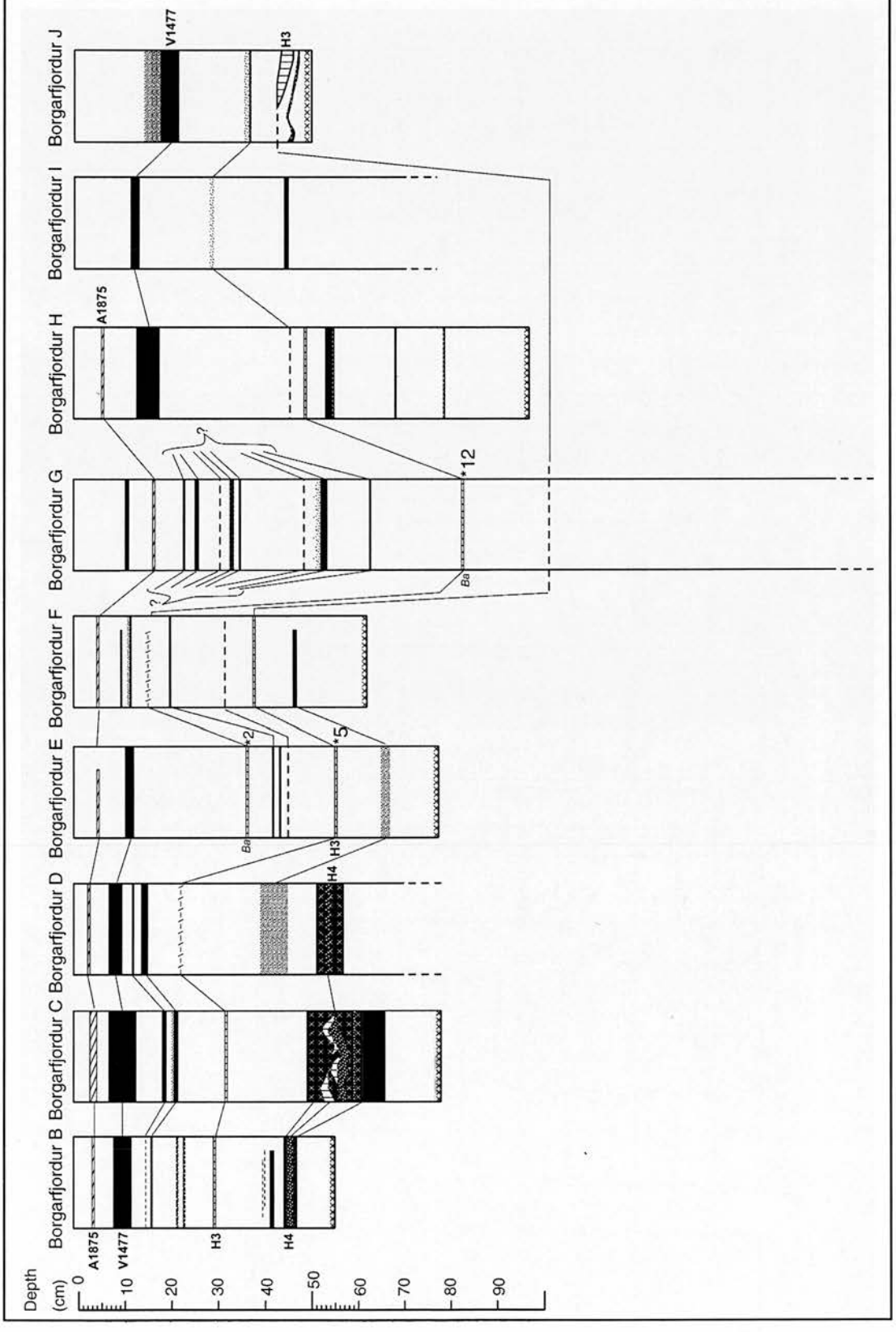

Figure 5.3-q (continued)

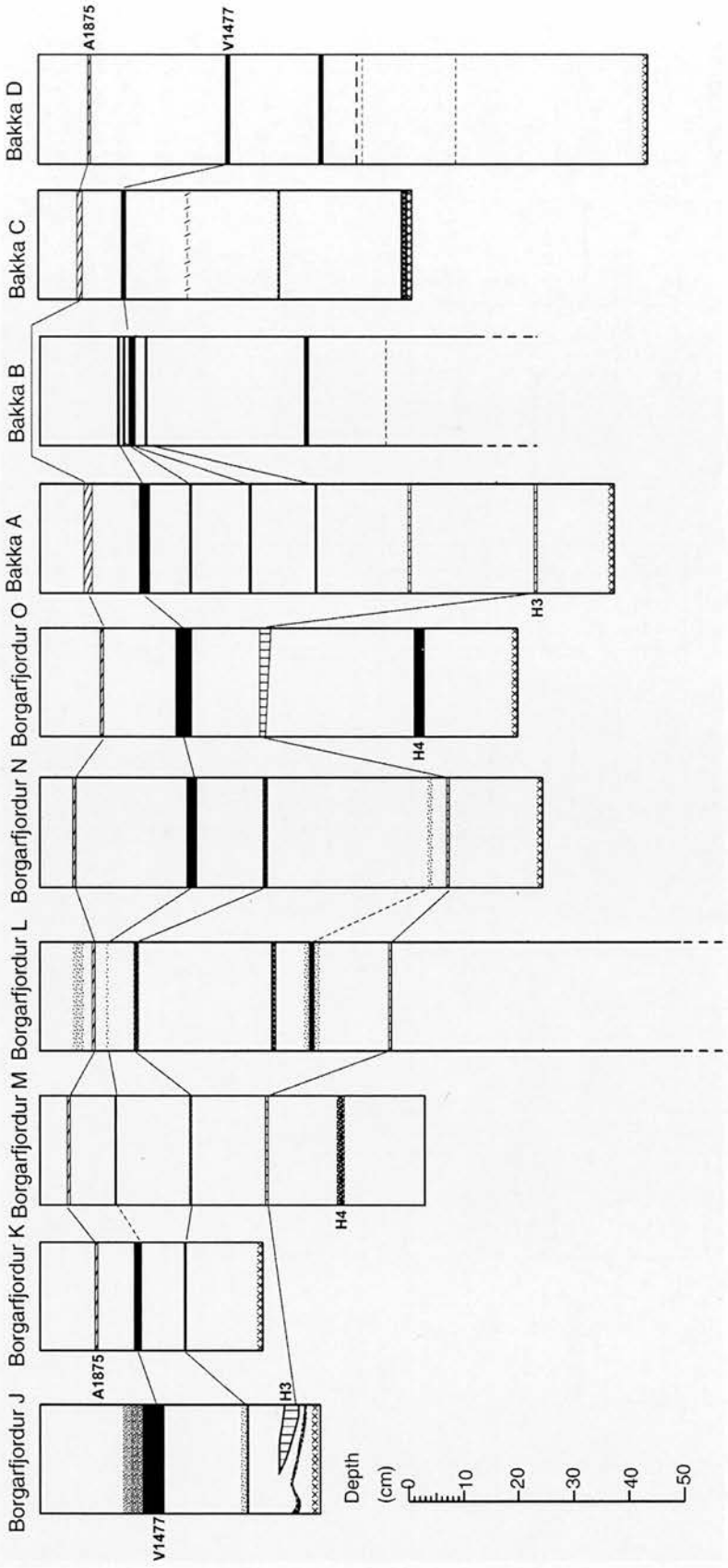

Figure 5.3-q (continued)

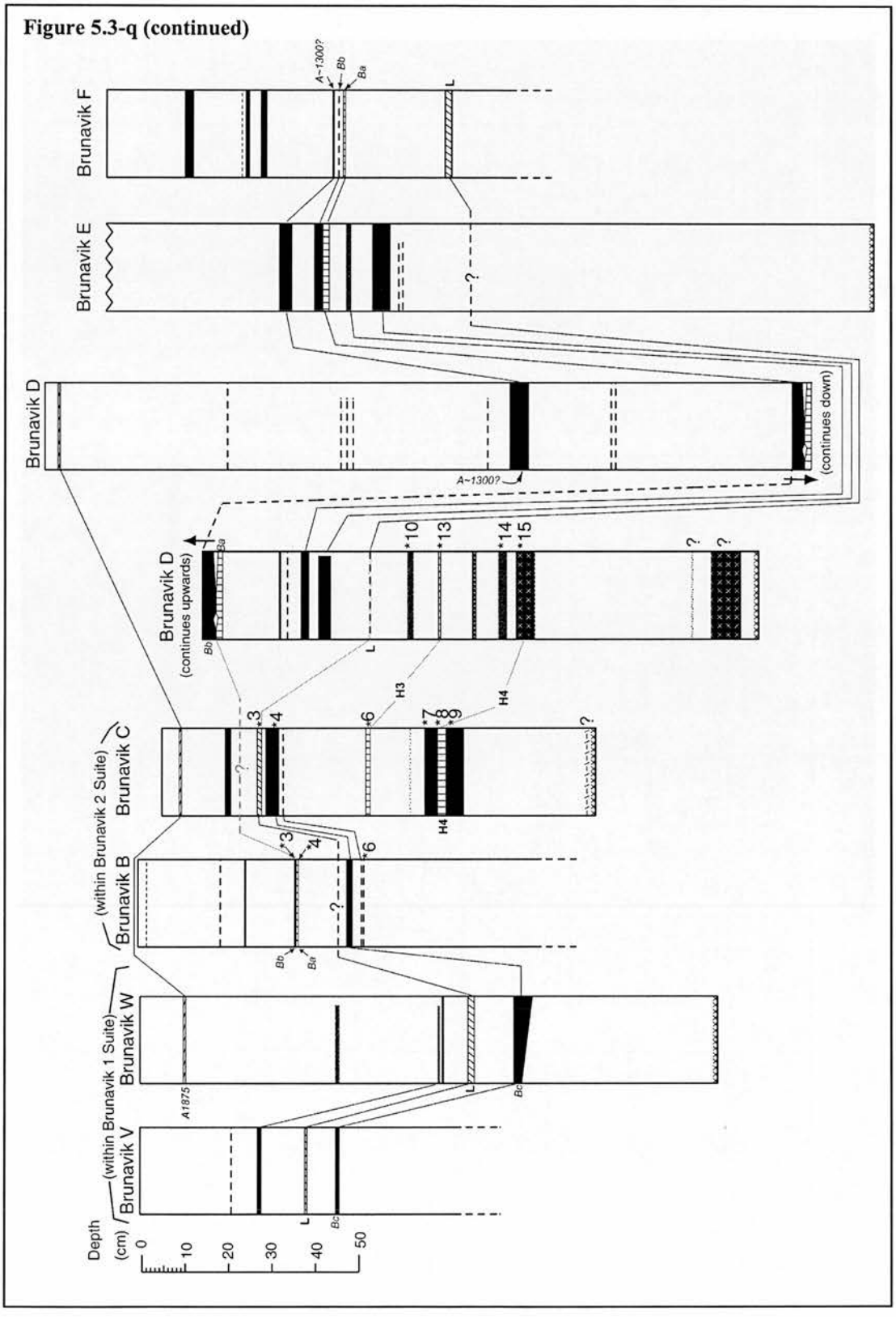

Figure 5.3-q (continued)

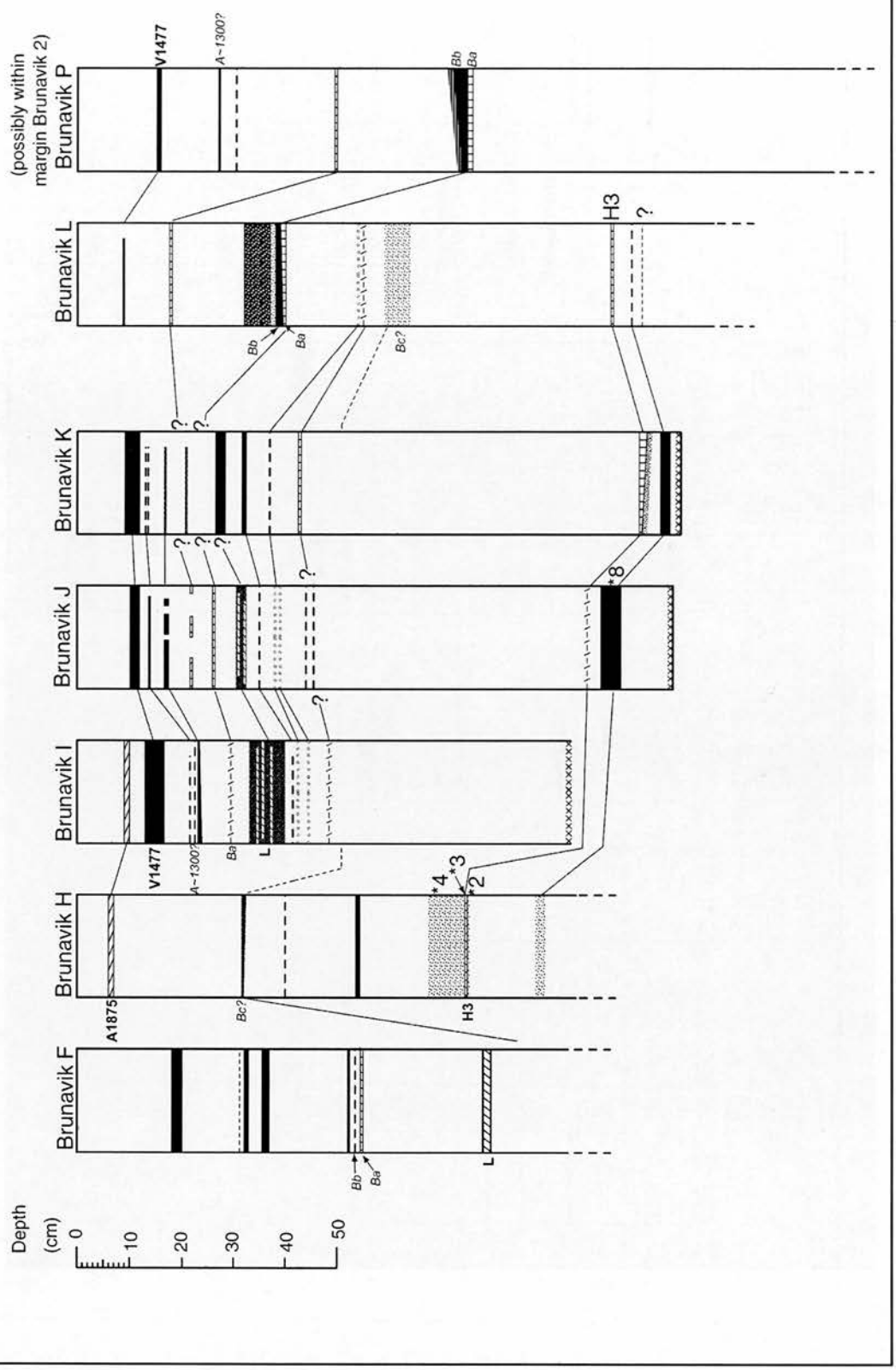

Figure 5.3-q (continued)

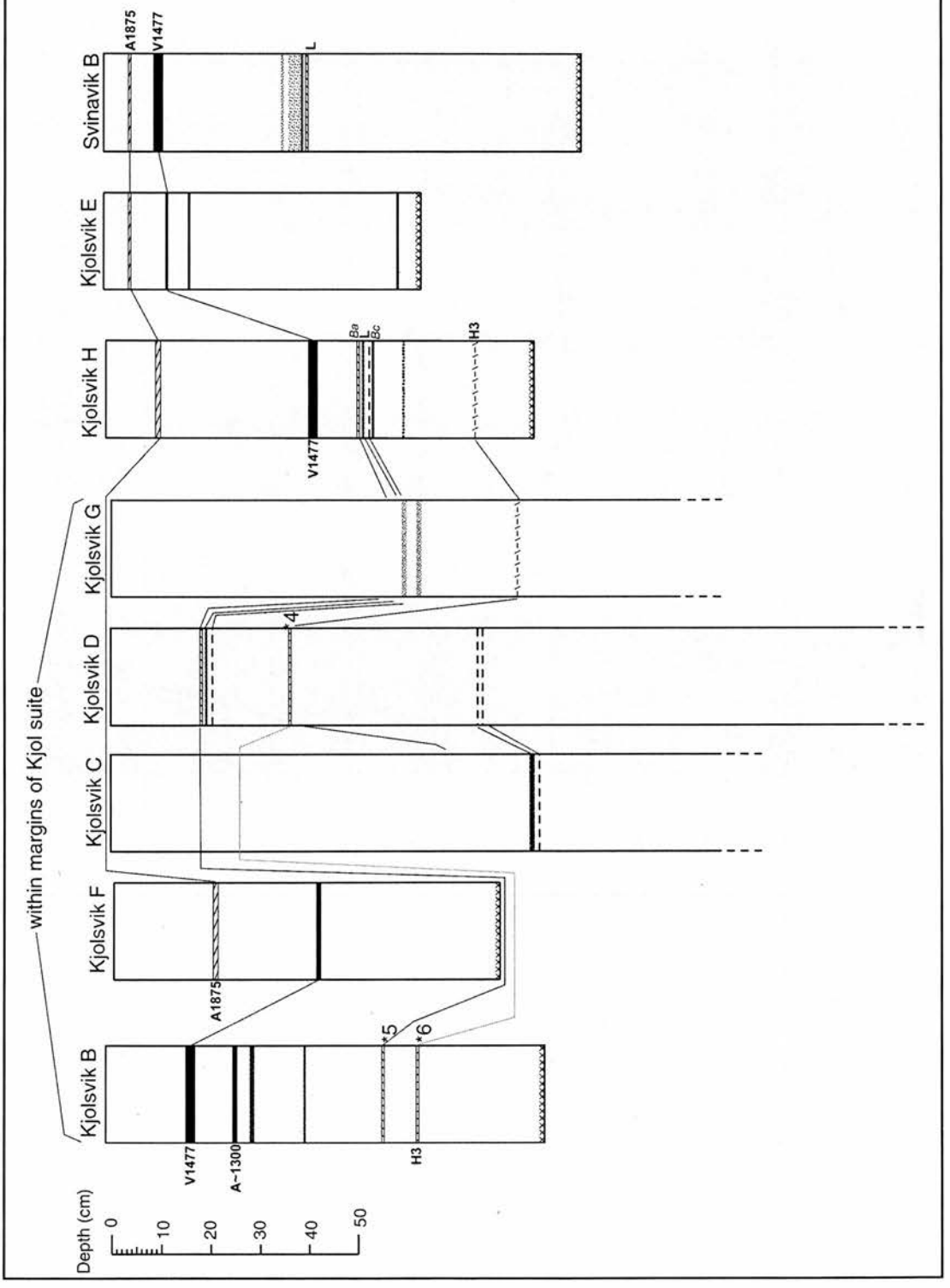

Figure 5.3-q (continued)

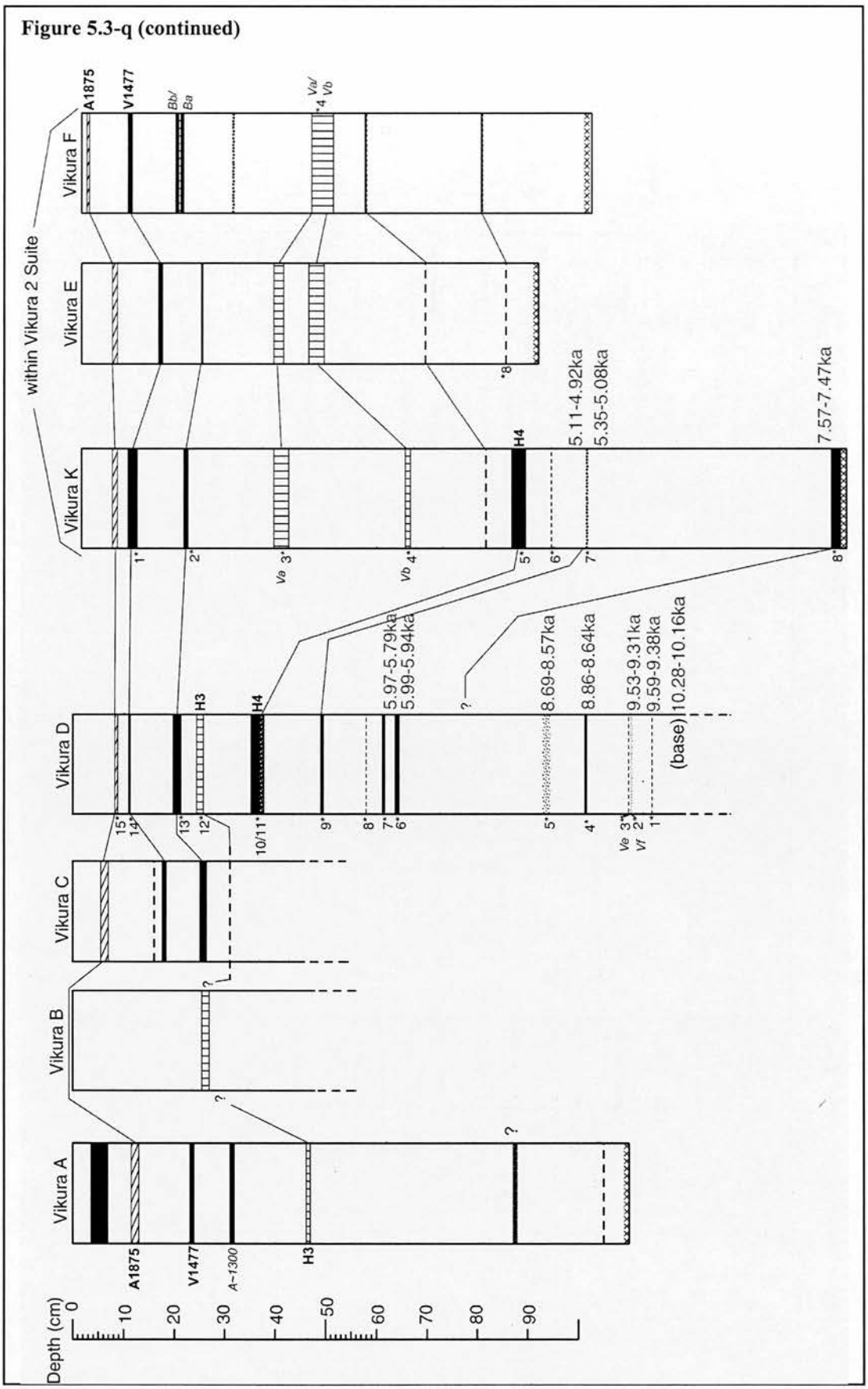

Figure 5.3-q (continued)

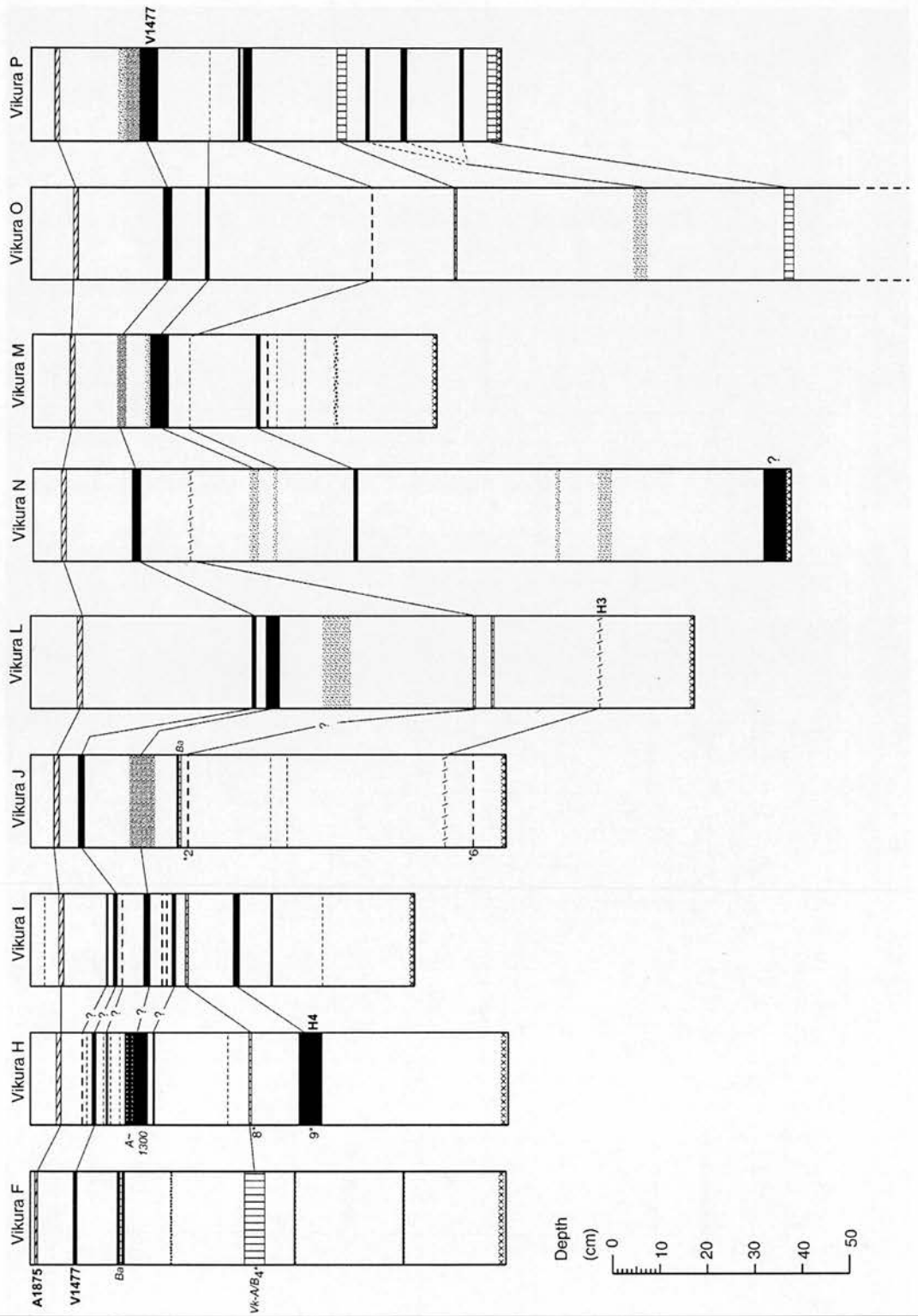

Figure 5.3-q (continued)

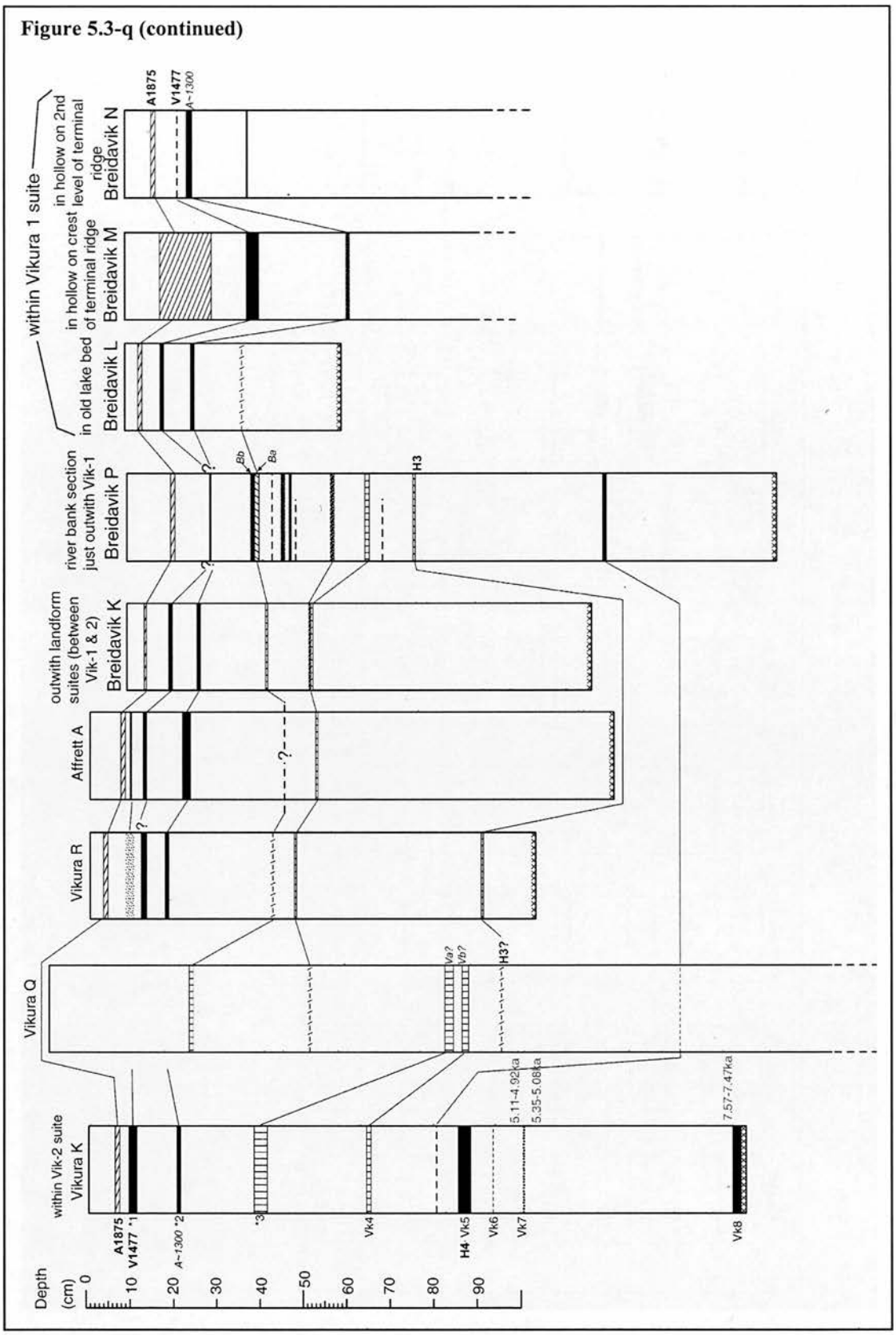

Figure 5.3-q (continued)

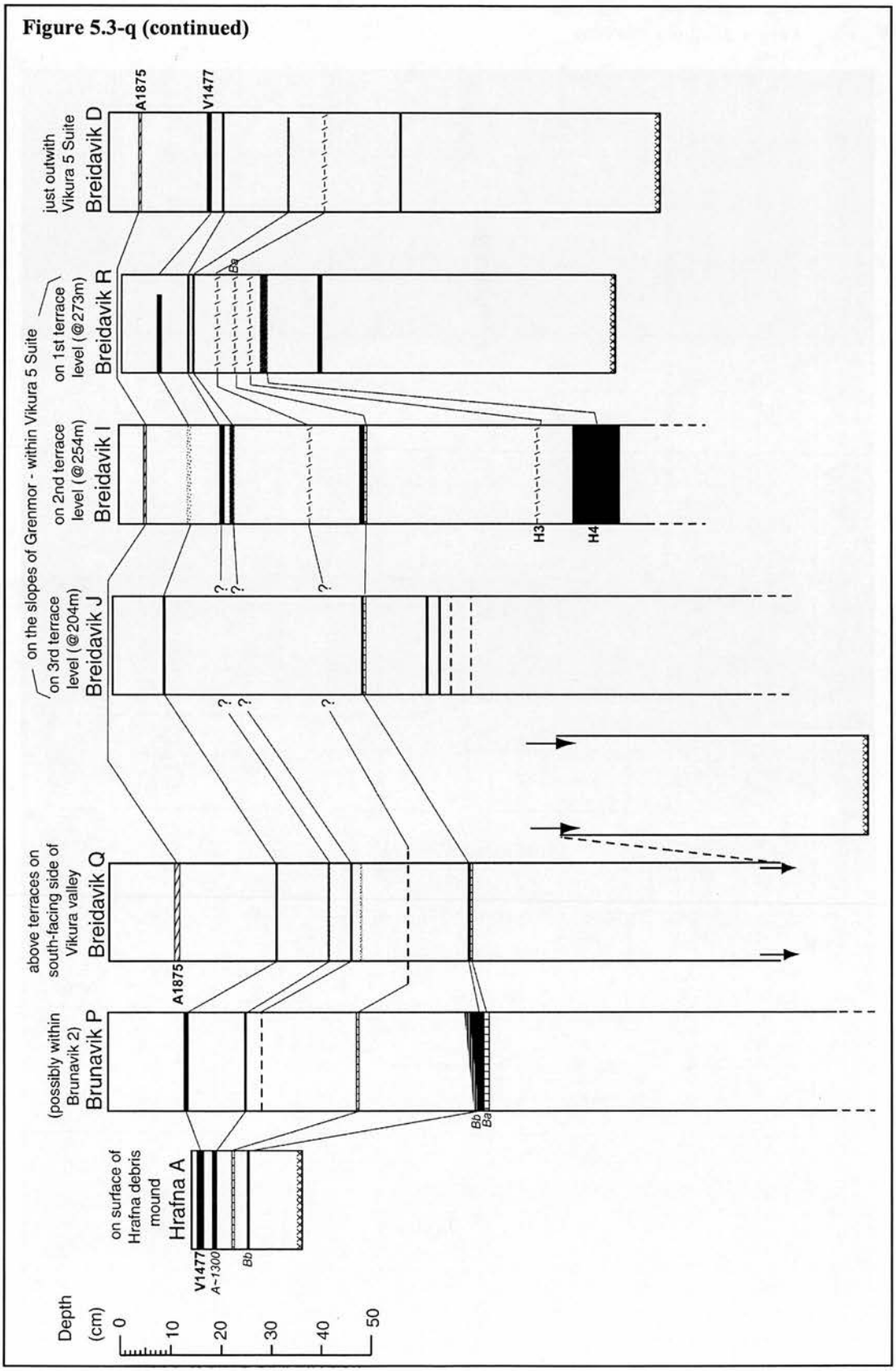

Figure 5.3-q (continued)

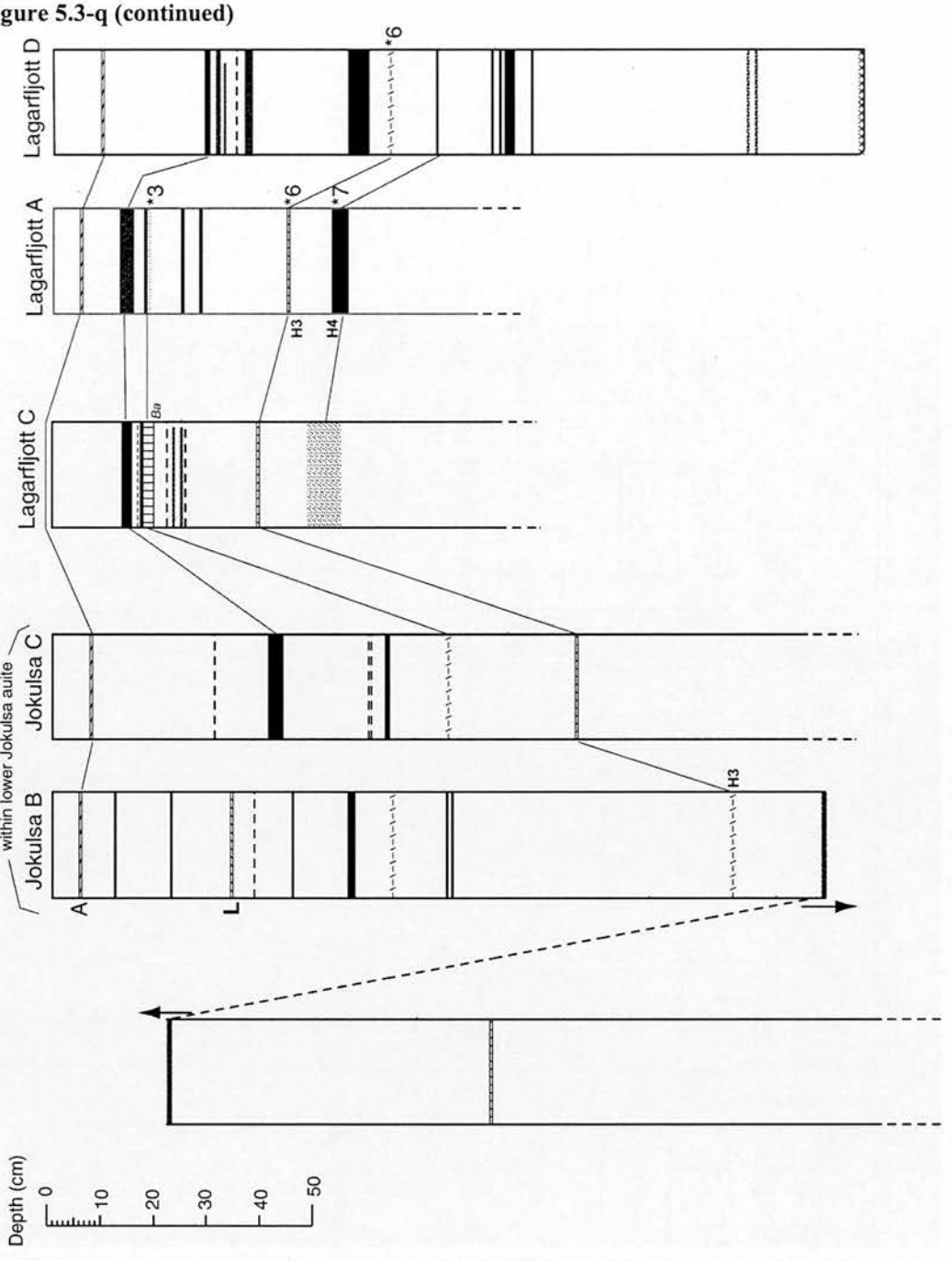

Figure 5.3-q (continued)

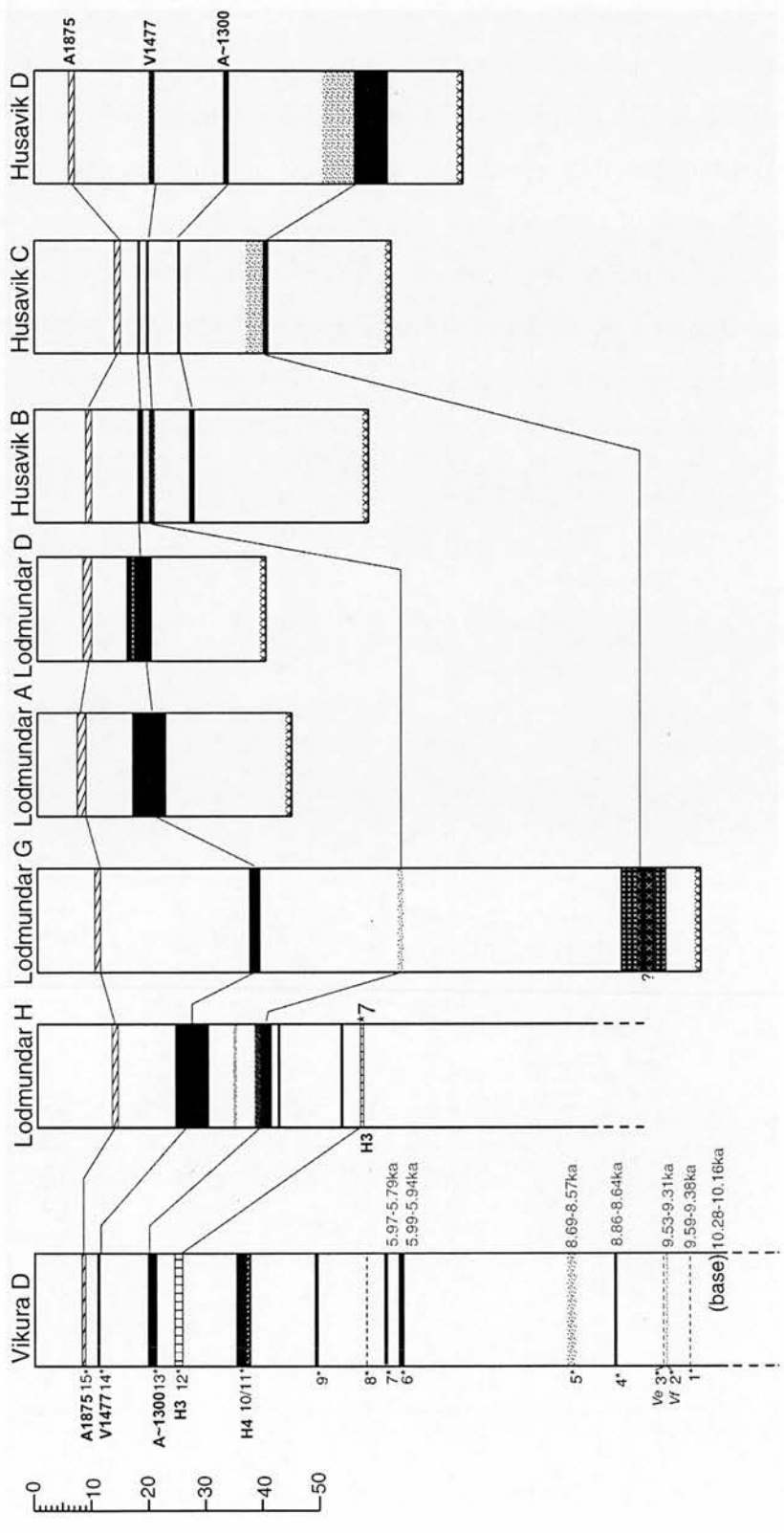

Following presentation of all the profiles above, a summary of the tephrostratigraphy of the field area is provided in Figure 5.3-r below, which provides information on the tephrostratigraphy of the four main valleys in the field area which contain dateable landform suites, Víkurá, Borgarfjörður, Brúnavík and Kjólsvík. This Figure does not represent an exact depth, but represents the relative depths between tephra layers when averaged across all the profiles. A time line is included on the left which highlights the ages of all key tephra layers in Years AD for historic age tephras, and Calendar Years Before Present for pre-historic tephras. The volcanic source of the tephra is included where this has been derived from the geochemical analysis in 5.3.2.

Figure 5.3-r: Composite tephra profiles for the Borgarfjörður Eystri region

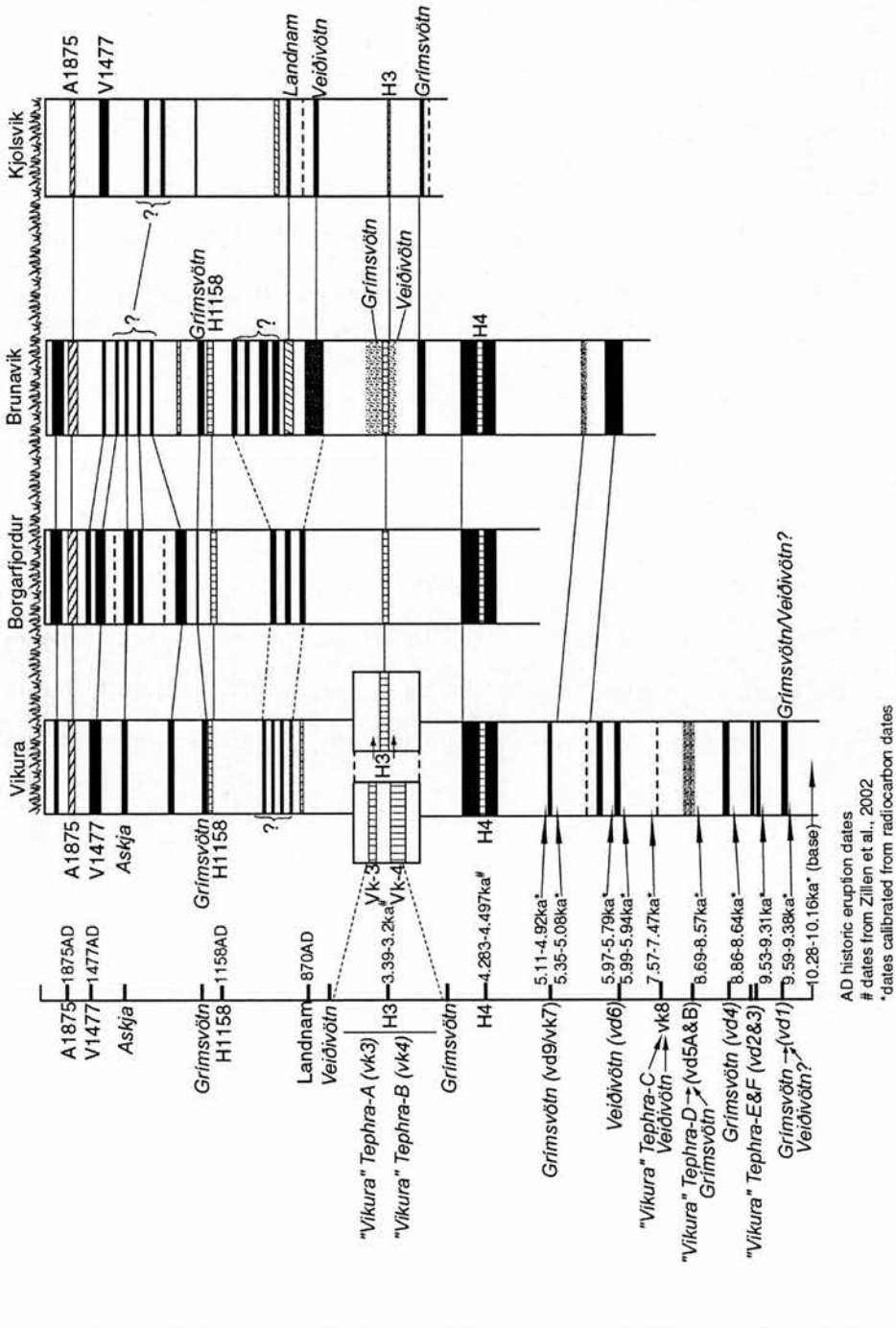

5.4. Geomorphic Implications

The implication of the dated stratigraphy in terms of the chronology of geomorphic events is discussed. Based on the dated tephrostratigraphic framework developed in 5.3, relative and absolute ages for the mapped landform suites and landform units are derived. Primarily, basal ages for key profiles which may enable dating of the mapped and dated landform suite and landform unit are presented. Each dated landform suite is then assessed individually, with sedimentological data from 5.2 drawn on where it aids the understanding of the sequence of geomorphic events.

5.4.1. Derivation of basal ages for key profiles

With a combination of data from tephrostratigraphy (5.3.4) and accumulation rate estimates (the determination of which is described in 5.3.3), putative ages were determined for unknown tephra layers of importance to dating landforms, and basal ages, where a tephra of known age was not present at the base. Where no dated tephras or radiocarbon dates area available to derive basal dates for profiles, estimated ages are based on accumulation rates. Accumulation rate estimates for each profile can be calculated based on the position of age-equivalent horizons (tephra layers or calibrated radiocarbon dates). These horizons are placed on a temporal scale, so that the "depth" of material between these horizons stretched or diminished depending on the accumulation rate (Figure 5.4-a). Taking into account the higher mid-Holocene accumulation rate discovered in 5.3.3, this derived accumulation rate can be applied to the lower sections of the profiles, which often have few known tephra layers, and basal ages estimated. These basal dates are presented in Figure 5.4-a, and represent a good indication of the relative differences in age between profiles.

The profiles selected and illustrated in 5.4-a are chosen based on the need to date units of the landform suites. This will enable determination of the chronology of landform genesis events, indicating the potential causal connections between the distinct geomorphic events and climatic change.

Figure 5.4-a: Ages for Landform Suites derived from stratigraphic framework
(i) Landform Suites Víkurá 2, Brúnavík 2 and Brúnavík 1

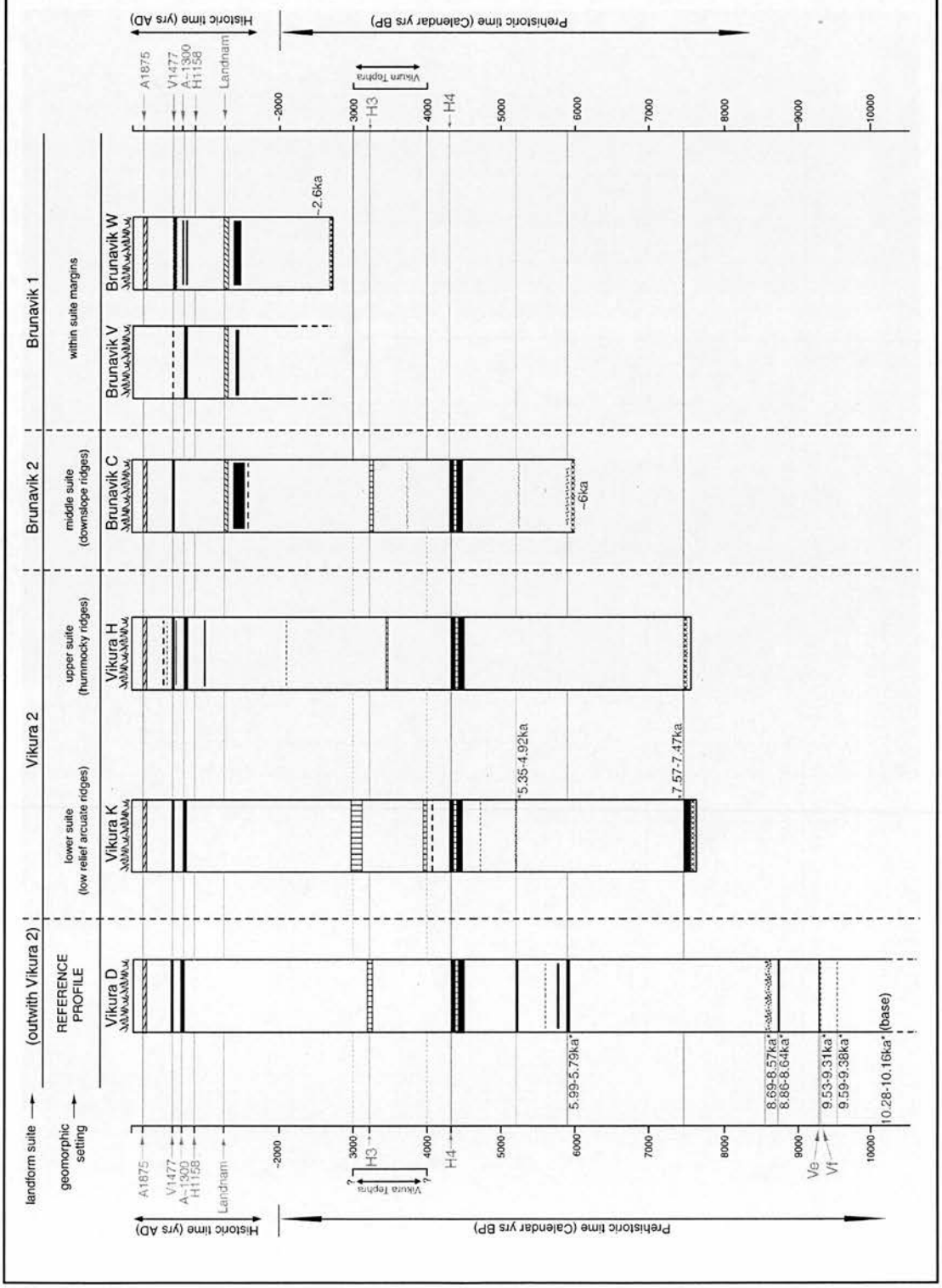

Figure 5.4-a: Ages for Landform Suites derived from stratigraphic framework
(ii) Landform Suites Víkurá 1, Víkurá 5, Svínavík

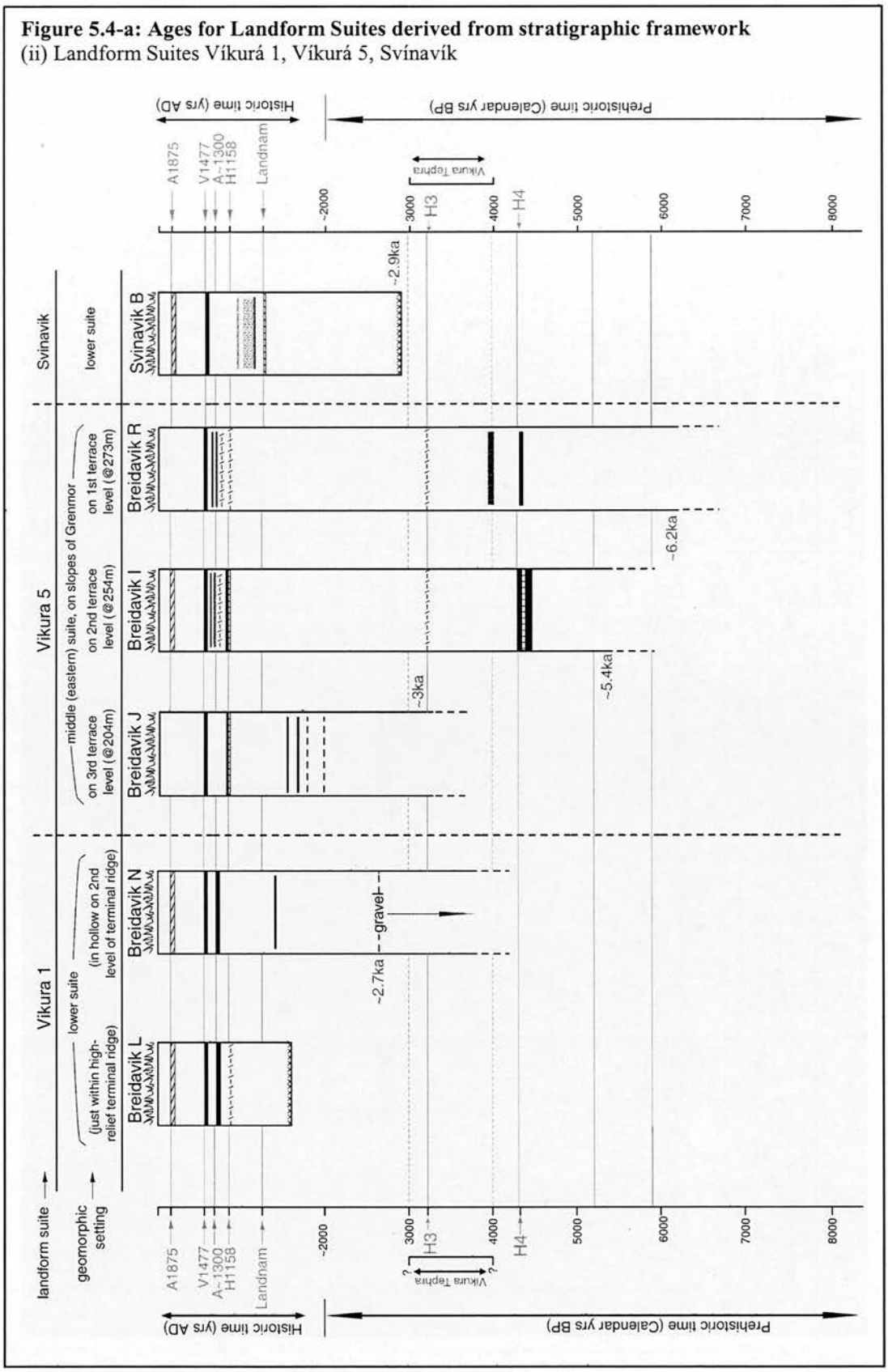

Figure 5.4-a: Ages for Landform Suites derived from stratigraphic framework
(iii) Kjólsvík and Borgarfjörður Landform Suites

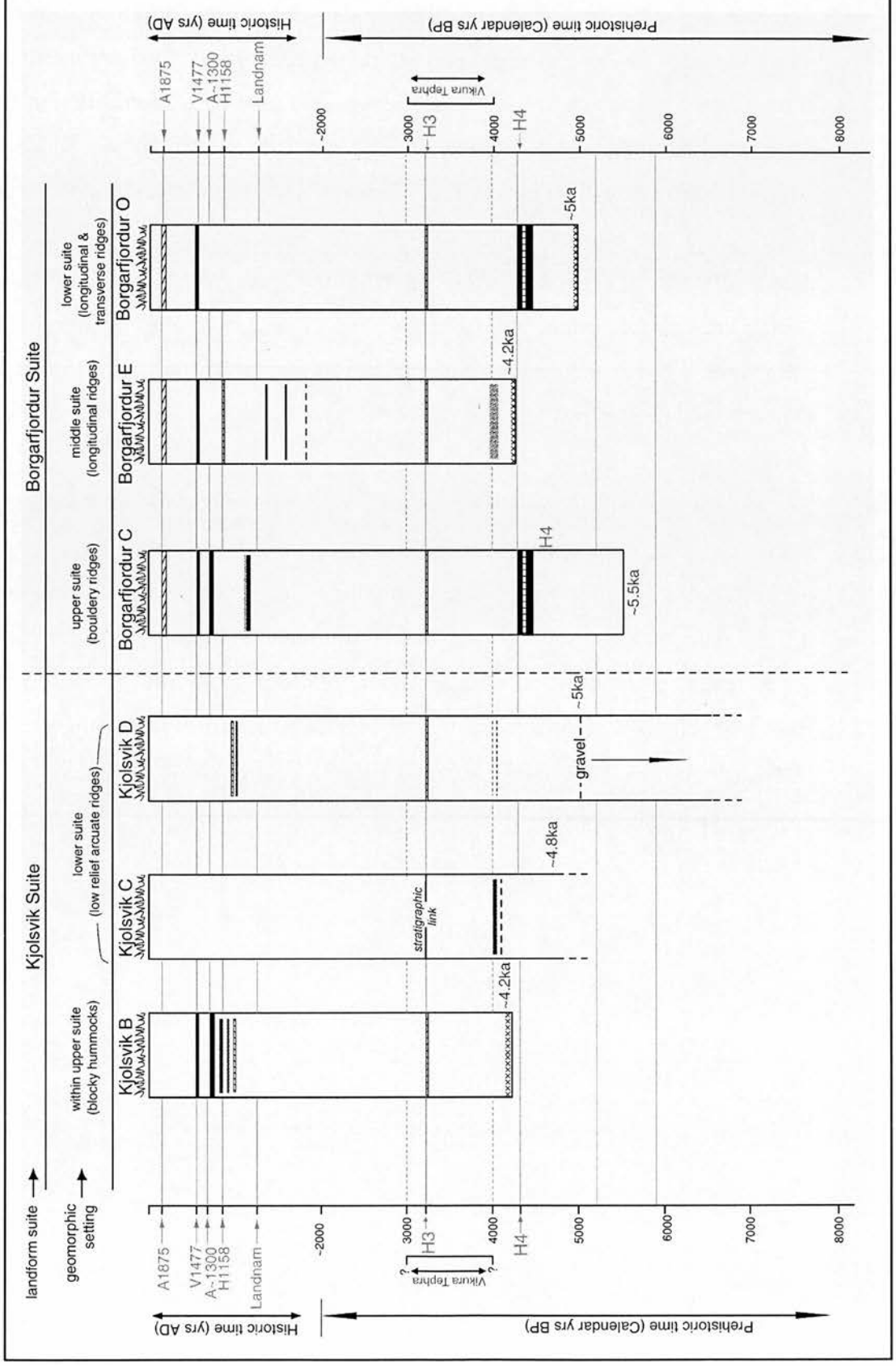

5.4.2. Value of basal ages to date Landform Suites

The use of basal ages from profiles to date landforms provides estimated and minimum ages for landform generation, but depends on the availability, quality and consistency of excavated profiles. Basal ages for profiles within different landform suites are presented in 5.4.1 above, and rely on tephrostratigraphy, radiocarbon and accumulation rate estimations. The following section assesses how representative these ages are of the real timing of landform genesis events. The profiles used to date landforms are evaluated in the context of the geomorphology and other available stratigraphic information, to determine the consistency and quality of the age estimation. Here, we outline potential errors associated with the utilised dating methods, and determine the value of the dates for dating the associated landforms.

Figure 5.4-b presents the initial estimated ages of all the dateable landform suites and landform units, based on the dating evidence, combined with information on the deepest (oldest) available well-dated tephra layer or peat layer which well-constrains the estimate, and information on whether an impenetrable base was reached or not. As a temporal framework within which to place these initial dating results, a Holocene climate record from the Greenland ice cap (Dansgaard et al. 1989; Dansgaard et al. 1993; GRIP.Members 1993; Grootes et al. 1993; Johnsen et al. 1997) is included on the right of the figure.

Figure 5.4-b: Initial age estimates of landform suites based on radiocarbon dates, tephrostratigraphy and accumulation rates: time-lags with climate

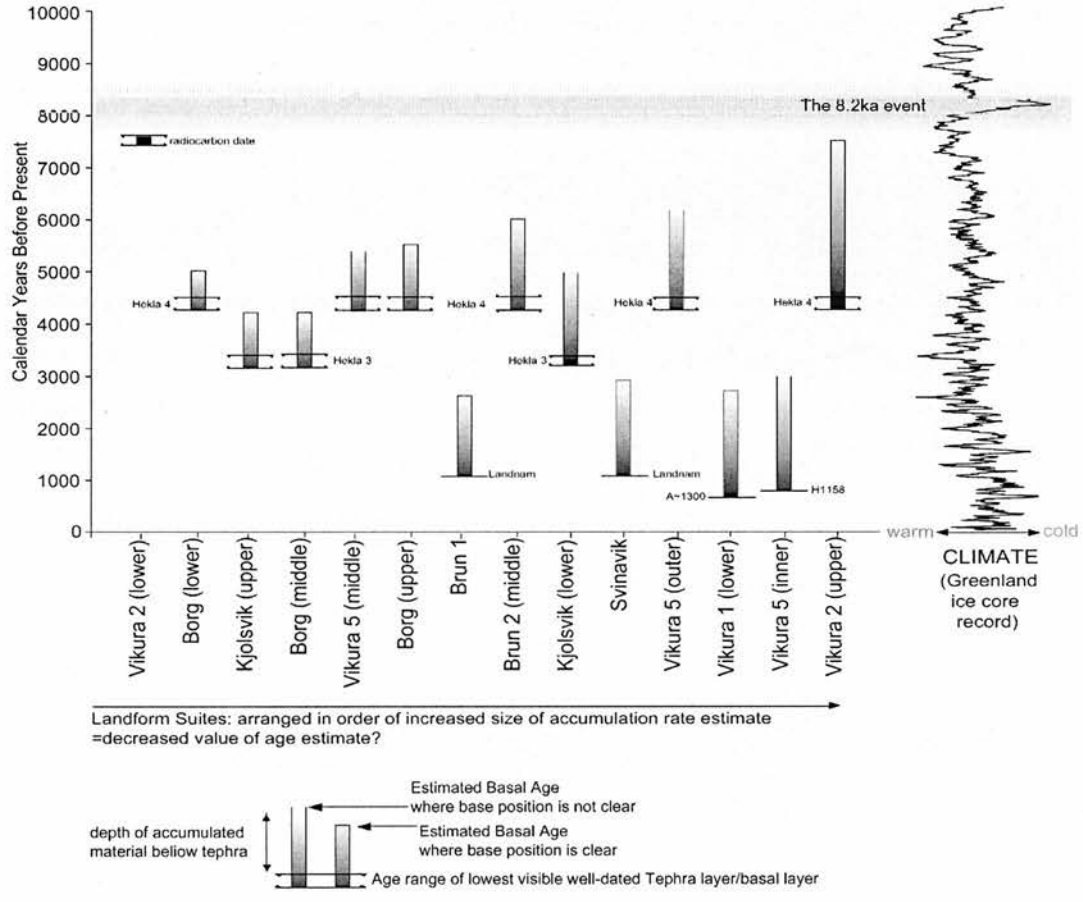

Dating errors associated with determination of the original landform surface

A basal age is expected to represent the age of the sedimentary layer which was laid down immediately on top of the landform surface when it has just been formed. However, determination of the original landform surface can be difficult. Where profiles within a landform suite reach a clear rocky base which extends for some depth, this is likely to represent the landform's original surface, and thus a minimum age for landform genesis can be derived with reasonable certainty. However, the observed rock may simply represent a rocky layer which has been super-imposed on a landform due to later processes, and therefore does no represent the true surface of the landform. In all cases, attempts were made to dig into or through the rock layers, to determine whether it represented a super-imposed layer or an impenetrable landform surface. Some rock layers are quite impenetrable however, so the

possibility must be considered that the base of the profile does not represent the landform surface. Similar problems are caused by indurated layers, or very solid iron layers, which can be impenetrable, again restricting access to the base, and the true landform surface.

A further set of problems arise from sand and gravel layers near the base of a profile. As discussed above, the accumulation rates can be very high, with large volumes being deposited in a short time. Excavating through great depths of such materials can be difficult and time-consuming, and in some cases, the "base" is not reached. Clay can also be present in great depths, with similar problems. These types of materials are potentially linked to the landform surface, or to some later geomorphic activity. However, if a basal layer is not reached beneath such materials, clear information on processes of genesis is not available.

Bearing these issues in mind, where gravels or sand are present at the base of a profile, an estimated basal age is derived for the peat layer immediately above, due to the uncertainties and potential variability in accumulation rates with such materials. As a result these estimates are minimum dates. Dates assigned to the profiles which were not excavated all the way to an impenetrable basal layer (illustrated by dotted lines in the lowest part of the profiles in Figure 5.4-a) again represent minimum ages. Ages derived from such profiles are highlighted in Figure 5.4-b, as having a base position which is "not clear", thus reducing their value.

Dating errors associated with using accumulation rate to estimate basal ages

There are inherent errors associated with dating using accumulation rate estimates, resulting in ages which may be misleading. Profiles may have sections missing from them due to post-depositional processes, resulting in ages which are significantly younger than the real landform age. Therefore, ages presented are generally minimum ages for landform genesis. Accumulation rates have most potential errors when they are relied upon to provide age estimates beneath the lowest well-dated horizon in a profile. As a means of quantifying the extent of these potential errors, the time-lags between the lowest known tephra layer and the estimated basal age are

calculated (shown in Figure 5.4-b). The length of this time-lag could represent the extent to which determination of the age relies on accumulation rate estimates. The greater the depth of material below the lowest time-markers, the more likely the basal date is to be erroneous. However, given the spatial variations in accumulation rate, this approach may require refinement if all profiles are to be compared against each other based purely on material depth. An attempt is made to "normalize" the quantified reliance on accumulation rates according to the known accumulation rates in the upper parts of profiles, the results of which are presented in Figure 5.4-c..

Figure 5.4-c: Summary of basal ages and their value

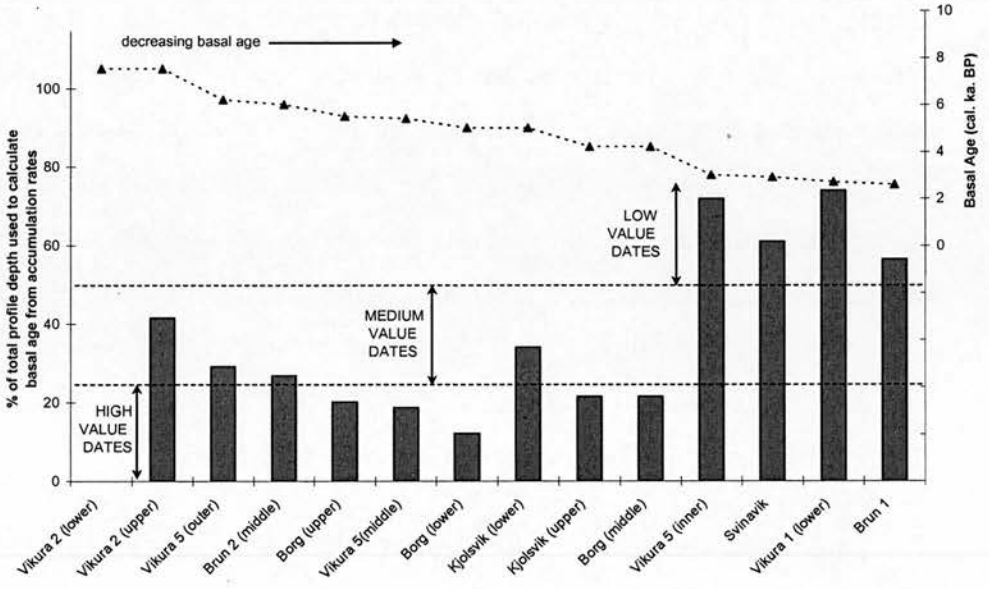

Figure 5.4-c compares the value of dates available for key profiles by ordering them according to the estimated basal age. Instead of measuring the value of the date in terms of the absolute depth of material beneath a known layer (as in Figure 5.4-b), this depth is measured as a proportion of the total profile depth. In this way it is anticipated that spatial variations in rate due to topography will be better 'normalized', as data on more recent (and better dated) accumulation rates is used. Three categories are highlighted, to distinguish between dates which are relatively high value (<25% profile depth estimated), medium value (~50-~25%) and low value (>~50%). NB there is no bar visible to represent Vikura 2 (lower) at the left hand side. This is because 0% of the age is based on accumulation rates.

It can be seen from Figure 5.4-c above, that there is a general trend where the profiles which rely more on accumulation rates to derive basal ages, appear to have younger ages. The four profiles which date landform suites Víkurá 5 (inner), Svinavik, Víkurá 1 (lower) and Brun 1, (on the right hand side in Figure 5.4-c), are

all revealed as having over 50% of their estimated age based on accumulation rates below the lowest visible tephra, making the value of these ages low. The basal ages which have been derived for these profiles all produce ages younger than 4 cal. ka BP, at least 4000 years after the 8.2ka event. These profiles are shown to have visibly younger age ranges than the remaining profiles in Figure 5.4-b.

The best constrained basal age in this study is associated with the lower part of the landform suite Víkurá 2 (left hand side of Figure 5.4-c). It is constrained by radiocarbon dates, and thus does not rely on accumulation rate estimates at all. The date derived for this suite is calibrated to between 7.47 and 7.57 cal. Ka BP, and is therefore the date which has the closest temporal link to the "8.2ka event", post-dating the climate event peak by around 600 years. Given the well-constrained nature of this basal age, and the resultant high "value" attributed to it, this age is thought to be well-representative of the landform suite age. The basal ages dating the Borgarfjörður (Borg) Suite are all classed as high value dates, given the relatively low reliance on accumulation rates, as are those dating the upper Kjólsvík Suite and the middle Víkurá 5 Suite.

5.4.3. Chronology of Landform Genesis Events

The purpose of this chapter was to determine a chronology of geomorphic events which generated the observed landforms. This information in combination with the interpretation of the geomorphic evidence (presented in Chapter 6), will develop understanding of the possible causal connections between processes which generated different landform units, and their relationship (if any) to the 8.2ka event.

In pursuit of this aim, a summary of the chronological information collected thus far (which relates to dating of the landform suites and units) is presented in Table 5.4-a below. Estimated ages (from basal dates) for the key mapped landform suites and, where possible, landform units within these suites, are shown in this table, alongside a valuation of the quality of the date. Bearing in mind the overall aim of the research, to test response to the 8.2ka event, lag-times between landform genesis and

8.2ka are included in the table. It must be noted that these lag-times are rough estimates. In addition to the variable value of landform age estimates, the peak date of the 8.2ka event may not have been at exactly 8.2ka, as assumed here, and its duration could have been as little as 60 years, or as much as 300 years or more. Nevertheless, high-value dates for landform genesis have been acquired, and these should be viewed as significant.

Table 5.4-a: Summary of estimated ages for landform suites

Landform Suite	Landform Unit	Estimated Age (cal. ka BP)	Value of Age estimate	Time-lag since 8.2 (cal. ka. BP)
Víkurá 1	lower	2.7	low	5.5
Víkurá 2	upper *lower*	7.5 *7.47-7.57*	medium *high*	0.5 *0.5*
Víkurá 3	-	No date	-	?
Víkurá 4	-	No date	-	?
Víkurá 5	inner *middle* outer	3 *5.4* 6.2	low *high* medium	5.2 *2.8* 2
Svínavík	lower	2.9	low	5.3
Mosdalur	-	-	No date	?
Kjólsvík	*upper* lower	*4.2* 5	*high* medium	*4* 3.2
Brúnavík 3	-	No date	-	?
Brúnavík 2	middle	6	medium	2.2
Brúnavík 1	middle	2.6	low	5.8
Borgarfjörður	*upper* *middle* *lower*	*5.5* *4.2* *5*	*high* *high* *high*	*2.7* *4* *3.2*

In the following section, an assessment of the dates presented in Table 5.4-a will be made, in the context of the geomorphological and stratigraphic evidence, to address the applicability of the dates described above to the landform suites as a whole. The assessment will take into account the number of available profiles within each landform suite, any evidence of recent erosional activity which may have removed materials and tephra layers, and any further chronological data retrievable from the stratigraphic materials. It is anticipated that following this assessment, initial conclusions can be drawn as to the chronology of landform genesis events, and their timings relative to the putative forcing mechanism, the 8.2ka event. These conclusions will be refined following full interpretation of the specific processes associated with generation of the observed landform suites (Chapter 6).

Víkurá 1

Figure 5.4-d: Location of key profiles in Víkurá 1 Landform Suite

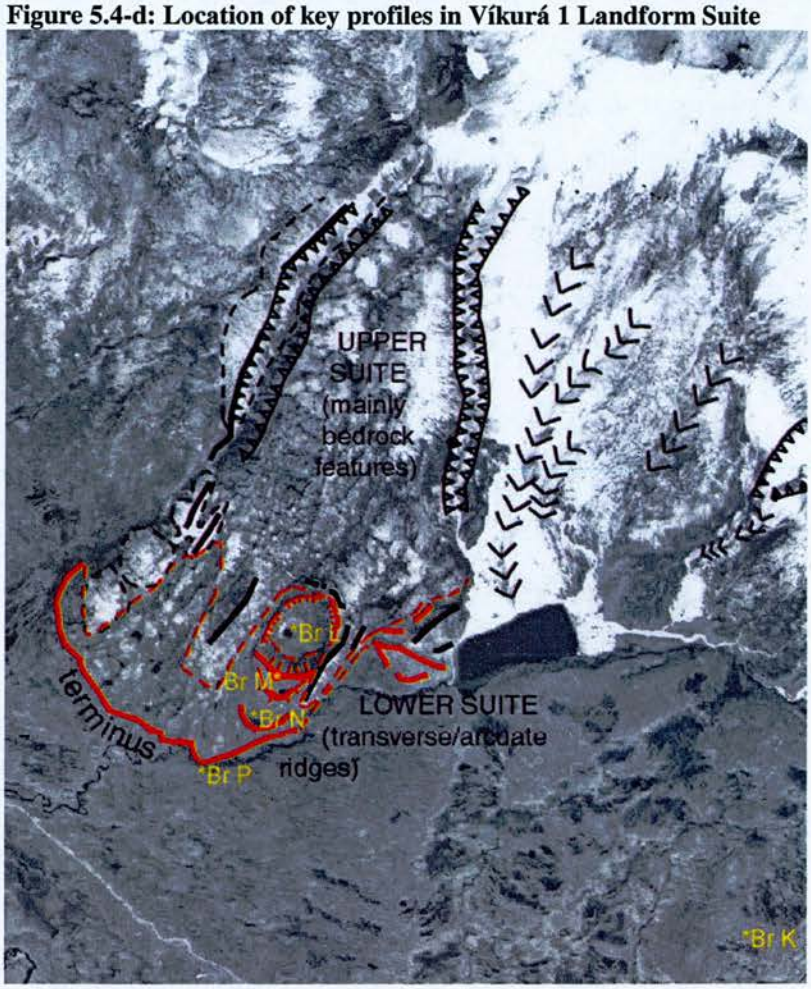

Despite attempts to excavate profiles at numerous sites in the upper Víkurá 2 suite, only a limited number were found in the 'lower' suite, and none in the 'upper' suite. As has been discussed, the basal dates derived from these profiles as indicators of the landform ages are of limited value, due to the extent to which they rely on estimates of accumulation rates. It can be seen in Figure 5.4-e that with the exception of profile "Breidavik L" (Br L) the profiles excavated within the lower limits of the suite contain a significant depth of gravely material, rendering estimation of basal age difficult. Further, the existence of such material suggests the occurrence of geomorphic (debris transport) activity.

Figure 5.4-e: Topographic setting of key profiles within Vikura 1 Landform Suite

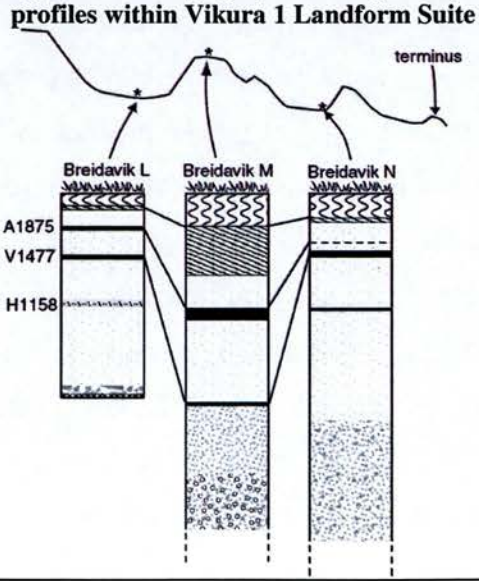

This occurred as recently as 1477 in the location of profile Br M, and at ~2.7 cal ka BP in profile Br N (estimated from soil accumulation rate). The lowest known tephra layer to be found within the suite limits is Hekla 1158, in profile Br L. At the base of this profile, a rocky layer was reached, and it should be ascertained whether this represents the real landform surface. The topographic setting in which this profiles was excavated is described in detail in Chapter 3, as an internally-draining, steep sided basin, surrounded on three sides by bedrock ridges (see 5.4-d). The surrounding bedrock features are heavily frost-shattered and the surfaces are covered in loose debris. In the light of this, it is possible that the rocky layer reached at the base in fact represents debris transported from these bedrock features.

Given the limited number of profiles available to date the Víkurá 1 landform suite, and the poor value of the basal age estimate, the age of ~2.7 cal ka BP is taken to be a minimum age for the landform suite. It is suggested that more recent geomorphic activity may have resulted in profiles which do not reach the original landform surface.

Víkurá 2

Figure 5.4-f: Location of key profiles in Víkurá 2 Landform Suite

Landform suite Víkurá 2 is has the best-constrained dating in the field area, as discussed in 5.4.2, with the availability of radiocarbon dates, and an extensive number of profiles excavated within and outwith the landform suite. Some of the key profiles are illustrated in Figure 5.4-f and Figure 5.4-g. It can be seen that profile Víkurá K (VK), which consists mostly of well-humified peat, is situated immediately inside the lower limit of the Víkurá 2 suite. It dates to 7.52+/-0.05 cal. ka BP, a date retrieved from radiocarbon dating of the basal peat layer. A thick dark tephra layer overlies an impenetrable rocky base immediately beneath this peat.

Figure 5.4-g: Topographic setting of key profiles in Víkurá 2 Landform Suite

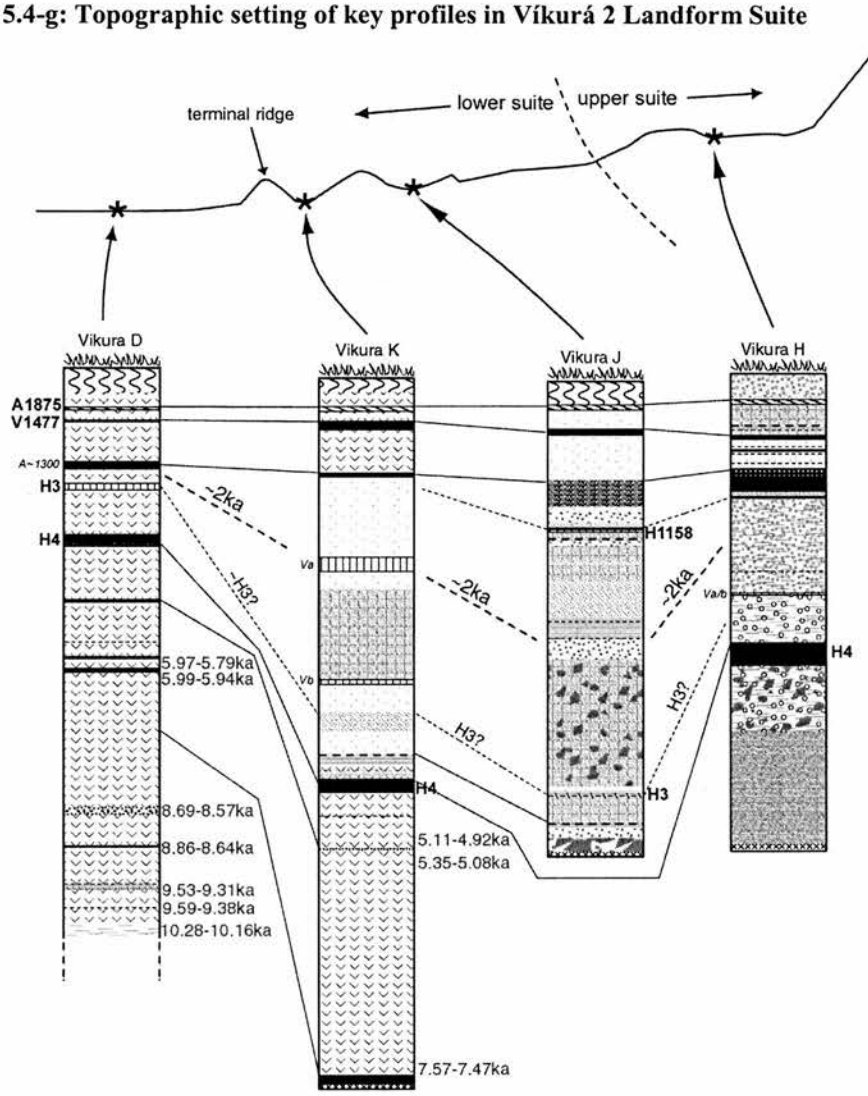

Moving up-slope, in profile Víkurá J (VJ) there is evidence for a mid-Holocene period of geomorphic activity. A rocky layer is found at the base of the profile followed by a sand layer just pre-dating H3 (~3.3 cal. ka BP). It may be significant that a sand layer of similar thickness is found within profile Víkurá K near the landform suite terminus. This stratigraphic connection may represent the same geomorphic event, and a temporal connection, as illustrated in Figure 5.4-g. Immediately above the Hekla 3 tephra in profile J, a further rocky layer probably dates to a maximum of ~2 cal. ka BP. In comparison, the same temporal section of profile K is mostly composed of fine sand. In profile J, the rocky layer is overlain by

sands, which continue from ~2 cal. ka BP until not long before the Hekla 1158 eruption.

Profile Víkurá H is the only profile to be found in the 'upper' Víkurá 2 suite, and the oldest known marker horizon in this profile is the Hekla 4 tephra. The mid-Holocene geomorphic activity evident in profile J, is also evident in H, though the timing appears to slightly pre-date activity lower down-slope. A rocky layer immediately pre-dates Hekla 4 (~4.3 cal. ka BP), underlain by gravely sands, which make up the remaining profile depth. Above Hekla 4, gravely clays make up the depth until around the time of the tephra Hekla 1158.

The basal age derived for profile Víkurá H of ~7.5 cal. ka BP is of low value, due to its reliance on the variable accumulation rate of gravel. Its initial determination was based on its association with profile Víkurá K, which has a high value basal date to back up this age estimate. This date can be viewed as a maximum basal age. The lack of peat or loess accumulation in the lower parts of profiles J and H, indicate general instability on these slopes before ~1158AD. During the mid-Holocene period from ~2 cal. ka BP, the middle and upper parts of the Víkurá 2 landform suite have been characterised by periods of activity resulting in the deposition of rock and sand layers. The lowest known tephra layer visible on the middle and upper slopes of Víkurá 2 is Hekla 4, and estimations of basal ages pre-dating this are problematic due to the variable rate of rock/gravel/sand accumulation. In contrast, the lowest region of the suite, consisting of the outer level of arcuate ridges, displays older basal ages, and mostly undisturbed peat accumulation back to ~7.5 cal. ka BP. It is most likely that significant geomorphic activity has occurred on the middle and upper slopes of the Víkurá 2 suite since 7.5ka, and that the associated landforms probably post-date the arcuate ridges at the lower suite margins. This conclusion is strengthened when the stratigraphic characteristics of other profiles from within the Víkurá 2 suite are observed.

Víkurá 5

Figure 5.4-h: Location of key profiles in the Víkurá 5 Landform Suite

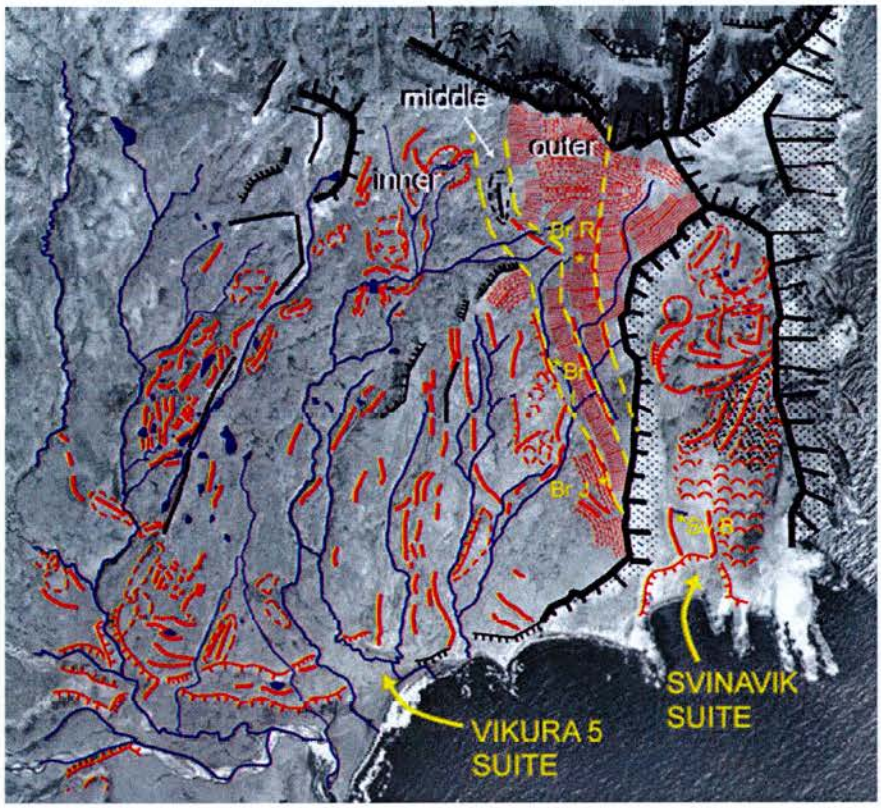

The best three profiles excavated within the Víkurá 5 suite are located respectively within three parallel lateral margins at the eastern edge of the suite, on the slopes of the mountain Grenmór (highlighted in yellow on Figure 5.4-h). Moving down-slope, and into the suite the basal ages derived for these three profiles becomes progressively younger, which is consistent with the geomorphic setting. The three terrace-like ridges represent the outer three lateral margins of the landform suite. It would be expected that any geomorphic activity responsible for creating the outer ridge would have removed any evidence of activity within this limit, and therefore must have occurred prior to generation of the middle and inner ridges. The highest value basal date acquired is that for the middle ridge, which dates to approximately 5.4 cal. ka BP (from accumulation rates), prior to the deposition of the distinctive Hekla 4 tephra. In profile Breidavik I (Figure 5.4-i), the section above H4 shows that environmental conditions enabled undisturbed peat and soil accumulation for ~4000

years until the present. However, beneath H4, the base of this profile was not reached due to the extensive clay deposits which could not be fully excavated. It suggests that conditions immediately pre-dating the Hekla 4 eruption were different from those afterwards. Hekla 4 provides an absolute minimum age for this ridge, and the true basal age may be a reasonable amount older. The outer ridge is estimated to be ~6.2 cal. ka BP, which is a minimum estimate based on accumulation rates. As can be seen in Figure 5.4-i, the accumulation rate for profile Breidavik R is very low, with layers thought to be H3 and H4 being observed in the upper third of the total depth. Beneath H4 are significant depths of peat and peaty clay, which would be likely to accumulate steadily over time. The real basal age may again be older than that suggested. The lack of any major tephra layers below Hekla 4 does make it unlikely, however, that any of these profiles date to pre-Holocene times.

Figure 5.4-i: Topographic setting of key profiles in Víkurá 5 Landform Suite

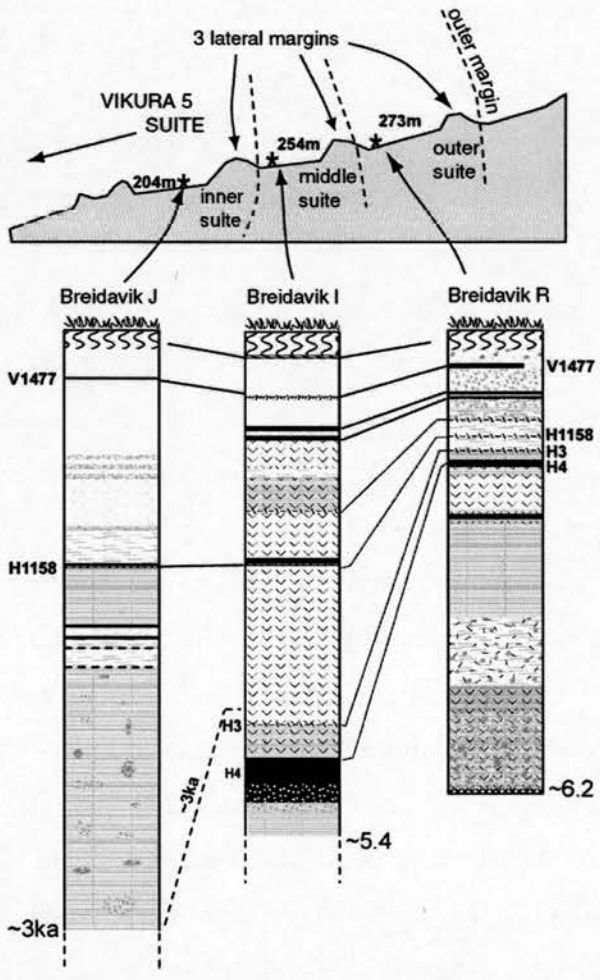

Svínavík

Figure 5.4-j: Svínavík B profile

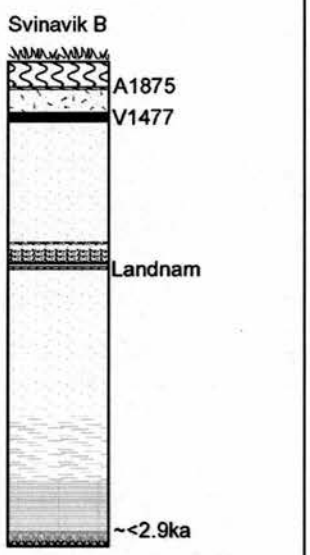

The location of a single profile, Sv B, excavated in the Svínavík suite is shown in Figure 5.4-h. The oldest identified tephra in this profile is Landnam, dating to ~870AD. The profile's basal age is estimated at ~2.9 cal. ka BP, based on a steady accumulation rate of soils and silts since deposition of the Landnam tephra. Many further profiles were excavated with little information being retrieved. Few profiles were deeper than ~50cm, and profile Sv B was the only one which contained tephras dating to before the Veiðivötn 1477 eruption. This may suggest that most of the Svínavík suite has been active until recent times.

Use of the basal age from Sv B to represent the age of the whole suite is problematic due to the lack of further available dates. However, generation of at least the lower part of the landform suite can be said to significantly precede Landnam. Due to the non-existence of Hekla 3 in this profile, there is no evidence to suggest that the Svinavik suite could have preceded this eruption.

Kjólsvík

Figure 5.4-k: Location of key profiles in Kjólsvík Suite

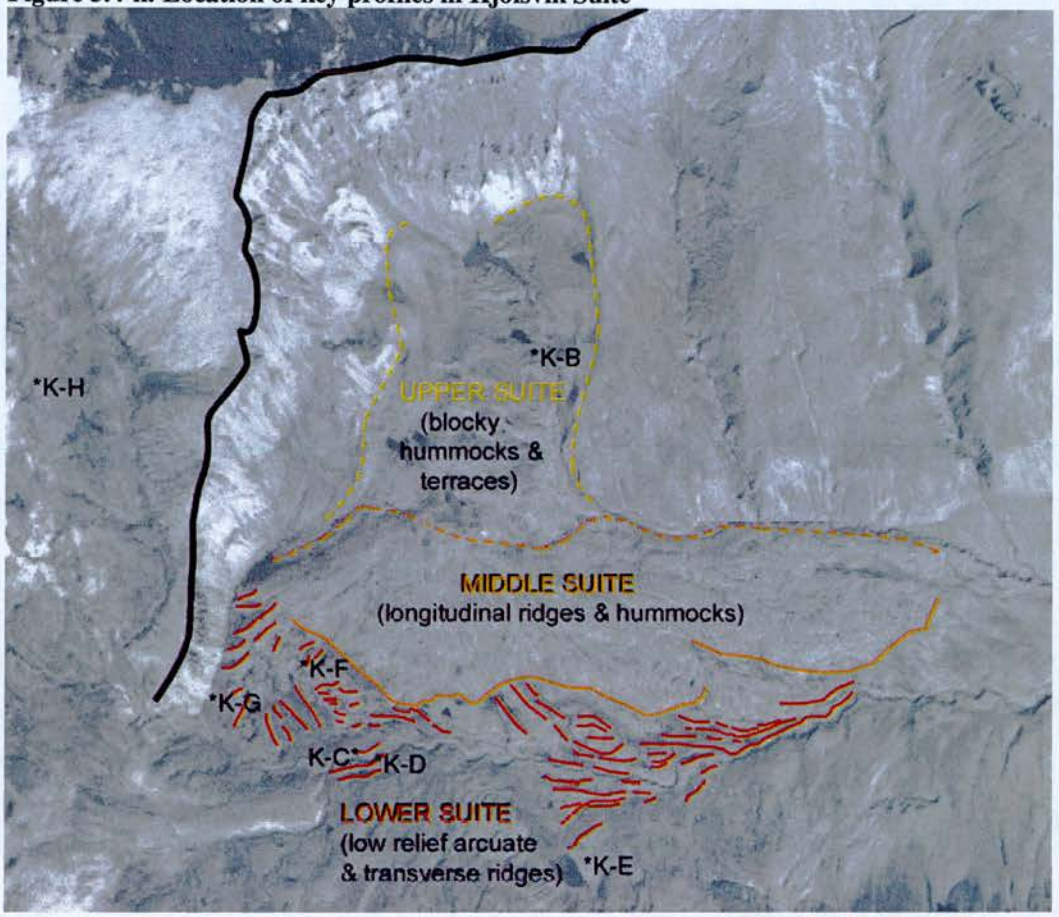

The upper part of the Kjólsvík landform suite is a distinct landform unit characterised by large blocky hummocks and terraces which contain rock blocks and surface debris, as discussed in Chapter 3 and 4. Only one useful stratigraphic profile was excavated in this upper part of the Kjólsvík suite, Kjólsvík B (K-B in Figure 5.4-k). This profile definitively contains the Hekla 3 tephra layer, providing a minimum age constraint on genesis of the upper unit of blocky landforms. As seen in Figure 5.4-l, beneath H3 is a depth of silty material which probably correlates to ~1000 years of accumulation (based on a well-constrained constant accumulation rate above H3). The basal age estimate of ~4.2ka is of relatively high value, as discussed in 5.4.2. The key marker horizon Hekla 4 is not found in this profile, indicating that the underlying surface probably post-dates this eruption.

The tephrostratigraphy of the lower part of the Kjólsvík suite is sparse, despite the excavation of a number of profiles. However, the existence of some key marker tephras enables the development of a chronology. Hekla 3 is again evident, overlying a rocky layer shown in profiles C and D in Figure 5.4-l below. This indicates that geomorphic (debris transport) activity occurred immediately prior to the deposition of Hekla 3 tephra. As can be seen, below this rock layer is a significant depth of undisturbed peat accumulation in both profiles C and D.

Figure 5.4-l: Topographic setting of key profiles in Kjólsvík Suite

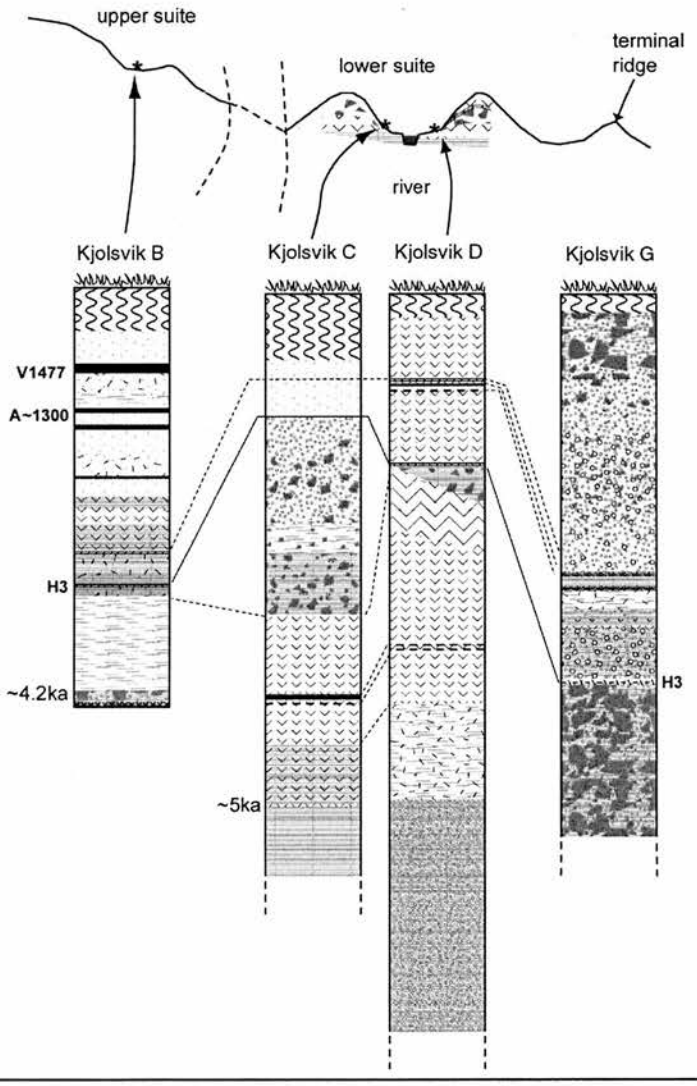

Two fine dark tephras are present within this lower peat section of profiles C and D, which are not seen in profile B (upper suite). The origin and age of these tephras was not identified, but their existence suggests that the lower part of the Kjólsvík suite pre-dates the upper suite.

Profile G (illustrated in Figure 5.4-l) was excavated at the western margin of the suite, and demonstrates the existence of significant geomorphic activity. The profile contains a rocky layer immediately prior to the deposition of Askja 1875, indicating

very recent activity. From this layer, the profile as far down as Hekla 3 consists mostly of sands, gravels and small stones. Beneath Hekla 3, as was seen in profiles C and D, is a further rocky layer. The rocks in this layer, in contrast to those in the other profiles, are larger, and become impenetrable. The thickness of the layer is greater than that found in C and D. It is evident that a great deal of geomorphic activity has occurred in the area where profile G is situated. When its location is observed in Figure 5.4-k, it can be seen that it is directly below a steep scree slope and cliff face, which may explain its high debris content. The basal age of this region, next to the cliff face, appears to be younger than the remaining part of the lower suite.

Based on accumulation rates, a tentative basal age of ~5 cal. ka is suggested for the lower suite around profiles B and C, within the region of arcuate and transverse ridges. However, without clear evidence for the existence of Hekla 4 in these profiles, this estimation is of low value. The upper suite, and the region in close proximity to the cliffs, has been active more recently.

Brúnavík 1 and 2

Many reference profiles were available in the Brúnavík valley, but few were excavated within the limits of the Brúnavík landform suites. Within Brúnavík 1 and 2 (shown in Figure 5.4-m), soil cover is mostly very thin, and a high rock content made many profiles impenetrable. The two best available profiles for dating these two landform suites are shown in Figure 5.4-n. As explained in 5.4.2, the value of the date derived for Brúnavík 1 is low, as the basal age relies largely on accumulation rate estimates. In addition, most profiles excavated within this suite were made up, in the lower part, of gravels (as in profile Brúnavík V, Figure 5.4-n).

Figure 5.4-m: Location of profiles within landform suites Brúnavík 1 and 2

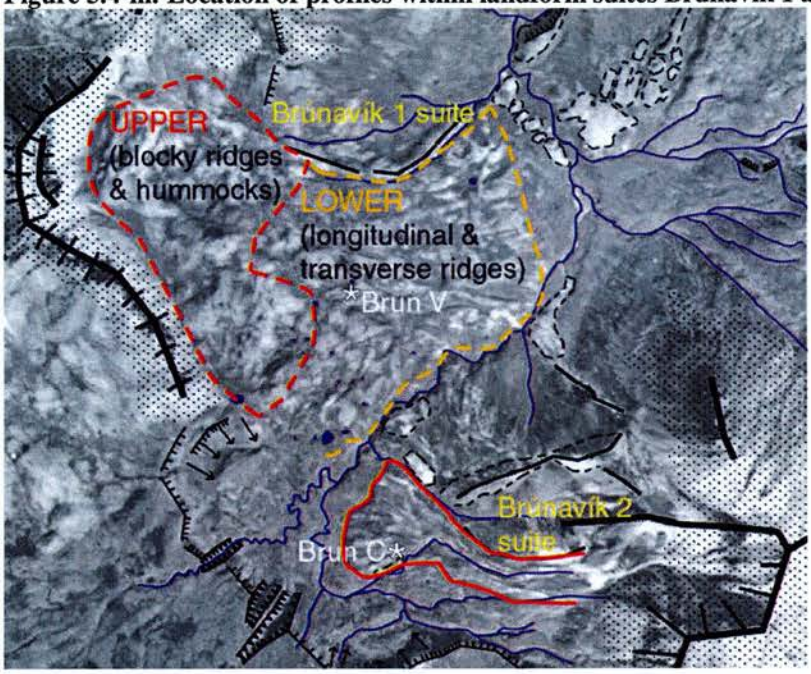

Figure 5.4-n: Profiles excavated from within the Brúnavík landform suites

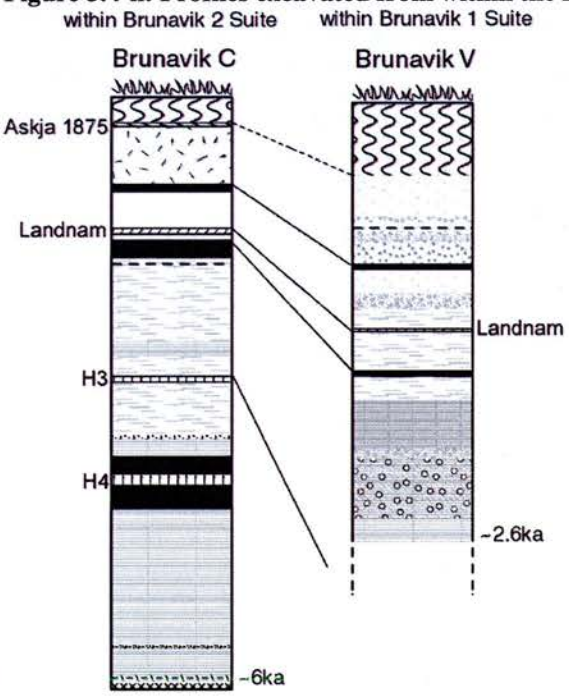

Profile Brúnavík V is within the area of longitudinal ridges in the lower Brúnavík 1 Suite, though it lies close to the margin with the upper suite, characterised by blocky hummocks and ridges. Based on the location of the Landnam tephra, an estimated

basal age of ~2.6ka is assigned to the profile. Given the difficulties encountered in reaching a rocky base representing the landform suite surface, this estimate is likely to be a minimum age.

In contrast, the profile providing an age for the Brúnavík 2 suite is better constrained. It reaches a clear basal layer and contains the well-known tephra Hekla 4 at two thirds of the profile depth. A further two tephras of unknown origin and age are present beneath H4. Based on accumulation rates, a basal age of ~6ka is postulated. This age is thought to represent a maximum landform suite age. Profiles from the inner part of the suite tend to show younger basal ages, which may suggest that the inner part is younger than the outer part, and therefore probably overlies or removed older landforms.

Borgarfjörður Suite

Three key dateable areas of the Borgarfjörður Suite are the upper (defined by large scale hummocks and ridges), middle (longitudinal ridges) and lower (transverse and arcuate ridges, with some hummocky terrain). In Figure 5.4-p, the stratigraphy of the key profiles is presented, the locations of which are shown in Figure 5.4-o. In the upper suite, H4 is clearly visible, providing a good marker horizon. The basal age of profile Borgarfjörður C, which reaches a clear rocky base, is estimated to have a basal age of ~5ka. The Borgarfjörður D profile does not reach a rocky base, and is estimated to be slightly older at ~5.5ka from accumulation rates. 5ka represents a high value minimum age estimate for the upper suite. In the middle suite, a high value age estimate of 4.2ka is based on the existence of Hekla 3, and a further layer beneath this, in profiles E and F, and the clear rocky base which is reached in both. Profile M may contain tephra layer H4, making its basal age older. However, the identification of H4 is only based on physical characteristics and cannot be clarified.

Figure 5.4-o: Location of key profiles within the Borgarfjörður Suite

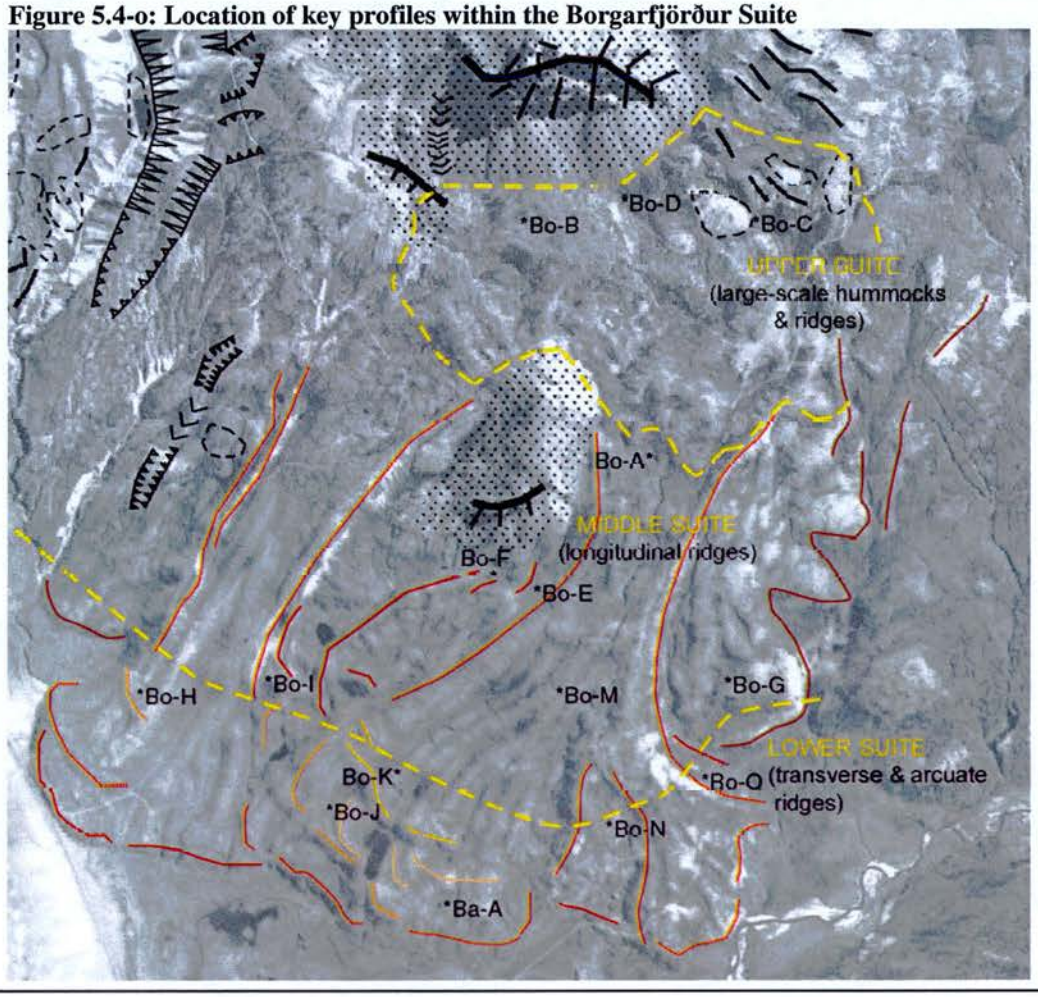

In the lower suite, profiles within the transverse ridges (Borgarfjörður J and Bakka A) are provided a high value minimum age by the existence of H3 and a clear base. Profiles N and O lie in the lower suite, but are not associated with transverse or arcuate ridges, instead lying within two distinct areas of hummocky, un-orientated terrain. While N has a basal age consistent with the rest of the lower suite, O suggests an older age due to the existence of H4 in the profile.

In conclusion, the upper suite is certainly of pre-H4 age, whilst the middle and lower suites may have been generated around the time of the Hekla 4 eruption, pre-dating Hekla 3 by ~1000 years. It is evident that in the lower suite, the hummocky, un-oriented terrain, may pre-date the genesis of the transverse and arcuate ridges. There is a strong geomorphological connection between the longitudinal ridges of the

middle suite, and the transverse and arcuate ridges of the lower suite, indicating they share a genetic origin. Given this shared 'process' origin, the longitudinal and transverse ridges are likely to have been formed simultaneously at ~4ka, just post-dating H4. The upper suite is older, pre-dating H4, and may have been generated simultaneously with the hummocky terrain found in small areas of the lower suite.

Figure 5.4-p: Stratigraphic profiles within the limits of the Borgarfjörður Suite

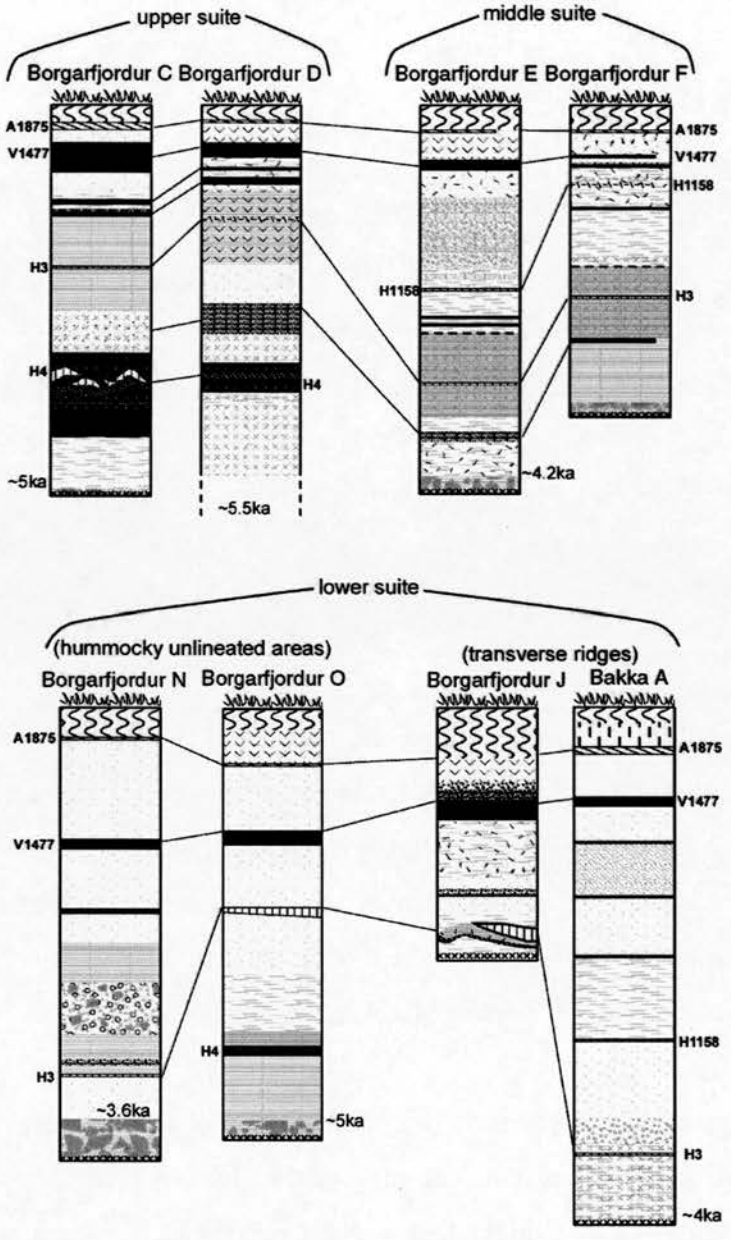

5.5. Summary

Figure 5.5-a: Summary of ages derived from basal ages for landform suites

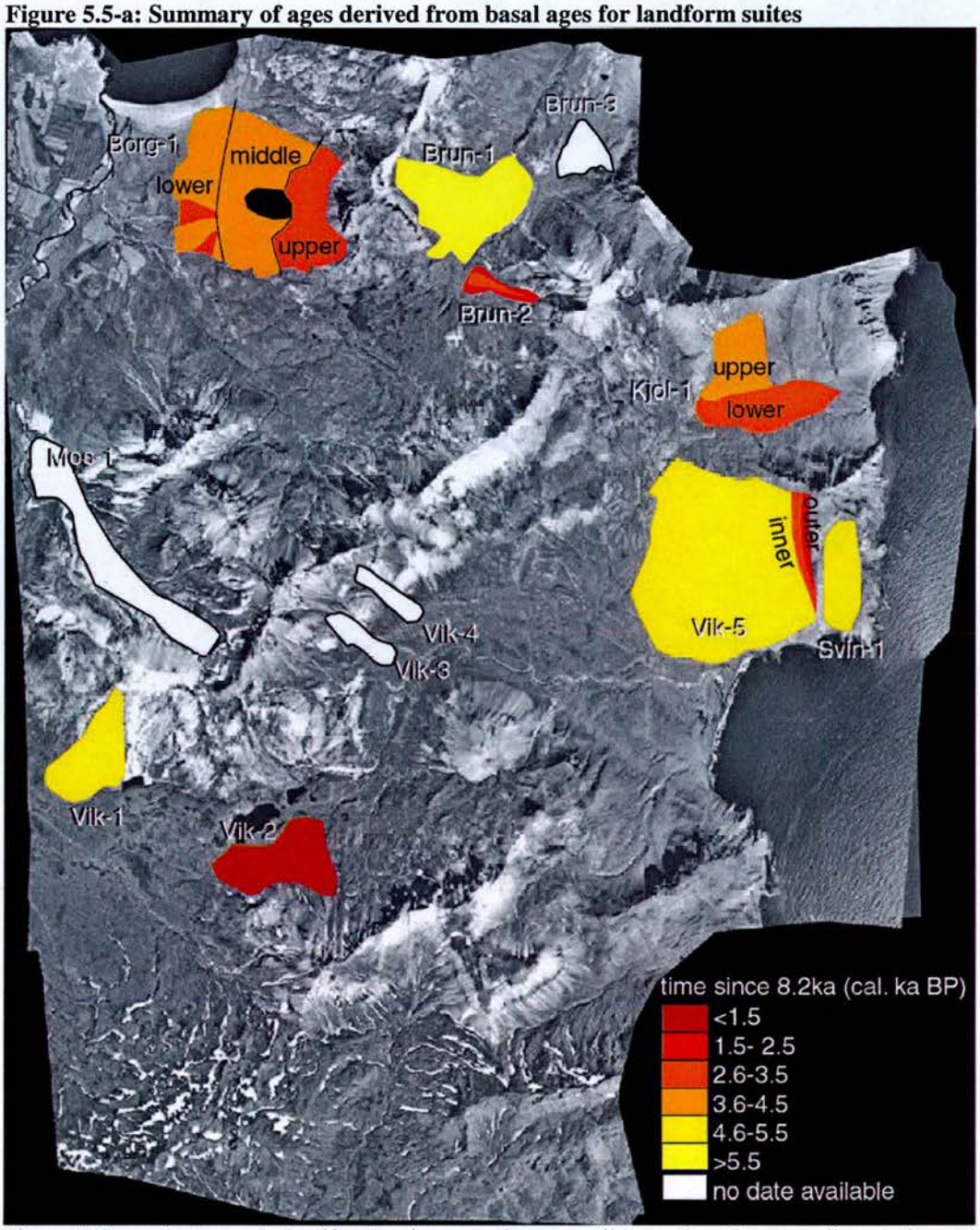

Figure 5.5-a colours each landform suite, or where possible each unit, according to its age derived from the stratigraphy. The dates are presented as 'years since the 8.2ka event', to provide a temporal context within which to compare ages.

Figure 5.5-a summarises the ages derived for the landform suites based on stratigraphic basal ages. It can be seen that the suite Víkurá-2 (Vik-2) appears to be

the most closely related to the 8.2ka event, chronologically. The Borgarfjörður (Borg-1), Brúnavík 2 (Brun-2) and Kjólsvík (Kjol-1) landform suites all show ages linking them to early-mid Holocene genesis, showing evidence of temporally distinct phases of activity producing different landform types. As discussed above, the landform suites which show ages far-removed form 8.2ka (eg Brun-1 and Vik-1) rely on poor value basal dates, and the ages presented are minimum ages. It is likely that these may in fact be older.

In Figure 5.5-b, the sedimentary information presented in 5.4 is summarised. The chronology of geomorphic events derived from basal ages is expanded, by including information on debris transport activity which has occurred since original landform genesis. Simplified stratigraphic profiles are presented, with depth converted to age, as in Figure 5.4-a. Sedimentary sequences representative of debris transport activity are highlighted (see areas of red stripes), with a distinction made between layers of sand/gravel, and layers of rocks. These layers within the profiles indicate phases of geomorphic activity which have super-imposed materials on top of the original landform surface. It can be seen that in addition to activity associated with landform suite generation, further phases of activity have occurred since, depositing layers of rocks and gravels on top of previously generated landforms. This activity occurs at various points in the mid-Holocene, centring at ~2.7ka, ~3.2ka, ~4.2ka and ~5-5.5ka in various locations. Two basal ages (from suite Brun-2 and Vik-5) reveal a period of geomorphic activity ceasing at ~6ka, and a further basal age shows activity which ended at ~7.5ka.

Figure 5.5-b: Phases of geomorphic activity in disparate landform suites

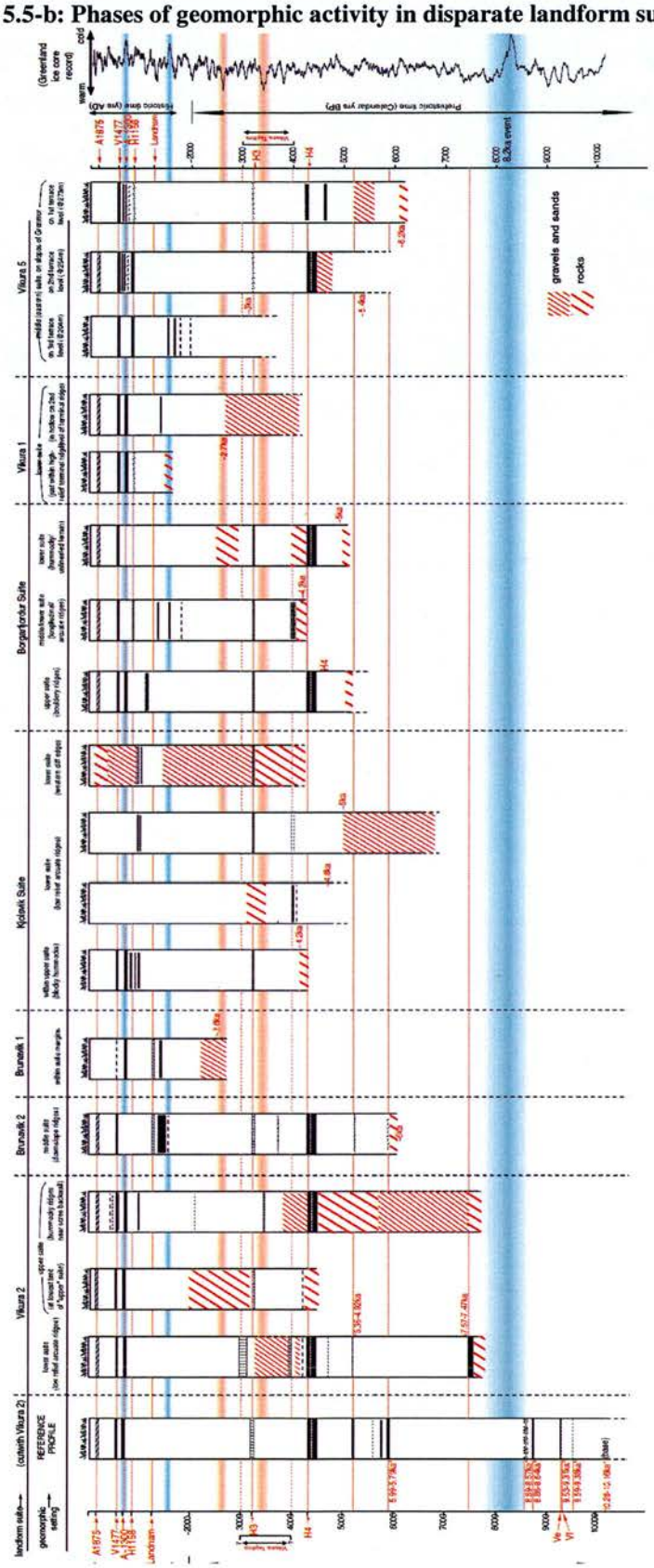

To place these phases of activity in a temporal context, a climate proxy from the Greenland ice core record (Dansgaard et al. 1989; Dansgaard et al. 1993; GRIP.Members 1993; Grootes et al. 1993; Johnsen et al. 1997) is included, highlighting some periods of cooler (shown in blue) and warmer (shown in red) temperatures. The nature of possible connections evident in Figure 5.5-b, between this climate record and the geomorphic record will be assessed in the following chapter. Chapter 6 will provide a detailed interpretation of the specific geomorphic processes responsible for generating the observed landform suites and sedimentary sequences. This information on process, combined with the chronological data presented in the current chapter, will enable development of a revised chronology of geomorphic events, and allow assessment to be made of the causal connections between distinct phases of geomorphic activity and climate.

6. Interpretation of Geomorphic Evidence

6.1. Introduction

Following detailed geomorphic mapping of the field area from aerial photographs and field observations, described in Chapter 3, key suites of landforms are identified which may be indicative of a complex geomorphic response mechanism to an Early Holocene climatic fluctuation. Various distinct landform units are found juxtaposed within each suite of features, which exhibit morphological characteristics of a number of different geomorphic processes. As outlined in Chapter 4, the disparities between and within landform suites indicate the activity of a number of geomorphic systems which are either (i) temporally separate or (ii) unique in system type and process. Chronological control (presented in Chapter 5) addresses (i) and in this chapter, interpretation and classification of system type address (ii). Neither of these outcomes rules out the possibility that the geomorphic activity is related, directly or indirectly, to a single climate event, and the two theories are not mutually exclusive. It is possible that multiple system types are responsible for generating the landforms, and that they were active non-synchronously.

The chronological evidence linked to the geomorphology, illustrated in Chapter 5, shows that although unique landforms are juxtaposed in space within the margins of each suite, the processes which generated them did not occur synchronously. It needs to be ascertained whether these suites of landforms are representative of the same process occurring non-synchronously, or whether the separate events may have involved distinct systems and associated processes. In order to extract a climatic signal from the geomorphic evidence, the way in which different types of geomorphic activity interact with climate needs to be established. Further, the extent that separate geomorphic events may be causally related, and therefore attributable to the same initial triggering mechanism, must be assessed.

The first part of this chapter tackles the problem of defining processes from geomorphic evidence, aiming to classify the systems and associated processes responsible for creating the observed landform suites. This is achieved through detailed study of the ways in which the landform record can provide information on process and system type. A series of detailed site-specific analyses of the geomorphic evidence will then be carried out as a means of interpreting the geomorphic process or processes which produced each observed landform type. Hypotheses are developed to explain the forcing mechanisms behind the observed landform suite generation. In the second part of the chapter, this interpretation of landforms enables assessment of the potential existence of causal links between separate geomorphic events, and their relation to external forcing. It is suggested that each distinct landform type could represent a specific phase in a complex multi-faceted response mechanism to some climatic perturbation. As is typical of environmental systems, it is plausible that such a complex series of events occurring over time is related to a simple external forcing, the effects of which propagate as a result of internal feedback within the system. For example, a geomorphic process is initially triggered by a single short-lived climatic fluctuation, and the subsequent instability in the system prompts further processes to occur in order to regain a more stable state. Testing of these hypotheses, regarding the nature of causal links, is possible with detailed knowledge of the timing of the geomorphic 'events', as presented in Chapter 5. The chronology of events can be compared and, where possible, correlated with climate records.

The climatic implications of this study are significant. If it is shown that there is a causal link between geomorphic events, the evidence is consistent with a time-transgressive response to a single climate (or other) forcing event. If a causal link is not evident, a series of unrelated geomorphic events are likely to have occurred in response to a series of climatic (or other) forcing events.

6.2. Background to classifying landforms

Classification of landforms in terms of processes of genesis is fundamental to understanding why the landform suites observed in the field have some morphological disparities. As suggested in Chapter 4.3, the observed landform suites in the field area are related to redistribution of debris, by a system (or systems) involving transportation of debris, ice and/or water. The aim of this section is to define the systems, by replacing the *generic* landform classifications outlined in Chapter 3, with *genetic* classifications relating to processes of landform genesis. In this way, it can be established whether the landforms represent (i) the response of one type of system regionally to a forcing mechanism, (ii) the response of multiple system types to a forcing mechanism, or (iii) a multitude of separate geomorphic events occurring in response to various un-related forcing mechanisms.

Figure 6.2-a: Interpretation of geomorphic evidence

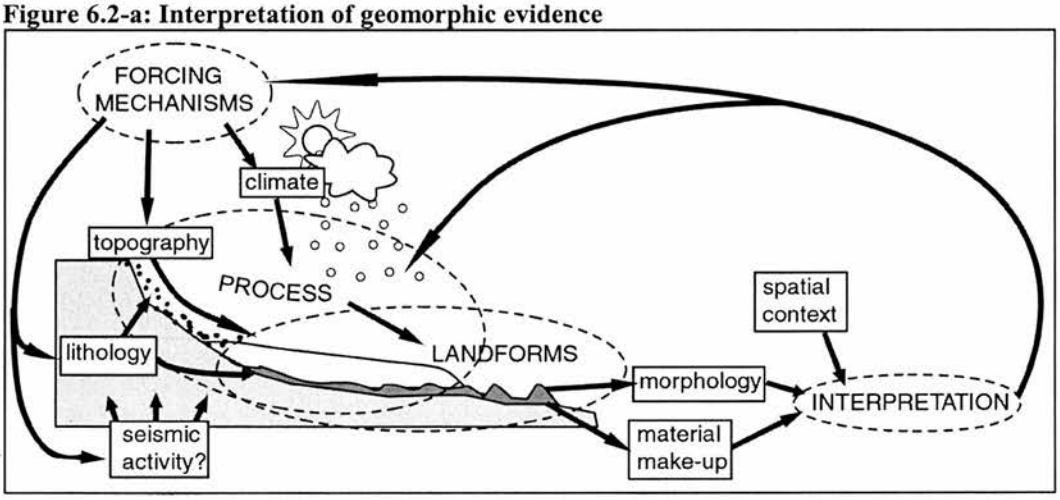

Figure 6.2-a above shows how various forcing mechanism influence geomorphic process, and these processes are reflected in the landform record. Interpretation of this record through reference to morphology, material make-up, and spatial context, enables hypotheses to be developed as to processes of landform genesis, and the forcing mechanisms which influenced these processes.

From the field evidence, detailed information is available on spatial context, morphology and, where possible, material make-up. The challenge of this chapter is to use this data to derive evidence of processes and system types involved in the landform genesis. Figure 6.2-a illustrates the methodology behind interpretation of

geomorphic evidence, which enables genetic classifications of landforms mapped in the field to be made.

Different classifications for the same landform can dramatically change the reconstruction of landscape environmental history. For example, classification of non-glacial forms such as landslide or avalanche deposits as glacial moraines, may support a theory of landscape evolution involving a glacial advance which did not occur. Such problems are outlined by (Hewitt 1999) who reclassifies landforms previously assigned as moraines indicating ice advances, to be rock avalanche debris deposits. The climatic implication of active debris redistribution by ice is significant compared with debris re-distribution by other means, as ice content is an indicator of climatic conditions. In this interpretation, particular attention is paid to the ice content of the system, as the aim is to derive the value of the climatic signal held in the geomorphic record.

Before attempting to make classifications pertaining to processes of landform genesis and system type, it is necessary to assess the expected morphological and sedimentological characteristics of landforms associated with different systems, derived from the literature. Here we outline the landform morphology and material make-up characteristics of landforms associated with the various possible debris-transport systems, from debris-covered glaciers to landslides and debris flows, based on current literature, in relation to the key processes of landform formation. From this information, a set of testable hypotheses are created (presented in Chapter 6.3) to enable classification of landforms found in the field by genetic origin. Once processes of formation are determined as so, claims can be made as to the possible forcing mechanisms behind the geomorphic activity, and the climatic and other conditions at the time of landform genesis.

It should be noted, however, that by discussing each system separately in the following sections, it is not also implied that the systems are always separate in terms of process. There is an underlying continuum in process which is linked to a continuum in morphology (Kirkbride 1989). In the context of this study, this

continuum of process is related to the relative ice/snow/debris content of different systems. The system's behavior may be altered by the influence of topography and lithology. The same general system type may be active, such as a glacier, but topography and lithology supply variable debris-cover. In effect, the glacial system may become a "debris-covered glacier", which responds to forcing mechanisms such as climate in a different way from a clean glacier. In contrast, there are some categories between which there is no continuum, where system types are fundamentally different in terms of the conditions necessary to trigger activity, and the nature of their behavior. For example, a glacier and a landslide have very different triggering mechanisms and related processes, so they interact with forcing mechanisms in different ways. As a structural framework, the debris-transport systems discussed here are split into those initiated by ice growth, which are thus the best climate indicators (6.2.1) and those initiated by slope failure (6.2.2).

6.2.1. Glacial Processes: Geomorphic Characteristics

The morphology of glacial deposits varies significantly depending on the nature of the ice, the basal melt, the underlying topography, the amount of supraglacial or englacial rock debris, and the varying associated glacial processes occurring. Here a brief overview is provided of key characteristics of glacial landforms which will aid classification of glacial indicators. This overview of glacial activity includes clean glaciers, debris-covered glaciers, and rock-glaciers, which will each be individually addressed.

Glaciers

There are well-documented ways of identifying glacial or fluvioglacial processes from the material make-up of their deposits, which are overviewed here. However, there are a number of difficulties with appealing to material make-up alone for deriving process information, especially in environments such as Iceland. Due to the geology of the field area and the current extent of frost-shattering processes, information retrieved on current material make-up is not representative of the materials deposited at the time of landform genesis, but rather an artefact of recent

weathering processes. Consequently, this study appeals mostly to morphological characteristics.

The nature of glacial landforms depends on the scale of the glacier. Corrie glaciers have different characteristics from glacial tongues feeding of ice sheets. In the Borgarfjörður Eystri region, the mapped landform suites extend from putative 'accumulation areas', which are often little more than small depressions on the hill-slope, backed by scree slopes and cliffs. The lower margins of the landform suites lie at or above the valley floor. Subsequently, if the suites do relate to glacial activity, it is likely to have been small-scale corrie glaciation.

Here the study does not attempt to provide a characterisation of all landform types one would expect to encounter related to glaciation, but outlines the main features which may indicate a glacial origin. Figure 6.2-b shown a simplified corrie glacier system in a topographic setting comparable to that observed in the field. Landform suites originate in very small depressions beneath steep scree slopes and cliffs, and are often constrained at their lateral margins by bedrock ridges.

Figure 6.2-b: Simplified corrie glacier system with some key landform types

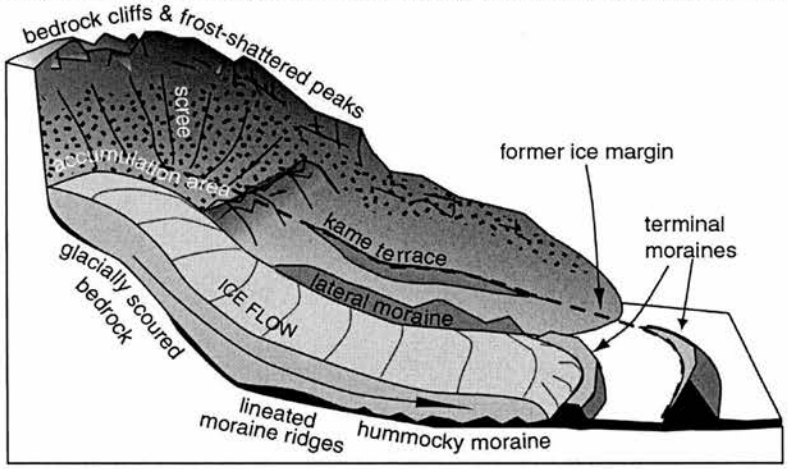

A brief overview is presented, of some key features illustrated in Figure 6.2-b. If the mapped landform suites represent glacial landforms, one would expect landforms representing glacial and fluvioglacial deposition beneath or proximal to the ice. In addition, eroded bedrock forms may be present, and glaciofluvial deposits are

possible beyond the terminus. Ice-marginal landforms which may occur include terminal moraines (arcuate and transverse), lateral moraines (longitudinal) and kame terraces. Sub-glacially formed features vary depending on whether the ice is active or stagnating, and on the extent of subglacial fluvial activity. Moraine beneath the glacier will be oriented downslope by an active glacier, while unlineated hummocky moraine may form under less active ice (Ham and Attig 1996). Kame and kettle topography is a feature of stagnating ice, where ice slowly wastes away within a mass of debris, resulting in chaotic morphology of hummocks and deep hollows (indicating the locations of former ice blocks). Fluvioglacial features such as eskers may be present on the valley floor where subglacial and englacial streams have deposited their debris loads.

Surface features of glacial landforms include erratics transported by ice, and further debris cover relating to post-depositional rock-fall from surrounding cliffs. Information on material composition helps determine between glacial, glaciofluvial and glaciolacustrine deposits, if accessible exposures can be found. Generally, glaciofluvial deposits are characterised by rounded clasts, and possibly sorting and bedding of materials. Landforms of glacial deposition contain unsorted and more angular matrix-supported clasts, whilst glaciolacustrine sediments are likely to be bedded and fine-grained. As has been discussed, such data is limited in the field area, but where it has been found, it will be discussed fully in relation to each specific site.

Debris Covered Glaciers

The morphology of a debris-covered glacier deposit differ from that of a clean glacier, reflecting the long residency times of debris-covered ice relative to clean ice, and the higher volumes of debris available for landform generation. Many studies have addressed the glaciological and geomorphic implications of debris cover on glaciers (Bozhinsky et al. 1986; Clark et al. 1994; Kirkbride 1995; Ackert Jr. 1998; Nakawo and Rana 1999; Shroder et al. 2000; Jansson and Fredin 2002; Everest and Bradwell 2003), and it is recognised that above a critical debris thickness, ablation at the glacier surface is reduced, allowing ice to remain, insulated, for a longer period

than clean ice. The main geomorphological difference one might expect between landforms indicative of debris covered glaciers as opposed to clean glaciers, is that there is likely to be more stagnating ice topography. Ice-cored debris may exist for a long time after the glacier is no longer active, resulting in morphology related to in situ stagnation of ice over time, ranging from ice-cored moraines to kames and kettle holes, and hummocky terrain (Kjær and Krüger 2001; Jansson et al. 2002). Such topography is evident in Figure 6.2-c which illustrated a debris-covered glacier in the Himalayas. Here a transition in morphology occurs from landforms associated with active ice (e.g. lineated ridges), to those related to in situ stagnating ice (chaotic hummocks and kettle holes).

Figure 6.2-c: Debris-covered glacier in the Himalayas

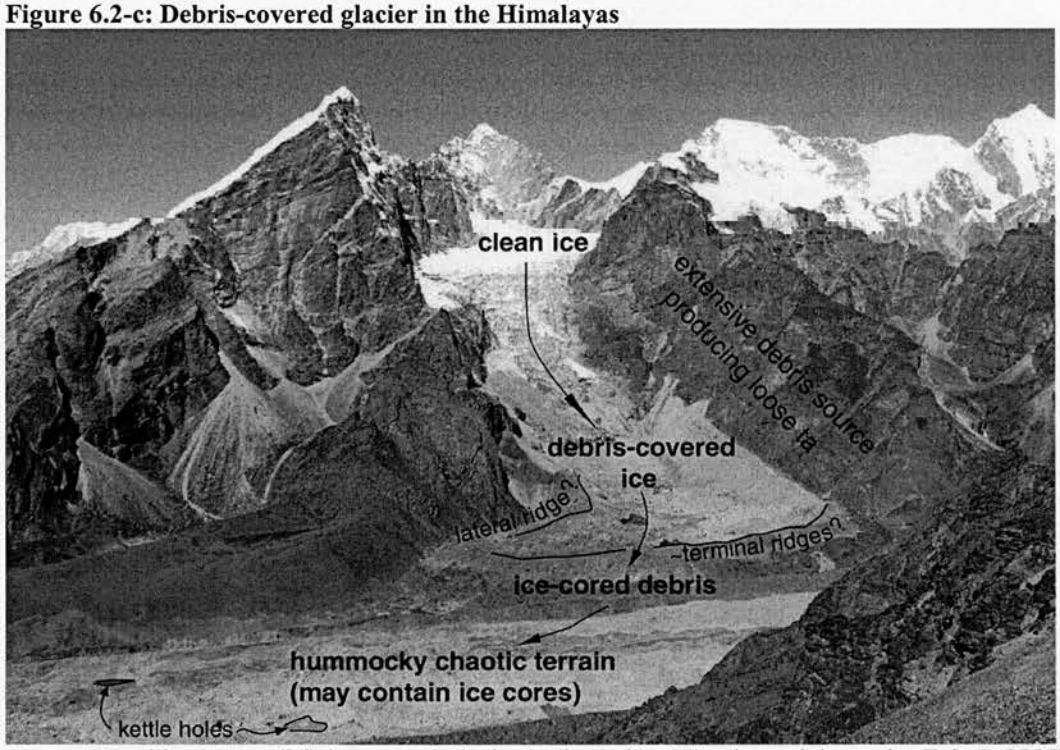

Figure 6.2-c illustrates a debris-covered glacier in the Indian Himalayas (picture by Tait, J, 2005). A transition is evident from clean ice near the glacier source, to debris-covered ice, to (ice-cored) debris ridges and hummocks. Eventually the extent of ice beneath the debris layer is uncertain, and hummocky stagnating ice topography is characteristic.

Jansson et al. (2002) suggest that the relatively high-relief ridges associated with debris-covered glaciers (in comparison to clean glaciers) highlight the volumes of debris available. If the glacier surface is crevassed, crevasse-fill ridges may form, where debris collects in the crevasses, and following ice melt and/or stagnation, debris ridges remain (Sharp 1985). Ridges may also form due to melt out of

englacial debris layers, although these are less likely to be clearly visible, and will probably become part of the generally hummocky terrain left by stagnating ice.

Figure 3.3-e from Chapter 3 is re-printed here as Figure 6.2-d, showing a small-scale currently active glacier on the Dyrfjöll massif in the field area, which may provide a modern analogue for glaciation of the field area in the early to mid Holocene. Dark bands through the ice are visible in Figure 6.2-d, which indicate englacial debris (and perhaps tephra) bands. It can be seen that at the snout there is a thick debris cover which is melting out of the ice. The rock debris making up this cover originates from the cliffs which surround the glacier. On closer inspection, much of the debris observed in Figure 6.2-d beyond the snout of the visible glacier is ice-cored, suggesting long-term insulation of ice (at a smaller-scale, but in a similar manner to the Himalayan example in Figure 6.2-c). About 15 metres beyond the snout, a small moraine ridge is visible, and beyond this, a further arcuate marginal moraine is evident, which indicate the former positions of the active glacier.

Figure 6.2-d: Debris covered glacier snout in field area

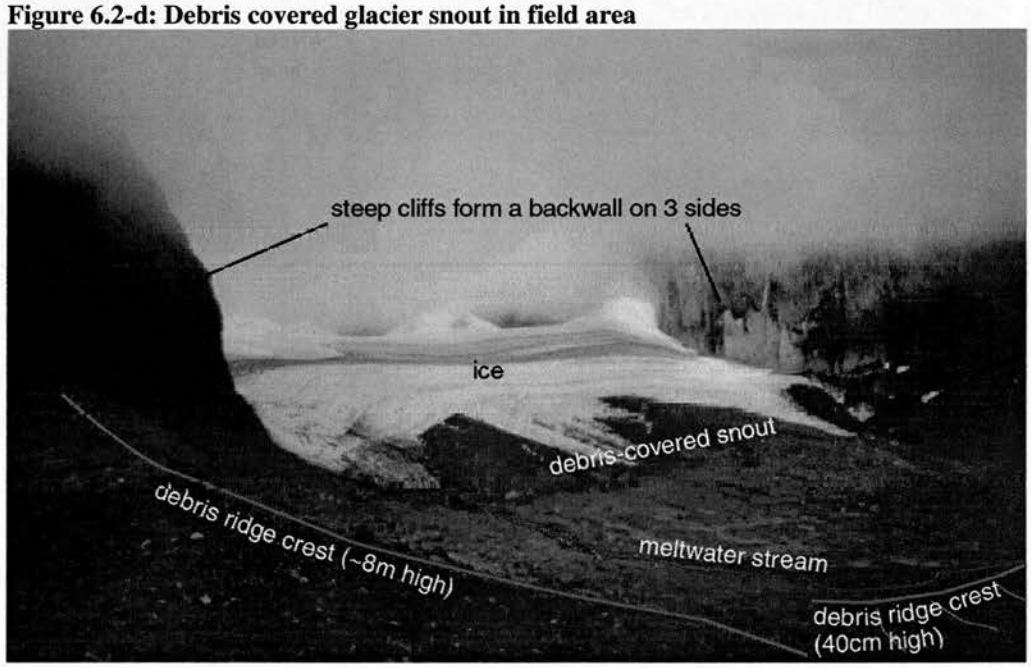

Rock Glaciers

There is much debate over the morphological signature of rock glaciers, due to the fact that their origins and mechanisms are poorly defined (Clark et al. 1998). This research shall not enter into this debate. They are defined here as distinct from debris-covered glaciers in that rock debris is not confined mostly to the ice surface, but forms a significant part of the moving matrix with the ice.

Given the controversy as to rock glacier origins, morphological characteristics are not clearly defined, being related to the specific genesis mechanism. Generally, a rock glacier is thought to be made up mainly of rock debris originating from rock fall activity, and may maintain a significant ice-core. They may have a distinct snout and lateral margins, and the surface is often made up of longitudinal and transverse ridges and furrows (Martin et al. 1991; Shroder et al. 2000). Rock glaciers may have evolved from debris-covered glaciers (Martin et al. 1991), which will assign them a morphology which may include glacial features such as moraines, unlike those generated through periglacial activity. The topographic surrounding of a putative rock glacier deposit is a good indicator of its process of genesis. If the deposit has an associated snow accumulation area above it, it is likely to have a glacial origin, as discussed by Martin et. al (1991), but if it is fed by steep talus slopes it may have a periglacial origin fed by snow avalanches and in situ freezing of moisture. This type of rock glacier extending from talus slopes may indicate the existence of permafrost (Ballantyne 1997). This appeal to topographic surrounding is an important consideration when assessing the possible genetic origin of the observed landform suites.

Summary

The specific interpretation of landform suites as having been generated by a glacial sytem has important climatic implications with regards to the extent the activity was climate-driven. As has been seen, the distinction between glaciers, debris-covered glaciers and rock glaciers is not clear as they form a continuum from systems made up mostly of ice (climate-driven) to systems made up mostly of rock debris (de-

coupled from climate). Figure 6.2-e summarises this transition, showing how two end-members can be defined clearly (high ice content or high debris content), but in between, an array of ice/debris ratios are found. As was seen in Figure 6.2-c, this transition of forms can exist within a single glacial system. The exact point at which the transition occurs from 'debris-covered glacier' to 'rock glacier' or 'ice-cored debris' cannot be clearly defined. In the interpretations presented in 6.4, the emphasis is placed on assessing the relative extent to which the systems may have been influenced by climate by using morphology to interpret putative ice/debris volumes.

Figure 6.2-e: The transition from climate-driven to de-coupled 'glacial' system

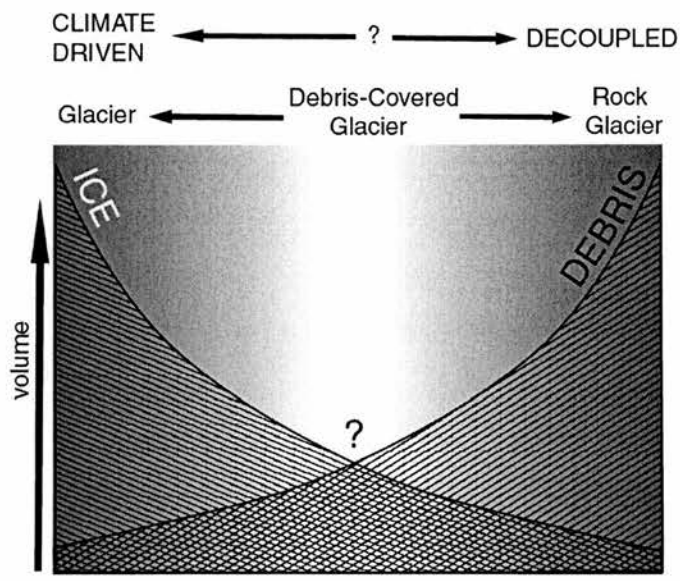

Figure 6.2-e represents the relationship between rock glaciers, debris-covered glaciers and clean glaciers, illustrating the uncertainties involved in climatic interpretation. Where the major material of the system is ice (in a clean glacier), it is highly climate-driven, and where the major material is debris it is de-coupled from climate. The point at which this transition occurs, and a system becomes uninfluenced by climate, is difficult to define.

6.2.2. Non-Glacial Processes: Geomorphic Characteristics

The non-glacial processes discussed here are those related to debris-transport activity caused initially by slope failure, although snow and ice may be involved in some situations. The geomorphic signature of this activity is highly variable and dependent on the specific processes occurring, which depends on the characteristics of the failure material, and the way in which the debris is transported and deposited. Three main processes of slope failure are identified, derived from Varnes (1978) and Cruden et al. (1996):

- Fall
- Slide
- Flow

In terms of morphological characteristics, the type of material involved in the failure is of major importance, so in the following discussion, these three slope failure processes are assessed in relation to material type. Failure affecting the bedrock will have a distinctly different geomorphic signature from that affecting only loose surficial debris, due to the likely existence of large blocks of intact rock within the deposit, as opposed to small fragments of loose rock or soil. The geomorphic signature of bedrock failure will have a high relief difference. The depth of slope which is affected by the failure has an obvious effect on the morphology, since it determines to some extent the size of rock blocks activated. The associated geology of the debris and the slope is of morphological importance in that it determines the extent of weathering, and therefore the propensity for the rock fragments and blocks to be further broken down, aiding the development of a smoother morphology over time.

The amount of water, snow or ice involved further influences the resultant geomorphology, so following a general overview of the geomorphic features of different types of slope failure, the morphological effects of this failure occurring on snow and ice is addressed. Snow and ice may affect morphology through its effect on frictional resistance, which influences the process of debris transportation, and the distance debris can travel.

Slide

Landslide deposits have a variable morphology depending on the composition of the failed slope material (bedrock blocks/soil/debris), the location of failure, and the initial geometry of the slope. Given the existence of bedrock cliffs surrounding many of the mapped landform suites, if landsliding processes have been responsible for landform genesis, a failure involving bedrock collapse is most likely. Figure 6.2-e below highlights the main characteristics of a "rotational" landslide. Large-scale landslides can affect the bedrock to depths of as much as 50 metres (Soldati et al.

2004), and thus they can maintain a high relief morphology. A number of geomorphological characteristics of landslide deposits are commonly used to classify landslides, often observable from aerial photo. These include tension cracks, steep hummocky topography, failed surface scarps, anomalous lumps, terraced slopes and disrupted vegetation cover (Dai et al. 2003).

Figure 6.2-f: Rotational Landslide Activity

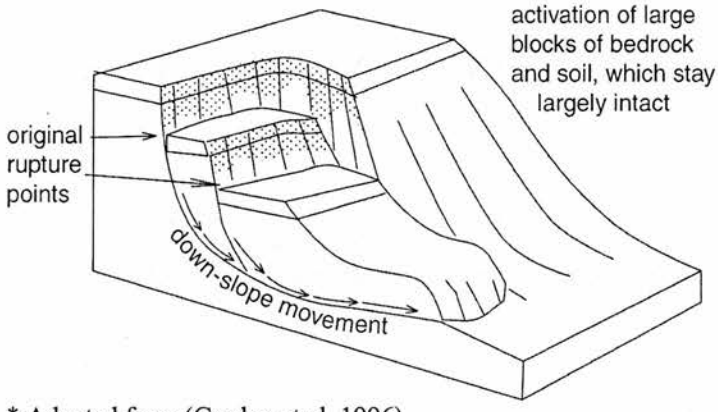

* Adapted from (Cruden et al. 1996).

Figure 6.2-f shows the main morphological characteristics of a deep-seated rotational bedrock landslide. Large blocks are activated following failure at some rupture point. These blocks slide as a whole mass down-slope, and thus the resultant morphology is likely to show old rupture sites, and may exhibit a step-like profile.

As shown in Figure 6.2-f, in the upper part of a landslide deposit, a series of steps and scarps, roughly parallel to the back wall (the main scarp), are likely to be found where failure occurred. Bentley et al. (1998) provide a number of key characteristics for landslides. They contain a steep back-wall or 'scoop' from the valley side, distinct from the normal valley side cross-profile, which is illustrated in Figure 6.2-f. In addition to morphological characteristics illustrated in Figure 6.2-f above, transverse and arcuate ridges are common around the lower edges of the landslide deposit (Varnes 1978).

The flow-direction, run-out distance, and final area covered by a landslide deposit is controlled by topography, material type, and frictional resistance, all of which are spatially variable. Landslides will flow down-hill, following the line of steepest descent. The may stop at the base of a slope, but they may continue beyond this point, becoming more of a "flow". The aerial spread of the deposit depends on how topographically constrained the flow-route is. If the slope is open and smooth, and the base of the slope has no obstructions, it is likely to spread widely at the base. In

contrast, it may be 'funnelled' down-slope and have restricted area to spread in a narrow valley. The morphology will then be very different.

The material composition of a landslide deposit is not likely to be uniform throughout, and is related to the specific material make-up of the slide. The upper part with scarps and terrace levels will have a high proportion of intact bedrock blocks, whilst lower in the deposit in the hummocky part, angular diamict with large boulders may be found (Bentley and Dugmore 1998). It is suggested (Bentley et al. 1998) that the transverse ridges at the terminus of the deposit are made up of different materials than the hummocky upper part. Larger blocks may travel faster down-slope following landslide initiation, and thus become incorporated in the deposit nearer the terminus of the deposit, while smaller materials will be in higher proportions in the upper part.

One problem associated with identifying and interpreting past landslide activity based on current geomorphology, is that only the largest landslides occurring in the past are likely to maintain morphological evidence of their existence today (Soldati et al. 2004). Less information is available on smaller landslide events.

Fall

A rock "fall", is defined as detachment and displacement of rock debris mainly by airfall, bouncing, or rolling down-slope (Cruden et al. 1996). The process involves a number of individual events where a piece of rock is detached from bedrock cliffs, and lands elsewhere, the exact location of its coming to rest dependent on the size and shape of the rock fragment, and the geometry of the slope on which it falls. As the rock fall activity does not occur as a continuous displaced mass, the resultant morphology is variable, and its overall shape and area is inherently random. However, the upper part of this rock-fall deposit is likely to form a scree or talus slope, which may lie at an angle of 35-40°, the traditionally cited angle of repose for course debris (Curry and Morris 2004).

As highlighted in Figure 6.2-g, debris produced from a rock fall is likely to become part of another debris-transport system which will re-work rock fall debris.

Figure 6.2-g: Rock-fall activity

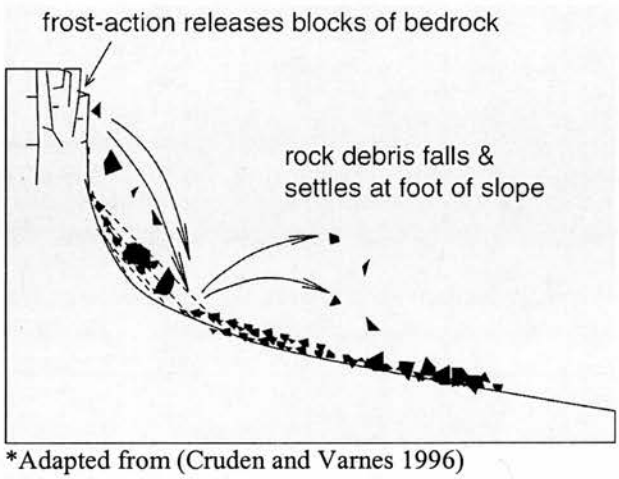

*Adapted from (Cruden and Varnes 1996)

Figure 6.2-g shows the basic processes involved in rock-fall activity. Existing joints and weaknesses in bedrock may be exploited by weathering processes such as frost action, which allow the release of rock debris, which falls and is deposited lower down the slope. The morphology of a rock fall will consist of piles of rock debris, and possible sorting of small from large rock fragments. The debris produced by the rock fall activity may become part of a different debris transport system, such as a debris flow, or become supraglacial debris.

Flow

Flow processes are largely involved in re-distribution of unstable slope materials. The material involved in this type of failure may either be made up of rock fragments or soil (Cruden et al. 1996), each of which behave differently. The volume of liquid or snow/ice contained within the debris further defines the specific failure process occurring, and subsequently influences the eventual morphology of the flow deposit. The liquid/snow/ice content of debris flows is related to the availability of an accumulation area for snow, and the climatic conditions at the time. Given the characteristics of the field area (low volumes of soil materials on slopes) this research is primarily concerned with flows involving rock debris as opposed to soil. These flows may take the form of debris flows, or debris/snow avalanches.

Figure 6.2-h: Debris Flow activity

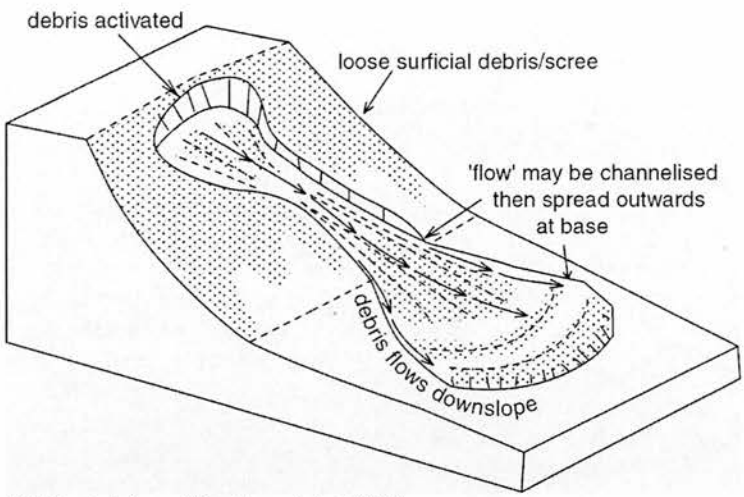

Figure 6.2-h shows the main processes involved in debris flow activity. Here, unstable surface debris may become activated, allowing it to flow like a liquid. The addition of water or snow may promote this flow-like behavior. The morphology may exhibit longitudinal 'flow-lines', and transverse/arcuate ridges may be generated from overlying flow lobes.

* Adapted from (Cruden et al. 1996)

A debris flow is defined here as a down-slope flow-like transportation of some combination of debris, sediments which possibly contains a liquid/snow/ice fraction. They may develop from shallow landslides, which become liquified and act like a flow (Ballantyne and Benn 1994). The characteristic morphology of a debris flow deposit depends on the mechanisms and nature of the flow, and on the type of debris involved. Debris flows are described as the most common sediment transfer mechanism on steep talus slopes, made up of poorly sorted debris (Ballantyne 1997). There are numerous examples of currently active debris flows in the field area. These can provide valuable information on the way this landscape responds to such activity, the types of debris involved, the topographic setting and the morphology of the subsequent deposits.

In the field area, the most common type of debris flow currently active involves the re-activation of loose rock detritus created by frost shattering, on unstable scree slopes. This type of failure probably occurs very quickly as a result of the crossing of a stability threshold. Current examples of this activity in the Borgarfjörður region are presented here based on observations in the field.

Figure 6.2-i: Currently Active Debris Flow

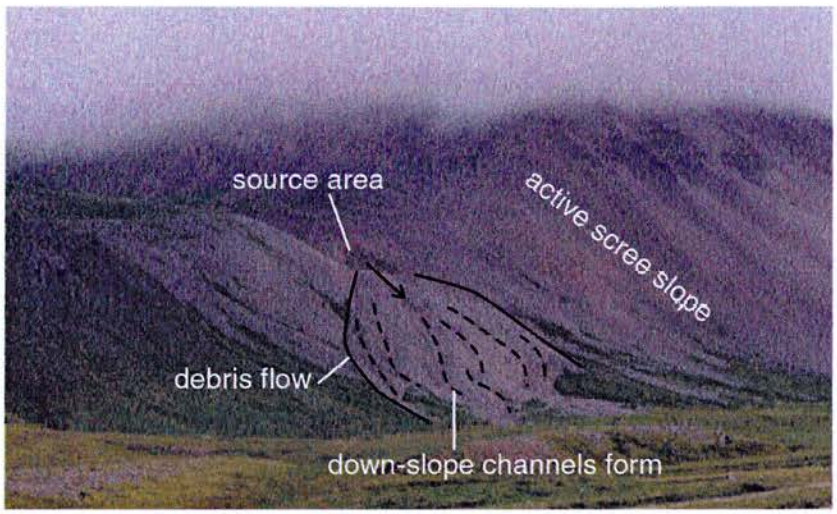

Figure 6.2-i shows a currently active debris flow observed in the field area. It originates from a gully cut into a scree slope. The scree material originates from bedrock outcrops visible just below the cloud line. Channels form on the surface in the direction of flow.

From Figures 6.2-i key morphological characteristics of debris flows in this environment are evident. There is no clear definition of lower margins in this example, with a series of 'tongues' extending towards the base. The surface morphology and flow path is defined by longitudinal parallel levées, which may be related to post-depositional fluvial activity, which cuts longitudinal channels into the debris. The debris flow originates in a narrow gully cut into bedrock or scree, and the flows widen towards the base into a fan shape. A similar debris flow morphology is observed by Ballantyne (1997) in the Cairngorms, Scotland, although terminal 'lobes' are also evident. These debris flows consist of relatively dry debris, and their activation appears to relate to some failure within the unstable scree slopes above. Figure 6.2-j shows more debris flow activity in the Börgarfjorður Eystri region, where repeated debris flow events have resulted in the development of debris 'cones' (Brazier and Ballantyne 1989).

Figure 6.2-j: Recently Active Debris Flow

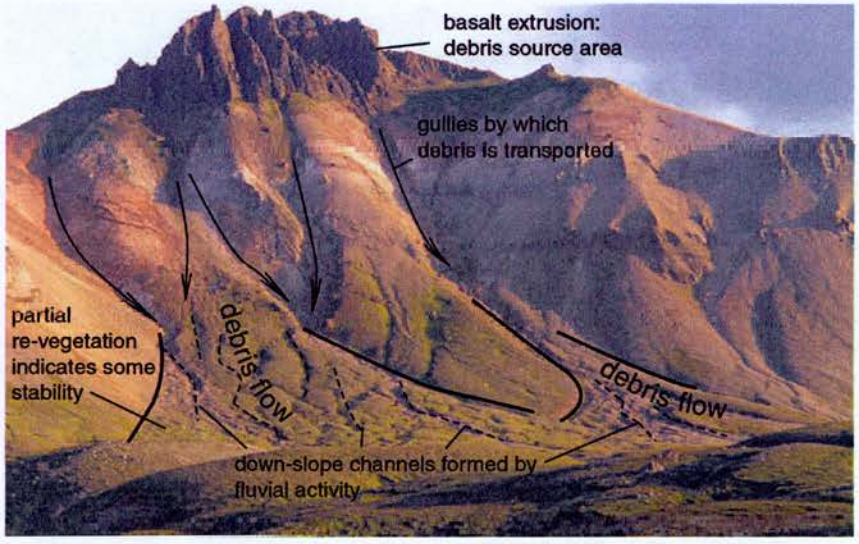

Figure 6.2-j shows a series of recently active debris flows, originating in a number of gullies which have constrained debris flow in the upper section. On the lower slopes, as can be seen, debris fans outwards. Channels cut into the deposits indicating the possible involvement of water in debris transportation. Much of the debris flow deposits maintain some vegetation, as seen from the colorization, indicating these have reached a stable enough state for vegetation growth to occur.

It has been seen that post-depositional fluvial activity helps shape the morphology of debris flow deposits by cutting longitudinal channels in the debris. Processes of solifluction and gelifluction (in response to wet-dry, and freeze-thaw cycles, respectively (Summerfield 1997)) may also re-distribute debris, forming arcuate lobes and transverse terraces (Ballantyne, C. K. 2002). Such activity may result in a series of parallel ridges or terraces, and a clearly defined lower margin, such as those illustrated in Figure 6.2-h. These terraces may also be evident as a result of recurrent flow events super-imposed on each other, without appeal to solifluction processes.

Slope failures involving rock debris, and/or snow and ice, may be categorised as avalanches, which are very fast and potentially highly erosive debris-transport systems (Summerfield 1997), involving lobes of debris which are transported beyond the lowest limit of the scree slope (Ballantyne 1997). Unlike slide processes, the failed material does not maintain a consistent mass, and is moved turbulently, resulting in unsorted and mixed material. Their run-out distance can be great (Ballantyne and Stone 2004) due to the speed at which movement occurs. Some

general morphological characteristics of rock avalanche deposits are outlined by Hewitt (1999), following his study in the Karakoram Himalaya. Deposits are likely to be thin relative to aerial extent, containing low (<5m) hummocks and transverse arcuate ridges and furrows. The margins are often raised, and the overall shape of the deposit is lobate, and possibly split into separate flow lobes as a result of topographic controls. The surface of such deposits is likely to exhibit large rock blocks and fragments, which may be oriented parallel or transverse to movement, and materials within the deposits will be un-sorted (Hewitt 1999).

An example of a recently active debris and snow avalanche is observed in the High Tatras Mountains of Slovakia, (Figure 6.2-k) exhibiting very similar characteristics to the active debris flows in the field area (Figure 6.2-j) in terms of topographic setting and morphology. It can be seen that there is high availability of rock debris in the steep cliffs and frost-shattered slopes above. The potential snow accumulation area is small and steep. Flow is channelled down-slope through a narrow chute, and widens towards the base into a debris fan (again, comparable to that seen in Figure 6.2-j). Limits of at least three distinct failure events with characteristics of flow-like behaviour are seen in Figure 6.2-k, numbered 1, 2 and 3. The materials making up the series of snow/debris avalanches is seen in the lower part of Figure 6.2-k, where blocks of ice, boulders, earth and wood are all observed. The fact that the debris and snow avalanche appears to have flattened a significant area of forest, indicates the catastrophic and high speed nature of the event.

Figure 6.2-k: Debris flow/avalanche onto snow in the High Tatras Mountains, Slovakia

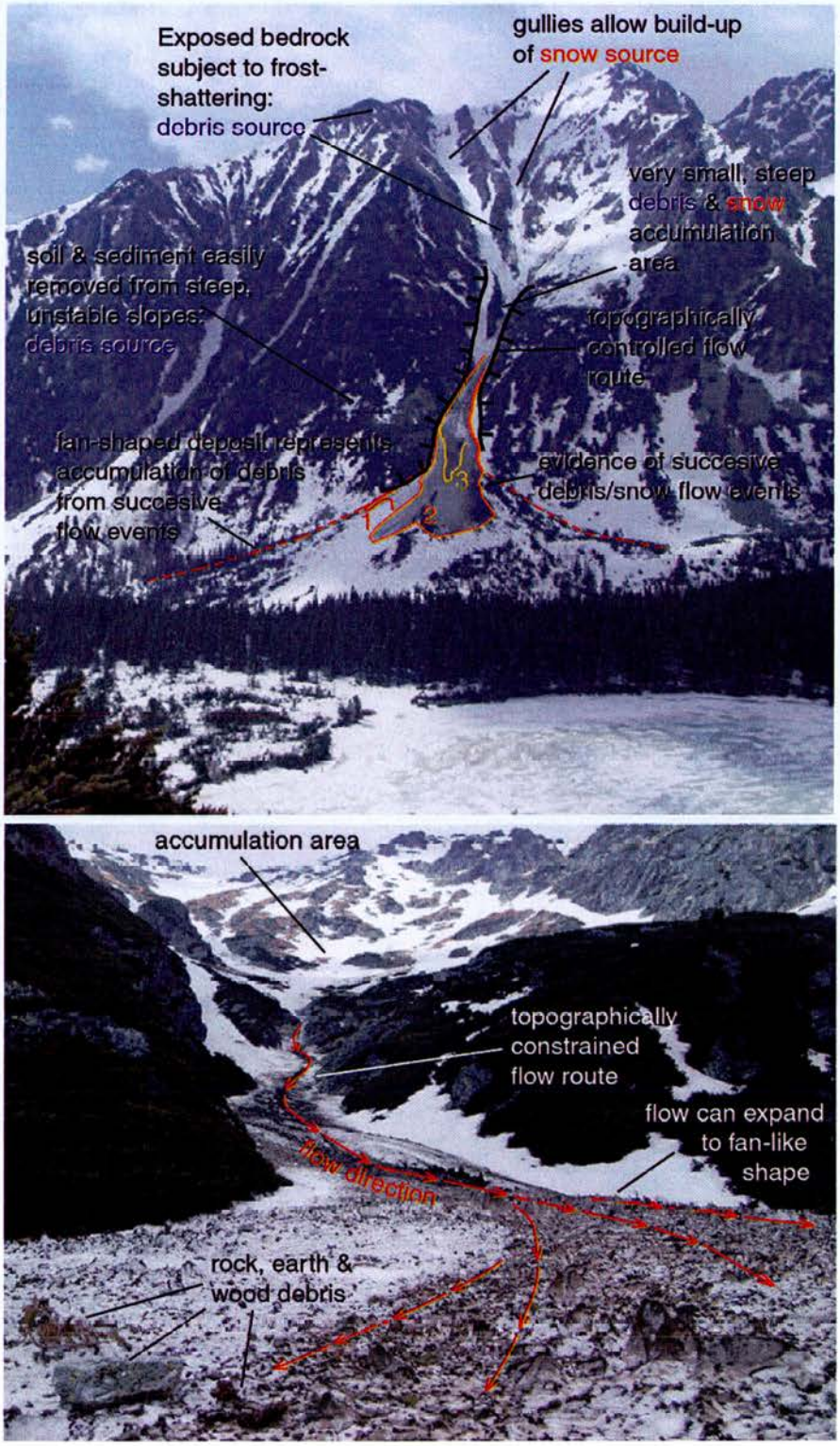

6.3. Defining processes of landform genesis based on field evidence

6.3.1. Approach: Spatial Context

This section aims to define the origins of the landform suites and associated landform elements in the field area in terms of specific processes and systems. In the approach to define process from geomorphic evidence, consideration is paid to the scale of study. Landform elements can be assessed individually on a small scale, or they can be assessed in the context of their associated landform suite, and in turn, at a large scale, in the context of the landscape as a whole. While studying individual landform elements and their associated characteristics provides useful information, placing this information in a spatial framework extends the value of this evidence. It also allows connections to be made with modelling results, which utilise the geomorphic evidence at a landscape scale. Given the limited access to material make-up data in the field area, spatial context is essential to interpretation of landform genesis processes.

Figure 6.3-a illustrates the importance of context in interpretation of geomorphic evidence. In stage 1, an individual landform element observed out of context could have many possible processes of formation. The evidence appealed to at this small scale is related to small-scale morphological characteristics, surface features, and where possible, material make-up. When this single element is viewed in relation to its proximity to other landform elements (stage 2), the number of potential processes of genesis is reduced. There are fewer explanations for the existence of a group of connected landform elements (a landform suite) than for a single element. Here, morphology of a single element can be viewed in relation to the morphology of nearby elements, and unit areas of landform types can be identified, with associated topographic characteristics. The single landform element has a location relative to the margins of the suite. In the final stage, the number of possible processes of genesis is further reduced because the landform suite is one of a series of similar suites in the landscape. Evidence is drawn from the overall morphology of the

landform suite in relation to other suites, and the topographic location. For example, the suites may all lie in small basins with steep back walls. In this study all possible evidence is evaluated on these three scales of landform elements, landform suites, and the landscape as a whole.

Figure 6.3-a: Reduction of explanation with increased reference to spatial context

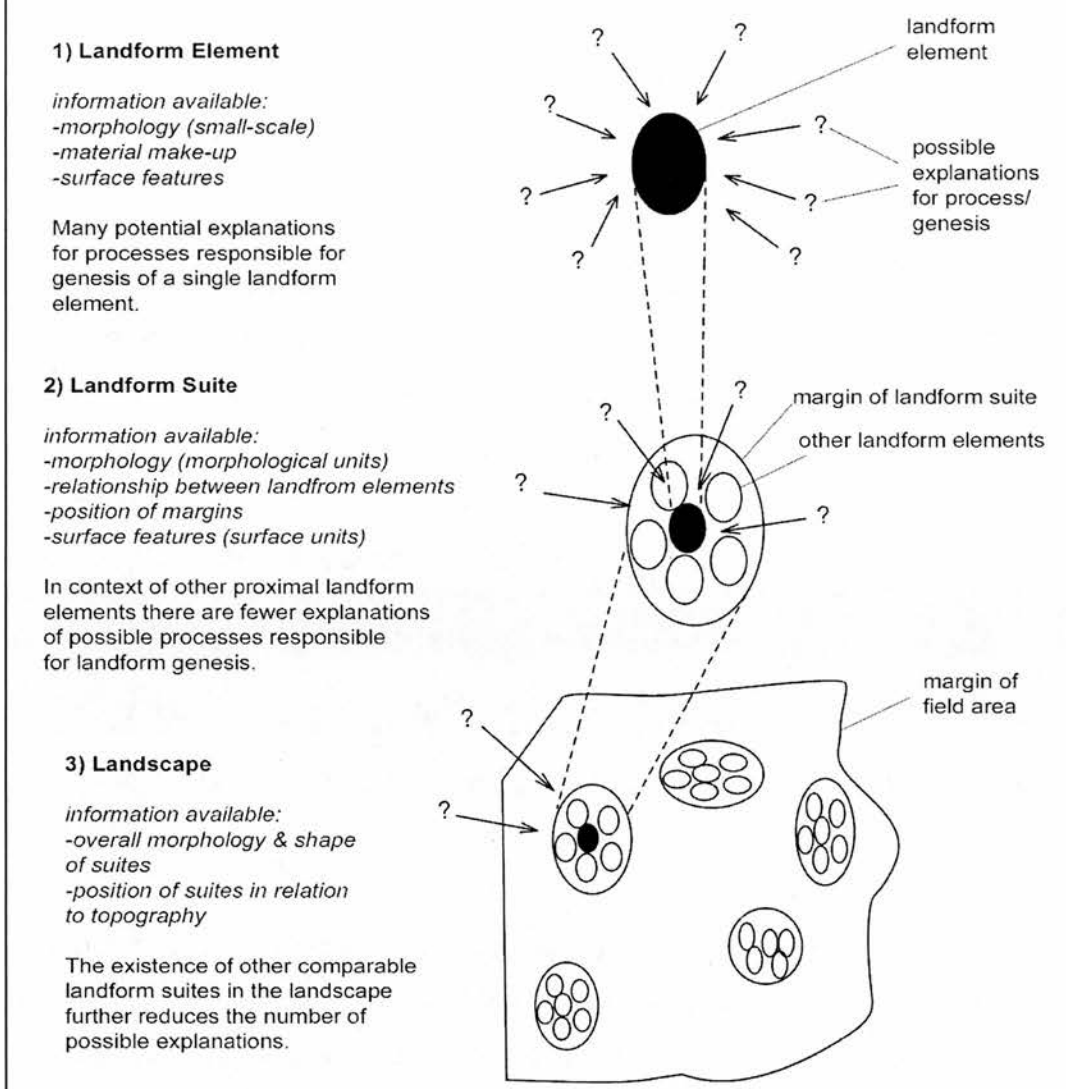

Explanations must be made for how limits are placed on the spatial extent of the field area, and thus how the limits of the "landscape", which form the context of the landforms, are defined. The field area is approximately fifteen square kilometres in area, which is thought to be an ideal study area size, because it covers enough area to be able to characterise regional response, yet is not so great in area that it has to deal

with numerous different system responses. As shown in Chapter 3 and 4, numerous suites of landforms sharing morphological characteristics are mapped in the field, which are situated in individual valleys or drainage basins. If the study area were smaller, whilst interesting data could be generated with regards to a single landform suite in a single valley, significantly more information can be derived from the study of thirteen similar landform suites across six main valleys. These numerous landform suites can be expected to represent a characteristic regional response to some forcing mechanism, whilst it is more difficult to derive explanations for the existence of a single landform suite (as shown in Figure 6.3-a). Conversely, if the area of study is much increased in area, explanation becomes more complex. The geomorphic diversity is increased to the point where the study is dealing with the response of very different systems, and characterisation of response becomes unrealistic. In the specific case of the field site, once the area is extended much beyond its present limits, the effects of large-scale ice streams become important evidence, which opens up new avenues which the scope of this study cannot achieve. Therefore it is postulated that the field area at its current spatial extent is the optimum area within which to study the nature of regional response to a specific climate event.

6.3.2. Hypotheses for Landform Genesis

The geomorphology of the field area is defined by units of land with specific morphological characteristics. Geomorphic mapping identified the existence of a number of key landform element types, which in collective units make up the body of the landform suites (Chapter 3.8). Figure 6.3-b represents a summary of the spatial distribution of these key landform types within the mapped landform suites (a figure repeated from Chapter 3).

Figure 6.3-b: Idealised Landform Suite

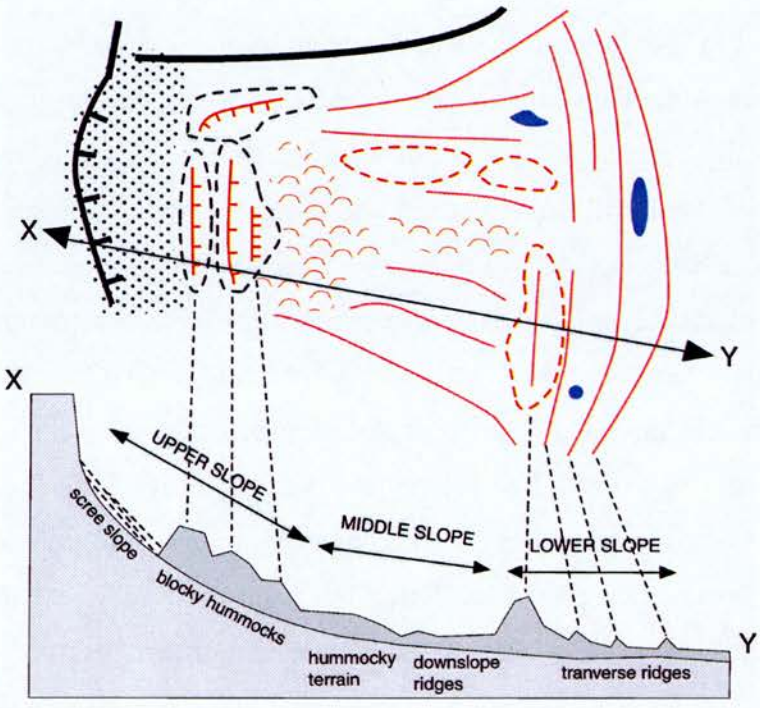

Figure 6.3-b, repeated from Chapter 3, Figure 3.4-a, for the purpose of this interpretation, illustrates an idealised landform suite based on the key characteristics of all landform suites observed in the field area. The upper slopes are characterized by blocky hummocky terrain. Down-slope ridges are found on the middle slopes, along with areas of hummocky terrain, with some lineations. Transverse and arcuit ridges are found on the lower slopes.

Interpretation of landform genesis processes from this geomorphic record is approached through testing of multiple working hypotheses. Hypotheses are developed to explain possible mechanisms for generation of each key landform type, within the context of the different debris-transport systems (glaciers, debris flows, landslides and avalanches). Table 6.3 illustrates these hypotheses within their system-type framework. The generation of each hypothesis is informed by the information presented in 6.2, on morphological characteristics of different system types. Using this approach for landform interpretation, it is possible to address all lines of evidence on the small and medium scales, while maintaining a view of the wider spatial context within which each landform element is placed. In the following discussion, landform suites are interpreted in relation to the multiple working hypotheses developed here.

Table 6.3-a: Testable hypotheses for landform genesis

Mapped Landform →	*Transverse /arcuate ridges*	*Down-slope/ Longitudinal ridges*	*Hummocky Terrain*	*Blocky hummocks/ridges*
SYSTEM ↓				
Debris-covered glacier -supraglacial debris input above ELA only	**1**-Terminal moraines **2**-Melted-out englacial debris bands	**1**-Subglacially oriented ridges (ice-directional) **2**-Subglacial stream deposits ~ eskers **3**-Medial/lateral moraines **4**-Kame terraces	**1**- Uneven melt out of englacial debris	**1**-Large-scale moraine ridges
Debris-covered glacier -supraglacial debris input above and below ELA	**1**-Terminal moraines	**1**-Crevasse-fill ridges **2**-Subglacially oriented ridges (ice-directional) **3**-Subglacial stream deposits ~ eskers **4**-Medial/lateral moraines **5**-Kame terraces	**1**-Uneven stagnation & melt of ice under varying debris-cover depths	**1**-Large intact blocks entrained in glacier
Debris/ice flow or avalanche	**1**-Gelifluction by freeze-thaw processes **2**-Repeated flow events	**1**-Selective erosion by surface fluvial activity **2**-Topographic control (i.e. following river channels)	**1**-Uneven stagnation & melt of ice blocks within debris	**1**-Gelifluction processes involving large-scale debris
Debris flow	**1**-Solifluction by wet-dry processes **2**-Repeated flow events	**1**-'Flow-lines' **2**- Post-depositional Fluvial activity	**1**-Transportation & deposition of debris blocks of varying sizes	**1**-Solifluction processes involving large-scale debris **2**-Repeated flow events with large-scale debris
Landslide	**1**-Series of large slope failures ~ large scale intact slope slides	**1**-Post-depositional fluvial activity	**1**-small-scale slope failure slides **2**-flow-like landslide (smaller blocks)	**1**-Rotational slides of intact rock masses
Other (i.e post-depostional) activity, fluvial activity	**1**-Post-depositional debris re-working by solifluction **2**-Selective bedrock erosion	**1**-Fluvial erosion **2**-Selective bedrock erosion	**1**-Selective bedrock erosion	
PROCESS ←		**LANDFORMS/ GENESIS**		→

6.4. Specific interpretation of field evidence

This section aims to interpret the specific processes occurring to produce the observed geomorphology, with reference to modern analogues from the literature and field observations. The approach described above is utilized, incorporating geomorphic and, where possible, sedimentological evidence from small to large scale, as a means of testing the working hypotheses for landform generation set out in Table 6.3. In keeping with the attempt to interpret landforms within their spatial context, each landform suite is discussed as a whole, with the main focus on interpretation of the genesis mechanisms for each key identified landform unit. As explained in Figure 6.3, the relationship between a single element and surrounding landforms, the associated landform suite, and the landscape as a whole are the factors which will allow useful interpretation of the processes responsible for creating the landform suites, and enable comparison between suites and the identification of common processes which may link the suites. This has implications for interpretation of the active debris transport processes which formed and modified the mapped landform suites, at a landscape scale. Section 6.5 will go on to evaluate the existence and nature of causal links between the processes and systems responsible for producing these landform suites.

The results from geomorphic mapping of the field area described in Chapter 3 highlight the existence of 13 suites of landforms occupying small basins within the main valleys which make up the field area. As outlined in Chapter 3.8, key landform types are identified which occupy major unit areas of each landform suite. Common characteristics of each landform type are shared in all landform suites at a landscape scale. With reference to each mapped landform suite, this section discusses the processes involved in the genesis of these characteristic landform types, evaluating the hypotheses postulated in 6.3.

Interpretation of the processes responsible for this landform type refers to the information presented in Chapter 3 and 4, and pays specific attention to spatial

variations in morphological characteristics of the landforms across the field area, and their topographic setting.

Note on post-genesis landform modification

Chapter 4 discussed the implications of variable preservation potential on the landform record. Various geomorphic agents are currently active in the field area, which may have modified (though not necessarily removed) landforms, with significant implications for interpretation of process. These include fluvial processes, various slope processes and periglacial activity. Consideration is paid to the observable extent of such activities, during the interpretative process.

6.4.1. Kjólsvík

Figure 6.4-a: Kjólsvík Suite - key geomorphological and topographic features

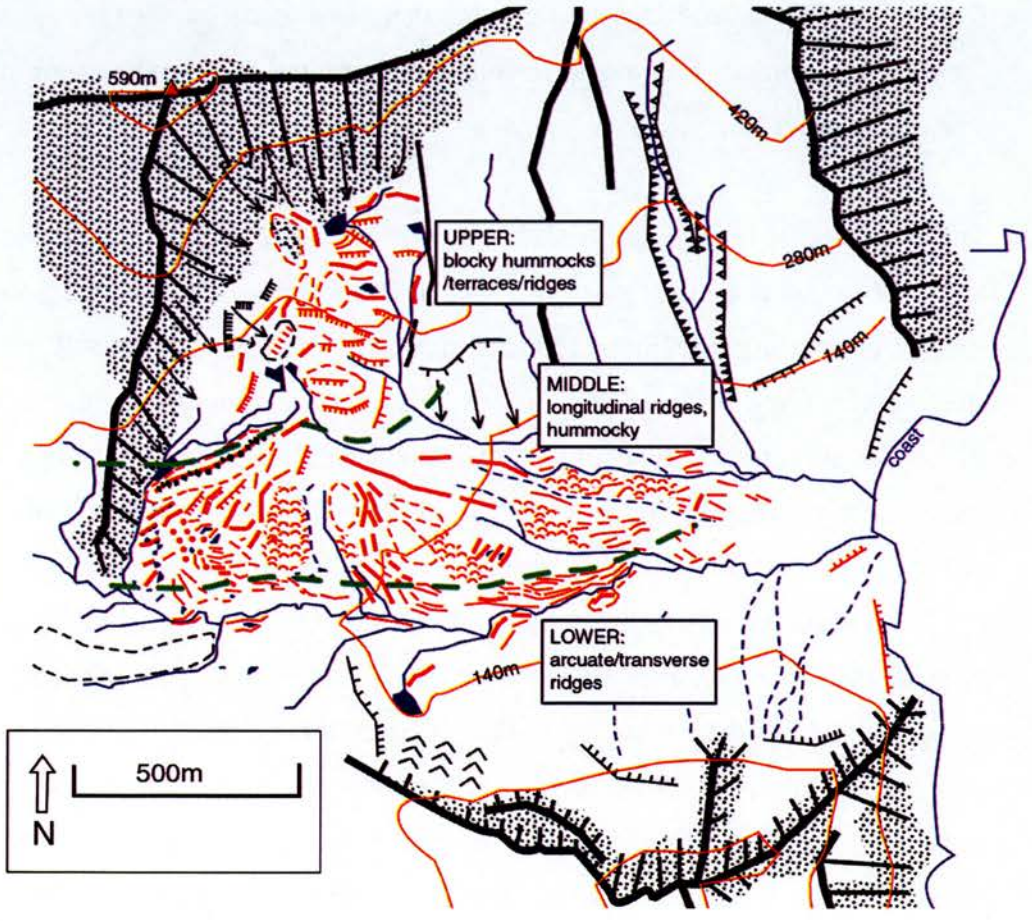

Observing the overall form and shape of the suite of connected landform elements named the "Kjolsvik" Suite, it maintains the lobate form characteristic of all suites in the field area, but has an unusual aspect ratio, where its width is greater than its length (the second highest aspect ratio of all the mapped suites). The suite of landforms exhibit a flow-like form in that the main ridge-lines appear to be lineated outwards in a fan shape from the source area, and on reaching the unconstrained valley floor, follow a line down-slope towards the sea. Figure 6.4-a highlights the existence of three main regions of the Kjolsvik suite, the upper, middle and lower, which all have very different characteristics.

Upper Suite

This landform suite has a clear source area backed by steep cliffs and slopes on three sides. The upper Kjolsvik suite is characterized by large blocky hummocks and terraces of varying orientations. In the context of the surrounding cliff faces on the North and West sides, it can be seen that there is a tendency for the orientations of the ridges and blocky hummocks to follow the orientation of the nearest cliff face, as was quantified in Chapter 4.

The existence of large intact rock blocks within the upper hummocks and terraces, and their orientations relative to the cliff faces indicates a link between source area (the cliffs) and deposit (the ridges and terraces). The cliffs give way in places to steep scree slopes made up of shattered rock fragments and large angular boulders, which also form the debris mantle on the deposits. This is representative of currently active debris transport by rock fall from the cliff to the slopes, indicating the instability of the cliff face. It is conceivable that the materials making up the ridge and hummocks, mainly large rock blocks and smaller rock fragments, originated up-slope as part of the cliff face. They were detached from the cliff face and slid in a rotational slide to their present location, hence the orientation following the nearest cliff-face orientation. When assessing the multiple working hypotheses set out in Table 6.3, the morphology of these blocky deposits, and their juxtaposition with steep cliffs, is not consistent with a glacial or flow-like process, but rather a removal of large blocks in a rotational landslide or series of smaller scale slides. The

morphology of the upper suite is comparable with the idealized rotational slide illustrated in Figure 6.2-f

Middle Suite

The middle section of the Kjolsvik suite consists mainly of hummocky terrain, with some units of down-slope-oriented ridges forming lineations outwards in a fan shape. The ridges in the middle suite are distinct from those in the lower suite in two key ways. Firstly they are of a much greater scale, rising up to four metres in height and being significantly than the lower ridges. Secondly, they appear to contain large blocks of intact rock blocks which form rocky outcrops and distinct terrace edges. The surface is generally "rougher", with a discontinuous mantle of loose debris on the surface.

Hummocky terrain and large-scale ridges have many potential origins, but more detailed study of the morphological variations within the middle section reveals valuable evidence. Figure 3.3.6 represents the transition in landform type from west to east across the middle section of the suite. As noted in Chapter 3.3, the western-most part of the middle section near the cliff is made up of large hummocks roughly oriented at a 45 degree angle to the cliff face. These contain large intact boulders and have a greater relief than the rest of the middle section. In terms of their scale and surface features, these hummocks have more morphological similarities to the upper suite than to the middle. It is significant therefore, that this area forms the western lateral margin of the suite and is juxtaposed with the cliff-face.

With increased distance from the cliff face, landforms become progressively smaller in scale and rock debris and boulder cover on the surface becomes less continuous, as shown in Chapter 3, Figure 3.2-i. This implies a debris-supply role for the cliff immediately above the hummocks, which is less significant further from the cliff. Stratigraphic evidence from Chapter 5 strengthens the hypothesis of a genetic link between cliff source and proximal landforms. Regular rocky layers from throughout the mid-Holocene period are found in profile Kjólsvík G (see Chapter 5), which is in close proximity to the cliff, indicating regular rock-fall activity. The sudden

transition from large rough hummocky ridges to the smaller conical hummocks and low ridge lines suggests abrupt change in process and in debris source. It is suggested that the hummocks proximal to the cliffs share a common process origin, which is mostly fed by cliff debris deposited in large blocks. The remainder of the middle section is more likely to share common process with the lower suite.

Moving east from the cliff face, and as visible in Figure 3.2-i, elongated cone-shaped hummocks are found in one morphological unit of the middle section, immediately east of the large hummocky ridges. These have morphological characteristics comparable to deposits found in front of Steinholtsjökull, an outflow glacier of the Eyjafjallajökull ice cap in Southern Iceland. These deposits are related to a landslide event in the route of the glacier which deposited material both on the ice and beyond it. As it has been suggested that the upper Kjólsvík suite is related to landsliding activity, the cone-like hummocks found juxtaposed with the landslide deposits may be indicative of a similar inter-relation between landslide activity and glaciers.

The eastern-most region of the middle suite is mostly made up of low hummocks and ridges, the orientations of which are debatable. Although ridges seem at first to be oriented west-east (down-slope), further lineations perpendicular to this are super-imposed on a smaller scale. Hummocks maintain some indication of transverse orientation, which has subsequently been cut through by channels giving the appearance of down-slope orientation. The key question is whether the landform elements are representative of the way they were initially deposited (as down-slope oriented ridges), or if original transverse ridges have been modified by subsequent processes to take on an appearance of down-slope lineation. It is difficult to define which hypothesis is most probably without reference to the wider context of the suite, so this problem is returned to.

Lower Suite

The "lower" suite is characterised by low-lying flat-topped ridge lines superimposed on subdued underlying topography on the valley floor. The lower part begins abruptly at the break of slope where the south-facing valley side meets the valley

floor. Figure 6.4-a clearly shows the series of stacked arcuate ridges in the lower section, which extend along the full width of the suite from East to West. These ridges form clear evidence of successive marginal deposits. Associated with these arcuate ridges are longitudinal ridges, which run parallel to each other and perpendicular to the arcuate ridges. When the working hypotheses outlined in Table 6.3 are referred to here, the most likely origin for the lower section ridges is glacial, for the following reasons: The ridges are superimposed on an almost flat topography, with symmetrical up- and down-slope ridge-sides, and being found at the margins of the suite. This indicates successive phases of deposition at ice margins. Successive debris flow events or solifluction activity would be expected to have a shallow up-slope side and steep down-slope side due to the mechanics of flow of this type of material. The longitudinal ridges indicate a down-slope flow direction either caused by erosion by overlying ice, or deposition during active flow. The juxtaposition of down-slope and arcuate ridges and their relative locations strengthen a glacial origin hypothesis.

Conclusions on genetic origin of the Kjolsvik Suite and chronological implications

To determine the processes responsible for the suite as a whole, the transitions from upper to middle to lower suite are studied in detail. There is an abrupt lower margin to the blocky upper deposits, which appear to overlie the hummocky terrain of the middle part of the suite, dropping off in a steep edge. The stratigraphic relationship between the upper and middle part is evidence that the landsliding activity responsible for the blocky hummocks post-dates the deposition of the hummocky terrain of the middle suite, and the transverse and arcuate ridges of the lower suite.

To return to the problem posed earlier with regards to the processes of formation of the eastern most part of the suite, it is now possible to connect the genesis of the observed morphology with the genesis of the rest of the suite. A glacier existed in the Kjolsvik basin which was responsible for creating the arcuate moraines at the base, and the hummocky and lineated moraines of the middle. Following the partial or complete removal of this glacier, some landsliding and small-scale slumping activity occurred, transporting large blocks of material from the cliff, and forming

the characteristic 'blocky' upper deposits, and the western-most hummocky ridges of the middle suite. It is conceivable that the heat generated from this mass-movement activity in the upper region promoted ablation of the ice masses, prompting meltwater outflow over the lower parts of the suite. On observation of the suite from a distance, channel-like forms radiate from the margins of the landslide deposits, which may signify key meltwater flow routes modifying the original glacial deposits. Figure 6.4-b illustrates such channels in the eastern part of the suite. In this way, the existence of the transverse ridges superimposed on downslope ridges in the eastern-most part of the suite can be explained. Originally transverse ridges may have been deposited by the glacier, and subsequent meltwater channels found routes through these ridges by multiple channels, creating new lineations.

Figure 6.4-b: Meltwater channels cut down-slope through eastern part of Kjolsvik suite

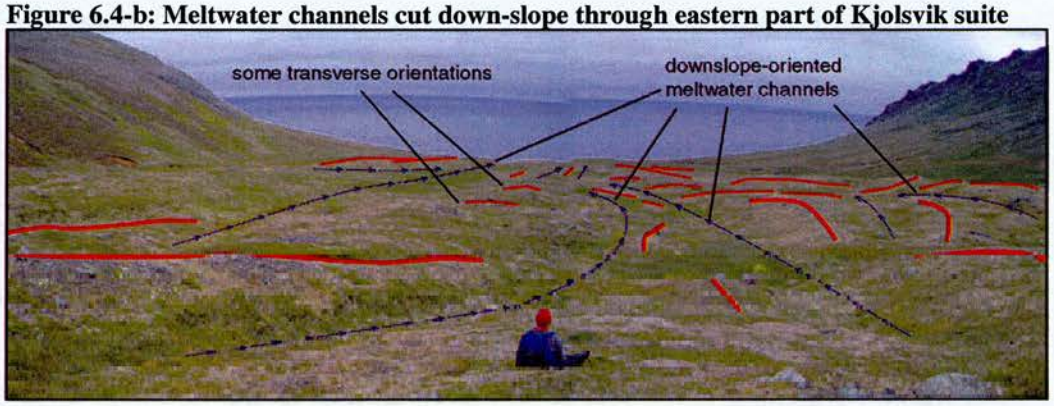

Chronostratigraphic evidence presented in Chapter 5 confirms the hypothesis that at least two distinct geomorphic events occurred to form the Kjolsvik landform suite. The upper suite dates to ~4.2cal. ka BP, while the lower suite has a minimum age of 5 cal. ka BP, indicating that a glacier was present in the Kjolsvik basin prior to a landsliding event, which involved the collapse of significant volumes of bedrock from the cliffs behind. In the upper suite, the large scale of the blocky terraces and hummocks, and their regularity and parallel orientations, indicate a large-scale failure event occurred, which may have had several phases of collapse. Given the existence, in the middle suite, of conical hummocks indicative of an interaction between landsliding and ice, it is possible that some ice still remained in the basin at the time of the landslide event. Following the large-scale landslide event, there were

probably further small-scale slumps and rock fall events which have occurred until the present day.

6.4.2. Svínavík

The Svínavík suite is unique from the others in that it occupies an individual drainage basin which is unconnected from the rest of the field area.

Figure 6.4-c: Svínavík landform suite – key geomorphological and topographic features

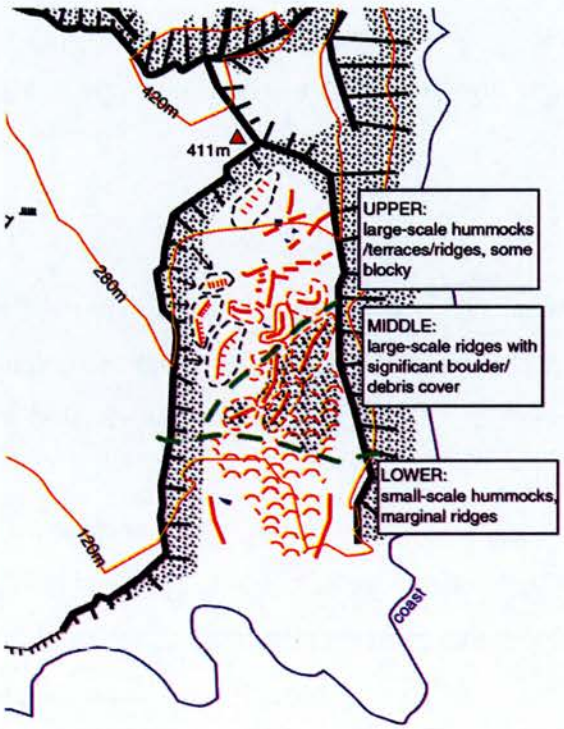

The basin is surrounded on two sides by steep basalt cliffs, and the entire floor of the valley is filled with large-scale hummocky terrain. Unlike many other suites it does not have a lobate overall form, but as can be seen, the basin is constrained laterally by bedrock cliffs. This topographic control evidently largely explains the overall suite shape, whose margins are juxtaposed with the foot of the cliffs or scree slopes.

Upper Suite

Figure 6.4-d: upper Svínavík suite - glacial vs landslide origin

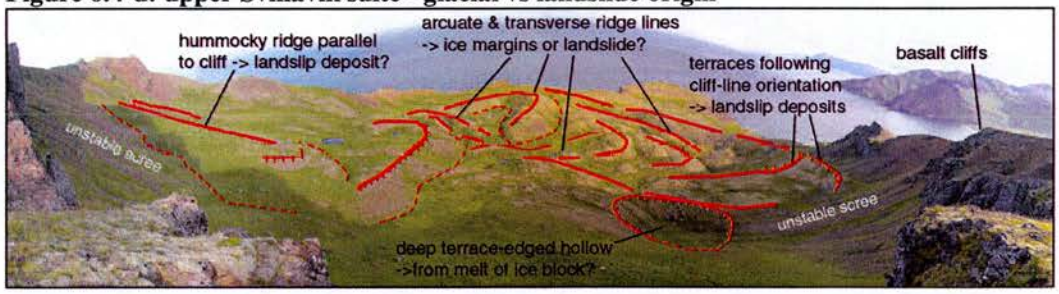

As in the Kjólsvík suite, there appears to be a relationship between orientation of ridges, hummocks and terraces, and proximity to cliff faces. As in other suites, the upper part of this landform suite contains characteristic blocky hummocks, ridges and terrace features, with orientations suggestive of a genetic link with the cliffs. Beyond these blocky terraces immediately next to the cliff, are further large-scale hummocky ridges with arcuate and transverse orientations. These landforms are consistent with landslide deposits, but also have characteristics reminiscent of glacial deposits, in their orientations and form. Notably, a relatively incongruous deep terrace-edged hollow is shown in Figure 6.4-d. The genetic origin of this hollow is difficult to explain without appeal to the existence of ice within a large volume of debris. The melting out of a single buried ice block would generate a deep hollow (kettle hole) such as that seen here.

Middle Suite

The middle part of the suite is characterised by large-scale debris-covered ridges, whose surface cover sets them apart from the upper suite, which maintains only the odd rock or boulder. This suggests these parts of the suite were generated in separate events. The most obvious origin for the debris cover is from rock-fall from the surrounding cliffs, but as seen in Figure 6.4-c, this region is not in close proximity to the cliffs, lying beyond the upper suite. On close inspection, the debris which covers the surface of the middle suite ridges, also makes up the body of the ridges (for as far as could be excavated). This debris must have been transported from the cliff source prior to the deposition of the blocky terraces above, which have little debris cover. These ridges are mostly oriented in a down-slope direction, which is consistent with ice-moulding by an active glacier, which evidently carried a high volume of debris. High debris volumes may have enabled ice to remain insulated for a long period, with the possibility of a rock glacier type system developing. It is possible, therefore, that the middle suite represents glacial deposits which have been overlaid in the upper suite by landslide deposits. Alternatively, the middle suite may represent the lower part of a landslide deposit, which may exhibit flow-like tendencies following the break up of the major rock blocks (Varnes 1978)

Lower Suite

In the lower suite, low-relief hummocky terrain prevails, with two lateral ridges curving towards each other at the base, where the hummocks become indistinct. These terminal ridges are consistent with landslide deposits, which often have arcuate ridges at the base. On review of the information presented in Table 6.3-a, however, these ridges may also be terminal moraines, recording a lower glacial limit.

Conclusions on genetic origin of the Svínavík Suite and chronological implications

The middle and lower units of the Svínavík suite have two potential origins: glacial activity or landsliding. If glacial activity is responsible, then a landslide event must have post-dated this to deposit the terrace and scarp features of the upper suite. If landsliding is responsible for the generation of the whole suite, the variation in form from the upper suite to the middle and lower suite must be explained. Bentley et al (1998) describe the spatial variability in landslide characteristics in different parts of a landslide deposit. The lower part of the deposit is made up of hummocky terrain, contains angular diamict and large boulders, whereas the upper part is characterized by terraces and scarps, with intact bedrock units. Bentley et al (1998) suggest that due to their increased traveling speed, larger rock blocks may find their way to the lowest slopes and become incorporated near the terminus of the landslide deposit, while smaller rock blocks will be more prevalent in the upper part. This description of landslide morphology compares well with the variable morphology of the middle and upper Svínavík Suite. However, the existence of ice as a transportation mechanism for debris to the middle suite cannot be ruled out. When the possibility of a glacier in the Svínavík basin is considered, it is easy to see how it could maintain a thick debris cover, due to the extensive surrounding cliffs. The putative kettle hole in the upper suite would back up this conclusion, being representative of in situ melting of an insulated ice block.

To fully assess the possibility of a glacial origin for the Svínavík landform suite it has to be viewed in the context of other landform suites. It is clear that landslides are responsible for generating at least the upper part of the suite. The middle and lower

regions may have been formed by the same landsliding event, but are also indicative of a glacial system with high debris content. The landslide event would have post-dated the glacier. If it is shown that glaciers existed in many basins in the study area, the likelihood of glacial activity in this basin is heightened. Chronostratigraphic information in this basin is limited, so does not help develop the events chronology.

6.4.3. Brúnavík

Figure 6.4-e: Brúnavík valley - Key topographic and geomorphological features

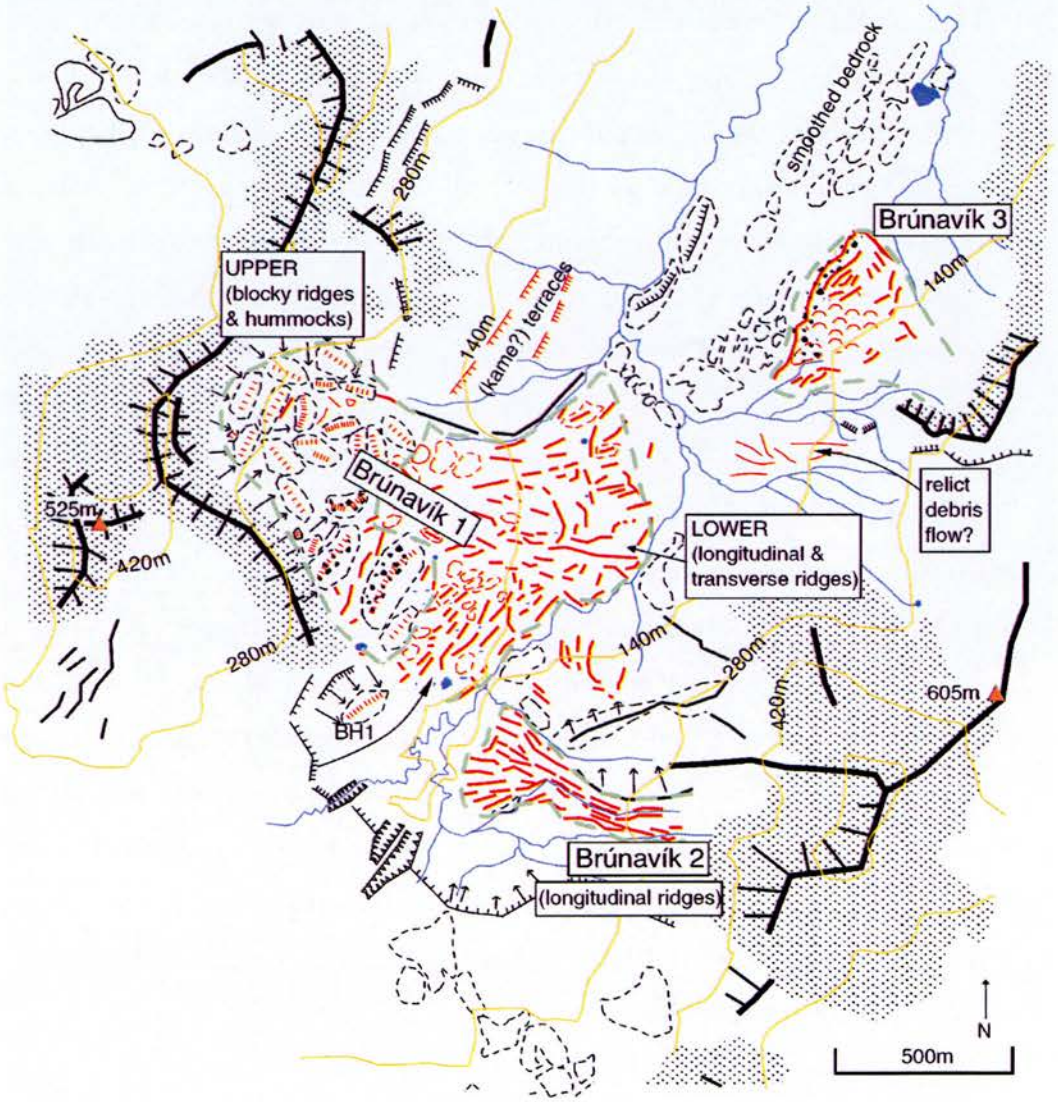

Brúnavík 1

The overall shape of the Brúnavík 1 Suite is lobate, constrained at the back and left flanks by steep basalt cliffs and scree slopes, and on the right flank by an extensive bedrock ridge. Its upper and lower regions have distinctly different geomorphological characteristics.

The upper part of the landform suite Brunavik 1 is characterized by blocky hummocks and terraces. As was seen in the upper Kjolsvik suite, the hummocks are oriented parallel to the orientation of the adjoining cliff face behind, and contain a number of large intact bedrock blocks, which match the geology of the cliffs. These factors again indicate that the bedrock cliffs are the source area of the blocky hummocks, which have been moved in a rotational landslide to their current locations. The slip-face for the slide is clearly evident in the steep back wall seen in Figure 6.4-e, though significant scree slopes have been built up through years of frost-weathering of the cliffs above.

The Brúnavík valley has further examples of 'blocky hummocks' outwith the landform suites, which are characterized by their terrace-like morphology, and their juxtaposition to an extensive bedrock terrace which crosses the Brúnavík valley. Given their scale and location relative to the bedrock terrace, the hummocks are most likely to share a genetic origin with the landforms of the upper Brúnavík 1 and Kjólsvík Suite, having been displaced in a continuous block from the bedrock terrace in a small-scale landslide. An example of one such small-scale slump is labeled "BH1" in Figure 6.4-e. The existence of these separate slide events outwith the landform suites indicates that such slide events are able to occur separately from events which generated the other landform types found within the suites, even when they are juxtaposed within the suite margins.

The lower Brúnavík 1 suite is characterised by transverse and longitudinal ridges made of till. A series of parallel transverse ridge lines are visible around the lower margins of the suite, which are interpreted as terminal moraines representing various

stages of glacial retreat. The ridges are distinct from those of the upper suite, and therefore do not represent landsliding. They are smaller in scale, with narrow crests and steep sides, and are often arcuate in shape. They do not contain large bedrock blocks but maintain a scattering of boulders and rock fragments. The longitudinal ridges represent moraine hummocks oriented in the direction of flow, and are associated with some transverse terminal moraine ridges.

The potential 'accumulation area' for a glacier producing the observed lower margins is large, sheltered and well-constrained by high cliffs on three sides. If temperatures were cool enough to enable ice to accumulate at between 200 and 280m, it is conceivable that an extensive glacier could be fed from this source. In general, the surface of the lower suite glacial deposits is rough and hummocky, geomorphology suggestive of stagnating ice under significant debris cover (Jansson et al. 2002). When the high level of available debris from proximal bedrock cliffs and scree slopes is observed, it is consistent with a debris-covered glacier hypothesis, which would enable long-term preservation of ice blocks. There is a clear element of bedrock control on the shape of this suite, as discussed in Chapter 4. The extensive bedrock ridge which runs along the (northern) lateral margin of the suite has formed a lateral control on the flow-route for the glacier, so that lateral ice margins run parallel to the bedrock ridge.

Chronologically, little data is available to absolutely date the glacial phase and the landslide phase of activity which generated the landform suite. A low value age of ~2.6ka is derived, which is thought to be an under-estimate of the true age. The landslide phase must necessarily have post-dated the glacial phase, but the extent to which it did is not clear. The 'blocks' of bedrock which have been moved by the landslides in the Brúnavík 1 Suite are smaller and more numerous than those evident in the Kjólsvík Suite, suggesting that 'slump' events may have occurred more often than at Kjólsvík and on a smaller scale, over a potentially long period of time, following the partial or full retreat of the Brúnavík 1 glacier.

The two suites clearly represent two main phases of activity which have resulted in the generation of distinctive upper and lower suites, and the better quality dating of the Kjolsvik Suite may provide dating evidence for the Brúnavík 2 Suite. The suites are comparable in terms of the landform types and their relative positions, the size of the accumulation area, the relationship with cliff-faces and bedrock features, the altitudinal range and the area covered by the putative former glaciers. It is suggested that given these connections, a climatic event which induced glacial activity in the Kjólsvík basin (dated to a minimum age of ~5ka), would have induced glacial activity at Brúnavík 1 at the same time. The landsliding activity occurred at Kjólsvík later, at around ~4.2ka, which may provide a rough age for the slumping at Brúnavík 1. However, the timing of such activity is inherently less regionally applicable than glacial activity, being more reliant on local thresholds and conditions than on climate.

Brúnavík 2

The Brúnavík 2 suite is one of the smallest landform suites in the field area, and extends from a well-defined though steep 'accumulation area'. Surrounding slopes are made up of unstable talus extending from high bedrock (rhyolite) ridges. The landform suite itself maintains a lobate form, and as discussed in Chapter 4, its 'flow' has probably been constrained at its northern margin by the bedrock ridge which extends almost to the Brúnavík valley floor. The suite is made up almost entirely of longitudinal ridges, which suggests that it was generated by a single type of process. Unlike most of the other suites, the lower margin of Brúnavík 2 is not defined by arcuate and transverse ridge-lines, but by a steep terrace-like edge, associated with the abrupt termination of longitudinal ridges which make up the suite body and lateral margins.

Figure 6.4-f: comparison between Brúnavík 2 landform suite (left) and debris/snow avalanche in the High Tatras Mountains (right)

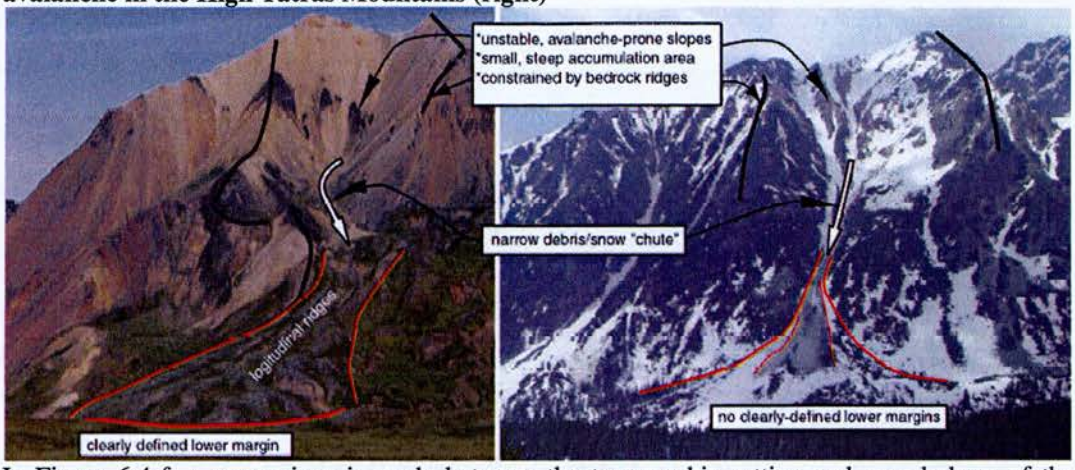

In Figure 6.4-f, a comparison is made between the topographic setting and morphology of the Brúnavík 2 landform suite, and a recently active debris/snow avalanche in the High Tatras Mountains. As can be seen, the size of the source area relative to the landform area is comparable, and both source areas are dominated by frost-shattered bedrock ridges and unstable slopes. In the Tatras example, the materials making up the unstable slopes are a combination of snow and rock-fall debris, which has been transported through a narrow chute and has become flow-like, widening towards the base. In the Brúnavík 2 Suite, a similar narrow chute is defined, through which rock (rhyolite) debris from the unstable talus slopes above is still actively transported. In both cases, the landforms spread towards the base in a fan-shape, and have irregular shaped margins. However their morphological characteristics are very different. The Brúnavík 2 suite has a clearly-defined high-relief lower margin, and is made up of longitudinal ridges, while the Tatras snow/rock avalanche has no clear lower margin relief and its surface contains no major ridge-lines.

From the similarities and between the Brúnavík 2 suite and the Tatras debris/snow avalanche, the conclusion is drawn that the source area of Brúnavík 2 is prone to failure through avalanching as in the Tatras example, and could readily transport a large volume of loose rock debris in the direction of the mapped landform suite. In colder climatic conditions, and in current winters, it is likely that such rock failure activities in this location also involve snow, which collects in gullies in the same way seen in the Tatras example.

In the High Tatras avalanche, it can be seen that the lower margins of each flow event are irregular and do not create significant morphology, with materials being spread thinly over the underlying topography. In Brúnavík 2, the lower margin does have significant relief, but does not form a smooth arcuate curve as in the lower margins of other suites, instead consisting of a series of longitudinal ridges which end abruptly, but not always in association with each other. This produces an

irregular margin as in the Tatras, which is seen clearly in Figure 6.4-i, and indicates genetic similarities.

One of the main ways in which the Brunavik 2 suite differs from the Tatras example is in surface morphology. Hypotheses are discussed to explain the existence of longitudinal lineations in the mapped landform suite, through reference to the hypotheses set out in Table 6.3-a. Given the climatic significance of glacial activity, the possibility is considered that the longitudinal ridges define 'crevasse-fill ridges', lineated hummocks, or sub-glacially formed eskers. However, with a glacial origin one would expect some arcuate/transverse ridges at the base representing the ice margins, which are notably absent. Further, the only potential accumulation area for snow and ice is poorly defined and small in area, so it would be difficult for it support a glacier which extended as far as the landform suite. Under current climate conditions, any winter snow accumulating in the source area would become associated with significant debris volumes, due to the high availability of friable rhyolite bedrock. This suggests that even under former 'glacial' conditions, any ice building up would have such a high debris content, it could not behave as a clean glacier, *per se*. Such conditions of high snow and debris availability foster rock glacier formation. However, the lineated surface morphology of the Brúnavík 2 suite is not reminiscent of a former rock glacier, which would be likely to have a far more chaotic surface, and probably contain transverse ridges.

The system generating Brúnavík 2 is likely to have relied on the rock debris source, with the input of snow and/or ice at least seasonally, as in the Tatras example described above. The lobate, topographically-controlled shape of the suite, and its longitudinally lineated surface morphology suggests that a large-scale flow process generated the observed longitudinal ridges (flow-lines), which are comparable to those seen in the idealized debris flow in Figure 6.2-h. This flow would have contained mostly rock debris, being enabled to flow by some moisture content from snow and ice melt or precipitation. It has been argued in Chapter 4 that bedrock is an important controlling factor in the shape of this landform suite, which one would

expect with debris flow activity. The relationship between bedrock and depositional forms is discussed in more details below.

Figure 6.4-g: debris flow overlying bedrock ridge

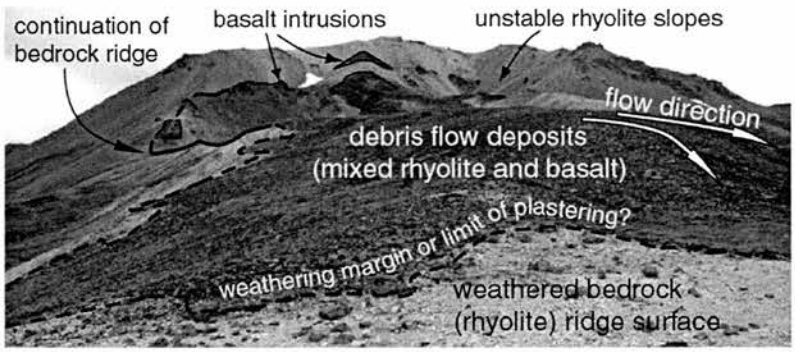

Figure 6.4-h: stratigraphic characteristics of Brúnavík 2 landform suite

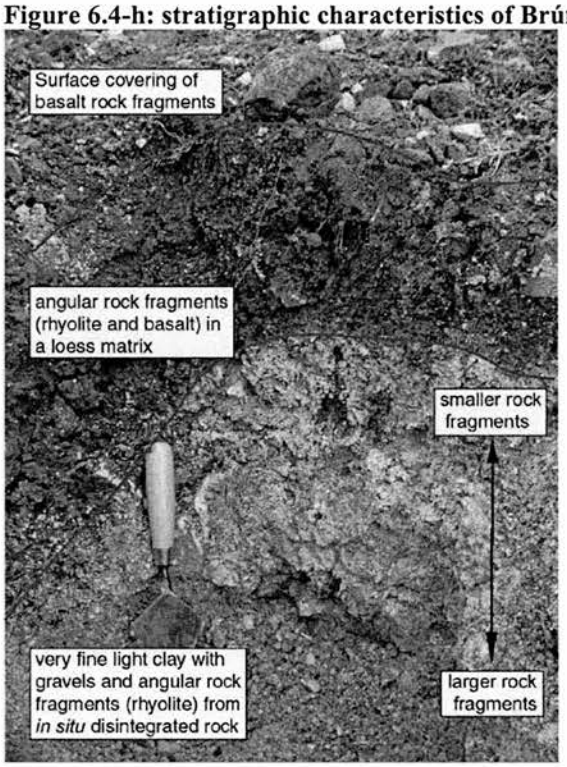

Figure 6.4-h shows a stratigraphic profile excavated on the outer (northern) ridge of the Brúnavík 2 suite, which is a bedrock ridge in the upper slopes, and exhibits depositional materials in the lower slopes. It is explained here as a bedrock ridge which has been overlain by debris flow deposits in the lower slopes. The upper layer is made up of a mixture of basalt and rhyolite rock fragments in a loessial matrix, while the lower section consists of only rhyolite fragments in a clay matrix. At the base of this profile the rhyolite clasts become so big the profile is impenetrable. The lower section is interpreted as the disintegrating surface of a bedrock (rhyolite) ridge, while the upper section is depositional and relates to the debris flow activity discussed above. The rock fragments which make up the upper section must have been transported from up-slope, as basalt intrusions exist in the upper slopes, visible in the dark sections on some ridge lines in Figure 6.4-g.

The chronostratigraphic information presented in Chapter 5 relating to this suite is limited, but a minimum age is derived of ~6ka near the outer margin of the suite, with the suggestion that the inner part of the suite has a younger basal age. This spatial relationship between the younger and older parts of the suite would be consistent with a debris flow origin, in that more recent flows may be super-imposed on older ones, following the main flow route down the centre of the suite. As

illustrated in Figure 6.4-i, the geomorphology suggests the existence of a second limit within the main suite, which may relate to this later flow event. This hypothesis is strengthened by the fact that at the lateral margins of the suite, materials representing depositional activity form thin layers over existing bedrock forms (see Figure 6.4-g and Figure 6.4-h), whilst in the central part of the landform suite, the ridges are entirely depositional, indicating a much greater depth of material in the central flow route.

Figure 6.4-i: Series of debris flow events generate Brúnavík 2 landform suite

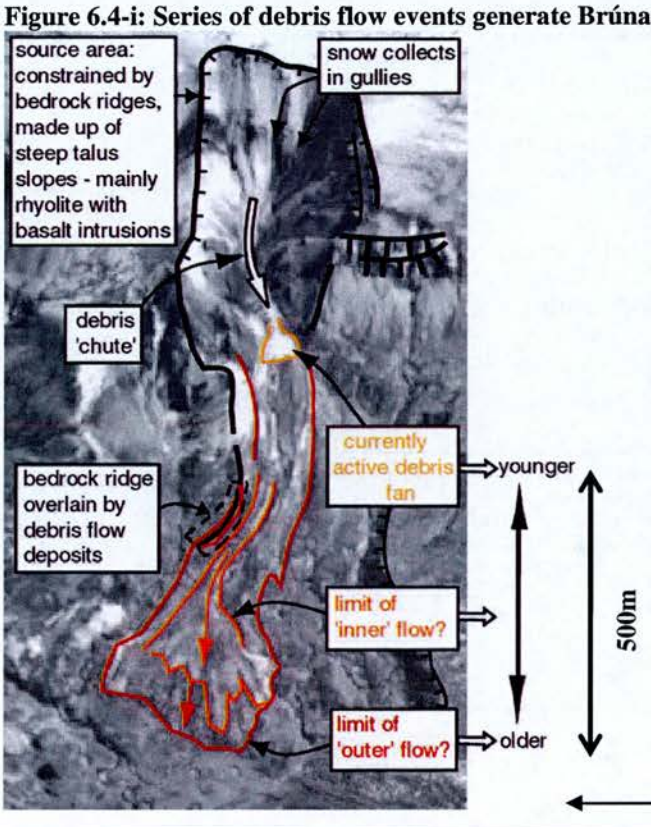

Figure 6.4-i summarises the genetic interpretation of the Brúnavík 2 landform suite. The 'outer' flow has been dated to ~6ka, and no dates were retrievable for the 'inner' flow. The suite is interpreted as a large-scale debris flow deposit, where the flow was fed by the extensive debris supplies above. Although the existence of snow and ice is likely within the debris flow, the exact volumes are difficult to quantify in a system which is controlled more by debris supply than by ice content.

Brúnavík 3

The Brúnavík 3 Suite has limited information. It has a well-constrained cliff-backed 'accumulation' area, well-defined lower margins, and a generally hummocky morphology, with some lineations. Given the morphological characteristics of the marginal ridges, it is probably of glacial origin. Though its accumulation area is small, it has a high level of available debris, which would enable it to survive and extend for longer than if it were a clean glacier.

6.4.4. Borgarfjörður

As discussed in Chapter 3, the body of the Borgarfjörður suite is made up of two distinctive lobate 'flows' made up of longitudinal ridges and associated transverse and arcuate ridges near the base. These two lobes are clearly evident when viewed from above as in Figure 6.4-j, and can be seen to share morphological characteristics with the Brúnavík 2 suite discussed above, which was interpreted as a set of debris flow deposits. The upper part of the suite has very different characteristics, consisting of less lineated and larger-scale hummocks and ridges, with more large rock-blocks visible and surface debris cover. Within the middle and lower suites there are some aerial units of larger-scale ridges and more chaotic hummocky terrain which are distinct from the main 'lobes' (described in Figure 6.4-j). It is suggested that, given the morphological similarities, these areas are remnants from the phase of activity that formed the upper suite. The lobes of the middle-lower suite appear to dissect these deposits, and are thus thought to have been super-imposed in a later phase of activity.

Figure 6.4-j: Borgarfjörður Suite - key topographic and geomorphological features

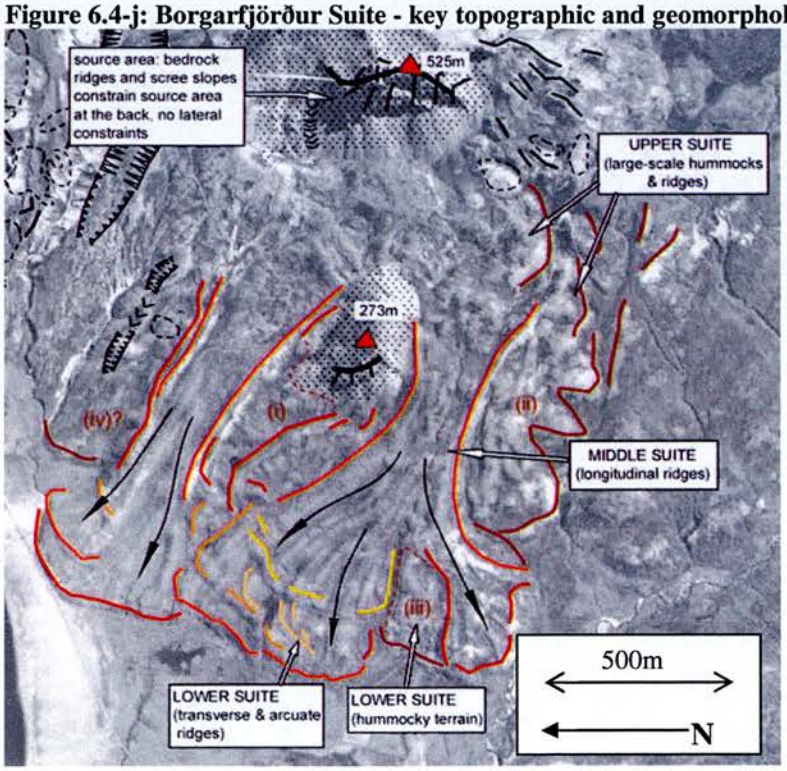

Figure 6.4-j illustrates the main features of the Borgarfjörður Suite. Two main lobes are visible on either side of the 273m bedrock knoll, the main trajectories of which are indicated by arrows. Distinct areas of less-lineated hummocks and large-scale hummocky ridges are labeled (i)-(iv) in the middle and lower suites, which share characteristics with the upper suite more than the longitudinal ridges of the main lobes.

On detailed inspection of the upper suite, and the areas (i) to (iv) of the middle-lower suite, they have characteristics of glacial deposits, which in the upper part, have been associated with a high level of debris from the scree and bedrock ridges which form the upper margin of the suite. There are clear lateral and terminal margins (exemplified in area (ii)), the generation of which is difficult to explain without appeal to glacial activity. The high-relief, steep-sided and boulder-crested lateral/terminal ridges, with deep sediment-filled hollows within their margins are typical of glacial deposits, as illustrated in Figure 6.4-k. Such margins are consistent with a glacier sourced immediately in front (down-slope) of the 525m peak, and just above the 273m bedrock knoll which is situated in the middle of the suite (as marked in Figure 6.4-j). This 'accumulation' area has no clear lateral constraints, but snow accumulates readily here in the winter months under current climates, so under colder climates it is conceivable that a glacier could grow, probably enabled to last longer and extend further due to the high level of debris provided by the bedrock ridges, peaks and knolls associated with this suite.

Figure 6.4-k: Glacial margins of the upper Borgarfjörður Suite

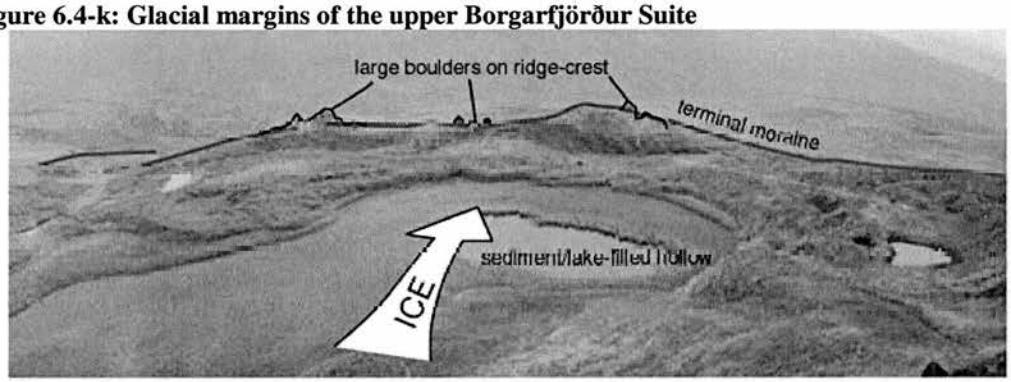

The lobes of the middle-lower suite are not interpreted as glacial, but as debris flow deposits, due to the existence of flow-lines (longitudinal ridges) and their lobate form, similar to the Brunavik 2 Suite. They have characteristics of flow processes involving debris and water rather than a significant volume of ice, in that the distinct flows always follow the quickest route down-slope, diverting around bedrock intrusions, and spreading fan-like near the base, often breaking into separate 'sub-lobes'. Their surface morphology is much smoother than that of the putative glacial deposits, and transverse ride lines tend to be terrace-like, with gentle up-slope angles and steep down-slope angles. Notably, the Brúnavík 2 debris flow contained no

transverse ridge lines as seen in the Borgarfjörður debris flows. This is explained by the fact that the Borgarfjörður flows extend a greater distance along gentler slopes and across the valley floor. When a debris flow terminates on steeper ground (as the Brunavik 2 suite does) it is less likely to maintain terminal ridges. As can be seen, a series of lobe margins are traceable, highlighted in progressively lighter colours in Figure 6.4-j, indicating that successive debris flow events occurred following possible glacial activity.

Figure 6.4-l: Reconstructed sequence of events which formed the Borgarfjörður Suite as observed today

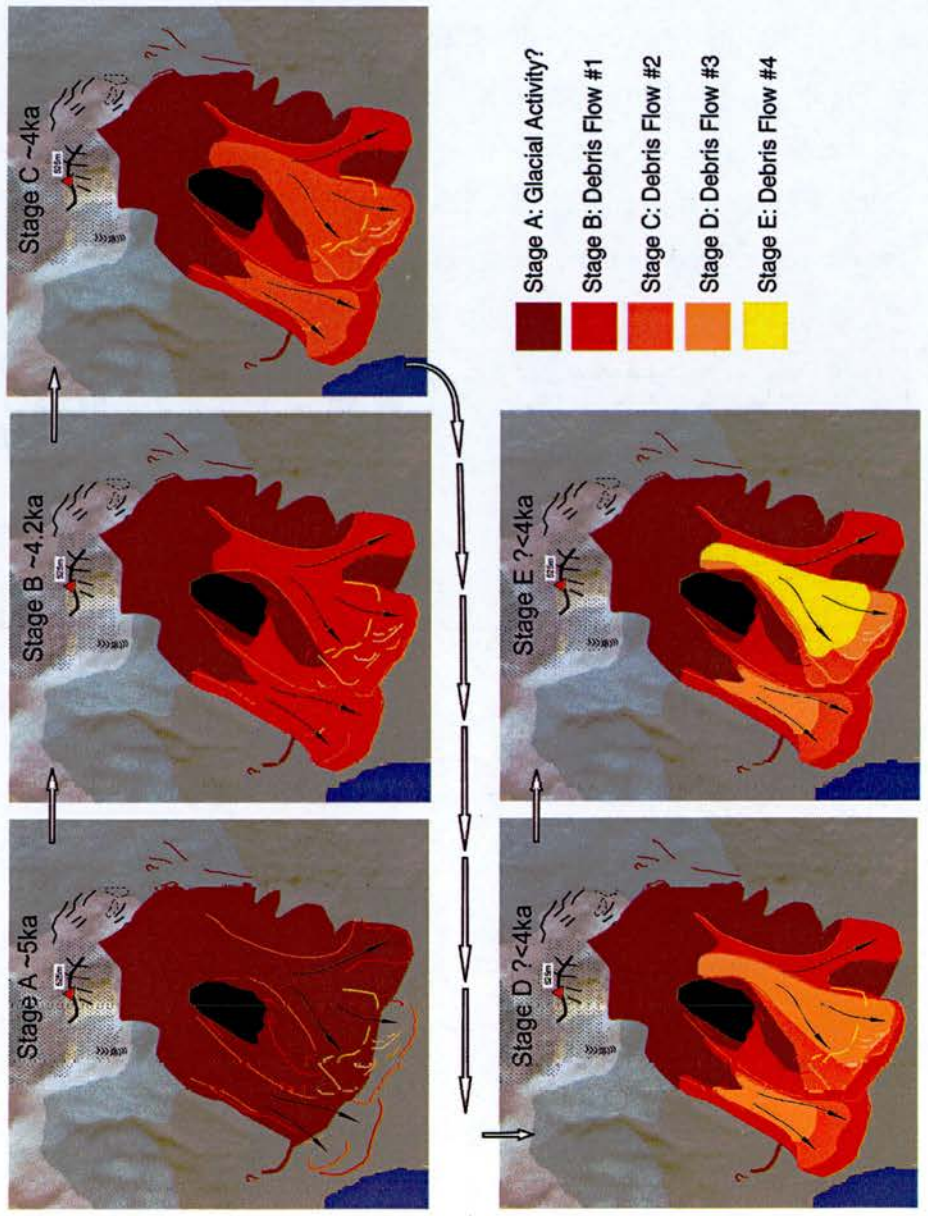

A chronology of events is presented in Figure 6.4-l, which utilizes the geomorphic and chronological evidence (from Chapter 5) to reconstruct and place age estimates on the phases of activity which formed the Borgarfjörður Suite. Chronostratigraphic evidence backs up the hypotheses of debris flows, preceded by glacial activity. The upper suite and the hummocky areas of the middle-lower suite, date to ~5.5-5k cal. Yrs. BP, based on available profiles, providing an age for the removal of ice from the area. The units of chaotic hummocky terrain in the lower suite, and the association of hummocky ridges with decaying bedrock ridges in the upper suite, suggest that ice probably remained in the area for a significant time, insulated by debris and decaying slowly. Initiation of the glacial phase may therefore have been a relatively long time prior to ~5ka, though the exact timing is hard to quantify. From Chapter 5, the landforms indicative of the debris flow events provide ages suggesting that the first phase of activity occurred at ~4.2k cal. yrs. BP. Within a second set of flow margins, a date of ~4k cal yrs. BP is derived in Chapter 5. Further flow margins are visible within these which are younger still, showing that the debris flow phase was probably not a single event, by a time-transgressive series of flows. An obvious moisture source to enable these flows would be the decaying glacial ice.

6.4.5. Mosdalur

The Mosdalur suite exhibits characteristics of glacial deposits. An arcuate marginal ridge at the terminus is interpreted as terminal moraine, behind which is an area of hummocky terrain reminiscent of ice-stagnation topography. In the upper region a series of longitudinally lineated hummocks probably represent moraine hummocks oriented by the over-riding ice. The source area for the putative glacier is an extensive cliff-backed basin with extensive scree slopes. In the upper and middle suite, there is evidence of debris flow activity, with a narrow "chute" evident between the source area and the lower deposits. This landform suite was not studied in detail and further data would be required to enable detailed chronological and process information to be derived on the nature of this putative debris flow. In the context of the field area and the known existence of other ice limits, it is highly

likely that, given the size of the potential accumulation area at Mosdalur, a glacier would have formed in this basin.

6.4.6. Víkurá

Víkurá 1

Figure 6.4-m: Víkurá 1 - key topographic and geomorphological features

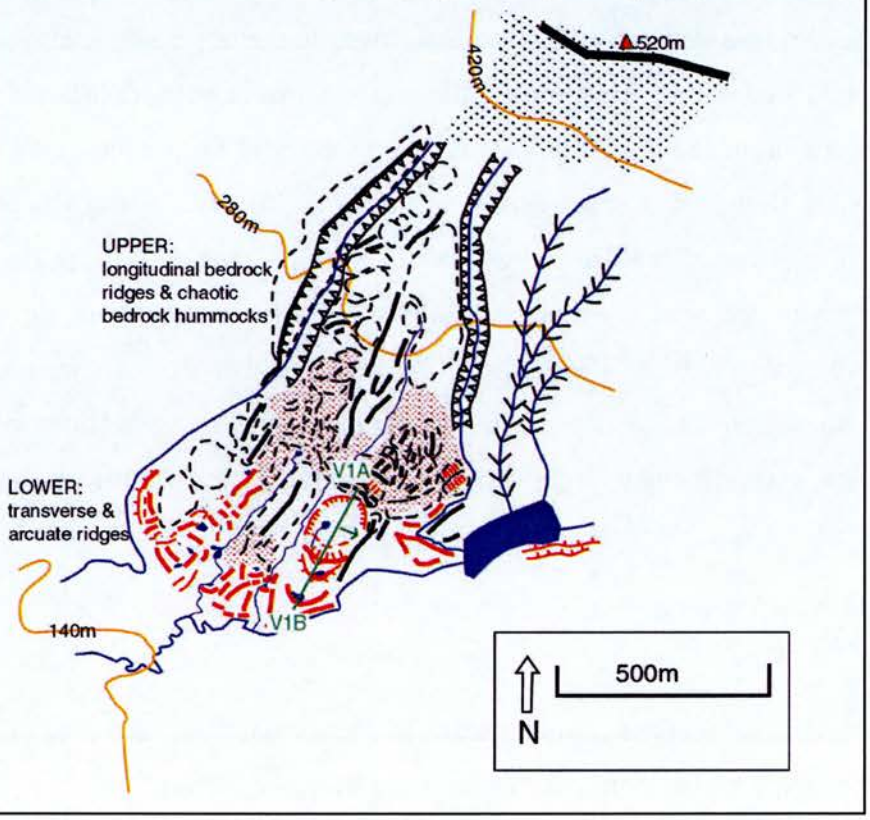

The Víkurá 1 landform suite differs from the other suites in the field area because it is made up of a high proportion of bedrock landforms, yet maintains the generally lobate form typical of the mapped landform suites, and is fronted by a series of marginal arcuate and transverse ridges (as seen in Figure 6.4-m). The upper region of the suite is made up of bedrock hummocks with no clear orientation, as discussed in Chapter 3.4.5. The most likely explanation for their morphology, given their bedrock origin, is selective erosion of less resistant rock either by a glacier or by other weathering processes. To the east and south of the main area of bedrock hummocks, a number of long bedrock ridges are visible with clear longitudinal

orientations, widening towards the base in a fan. They are in some places reduced to piles of large boulders, but a clear continuity and structure enables the bedrock interpretation. These are probably ridges of more resistant basaltic rock which have a fan-like structure due to their association with the old central volcanoes. The rhyolitic rock in between the ridges is more readily weathered or eroded. If a glacial hypothesis is considered, erosion by ice may cause this selective erosion, which smooths the bedrock into ridges and furrows in the direction of flow. These opposing hypotheses for landform genesis, of glacial activity versus weathering are discussed further in the following section. It is possible that both processes have occurred.

In the lower region of the suite, as seen in Chapter 3.4.5, non-bedrock ridges are observed which follow a down-slope orientation in line with the bedrock ridges. The have a starkly different character to the bedrock ridges, being smoother in profile, and being of lower relief. In terms of material make-up, information is very hard to gather on these ridges, as the surface is made up of a thick and mostly impenetrable layer of shattered rock debris. Further evidence can be derived from the link between these ridges and transverse ridges at the margins of the suite. The steep transverse and arcuate ridges at the lower margins of the suites are connected to the longitudinal ridges, indicating they share a common process origin.

Figure 6.4-n: The arcuate ridges of the lower Víkurá 1 Suite - evidence of glacial activity?

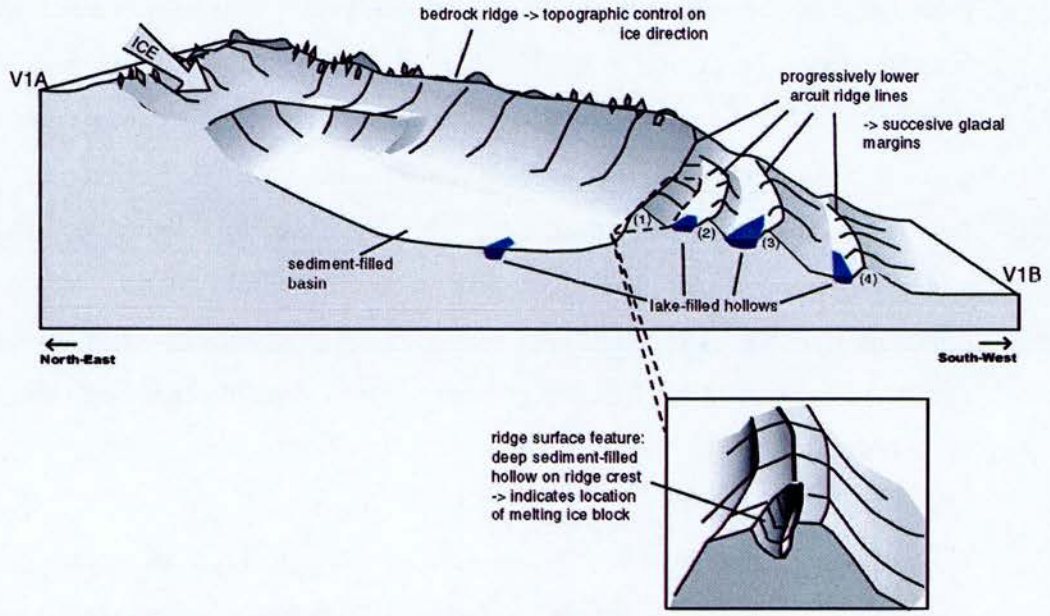

The cross section shown here is taken from the point V1A to V1B, the locations of which are shown in Figure 6.4-m, in the context of the whole suite.

Figure 6.4-o: Terminal Moraine and bedrock control in the Víkurá 2 Suite

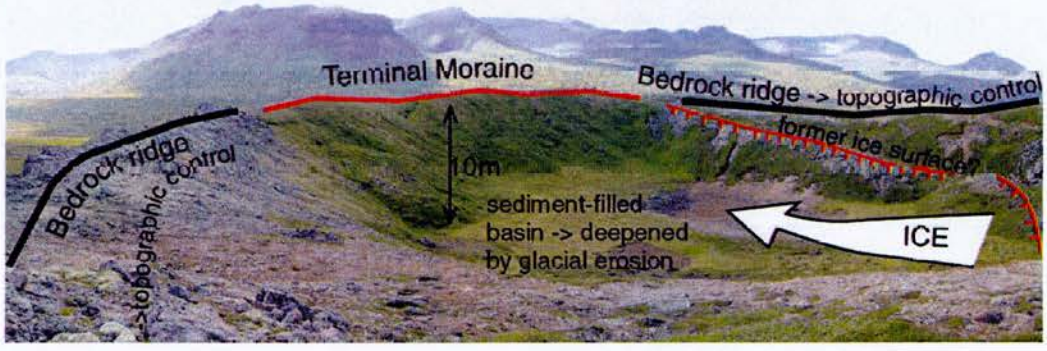

The arcuate ridges at the margins of the suite are typified by steep sided ridges rising six to ten meters from the base on the up-slope side. On the down-slope side, a series of four progressively lower terrace-like forms drop (as illustrated in Figure 6.4-n), fronted by arcuate ridges, with sediment and lake filled hollows behind. These ridges have been confirmed to be debris ridges rather than bedrock, following excavation, so the possibility of these landform elements representing the lower margins of an old lava flow is ruled out (although bedrock features within the suite may still be related to such an event). There are a number of potential mechanisms for the generation and deposition of these progressively lower arcuate terrace-like

ridges. From assessment of Table 6.3-a, glacial activity, solifluction or landsliding may produce arcuate or transverse ridges near their margins. Here, these hypotheses are assessed in detail.

On the upper ridge-crest numbered as ridge (1) in Figure 6.4-n, is a sediment-filled hollow of approximately two metres deep, two metres long and one metre wide. This small feature lends significant information to the interpretation of the ridge's origin. The most obvious explanation for the existence of such an incongruous hollow is that it was formed when an ice block within the ridge debris melted out. On observation of the up-slope side of this main arcuate ridge (shown clearly in Figure 6.4-o), its steepness and height make solifluction processes an unlikely genetic origin. Given the extent of bedrock ridges and features which controlled and were selectively eroded by ice flow, ice existing in this area would have high debris content, allowing the deposition of high terminal moraines such as this. Another process which may produce steep high transverse ridges is landsliding, where such ridges may occur in the lower deposits. However, there is no evidence of landsliding up-slope, so this is ruled out. The morphology of these ridges, combined with the fact that a series of similar progressively lower marginal ridges front the suite for its full width, is taken as evidence of a glacial origin for deposits in the lower region of the suite.

If it is accepted that a glacier did exist in this region, the relationship between this glacial activity and the large number of bedrock forms which define most of the rest of the landform suite must be considered. The volume of bedrock outcrops signifies significant bedrock control on all processes occurring in this region. For ice to have existed in the lower suite, to deposit the clear glacial moraines, it must have existed in the upper suite. There is no clear accumulation area for snow and ice however, and the upper suite is constrained laterally only by bedrock ridges. The validity of the hypothesized glacial activity as a genesis mechanism for theVik-1 suite is re-addressed in the context of the landscape as a whole in 6.6, and further tested with modeling in Chapter 7. In the mean time it is suggested that ice did exist here, and snow accumulation may have occurred in small basins sheltered by bedrock features.

Alternatively ice may have been fed from a small ice cap centered on the 520m peak behind the landform suite. Glacial ice in this region would have undoubtedly been strongly influenced by bedrock features. For example, from Figure 6.4-o, it can be seen that the steep (glacial) terminal ridge is associated with two longitudinal bedrock ridges, which would have directionally controlled glacier flow. A small terrace level is highlighted at the right hand side of Figure 6.4-o, which may potentially represent a small-scale kame terrace, deposited at the surface of decaying ice which remained in the basin. The upper part of the suite contains few depositional forms, representing the erosive phase of the glacier, and the lower suite represents the depositional phase, where the debris transported from up-slope is deposited. Chronostratigraphic evidence for this suite is limited due to an inability to excavate many profiles. This is due, in part, to the composition of the suite, which in the upper and middle parts of the suite, is made up of large, frost-weathered boulders, maintaining little soil cover.

Víkurá 2

As explained in Chapter 5, the Víkurá 2 landform suite has the best chronological control of all the suites. As will be demonstrated, it also contains the most convincing evidence of glacial activity, and these two factors combined make this set of landforms an invaluable environmental indicator in the context of this study. The suite maintains a roughly lobate form, containing two main 'lobes' with ridged lower margins, of which the easterly lobe is most well-defined. Lateral margins are not clear as they are in some of the other suites (e.g. the suites Brúnavík 1, Brúnavík 2 and Borgarfjörður).

Figure 6.4-p: Víkurá 2 Suite – key topographic and geomorphological features

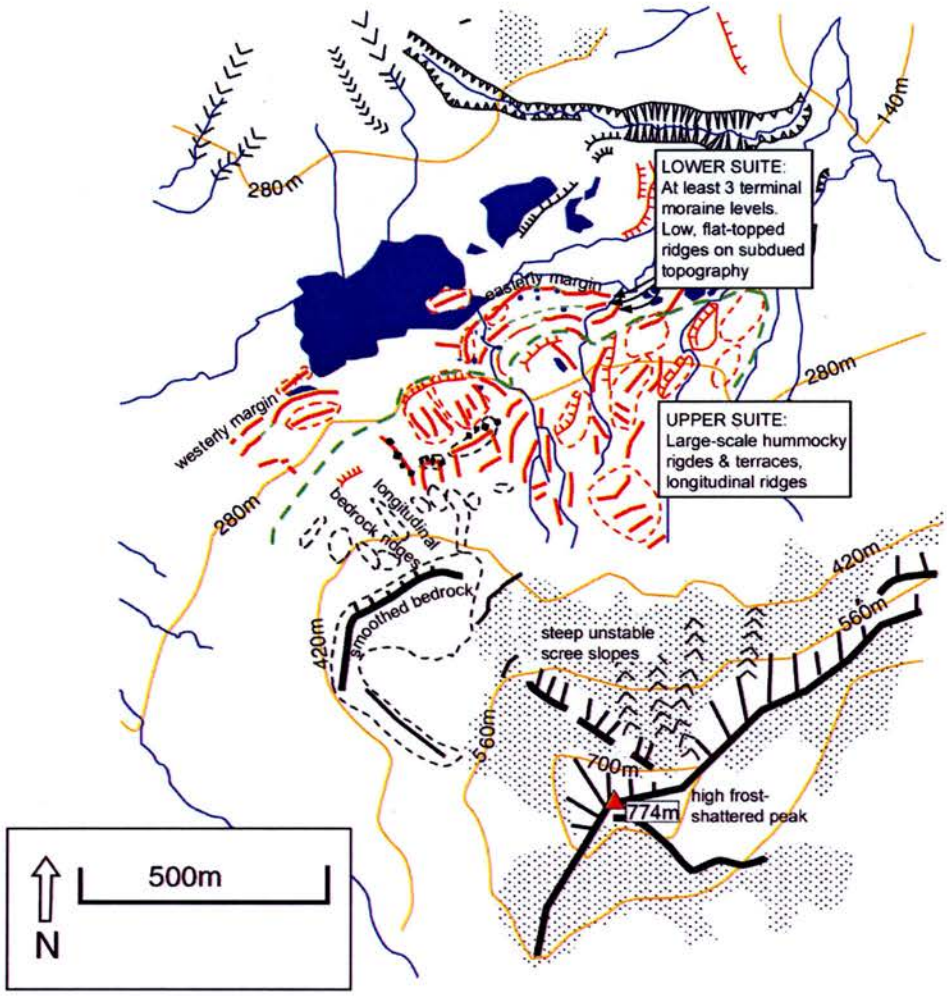

Figure 6.4-q: The glacial limits of the Víkurá 2 Suite (eastern lobe)

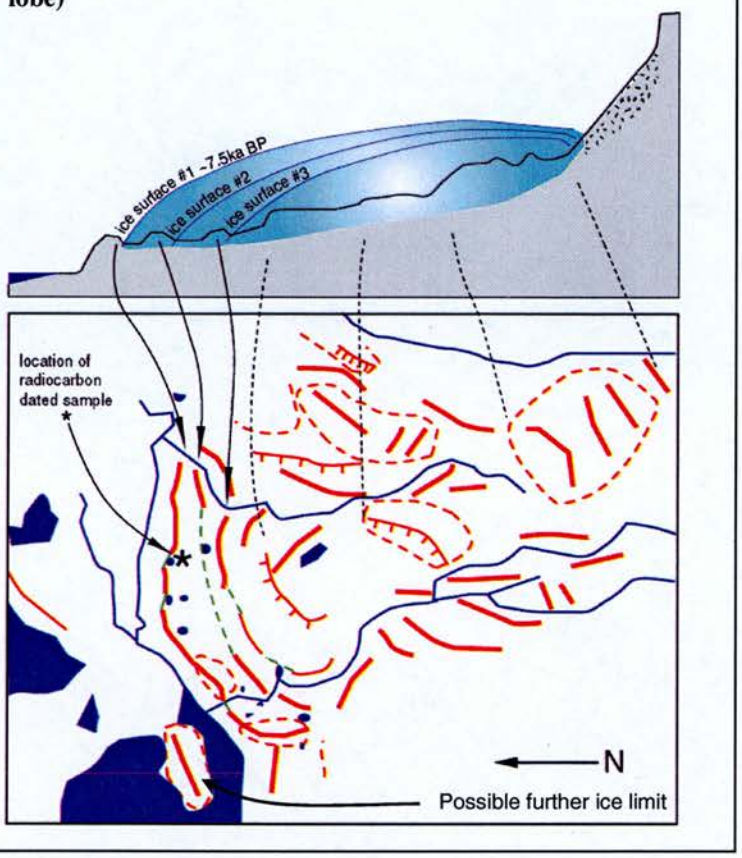

Lower Suite

The lower region of the suite is dominated by a series of low-relief, flat-topped arcuate and transverse ridge lines. At least three levels of ridge are clearly visible, the outer of which has a steep flank which drops around four metres to the lake edge, as shown in profile in Figure 6.4-q. The height of the outermost ridge relative to the lake edge suggests that the ridges may be of higher relief than is currently seen, but the hollows between ridges have been filled in by significant volumes of sediment. One further ridge line at a lower level may represent a more extensive glacial limit (highlighted in Figure 6.4-q). These ridges are morphologically very similar to the low-relief arcuate ridges found in the lower Kjólsvík suite, which have been interpreted as glacial margins. Following assessment of the multiple working hypotheses presented in Table 6.3-a, glacial activity is again thought to be the most

likely genetic origin of the Víkurá 2 arcuate ridges. Figure 6.4-q reconstructs estimated ice positions at the time of deposition of the three distinct margins.

Upper Suite

The upper part of the suite in the eastern lobe is dominated by large-scale, boulder-covered hummocky terrain and some longitudinal ridges. As seen in Figure 6.4-q, the area of the upper suite would have been ice-covered at the time of deposition of the terminal ridges. The hummocky terrain probably represents moraine deposits, and the lineated ridges are moraine ridges which have been shaped in the direction of flow by active ice. It is also possible that some of these represent lateral moraine deposits. In the western lobe of the Víkurá 2 suite, the upper region does not contain depositional landforms, but a large area of bedrock forms. The lineations evident in some of the smoothed bedrock forms are consistent with glacial erosion features, which were probably formed during the glacial phase which deposited the lower suite terminal moraines.

Chronostratigraphic Evidence

Figure 6.4-r: sedimentary properties of upper and lower Vik-2 suite (section of Figure 5.5-b repeated)

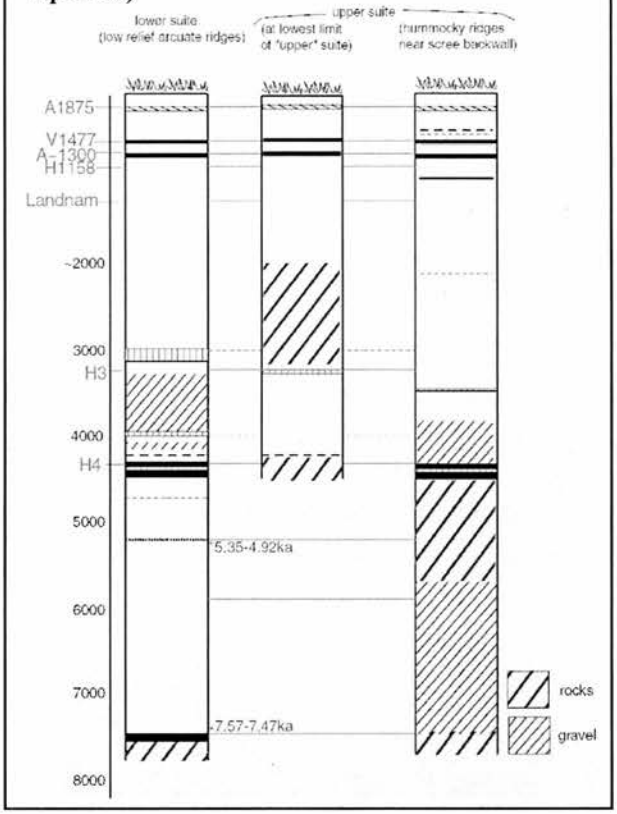

From Chapter 5, it has been seen that the upper suite has experienced a significant amount more post-depositional geomorphic activity than the lower suite. Referring back to Figure 5.5-b in Chapter 5, during most of the mid to early Holocene, layers of gravels and rocks have been superimposed on the upper suite landforms, whereas in the lower suite, mostly undisturbed peat accumulation has occurred since ~7.5ka.

This suggests that whilst the upper and lower units of the landform suite may initially have been generated synchronously, further debris-transport processes have affected the upper suite from its time of deposition until the mid-Holocene. In particular, the deposition of a layer of rocks which occurred between 6000 and 4000 cal. yrs BP suggests a period of enhanced geomorphic activity. The rock layer does not have the characteristics of glacial till, being made up of small angular rock fragments in a gravelly matrix, and is probably related to rock fall or debris flow deposits from the scree slopes and cliffs behind. As discussed in Chapter 5, the basal age derived for the upper suite is of lesser worth than that for the lower suite, rendering the estimation a maximum age. It is conceivable that the upper suite owes its form to processes occurring after the lower suite had been deposited and stabilized. Given the proximity to an unstable scree slope, it is likely that ice remaining in the upper slopes of the suite following retreat from the terminal moraines was covered in

debris and may have remained for an extended period of time as such. The larger-scale hummocky morphology of the upper Víkurá 2 suite supports the hypothesis that geomorphic activity continued on the upper slopes of this suite after the retreat of ice from the lower margins.

Víkurá 3 & 4

The landform suites Víkurá 3 and 4 are very similar in form and aerial extent, and have source areas in adjoining valleys. They have dissected but traceable marginal (arcuate) ridges which lie not at the valley floor (as in other suites), but on the steep valley side, as shown in Figure 6.4-s. The main body of the suite is not well-defined, with only sparsely distributed hummocks and ridges. As discussed in Chapter 4, the lack of landforms within these suites is attributable to the poor preservation potential on such steep slopes. The landform suites appear to dissect a series of parallel terraces, which run much of the length of the Víkurá valley on the north side (we return to the origin of these in 6.4.6), showing that the suites were generated after the creation of the terraces. Both Víkurá 3 and 4 have very large accumulation areas relative to the aerial extent of the landform suites, originating in large sheltered basins beneath steep scree slopes. Unlike in other suites, the lower limit of the accumulation area is well-defined by a bedrock ridge feature, illustrated in Figure 6.4-s, on which depositional hummocks are found.

On the basis of the morphological characteristics of the landforms, particularly the lower margins, and the potential accumulation area, glacial activity is thought to be the genetic origin of the landform suites. A reconstruction of the ice margin positions is presented in Figure 6.4-s (lower part). The hummocky terrain found super-imposed on the corrie 'lip' is interpreted as morainic material deposited by retreating ice.

Figure 6.4-s: Landforms indicative of glacial activity: Illustration of the topographic setting of the Víkurá 3 Suite (above), and reconstructed ice margins (below)

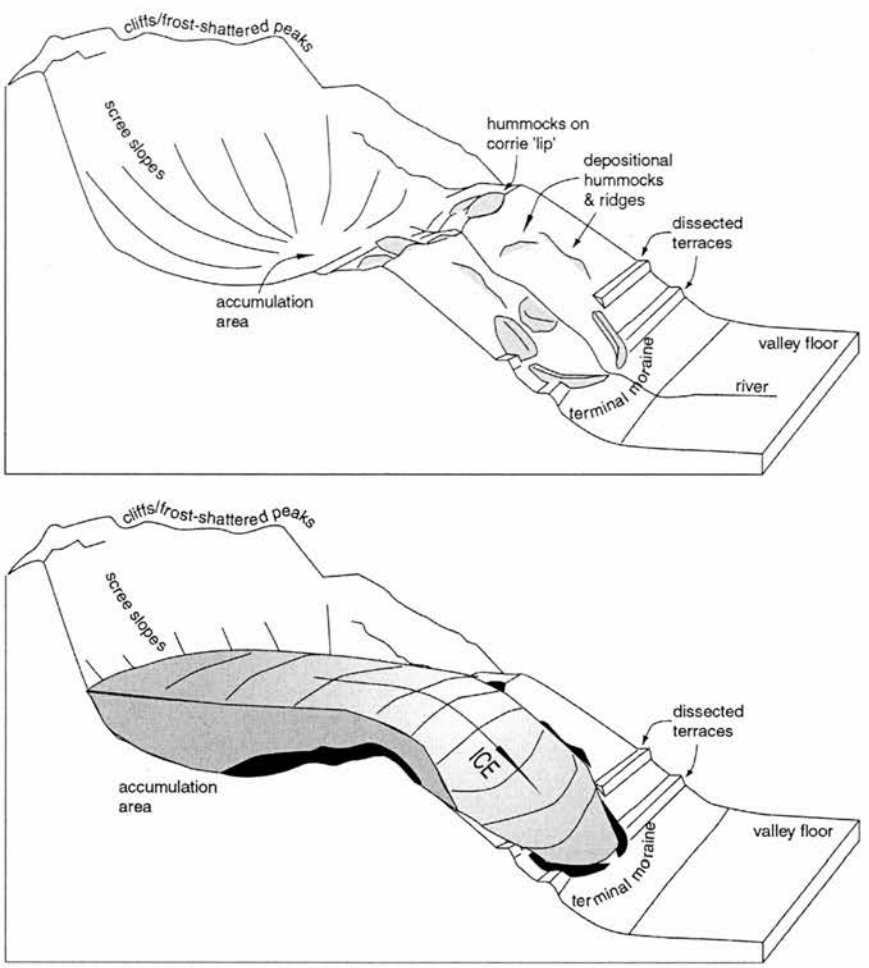

Víkurá 5

The Víkurá 5 suite covers the largest area of all the mapped suites, and its source area is less clear than in other suites. While its lower margins and lateral margins to the east are well-defined, its lateral margin to the west is difficult to reconstruct. Its lowest margins are defined by a series of steep-sided, transverse, boulder-crested ridges, on a gently sloping topography. They are of too high-relief, and lie on too gentle a slope to be related to solifluction activity or debris flows, and have no clear cliff source area for landsliding activity. They are interpreted as glacial moraines, and the remaining landform elements within the suite are consistent with this interpretation. At the easterly lateral margins of the suite, near the cliff edge which drops into the Svínavík basin to the east, parallel ridges run perpendicular to the

lower margins, at progressively lower altitudes, on the slopes of Grenmór. The two hypotheses for their generation are solifluction terraces, or kame terrace features. As the orientation taken by the ridge lines is not directly down-slope or transverse (in the context of the local slope aspect), as would be expected of solifluction processes, kame terraces are the more likely cause. This is consistent with the known existence of the terminal moraine ridges at the base of the slope.

The characteristics of the Víkurá 5 suite are distinct from other suites interpreted as glacial, which tend to contain more landform elements within the limits, with a greater proportion of chaotic hummocky terrain and lineated ridges and hummocks. In comparison, Víkurá 5 has a large amount of land without significant relief. This is explained by the relative lack of available debris for glaciers in this location, so that their debris load is less, and there is less likely to have been long-term buried ice stagnation. The local accumulation area is low altitude and small, containing only limited bedrock exposures.

Figure 6.4-t illustrated the many glacial margins traceable from the terminal and lateral moraines, and kame terraces. As many as 14 different limits are visible, representing ice at different stages of decay. The potential accumulation area for ice in this basin is limited to a number of small bedrock basins which are highlighted in Figure 6.4-t, and all lie at very low altitude (relative to other landform suite source areas) at around 250m. As can be seen, the outer series of mapped glacial limits represent former glaciers far too big to have been fed by these limited accumulation zones, and it is postulated that at the time these limits were generated, ice was sourced in the larger and higher altitude Kjólsvík basin to the north, and crossed the low col towards the Víkurá valley (as highlighted by the ice breached col in Figure 6.4-t). Given the existence of a glacial margin in the Kjolsvik basin (the location of which is shown in Figure 6.4-t), the ice must have breached this col prior to the generation of the Kjolsvik moraines, which are dated to ~5ka. By this time, the Víkurá 5 ice must have become separate and been sourced only by its own limited accumulation zones. Dating evidence for the Víkurá 5 suite relies on three dates from the outer 3 kame terrace levels, and the dates retrieved, when viewed in the

context of the whole field area, appear to be younger than expected. The dates for three lateral ice margins are illustrated in Figure 6.4-t, as 6.2ka, 5.4ka and 3ka, working progressively inwards into the suite. It can be seen that the glacier responsible for the generation of lateral ice margins at the observed altitudes (between 180 and 320m) must have reached the sea, as the ridges terminate abruptly at the cliff edge. Continuing the ice margins up-slope to find a possible source area, it appears that ice must have originated beyond the immediate Víkurá 5 basin, crossing the low col from the Kjólsvík valley. The lateral margins do not connect with any terminal moraine in the lower suite, implying that these limits relate to a later phase of glacial retreat.

Figure 6.4-t: Glacial Limits of the Víkurá 5 Suite

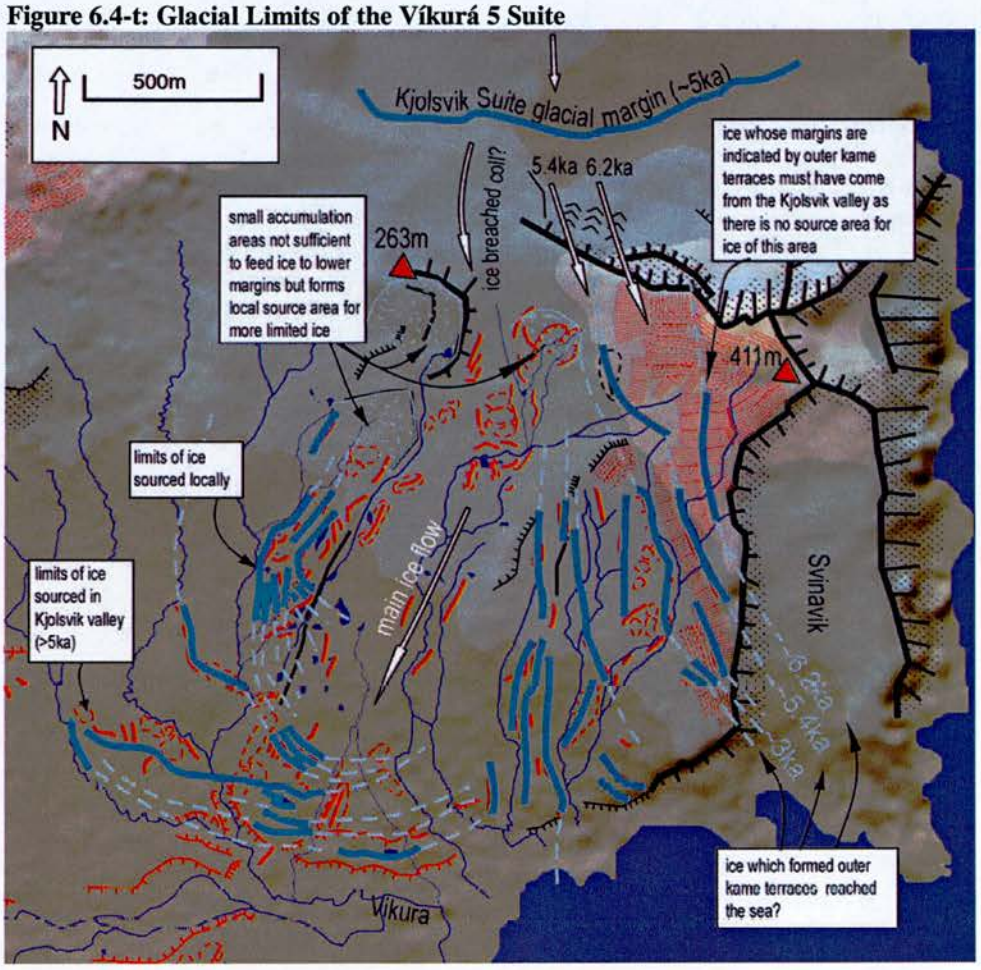

As was discussed in Chapter 1, the last time valley glaciers are thought to have reached the sea in this part of Iceland, as suggested by the kame terrace levels, was during the Younger Dryas, or at the latest during the Preboreal period, which ended

prior to 11k cal. Yrs BP (Björck et al. 1997; Gulliksen et al. 1998; Norðdahl and Einarsson 2001), making an age of 6.2k cal. Yrs BP for the outer limit seem unlikely. There are major glaciological implications for the rest of the field area, if ice reached the sea at 6.2ka, and no evidence has been found elsewhere of such extensive ice so recently.

To derive ages for the terminal moraines, it is postulated that to maintain a glacier which extended to the lowest margins of the landform suite very close to the sea, the accumulation zone would have to be bigger than that provided by the small, low-altitude bedrock hollows illustrated in Figure 6.4-t. Therefore, the ice which formed these limits must also have come from the Kjólsvík basin. Due to the existence of smaller-scale glacial limits within the Kjólsvík valley, which are dated to a minimum age of ~5ka, the glacier must have retreated from the Kjolsvik-Víkurá col a significant time prior to 5ka. A second set of glacial limits are found some distance within these lower limits, illustrated in Figure 6.4-t. These indicate the existence of a smaller-scale glacier, which may have fed from a more local source area, in the small bedrock basins highlighted in Figure 6.4-t. It is likely that this ice probably existed at a similar time to the Kjólsvík ice.

6.5. Context: Past and Present geomorphic activity

6.5.1. Currently active processes in Borgarfjörður Eystri: Geomorphic processes since landform suite generation

A brief overview is provided of the currently active geomorphic processes occurring in the field area. The extent of current periglacial and glacial activity in the field area under modern climatic conditions provides an indicator of current interactions between climate and geomorphic process, and may show how close to the threshold the field area is to becoming glaciated again. In addition, knowledge of currently active processes enables assessment of the extent of post-depositional modification which the mapped landform suites may have been subject to, a factor which should be considered during interpretation of genetic process.

Current glacial activity

There is limited current glacial activity just outwith the immediate field area, on the Dyrfjöll massif, at altitudes above ~800 metres. Although these are not significant erosive or depositional agents in modern times, they are active glaciers which have deposited small marginal moraines very recently, and which have, in the past, extended much further. The existence of these small glaciers at ~800m and above highlights the existence of a minimum altitude for glacier activity under current climatic conditions. The highest peaks in the main field area lie just below 800m (at a maximum height of 775m), which shows that the region is probably just below the altitude necessary for significant glacial activity to occur. In Chapter 7, modeling experiments will be carried out as a means of testing the climatic deterioration necessary for glaciers to initiate in the main field area.

Hrafná Basin

The Hrafná basin is briefly discussed in this section because the hummocky landform suite observed in this basin is interpreted to be a recently active rock glacier, possibly relating to the Little Ice Age cooling. Its much younger age is evident in the lack of vegetation cover on the surface. It is in an ideal location for rock glacier generation, with extensive talus slopes surrounding a small sheltered basin in which ice could easily build up. It is distinct in form from other mapped landform suites in the field, not being lobate in shape, and not showing clear evidence of flow-like behaviour. It is possible that it may contain ice-cores buried under the thick debris.

Periglacial processes

Periglacial processes are extensively active in the field area, and evidence exists for larger-scale periglacial activity in the past. In areas above ~600m, permanent snow patches are common, promoting periglacial activity such as solifluction on the saturated ground. Where permanent snow patches are associated with talus slopes, such processes are extensive. Talus slopes are a product of periglacial activity, and are the most noticeable feature of the hill sides in the field area. They originate from in situ fracturing rocks, or rock fall from cliffs above, caused by ice forming in

cracks in the rock and forcing it apart. Generally larger basaltic boulders build up at the foot of slopes, falling from the tops where basaltic intrusions are common. Small angular fragments of rhyolitic bedrock make up the main hill-slopes.

There is evidence of small-scale periglacial processes as low as sea level, as demonstrated by the stone stripes and stone circles in Figure 6.5-a and Figure 6.5-b. This leaves scope for significant slope modification to have occurred since the landform suites were deposited. For example, polygons have formed in the stone and gravel car park in the village of Bakkagerði in Borgarfjorður, at 5 metres altitude. At higher altitudes, forms become larger and more extensive. These grade into terraces and solifluction lobes on steeper slopes. Solifluction processes can significantly alter slope form and the terraces and ridges formed by these processes could be mistaken for arcuate moraine formations. It is highly likely that any of the landforms characteristic to this study have been modified in some way by periglacial processes. The existence of such forms proves the existence of at least semi-permanent ground ice (if not permafrost) as low as sea level.

Figure 6.5-a: Stone Stripes in Brúnavík valley

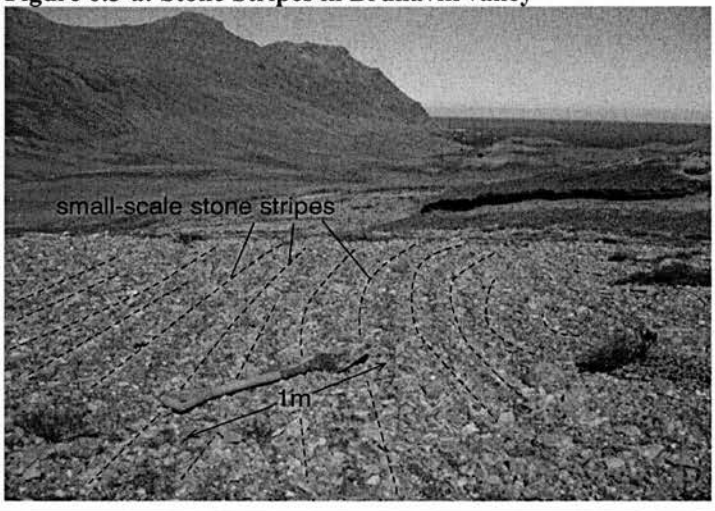

Figure 6.5-a shows stone-stripes, representative of the characteristics of such small-scale periglacial activity in the field area as a whole. These are found oriented in a down-slope direction on a gentle slope gradient.

Figure 6.5-b: Stone Circles in Víkurá valley

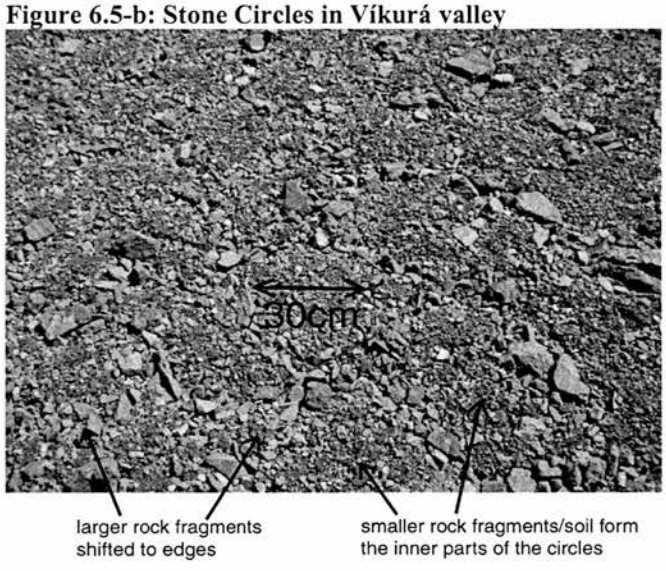

Figure 6.5-b shows an example of small-scale stone circles or polygons, found on mostly gently sloping or flat ground in the field area. Sorting of large from small debris occurs, as in Figure 6.5-a, by freeze-thaw action.

The known existence of ground ice at sea level, and permanent snow patches above 600m, implies that current climatic conditions are sufficient to induce significant periglacial activity. It can be assumed that, given the extent of such activity under the current climate, during a Holocene cold fluctuation, periglaciation would have played a key role in landscape modification, perhaps even more so than glaciation.

6.5.2. Previously active processes in Borgarfjörður Eystri: Glacial activity prior to landform suite generation

The initial environmental (particularly glacial) conditions prior to and at the time of landform suite generation, have major implications for the type and extent of geomorphic processes which can occur. Knowledge of the timing and extent of glacial activity prior to landform suite generation will therefore provide information on the environmental conditions in the region prior to generation of the mapped landform suites. In the following section, landforms mapped in the field thought to be indicative of previous glacial activity are described, and the glacial and climatic implications assessed.

Landforms

At least two levels of dissected parallel terraces on the valley sides have been mapped in the Víkurá valley and in the Brunavik valley (as shown in Figure 6.5-c).

These are interpreted as kame terraces, marking former ice surface altitudes. This conclusion is drawn because of the terrace surface slope angle, gently dipping down-slope towards the sea, and where it was possible to excavate, the materials making up the terraces were morainic in nature.

Figure 6.5-c: The kame terraces of the Víkurá valley

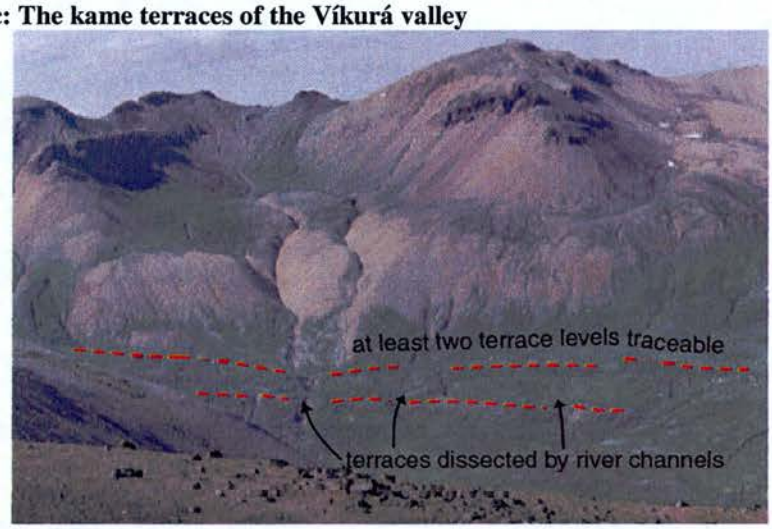

Terrace features with very different characteristics were mapped at the head of the Víkurá, Kjólsvík, Brúnavík and Borgarfjörður valleys, which are interpreted as raised beach deposits (an example of which is presented in Figure 6.5-d).

Figure 6.5-d: Topographic setting of raised beach at the head of the Víkurá valley

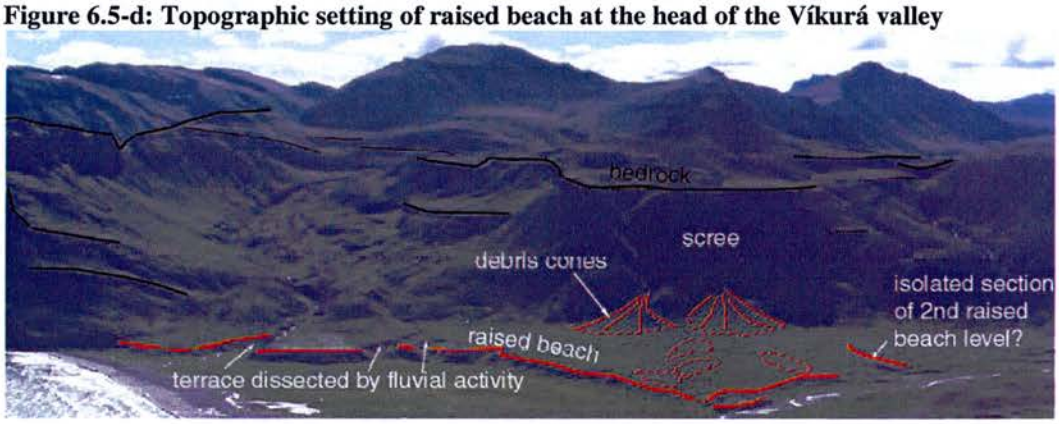

Figure 6.5-e: Sedimentary properties of 'raised beach' at head of Víkurá valley

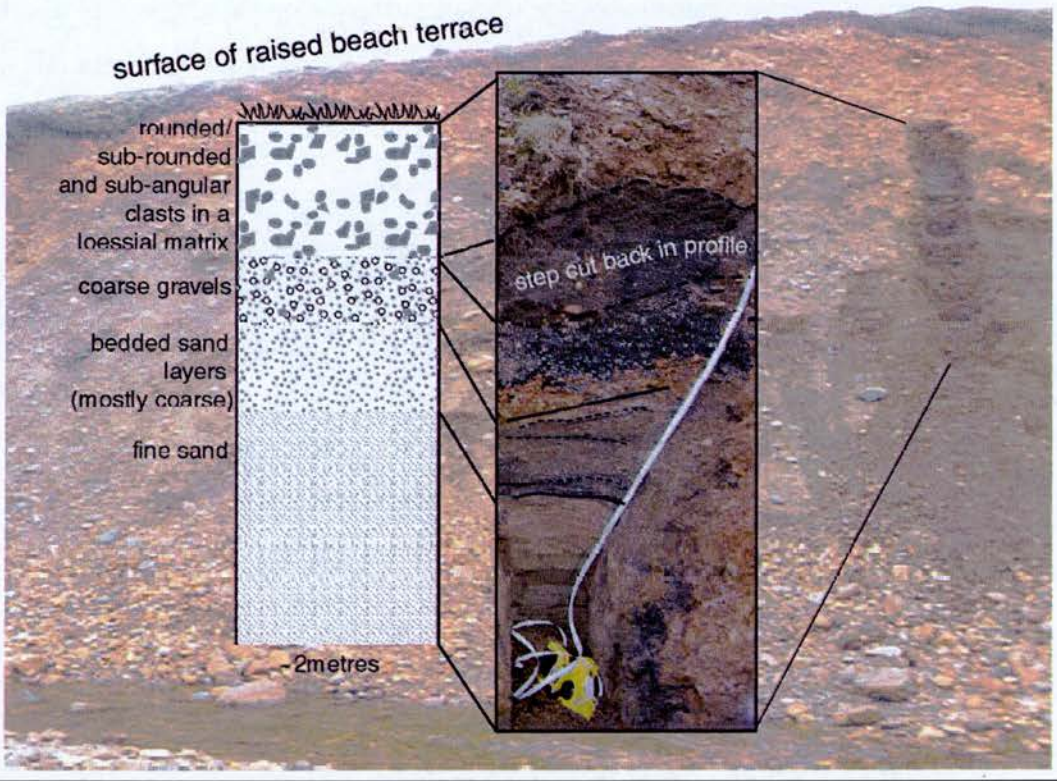

Morphologically, they occur near the coast and have been dissected by fluvial activity, so are often quite fragmented. Unlike the kame terraces, which were found on valley sides with a steadily dipping surface angle, these terraces are features of the valley floor, lying at an altitude of between 40 to 60m, with no particular dip direction. As shown in Figure 6.5-e, much of the Víkurá terrace is composed of sands, typical of beach deposits. A thin layer of rocks and loess are superimposed on the surface of the sandy deposits, which has the characteristics of glacial till. A similar sedimentary pattern of glacial till overlying beach deposits is observed at the head of the Kjólsvík valley. This suggests that at the time when this raised terrace represented the real beach level, valley glaciers reached the sea and deposited morainic material. Elongated hummocks found on the surface of the Víkurá raised beach (pictured in Figure 6.5-d) probably represent moraines deposited by retreating ice. In the Víkurá and Börgarfjorður valleys, a second, more dissected terrace level is found further up-valley, which may represent a second raised beach level from a previous sea level phase.

Chronology of Events

The kame terraces and raised beaches mapped in the Borgarfjörður region (see Figure 6.5-f) are thought to have pre-dated the generation of the observed landform suites. In many locations, (for example in the Brúnavík valley to the north of the Brun-1 Suite, and in the Víkurá valley around the Vik-3 and Vik-4 Suites) the margins of landform suites can be seen to dissect terrace levels, showing that the terraces must have been present before the landform suites. The kame terraces provide evidence of valley glacier surface positions on the hill-slopes, indicating extreme glacial conditions. In addition, outer kame terrace levels mapped at the lateral margins of the Víkurá 5 suite are interpreted as lateral ice limits dating to this pre-landform suite time-period, when valley glaciers reached the sea, and breached the col between the Kjólsvík and Víkurá valleys. The former glacier surface heights are estimated based on the kame terrace locations illustrated in Figure 6.5-f. As there is strong evidence for glaciers in the Víkurá and Brúnavík valleys, there must have also been connected glaciers in other valleys, the evidence for which has been removed by more recent processes. The main Borgarfjörður valley probably contained an ice stream which fed the valley glaciers. It is known, given the stratigraphic relationship between moraine materials and beach deposits, that glaciers reached the sea at the time of the higher relative sea level which created the raised beaches. The kame terraces are thought to represent the surface altitude of the same glaciers (at varying stages of retreat) which deposited the moraine materials near the sea. In the northerly part of the Brúnavík basin, smoothed bedrock hummocks, oriented in the direction of ice-flow, are evident on the valley floor, representing erosion by the over-riding ice.

Figure 6.5-f: Raised Beaches and Kame Terraces representative of former sea level and former ice surfaces in the Borgarfjörður Eystri region

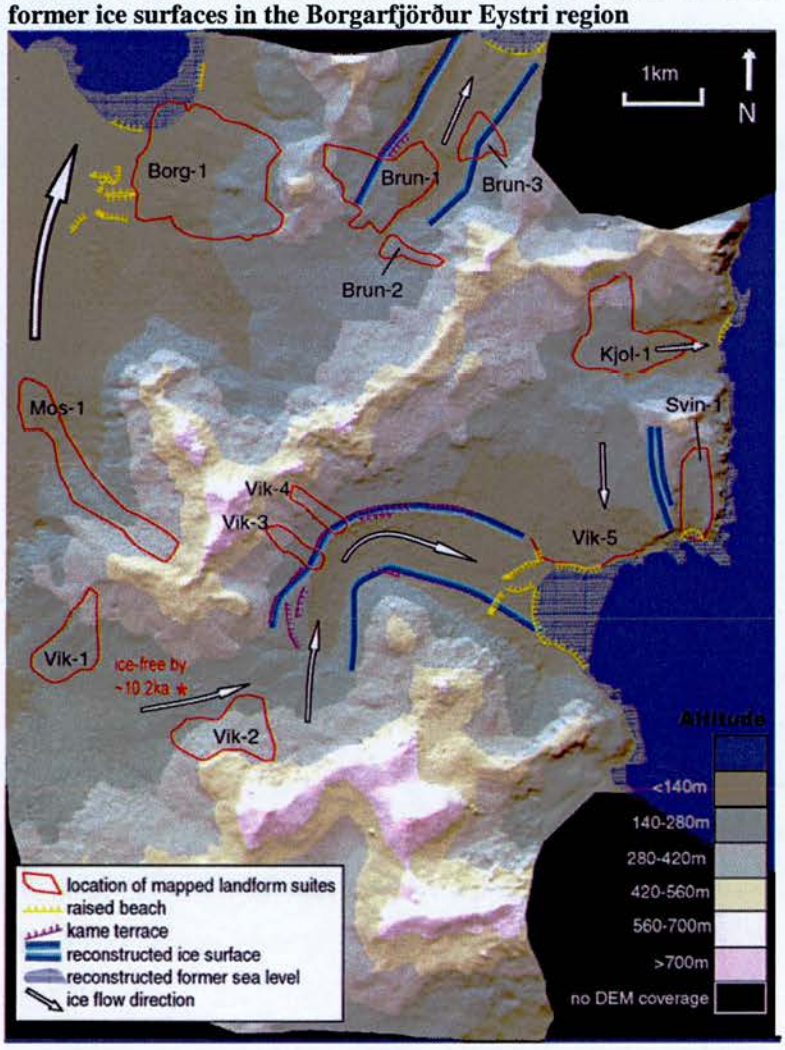

Figure 6.5-f illustrates the mapped kame terraces and raised beaches in the field area, and shows the location of landform suites. Estimated sea levels and ice surface levels derived from the positions of the kame terraces and raised beaches are highlighted. The "*" represents the site at which basal peat was excavated for radiocarbon dating. It is calibrated to 10.22+/-0.06 cal. yrs. BP, showing that this valley was ice free by ~10.2ka, following final deglaciation. As the valley floor from which this basal date was derived is the highest altitude valley floor in the field area, by implication, the remaining valleys in the field area must also have been ice free by this time.

It is unlikely that such extensive glacial activity could have occurred only locally, and it is suggested that such glaciers must have fed off the Flótsdalur ice stream (west of the Dyrfjöll massif), which extended from an Icelandic ice sheet. Therefore, these kame terraces must have existed at a time while there was an Icelandic ice sheet, which provides chronological constraint on the possible ages of the kame terraces and raised beaches. The glacial limits may relate to the Preboreal advance or the Younger Dryas. The locations and relative altitudes of the raised beaches in the Borgarfjörður Eystri region are comparable with those mapped by Norðdahl et al (2001) in the more southerly parts of the eastern fjords. Two levels of raised beach were presented by Norðdahl et al (2001), one relating to the Younger Dryas advance, which terminated at 11,500-11,600 cal. Yrs. BP (Gulliksen et al. 1998), and one

relating to the Preboreal climatic cooling, at 11,300-11,150 cal. Yrs. BP (Björck et al. 1997).

Based on the available geomorphic evidence, it is possible that the lower kame terrace level and associated upper raised beach level could relate to the Preboreal advance, while the upper kame terrace and lower raised beach may relate to the Younger Dryas. However, as postulated in Chapter 1, in the context of other studies of the Preboreal glaciation of eastern Iceland (Norðdahl et al. 2001), this climate oscillation may have had limited effect in the Borgarfjörður Eystri region, due to the region's proximity to the coast, and relatively low altitude. Thus all the terrace levels and raised beaches may still relate to the Younger Dryas.

A radiocarbon-dated basal age derived from a profile in the main Víkurá valley floor (the location of which is shown in Figure 6.5-f), is calibrated to 10.22+/-0.06 cal. Yrs. BP, post-dating both the Preboreal and Younger Dryas periods. This shows that the valley floor beneath the kame terraces has remained ice-free since at least ~10.22ka, around 1000 years after the Preboreal. This does not necessarily confirm the existence of Preboreal valley glaciers, but does confirm that by 8.2ka, there had been no remnants of valley glaciers from Younger Dryas or Preboreal advances for around 2000 years. This means that any ice remaining in the Borgarfjörður region leading up to 8.2ka, was restricted to small-scale corrie glacier activity at the most. In modeling experiments presented in Chapter 7, comparisons can be made between the climatic deterioration required to promote corrie glaciation such as that which generated the glacial moraines at the terminus of many landform suites, and that which could initiate valley-scale glaciation.

6.6. Causal relationships between Glacial Activity, Slope Failure Events and Climate

It has thus-far been shown that the landform suites observed in the field represent a series of temporally separate events involving different types of geomorphic system.

If this evidence is to be compatible with the Key Hypothesis that all landforms represent geomorphic activity in response to the 8.2ka event, then establishing the existence (or non-existence) of causal relationships between the separate geomorphic events, and evaluating their interactions with climate, is crucial. This discussion will develop testable hypotheses with which to investigate glacial response to the "8.2ka event", information which will constrain and inform the ice flow modelling experiments in Chapter 7. Initial conclusions will be drawn with regards to the causal links between events, and the climatic implications of these.

6.6.1. Climatic Implications of glacial activity

In the following section, the aim is to assess the climatic implications of the observed glacial limits. The geomorphic evidence recorded in the field represents a series of early-mid Holocene glaciers, which significantly post-date the Younger Dryas or Preboreal cold periods, while basal ages within the glacial deposits show that the glaciers existed a long time prior to the Little Ice Age (which is often cited as a trigger for glacial advances in Iceland). Climatic conditions are thought to have been comparable to conditions today in the period following the Preboreal, meaning that glacial activity was minimal prior to the initiation of the observed glaciers. As has been discussed, the glacial limits of the Víkurá 2 suite are some of the best-defined and best-dated ice limits in the field area. The lower limits of this glacier dates to ~7500 cal. yrs. BP, based on high value radiocarbon dates combined with tephrochronology. It is unlikely that a glacier advance occurred in this location at this time independently of any glacial activity elsewhere, as if climatic conditions were sufficient to allow ice to accumulate here, it must also have accumulated in other similar locations within the field area. This leads to the putative conclusion that other observed ice margins in the field may have related to the same climatic deterioration.

Figure 6.6-a: Glacial Limits

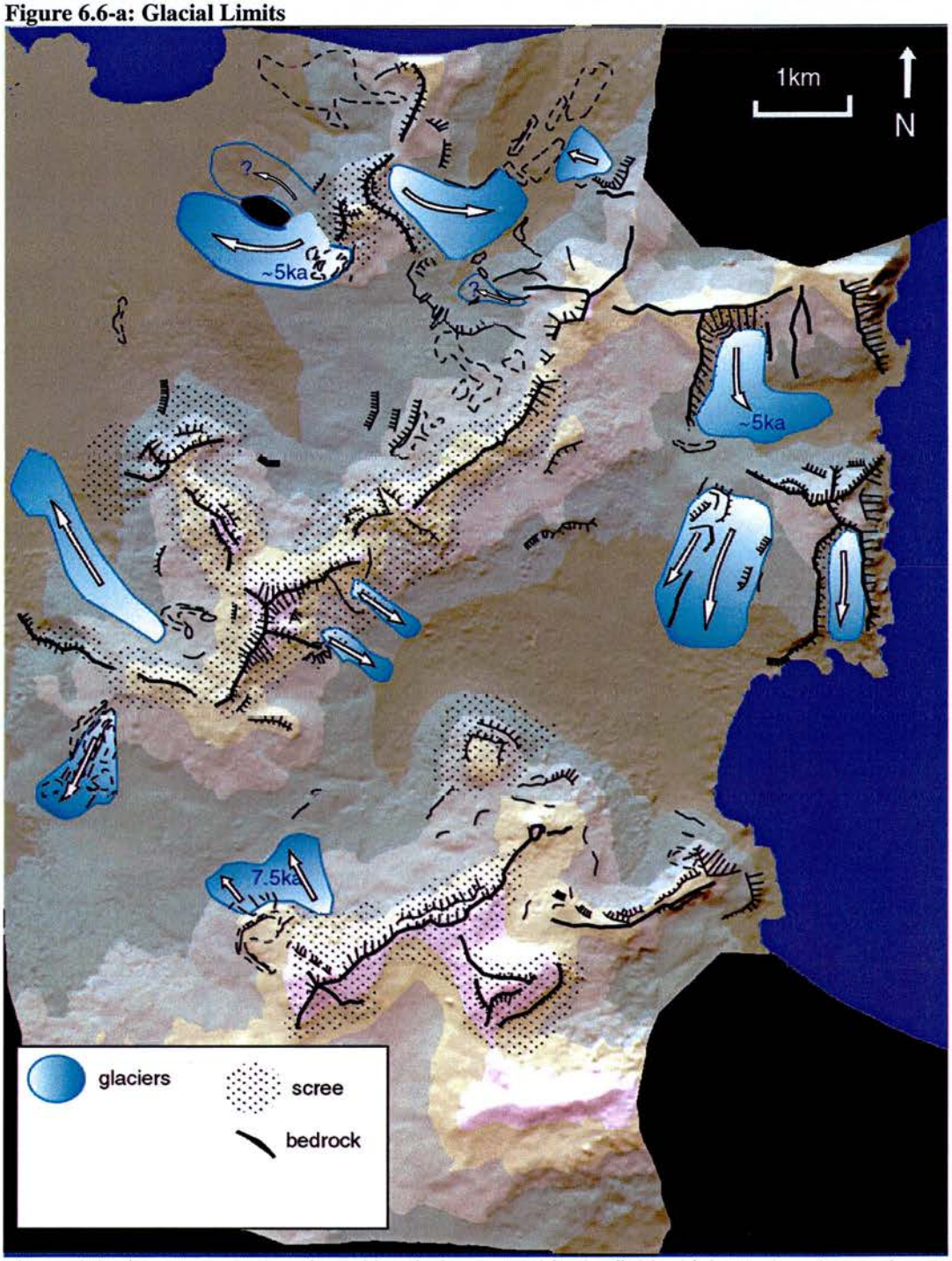

Figure 6.6-a illustrates the location of ice limits mapped in the field which are thought to relate to Holocene glacier advances. The dates included within the limits are in cal. ka. BP, and only the highest value dates are included in the figure. Cliffs, bedrock ridges and current scree deposits are shown, given the apparent importance of debris cover to glacial process in this area.

As seen in Figure 6.6-a, evidence exists for eleven corrie glacier advances occurring in many sub-basins of the field area. Given glacial systems' inherent reliance on ice growth, the glaciers would have required some climatic deterioration to advance,

which lowered the critical altitude above which ice could accumulate (currently this threshold altitude lies just above most of the field area, at ~800m). If the observed series of glacier advances occurred in direct response to a single climate event like the 8.2ka event, then given equal sized accumulation areas within the same altitudinal ranges across the field area, glaciers would be expected to have comparable Equilibrium Line Altitudes (ELAs) and, in an ideal case, have similar lower margin altitudes.

The observed glacial landforms maintain putative accumulation areas at altitudes mostly lying at around ~400m (with variation between 290 and 450m), but lower margin altitudes are much more variable, at between 4m and 250m. Based on the available chronological data, ice limits are dated to between ~7500 and 5000 cal. yrs. BP. Some dates indicate ages of younger than 3000 years, but as discussed in Chapter 5, these younger ages are low value estimates and not considered representative. The disparities in apparent age and lower limit altitude need to be explained if the glacial limits are to be attributed to a single climatic trigger such as the 8.2ka event.

Based on the interpretations presented in this Chapter, the most important factor in influencing glacial process, besides climate, is debris volume, which inevitably served to de-couple the glaciers from climate. This existence of a high level of debris in the glacial systems may explain the differences in margin altitude and age discussed above. The continuum in process identified by Kirkbride (1989), related to the relative ice/snow/debris content of a system, is evident in the range of processes which have occurred in the Borgarfjörður region to produce the observed landform suites. This continuum in process related to relative ice volume, could be seen as a continuum in climatic control, with those systems involving the lowest debris content, being the most climatically significant.

Evidence for ice stagnation under thick debris cover is common in the field area, in the form of chaotic hummocky moraine, and kame and kettle topography, exemplified in the Borgarfjörður suite, the Brúnavík 1 Suite, the Víkurá 1 suite and

the Svínavík suite amongst others. The ice in such cases is likely to have lasted for longer than in the equivalent clean glaciers. This suggests that dates derived for such landforms may be significantly younger than the age of glacier initiation, representing the date at which the landforms became stable and inactive.

The other important implication of high levels of debris cover is that it can promote glacier growth even under climatic conditions which would cause a clean glacier to retreat (Jansson et al. 2002). With a continued high debris input, a glacial system can become a system more defined and controlled by debris availability than by ice growth, through a continuum of processes as discussed by Kirkbride (1989). This results in glacial margins which do not reflect realistic glacier E.L.As, but reflect the controls of topography and debris supply.

Conclusions: The link between climate and glacier initiation

This date of ~7500 cal. yrs. BP may represent the closest available date to the onset of the climate event which induced regional corrie-glacier initiation. The only known climate fluctuation in the early Holocene period is the 8.2ka event, making it a potential triggering mechanism for glacier initiation. The dated glacial advance post-dates the peak of the 8.2ka event (8200 cal. yrs. BP as suggested by Alley et al, 1997) by ~700 years. It is concluded that, in the light of well-dated and strong geomorphic evidence for an ice advance at Víkurá 2, that ice growth was probably initiated in other basins at the same time, resulting in the other observed glacial limits. Given the variable topographic and lithologic conditions in different basins, many other glaciers became de-coupled from climate and remained 'active' for a greater time, controlled by debris content rather than ice growth and climate. Dates suggest that some ice limits (Kjólsvík and Borgarfjörður) date to ~5000 cal. yrs. BP. These ages are thought to be minimum ages, but still suggest that ice may have survived for thousands of years under debris cover. Further good quality basal dates from within the landform suites are necessary to confirm this speculation. It is suggested that glaciers may have also existed in other areas, such as the Leirfjall basin, but poor preservation potential (as discussed in Chapter 4) has resulted in a lack of visible geomorphic evidence.

The results presented in this section, provide input data for ice sheet modelling experiments to be presented in Chapter 7. These experiments are designed to test the amount of climatic cooling required to initiate glaciers in the observed locations. A key conclusion which can be drawn from the detailed geomorphological work is that the nature of ice-growth in the source area is a greater climatic indicator than the position of the lower limits of glaciers. The lower limits often reflect debris cover conditions rather than the position of a glacier in equilibrium with climate. Modelling experiments will therefore enhance this interpretation of glacier/climate interactions which have been derived from this chapter.

6.6.2. Climatic implications of slope failure activity

Besides glacial limits, evidence also exists for landslide and debris flow activity in the field area, the limits of which are shown in Figure 6.6-b. These events cannot be linked to the continuum of process relating to debris/ice volumes, as the processes involved are inherently distinct. While glaciers are fundamentally initiated by ice growth, with an inevitable connection to climate, slope failure events become active as a result of the crossing of a stability threshold in a slope or rock face, and can occur independently of climate. The observed slope failure events have mostly occurred in locations where former glaciers have been reconstructed, post-dating the glacial retreat and overlying glacial landforms (exemplified clearly in the Kjólsvík Suite). Figure 6.6-b shows this relationship clearly. Evidence suggests that a series of major slope failure events post-date glaciers in the region, dating to between ~6000 and ~4200 cal. yrs. BP (again far outwith the dates for the Little Ice Age, which is commonly a trigger of such activity in Iceland). Further low value dates indicate younger ages of 2000-3000 cal. yrs. BP, but as with the glacial margin dates, these are thought to be under-estimates of age. In addition to some major relict debris flows and landslides, the geomorphology shows that smaller-scale slope failure events such as slumping and rock falls have occurred frequently throughout the Holocene, evidence for which often exists in the sedimentary records.

Figure 6.6-b: Mass Movement events post-dating glaciers

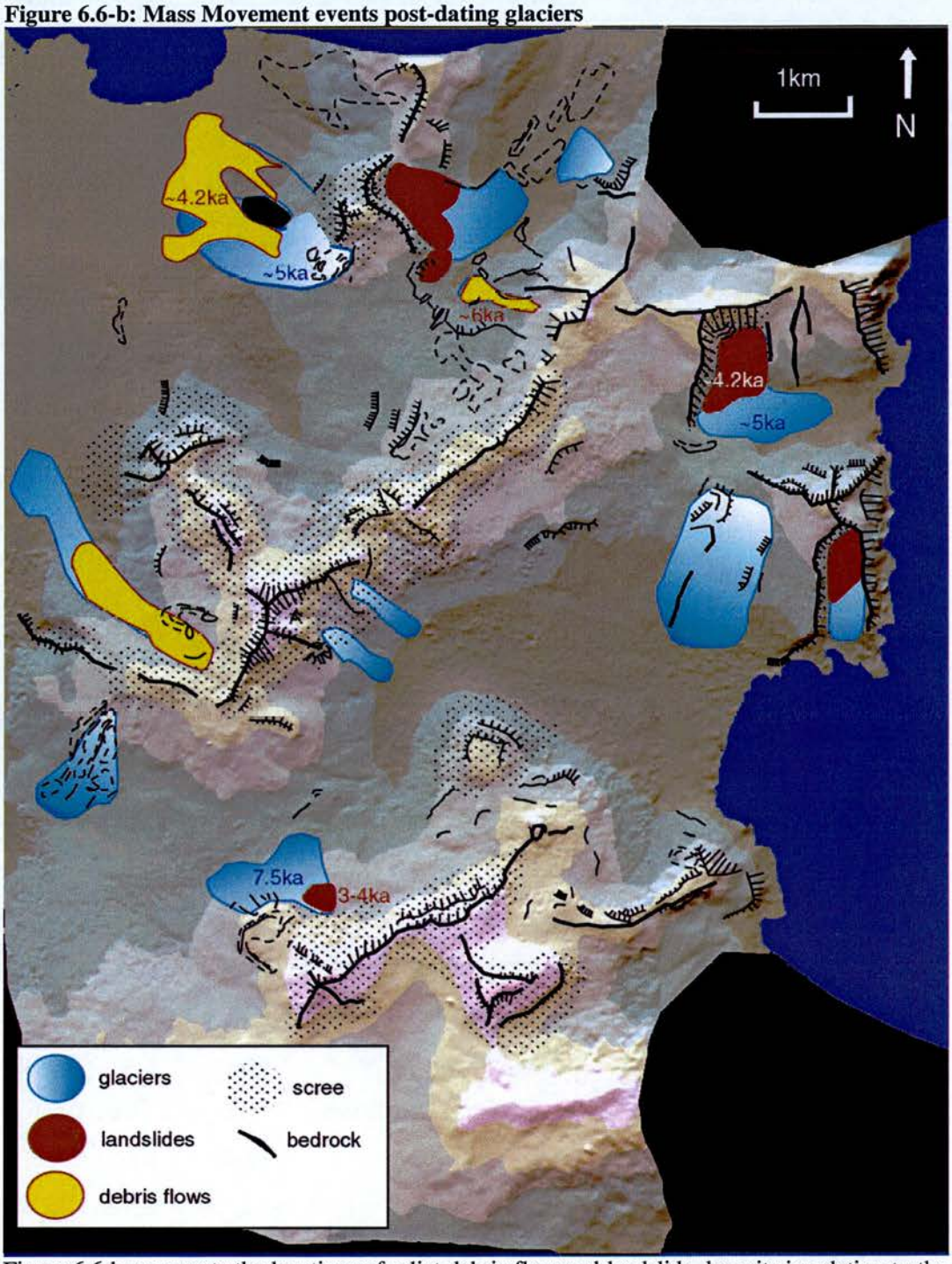

Figure 6.6-b represents the locations of relict debris flow and landslide deposits in relation to the locations of former glaciers. Where dates have been available for these events, they are included in the figure (in cal. ka. BP). This figure only illustrates mass movement events for which there is geomorphological evidence in the form of a landform unit within clear margins. As shown in Chapter 5, sedimentological data reveals that various other debris-transport processes have been active since the glaciers were removed, depositing layers of rocks and gravels on older deposits.

This section investigates the potential causal link between glacial activity and the slope failure events shown in Figure 6.6-b. Triggering mechanisms and influences

on slope failure events are first outlined, including climatic and non-climatic factors. Given the association of landforms indicating slope failure events with some glacial limits, it is conceivable that the slope failures and the glacial activity may be attributable to the same cause. However, from the chronological results, slope failure events always post-date glacial events, where evidence for both in the same basin remains. Evidence for slope failure activity also exists in locations where there is no existing evidence of glacial activity, suggesting it can occur independently. Two hypotheses are developed to explain the observed geomorphological and chronological evidence:

(i) Slope failures events occurred independently of glacial activity, sometimes occurring co-incidentally in the same locations as former glaciers. Events may have been induced by climatic factors, or due to inherent instabilities in the slopes.

(ii) Slope failures are causally related to the glacial activity which pre-dates them, a result of post-glacial/paraglacial slope instabilities. In some locations, the slope failure event removed or overlaid any evidence of former glaciers.

Large-scale past slope failure events are recorded in the landscape record of the Borgarfjörður region as relict landslide and debris flow deposits. It is acknowledged that there are various types and scales of slope failures (Flageollet et al. 1999), and triggering mechanisms and time-scales for all cannot necessarily be comparable. Nevertheless, with an aim to test the above hypotheses, this section discusses the variable influence of inherent slope properties, climate and glacial activity on the propensity for slope failure, factors which are thought to be generic controlling factors which can be applied to varying spatial and temporal scales. In this way the study aims to determine the relationship between the observed glacial limits, the slope failure events, and climate (particularly the 8.2ka event). Differentiation will be made between the two main types of failure for which evidence exists in the field area, debris flow events and rotational landslides/slumping, to determine whether different types of slope failure events respond differently.

The Nature of Slope Stability Thresholds

Slopes exist in quasi-equilibrium states, maintaining a level of stability despite gradual change in exogenic variables. This 'self-organized criticality' means the system can exist 'on the edge of chaos' (Scheidegger 1998), until an inherent threshold is crossed and the system is forced to find a new quasi-equilibrium state. A slope failure event represents the system's search for a new equilibrium state, in response to some internal or external forcing mechanism. Understanding the mechanisms triggering crossing of this threshold is key to determining the specific links between system behaviour and external variables such as climate or glacial activity. Although slope failure can be a catastrophic high magnitude/low-frequency event, the trigger is not necessarily catastrophic, but can be a gradual long-term change, eventually resulting in the crossing of a stability threshold. As a consequence, the catastrophic nature of slope failure event does not necessarily imply an abrupt change in forcing.

The influence of Inherent slope properties on slope failure

The initial condition of the slope before a landslide event is critical in defining the position of the inherent stability threshold, the point beyond which the slope becomes unstable and landsliding occurs. Landslides can occur as bedrock failures or surficial failures (Holm et al. 2004), and the following factors are important in controlling the occurrence of these events.

Slope morphology and angle

Initially the slope angle is most important in defining failure susceptibility. A slope is constantly attempting to reach an equilibrium angle of repose at which it is stable, and processes such as mass-movement which are triggered internally will occur as a mechanism by which the slope can regain its stability. Slopes which are steeper are generally more unstable, but only slopes within a certain steepness bracket will be susceptible to landslides as such. Very steep slopes will reach a stable state as a cliff-face, not prone to landsliding, though prone to rock failure. One unanimous threshold slope angle has not been discovered, but an indication suggests slopes

above 30°, where other conditions are sufficient, are likely to landslide (Holm et al. 2004).

The overall morphology of the slope is also significant. A high level of concavity in a slope (in profile and in planform) may increase the propensity to failure because it will cause groundwater and run-off to converge, increasing porewater pressure (Dai et al. 2003). In addition, the relative 'roughness' and uniformity of the slope is of key importance, as illustrated by Scheideggar (1998), who highlights the divergences in the geomorphic evolution of slopes with slight initial morphological differences, under the same changing climatic conditions. Slight unconformities such as a ditch in a slope can result in positive feedback with increased erosion surrounding the ditch. Gradual over-steepening from erosion at this point on a slope can be sufficient to cause the stability threshold to be reached sooner than it would be in the slope without the ditch.

Geology

The local geology is a key factor in promoting or negating slope instability in terms of its susceptibility to weathering, erosion, frost-shattering, or other mass wasting processes (Rowbotham and Dudycha 1998). More solid rocks are less susceptible to such processes and thus are likely to retain more stable slopes. On the other hand, soft rock such as the largely volcanic material which characterises much of the field area of this study, have a higher propensity to weathering, erosion and frost action, and thus may more easily become unstable and prone to bedrock failure and landsliding. This is illustrated by (Holm et al. 2004) in British Columbia, who find that landslide frequency and magnitude is much higher in the volcanic complex area than in the granite basins.

Rock strengths and jointing patterns influence the way in which a slope fails (Augustinas 1995), and within volcanic areas, this can be variable. As explained in Chapter 1, the Borgarfjörður region is within the eastern Icelandic Tertiary basalt region, highlighted as an area with high debris flow and rock fall hazard levels, attributable to its geology (Saemundsson et al. 2003). Dominated by the rhyolitic old

central volcano domains, the region is characterised by a mixture of basalt and rhyolite, each of which have distinct properties in terms of stability, with associated variable impacts on the type of failures which occur. Basalt is a stronger, less erodable rock than rhyolite, susceptible to deep-seated bedrock landsliding which utilises existing jointing patterns and involves large rock blocks which retain their form. The increased mass-wasting activity on rhyolite lithologies creates more loose and unstable surficial debris on slopes, promoting surficial slope failure involving the transportation of weathered rock fragments.

Differences between rhyolite and basalt are further highlighted by the influence of permeability on slope failure. In rock with significant jointing such as basalt, water is held within the rock joints, promoting weathering and, on freezing, frost-shattering. The porosity of loose slope materials (characterised by the extensive talus slopes in the field area), is highlighted as an important influence on failure rates, as in experiments where the same precipitation input was forced on slopes with differing porosities, failure rates were very different (Iverson et al. 2000). Loose surficial debris which is saturated will 'flow' better than material not retaining water.

Altitude and Aspect

Altitude and aspect affect susceptibility to slope failure because of their effects on microclimate. Higher altitudes and aspects which retain less insolation are at a colder temperature, so will maintain less vegetation, and have increased snow cover and frost action, promoting instability.

Seismic or Volcanic activity

In areas prone to such activity, these high-magnitude events may be a trigger for catastrophic landslides, dramatically altering the stability threshold of a landscape. This type of activity is noted as a potential trigger for debris flow activity in Western Norway, where seismic shaking may have caused a reduction of frictional strength, and 'liquification' of debris (Sletten et al. 2003). Iceland is prone to regular seismic activity due to its location on a plate boundary, and mass movement events have

been linked to such activity in Iceland (Saemundsson et al. 2003). Such a triggering mechanism for mass movement events in the field area cannot be ruled out.

The influence of climate on slope failure

Landslide activity has been used as an indicator of climate change (Bentley et al. 1998; Flageollet et al. 1999; Trauth et al. 2000; Holm et al. 2004; Soldati et al. 2004), where it is suggested that a change in climatic conditions is responsible for pushing a slope beyond its threshold of stability. The 8.2ka event was a short cooling period lasting about two centuries, which may have itself triggered slope failure at the time of the event. However, it is also possible that this cooling served to destabilise slopes through glacial activity and increased frost action, so that failure occurred later, during or following deglaciation, as an indirect effect of climate. Climatic influence on slope failure is manifested through the existence of water, snow and ice on and within slopes and slope materials, and the associated processes which are thus enabled.

Precipitation

Precipitation can be sufficient to push the slope beyond its stability threshold, inducing rapid failure, and the initiation of slope failure activity has been causally linked to periods of intense rainfall in a number of studies (Wieczorek 1996; Ballantyne 1997; Asch et al. 1999; Flageollet et al. 1999; Ocakoglu et al. 2002; Dai et al. 2003; Soldati et al. 2004). The addition of water (direct from rain, or from snow melt) increases porewater pressure, which in turn reduces effective normal stress, and therefore the shear strength of the slope material, increasing the propensity for materials to 'flow' down-slope (Ballantyne et al. 1994; Sletten et al. 2003). The threshold value for triggering of slope failure by precipitation is influenced by a number of factors, namely initial topography, and the type of material making up the slope (Sletten et al. 2003). On steeper slopes or where soils are less able to retain moisture, water from precipitation will act as an erosive agent, removing soil cover and rendering rock debris more unstable as the removal of soil leaves it exposed and unconsolidated. Higher runoff due to increased precipitation results in enhanced erosion and eventual undercutting of slopes, altering cross-profile

slope morphology to make it more susceptible to landsliding (Trauth et al, 2000). The type of material making up the slopes is a strong influence in terms of the porosity of loose slope debris. In experiments where the same precipitation input was forced on slopes with differing porosities, failure rates were very different (Iverson et al. 2000). Loose surficial debris which is saturated will 'flow' better than material not retaining water.

A threshold precipitation level for debris flow initiation was suggested based on based on a study in Seydisfjorður, Eastern Iceland (Saemundsson et al. 2003), immediately south of the Borgarfjörður field area. They suggested that the required precipitation level was to exceed 50mm over 24 hours, and temperature had to exceed 4°C. Precipitation in Iceland has seasonal variations which impacts on the occurrence and timing of slope failure events. Saemundsson et al. (2003) highlights the significance in modern-day Iceland of precipitation as a trigger for debris flows and rock falls during the heavy rains between May and October, with activity peaking in the Autumn.

Heavy snowfall in winter increases snow avalanche occurrence from October to April (Saemundsson et al. 2003), which can be responsible for significant debris transport (Blikra and Nemec 1998). During the spring warming, the increased moisture input from seasonal snow melt has been shown to be an important triggering factor for debris flows, rock falls and avalanches (Saemundsson et al. 2003). It is suggested that snow melt can provide moisture supply for a longer period than rain infiltration (Wieczorek 1996), potentially enabling longer-term or larger-scale slope failure events to occur. The field area may be particularly prone to moisture input from snow melt, given that the topographic characteristics of the Tertiary basalt regions have been found to be favourable to snow accumulation, having the highest level of avalanche occurrence in Iceland (Bjornsson 1980).

The impact of seasonal precipitation variations on slope failure events may be a small-scale indicator of the impact of a climate fluctuation such as the 8.2ka event. During the intense cold period at the peak of the climate oscillation, increased snow

fall, accumulation and ice growth would be expected. Perhaps most significantly, the rapid warming period and associated melt of snow and ice at the end of such a climatic cooling event would provide a large moisture input and could act as a major trigger for slope failure events in the same way as spring-time warming and snow-melt induces small-scale slope failure (mainly debris flow) activity under modern climatic conditions.

Permafrost/Ground Ice/Frost-shattering

Reduction in temperature induces the growth of permafrost or extensive ground ice, which has a considerable effect on the stability of slope materials. Permafrost encourages various periglacial mass-movement processes such as solifluction, which can destabilise and relocate large boulders, while ground ice can up-heave soil and rock fragments, encouraging smaller scale mass-movement. The destabilising effect of ice growth and decay in the ground creates ideal conditions for initiation of slope failure (Matthews and Shakesby 2004). Melting of ground ice and permafrost will influence slope moisture content in a similar way to snow melt, increasing the propensity for failure to occur. As has been seen, the Borgarfjörður region is subject to a high level of periglacial activity under modern conditions, so under slightly colder conditions there may be significant activity related to growth and decay of permafrost and ground-ice.

Colder temperatures also result in increased frost action on bedrock and exposed boulders, which is observable today. Freeze-thaw action acts on rock weaknesses and joints, breaking it apart, which in turn weakens the bedrock promoting bedrock failure. It also produces high levels of loose slope debris, which characterises the field area in modern times, and is highly susceptible to failure.

Glacier activity

Slope failure processes conditioned or intensified by glacial activity are collectively termed as "paraglacial" (Ballantyne et al. 1994; Ballantyne, C.K. 2002; Ballantyne, C. K. 2002; Matthews et al. 2004). Landscapes tend towards equilibrium states, and when a glacier is present in a corrie or valley, the slopes around it will tend towards a

stable angle in response to the glacial processes of erosion and deposition. Fast retreat of ice can leave slopes very unstable while they try to reach a new equilibrium. This instability may arise from over-steepening and debutressing of slopes by ice, and the development of pressure-release jointing when ice is removed, resulting in a weakening of the bedrock and a higher susceptibility to failure (Augustinas 1995; Matthews et al. 2004). Higher instances of landsliding are common in areas where ice has recently retreated leaving unstable valley walls. Increased instances of landslide activity were recorded by Soldati et al (2003) in the Italian Dolomites following Late Glacial ice retreat at the beginning of the Holocene. Holm et al. (2004) found a high incidence of catastrophic rock slope failure in areas just above Little Ice Age glacial trim lines. Further, glaciers tend to leave a covering of loose morainic material and/or a debris mantle which is highly susceptible to mass-movement (Holm et al. 2004).

Slope failure may occur immediately after the ice has gone, but it is more likely that there is a time-lag. Initial weakening of the bedrock and surface materials may gradually increase until an inherent slope stability threshold is crossed, resulting in sudden failure. Alternatively, paraglacial instabilities may be accentuated by a sudden climatic or seismic event which finally triggers failure. It has been suggested that much of the relict rock fall and debris flow deposits that characterise the landscape of the eastern Icelandic fjords area (including the field area) occurred soon after deglaciation (Saemundsson et al. 2003), indicating a causal link between mass movement activity and deglaciation.

Specific triggers for the mapped debris flows and landslides in Borgarfjörður Eystri

In the light of the discussion regarding triggering factors for slope failure, it is postulated that the series of large-scale relict debris flow and landslide events observed in the field area are indicative of a time-transgressive response to the early-mid Holocene retreat of corrie glaciers and melting of snow and ice in the Borgarfjörður Eystri region.

Deep-seated rotational bedrock landslides are evident at the Kjólsvík suite, the Svínavík suite and the Borgarfjörður suite, the suites which were backed by extensive basalt cliffs. They exploited weaknesses in the bedrock following glacial retreat, and were promoted by the accentuation of bedrock jointing by frost-action under the colder glacial climate. In this way landsliding can be seen as an indirect response to climate and the existence of glaciers.

Relict debris flows were observed at the Brúnavík 2 suite and the Borgarfjörður suite, in locations with high availability of rhyolite bedrock, associated with extensive talus deposits. These debris flows are thought to represent collapse of significant amounts of loose rock debris activated by moisture input. As has been seen, moisture input is known to be a key trigger for debris flow activity, and in the case of the landform suites, this is most likely to have been from melting snow and ice during the glacial retreat phase. In the case of the Borgarfjörður Suite, evidence exists for the existence of a debris-covered glacier underlying the debris flow deposit. It is suggested that the debris flow occurring here exploited the extensive loose debris associated with the glacier, reworking materials which were de-stabilised and "liquefied" by the melting ice. In the case of Brunavik 2, the existence of a glacier is not clear. However, as discussed, there is likely to have been at least significant snow accumulation in this area at a time when glaciers were being initiated nearby. Therefore snow melt is a likely source of moisture which enabled the flow events to occur.

Selective preservation of evidence for slope failure events

A phase of major slope failure events occurred in time-transgressive response to glacial retreat and paraglacial instabilities. During this mid-Holocene phase discussed above, smaller-scale failure events are also likely to have occurred, such as rock falls, small-scale debris flows and small slumps. The geomorphic record of past slope failures is biased towards the largest events, as these are more likely to preserve landforms to the present day. As has been seen, under modern climate, a great deal of small-scale slope failure activity occurs on a regular basis, so the implication is that this small-scale activity also occurred in the past, especially in the

mid-Holocene period of apparently enhanced geomorphic activity. These events would not have been significant enough to remove glacial landforms all together, or to leave remaining morphological evidence. However, evidence exists for this smaller-scale activity, as shown in the stratigraphic records presented in Chapter 5 (see Figure 5.5-b), showing significant debris transport activity during the mid-Holocene across the field area. Stratigraphic sections show evidence of erosive and depositional activity at this time, through the existence of distinct rock and gravel layers in the lower and middle sections. Such activity may have removed lower units of stratigraphic profiles, resulting in unrealistically young basal ages. This may further help to explain the disparities in age derived for glacial limits (between 7500 and 5000 cal. yrs BP for the highest value dates) which, it is suggested, are related to the same climatic fluctuation.

6.6.3. Conclusions: Slope Failure events, Climate and Glaciers

The 8.2ka cold event is cited as the most likely trigger for initiation of a series of corrie glacier advances in the Borgarfjörður Eystri region, given the known age of some key moraine limits at ~7.5ka. Advances dated to ~5ka may have been related to a further advance, but may simply reflect long-term stagnation of insulated ice. The Little Ice Age has been seen to have had limited impact in the Borgarfjörður region, with potential implications for other interpretations of LIA activity in comparable regions of Iceland. The early-mid Holocene glaciers were debris-covered in most cases, enabling ice to survive for a long period of time after glacier initiation, effectively becoming de-coupled with climate. The melting of snow and ice and weakening of bedrock which triggered slope failure may have been associated with the warming leg of the climatic reversal, possibly the 8.2ka event. However, it is evident that the type, timing and extent of slope failure is also conditioned by and controlled by inherent slope properties, defined by the specific topography and lithology. Basalt catchments have been seen to be prone to landsliding, while rhyolite enables surficial debris flows. The run-out extent of these failure events is also conditioned mainly by debris volumes and local topography. Spatially variable local conditions influence the timing of these events, which has

been seen not to be regionally synchronous. This temporal variation is due to the fact that the triggering of slope failure events relies on the positions of locally specific (and highly variable) stability thresholds. Consequently, the slope failure events discussed in this section can be seen as secondary effects of a climatic fluctuation and associated enhanced glacial activity, whilst the specific timing, nature and extent of these events is conditioned by local topography and lithology.

7 Ice Sheet Modelling

7.1. Introduction

The geomorphological and chronological evidence outlined in previous chapters has established the existence of a geomorphic, and specifically glacial, response in the Borgarfjorður region to some early Holocene climatic forcing, possibly the 8.2ka event. Ice sheet and climate modelling experiments carried out in this chapter aim to extend the value of this empirical evidence by investigating the climatic conditions necessary to produce such glacial limits. Through combining high resolution empirical field data defining the locations and ages of ice limits, with data from controlled ice sheet modelling experiments, a better understanding will be gained of the nature of interactions between climate and ice growth, in the context of the specific field area. Specifically, the ice sheet model GLIMMER is used in combination with a climate model (Casely 2006) to assess the spatial patterns of snow accumulation and ice growth in the Borgarfjörður Eystri region which emerge in response to modelled climate fluctuations of varying magnitude and duration.

Aims and Approach

Figure 7.1-a: Input data for modelling experiments and generation of testable hypotheses

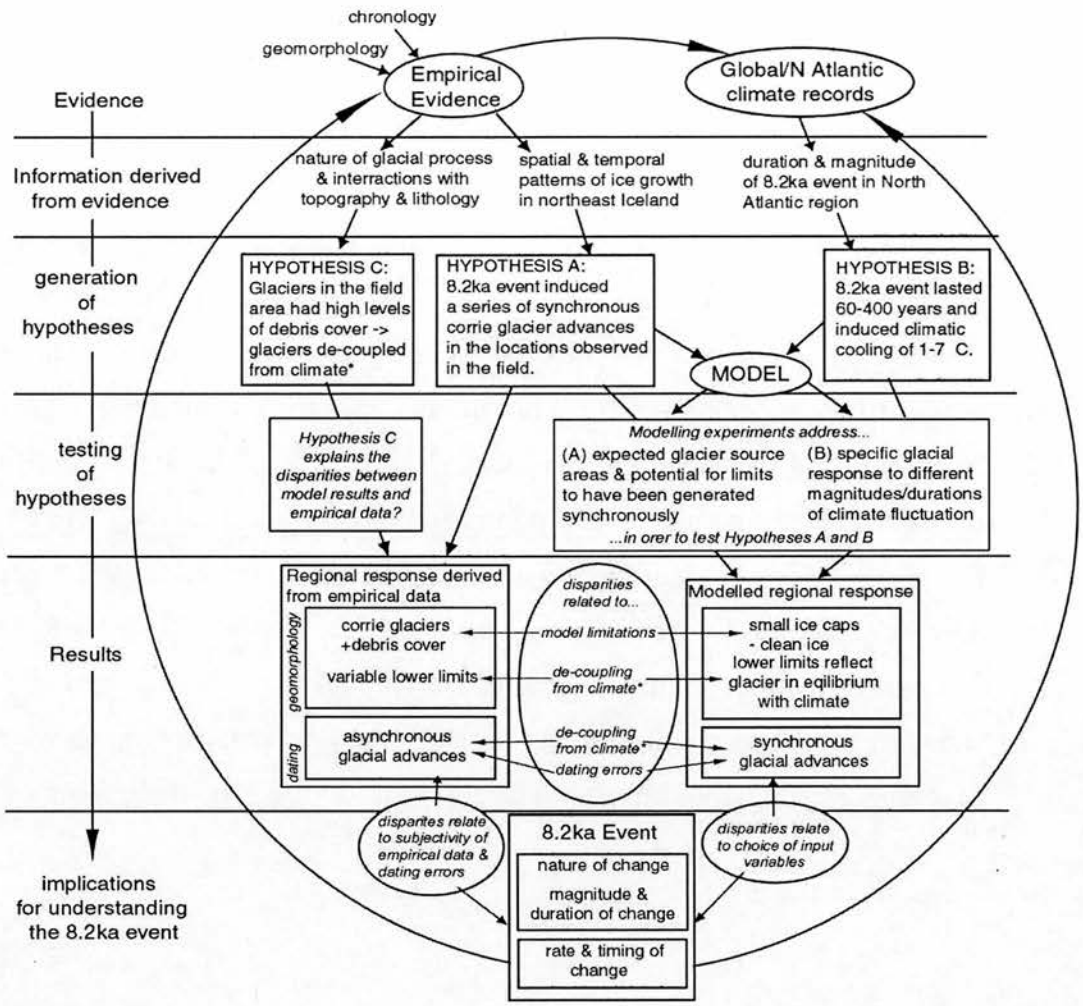

Figure 7.1-a illustrates the connections between the different strands of evidence (from empirical data and other environmental records) which, combined, enable generation of testable hypotheses regarding the characteristics of the 8.2ka event, which motivate modelling experiments. The evidence displayed in the upper part of the figure informs the generation of 3 hypotheses, A-C. Hypothesis A is derived from the geomorphic record, and B is developed through assessment of other environmental records, and both can be tested specifically with controlled modelling experiments. Hypothesis C, based on the geomorphic evidence, suggests that the observed glacial limits represent glaciers which were, to a variable extent, de-coupled from climate, which may ultimately explain some of the disparities between the empirical and modelling results. The results section indicates some of these differences between empirical and modelling data, and highlights reasons for such differences (a topic which shall be discussed in more detail in following sections). It further highlights that there likely are disparities between the modelled and empirically derived glacial response to the 8.2ka event, and the actual response to the event, which can only be known through subjective interpretation.

Modelling experiments are carried out with the aim of testing hypotheses regarding the magnitude and duration of the 8.2ka climatic cooling event in Iceland, and the

nature of Icelandic glacial response to it. Figure 7.1-a illustrates how chronological and geomorphological data derived from the empirical evidence (described and explained in Chapters 3 to 6) combines with other data regarding the global expression of the 8.2ka event (described in Chapter 1) to generate hypotheses to be tested in the modelling experiments.

Key research aims to be achieved in this chapter stem from each of the hypotheses described in Figure 7.1-a. These are to:

- Assess the nature of Icelandic glacial response to the 8.2ka event (Hypothesis A).
- Determine the climatic parameters necessary to produce the observed ice limits (Hypothesis B).
- Improve understanding of glacial process and the factors which influence it (Hypothesis C).

In the following sections, I outline key information derived from the two main strands of evidence which constrain the model input data (highlighted in Figure 7.1-a), empirical evidence and climate data. The relative value of each data type as model input data for achieving the research aims described above is assessed. This part of the study involves association of discrete units of high resolution empirical data with climate records from distant locations, to produce lower resolution but spatially continuous modelling data which, it is anticipated, will improves understanding of the nature of glacial response in Iceland to the 8.2ka event, or indeed any short-lived climate fluctuation.

7.2. Empirical Evidence as a model constraint

Empirical evidence provides detailed data on the timing, duration and nature of glacial and geomorphic response mechanisms to climate change. This landform record (discussed in Chapters 3 to 6) provides constraint on the numerical modelling by presenting the spatial and temporal patterns of geomorphic activity derived from

the geomorphological and chronological data. In the following section, the value of this data is as model input is assessed, in terms of the extent to which it can aid extraction of a climatic signal. We address the methodological issues related to the association of high resolution empirical data with lower resolution model data, and climate records from disparate regions.

7.2.1. Extracting an initial climate signal from the empirical evidence

In Chapter 6, initial causal links were forged between climate and glacial activity observed in the field. A geomorphic signal with climatic indications was retrievable from two empirical sources:

1. The geomorphic record: The positive identification of glacial margins (Chapter 6), provides a real-world 'control' for the spatial patterns of modelled ice growth and snow accumulation
2. The chronostratigraphic record: Good dating control on some ice limits (Chapter 5), indicates temporal patterns of ice growth and decay, and enables linkages to be drawn with specific climate events.

The putative geomorphic "response" to climate change (specifically the 8.2ka event) derived from these sources revealed phases of activity relating to glaciers, landslides and debris flows. These occurred between ~7.5 cal. ka BP and at least ~4 cal. ka BP, and the initial (glacial) phase has been tentatively associated with the 8.2ka event. Figure 7.2-a illustrates the steps made between the collection of this empirical data, and the interpretation of an initial climatic signal. The climate signal from this study can be compared with other climate proxies characterising the 8.2ka event, informing interpretation of the global expression of the event. The potential errors associated with making each step from present day empirical data to process (essentially characterising the environment at 8.2ka), and from process to climate are discussed here, testing the climatic significance of the field evidence. Modelling experiments will further test these associations between landforms, process and climate.

Figure 7.2-a: Use of empirical data to reconstruct glacial limits and climatic conditions

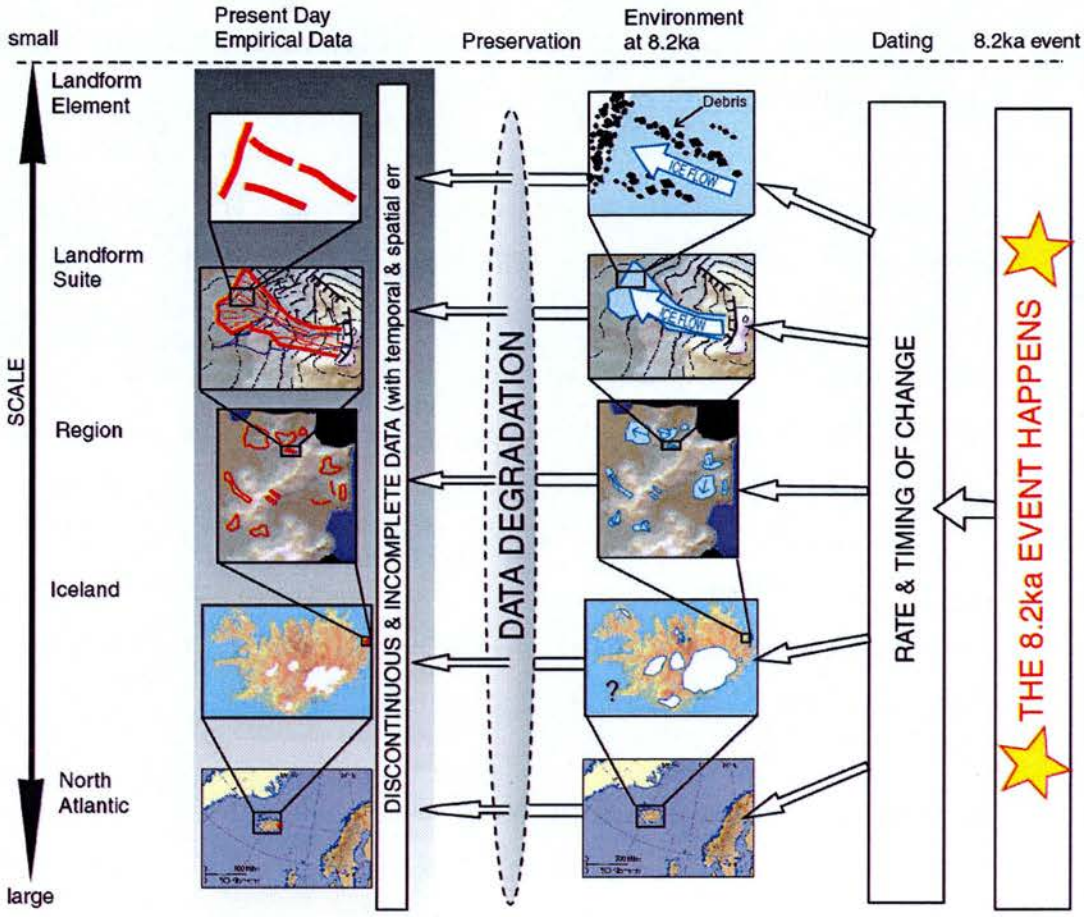

Figure 7.2-a represents the theoretical causal connections between the nature of the putative forcing mechanism ("8.2ka event"), the environmental response to it ("environment at 8.2ka"), and the preserved evidence of this response ("present day empirical data"). The study aims to use the present day empirical data (the final step) to retrieve information on the nature of the causal trigger (the 8.2ka event – the initial step). The connections between present day field evidence and the climate trigger are evident across a spectrum of scales, from landform elements and landform suites, which can reveal information on specific geomorphic processes, through regional- and Icelandic-scale data, to the wider North Atlantic region for which climate records on the nature of the 8.2ka event are available for comparison.

Inferring the 'environment at 8.2ka' from present day empirical evidence

Using present day empirical evidence to infer the processes of landform genesis (and thus the nature of the environment at the time) has limitations relating to variable preservation potential of landforms and sediments. As illustrated in Figure 7.2-a (and discussed in Chapter 4), geomorphic evidence regarding past process is

degraded through time as a result of poor preservation, resulting in present day spatial distribution of landforms which are only a partial representation of the true extent of past activity. The conceptual modelling of preservation potential and topographic control in Chapter 4 allowed the location of well-defined limits to inform estimations of the likely extent of glacial activity across the whole field area, including basins which no longer maintain evidence. The results of this study are considered when comparing mapped ice limits with modelled ice limits.

In terms of chronological constraint, which enables association of the inferred geomorphic activity with a specific time period, there are errors associated with the restricted dating potential on many landform suites, and the error margins associated with the retrieved dates (Chapter 5). These influence the derived chronological signal, giving a potentially erroneous view of the temporal distribution of activity. As a means of minimising these potential errors, Chapter 5 assessed and determined the relative values of derived ages for landform suites.

Following consideration of such potential errors, a summary of the temporal and spatial distribution of glaciers can be presented based on the highest value evidence. Eleven landform suites were identified which contained clear glacial limits (see Figure 6.6-a), one of which (Víkurá 2) was well-dated to 7.52+/-0.05 ka, and tentatively connected to the '8.2ka event'. It is suggested in Chapter 6, that climatic conditions sufficient to cause a glacier advance at ~7.5ka, must have also initiated glacial activity in other parts of the field area at the same time. Dating evidence suggests that other ice limits date to at least 5ka, but that glacier initiation probably occurred significantly earlier than this.

Inferring the nature of the 8.2ka event from the interpreted 'environment at 8.2ka'.

The key aim of the modelling is to aid development of the link between the 'environment at 8.2ka' and the climatic conditions at the time, with implications for interpretation of the nature of the 8.2ka event. To make the step from the interpreted spatiotemporal patterns of geomorphic activity, to specific climatic conditions and climatic triggers, and so that meaningful comparisons can be made with empirically-

derived and modelled ice limits, the extent to which the inferred activity was controlled by climate must be determined.

As discussed in Chapter 6, the association of high levels of debris cover with glacial activity to generate many suites may have resulted in young ages and lower limits which do not reflect glaciers in equilibrium with climate (Hypothesis C in 7.1 above). The value of each landform suite as a modelling constraint which represents climatically induced ice limits can be assessed because the high resolution empirical data provides information on process. The "value" of the landform suite for this purpose is defined as the inherent degree of climatic sensitivity of the former glacier, depending on extent of debris cover. While some suites contain clear glacial limits which are thought to provide a good indication of climatic conditions, as discussed in Chapter 6, most show evidence of extensive debris cover and long-term stagnation, with ice having lasted as long as several thousand years independent of climate, and well beyond the time of glacier initiation.

Despite these limitations on use of empirical data as climatic parameters, it is still possible to derive climatic information from the available evidence. There is inherent reliance on climate to *initiate* ice growth, even if it becomes de-coupled with climate through time. It is anticipated, therefore, that although glacier lower limits may not be indicative of climatic conditions, ice sheet modelling experiments carried out on a digital elevation model of the field area will promote greater understanding of spatial and temporal patterns of ice growth and glacier initiation in response to specific climate scenarios. Through modelling experiments, the likelihood of ice accumulating in all of the observed locations synchronously can be assessed. If this is possible, there is more evidence to suggest that glaciers were de-coupled from climate to varying extents, resulting in apparently asynchronous dates. In this way, modelling experiments, will help improve understanding of the connections between the empirically-derived 'response' to a climate forcing (the reconstructed "environment at 8.2ka" in Figure 7.2-a), and the specific climate parameters associated with the climate forcing.

7.2.2. Value of modelling data as an interpretive tool

As discussed, modelling experiments aim to enhance the interpretation of a climate signal derived from the empirical record. The value of numerical modelling as an interpretive tool in the context of a regional empirical study is discussed here. Firstly, specific attention is paid to the variable scales at which modelling data and climate data can be combined with empirical data (illustrated in Figure 7.2-b). This section goes on to discuss the discrepancies between glacial processes interpreted from empirical data, and the types of glacial processes which can be modelled using GLIMMER.

Applicable scale of different data sources

There are methodological issues to be considered when interpreting and comparing model data with the field data, related to the inherently different achievable resolutions of the data sources, and the associated discrepancies between the modelled topography and the true topography. As a result, the different scales at which model data and empirical data can be viewed must be considered.

At the smallest scale (landform elements and landform suites), the empirical evidence contains a series of discrete areas of very high resolution data, a manifestation of the field collection method. These highly detailed case-studies of glacial processes and small-scale interactions with topography, lithology and climate have enabled the development of hypotheses to describe the relationship between glacier extent and climate, and to explain the spatial distribution and extent of glacial activity (Hypotheses A and C in Figure 7.1-a).

Figure 7.2-b: Modelling as a tool in relating empirical evidence to climatic conditions

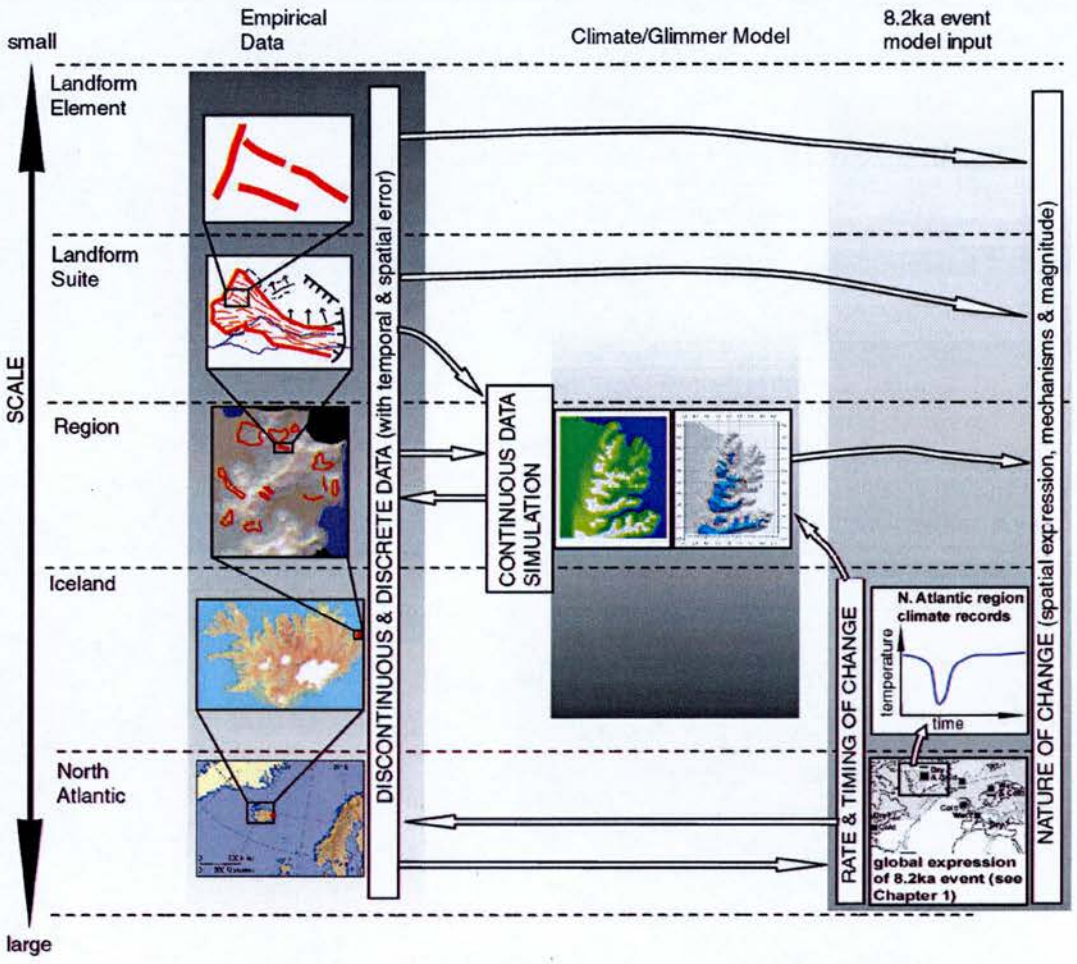

Figure 7.2-b shows the connections between empirical data, model data and the 8.2ka forcing. Empirical data provides information on glacial process at the scale of landform elements and landform suites, which aids interpretation of the nature of the climate forcing (information is seen to feed back to the "8.2ka model input". As can be seen, model data from both GLIMMER and the climate model are linkable with the empirical data only at a regional scale, because of their reliance on 250x250m resolution DEMs. At this scale, empirical data provides real-world constraints on modelled ice limits. Experiments to model snow and ice patterns under different climatic conditions further provide information on the nature of the forcing mechanism. Climate data for the 8.2ka event, which should provide real world constraints on the nature of the forcing mechanism, are only available for disparate North Atlantic regions, so their application to one part of Iceland is undertaken with caution, and only in the context of the wider region. The specific magnitude and duration of change can be used as input climate model constraints, but cannot be assumed to represent climatic conditions at the scale of landform elements and landform suites.

When viewed on a larger scale, the landform suites are of increased climatic significance, representing a regional response mechanism to climate forcing. At this regional scale, the application of the empirical results can be further enhanced with the use of numerical modelling, which is run using a Digital Elevation Model (DEM)

of the Borgarfjörður Eystri region at a maximum resolution of 250mx250m. Because of the relatively low achievable resolution for modelling data, model results are not directly comparable with empirical evidence at the scale of individual landform suites and landform elements. It has been seen that many reconstructed glaciers extend from minimal accumulation basins, which are often less than 250m^2 in area. The accumulation basins visible in the field may be smoothed over by the low resolution DEM representation, as shown in Figure 7.2-c, so that modelled ice cannot accumulate in that area.

Figure 7.2-c: Discrepancies between modelled topography (i) and topography derived from field work (ii)

(i) 250mx250m DEM- ice sheet & climate modelling (ii) 7mx7m DEM – conceptual modelling

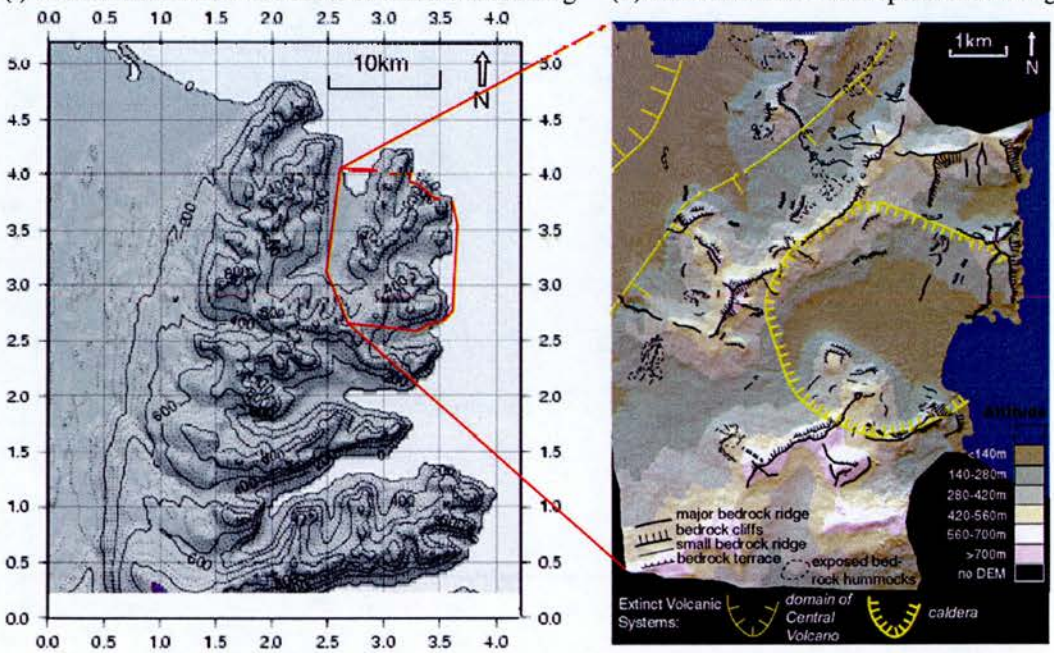

Figure 7.2-c (i) shows the DEM representation of the Borgarfjörður Eystri region which is used as the base topography fro ice sheet and climate modelling. Figure 7.2-c (ii) illustrates the high resolution DEM generated by the author from air photo analysis and field collection of GPS data, which is used as a base topography for analysis of geomorphic data (see Chapter 4). The value of this high resolution DEM is further extended by the addition of data on geological characteristics, which are important controls on accumulation areas and glacial flow direction. It can be seen that the model DEM smooths the topography substantially. It has thus-far been shown that the distribution of bedrock and cliffs is of key importance in defining areas of ice growth. The absence of this information in the model DEM causes further discrepancies between modelled ice accumulation zones and those mapped from the empirical evidence.

Despite these limitations, modelling is still a useful tool for interpretation, as it can be used to test the hypotheses developed from the high resolution empirical evidence, at the larger scale of a continuous modelled data simulation. As will be seen in the results section, although modelled ice may not be able to accumulate in

all areas indicated by the empirical evidence (as a result of the low resolution topography), the major source areas at which ice is most likely to accumulate, and the relative timing of ice initiation in different parts of the field area can be examined.

Other scale-related problems associated with direct comparison between model data and field data relate to the type of glacial process which can be modelled using Glimmer and the climate model. Glimmer is designed to model large ice sheets, and its application to a small region showing evidence of corrie glaciation is experimental. Ice accumulates in response to altitudinal temperature variations, allowing ice to initiate only on the tops of mountains, rather than in sheltered basins. In terms of compatibility with empirical evidence, this type of accumulation pattern is not representative of the former glacial activity observed in the field, which has not involved glaciers extending from ice caps and ice sheets, but a series of distinct corrie glaciers. Use of the climate model to investigate snow accumulation patterns is useful in combination with the Glimmer ice sheet model, because snow can be forced to accumulate in basins and on slopes rather than only on the peaks of mountains.

7.2.3. Climate Data as a model input

As has been discussed, evidence suggests that climatic conditions prior to the 8.2ka event were comparable to modern day conditions, so the modern climate may provide a good representation of conditions immediately prior to the onset of cooling which initiated or grew the mapped glaciers. The climate oscillation used to force the model will thus be represented as a relative variation from 'modern' conditions. Climate input to the models therefore relies on the value of parameters which define these 'modern' climatic conditions, and on the magnitude and duration of the modelled climate forcing associated with initiation or growth of snow and ice.

Defining 'modern' climatic conditions in Borgarfjörður Eystri

Modern climate is derived from weather station data provided by the Icelandic Meteorological Office (REF). Various weather stations exist around the field area but not all of them record all the necessary data for a long enough time period to derive meaningful values. Data is compared from the three weather stations which do provide detailed data, and are in close proximity to the field area. The locations of these stations, Seyðisfjörður, Dalatangi and Egilsstaðir, are shown in Figure 7.2-d, and the weather data from which average values are determined is illustrated in Figure 7.2-e.

Figure 7.2-d: Location of weather stations near the field area

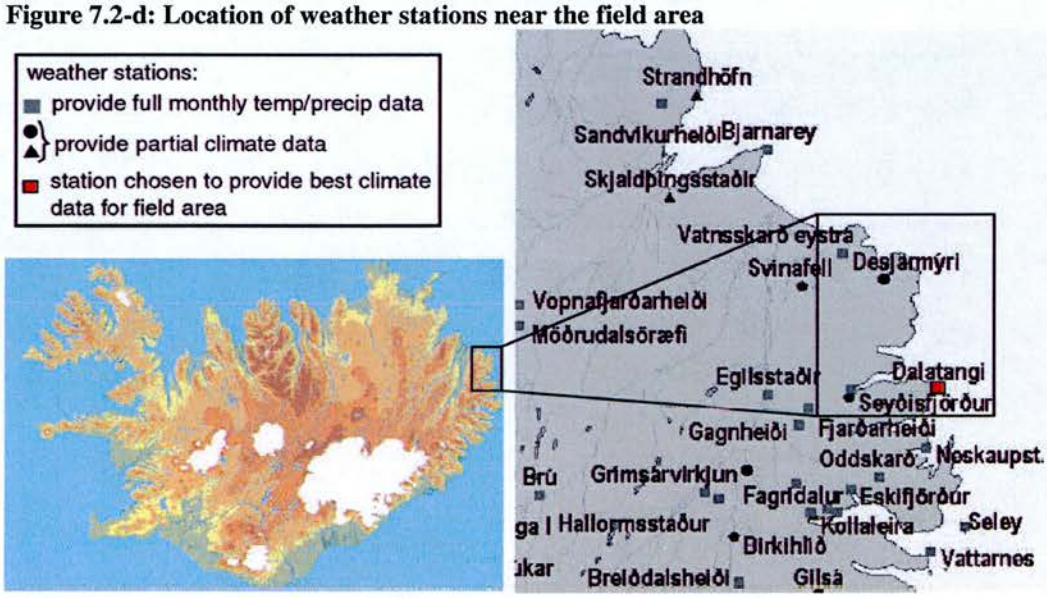

Figure 7.2-d shows the location of the weather stations nearest the field area, as adapted from The Icelandic Meteorological Office (www.vedur.is). The stations near the field area which provide full climate data are Seyðisfjörður, Dalatangi and Egilsstaðir, the precipitation and temperature data for which is illustrated in Figure 7.2-e.

Figure 7.2-e: Range of data considered during derivation of 'modern' climate conditions
(i) 1961-2003 Temperature data 1961-2003

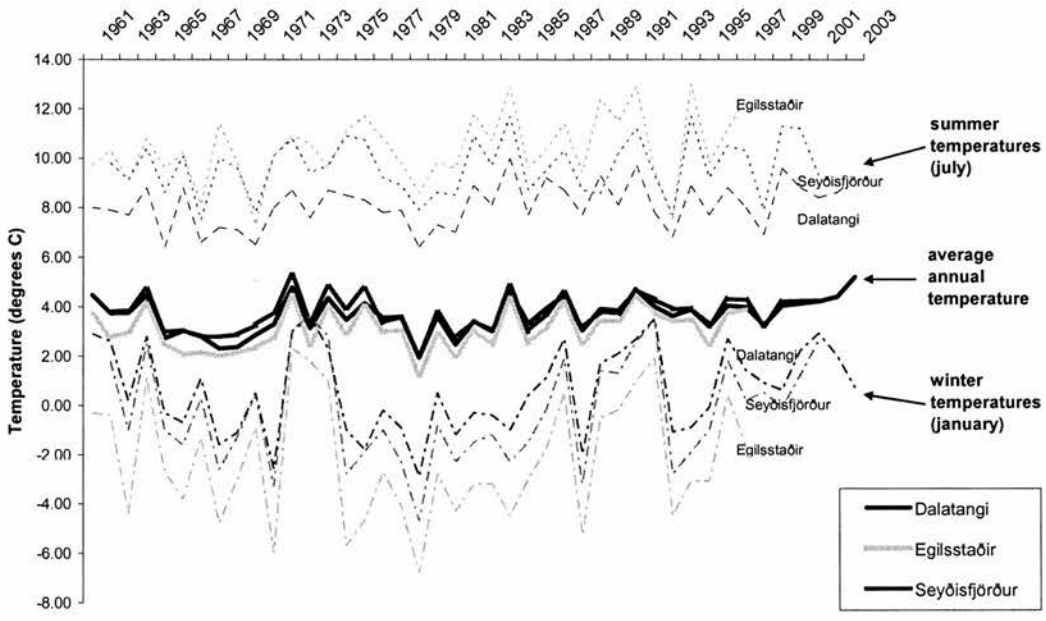

(ii) Precipitation data 1961-1963

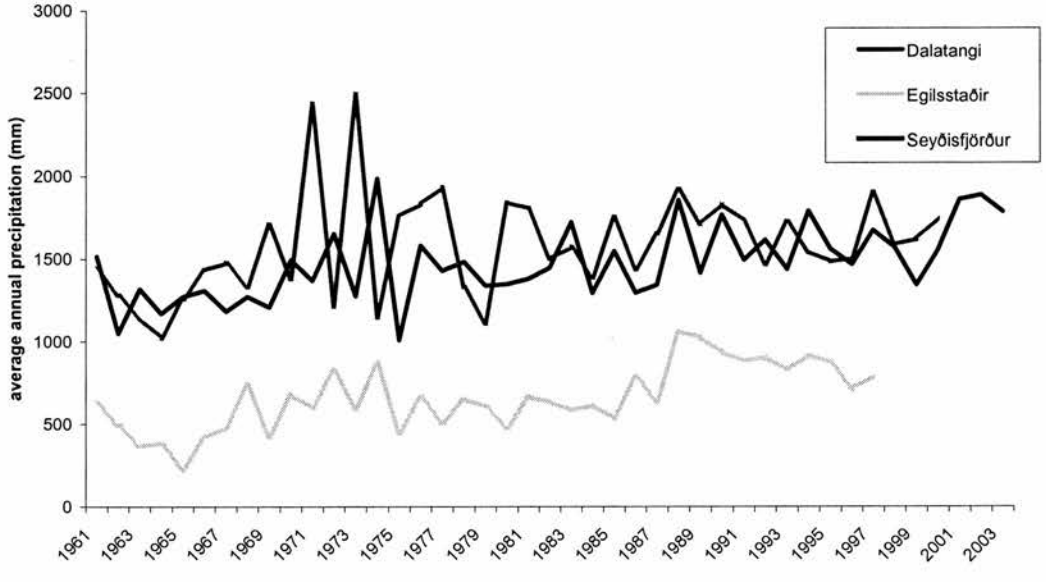

As can be seen from Figure 7.2-d, the three stations for which data is derived are located progressively further inland, and a clear associated climate gradient is visible on assessment of Figure 7.2-e. A temperature gradient is most evident in the temperature range data, presented in Figure 7.2-e (i), with Egilsstaðir, the furthest inland station, having the largest variation between summer and winter temperatures,

compared to Dalatangi, the most coastal station, which has a much lower winter/summer variation. A strong precipitation gradient is evident in Figure 7.2-e (ii), where Egilsstaðir has as little as half the annual precipitation received by the more coastal Dalatangi and Seyðisfjörður.

In the light of the strong climate gradient related to distance from the coast, the Dalatangi or Seyðisfjörður stations are thought to be best representative of climate in the Borgarfjörður Eystri region, given its proximity to the coast. Modern climate is based on Dalatangi data, and though Seyðisfjörður data would be equally applicable, the variation between them is negligible. Modern day climate conditions are defined based on mean temperature/precipitation values from 1962 to 2001, and are as follows:

*Average Annual Temperature = 3.57°C

*Average Annual Temperature Range = 7.3°C

*Average Annual Precipitation = 1452mm

*Average Annual Precipitation Range = 44.1mm

The climate data presented above is used to develop a simple Degree Day Model, which assumes that daily air temperatures follow a sinusoidal cycle with a set standard deviation. Mass balance is calculated as the difference between total annual ablation and total annual precipitation.

Defining the magnitude and duration of the climate fluctuation signal

Based on the geomorphological and chronological data from empirical evidence, a glacial advance is known to have occurred ~700 years after the peak of the '8.2ka event', rendering this major early Holocene climate fluctuation a likely trigger for the observed glacial advances. As discussed in Chapter 1, palaeoenvironmental proxies which may record effects of the "8.2ka event" indicate a potentially global climatic event with spatially variable environmental effects. The exact magnitude, duration and manifestation of the event is hard to quantify given its variable manifestations in climate proxy records (see Chapter 1). Deriving a specific temperature and precipitation value for the 8.2ka event is difficult when the climate records come

from different sources and rely on subjective interpretation of proxy data. To derive the climate in Iceland around 8.2ka is made more difficult given the relative lack of good Icelandic climate records for this time period, and the difficulties associated with inferring links between disparate records (discussed in Chapter 1).

The most cited source for proxy records of the 8.2ka event (Alley et al. 1997), suggests a 5°C temperature drop on the Greenland ice sheet. Records from the North Atlantic region suggest it may have lasted for between 60 and 400 years (e.g. Alley et al. 1997; Matthews et al. 2000; McDermott et al. 2001). Quantification of the precipitation patterns associated with the 8.2ka event is less well-defined than temperature changes, from the records discussed in Chapter 1. Various records suggesting it was dryer than at present in Greenland (Blunier et al. 1995; Alley et al. 1997) and wetter in Scandinavia (Dahl and Nesje 1994; 1996; Nesje and Dahl 2001), while various other records reveal mixed precipitation signals across the North Atlantic region at the time of the "8.2ka event", so the conditions in Iceland are not clear.

From the available literature, an "8.2ka signal" from one North Atlantic location cannot be automatically transferred to Iceland. Rather than attempting to exactly reproduce the 8.2ka climate fluctuation in Iceland, and view the modelled glaciological response, the modelling is approached from the other direction, aiming to investigate the climate scenarios necessary to produce the ice volumes which have been indicated by the empirical evidence. Experiments are run using a range of modelled climate fluctuations of variable duration and magnitude, to represent a putative '8.2ka event'. It is anticipated that this approach will provide an indication of the characteristics of the climate in Iceland at ~8.2ka which were able to induce such glacial activity.

7.3. Modelling Strategy

Since there is no clear climatic signal relating to the 8.2ka event in terrestrial Iceland, modelling experiments are carried out to assess ice growth and snow accumulation under a range of climatic conditions, in order to find the climate that best produce ice limits comparable with the empirical record. The limitations described in 7.1 are borne in mind, and an exact re-production of reconstructed limits is not expected. Experiments assume a spatially uniform sea-level climate across the field area, and given the relatively small size of the field area, this assumption is thought to provide a reasonable representation of the regional climate. In the climate model, it is possible to use a spatially variable precipitation factor, discussed in more detail later.

7.3.1. Simulating the 8.2ka climate fluctuation

Climate variables which can be altered to simulate the climate fluctuation are temperature and precipitation, within which the average annual value and the range can be changed. In addition, the duration of the event can be varied. A range of climate scenarios involving temperature drops of 1°C to 7°C below modern day are investigated.

As has been discussed, an envelope of climatic conditions is investigated for variable lengths of time, to represent the putative 8.2ka signal. Initially model runs of Glimmer and of the Climate Model employ a constant input climate signal run for 400 model years. Figure 7.3-a illustrates the structure in which these model experiments are carried out, and presents hypothesised relationships between relative ice volume and climate fluctuation magnitude/duration. The rate and extent of ice growth in response to climate change is assessed in a series of experiments in which temperatures are dropped by between 1 and 7°C. At each temperature drop stage, the spatial distribution of ice is investigated for durations of between 60 and 400years. The 8.2ka event may have lasted as little as 60 years, and as such it is important to get an indication of the magnitude of temperature drop sufficient to produce ice volumes comparable to those expected to have occurred in the field, in such a short

time period. By running the model for longer than the expected duration of the event, the study tests whether the glaciers in their observed locations were able to have reached an equilibrium state with the climate at 8.2ka, or if the duration of the event was insufficient.

Figure 7.3-a: Relationship between ice volume and magnitude/duration of climate forcing

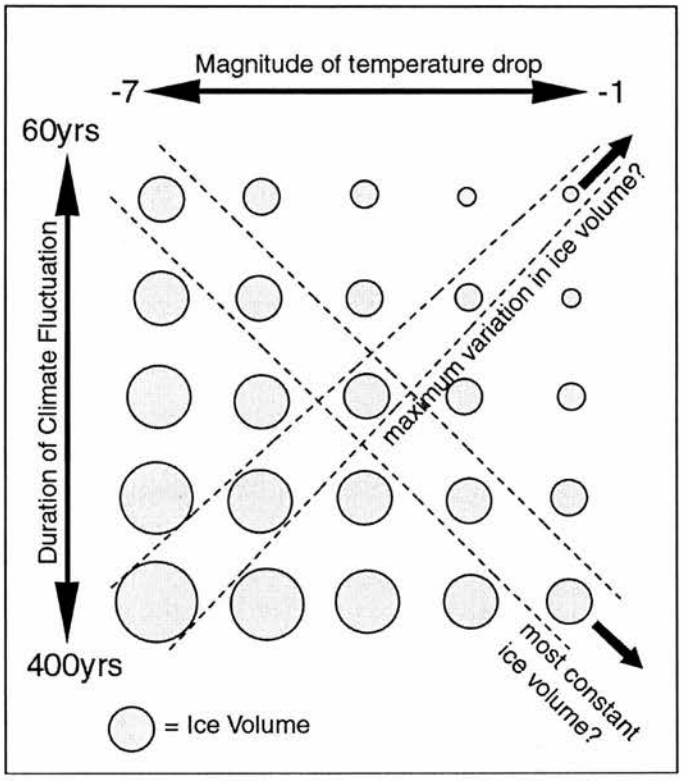

Figure 7.3-a represents the expected relative ice volume of a set of model runs using different magnitudes and durations of climate forcing. One would expect the largest volume of ice to build up where the climate forcing was of the largest magnitude (-7°C temperature drop), and of the longest duration (400 years), while the smallest ice volumes may be expected where a low magnitude, short-duration event had occurred.

Following these 'equilibrium' experiments with a constant temperature input, an attempt is made to re-create a dynamic climate signal as input to the model, representing the cooling and warming phase of the 8.2ka event seen in high resolution climate proxies (Alley et al. 1997; McDermott et al. 2001). Model runs are "hot-started" under modern climate conditions after 60, 200 and 400 model years having been run at a temperature constantly cooled by 1 to 7°C (see 7.5.2). This stepped temperature change from cool to warm is not strictly representative of the more gradual rate of change of the 8.2ka climate fluctuation over period of decades, but given the short duration of the 8.2ka event and its apparently rapid return to warmer temperatures less than ~100 years after cooling (Alley et al. 1997), these

experiments should provide an indication of the survival time of glacial response to rapid warming.

7.3.2. Testing the Model

Within the framework for modelling experiments described above, further investigations are carried out into the relative importance of other climate variables for forcing change in ice mass and properties. Climate data indicative of the precipitation values associated with the 8.2ka event are non-conclusive, as discussed in 7.2.3. Initially, precipitation values are kept at modern-day value in a uniform distribution while temperature change is investigated, but further experiments are run to assess the model's sensitivity to changes in precipitation, particularly its spatial patterns in response to the topography.

7.4. Modelling Results

In the following section, model results for Glimmer and the climate model are presented in combination, so comparison can easily be made between the effects of different climatic conditions on modelled ice and modelled snow accumulation.

7.4.1. Modern Climate Runs

To test the ability of the model to reproduce realistic ice distribution under each climatic regime, a test run is carried out under modern climatic conditions. Current glacial activity in the Borgarfjörður Eystri region has been seen to be constrained to high corries on the Dyrfjöll massif. Model runs under a modern climate (as defined in 7.2.3) should produce similar limited glaciation. Model runs using Glimmer and the climate model both revealed no ice growth and no positive mass balance snow accumulation under modern conditions. This could be due to the models' inherent difference from reality, but could also be an artefact of the poor model resolution. The currently active glaciers observed in the field (around Dyrfjöll) reach a maximum aerial extent of around $300m^2$, and are mostly smaller than this. The

model run under modern conditions fails to produce these glaciers. This may be an artefact of the low-resolution modelling topography, which is an inevitable limitation on the model's ability to re-produce very small glaciers. It is also possible that these glaciers remain in the field area as 'relicts' from the recent Little Ice Age cooling, and that if these were melted now, they could not re-initiate under modern conditions.

The inability of the model to reproduce small-scale glaciers due to its low resolution may cause problems for linking empirical and modelling evidence. If glaciers of such limited extent were induced by the 8.2ka event, as suggested by some small landform suites, the model could not be expected to reproduce these. It is important to assess how much temperature depression is necessary to create some (limited) positive mass balance on the modelled topography, to test the extent to which the model results are distinct from the real world. Testing both models in this way will assess the compatibility of Glimmer and the climate model. From these experiments, although the model will not resolve some of the smaller reconstructed glaciers, further insight will be gained into the locations most susceptible to initial snow and ice accumulation.

Model runs were carried out in Glimmer and in the climate model by keeping all variables the same except temperature, which was decreased by 1°C from modern conditions in the first run, and by a further 1°C on each subsequent run. The results were recorded in terms of the spatial distribution of positive mass balance and ice accumulation generated in the models. Figure 7.3-a represents the spatial distribution of ice and snow produced by the climate model with a 2°C cooling, with limited snow patches on hills of ~1100m and above. A 3°C drop produced more extensive snow patches, including the growth of snow on Dyrfjöll, where currently active glaciers are found (Figure 7.4-b (i)). Glimmer produced no ice with a 2°C cooling, requiring at least a 3°C drop in temperature to induce any ice growth on the modelled topography (results of which are presented in Figure 7.4-b (ii)).

Figure 7.4-a: Model results for temperature drop of 2°C
(i) Climate Model

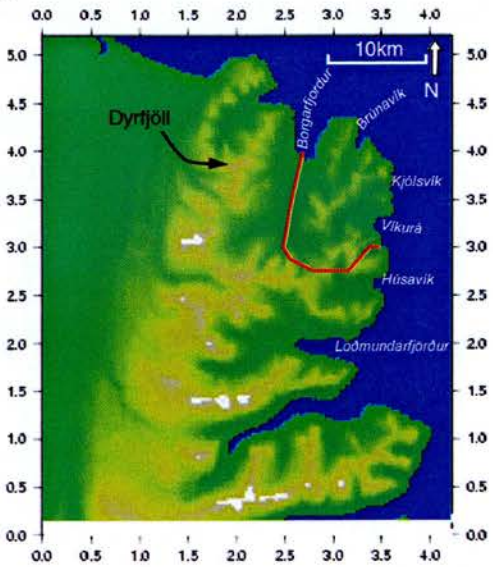

As can be seen the modelled snow accumulated with a 2°C temperature drop is minimal, and none occurs in the Dyrfjöll region (highlighted) where permanent snow and ice exists under modern climates.

White areas are permanent snow patches. The red line indicates the margin of the area assessed in greatest detail by the empirical studies. All further Climate Model output images will contain the same key.

Figure 7.4-b: Model results for temperature drop of 3°C

(i)Climate Model

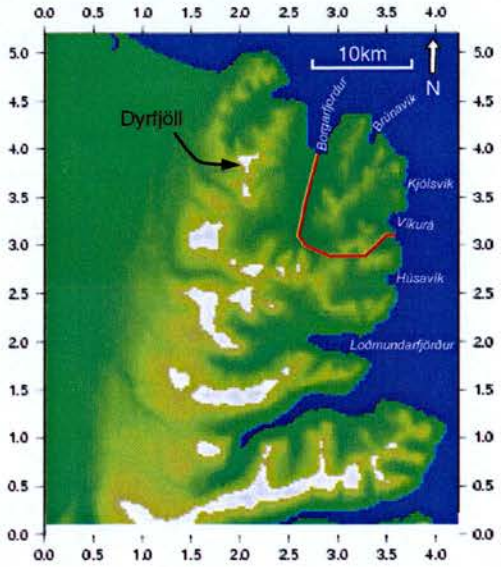

(ii)GLIMMER

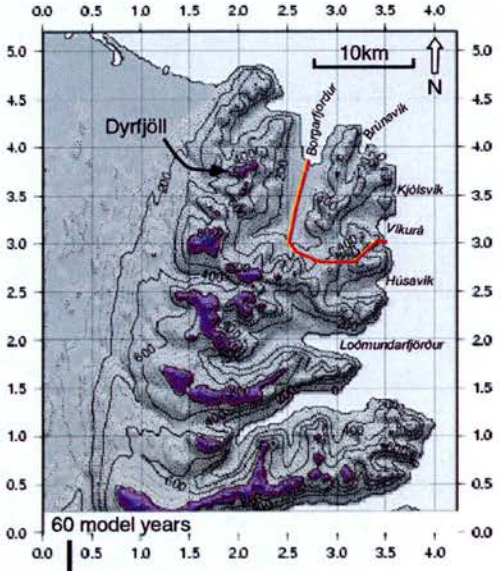

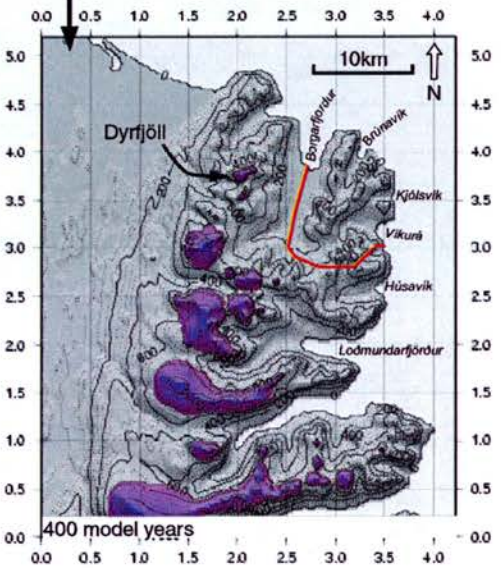

Under a 3°C cooling, snow and ice begin to accumulate on the Dyrfjöll massif, as highlighted. The distribution of positive mass balance created by the climate model compares well with the distribution of ice which has been modelled in Glimmer after 60 years at the same temperature. Following 400 model years, ice is more extensive in the Glimmer run, though crucially, no new source areas have been created.

7.4.2. Further temperature reduction model runs

As has been discussed, the primary concern in modelling experiments is to reproduce glacial source areas rather than the specific lower limits indicated by the empirical evidence. In the following set of experiments the aim is to derive the source areas most favourable to ice growth, and the relative magnitude of climate cooling necessary to glaciate the source areas identified. With each incremental

decrease in temperature, the new source areas which become able to support ice and snow are highlighted. Following these experiments, other factors influencing modelled ice and snow distribution are outlined. The distribution of snow and ice in the main field area is viewed in the context of the distribution in the wider region.

Temperature Reduced by 4°C

Figure 7.4-c: Model results for temperature drop of 4°C

(i)Climate Model (ii)GLIMMER

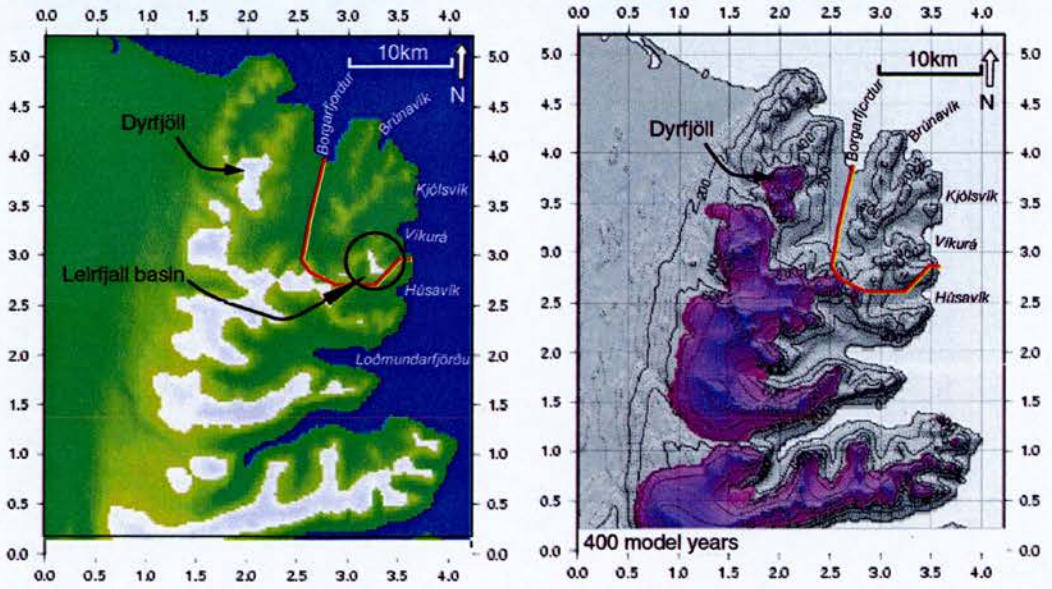

Figure 7.4-c shows that a temperature drop of 4°C induces significant positive mass balance in the climate model on mountains above ~800m. Snow begins to accumulate in the Leirfjall basin, which contained no empirical evidence for glaciation. This basin is highlighted in Chapter 4, however, as a basin which is likely to have contained a glacier but for which evidence no longer remains due to poor preservation potential. In Glimmer, the 400yr model run is presented, and as can be seen, in the main field area no ice accumulates even after this time, although outwith the immediate field area large ice caps have built up. This highlights the difficulty of initiating ice growth as opposed to expanding existing ice.

Temperature reduced by 5°C

Figure 7.4-d: Model results for temperature drop of 5°C

(i)Climate Model

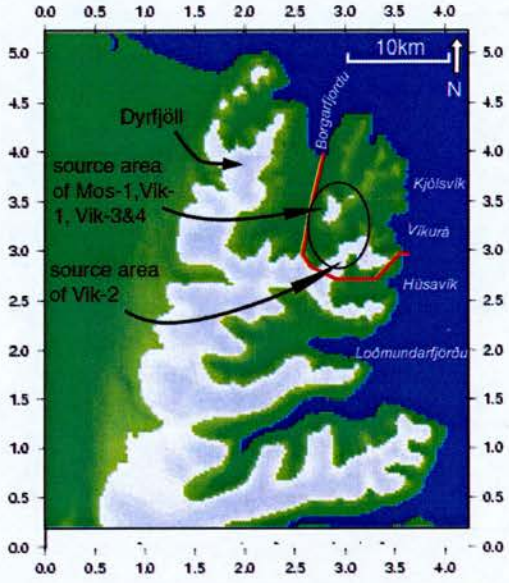

(ii)GLIMMER

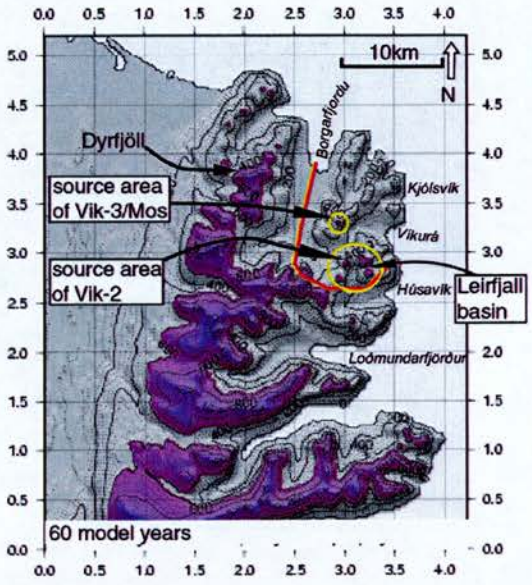

With a temperature drop of 5°C, modelled snow cover in the climate model continues to expand on high peaks, with extensive snow cover reaching the source area for the Víkurá 2 glacier, as highlighted in Figure 7.4-d (i), the peak Hvítserkur. In Glimmer (Figure 7.4-d (ii)), the ice-cover after 60 years is limited to small ice caps on the highest peaks, and ice does no connect to the large nearby ice caps. It is noted that the ice volumes produced for the 60 year run at 5°C temperature drop are smaller than the volumes produced after 400 years at a warmer 4°C temperature drop (see Figure 7.4-c).

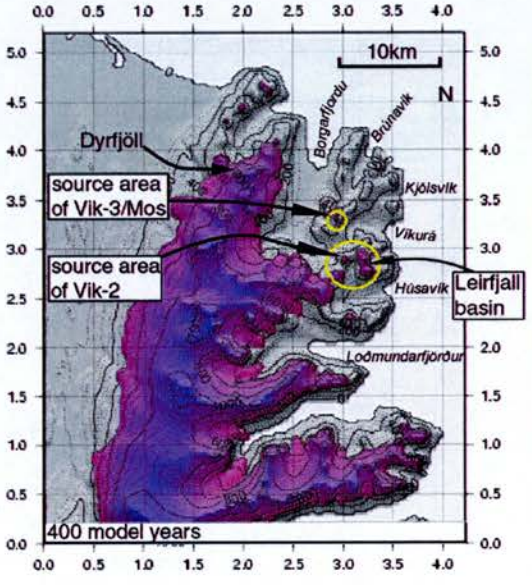

New independent snow patches are developed in the climate model, to the north of Hvítserkur, at altitudes of above ~520m, where the peak lies above ~700m. Specifically, snow has built up on the mountain Bàlkur (731m), and its associated ridge lines, which forms the source area for the glaciers reconstructed from the landform suites Víkurá 1, Mosdalur, and Víkurá 3 and 4.

In the Glimmer runs, after 400 model years an extensive ice cap has grown, with glaciers extending almost to sea level in the southern region. In the main field area however, in the North-Eastern corner of the model topography, only minimal ice patches are maintained at a temperature drop of 5°C. Ice does not expand beyond the summit of Bàlkur, forming a minimal initial source for the Víkurá 3 and Mosdalur glaciers, but not expanding far enough South-West to form a source for the Víkurá 1 glacier, or far enough East to source the Víkurá 4 glacier.

Temperature reduced by 6°C

Figure 7.4-e: Model results for temperature drop of 6°C

(i) Climate Model

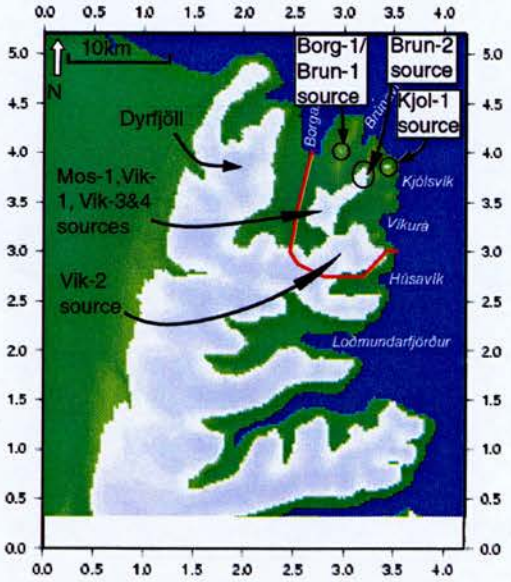

(ii) Glimmer – 60 model years

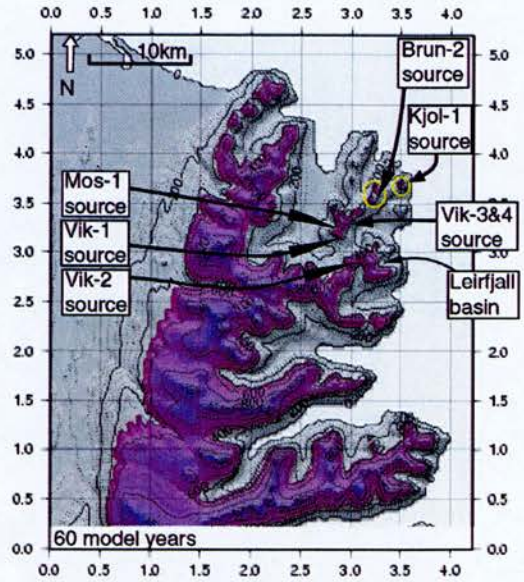

(iii) Glimmer – 200 model years

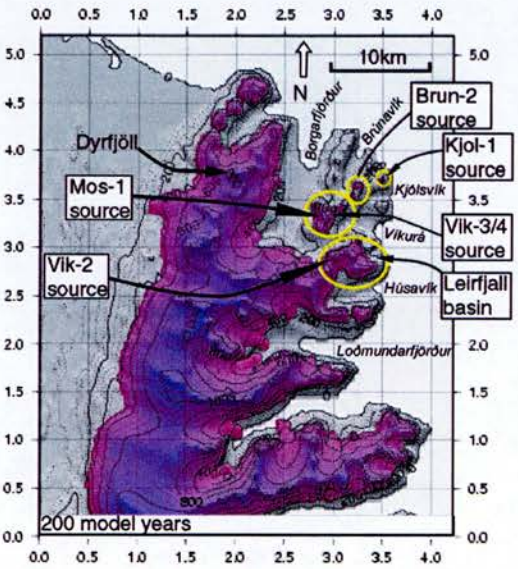

(iv) Glimmer – 400 model years

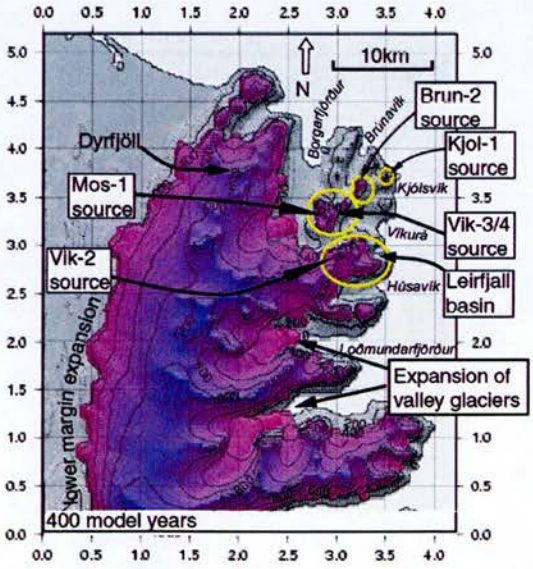

A temperature drop of a further degree enables expansion of modelled snow cover in the climate model to incorporate a source area for the Brunavik 2 landform suite, and new limited snow patches to develop at the source areas for the Kjólsvik, Borgarfjörður and Brúnavík 1 glaciers. In Glimmer, the independent ice cap centred on Bàlkur expands to source the putative Víkurá 1 and Víkurá 4 glaciers, and extends the ice source for the Mosdalur and Víkurá 3 glaciers. New independent ice caps are formed within 60 years, sourcing the Kjólsvík and Brúnavík 2 glaciers, though no ice is developed at Borgarfjörður as in the climate model. As shown, the ice sheet over the southern and western mountains expands dramatically over ~300 model years, while the independent ice caps in the field area have limited growth. By 300 model years the ice sheet ceases to expand and fluctuates around a mean at the extent illustrated in Figure 7.4-e (iv).

Temperature reduced by 7°C

Figure 7.4-f: Model results for temperature drop of 7°C

(i) Climate Model

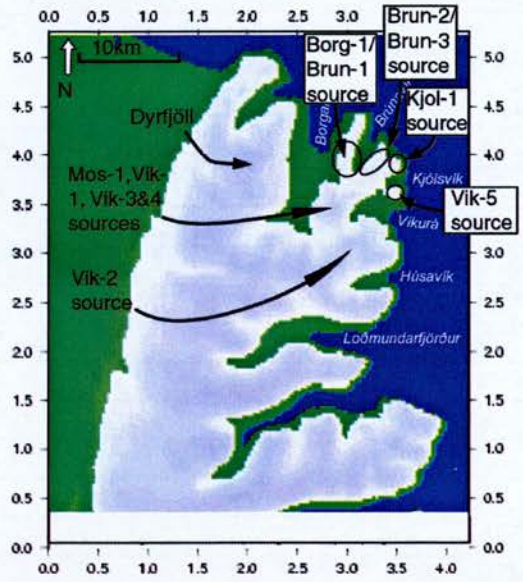

(ii) Glimmer – 60 model years

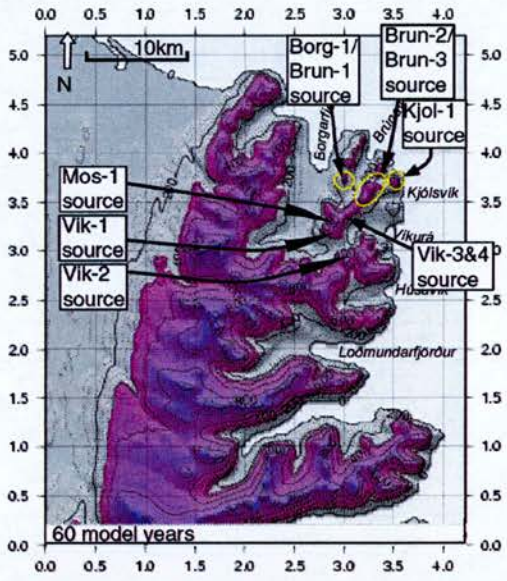

(iii) Glimmer – 400 model years

(iv) Glimmer – 400 model years/basal velocity

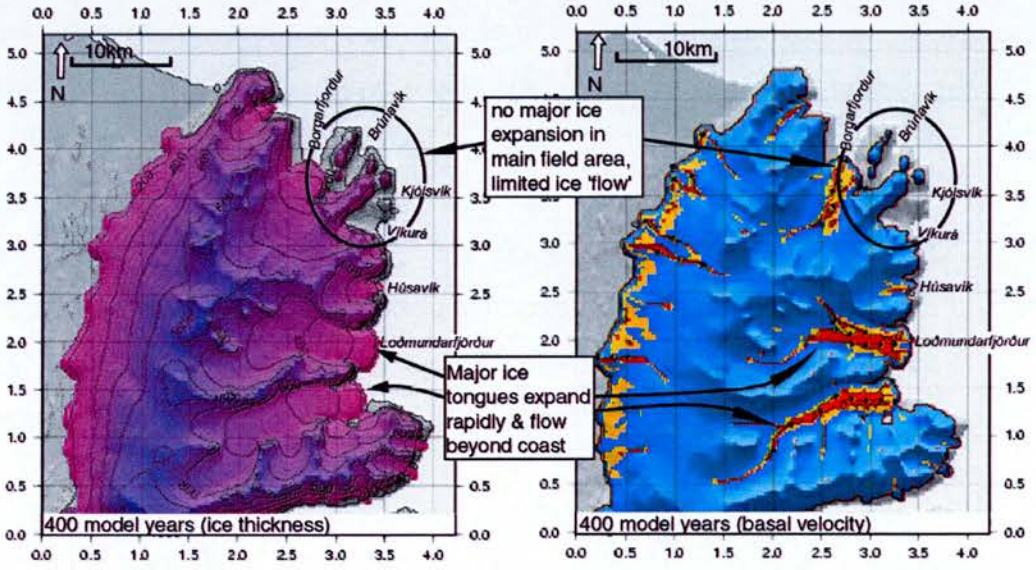

A 7°C temperature drop (to an average annual temperature of -3.57) creates continuous positive mass balance over all major peaks and ridges on the modelled topography in the climate model, with source areas for all reconstructed glaciers with the exception of Svínavík. The Glimmer results show that despite the major expansion of the southern/western ice sheet over ~400 years, the majority of the main field area still maintains only very small ice caps on the main ridges, which expand little between 60 and 400 model years. There is limited ice flow in the main field area, as shown in Figure 7.4-f (iv). While in the main Borgarfjörður valley, in Loðmundarfjörður and to a lesser extent in the Húsavík valley, after 400 years, glacial tongues flow well beyond the coastline, in the main field area no major flow is evident, with only static ice caps being maintained.

7.4.3. Summary

Table 7.4-a: Summary of initial model results

Rank	Glacier/basin name	Upper altitude of glaciated peak	Temperature drop (°C) required to induce ice/snow growth	
			Climate Model	*Glimmer*
1	Dyrfjöll	1136	-3	-4
2	Leirfjall	775	-4	-5
3	Víkurá 2	774	-5	-5
4	Mosdalur	731	-5	-5
5	Víkurá 3	731	-5	-5
6	Víkurá 4	611	-5	-6
6	Víkurá 1	521	-5	-6
8	Brúnavík 2	425	-6	-6
9	Kjol-1	590	-6	-6
10	Brúnavík 1	525	-6	-7
10	Borgarfjörður	525	-6	-7
11	Brúnavík 3	420	-7	-7
12	Víkurá 5	265	-7	-
13	Svínavík	410	-	-

Table 7.4-a summarises the key results of the modelling experiments carried out in the section above, in terms of their relationship to the glaciers reconstructed from empirical evidence. The "rank" refers to the magnitude of temperature drop required for snow or ice to develop at the source area, where 1 is the smallest magnitude change, and 13 the largest magnitude change. Where the temperature drop required to induce ice growth is the same for two glaciers, the largest ice/snow patch is ranked as requiring a lower magnitude forcing. It can be seen that in general, the regions requiring the lowest magnitude forcing to induce ice are those containing the highest altitude peak.

Relative value of results from Glimmer, Climate Model and Empirical Evidence

It is seen from the results above that positive mass balance accumulates more easily in the climate model than in Glimmer, suggesting that the climate model is more sensitive to temperature changes. A temperature drop of 3°C is required, in both Glimmer and the climate model, to produce any snow and ice accumulation on the Dyrfjöll massif, where currently active glaciers exist. This highlights some limitations inherent to the models in their ability to re-produce current

climate/glacier interactions. However, knowledge of this 3 degree 'lapse' may aid understanding of the glacial effects of a more extreme climate reversal which could have generated the glaciers associated with observed landform suites. The climate depressions necessary to induce ice/snow accumulation suggested in Table 7.4-a are probably over-estimates of the magnitude of climate change necessary.

7.5. Modelled glaciation of the field area in a wider context

It can be seen from the results presented above that there is a marked difference in modelled glacial extent between the specific field area, and the wider area. Glaciers reconstructed from the empirical evidence are ranked 1-13 in 7.4.2 above. In order to generate limited positive ice accumulation in the model at the source areas for all of the observed landform suites, extreme conditions are required, with a temperature reduction of ~7°C.

Figure 7.5-a: Comparison of empirical evidence with modelling results (7°C temperature decrease)

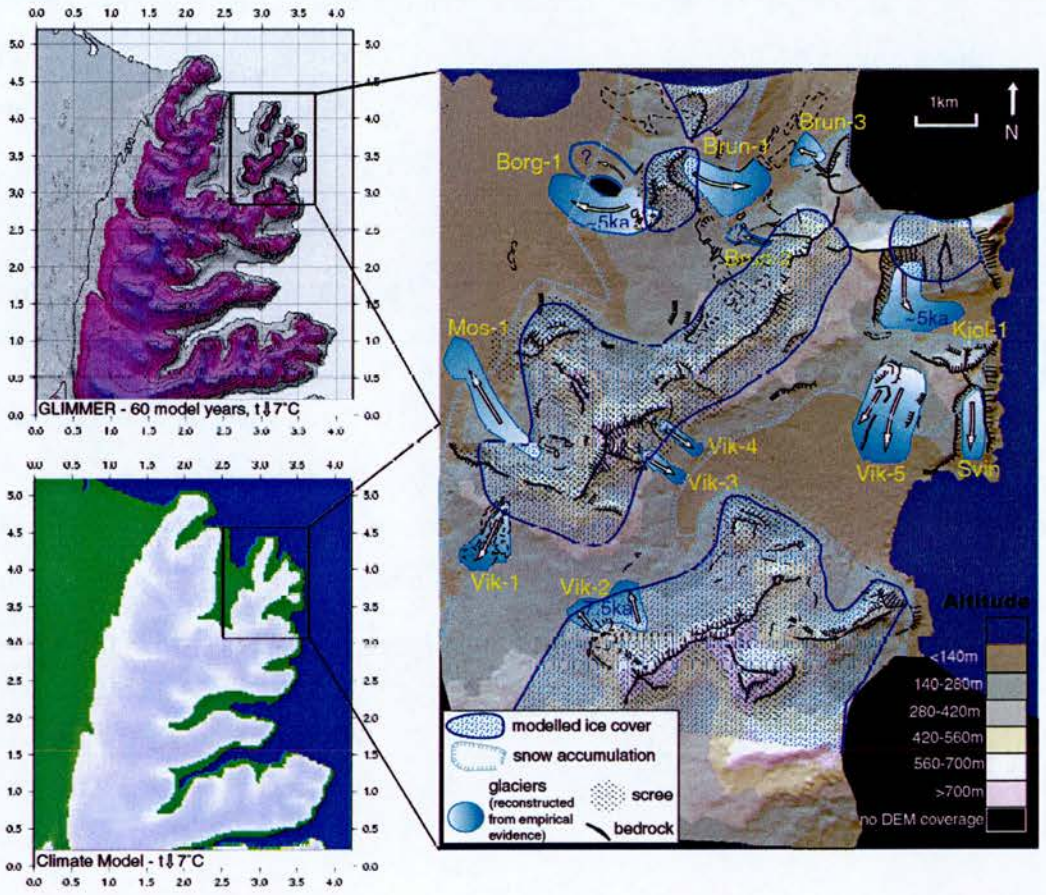

In Glimmer, even with a temperature drop of 7°C run for 400 years, no ice can be made to accumulate at the source area for the Víkurá 5 glacier, at 263m. In the climate model, a positive mass balance is only achieved here when temperatures are reduced by 7°C, at which temperature much of the field area can support snow. A source for the Svínavík glacier is not re-produced in Glimmer or in the climate model. As was seen however, this glacier relied on the sheltered cliff-backed basin for snow accumulation. This basin is too small to be re-produced in the low resolution model topography and thus modelled ice accumulation here is not expected.

7.5.1. Experiments with a spatially variable precipitation

As has been discussed, the snow and ice distribution developed in modelling experiments (accumulating on mountain and ridge tops), does not represent the nature of the glaciation reflected in the empirical evidence (corries glaciers). Model results represent the source areas in which snow can accumulate, above which there is positive mass balance. In the climate model, it is possible to implement a *spatially variable* precipitation parameter, where a strong aspect-related wind effectively forces precipitation (and thus accumulation) away from the mountain tops and towards slopes and basins of certain sheltered aspects. It is anticipated that if this precipitation distribution is implemented in Glimmer, the spatial patterns of ice growth will be more realistic with regards to the spatial patterns of snow accumulation associated with generation of the glaciers observed in the field

Figure 7.5-b: Snow distribution with an aspect-related wind forcing

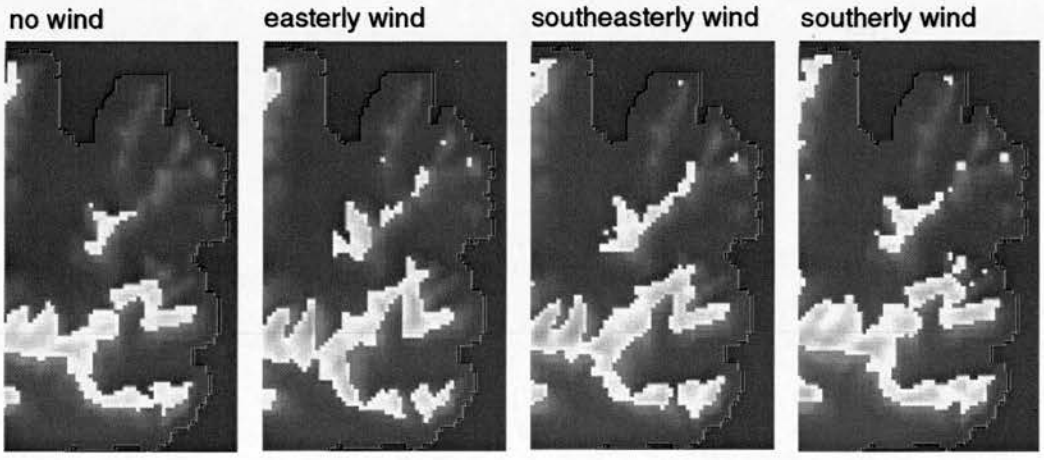

The four model runs illustrated here present snow accumulation patterns in a section of the field area, with a temperature reduction of 5°C. The effects on snow accumulation patterns of adding an aspect parameter to the model input are shown. Three examples use easterly, south-easterly and southerly winds. A southerly wind, for example, promotes accumulation on north-facing slopes. It can be seen that small snow patched appear in regions which grew no snow under a 'no wind' scenario.

Figure 7.5-b shows the results of such climate modelling experiments, combining different wind-direction parameters with the same climate input. It is seen that discrete units of positive mass balance are generated on ridge-lines which maintain no snow under a 'no wind' scenario. The variable precipitation distribution

generated by the climate model runs (seen in Figure 7.5-c) are input to Glimmer to assess ice growth, in response to this changed precipitation.

Figure 7.5-c: Spatially variable precipitation values related to south-easterly and north-westerly aspect wind forcing

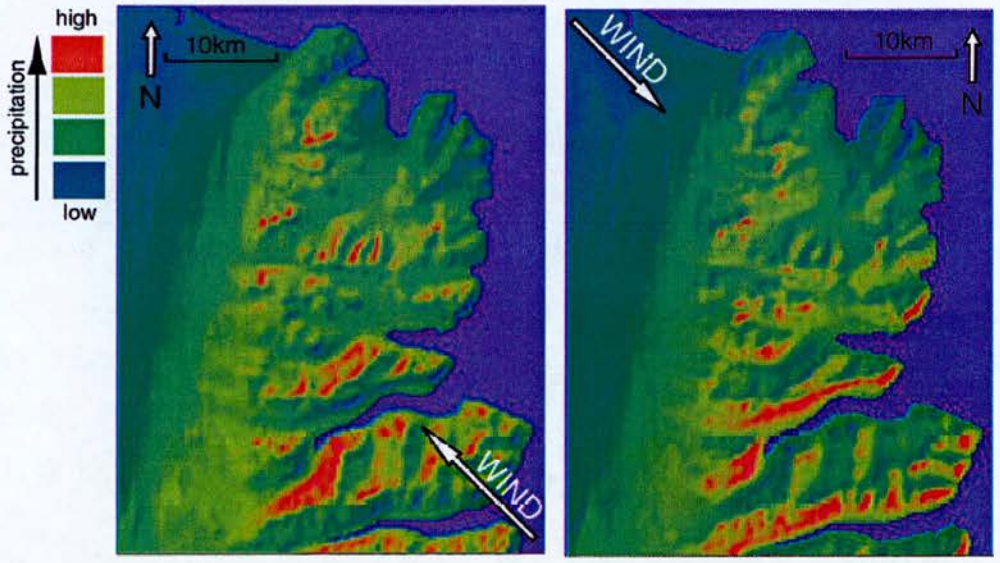

In Figure 7.5-c, two examples of the spatially variable precipitation values associated with applying a strong aspect-related wind to the climate model are presented. As can be seen, the main field area in the north-easterly corner is relatively dry compared to the remaining area.

Glimmer modelling experiments up to this point have assumed a constant relationship between altitude and mass balance, but by incorporating a spatially variable precipitation parameter, favourable ice growth can be generated on sheltered aspects, and ice accumulates less on mountain tops and exposed aspects. Model runs are carried out using the two variable precipitation models presented in Figure 7.5-c above, at a temperature reduced by 6°C, a temperature reduction sufficient to initiate ice growth on most key ridge lines in the field area in previous model runs. Selected results are presented in Figures 7.5-d and 7.5-e, highlighting the increased modelled ice volumes attainable by implementing a spatially variable precipitation field.

Figure 7.5-d: 200 year Glimmer runs with different aspect influence (av. an. temp. -2.57°C)

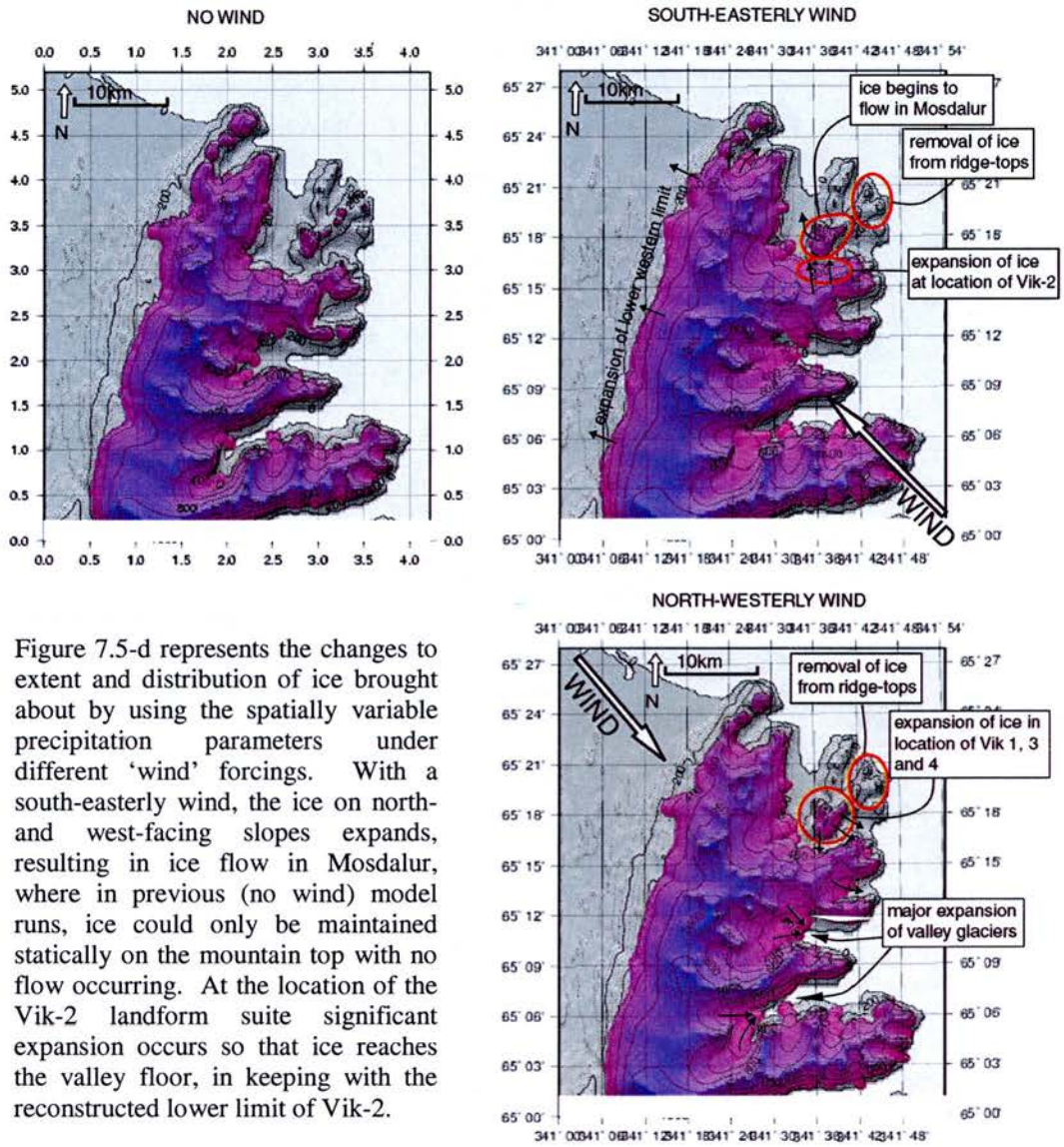

Figure 7.5-d represents the changes to extent and distribution of ice brought about by using the spatially variable precipitation parameters under different 'wind' forcings. With a south-easterly wind, the ice on north- and west-facing slopes expands, resulting in ice flow in Mosdalur, where in previous (no wind) model runs, ice could only be maintained statically on the mountain top with no flow occurring. At the location of the Vik-2 landform suite significant expansion occurs so that ice reaches the valley floor, in keeping with the reconstructed lower limit of Vik-2.

With north-westerly wind, expansion of ice at Vik-1, Vik-3 and Vik-4 occurs. In both wind scenarios, the small ice patches on ridge tops in the north-eastern corner of the area are removed completely, whilst significant expansion of valley glaciers occurs in the deep sheltered fjords of the southern area.

Figure 7.5-e: Variable ice growth at -2.57 (av.an temp) under different 'wind' conditions

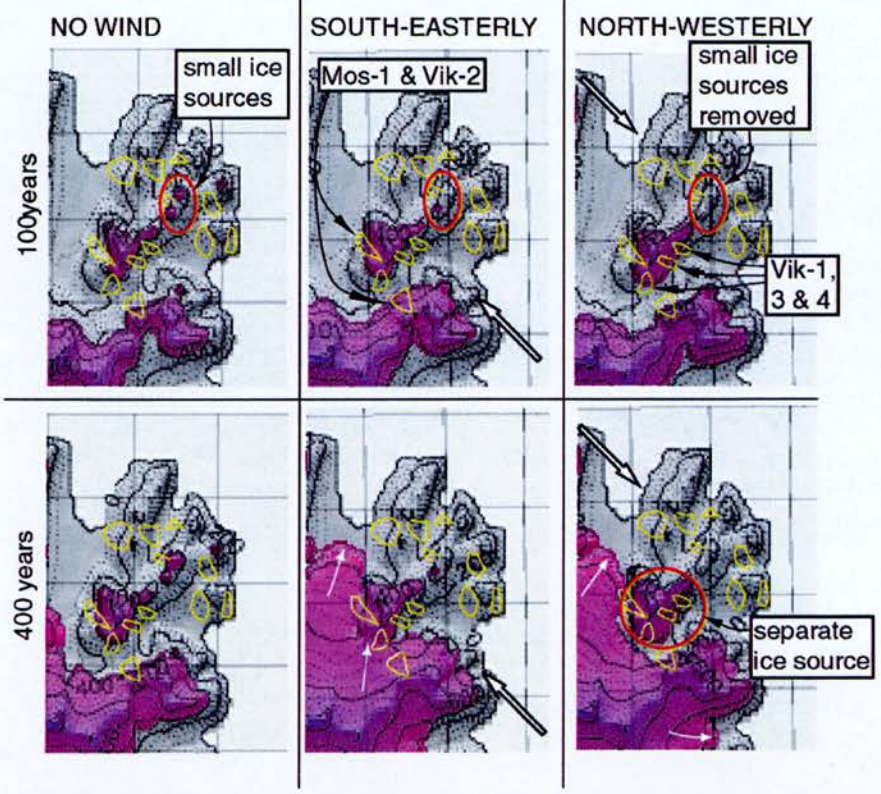

Figure 7.5-e illustrates modelled ice growth for the main field area with temperature reduced by 6°C from modern climate, under different 'wind' conditions. Yellow polygons represent the margins of glaciers reconstructed from empirical evidence. It can be seen that by utilising spatially variable precipitation, although small ice sources are removed from ridge-tops, modelled ice limits become more compatible with the empirically-deduced ice limits. After 100 model years, the precipitation distribution associated with a south-easterly wind produces ice flow in the location of the Mos-1 and Vik-2 glaciers, with the lower ice limit almost matching that interpreted from empirical evidence. Under a north-westerly wind, the precipitation distribution enables expansion of ice to the limits of the Vik-1, Vik-3 and Vik-4 glaciers. The nature and locations of ice expansion after only 100 years in these examples is a better representation of the empirically-derived glacier distribution than the expansion which occurs after 400 years with 'no wind', as shown in the lower left example in Figure 7.5-e. It is evident that ice centred in the higher more southern hills is able to expand significantly further under a spatially variable precipitation scenario, as after only 100 years the lower limits of this ice has dropped by ~100m or more. In the 400 year model runs, ice has expanded to near sea level in the spatially variable precipitation scenarios (the main expansion trajectories are indicated by white arrows), while its remains restricted and mostly above 200m under uniform precipitation.

There are some discrepancies between the climate model and ice sheet model in terms of the distribution of positive mass balance. The number if individual ice source areas produced by Glimmer under a set climate scenario are reduced when implementing the aspect-related variable precipitation, because ice can accumulate less easily on mountain tops. The smallest source areas (which formed sources for the Kjólsvík, Brúnavík and Borgarfjörður glaciers) are removed completely with a

strong wind influence. Where the source area is large enough however, the wind influence promotes growth. In the climate model, in contrast, the number of individual snow source areas is increased by the variable precipitation. It is anticipated that, in Glimmer, with a stronger aspect influence, it may be possible to maintain modelled ice on sheltered slopes in the more marginal parts of the field area.

The key conclusion to be drawn from this study is that with the use of spatially variable precipitation, modelling can better re-produce the empirically-derived ice limits. Ice (and snow) generated under a strong aspect-influenced precipitation pattern can expand far beyond the limits reached under a constant uniform precipitation, which means that a lower magnitude climate forcing is required to generate the same ice limits. These experiments further confirm that only a short-duration climate reduction is necessary to promote ice growth of the magnitude observed from field evidence. When the spatially variable precipitation experiments are carried out for a few hundred years the volumes of ice produced are much greater than volumes suggested by the empirical evidence.

7.5.2. Hot-starting experiments

From the experiments carried out thus far, it is shown that a significant amount of ice can build up in the field area over a short (sixty to one-hundred year) period when temperatures are reduced enough. A series of further experiments are carried out to test the stability of the modelled ice and its sensitivity to suddenly warming. After large ice masses have been allowed to build up under cool conditions, the model is "hot-started" with a much warmer temperature (representing modern climatic conditions). The length of time for the topography to fully deglaciate can be assessed, which has implications for the residency time of ice in the field area following a short-lived cold spell such as the 8.2ka event.

Model runs described in 7.4 are paused at various points through their runs once ice has built up (at between 100 and 400 model years), the temperatures are increased to

modern day values, and the models are re-started, to assess how long the existing model ice takes to melt. Similar results were discovered in every hot-starting experiment carried out. All ice formerly built up under cooler conditions, had melted after a maximum of 70 years under a modern climate. Results from these experiments are presented in Figure 7.5-f, showing that even with a significant initial ice sheet, when temperatures are returned to their modern values, ice cannot survive for a long period. The fact that such an ice sheet can disappear so quickly indicates that the smaller corrie glaciers revealed by empirical evidence would last even less time, under these model conditions. The speed of deglaciation is probably due to the fact that the ice sheets developed in the modelling are relatively thin, so a short warming would be sufficient to remove them.

Figure 7.5-f: Modelling in Glimmer the effects of sudden warming on an ice sheet built up over 400 years at an average annual temperature of -2.57 (depressed from modern by 6°C)

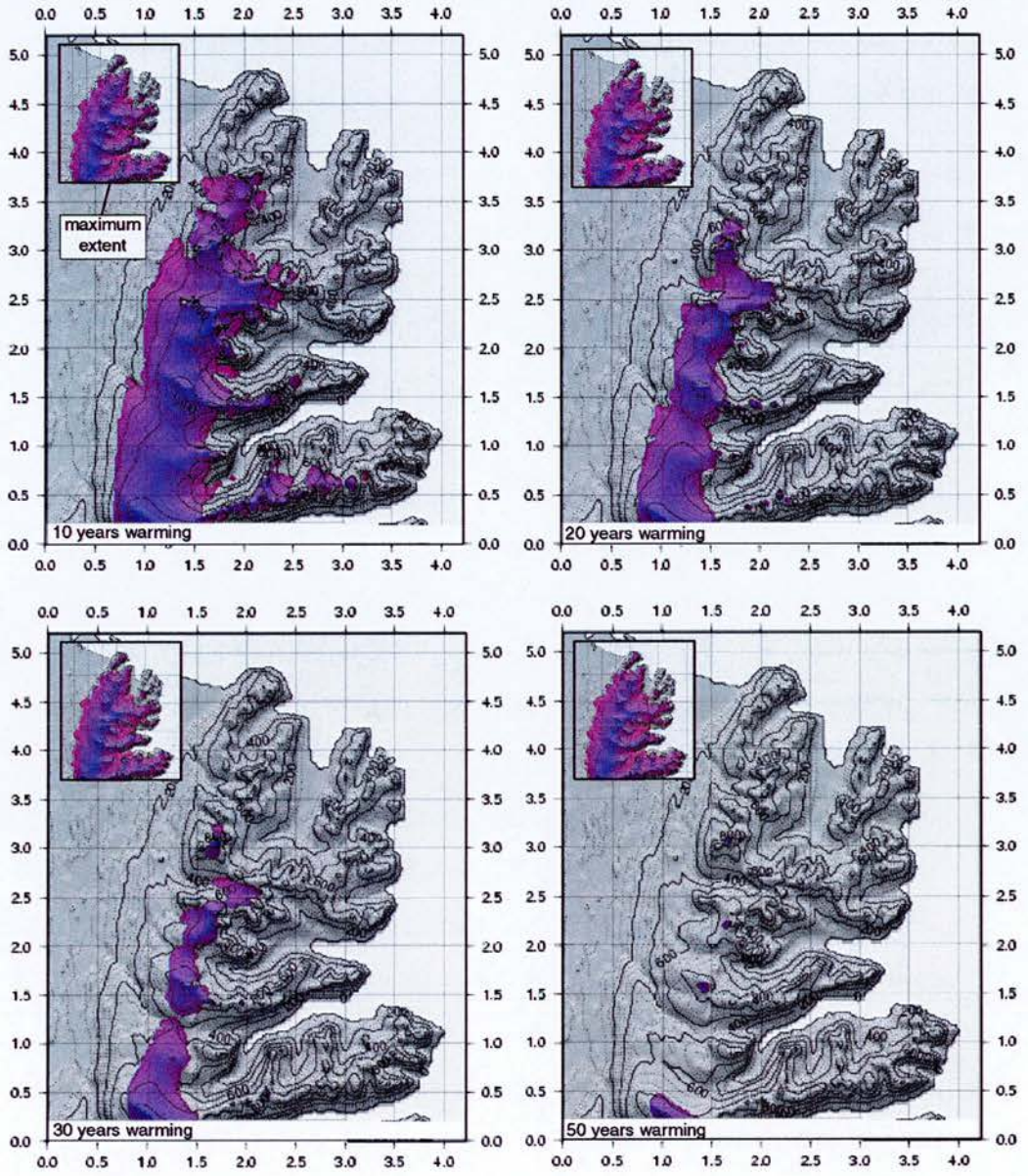

Figure 7.5-f represents four stages in the deglaciation of an ice sheet built up following 400 model years with a temperature reduced from modern values by 6°C. The model is hot-started from this 400 year glacial maximum under modern climatic conditions, and the majority of the ice is removed within 50 years. The remainder lasts only a further 20 years.

The empirical evidence suggests that ice in the main field area lasted for a longer period of time than indicated by modelling experiments, surviving until ~7.5ka or longer, 700 years after the peak of the 8.2ka cooling, an order of magnitude longer than the modelled deglaciation time. The disparities between model and empirical data can be explained with reference to the detailed geomorphic evidence. The

model assumes that the ice is clean, and so will melt quickly when warming occurs. In reality, empirical evidence suggests processes involving a thick debris cover associated with the glacial ice in the field area, which enables ice to survive, insulated, for long periods of time.

7.6. Discussion

Two key conclusions were drawn from the modelling experiments. Regarding the magnitude and duration of the climate forcing, a high magnitude but short-duration climatic cooling was sufficient to promote a limited amount of ice growth in the main field area. Using a spatially uniform precipitation input, an extreme climatic cooling with a temperature drop of as much as 7°C is necessary to enable modelled ice accumulation at the source areas for *all* former glaciers. By implementing spatially variable precipitation however, modelled ice can better represent the ice limits observed in the field, and the magnitude of climate forcing required to promote this ice growth is lower. Further, disparities between the modelled and real world ice/climate relationships lead to the conclusion that a lower magnitude temperature drop (tentatively estimated at ~5 °C) may have been sufficient to promote ice growth. The event duration may have been as short as 60 years, which was sufficient to produce limited glacial activity if the magnitude of climatic cooling was high.

Modelling highlighted the clear distinction between the main field area, Borgarfjörður Eystri, and the remaining Eastern Fjords, in terms of their susceptibility to glaciation. The field area is difficult to glaciate because of its low altitude and proximity to the sea. In order to produce limited ice/snow in this region using Glimmer or the climate model, the temperature reduction required necessitates the concurrent existence of much larger ice sheets in the surrounding Eastern Fjords, which implies the associated expansion of other major ice centres further afield in Iceland at the same time. This difference between the main field area and the remaining area in terms of glacial extent may serve to explain the differences

between the spatial patterns of response to the Little Ice Age and to the 8.2ka cooling event.

The 8.2ka event is thought to have been a short-lived high magnitude climate reversal (Alley et al. 1997), and modelling evidence supports the postulation that it was a short-lived (<100 years) and high-magnitude (5-7°C temperature drop) event. The LIA was, in contrast, a longer-duration but low-magnitude cooling. It was the last major climatic event in Iceland, consisting of a 2-3°C temperature drop lasting from around 1550-1850 (Ogilvie and Jónsson 2001) for a minimum duration of 300 years, and perhaps longer (Grove 2001). It induced widespread glacial response in Iceland, and is attributed as a trigger for much geomorphic activity. Lack of evidence for the 8.2ka event in Iceland is attributed to the fact that Little Ice Age glaciers removed evidence of 8.2ka activity, implying that the LIA must have induced a higher magnitude glacial response than the 8.2ka event. Therefore, the lack of LIA response in Borgarfjörður Eystri must be explained, if a response to the 8.2ka event there is postulated.

Modelling experiments have helped to explain this lack of LIA evidence, by addressing the relative glacial impact of short-lived high magnitude climate events versus long-duration low magnitude events. In the main field area, a low magnitude, long-lived cold spell (like the LIA) was not able to re-produce the ice source areas produced by a short-duration high magnitude event (like the 8.2ka event). Specifically, model runs implementing a -3°C and -4°C temperature drop, comparable to the LIA, promote glaciers on the Dyrfjöll massif, and large discrete ice sheets further south. These temperature reductions produce no ice in the main field area even after 400 years, when the ice elsewhere has expanded significantly. In contrast, a much more extreme climatic cooling is necessary to create ice in the main field area. A higher magnitude climate event could produce new ice source areas in the main field area within 60 years, but in this time the ice sheet in the surrounding region may not reach the same extent as the ice sheet grown after 400 years at a warmer temperature (for example, there is greater ice sheet volume after 400 years @ -4°C than after 60 years at -5°C).

It could therefore be suggested that while the 8.2ka event was high magnitude enough to initiate ice growth in the main field area as observed, it was not of sufficient duration to cause ice elsewhere to expand beyond the yet-to-come Little Ice Age limits. The Little Ice Age was of too low a magnitude to induce any glacial response in the main field area, but was of sufficient duration to cause ice elsewhere to expand beyond 8.2ka limits.

Discrepancies between the modelling results and the empirical evidence are evident with regards deglaciation rates. Modelling indicates rapid melting of all ice on the modelled topography within less than 100 years in response to sudden warming, but empirical evidence suggested that ice may have survived in the field area for a thousand years or more. This disparity can be explained with reference to the detailed empirical evidence. Borgarfjörður's mainly rhyolite geology produces high levels of rock debris relative to the volumes produced in the remaining Eastern Fjords, which would enable greater insulation of ice in the main field area, and an associated change in process from a climate-driven glacial system to a debris-controlled system. The conclusion is drawn that ice initiated during a short-lived high magnitude cooling event was able to survive and expand even when warming occurred, due to the extensive insulating debris cover. The rapid ice retreat in the model may be realistic for cleaner ice of the Eastern Fjords, but the model cannot re-produce the effects of debris insulation which enabled the ice to survive in the main field area for a much longer time period following warming.

8 Conclusions and Implications

8.1. Research Objectives

The overall aim of the research is to test the hypothesis that there was a geomorphic response mechanism to the 8.2ka cooling event in Iceland. The key objectives are to:

1. Quantify the magnitude and mechanisms of environmental response to the 8.2ka event in Iceland, by studying the potential causal connection between this Early Holocene cooling event and glacial activity occurring at this time.
2. Determine the specific glacial processes involved in manifesting response to the 8.2ka event.
3. Assess the extent to which non-glacial geomorphic activity in the field area at this time was triggered or intensified (directly or indirectly) by the 8.2ka event.
4. Determine the value of geomorphic evidence for reconstructing past environmental changes in response to rapid climate fluctuations.
5. Provide a case-study of specific response mechanisms to an extreme climate event, and assess the implications of these results for predicting the potential effects of future climate changes of comparable magnitude.

8.2. Summary of key results

The geomorphology of the Borgarfjörður Eystri region includes thirteen key landform suites indicative of debris-transport processes which occurred in response to climatic forcing. The suites are lobate in shape, exhibiting clear lateral and terminal margins, and originate in small accumulation basins, expanding towards the base as the slopes become gentler. Within these landform suites, distinct units of landform elements are juxtaposed, and the same spatial pattern is evident across many of the suites. Upper suites are associated with large blocky hummocky terrain, while the middle suites are dominated by small-scale hummocks and/or longitudinal

ridges. Lower suites are generally defined by transverse and arcuate ridges on subdued topography near the valley floor.

There is the possibility that the landform suites represent glacial and geomorphic (debris transport) processes which were triggered by the 8.2ka event. Specifically:

i. The spatial distribution of landform suites represents the real spatial distribution of geomorphic activity which occurred in response to the climate fluctuation
ii. The landform suites were formed by the same type of process (uniformity of the 'response')
iii. Landform suite generation occurred synchronously (timing of the 'response')

Preservation potential of geomorphic evidence provides a test for hypothesis (i). It reveals that slope angle was the key factor affecting preservation of landforms. A number of basins in the field area in which geomorphic activity was likely to have occurred contain no evidence for the activity because of poor preservation. Hypothesis (i) is therefore disproved, and the true extent of geomorphic activity which occurred is shown to have been greater than the landform record would suggest.

An alternative explanation for the existence of distinct landform units within each landform suite, and the variation in size, shape and extent of the suites, is the impact of spatially variable topographic and lithological factors. This study revealed a high level of topographic and lithological control on landform suites as a whole. Slope angle, the size of the putative accumulation zone and bedrock control were shown to exert a strong influence on landform suite size and shape. However, although topography and lithology were shown to be an influencing factor in the processes of generation of landform elements, these factors could not explain completely the existence of distinct landform units within each suite. Thus, the observed landform suites represented a series of separate geomorphic events, which generated the distinct landform units, disproving Hypothesis (ii).

The chronology of geomorphic events from tephrostratigraphy and radiometric dating tested Hypothesis (iii). This revealed asynchrony in landform genesis processes, and a time-transgressive response mechanism to the 8.2ka cooling event, thus disproving Hypothesis (iii). Phases of activity began around 700 years after the peak of the 8.2ka event, and further events occurred throughout the mid-Holocene.

The landforms may result from:

1. A *causal trigger* - the climate reversal at 8.2ka.
2. A *primary geomorphic response* - debris-covered glacial expansion initiated following the 8.2ka cooling, by at least 7.5ka.
3. A *secondary geomorphic response* - mass-movement events between 6ka and 4.2ka triggered by post-glacial instabilities and the existence of melting snow and ice under thick loose debris cover.

Ice sheet modelling experiments extend the value of the empirical evidence and reveal that the climate fluctuation (the 8.2ka event) which triggered the primary (glacial) response was an event of high magnitude (5-7 °C temperature drop) but short-duration (as little as 60 years). Modelling highlights the difference in glacial response to this event found in the main field area (limited, discrete ice sources), compared with the remaining Eastern Fjords (where extensive ice sheets were generated).

8.3. Main Conclusions

8.3.1. Primary Response

- A series of debris-covered corrie glaciers (in the order of ~500 to 200o square metres in area) expanded in the Early to Mid-Holocene in the Borgarfjörður Eystri region in response to the 8.2ka event. They were responsible for

generating (at least) the lower units of most of the mapped landform suites, characterised by arcuate and transverse terminal ridges.

Timing of primary response

- A well-constrained and dated glacial limit has an age of 7.47-7.57ka, post-dating the peak of the 8.2ka event by around 700 years.
- Glacial advances significantly pre-date late Holocene cooling events such as the Little Ice Age, which accounts for much of Iceland's surviving evidence for corrie glacier activity.
- The glacial phase well post-dates the Preboreal and Younger Dryas cold spells.

Nature of primary response

- The high level of debris-cover on these glaciers was an artefact of the local highly erodable rhyolite geology, associated with old central volcano domains.
- Debris-cover enabled ice to last, insulated, for an extended period of time, effectively de-coupling the glaciers from climate and resulting in asynchronous patterns of glacial retreat dating to between 7.5ka and 5ka.
- As a result of the extended survival of ice (and snow) under debris, long-term ice stagnation occurred, generating chaotic hummocky terrain.

8.3.2. Secondary Response

- Slope instabilities, promoted by the glacial activity, resulted in the eventual crossing of stability thresholds and the triggering Mid-Holocene slope/rock failure events, which generated the upper units of many landform suites, overlying or removing glacial deposits.

Timing of secondary response

- The timing of these events was not synchronous across the field area, dating to between 6ka and 4.2ka, with further smaller-scale slope failure events occurring throughout the mid-Holocene until at least 3ka.

- The asynchrony of slope failures is due to the fact their occurrence is controlled by locally specific stability thresholds relating to the individual topographic and lithological setting, rather than by climate.
- Slope failure events occurred before all ice from the former glaciers had retreated.

Nature of secondary response

- As ice and snow still remained at the time of the slope failure events, in some cases the meltwater and debris from the former glaciers were incorporated in, and/or defined the collapse material.
- Where landform suites were backed by basalt cliffs, rotational bedrock failure occurred, which generated the blocky hummocks of many of the upper units of the landform suites.
- Where landform suites originated on rhyolite hill-slopes, debris flows occurred, generating longitudinal and transverse ridge lines, and clear lobate flows.

8.3.3. Climatic Implications

Nature of the 8.2ka event

- The 8.2ka event was a high magnitude climate fluctuation, of sufficient magnitude to promote small scale corrie glacier expansion in the Borgarfjörður region, and concurrently promote significant ice sheet glaciation in the wider region, and probably across much of Iceland.
- The event was short-lived however, and in the wider region of the Eastern Fjords, deglaciation occurred quickly.
- Due to the high level of debris available in the Borgarfjörður region, the limited glaciers in this region were able to last for a longer period.

The 8.2ka event and the Little Ice Age

- The Little Ice Age was of lesser magnitude than the 8.2ka event, and was insufficient to induce glacial activity in the Borgarfjörður region, although the wider area was affected significantly.
- The Little Ice Age lasted for a much greater period of time than the 8.2ka event. Due to the fact that ice sheets can expand more easily from an existing ice source than from a 'no ice' scenario, ice growth which was initiated at the start of the LIA may have been able to expand beyond the former 8.2ka ice limits, removing evidence of the 8.2ka event in these locations. In the main field area, however, because the magnitude of the LIA was insufficient to initiate any ice growth, the 8.2ka event limits survived.

8.4. Global Implications

The detailed case-study of regional response to a short-lived high magnitude climatic cooling presented in this thesis highlights the significance of short-lived, extreme climate events as triggers for widespread glacial and geomorphic activity. The research provides evidence for a significant glacial response to the 8.2ka cold event in Iceland. In much of the country, the Little Ice Age induced large-scale glacial response, which removed evidence of earlier Holocene activity. However, Borgarfjörður Eystri provides a unique record of Early to Mid-Holocene glacial and geomorphic activity in a region which, owing to its relatively low altitude and coastal location away from major ice sources, had limited response to the Little Ice Age. It is suggested that further evidence of this widespread Early Holocene glacial activity is likely to exist in other coastal parts of Iceland within a similar altitudinal range.

The research has also highlighted the existence of a Mid-Holocene period of mass-movement activity, related to slope instabilities caused by the preceding glacial activity. These landslides and debris flows are thus seen as 'secondary responses' to climatic cooling, processes occurring as part of landscape re-adjustment over thousands of years, following a short but extreme climate cooling.

The variable ice/debris ratios of the systems responsible for generating the landform suites result in a continuum of processes, from climate-driven 'glacial' systems, to systems which are controlled mostly by debris supply and are thus de-coupled from climate. This results in an asynchronous and spatially variable geomorphic signal. This has implications for understanding the extent to which lithology and topography control the nature, timing and extent of glacial 'response' to climate fluctuations.

The research has provided the first evidence for a glacial response in Iceland to the "8.2ka event", a globally significant early Holocene climate fluctuation. The existence of such a response in a sensitive terrestrial environment in the North Atlantic provides a new constraint on interpretations of the spatial and temporal patterns of environmental change which were triggered by this event. On the smallest scale, a phase of corrie glacier advances has been identified in north-east Iceland, which occurred in response to the 8.2ka cooling. By implication, and on a larger scale, this response was probably Iceland-wide, inducing advance of the major ice sources and corrie glacier initiation. Early Holocene geomorphic evidence is not well-preserved in much of Iceland, but evidence for the response may exist in other marginal parts of Iceland which had limited response to the Little Ice Age. Given the existence of a clear 8.2ka signal in offshore climate proxies, and the known glacial advances, the biostratigraphic record may also show evidence of climatic cooling.

The research supports the hypothesis that the 8.2ka event was a short-lived but high magnitude climate reversal in the North Atlantic region, while highlighting the spatial variations in nature and timing of response even within a small region. The variable expression of response to the event, which is mirrored at a larger scale in the North Atlantic and globally, may be a manifestation of the structure of the climate reversal. The short duration of the extreme cooling would have variable impact on the environment depending on the speed at which the specific system could respond to sudden change. Systems which are slow to respond to such climatic change may have shown no response at all, since the climate returned to 'modern' conditions within such a short time period. In contrast, systems which can respond quickly may

continue 'responding' long after the climate event has ended, as has been shown in this study. The long-term preservation of ice under debris cover following glacier initiation, and the occurrence of secondary response mechanisms to the 8.2ka event in the field area signifies the long-term environmental impact of a relatively short climate fluctuation as the landscape attempts to regain stability. It highlights the locally-specific nature of response mechanisms to climate change and provides an explanation for the spatially and temporally variable global expression of the 8.2ka event.

References

Abbott, M. B., Wolfe, B. B., Wolfe, A. P., Seltzer, G. O., Aravena, R., Mark, B. G., Polissar, P. J., Rodbell, D. T., Rowe, H. D. and Vuille, M. 2003. Holocene paleohydrology and glacial history of the central Andes using multiproxy lake sediment studies. *Palaeogeography, Palaeoclimatology, Palaeoecology* **194**(1-3): 123-138.

Ackert Jr., R. P. 1998. A rock glacier/debris-covered glacier system at Galena Creek, Absaroka Mountains, Wyoming. *Geografiska Annaler* **80**(3-4).

Alley, R., Mayewski, P., Sowers, T., Stuiver, M., Taylor, K. and Clark, P. 1997. Holocene climatic instability: A prominent, widespread event 8200 yr ago. *Geology* **25**: 483-486.

Alley, R. B. and Agustsdottir, A. M. 2005. The 8k event: cause and consequences of a major Holocene abrupt climate change. *Quaternary Science Reviews* **24**(10-11): 1123-1149.

Andruleit, H. A. and Baumann, K.-H. 1998. History of the Last Deglaciation and Holocene in the Nordic seas as revealed by coccolithophore assemblages. *Marine Micropaleontology* **35**(3-4): 179-201.

Argollo, J. and Mourguiart, P. 2000. Late Quaternary climate history of the Bolivian Altiplano. *Quaternary International* **72**(1): 37-51.

Asch, T., Buma, J. and Van Beek, L. 1999. A view on some hydrological triggering systems in landslides. *Geomorphology* **30**: 25-32.

Augustinas, P. 1995. Glacial valley cross-profile development: the influence of in situ rock stress and rock mass strength, with examples from the Southern Alps, New Zealand. *Geomorphology* **14**: 87-97.

Baker, P. A., Rigsby, C. R., Seltzer, G. O., Fritz, S., Lowenstein, T. K., Bacher, N. P. and Veliz, C. 2001. Tropical climate changes at millennial and orbital timescales on the Bolivian Altiplano. *Nature* **409**: 698-701.

Baldini, J. U. L., McDermott, F. and Fairchild, I. J. 2002. Structure of the 8200-Year Cold Event Revealed by a Speleothem Trace Element Record. *Science* **296**(5576): 2203-2206.

Ballantyne, C. K. (1997). The Periglacial Geomorphology of Scotland. Reflections on the Ice Age in Scotland. J. E. Gordon. Glasgow, The Scottish Association of Geography Teachers and Scottish Natural Heritage: 166-178.

Ballantyne, C. K. 2002. A general model of paraglacial landscape response. *The Holocene* **12**(3): 371-376.

Ballantyne, C. K. 2002. Paraglacial geomorphology. *Quaternary Science Reviews* **21**(18-19): 1935-2017.

Ballantyne, C. K. and Benn, D. I. 1994. Paraglacial slope adjustment and resedimentation following recent glacier retreat, Fårbergstølsdalen, Norway. *Arctic and Alpine Research* **26**(3): 255-269.

Ballantyne, C. K. and Stone, J. O. 2004. The Beinn Alligin rock avalanche, NW Scotland: cosmogenic 10Be dating, interpretation and significance. *The Holocene* **14**(3): 448-453.

Barber, D. C., Dyke, A., Hillaire-Marcel, C., Jennings, A. E., Andrews, J. T., Kerwin, M. W., Bilodeau, G., McNeely, R., Southon, J., Morehead, M. D.

and Gagnon, J.-M. 1999. Forcing of the cold event of 8,200 years ago by catastrophic drainage of Laurentide lakes. *Nature* **400**(6742): 344-348.

Barnett, C., Dumayne-Peaty, L. and Matthews, J. A. 2001. Holocene climatic change and tree-line response in Leirdalen, central Jotunheimen, south central Norway. *Review of Palaeobotany and Palynology* **117**(1-3): 119-137.

Barron, J. A., Bukry, D. and Bischoff, J. L. 2004. High resolution paleoceanography of the Guaymas Basin, Gulf of California, during the past 15000 years. *Marine Micropaleontology* **50**(3-4): 185-207.

Bauch, H. A. and Weinelt, M. S. 1997. Surface water changes in the Norwegian sea during last deglacial and holocene times. *Quaternary Science Reviews* **16**(10): 1115-1124.

Benjamínsson, J. (1980). Tephra Layer "a". Proceedings of the NATO Advanced Study Institute "Tephra Studies as a Tool in Quaternary Research", Laugarvatn and Reykjavík, Iceland, D. Reidel Publishing Company.

Bentley, M. and Dugmore, A. 1998. Landslides and the rate of glacial trough formation in Iceland. *Quaternary Proceedings* **6**: 11-15.

Bergman, J., Wastegard, S., Hammarlund, D., Wohlfarth, B. and Roberts, S. 2004. Holocene tephra horizons at Klocka Bog, west-central Sweden: aspects of reproducibility in subarctic peat deposits. *Journal of Quaternary Science* **19**(3): 241-249.

Bianchi, G. G. and McCave, I. N. 1999. Holocene periodicity in North Atlantic climate and deep-ocean flow south of Iceland. *Nature* **397**(6719): 515-517.

Birks, C. and Koç, N. 2002. A high-resolution diatom record of late-Quaternary sea-surface temperatures and oceanographic conditions from the eastern Norwegian Sea. *Boreas* **31**: 323-344.

Birks, H., Gulliksen, S., Haflidason, H., Mangerud, J. and Possnert, G. 1996. New Radiocarbon dates for the Saksunarvatn Ash from west Norway. *Quaternary Research* **45**: 119-127.

Björck, S., Kromer, B., Johnsen, S., Bennike, O., Hammarlund, D., Lemdahl, G., Possnert, G., Rasmussen, T. L., Wohlfarth, B., Hammer, C. U. and Spurk, M. 1996. Synchronized TerrestrialAtmospheric Deglacial Records Around the North Atlantic. *Science* **274**(5290): 1155-1160.

Björck, S., Rundgren, M., Ingolfsson, O. and Funder, S. 1997. The Preboreal oscillation around the Nordic Seas: terrestrial and lacustrine responses. *Journal of Quaternary Science* **12**(6): 455-465.

Bjornsson, H. 1980. Avalanche activity in Iceland, climate conditions, and terrain features. *Journal of Glaciology* **26**(94): 13-23.

Blikra, L. H. and Nemec, W. 1998. Postglacial colluvium in western Norway: depositional processes, facies and palaeoclimatic record. *Sedimentology* **45**: 909-959.

Blunier, T., Chappellaz, J., Schwander, J., Stauffer, B. and Raynaud, D. 1995. Variations in atmospheric methane concentration during the Holocene epoch. *Nature* **374**: 46-49.

Boygle, J. (1994). Tephra in lake sediments: An unambiguous geochronological marker? Edinburgh, University of Edinburgh.

Boygle, J. 2004. Towards a Holocene tephrochronology for Sweden: geochemistry and correlation with the North Atlantic tephra stratigraphy. *Journal of Quaternary Science* **19**(2): 103-109.

Bozhinsky, A. N., Krass, M. S. and Popovnin, V. V. 1986. Role of debris cover in the thermal physics of glaciers. *Journal of Glaciology* **32**(111): 255-266.

Brazier, V. and Ballantyne, C. K. 1989. Late Holocene debris cone evolution in Glen Feshie, western Cairngorm Mountains, Scotland. *Transactions of the Royal Society of Edinburgh, Earth Sciences* **80**: 17-24.

Bronk Ramsey, C. 1995. Radiocarbon calibration and analysis of stratigraphy: the OxCal programme. *Radiocarbon* **37**: 425-430.

Caseldine, C., Geirsdottir, A. and Langdon, P. 2003. Efstadalsvatn – a multi-proxy study of a Holocene lacustrine sequence from NW Iceland. *Journal of Paleolimnology* **30**(1): 55-73.

Casely, A. (2006). Medieval climate and settlement in Iceland. School of Geosciences. Edinburgh, Edinburgh University.

Chambers, F. M., Daniell, J. R. G., Hunt, J. B., Molloy, K. and O'Connell, M. 2004. Tephrostratigraphy of An Loch Mór, Inis Oírr, western Ireland: implications for Holocene tephrochronology in the northeastern Atlantic region. *The Holocene* **14**(5): 703-720.

Clark, D. H., Clark, M. M. and Gillespie, A. R. 1994. Debris-Covered Glaciers in the Sierra Nevada, California, and Their Implications for Snowline Reconstructions. *Quaternary Research* **41**(2): 139-153.

Clark, D. H., Steig, E. J., Potter, P. and Gillespie, A. R. 1998. Genetic variability of rock glaciers. *Geografiska Annaler* **80A**(3-4): 175-184.

Clark, P., Pisias, N., Stocker, T. and Weaver, A. 2002. The role of the thermohaline circulation in abrupt climate change. *Nature* **415**: 863 - 869.

Cross, S. L., Baker, P. A., Seltzer, G. O., Fritz, S. C. and Dunbar, R. B. 2001. Late Quaternary Climate and Hydrology of Tropical South America Inferred from an Isotopic and Chemical Model of Lake Titicaca, Bolivia and Peru. *Quaternary Research* **56**(1): 1-9.

Cruden, D. and Varnes, D. (1996). Landslide Type and Process. Landslides: Investigation and Mitigation. A. Turner and R. Schuster. Washington D. C., National Academy Press. **Special Report 247:** 76-90.

Curry, A. M. and Morris, C. J. 2004. Lateglacial and Holocene talus slope development and rockwall retreat on Mynydd Du, UK. *Geomorphology* **58**(1-4): 85-106.

Dahl, O. and Nesje, A. 1994. Holocene glacier fluctuations at Hardangerjøkulen, central-southern Norway: a high-resolution composite chronology from lacustrine and terrestrial deposits. *The Holocene* **4**: 269-277.

Dahl, O. and Nesje, A. 1996. A new approach to calculating Holocene winter precipitation by combining glacier equilibrium-line altitudes and pine-tree limits: a case study from Hardangerjøkulen, central southern Norway. *The Holocene* **6**(4): 381-398.

Dahl, O., Nesje, A., Øyvind, L., Fjordheim, K. and Matthews, J. A. 2002. Timing, equilibrium-line altitudes and climatic implications of two early-Holocene glacier readvances during the Erdalen Event at Jostedalsbreen, western Norway. *The Holocene* **12**(1): 17-25.

Dai, F. C., Lee, C. F. and Wang, S. J. 2003. Characterization of rainfall-induced landslides. *International Journal of Remote Sensing* **24**(23): 4817-4834.

Dansgaard, W., Johnsen, S., Clausen, H., Dahl-Jensen, D., Gundestrup, N., Hammer, C., Hvidberg, C., Steffensen, J., Sveinbjornsdottir, A., Jouzel, J. and Bond, G. 1993. Evidence for general instability of past climate from a 250 kyr ice-core record. *Nature* **264**: 218-220.

Dansgaard, W., White, J. and Johnsen, S. 1989. The abrupt termination of the Younger Dryas climate event. *Nature* **339**(532-533).

Davies, S. M., Branch, N. P., Lowe, J. J. and Turney, C. S. M. 2002. Towards a European tephrochronological framework for Termination 1 and the Early Holocene. *Philosophical Transactions of the Royal Society of London* **360**: 767-802.

Davies, S. M., Wastegard, S. and Wohlfarth, B. 2003. Extending the limits of the Borrobol Tephra to Scandinavia and detection of new early Holocene tephras. *Quaternary Research* **59**(3): 345-352.

Dugmore, A., Larsen, G. and Newton, A. 1995. Seven tephra isochrones in Scotland. *The Holocene* **5**(3): 257-266.

Dugmore, A. and Newton, A. 1992a. Thin tephra layers in peat revealed by X-radiography. *Journal of Archaeological Science* **19**(2): 163-170.

Dugmore, A. and Newton, A. 1997. Holocene tephra layers in the Faroe Islands. *Frodskaparrit* **45**: 141-154.

Dugmore, A., Newton, A. and Sugden, D. 1992b. Geochemical stability of fine-grained silicic Holocene tephra in Iceland and Scotland. *Journal of Quaternary Science* **7**(2): 173-183.

Eiríksson, J., Knudsen, K. L., Haflidason, H. and Henriksen, P. 2000. Late-glacial and Holocene palaeoceanography of the North Iceland shelf. *Journal of Quaternary Science* **15**(1): 23-42.

Everest, J. and Bradwell, T. 2003. Buried glacier ice in southern Iceland and its wider significance. *Geomorphology* **52**(3-4): 347-358.

Fisher, T. G., Smith, D. G. and Andrews, J. T. 2002. Preboreal oscillation caused by a glacial Lake Agassiz flood. *Quaternary Science Reviews* **21**(8-9): 873-878.

Flageollet, J.-C., Maquaire, O., Martin, B. and Weber, D. 1999. Landslides and climatic conditions in the Barcelonnette and Vars basins (Southern French Alps, France). *Geomorphology* **30**(1-2): 65-78.

Gasse, F. 2000. Hydrological changes in the African tropics since the Last Glacial Maximum. *Quaternary Science Reviews* **19**(1-5): 189-211.

Gasse, F., Fontes, J. C., Van Campo, E. and Wei, K. 1996. Holocene environmental changes in Bangong Co basin (Western Tibet). Part 4: Discussion and conclusions. *Palaeogeography, Palaeoclimatology, Palaeoecology* **120**(1-2): 79-92.

Glasser, N. F. and Hambrey, M. J. 2002. Sedimentary facies and landform genesis at a temperate outlet glacier: Soler Glacier, North Patagonian Icefield. *Sedimentology* **49**(1): 43-64.

Glasser, N. F., Harrison, S., Winchester, V. and Aniya, M. 2004. Late Pleistocene and Holocene palaeoclimate and glacier fluctuations in Patagonia. *Global and Planetary Change* **43**(1-2): 79-101.

GRIP.Members 1993. Climate instability during the last interglacial period recorded in the GRIP ice core. *Nature.* **364**: 203-207.

Grönvold, K., Óskarsson, N., Johnsen, S. J., Clausen, H. B., Hammer, C. U., Bond, G. and Bard, E. 1995. Ash layers from Iceland in the Greenland GRIP ice core correlated with oceanic and land sediments. *Earth and Planetary Science Letters* **135**(1-4): 149-155.

Grootes, P. M., Steig, E. J., Stuiver, M., Waddington, E. D., Morse, D. L. and Nadeau, M.-J. 2001. The Taylor Dome Antarctic 18O Record and Globally Synchronous Changes in Climate. *Quaternary Research* **56**(3): 289-298.

Grootes, P. M., Stuiver, M., White, J., Johnsen, S. and Jouzel, J. 1993. Comparison of oxygen isotope records from the GISP2 and GRIP Greenland ice cores. *Nature* **366**: 552-554.

Grove, J. 2001. The Initiation of the "Little Ice Age" in Regions Round the North Atlantic. *Climatic Change* **48**(1): 53-82.

Gudmundsson, H. J. 1997. A review of the Holocene environmental history of Iceland. *Quaternary Science Reviews* **16**(1): 81-92.

Gulliksen, S., Birks, H., Possnert, G. and Mangerud, J. 1998. A calendar age estimate of the Younger Dryas-Holocene boundary at Kråkenes, western Norway. *The Holocene* **8**(3): 249-259.

Gupta, A. K., Anderson, D. M. and Overpeck, J. T. 2003. Abrupt changes in the Asian southwest monsoon during the Holocene and their links to the North Atlantic Ocean. *Nature* **421**(6921): 354-357.

Gyte, N. (2005). School of Geosciences. Edinburgh, University of Edinburgh.

Haas, J., Richoz, I., Tinner, W. and Wick, L. 1998. Synchronous Holocene climatic oscillations recorded on the Swiss Plateau and at timberline in the Alps. *The Holocene* **8**(3): 301-309.

Haflidason, H., Eiriksson, J. and Van Kreveld, S. 2000. The tephrochronology of Iceland and the North Atlantic region during the Middle and Late Quaternary: a review. *Journal of Quaternary Science* **15**(1): 3-22.

Haflidason, H., Sejrup, H., Klitgaard-Kristensen, D. and Johnsen, S. 1995. Coupled response of the late glacial climatic shifts of northwest Europe reflected in Greenland ice cores: Evidence from the northern North Sea. *Geology* **23**(12): 1059-1062.

Hall, V. and Pilcher, J. 2002. Late-Quaternary Icelandic tephras in Ireland and Great Britain: detection, characterization and usefulness. *The Holocene* **12**: 223-230.

Ham, N. R. and Attig, J. W. 1996. Ice wastage and landscape evolution along the southern margin of the Laurentide Ice Sheet, north-central Wisconsin. *Boreas* **25**(3): 171-186.

Hammarlund, D., Bjorck, S., Buchardt, B., Israelson, C. and Thomsen, C. T. 2003. Rapid hydrological changes during the Holocene revealed by stable isotope records of lacustrine carbonates from Lake Igelsjon, southern Sweden. *Quaternary Science Reviews* **22**(2-4): 353-370.

Hannon, G., Hermanns-Audardottir, M. and Wastegard, S. 1998. Human impact at Tjornvik in the Faroe Islands. *Frodskaparrit* **46**: 215-228.

Hansen, B. C. S. and Engstrom, D. R. 1996. Vegetation History of Pleasant Island, Southeastern Alaska, since 13,000 yr B.P. *Quaternary Research* **46**(2): 161-175.

Heusser, C. J. 1995. Three Late Quaternary pollen diagrams from Southern Patagonia and their palaeoecological implications. *Palaeogeography, Palaeoclimatology, Palaeoecology* **118**(1-2): 1-24.

Hewitt, K. 1999. Quaternary Moraines vs Catastrophic Rock Avalanches in the Karakoram Himalaya, Northern Pakistan*1. *Quaternary Research* **51**(3): 220-237.

Hjartarson, Á. and Ingólfsson, Ó. 1988. Preboreal Glaciation of Southern Iceland. *Jökull* **38**: 1-13.

Holm, K., Bovis, M. and Jakob, M. 2004. The landslide response of alpine basins to post-Little Ice Age glacial thinning and retreat in southwestern British Columbia. *Geomorphology* **57**(3-4): 201-216.

Hu, F. S., Slawinski, D., Wright, H. E., Jr, Ito, E., Johnson, R. G., Kelts, K. R., McEwan, R. F. and Boedigheimer, A. 1999. Abrupt changes in North American climate during early Holocene times. *Nature* **400**(6743): 437-440.

Huang, C. C., Pang, J. and Huang, P. 2002. An early Holocene erosion phase on the loess tablelands in the southern Loess Plateau of China. *Geomorphology* **43**(3-4): 209-218.

Hulton, N., Sugden, D. and Purves, R. 2003. The role of icesheet/climate models in Quaternary research. *Quaternary Science Reviews* **22**(5-7): 755-757.

Ingólfsson, Ó., Björck, S., Haflidason, H. and Rundgren, M. 1997. Glacial and climatic events in Iceland reflecting regional North Atlantic climatic shifts during the pleistocene-holocene transition. *Quaternary Science Reviews* **16**(10): 1135-1144.

Ingólfsson, Ó. and Norðdahl, H. 1994. A review of the environmental history of Iceland, 13,000-9000 yr BP. *Journal of Quaternary Science* **9**: 147-150.

Ingólfsson, Ó., Norðdahl, H. and Haflidason, H. 1995. Rapid isostatic rebound in southwestern Iceland at the end of the last glaciation. *Boreas* **24**: 245-259.

Iverson, R., Reid, M., Iverson, N., LaHousen, R., Logan, M., Mann, J. and Brien, D. 2000. Acute sensitivity of Landslide Rates to Initial Soil Porosity. *Science* **290**: 513-516.

Jansson, P. and Fredin, O. 2002. Ice sheet growth under dirty conditions: implications of debris cover for early glaciation advances. *Quaternary International* **95-96**: 35-42.

Johannesson, H. and Saemundsson, K. Geological Map of Iceland, Icelandic Institute of Natural History.

Johnsen, S. 1992. Irregular glacial interstadials recorded in a new Greenland ice core. *Nature* **359**: 311-313.

Johnsen, S., Dahl-Jensen, D., Gundestrup, N., Steffensen, J., Clausen, H., Miller, H., Masson-Delmotte, V., Sveinbjörnsdottir , A. and White, J. 2001. Oxygen isotope and palaeotemperature records from six Greenland ice-core stations: Camp Century, Dye-3, GRIP, GISP2, Renland and NorthGRIP. *Journal of Quaternary Science* **16**(4): 299-307.

Johnsen, S. J., Clausen, H. B., Dansgaard, W., Gundestrup, N. S., Hammer, C. U., Shoji, U., Sveinbjörnsdóttir, A., White, J. W. C., Jouzel, J. and Fisher, D.

1997. The d18O record along the Greenland Ice Core Pproject deep ice core and the problem of possible Eemian climatic instability. *Journal of Geophysical Research* **102**: 26397-26410.

Kaldal, I. and Vikingsson, S. 1991. Early Holocene deglaciation in Central Iceland. *Jökull* **40**: 51-66.

Karlén, W. 1976. lacustrine sediments and tree-limit variations as indicators of Holocene climatic fluctuations in Lappland, Northern Sweden. *Geografiska Annaler* **58A**: 1-34.

Kirkbride, M. 1989. About the concepts of continuum and age. *Boreas* **18**: 87-88.

Kirkbride, M. 1995. Ice flow vectors on the debris-mantled Tasman glacier, 1957-1986. *Geografiska Annaler* **77A**(3): 147-157.

Kirkbride, M. and Dugmore, A. 2001. Timing and significance of Mid-Holocene glacier advances in northern and central Iceland. *Journal of Quaternary Science* **16**(2): 145-153.

Kjær, K. H. and Krüger, J. 2001. The final phase of dead-ice moraine development: processes and sediment architecture, Kötlujökull, Iceland. *Sedimentology* **48**(5): 935-952.

Klitgaard-Kristensen, D., Sejrup, H., Halfidson, H., Johnsen, S. and Spurk, M. 1998. A regional 8200 cal. yr BP cooling event in northwest Europe, induced by final stages of the Laurentide ice-sheet deglaciation? *Journal of Quaternary Science* **13**: 165-169.

Kneller, M. and Peteet, D. 1999. Late-Glacial to Early Holocene Climate Changes from a Central Appalachian Pollen and Macrofossil Record*1. *Quaternary Research* **51**(2): 133-147.

Knudsen, K. L. and Eiriksson, J. 2002. Application of tephrochronology to the timing and correlation of palaeoceanographic events recorded in Holocene and Late Glacial shelf sediments off North Iceland. *Marine Geology* **191**(3-4): 165-188.

Korhola, A., Weckstrom, J., Holmstrom, L. and Erasto, P. 2000. A Quantitative Holocene Climatic Record from Diatoms in Northern Fennoscandia. *Quaternary Research* **54**(2): 284-294.

Kurek, J., Cwynar, L. C. and Spear, R. W. 2004. The 8200 cal yr BP cooling event in eastern North America and the utility of midge analysis for Holocene temperature reconstructions. *Quaternary Science Reviews* **23**(5-6): 627-639.

Lacasse, C. 2001. Influence of climate variability on the atmospheric transport of Icelandic tephra in the subpolar North Atlantic. *Global and Planetary Change* **29**(1-2): 31-55.

Lacasse, C., Werner, R., Paterne, M., Sigurdsson, H., Carey, S. and Pinte, G. 1998. Long-range transport of Icelandic tephra to the Irminger basin, site 919. *Proceedings of the Ocean Drilling Program, Scientific Results* **132**: 52-65.

Laird, K., Fritz, S., Cumming, B. and Grimm, E. 1998. Early-Holocene limnological and climatic variability in the Northern Great Plains. *The Holocene* **8**(3): 275-285.

Lamb, H., Gasse, F., Benkaddour, A., El Hamouti, N., van der Kaars, S., Perkins, W. T., Pearce, N. J. and Roberts, C. N. 1995. Relation between century-scale Holocene arid intervals in tropical and temperate zones. *Nature* **373**: 134-137.

Larsen, G. (2000). Holocene Volcanism in Iceland and Tephrochronology as a tool in Volcanology. Iceland 2000, Modern Processes and Past Environments, Keele University.

Larsen, G., Dugmore, A. and Newton, A. 1999. Geochemistry of historical-age silicic tephras in Iceland. *The Holocene* **9**(4): 463-471.

Larsen, G., Gudmundsson, H. J. and Björnsson, H. 1998. Eight centuries of periodic volcanism at the center of the Iceland hotspot revealed by glacier tephrostratigraphy. *Geology* **26**(10): 943-946.

Larsen, G., Newton, A., Dugmore, A. and Vilmundardottir, E. 2001. Geochemistry, dispersal, volumes and chronology of Holocene silicic tephra layers from the Katla volcanic system, Iceland. *Journal of Quaternary Science* **16**(2): 119-132.

Lehmkuhl, F. 1997. Late Pleistocene, Late-Glacial and Holocene glacier advances on the Tibetan Plateau. *Quaternary International* **38/39**: 77-83.

Lowe, J. and Turney, C. 1997. Vedde Ash layer discovered in a small lake basin on the Scottish mainland. *Journal of the Geological Society, London* **154**(4): 605-612.

Magri, D. and Parra, I. 2002. Late Quaternary western Mediterranean pollen records and African winds. *Earth and Planetary Science Letters* **200**(3-4): 401-408.

Mann, D. H. and Hamilton, T. D. 1995. Late Pleistocene and Holocene paleoenvironments of the North Pacific coast. *Quaternary Science Reviews* **14**(5): 449-471.

Markgraf, V. 1993. Palaeoenvironments and palaeoclimates in Tierra del Fuego and southernmost Patagonia, South America. *Palaeogeography, Palaeoclimatology, Palaeoecology* **102**: 53-68.

Markgraf, V., Bradbury, J. P., Schwalb, A., Burns, S. J., Stern, C., Ariztegui, D., Gilli, A., Anselmetti, F. S., Stine, S. and Maidana, N. 2003. Holocene palaeoclimates of southern Patagonia: limnological and environmental history of Lago Cardiel, Argentina. *The Holocene* **13**(4): 581-591.

Markgraf, V., Webb, R. S., Anderson, K. H. and Anderson, L. 2002. Modern pollen/climate calibration for southern South America. *Palaeogeography, Palaeoclimatology, Palaeoecology* **181**(4): 375-397.

Martin, H. E., Whalley, W. B. and Caseldine, C. (1991). Glacier fluctuations and rock glaciers in Trollaskagi, Northern Iceland, with special reference to 1946-1986. Environmental Change in Iceland: Past and Present. J. K. Maizels and C. Caseldine. Netherlands, Kluwer Academic Press: 255-265.

Masson, V., Vimeux, F., Jouzel, J., Morgan, V., Delmotte, M., Ciais, P., Hammer, C., Johnsen, S., Lipenkov, V. Y. and Mosley-Thompson, E. 2000. Holocene Climate Variability in Antarctica Based on 11 Ice-Core Isotopic Records. *Quaternary Research* **54**(3): 348-358.

Matthews, J. A., Dahl, O., Nesje, A., Berrisford, M. S. and Andersson, C. 2000. Holocene glacier variations in central Jotunheimen, southern Norway based on distal glaciolacustrine sediment cores*1. *Quaternary Science Reviews* **19**(16): 1625-1647.

Matthews, J. A. and Shakesby, R. A. 2004. A twentieth-century neoparaglacial rock topple on a glacier foreland, Ötztal Alps, Austria. *The Holocene* **14**(3): 454-458.

McDermott, F., Frisia, S., Huang, Y., Longinelli, A., Spiro, B., Heaton, T. H. E., Hawkesworth, C. J., Borsato, A., Keppens, E. and Fairchild, I. J. 1999. Holocene climate variability in Europe: Evidence from [delta]18O, textural and extension-rate variations in three speleothems. *Quaternary Science Reviews* **18**(8-9): 1021-1038.

McDermott, F., Mattey, D. P. and Hawkesworth, C. 2001. Centennial-Scale Holocene Climate Variability Revealed by a High-Resolution Speleothem delta 18O Record from SW Ireland. *Science* **294**(5545): 1328-1331.

Menounos, B., Koch, J., Osborn, G., Clague, J. J. J. J. and Mazzucchi, D. 2004. Early Holocene glacier advance, southern Coast Mountains, British Columbia, Canada. *Quaternary Science Reviews* **23**(14-15): 1543-1550.

Mikolajewicz, U., Crowley, T., Schiller, A. and Voss, R. 1997. Modelling teleconnections between the North Atlantic and North Pacific during the Younger Dryas. *Nature* **387**: 384-387.

Moreno, P. I. 2004. Millenial-scale climate variability in northwest Patagonia over the last 15 000 yr. *Journal of Quaternary Science* **19**(1): 35-47.

Muscheler, R., Beer, J. and Vonmoos, M. 2004. Causes and timing of the 8200 yr BP event inferred from the comparison of the GRIP 10Be and the tree ring [Delta]14C record. *Quaternary Science Reviews* **23**(20-22): 2101-2111.

Nakawo, M. and Rana, B. 1999. Estimate of ablation rate of glacier ice under a supraglacial debris layer. *Geografiska Annaler* **81A**(4): 695-701.

Neff, U., Burns, S. J., Mangini, A., Mudelsee, M., Fleitmann, D. and Matter, A. 2001. Strong coherence between solar variability and the monsoon in Oman between 9 and 6k yr ago. *Nature* **411**(6835): 290-293.

Nesje, A. and Dahl, O. 2001a. The Greenland 8200 cal. yr BP event detected in loss-on-ignition profiles in Norwegian lacustrine sediment sequences. *Journal of Quaternary Science* **16**(2): 155-166.

Nesje, A., Dahl, O., Andersson, C. and Matthews, J. A. 2000. The lacustrine sedimentary sequence in Sygneskardvatnet, western Norway: a continuous, high-resolution record of the Jostedalsbreen ice cap during the Holocene. *Quaternary Science Reviews* **19**(11): 1047-1065.

Nesje, A., Matthews, J. A., Dahl, O., Berrisford, M. S. and Andersson, C. 2001b. Holocene glacier fluctuations of Flatebreen and winter-precipitation changes in the Jostedalsbreen region, western Norway, based on glaciolacustrine sediment records. *The Holocene* **11**(3): 267-280.

Norðdahl, H. 1990. Late Weichselian and Early Holocene deglaciation history of Iceland. *Jökull* **40**: 27-48.

Norðdahl, H. 1991. Late Weichselian and Early Holocene deglaciation history of Iceland. *Jökull* **40**: 27-48.

Norðdahl, H. and Einarsson, T. 2001. Changes of relative sea-level and glacier extent at the Weichselian-Holocene boundary at Berufjörður, Eastern Iceland. *Quaternary Science Reviews* **20**: 1607-1622.

Norðdahl, H. and Hjort, C. 1993. Lateglacial raised beaches and glacier recession in the Þistilfjörður-Bakkaflói area, Northeast Iceland. *Jökull* **43**: 33-44.

Nott, J., Bryant, E. and Price, D. 1999. Early-Holocene aridity in tropical northern Australia. *The Holocene* **9**(2): 231-236.

Ocakoglu, F., Gokceoglu, C. and Ercanoglu, M. 2002. Dynamics of a complex mass movement triggered by heavy rainfall: a case study from NW Turkey. *Geomorphology* **42**: 329-341.

Ogilvie, A. and Jónsson, T. 2001. "Little Ice Age" Research: A Perspective from Iceland. *Climatic Change* **48**(1): 9-52.

Palmer, S., Walker, I., Heinrichs, M., Hebda, R. and Scudder, G. 2002. Postglacial midge community change and Holocene palaeotemperature reconstructions near treeline, Southern British Columbia (Canada). *Journal of Paleolimnology* **28**: 469-490.

Pellatt, M. G., Hebda, R. J. and Mathewes, R. W. 2001. High-resolution Holocene vegetation history and climate from Hole 1034B, ODP leg 169S, Saanich Inlet, Canada. *Marine Geology* **174**(1-4): 211-222.

Pendall, E., Markgraf, V., White, J. W. C., Dreier, M. and Kenny, R. 2001. Multiproxy Record of Late Pleistocene-Holocene Climate and Vegetation Changes from a Peat Bog in Patagonia. *Quaternary Research* **55**(2): 168-178.

Pilcher, J. and Hall, V. 1996a. Tephrochronological studies in northern England. *The Holocene* **6**(1): 100-105.

Pilcher, J., Hall, V. and McCormac, F. 1995. Dates of Holocene Icelandic volcanic eruptions from tephra layers in Irish peats. *The Holocene* **5**(1): 103-110.

Pilcher, J., Hall, V. and McCormac, F. 1996b. An outline tephrochronology for the Holocene of the north of Ireland. *Journal of Quaternary Science* **11**(6): 485-494.

Porter, S. and Zhisheng 1995. Correlation between climate events in the North Atlantic and China during the last glaciation. *Nature* **375**: 305-308.

Porter, S. C. 2001. Chinese loess record of monsoon climate during the last glacial-interglacial cycle. *Earth-Science Reviews* **54**(1-3): 115-128.

Ramirez, E., Hoffmann, G., Taupin, J. D., Francou, B., Ribstein, P., Caillon, N., Ferron, F. A., Landais, A., Petit, J. R. and Pouyaud, B. 2003. A new Andean deep ice core from Nevado Illimani (6350 m), Bolivia. *Earth and Planetary Science Letters* **212**(3-4): 337-350.

Renssen, H., Goose, H., Fichefet, T. and Campin, J. M. 2001. The 8.2 kyr BP event simulated by a global atmosphere-sea-ocean model. *Geophysical Research Letters* **28**(8): 1567-1570.

Rousseau, D.-D., Limondin, N., Magnin, F. and Puissegur, J.-J. 1994. Temperature oscillations over the last 10,000 years in western Europe estimated from terrestrial mollusc assemblages. *Boreas* **23**: 66-73.

Rousseau, D.-D., Limondin, N. and Puissegur, J.-J. 1993. Holocene Environmental Signals from Mollusk Assemblages in Burgundy (France). *Quaternary Research* **40**(2): 237-253.

Rousseau, D.-D., Preece, R. and Limondin-Lozouet, N. 1998. British late glacial and Holocene climatic history reconstructed from land snail assemblages. *Geology* **26**(7): 651-654.

Rowbotham, D. N. and Dudycha, D. 1998. GIS modelling of slope stability in Phewa Tal watershed, Nepal. *Geomorphology* **26**(1-3): 151-170.

Rundgren, M., Ingólfsson, Ó., Björck, S., Jiang, H. and Haflidason, H. 1997. Dynamic sea-level change during the last deglaciation of northern Iceland. *Boreas* **26**: 201-215.

Saemundsson, T., Petursson, H. and Decauline, A. (2003). Triggering factors for rapid mass movement in Iceland. Debris-flow hazards mitigation: Mechanims, Prediction and Assessment. Rickenmann and Chen. Rotterdam, Millpress: 167-178.

Scheidegger, A. E. 1998. Tectonic predesign of mass movements, with examples from the Chinese Himalaya. *Geomorphology* **26**(1-3): 37-46.

Seierstad, J., Nesje, A., Dahl, S. O. and Simonsen, J. R. 2002. Holocene glacier fluctuations of Grovabreen and Holocene snow-avalanche activity reconstructed from lake sediments in Grøningstølsvatnet, western Norway. *The Holocene* **12**(2): 211-222.

Seppä, H., Cwynar, L. and MacDonald, G. 2003. Post-glacial vegetation reconstruction and a possible 8200 cal. yr BP event from the low arctic of continental Nunavut, Canada. *Journal of Quaternary Science* **18**(7): 621-629.

Sharp, M. 1985. "Crevasse-Fill" Ridges: A landform type characteristic of surging glaciers? *Geografiska Annaler* **67**(3/4): 213-220.

Shroder, J. F., Bishop, M. P., Copland, M. P. and Sloan, V. F. 2000. Debris-covered glaciers and rock glaciers in the Nanga Parbat Himalaya, Pakistan. *Geografiska Annaler* **82A**(1): 17-31.

Sletten, K., Blikra, L. H., Ballantyne, C. K., Nesje, A. and Dahl, S. O. 2003. Holocene debris flows recognized in a lacustrine sedimentary succession: sedimentology, chronostratigraphy and cause of triggering. *The Holocene* **13**(6): 907-920.

Snowball, I., Zillén, L. and Gaillard, M.-J. 2002. Rapid early-Holocene environmental changes in northern Sweden based on studies of two varved lake-sediment sequences. *The Holocene* **12**(1): 7-16.

Soldati, M., Corsini, A. and Pasuto, A. 2004. Landslides and climate change in the Italian Dolomites since the Late glacial. *CATENA* **55**(2): 141-161.

Stager, J. C., Cumming, B. F. and Meeker, L. D. 2003. A 10,000-year high-resolution diatom record from Pilkington Bay, Lake Victoria, East Africa. *Quaternary Research* **59**(2): 172-181.

Street-Perrot, F. and Perrott, R. 1990. Abrupt climate fluctuations in the tropics: the influence of Atlantic Ocean circulation. *Nature* **343**: 607-612.

Stuiver, M. and Reimer, P. J. 1993. Extended 14C data base and revised radiocarbon age calibration program. *Radiocarbon* **35**: 215-230.

Stuiver, M., Reimer, P. J., Bard, E., Beck, J. W., Burr, G. S., Hughen, K. A., Kromer, B., McCormac, G., Van Der Plicht, J. and Spurk, M. 1998. INTCAL98 radiocarbon age calibration, 24,000-0 cal BP. *Radiocarbon* **40**(3): 1041-1083.

Summerfield, M. A. (1997). Global Geomorphology. Singapore, Longman.

Sveinbjörnsdóttir, A. and Johnsen, S. 1990. The late glacial history of Iceland. Comparison with isotopic data from Greenland and Europe, and deep sea sediments. *Jökull* **40**: 83-96.

Taylor, F., Whitehead, J. and Domack, E. 2001. Holocene paleoclimate change in the Antarctic Peninsula: evidence from the diatom, sedimentary and geochemical record. *Marine Micropaleontology* **41**(1-2): 25-43.

Teller, J. T. and Leverington, D. W. 2003. Glacial Lake Agassiz: A 5000 yr history of change and its relationship to the ?18O record of Greenland. *Geological Society of America Bulletin* **116**(5): 729-742.

Thompson, L., Mosley-Thompson, E. and Henderson, K. 2000. Ice-core palaeoclimate records in tropical South America since the Last Glacial Maximum. *Journal of Quaternary Science* **15**(4): 377-394.

Thompson, L. G., Davis, M. E., Mosley-Thompson, E., Sowers, T. A., Henderson, K. A., Zagorodnov, V. S., Lin, P.-N., Mikhalenko, V. N., Campen, R. K., Bolzan, J. F., Cole-Dai, J. and Francou, B. 1998. A 25,000-Year Tropical Climate History from Bolivian Ice Cores. *Science* **282**(5395): 1858-1864.

Thompson, L. G., Yao, T., Davis, M. E., Henderson, K. A., Mosley-Thompson, E., Lin, P.-N., Beer, J., Synal, H.-A., Cole-Dai, J. and Bolzan, J. F. 1997. Tropical Climate Instability: The Last Glacial Cycle from a Qinghai-Tibetan Ice Core. *Science* **276**(5320): 1821-1825.

Thorarinsson, S. 1958. The Öræfajökull eruption of 1362. *Acta Naturalia Islandica* **II**(2): 1-99.

Thórarinsson, S. 1944. Tefrokronologiska studier på Island. *Geografiska Annaler* **26**: 1-217.

Thórarinsson, S. 1979. Tephrochronology and its application in Iceland. *Jökull* **29**: 33-36.

Thórarinsson, S. (1981). The application of tephrochronology in Iceland. Proceedings of the NATO advanced Study Institute "Tephra Studies as a Tool in Quaternary Research", Laugarvatn and Reykjavik, Iceland, D. Reidel Publishing Company.

Trauth, M. H., Alonso, R. A., Haselton, K. R., Hermanns, R. L. and Strecker, M. R. 2000. Climate change and mass movements in the NW Argentine Andes. *Earth and Planetary Science Letters* **179**(2): 243-256.

Van Campo, E., Cour, P. and Sixuan, H. 1996. Holocene environmental changes in Bangong Co basin (Western Tibet). Part 2: The pollen record. *Palaeogeography, Palaeoclimatology, Palaeoecology* **120**(1-2): 49-63.

Van Campo, E. and Gasse, F. 1993. Pollen- and Diatom-Inferred Climatic and Hydrological Changes in Sumxi Co Basin (Western Tibet) since 13,000 yr B.P. *Quaternary Research* **39**(3): 300-313.

van den Bogaard, C. and Schmincke, H. 2002. Linking the North Atlantic to central Europe: a high-resolution Holocene tephrochronological record from northern Germany. *Journal of Quaternary Science* **17**(1): 3-20.

Varnes, D. (1978). Slope Movement Types and Processes. Landslides: Analysis and Control. R. Schuster and R. Krizek. Washington D.C., National Research Council. **Special Report 176**.

Von Grafenstein, U., Erlenkeuser, H., Muller, J., Jouzel, J. and Johnsen, S. 1998. The cold event 8200 years ago documented in oxygen isotope records of precipitation in Europe and Greenland,. *Climate Dynamics* **14**: 73-81.

Wagner, F., Aaby, B. and Visscher, H. 2002. Rapid atmospheric CO2 changes associated with the 8,200-years-B.P. cooling event. *Proceedings of the National Academy of Sciences* **99**(19): 12011-12014.

Wastegård, S. 2002. Early to middle Holocene silicic tephra horizons from the Katla volcanic system, Iceland: new results from the Faroe Islands. *Journal of Quaternary Science* **17**(8): 723-730.

Wastegård, S., Björck, S., Grauert, M. and Hannon, G. 2001. The Mjáuvøtn tephra and other Holocene tephra horizons from the Faroe Islands: a link between

the Icelandic source region, the Nordic Seas, and the European continent. *The Holocene* **11**(1): 101-109.

Wieczorek, G. (1996). Landslide Triggering Mechanisms. Landslides: Investigation and Mitigation. R. Schuster. Washington, National Academy Press: 76-90.

Winn, K., Sarnthein, M. and Erlenkeuser, H. 1991. 180 stratigraphy and age control of Kiel sediment cores in the east Atlantic. *Ber. Rep. -Paläontol. Inst. Univ. Kiel* **45**: 99 pp.

Yi, S., Saito, Y., Zhao, Q. and Wang, P. 2003. Vegetation and climate changes in the Changjiang (Yangtze River) Delta, China, during the past 13,000 years inferred from pollen records. *Quaternary Science Reviews* **22**(14): 1501-1519.

Zahn, R. 2003. Global Change: Monsoon Linkages. *Nature* **421**: 324-325.

Zhang, H. C., Ma, Y. Z., Wunnemann, B. and Pachur, H.-J. 2000. A Holocene climatic record from arid northwestern China. *Palaeogeography, Palaeoclimatology, Palaeoecology* **162**(3-4): 389-401.

Zillen, L. M., Wastegard, S. and Snowball, I. 2002. Calendar year ages of three mid-Holocene tephra layers identified in varved lake sediments in west central Sweden. *Quaternary Science Reviews* **21**(14): 1583-1591.

APPENDIX I: Summary of recorded environmental change around the time of the 8.2ka event (references, type of proxy, resolution, timing, expression)

Region	*References*	*Type of record*	*Resolution*	*Dates (cal. ka BP)*	*Description/Climatic Conditions*
Greenland	Alley et al., 1997 Johnsen et al., 1992 Dansegaard, 1987	Ice core Ice core Ice core	High High High	Peak: 8.25 Peak: 8.21+/- 0.03 Peak: 8.23+/- 0.05	• Cold (Temperature drop of 4-8°C) • Dry (20% drop in accumulation) • Windy (increase in windblown chemical indicators) • Drop in atmospheric methane concentrations
Scandinavia	Dahl & Nesje (1994; 1996; 2001)	Glacier advance	Medium	3 ice advances: 8.4, 8.4-8 and 8.5-8.3	• Named the "Finse Event" • Cold & wet • Hardagnerjøkulen glacial advance • Changing pine tree limits
	Seierstad et al., 2002 Nesje et al., 2000	Lacustrine Lacustrine	Medium Medium	~8.44-7.88 3 advances: 8.5, 8.4 & 8.2	• Cold: Glacial advance inferred from Grøningstølsvatnet (Seierstad et al., 2002) and Sygneskardvatnet (Nesje et al., 2000) lake sediments.
	Matthews et al., 2000	Glacier advance	Medium	8.4-8	• Cold: Glacial advance episode on Smørstabbtinden massif
	Seierstad et al., 2002	Avalanche occurrence	Low	Peak: 8	• Cold: Increased snow avalanche activity recorded
	Korhola et. al., 2000	Lacustrine	Medium	8.45-8.15	• Cold: changes in tree-line inferred from lacustrine sediment core in Fennoscandian lake suggests temperature drop
	Snowball et al, 2002	Lacustrine Pollen	Medium	8-7.7	• Cold:Period of increased erosion – caused by increased snow in drainage basin

Scandinavia (continued)					during severe winters, and response of boreal forest to cooling
	Hammarlund et al, 2003	Lacustrine	Medium	8.3-8	• Cold: Isotope records reveal decreased evaporation due to cooler temperatures
	Karlen,1976	Glacial, Lacustrine and Pollen	Medium	8.575-8.375	• Cold: decrease in organic material, low pine tree limits and glacier advance (dated moraine limits)
	Barnett et al., 2001	Pollen	Medium	Peak: 8.38+/-0.164	• Cold: Decrease in arboreal pollen indicates tree-line movement to lower altitude
Europe (mainland)	von Grafenstein et al., 1998; 1999	Lacustrine	High	Peak: 8.2+/-0.13	• Cold: $\delta^{18}O$ ratios from the Amersee lakes, Germany
	Schettler et al, 1999	Lacustrine	Medium	8.5: Wet 8.1-7.3: Dry	• Wet phase followed by cold phase
	Haas et al, 1998	Lacustrine & Pollen	Medium	8.4-7.7	• Wet & Cold: increased precipitation and cooling inferred from tree pollens in the Swiss Alps
	Rousseau et al, 1993; 1994	Invertebrate	Medium	8.5-8	• Cold: temperature drop inferred from mollusc assemblages, France
	Wagner et al., 2002	Lacustrine (stomata)	Medium	8.4-8	• Cold: Temperature drop recorded in CO_2 levels, Denmark
	Magri & Parra, 2002	Pollen	Medium	Peak: 8.1	• Dry: Italian pollen records indicate deforestation in response to aridity phase and enhanced by increase in African

					winds in Mediterranean region.
UK & Ireland	Rousseau et al., 1998	Invertebrate	Medium	8.5-8	• Cold: temperature drop inferred from land snail assemblages, England
	McDermott et al., 2001	Speleothem	High	Peak: 8.32+/- 0.12	• Cold: Temperature drop inferred from stalagmite isotope records, Ireland
	Baldini et al., 2002	Speleothem	Very High (seasonal)	8.35+/- 0.08 – 8.31+/- 0.08 Peak: 8.33+/- 0.08	• Cold & Dry: Trace element record from western Ireland stalagmite shows evidence for decrease in precipitation, temperature & vegetation cover.
North Atlantic Sea	Klitgaard-Kristensen et al., 1998	Marine	High	Peak: 8.26+/- 0.06	• Cold: Marine isotope record calibrated against German tree-ring data & Greenland ice cores
	Bianchi & McCave, 1999	Marine	Medium	8.8-7.8+/- 0.3	• Faster/Colder ocean circulation: sediment grain-size data from the Iceland basin reconstruct changes in ocean circulation
	Andruleit & Baumann, 1998	Marine	Medium	Peak: 8.5	• Cold: decrease in coccolithophore assemblages in Eastern North Atlantic
Iceland	*Caseldine et al., 2003*	Lacustrine	ow	Around 8.2	• no conclusive biostratigraphic evidence for the 8.2ka event, but changes in some parameters may be an indicator or a response in vegetation

North America (East)	Hu et al., 1999	Lacustrine	Medium	8.9-8.3 Peak: 8.2	• Cold 8.9-8.3ka: $\delta^{18}O$ reversal representing a temperature drop,
	Laird et al., 1998	Lacustrine	Medium	9.8-7.95 Peak: 8.275+/- 0.125	• Dry 8.2: increase in varve thickness indicating increased aeolian activity due to drought
	Kneller and Peteet, 1999	Pollen	Medium	8.34+/- 0.11	• General climatic instability indicated by diatom salinity record showing several freshwater intervals
	Kurek et al., 2004	Lacustrine	Medium	8.4-8	• Cold & Wet: Macrofossils & pollen in Appalachians indicate colder climate & increased precipitation. • Cold: Drop in organic content at 2 White Mountain lakes, indicate temperature drop
North America (Central)	Seppä et al., 2003	Pollen/ Lacustrine	Medium	.1-7.9	• Cold: Sudden decline in *Betula* population, Northern Canada
North America (West)	Menounos et al, 2004	Glacio-lacustrine	Medium	8.63-8.02	• Cold: Glacial advance in BC, Western Canada
Tibet/China	Thompson et al, 1997	Ice core	High	Peak: 8.25	• Cold: $\delta^{18}O$ records from Guliya ice cap on the Quinghai-Tibetan plateau indicate temperature drop. (General trend in ice core record becomes more like South American records, getting cooler after 7ka)

Tibet/China (continued)	Van Campo and Gasse,1993	Pollen/ Lacustrine	Medium	8.95-8.57	• Dry: Sumxi Co, Tibet, lake record
	Gasse et al, 1996; Van Campo et al, 1996	Lacustrine	Medium	8.95-8.57	• Dry: Bangong Co, Tibet, lake record
	Zhang et al, 2000	Pollen	Low	8.45-7.95	• Dry: Increased aeolian transported material indicating dryer conditions, China
	Lehmkuhl, 1997	Glacial Advance	Low	9.175-7.865	• Glacial advances dated to this time and correlated with period of increased aeolian activity
	Yi et al, 2003	Pollen	Low	9-7.6	• Cold & Dry: inferred from Chinese Changjiang Delta records
Arabia	Gupta et.al, 2003	Marine	High	8.4-8	• Weakening of Asian Southwest monsoon recorded in shells from Arabian Sea sediment section.
	Neff et. al, 2001	Speleotherm	High	8.4-7.96	• Weakening of monsoon: isotope record form Omani speleothem indicates reduced precipitation
Tropical Africa	Street-Perrott and Perrott, 1990	Lacustrine	Low	8.9-8.7 9.1-7.9 9.5-7.5	• Dry: Low lake levels and low organic content recorded in 3 lake records in: • Ethiopia • Ghana • Kenya
	Stager, 2003	Lacustrine		8.3-7.8	• Dry: Diatom record from Lake Victoria shows dry phase & climatic reorganization following early Holocene humidity maximum.

Tropical Africa (continued)	Gasse, 2000	Lacustrine		8.5-7.8 8.5-8	• Dry: Lake Level records indicate dry phase widespread across tropical Africa. For example: • Lake Victoria, East Africa • Northern Sahara
Tropical Atlantic	Hughen et al, 1996	Marine	High	Peak: 8.2	• Cold: evidence in sediment record of Cariaco Basin
	Street-Perrott and Perrott, 1990	Lacustrine	Low	Peak: 8	• Dry: Low lake levels recorded in Lake Chalco, Mexico
Antarctic	Masson et al., 2000	Ice core	Medium	Peak: ~8+/-0.5, averaged. Separate peaks: 8 7.5 & 8.3 8.2 7.2 8.2	• Cold: Ice core isotope records from Eastern Antarctic show distinct isotope minimum about 8ka BP (averaged). Taken from 11 separate ice cores, including the following:
	Taylor et al., 2001	Marine	Medium	8.85 & 8.46	• Vostok • Komosomolkaia • Byrd • Law • Taylor • Cold & Windy: inferred from 2 phases of deposition of unusual diatom assemblages, Antarctic peninsula
Australia/NZ	Nott et al., 1999	Terrestrial sediments	Low	8-5.9ka	• Aridity inferred from period of dune formation
South America	Pendall et al., 2001	Pollen & Isotope	Medium	Peak: ~8 End: ~7.9, start date less clear +/-0.11	• Cold & Dry: Vegetation change indicates brief cooling episode during South American Holocene optimum, Patagonia

APPENDIX II: Geochemical Data

Full geochemical data for each analysed tephra sample is presented here. Where the eruption is known, its name is included at the top of each table, and where geochemistry and stratigraphy reveals possible genetic connections between layers from different profiles, these layers have been grouped. Geochemical tables are arranged with the youngest layers first as far as possible. Where four or more tephra grains are found with identifiably similar geochemistries, an average figure and standard deviation are presented for each element.

Askja 1875

Sample	*SiO2*	*TiO2*	*Al2O3*	*FeO*	*MnO*	*MgO*	*CaO*	*Na2O*	*K2O*	*Total*
Vik D-15										
	72.08	0.79	12.45	3.34	0.15	0.72	2.35	3.61	2.37	98.01
	72.313	0.782	12.466	3.191	0.12	0.624	2.307	3.562	2.411	97.907
	71.238	0.884	12.473	3.956	0.053	0.83	2.743	2.841	2.315	97.573
	73.046	0.727	12.247	3.221	0.065	0.628	2.296	3.386	2.373	98.179
	73.892	0.693	12.049	2.738	0.053	0.478	1.983	3.529	2.592	98.135
	73.483	0.738	12.043	3.134	0.08	0.614	2.159	3.755	2.37	98.514
	72.546	0.717	12.042	3.151	0.091	0.617	2.213	3.094	2.311	96.908
	72.857	0.801	12.012	3.209	0.11	0.626	2.257	3.763	2.448	98.239
	72.305	0.804	12.431	3.635	0.099	0.726	2.674	3.485	2.275	98.609
	73.253	0.779	12.14	3.321	0.044	0.679	2.369	3.798	2.472	99.006
	71.888	0.794	12.392	3.554	0.169	0.644	2.399	3.682	2.35	97.975
average	*72.63*	*0.77*	*12.25*	*3.31*	*0.09*	*0.65*	*2.34*	*3.50*	*2.39*	*98.10*
std dev	*0.735*	*0.050*	*0.186*	*0.301*	*0.039*	*0.084*	*0.206*	*0.284*	*0.085*	*0.525*

Veiðivötn 1477

Sample	*SiO2*	*TiO2*	*Al2O3*	*FeO*	*MnO*	*MgO*	*CaO*	*Na2O*	*K2O*	*Total*

Vik D-14	49.327	1.969	13.259	12.981	0.22	6.433	11.068	2.653	0.277	98.503
	49.368	1.903	13.458	12.693	0.196	6.69	11.248	2.458	0.23	98.552
	49.586	1.965	13.278	12.943	0.192	6.549	11.199	2.573	0.256	98.865
	49.597	1.976	13.42	13.093	0.221	6.467	10.991	2.407	0.205	98.647
	50.247	1.998	14.19	13.293	0.301	6.088	11.319	1.82	0.224	99.75
	49.981	2.008	13.477	13.444	0.224	6.387	11.174	1.981	0.264	99.232
	49.793	1.874	13.334	12.599	0.237	6.439	11.086	2.484	0.206	98.307
	49.372	1.938	13.528	13.007	0.24	6.511	11.101	2.551	0.252	98.768
	49.082	2.024	13.155	13.113	0.241	6.407	10.984	2.515	0.263	98.081
	48.669	2.214	13.95	11.911	0.23	6.71	11.285	2.681	0.327	98.274
average	*49.5022*	*1.9869*	*13.5049*	*12.9077*	*0.2302*	*6.4681*	*11.1455*	*2.4123*	*0.2504*	*98.6979*
std dev	*0.426731*	*0.08753*	*0.306885*	*0.407902*	*0.028509*	*0.165229*	*0.111903*	*0.270156*	*0.034783*	*0.469035*

Askja ~1300

Sample	*SiO2*	*TiO2*	*Al2O3*	*FeO*	*MnO*	*MgO*	*CaO*	*Na2O*	*K2O*	*Total*
Vik D-13...	73.588	0.665	12.014	2.877	0.072	0.598	1.981	3.038	2.387	97.352
	73.433	0.776	12.207	3.263	0.098	0.675	2.345	3.331	2.401	98.684
	73.18	0.758	12	3.053	0.112	0.598	2.091	2.955	2.366	97.272
	72.962	0.727	12.209	3.164	0.108	0.614	2.242	3.33	2.457	97.978
	72.795	0.768	12.222	3.353	0.089	0.646	2.453	3.755	2.374	98.626
	72.692	0.725	12.181	2.816	0.115	0.484	1.91	3.141	2.529	96.669
	72.567	0.783	12.006	3.396	0.125	0.646	2.279	3.659	2.364	98.007
	72.553	0.758	12.494	3.259	0.104	0.64	2.266	3.603	2.507	98.352
	71.904	0.806	12.143	3.29	0.07	0.583	2.321	3.608	2.558	97.493
	71.348	0.769	12.142	3.19	0.095	0.685	2.403	2.944	2.32	96.047
average	*72.7022*	*0.7535*	*12.1618*	*3.1661*	*0.0988*	*0.6169*	*2.2291*	*3.3364*	*2.4263*	*97.648*
std dev	*0.643019*	*0.037377*	*0.138443*	*0.184573*	*0.017011*	*0.054566*	*0.169917*	*0.291698*	*0.076866*	*0.808569*
	49.666	1.986	13.261	13.466	0.204	6.065	10.524	2.772	0.337	98.611

Brun B-3

Sample	*SiO2*	*TiO2*	*Al2O3*	*FeO*	*MnO*	*MgO*	*CaO*	*Na2O*	*K2O*	*Total*
Brun B-3..	48.427	2.401	13.362	12.188	0.262	6.38	11.117	2.768	0.304	97.597
	48.763	2.372	13.481	12.055	0.141	6.761	11.502	2.698	0.266	98.437
	48.845	2.348	13.371	12.109	0.202	6.582	11.249	2.781	0.332	98.146
	48.979	2.416	13.441	12.028	0.252	6.487	11.13	2.795	0.312	98.146
	49.115	2.827	13.031	13.462	0.124	5.82	10.177	2.851	0.468	98.335
	49.171	2.433	13.44	12.241	0.293	6.515	11.284	2.905	0.365	99.005
	49.172	2.502	13.122	12.608	0.143	6.632	11.286	2.66	0.298	98.76
	49.338	2.319	13.197	12.315	0.125	6.581	11.284	2.622	0.333	98.512
	49.347	2.374	13.545	11.652	0.16	6.988	11.391	2.69	0.261	98.764
average	*49.01744*	*2.443556*	*13.33222*	*12.29533*	*0.189111*	*6.527333*	*11.15778*	*2.752222*	*0.326556*	*98.41133*
std dev	*0.28145*	*0.144426*	*0.165483*	*0.477442*	*0.061341*	*0.299526*	*0.364214*	*0.087101*	*0.058743*	*0.397065*

Hekla 1158

Sample	*SiO2*	*TiO2*	*Al2O3*	*FeO*	*MnO*	*MgO*	*CaO*	*Na2O*	*K2O*	*Total*
Brun B-4	67.567	0.49	14.428	5.492	0.151	0.439	3.096	5.112	2.172	99.098
	67.324	0.463	14.416	5.617	0.233	0.438	3.075	5.181	2.099	98.945
	67.15	0.45	14.755	5.751	0.192	0.453	3.024	5.119	2.278	99.278
	67.148	0.374	14.319	5.43	0.189	0.42	2.906	4.82	2.162	97.878
	66.842	0.474	14.212	5.391	0.227	0.428	3.044	4.991	2.209	97.898
	66.784	0.398	14.397	5.641	0.16	0.438	3.066	5.282	2.095	98.376
	66.585	0.457	14.427	5.523	0.17	0.437	3.047	5.2	2.363	98.264
	66.524	0.441	14.27	5.58	0.148	0.473	3.01	5.137	2.458	98.098
	66.296	0.449	14.198	5.471	0.154	0.452	3.032	5.119	2.076	97.392
	65.804	0.456	14.615	5.338	0.189	0.409	3.062	5.073	2.117	97.22
average	*66.8024*	*0.4452*	*14.4037*	*5.5234*	*0.1813*	*0.4387*	*3.0362*	*5.1034*	*2.2029*	*98.2447*

std dev	*0.497681*	*0.032805*	*0.165378*	*0.119145*	*0.028893*	*0.017053*	*0.049616*	*0.119505*	*0.120388*	*0.660088*
La-A3	68.276	0.377	14.912	5.343	0.202	0.464	3.036	4.7	2.287	99.728
	68.133	0.446	12.93	6.206	0.183	0.49	2.543	4.842	2.431	98.32
	67.911	0.476	14.733	5.478	0.18	0.441	3.092	5.12	2.23	99.801
	67.718	0.464	14.355	5.536	0.199	0.442	3.073	4.91	2.166	98.995
	67.446	0.423	14.936	4.821	0.234	0.384	3.187	5.22	1.955	98.679
	66.801	0.408	14.499	5.419	0.218	0.402	3.021	5.207	2.25	98.324
	65.922	0.408	14.085	5.178	0.193	0.425	2.969	5.223	2.296	96.786
	65.913	0.364	15.247	4.867	0.032	0.341	3.324	5.976	2.124	98.3
	65.652	0.492	14.114	5.365	0.196	0.429	3.093	5.094	2.322	96.901
	64.89	0.432	13.785	5.376	0.177	0.441	2.956	4.778	2.125	95.036
average	*66.8662*	*0.429*	*14.3596*	*5.3589*	*0.1814*	*0.4259*	*3.0294*	*5.107*	*2.2186*	*98.087*
std dev	*1.137087*	*0.039431*	*0.639796*	*0.364877*	*0.052471*	*0.039775*	*0.191632*	*0.342731*	*0.12552*	*1.391734*
	48.987	1.555	13.74	10.777	0.031	7.395	12.456	2.317	0.224	97.749
	48.642	2.419	12.909	12.021	0.25	6.77	11.159	2.687	0.325	97.556
Borg E-2	68.189	0.497	14.02	6.149	0.199	0.463	2.784	4.813	2.388	99.602
	67.704	0.423	14.478	5.487	0.177	0.388	3.051	5.068	2.148	99.042
	67.543	0.49	14.639	5.819	0.136	0.428	3.051	4.897	2.344	99.461
	67.496	0.47	14.082	6.084	0.196	0.478	2.77	4.841	2.464	99.032
	67.442	0.464	14.493	5.379	0.145	0.44	2.932	5.042	2.286	98.771
	67.437	0.525	14.446	5.467	0.202	0.432	3.053	5.033	2.232	98.982
	67.353	0.487	14.499	5.585	0.123	0.44	2.996	4.961	2.134	98.636
	66.866	0.409	15.429	5.064	0.133	0.425	3.46	5.296	2.292	99.467
	63.174	0.403	13.596	4.895	0.158	0.358	2.616	3.898	2.064	91.24
average	*67.02267*	*0.463111*	*14.40911*	*5.547667*	*0.163222*	*0.428*	*2.968111*	*4.872111*	*2.261333*	*98.24811*
std dev	*1.398918*	*0.040098*	*0.475372*	*0.397606*	*0.029211*	*0.034218*	*0.226596*	*0.370387*	*0.122184*	*2.496901*
Borg G-12	67.44	0.425	14.745	5.143	0.117	0.428	3.2	5.151	2.065	98.834
	66.926	0.421	15.477	4.537	0.127	0.372	3.449	5.363	1.893	98.679

	66.735	0.434	14.39	5.631	0.148	0.429	2.986	4.694	2.258	97.788
	66.445	0.449	14.197	5.604	0.186	0.408	3.102	5.084	2.346	97.949
	66.212	0.38	15.861	4.788	0.108	0.323	3.561	5.466	1.982	98.825
	65.697	0.438	14.189	5.414	0.171	0.388	2.876	4.85	2.27	96.322
	65.566	0.446	13.984	5.299	0.259	0.391	2.992	4.966	2.33	96.337
	61.324	0.384	13.06	5.04	0.237	0.415	2.612	4.301	2.181	89.712
	61.195	0.362	16.008	3.607	0.165	0.244	3.7	5.494	1.581	92.418
average	*65.28222*	*0.415444*	*14.65678*	*5.007*	*0.168667*	*0.377556*	*3.164222*	*5.041*	*2.100667*	*96.31822*
std dev	*2.218873*	*0.030067*	*0.910446*	*0.600476*	*0.04906*	*0.056425*	*0.330014*	*0.367209*	*0.235984*	*3.015889*
	65.197	0.311	17.458	5.248	0.177	0.572	4.568	5.723	1.637	101.015

Brun B-6

Sample	*SiO2*	*TiO2*	*Al2O3*	*FeO*	*MnO*	*MgO*	*CaO*	*Na2O*	*K2O*	*Total*
Brun B-6 .	48.573	2.019	13.644	11.158	0.206	7.108	11.902	2.606	0.349	97.891
	48.882	1.99	13.961	11.098	0.226	7.149	11.958	2.477	0.347	98.444
	48.956	2.11	13.596	11.25	0.232	7.285	11.953	2.534	0.216	98.411
	49.041	2.035	13.504	11.146	0.15	7.313	12.17	2.65	0.332	98.681
	49.052	2.071	13.904	11.201	0.178	7.297	12.112	2.665	0.333	99.071
	49.117	2.099	13.832	11.121	0.166	7.282	11.992	2.573	0.274	98.763
	49.174	2.053	13.66	11.011	0.172	7.424	11.876	2.604	0.288	98.57
	49.179	2.075	13.956	11.409	0.225	7.267	11.874	2.559	0.283	99.136
	49.223	2.059	13.947	10.999	0.257	7.231	11.816	2.63	0.375	98.892
	49.384	1.964	13.463	11.288	0.203	7.321	11.969	2.513	0.305	98.774
average	*49.0581*	*2.0475*	*13.7467*	*11.1681*	*0.2015*	*7.2677*	*11.9622*	*2.5811*	*0.3102*	*98.6633*
std dev	*0.21024*	*0.043905*	*0.184942*	*0.118826*	*0.032435*	*0.084632*	*0.103376*	*0.057939*	*0.044156*	*0.343712*

Landnam

	SiO2	*TiO2*	*Al2O3*	*FeO*	*MnO*	*MgO*	*CaO*	*Na2O*	*K2O*	*Total*
Brun D-10	48.177	1.754	13.318	12.071	0.153	7.277	11.736	2.45	0.184	97.388
	48.553	1.753	13.445	12.345	0.227	7.123	11.723	2.514	0.265	98.276
	48.598	1.781	13.424	12.58	0.177	7.121	11.927	2.516	0.17	98.525
	48.68	1.43	13.98	10.42	0.16	8.24	12.98	2.17	0.16	98.47
	48.723	1.718	13.279	11.974	0.171	7.291	12.004	2.551	0.237	98.235
	48.998	1.835	13.381	12.197	0.156	6.968	11.924	2.639	0.198	98.616
	49.013	1.747	13.602	12.11	0.24	7.162	11.951	2.416	0.156	98.682
	49.201	1.729	13.618	12.72	0.199	7.292	11.88	2.597	0.212	99.743
	49.22	1.798	13.681	12.447	0.265	7.207	11.84	2.506	0.184	99.456
	49.316	1.795	13.576	12.157	0.243	7.183	11.902	2.306	0.173	98.926
	49.70	1.78	13.35	12.06	0.24	7.09	11.70	2.58	0.22	99.03
average	*48.92591*	*1.738182*	*13.51445*	*12.09755*	*0.203091*	*7.267818*	*11.96036*	*2.477273*	*0.196545*	*98.66764*
std dev	*0.408836*	*0.103215*	*0.194976*	*0.577017*	*0.03906*	*0.320291*	*0.336355*	*0.130378*	*0.032776*	*0.604086*
Brun C-3	50.931	1.69	13.87	12.147	0.275	6.656	11.333	2.374	0.171	99.783
	50.601	1.727	14.042	11.877	0.244	6.444	11.54	2.54	0.196	99.514
	50.37	1.972	13.813	13.007	0.215	6.37	11.017	2.608	0.243	99.859
	50.33	1.708	13.603	12.076	0.175	6.777	11.538	2.326	0.185	98.953
	49.973	1.744	13.785	12.017	0.315	6.575	11.317	2.459	0.227	98.732
	49.783	1.646	13.859	11.743	0.272	6.749	11.746	2.401	0.179	98.647
	49.749	1.989	13.314	12.839	0.193	6.157	10.714	2.634	0.229	98.138
	49.651	1.612	13.968	11.99	0.206	6.907	11.888	2.367	0.201	99.089
	49.522	1.695	14.071	11.935	0.172	6.882	11.68	2.114	0.162	98.467
average	*50.10111*	*1.753667*	*13.81389*	*12.18122*	*0.229667*	*6.613*	*11.41922*	*2.424778*	*0.199222*	*99.02022*
std dev	*0.452506*	*0.126972*	*0.221679*	*0.413061*	*0.046866*	*0.236415*	*0.349641*	*0.150781*	*0.026628*	*0.562256*
	50.326	2.576	13.55	12.448	0.203	5.874	10.734	2.674	0.431	99.168

Brun C-4

	SiO2	*TiO2*	*Al2O3*	*FeO*	*MnO*	*MgO*	*CaO*	*Na2O*	*K2O*	*Total*
Brun C-4..	49.847	2.008	13.217	13.293	0.318	5.946	10.88	2.504	0.243	98.54
	49.252	1.959	13.293	13.22	0.252	6.272	10.864	2.484	0.293	98.162
	49.33	1.887	13.831	12.476	0.265	5.974	11.405	2.446	0.238	98.101
	49.401	1.961	13.44	13.502	0.237	5.863	10.906	2.531	0.24	98.376
	49.183	1.944	13.036	13.17	0.19	6.007	11.139	2.567	0.24	97.735
	49.68	1.891	13.372	12.73	0.203	6.208	11.056	2.479	0.263	98.187
	49.662	2.003	13.485	13.154	0.299	6.001	10.835	2.499	0.285	98.51
	49.677	1.889	13.678	13.149	0.302	6.255	11.169	2.594	0.179	99.149
	49.606	2.005	13.003	13.294	0.196	6.024	11.156	2.598	0.223	98.421
average	*49.51533*	*1.949667*	*13.37278*	*13.10978*	*0.251333*	*6.061111*	*11.04556*	*2.522444*	*0.244889*	*98.35344*
std dev	*0.216075*	*0.047849*	*0.25842*	*0.29562*	*0.045748*	*0.138102*	*0.1794*	*0.050537*	*0.031922*	*0.366341*

Kjol B-5

	SiO2	*TiO2*	*Al2O3*	*FeO*	*MnO*	*MgO*	*CaO*	*Na2O*	*K2O*	*Total*
Kjol B-5...	45.747	2.552	15.591	12.417	0.122	7.28	10.829	2.902	0.422	98.234
	45.689	2.686	14.699	13.059	0.181	7.129	10.933	2.832	0.377	97.972
	45.397	2.465	15.694	12.545	0.234	7.667	10.914	2.694	0.414	98.412
	45.373	2.611	15.333	12.976	0.193	7.305	10.837	2.759	0.358	98.076
	45.234	2.765	14.577	13.23	0.256	7.018	10.391	3.015	0.463	97.338
	44.693	2.59	14.718	13.047	0.137	7.489	10.658	2.921	0.391	97.001
average	*45.3555*	*2.6115*	*15.102*	*12.879*	*0.187167*	*7.314667*	*10.76033*	*2.853833*	*0.404167*	*97.83883*
std dev	*0.346456*	*0.095374*	*0.452481*	*0.293892*	*0.047901*	*0.215372*	*0.187483*	*0.106319*	*0.033958*	*0.501906*
	53.342	1.916	16.222	9.946	0.266	2.686	7.8	4.589	1.007	98.968
	52.65	2.255	13.973	11.631	0.228	3.309	7.17	4.142	1.183	97.905
	50.081	1.811	13.304	12.153	0.138	6.459	10.782	2.807	0.334	98.142
	48.901	1.724	13.437	11.625	0.175	7.503	11.978	2.348	0.249	98.218

La D-6

	SiO2	*TiO2*	*Al2O3*	*FeO*	*MnO*	*MgO*	*CaO*	*Na2O*	*K2O*	*Total*
La D-6...	49.825	1.725	13.487	12.016	0.238	6.351	11.127	2.517	0.197	97.775
	48.995	1.752	13.749	12.562	0.247	6.872	11.287	2.819	0.241	98.839
	48.94	1.723	13.609	12.147	0.254	6.733	11.531	2.428	0.188	97.783
	48.707	1.804	13.509	12.158	0.248	6.81	11.262	2.513	0.177	97.452
	48.439	1.764	13.01	12.31	0.213	6.902	11.389	2.524	0.171	96.997
	48.359	2.189	13.465	10.988	0.229	6.943	11.547	2.494	0.247	96.759
	47.937	2.275	13.519	11.968	0.251	6.42	10.914	2.614	0.384	96.604
	47.836	1.711	13.292	12.179	0.244	6.944	11.374	2.623	0.18	96.714
	47.474	1.999	13.404	11.445	0.229	7.081	11.821	2.692	0.353	96.784
	47.448	2.981	12.821	13.717	0.184	5.962	10.11	3.148	0.425	97.263
	47.392	1.752	12.604	11.726	0.288	6.851	11.561	2.599	0.21	95.215
	46.962	2.042	13.511	11.359	0.237	7.174	11.974	2.642	0.279	96.461
average	*48.19283*	*1.976417*	*13.33167*	*12.04792*	*0.2385*	*6.753583*	*11.32475*	*2.634417*	*0.254333*	*97.05383*
std dev	*0.797853*	*0.356112*	*0.328157*	*0.660208*	*0.02388*	*0.329797*	*0.457429*	*0.183952*	*0.083974*	*0.849237*

Vik K 3 & 4

	SiO2	*TiO2*	*Al2O3*	*FeO*	*MnO*	*MgO*	*CaO*	*Na2O*	*K2O*	*Total*
Vik K-4	73.425	0.047	11.981	0.806	0.052	0.033	0.357	3.741	4.209	94.652
	73.144	0.03	11.295	1.037	0.028	0.033	0.576	3.57	4.641	94.354
	72.997	0.046	11.83	1.001	0.031	0.04	0.508	4.003	4.374	94.839
	72.899	0.067	11.846	0.867	0.063	0.029	0.447	3.795	4.285	94.297
	72.78	0.028	11.632	1.183	0	0.034	0.519	3.542	4.213	93.935
	72.758	0.069	11.435	1.068	0.055	0.04	0.566	3.893	4.163	94.046
	70.921	0.053	11.476	1.131	0.068	0.025	0.561	3.508	4.316	92.076
average	*72.7034286*	*0.048571*	*11.64214*	*1.013286*	*0.042429*	*0.033429*	*0.504857*	*3.721714*	*4.314429*	*94.02843*

std dev	*0.75829637*	*0.014898*	*0.233848*	*0.125774*	*0.022251*	*0.005039*	*0.073066*	*0.175333*	*0.148997*	*0.84895*
Vik K-3	74.495	0.05	11.552	0.965	0.048	0.055	0.477	3.696	4.336	95.675
	73.585	0.019	11.781	1.091	0.01	0.006	0.479	3.838	4.34	95.161
	73.565	0.014	11.761	1.065	0.006	0.026	0.489	4.091	4.413	95.43
	73.516	0.058	11.561	1.052	0.045	0.003	0.521	3.743	4.306	94.827
	73.467	0.04	11.324	0.978	0.064	0.039	0.469	3.356	3.991	93.747
	73.32	0.047	11.472	0.673	0.064	0.015	0.466	3.839	4.499	94.398
	72.986	0.052	11.536	0.788	0.016	0.024	0.54	3.606	4.227	93.776
	72.985	0.034	11.845	1.191	0	0.023	0.559	3.93	4.095	94.672
	72.571	0.034	11.419	0.963	0	0.039	0.521	3.473	4.426	93.447
	63.495	0.506	15.231	4.507	0.21	0.428	2	5.594	3.949	96.018
average	*72.3985*	*0.0854*	*11.9482*	*1.3273*	*0.0463*	*0.0658*	*0.6521*	*3.9166*	*4.2582*	*94.7151*
std dev	*3.00657088*	*0.140837*	*1.105607*	*1.069319*	*0.059646*	*0.121658*	*0.450314*	*0.595214*	*0.178813*	*0.828915*
Vik H-8	74.486	0.051	11.767	1.089	0.071	0.036	0.577	3.703	4.539	96.319
	74.298	0.031	11.549	0.857	0.016	0.046	0.549	3.578	4.749	95.672
	73.789	0.038	11.625	1.196	0.01	0.059	0.629	3.871	4.44	95.657
	73.789	0.038	11.625	1.196	0.01	0.059	0.629	3.871	4.44	95.657
	73.05	0.033	11.752	1.163	0.074	0.021	0.558	3.635	4.569	94.856
	72.558	0.044	11.683	0.937	0.019	0.017	0.573	3.616	4.75	94.198
Average	*73.6616667*	*0.039167*	*11.66683*	*1.073*	*0.033333*	*0.039667*	*0.585833*	*3.712333*	*4.581167*	*95.39317*
std dev	*0.67194858*	*0.006719*	*0.076303*	*0.131508*	*0.027891*	*0.01665*	*0.031887*	*0.118141*	*0.128098*	*0.682044*
	49.165	2.401	12.96	12.409	0.165	6.484	11.187	2.718	0.374	98.197
Vik F-4	74.092	0.066	11.828	0.883	0.074	0.036	0.561	3.746	4.176	95.505
	73.878	0.071	11.598	0.992	0.048	0.021	0.577	3.797	4.61	95.593
	73.611	0.024	11.472	0.961	0.013	0.035	0.6	2.21	5.048	93.973
	73.563	0.045	11.851	1.238	0.1	0.049	0.531	4	4.644	96.046
	73.498	0.068	11.409	1.006	0	0.01	0.527	3.822	4.578	94.918
	73.451	0.029	11.703	1.073	0.013	0	0.52	3.961	4.657	95.408

	73.32	0.027	11.732	1.058	0.064	0.012	0.541	3.631	4.168	94.554
	73.29	0.03	11.605	1.157	0.074	0.034	0.512	3.864	4.536	95.101
	73.035	0.07	11.385	1.044	0.035	0.029	0.48	3.881	4.67	94.63
	72.854	0.052	11.505	1.062	0.052	0.03	0.524	3.257	4.32	93.654
average	*73.4592*	*0.0482*	*11.6088*	*1.0474*	*0.0473*	*0.0256*	*0.5373*	*3.6169*	*4.5407*	*94.9382*
std dev	*0.34719412*	*0.018611*	*0.158236*	*0.094132*	*0.030407*	*0.013966*	*0.032601*	*0.509533*	*0.250021*	*0.71051*
	49.564	1.808	13.517	13.031	0.073	6.556	11.473	2.483	0.261	99.057
Vik J-2	74.012	0.049	11.74	0.959	0.026	0.044	0.558	4.193	4.206	95.787
	73.538	0.038	11.849	1.087	0.003	0.068	0.634	4.081	4.516	95.847
	73.372	0.058	11.74	1.052	0.006	0.032	0.539	3.746	4.161	94.71
	73.322	0.047	11.725	0.983	0	0.022	0.601	4.08	4.562	95.342
	73.244	0.005	11.325	1.1	0.123	0.025	0.556	4.007	4.306	94.698
	73.179	0.081	11.663	1.172	0.045	0.061	0.57	4.217	4.212	95.2
	73.06	0.038	11.612	1.019	0.071	0.043	0.605	4.083	4.172	94.718
	72.954	0.018	11.7	1.089	0.116	0	0.505	3.924	4.959	95.266
	72.911	0.076	11.325	1.019	0.013	0.006	0.487	3.245	4.337	93.419
	72.824	0.048	11.631	0.997	0	0.015	0.615	3.992	4.522	94.646
average	*73.2416*	*0.0458*	*11.631*	*1.0477*	*0.0403*	*0.0316*	*0.567*	*3.9568*	*4.3953*	*94.9633*
std dev	*0.33288743*	*0.022081*	*0.16539*	*0.061422*	*0.045056*	*0.021304*	*0.045422*	*0.269436*	*0.237009*	*0.665638*
Vik J-6	*75.83*	*0.031*	*11.688*	*0*	*0*	*0.065*	*0.575*	*3.915*	*0*	*92.104*
	74.083	0.056	11.607	1.131	0.09	0.025	0.554	4.149	4.551	96.247
	73.892	0.028	11.681	1.226	0	0.044	0.642	3.958	4.521	96.02
	73.463	0.044	11.338	1.259	0.055	0.002	0.485	4.368	3.922	94.935
	73.415	0.052	11.532	1.019	0.077	0.016	0.521	4.249	4.434	95.316
	73.058	0.102	11.631	1.107	0.113	0.014	0.583	3.285	4.356	94.262
	72.743	*0.059*	*11.181*	*0.989*	*0.032*	*0.017*	*0.421*	*3.513*	*4.446*	*93.402*
	72.305	*0.045*	*11.152*	*0.892*	*0.048*	*0*	*0.442*	*3.545*	*4.657*	*93.087*
	69.902	0.241	13.27	4.197	0.186	0.145	1.352	5.522	3.808	98.643
	69.452	*0.047*	*10.63*	*1.05*	*0.048*	*0.026*	*0.436*	*3.945*	*4.323*	*89.985*
	68.96	*0.025*	*11.058*	*0.818*	*0.032*	*0.057*	*0.53*	*3.193*	*3.903*	*88.577*

average	*72.4639091*	*0.066364*	*11.52436*	*1.244364*	*0.061909*	*0.037364*	*0.594636*	*3.967455*	*3.901909*	*93.87073*
std dev	*2.05077956*	*0.058698*	*0.634284*	*0.988962*	*0.05127*	*0.039456*	*0.248312*	*0.613717*	*1.263888*	*2.755043*

Brun H-4, Vik E-8, Brun D-14

	SiO2	*TiO2*	*Al2O3*	*FeO*	*MnO*	*MgO*	*CaO*	*Na2O*	*K2O*	*Total*
Brun H-4	50.079	2.687	12.913	13.296	0.081	5.45	9.921	3.117	0.325	98.236
	49.586	2.349	13.28	12.364	0.184	6.761	11.327	2.661	0.26	99.137
	49.546	2.781	13.153	13.471	0.184	5.89	10.095	2.895	0.441	98.864
	49.512	2.774	13.054	13.507	0.261	5.668	9.839	2.924	0.371	98.285
	49.356	2.812	13.174	13.489	0.177	5.547	10.007	2.911	0.402	98.29
	49.343	2.672	13.035	13.436	0.292	5.584	9.859	3.042	0.441	98.092
	49.223	2.844	13.051	13.687	0.273	5.384	9.867	3.196	0.396	98.327
	49.195	2.941	12.525	13.644	0.205	5.236	9.887	3.25	0.402	97.677
	49.168	2.783	11.913	13.422	0.233	6.691	10.309	2.843	0.416	98.178
	49.146	2.835	12.809	13.769	0.208	5.557	9.971	3.022	0.469	98.19
average	*49.4154*	*2.7478*	*12.8907*	*13.4085*	*0.2098*	*5.7768*	*10.1082*	*2.9861*	*0.3923*	*98.3276*
std dev	*0.269073*	*0.151597*	*0.383485*	*0.372511*	*0.057388*	*0.502087*	*0.42799*	*0.167097*	*0.058203*	*0.384002*
Vik E-8	49.828	2.565	13.254	12.317	0.232	5.851	10.224	2.97	0.541	98.162
	49.187	2.816	12.849	13.325	0.247	5.882	10.59	2.938	0.426	98.662
	49.022	3.036	12.778	13.965	0.243	5.51	10.009	2.94	0.419	98.381
	48.88	3.082	12.79	13.915	0.264	5.432	10.011	2.981	0.408	98.176
	48.714	2.988	12.442	13.687	0.251	5.676	10.141	2.952	0.408	97.642
	48.674	2.626	13.23	12.792	0.237	6.278	10.903	2.818	0.412	98.338
	48.658	3.073	12.662	13.815	0.2	5.403	9.992	3.03	0.459	97.718
	48.607	2.696	13.042	12.546	0.223	6.289	10.961	2.785	0.357	97.876
	48.583	2.899	12.75	13.264	0.245	5.884	10.127	3.039	0.405	97.584
average	*49.1854*	*2.8411*	*12.9309*	*13.1776*	*0.2341*	*5.6746*	*10.164*	*2.9804*	*0.4628*	*98.0558*
std dev	*0.912167*	*0.19065*	*0.306246*	*0.648299*	*0.020186*	*0.480034*	*0.603461*	*0.14565*	*0.118977*	*0.334696*

Brun D-14	48.288	2.317	13.55	12.296	0.268	6.773	11.004	2.956	0.304	98.099
	48.68	2.553	12.892	13.118	0.205	6.053	10.535	2.889	0.256	97.603
	48.782	2.574	13.373	13.707	0.304	5.962	10.381	3.075	0.39	98.906
	49.023	2.641	12.957	13.332	0.258	5.838	10.129	3.099	0.388	98.04
	49.09	2.329	13.658	12.393	0.221	6.662	11.431	2.816	0.326	99.281
	49.39	2.262	13.817	12.241	0.146	6.835	11.406	2.79	0.301	99.505
	49.727	2.609	12.984	12.965	0.252	5.852	10.449	2.913	0.363	98.496
	50.935	2.536	13.145	13.582	0.301	4.608	8.761	3.239	0.633	98.343
	51.462	2.644	13.25	13.858	0.251	4.434	8.972	3.249	0.576	99.344
average	*49.48633*	*2.496111*	*13.29178*	*13.05467*	*0.245111*	*5.890778*	*10.34089*	*3.002889*	*0.393*	*98.62411*
std dev	*1.001283*	*0.141938*	*0.311478*	*0.588157*	*0.0464*	*0.821114*	*0.896183*	*0.161333*	*0.120953*	*0.62895*
	50.725	1.665	9.058	9.85	0.191	11.727	15.933	1.267	0.175	100.836

Hekla 3

	SiO2	*TiO2*	*Al2O3*	*FeO*	*MnO*	*MgO*	*CaO*	*Na2O*	*K2O*	*Total*
Brun C-6	74.015	0.052	12.141	1.178	0.045	0.064	0.536	3.63	4.282	95.942
	72.372	0.144	14.564	2.886	0.073	0.155	2.047	5.18	2.372	99.823
	71.961	0.19	14.1	2.965	0.155	0.118	2.04	5.129	2.592	99.25
	71.767	0.163	13.909	3.236	0.136	0.126	1.938	5.03	2.508	98.832
	71.763	0.211	14.001	2.876	0.089	0.121	2.08	4.987	2.487	98.694
	71.638	0.154	14.042	2.974	0.165	0.133	1.882	4.793	2.402	98.186
	71.456	0.2	14.262	2.982	0.063	0.162	2.114	4.835	2.558	98.691
	71.024	0.193	14.9	1.852	0.025	0.109	3.005	5.046	2.463	99.053
	68.891	0.165	13.163	2.711	0.067	0.116	1.881	5.066	2.343	94.402
	68.704	0.181	13.447	2.93	0.085	0.163	1.843	4.641	2.287	94.311
	67.491	0.139	12.852	2.784	0.048	0.124	1.777	4.755	2.307	92.326
av	*71.00745*	*0.162909*	*13.76191*	*2.670364*	*0.086455*	*0.126455*	*1.922091*	*4.826545*	*2.600091*	*97.22818*
std dev	*1.801871*	*0.041526*	*0.761183*	*0.577116*	*0.044122*	*0.026763*	*0.540712*	*0.411374*	*0.540371*	*2.414197*

	49.576	1.752	13.981	11.302	0.331	7.036	11.942	2.414	0.246	98.878
Brun D-13	72.46	0.143	14.12	3.105	0	0.141	2.015	5.37	2.435	99.866
	72.26	0.166	14.096	3.002	0.073	0.131	1.945	5.159	2.538	99.445
	71.845	0.141	14.338	3.13	0.07	0.158	2.05	5.104	2.455	99.313
	71.655	0.167	14.055	2.836	0.057	0.117	1.876	4.853	2.425	98.106
	71.528	0.206	13.766	3.032	0.142	0.137	2.066	3.631	2.371	96.896
	71.257	0.182	13.945	2.822	0.123	0.14	1.925	5.158	2.372	97.941
	70.922	0.193	14.081	3.021	0.114	0.14	1.936	5.246	2.456	98.109
	70.366	0.188	13.723	3.08	0.117	0.153	1.936	4.664	2.489	96.784
	69.786	0.156	13.36	2.904	0.098	0.155	1.849	5.143	2.339	95.8
	69.391	0.132	13.331	2.888	0.108	0.116	1.849	3.253	2.286	93.367
average	*71.147*	*0.1674*	*13.8815*	*2.982*	*0.0902*	*0.1388*	*1.9447*	*4.7581*	*2.4166*	*97.5627*
std dev	*0.972713*	*0.023367*	*0.316021*	*0.106252*	*0.039196*	*0.013783*	*0.073702*	*0.689525*	*0.071107*	*1.855004*
Kjol B-6	73.173	0.781	12.308	3.185	0.086	0.639	2.32	4.237	2.439	99.331
	71.551	0.218	13.935	3.249	0.143	0.156	2.036	5.379	2.706	99.403
	71.13	0.18	14.002	3.132	0.124	0.144	2.066	5.281	2.488	98.554
	71.033	0.151	13.991	3.163	0.136	0.122	2.001	5.333	2.403	98.387
	70.666	0.163	13.79	2.984	0.105	0.116	1.855	5.156	2.364	97.247
	70.155	0.184	13.717	3.109	0.095	0.148	2.023	5.126	2.668	97.278
	70.011	0.167	13.513	2.911	0.19	0.138	1.928	5.249	2.465	96.604
	69.871	0.171	13.602	3.23	0.092	0.112	2.016	5.049	2.644	96.808
	68.437	0.134	16.247	2.399	0.175	0.136	3.37	5.621	1.848	98.41
average	*70.670*	*0.239*	*13.901*	*3.040*	*0.127*	*0.190*	*2.179*	*5.159*	*2.447*	*98.002*
std dev	*1.234*	*0.193*	*0.963*	*0.249*	*0.035*	*0.159*	*0.437*	*0.362*	*0.241*	*0.990*
Kjol D-4	71.159	0.197	13.933	2.75	0.089	0.147	1.959	5.175	2.724	98.149
	71.105	0.192	13.967	3.246	0.187	0.174	1.984	5.239	2.606	98.74
	71.069	0.19	13.754	2.853	0	0.14	1.96	4.908	2.575	97.489
	70.865	0.118	15.553	2.361	0.108	0.128	2.617	5.947	2.034	99.794

	70.598	0.132	13.717	2.849	0.051	0.119	1.939	5.102	2.425	96.962
	70.238	0.147	13.778	2.972	0.124	0.144	2	5.1	2.552	97.085
	68.313	0.193	13.344	2.952	0.029	0.124	1.914	4.827	2.381	94.123
average	*70.47814*	*0.167*	*14.00657*	*2.854714*	*0.084*	*0.139429*	*2.053286*	*5.185429*	*2.471*	*97.47743*
std dev	*0.934663*	*0.031067*	*0.658712*	*0.248159*	*0.05853*	*0.017154*	*0.231599*	*0.338624*	*0.207294*	*1.651129*
	60.069	0.891	14.371	9.083	0.266	1.325	4.818	4.71	1.722	97.715
Borg E-5	72.978	0.145	14.385	3.009	0.108	0.159	1.888	4.804	2.345	99.868
	72.406	0.187	14.071	2.863	0.127	0.129	1.907	4.945	2.601	99.236
	71.714	0.153	13.752	2.711	0.216	0.141	1.975	5.014	2.41	98.087
	70.952	0.153	13.691	2.762	0.105	0.162	1.868	4.935	2.44	97.096
	70.949	0.176	13.753	2.97	0.124	0.108	1.909	5.141	2.433	97.592
	70.905	0.2	13.635	3.006	0.102	0.112	1.904	4.753	2.378	97.057
	70.626	0.192	13.957	2.979	0.079	0.123	1.951	5.021	2.521	97.477
	70.145	0.158	13.382	2.748	0.114	0.127	1.882	4.92	2.335	95.821
	69.905	0.182	13.807	3.028	0.095	0.148	1.982	5.107	2.45	96.723
	67.885	0.152	12.936	2.756	0.079	0.115	1.74	4.69	2.321	92.705
average	*70.8465*	*0.1698*	*13.7369*	*2.8832*	*0.1149*	*0.1324*	*1.9006*	*4.933*	*2.4234*	*97.1662*
std dev	*1.339798*	*0.018771*	*0.369511*	*0.12157*	*0.037063*	*0.018288*	*0.06495*	*0.14009*	*0.082964*	*1.861041*
	49.052	1.754	13.709	11.116	0.151	7.484	12.559	2.352	0.14	98.571
	48.852	1.701	14.248	10.734	0.154	7.051	12.578	2.426	0.168	98.196
Brun H-3	71.518	0.167	14.074	2.945	0.139	0.134	1.987	5.203	2.414	98.615
	71.294	0.203	13.872	2.935	0.092	0.126	1.957	4.994	2.575	98.094
	71.185	0.158	14.011	3.129	0.12	0.141	1.989	5.058	2.558	98.354
	71.136	0.164	13.955	3.236	0.155	0.107	1.928	5.229	2.468	98.4
	70.945	0.179	13.609	3.117	0.038	0.135	1.864	5.173	2.537	97.607
	69.745	0.15	13.49	2.926	0.127	0.147	2.023	5.026	2.478	96.14
	68.876	0.12	13.377	2.994	0.108	0.155	1.9	5.083	2.435	95.13
	60.947	0.893	14.528	8.554	0.238	1.348	4.736	4.661	1.672	97.966
	60.446	1.792	11.456	10.209	0.245	2.303	4.648	3.734	1.436	96.91

average	*68.45467*	*0.425111*	*13.59689*	*4.449444*	*0.140222*	*0.510667*	*2.559111*	*4.906778*	*2.285889*	*97.46844*
std dev	*4.22477*	*0.534596*	*0.824173*	*2.66682*	*0.062499*	*0.738084*	*1.141174*	*0.443973*	*0.39841*	*1.114033*
	49.102	1.733	13.457	11.491	0.312	7.712	12.412	2.547	0.14	99.131
Lo H-7	72.076	0.191	14.154	3.052	0.111	0.128	2.031	5.53	2.514	99.791
	72.009	0.205	14.15	3.128	0.193	0.148	1.952	5.082	2.403	99.334
	71.643	0.192	13.67	2.882	0.101	0.136	1.972	5.275	2.281	98.152
	71.387	0.171	13.967	2.986	0.177	0.152	2.054	5.195	2.463	98.643
	71.316	0.147	13.435	2.948	0.089	0.123	1.932	5.236	2.573	97.87
	70.896	0.186	13.578	2.842	0.095	0.151	1.902	5.125	2.285	97.094
	70.744	0.166	13.93	2.88	0.092	0.111	1.946	5.157	2.668	97.696
	70.186	0.134	13.491	2.848	0.054	0.129	1.907	5.165	2.535	96.449
	69.723	0.177	13.497	2.965	0.092	0.145	1.901	5.017	2.325	95.891
	69.211	0.192	13.331	3.046	0.101	0.077	1.91	5.262	2.489	95.657
	68.45	0.145	13.382	2.887	0.044	0.15	1.862	5.192	2.4	94.57
	65.935	0.313	14.437	5.171	0.101	0.315	2.95	5.243	2.056	96.577
	63.764	0.518	15.581	5.903	0.167	0.664	4.625	5.104	1.436	97.988
average	*69.79538*	*0.210538*	*13.89254*	*3.349077*	*0.109*	*0.186846*	*2.226462*	*5.198692*	*2.340615*	*97.36246*
std dev	*2.386843*	*0.098291*	*0.590983*	*0.947508*	*0.042665*	*0.147415*	*0.744008*	*0.119907*	*0.301237*	*1.446564*
	49.614	1.618	14.003	10.974	0.219	7.828	12.296	2.371	0.215	99.379
La-A6	71.606	0.158	13.942	3.168	0.162	0.149	1.967	4.949	2.434	98.568
	70.541	0.146	13.437	3.076	0.13	0.135	1.854	4.763	2.416	96.557
	70.422	0.209	13.91	2.953	0.172	0.132	1.983	5.338	2.517	97.655
	70.348	0.186	13.59	3.039	0.159	0.111	1.993	5.232	2.453	97.141
	70.189	0.147	13.581	3.133	0.079	0.139	1.969	5.31	2.596	97.159
	69.86	0.202	13.295	2.881	0.127	0.124	1.97	4.988	2.398	95.872
	69.815	0.139	13.768	3.141	0.159	0.13	1.938	5.22	2.643	96.975
	69.084	0.15	13.694	2.92	0.108	0.155	1.919	5.117	2.5	95.648
	68.831	0.17	13.302	2.922	0.12	0.172	2.012	5.314	2.525	95.391
	66.122	0.646	12.655	5.236	0.174	0.695	2.725	4.558	2.122	95.056
	59.751	0.941	14.74	8.732	0.186	1.306	4.889	4.677	1.643	97.282

average	*68.779*	*0.281273*	*13.62855*	*3.745545*	*0.143273*	*0.295273*	*2.292636*	*5.042364*	*2.386091*	*96.664*
std dev	*3.150006*	*0.250496*	*0.490143*	*1.701423*	*0.031331*	*0.357389*	*0.850941*	*0.263494*	*0.267855*	*1.01961*
Vik D-12	71.851	0.168	13.893	2.955	0.141	0.118	1.978	3.299	2.484	96.922
	71.215	0.173	13.265	3.147	0.102	0.136	1.967	4.7	2.346	97.088
	71.924	0.17	13.658	3.068	0.108	0.122	1.991	4.749	2.342	98.161
	71.688	0.176	13.702	2.985	0.112	0.117	1.912	4.526	2.571	97.835
	71.89	0.17	13.749	3.213	0.116	0.168	2.002	4.482	2.581	98.371
	70.976	0.153	13.607	2.902	0.123	0.127	1.924	4.556	2.495	96.94
	71.527	0.167	13.74	2.953	0.123	0.151	1.989	4.241	2.421	97.361
	72.395	0.184	13.797	2.822	0.121	0.111	1.982	4.237	2.541	98.205
	71.574	0.167	13.735	3.116	0.078	0.116	1.996	4.326	2.483	97.636
average	*71.67111*	*0.169778*	*13.68289*	*3.017889*	*0.113778*	*0.129556*	*1.971222*	*4.346222*	*2.473778*	*97.61322*
std dev	*0.392986*	*0.007828*	*0.166297*	*0.119222*	*0.01641*	*0.017833*	*0.030158*	*0.408552*	*0.08339*	*0.531735*

Brun H-2

	SiO2	*TiO2*	*Al2O3*	*FeO*	*MnO*	*MgO*	*CaO*	*Na2O*	*K2O*	*Total*
Brun H-2..	49.591	2.307	13.722	11.557	0.187	6.802	11.538	2.647	0.344	99.066
	49.427	1.599	13.381	11.8	0.203	7.202	11.801	2.398	0.249	98.376
	48.971	1.751	13.288	12.135	0.19	7.138	11.841	2.43	0.221	98.25
	48.885	1.625	13.411	11.103	0.178	7.432	12.386	2.318	0.165	97.785
	48.874	1.707	13.514	11.101	0.213	7.582	12.418	2.416	0.182	98.255
	48.796	1.683	13.834	11.637	0.197	7.427	12.159	2.391	0.162	98.619
	48.771	2.517	13.501	12.223	0.137	6.549	11.061	2.764	0.274	98.162
	48.598	1.759	13.359	11.748	0.294	7.177	12.211	2.4	0.179	98.004
	48.593	1.577	13.583	12.168	0.194	7.15	12.238	2.369	0.226	98.381
	48.452	1.692	13.509	11.695	0.235	7.414	12.265	2.36	0.199	98.071
average	*48.8958*	*1.8217*	*13.5102*	*11.7167*	*0.2028*	*7.1873*	*11.9918*	*2.4493*	*0.2201*	*98.2969*
std dev	*0.342723*	*0.304182*	*0.159334*	*0.378278*	*0.038636*	*0.297413*	*0.409849*	*0.134062*	*0.053967*	*0.336097*

Brun D-10

	SiO2	*TiO2*	*Al2O3*	*FeO*	*MnO*	*MgO*	*CaO*	*Na2O*	*K2O*	*Total*
Brun D-14	48.288	2.317	13.55	12.296	0.268	6.773	11.004	2.956	0.304	98.099
	48.68	2.553	12.892	13.118	0.205	6.053	10.535	2.889	0.256	97.603
	48.782	2.574	13.373	13.707	0.304	5.962	10.381	3.075	0.39	98.906
	49.023	2.641	12.957	13.332	0.258	5.838	10.129	3.099	0.388	98.04
	49.09	2.329	13.658	12.393	0.221	6.662	11.431	2.816	0.326	99.281
	49.39	2.262	13.817	12.241	0.146	6.835	11.406	2.79	0.301	99.505
	49.727	2.609	12.984	12.965	0.252	5.852	10.449	2.913	0.363	98.496
	50.935	2.536	13.145	13.582	0.301	4.608	8.761	3.239	0.633	98.343
	51.462	2.644	13.25	13.858	0.251	4.434	8.972	3.249	0.576	99.344
average	*49.48633*	*2.496111*	*13.29178*	*13.05467*	*0.245111*	*5.890778*	*10.34089*	*3.002889*	*0.393*	*98.62411*
std dev	*1.001283*	*0.141938*	*0.311478*	*0.588157*	*0.0464*	*0.821114*	*0.896183*	*0.161333*	*0.120953*	*0.62895*
	50.725	1.665	9.058	9.85	0.191	11.727	15.933	1.267	0.175	100.836

Hekla 4 *(tephra shards assigned "a" and "b" represent the two distinct groups of geochemistries)*

	SiO2	*TiO2*	*Al2O3*	*FeO*	*MnO*	*MgO*	*CaO*	*Na2O*	*K2O*	*Total*
La-A7										
a	72.09	0.08	12.805	1.931	0.089	0.045	1.293	5.011	2.911	96.274
b	62.175	0.77	14.835	7.89	0.217	0.865	4.712	5.065	1.524	98.352
b	60.956	0.818	14.363	8.339	0.299	1.019	4.296	4.866	1.682	96.941
b	60.722	0.812	14.397	8.02	0.233	0.965	4.205	4.768	1.634	96.045
b	59.762	0.86	14.815	8.242	0.309	1.087	4.805	4.974	1.409	96.601
b	59.518	1.031	14.565	9.614	0.289	1.375	4.869	4.384	1.515	97.684
b	59.441	1.167	13.619	9.636	0.305	1.577	4.603	4.589	1.767	97.278
b	59.433	0.799	13.943	8.146	0.239	1.044	4.48	4.795	1.716	95.059

b	57.912	0.872	14.2	9.483	0.301	1.186	4.494	4.74	1.59	95.174
b	57.664	1.129	14.387	10.095	0.342	1.595	5.109	4.281	1.394	96.601
b	56.326	1.358	14.318	11.281	0.263	1.364	4.957	4.889	1.327	96.548
average	*59.3909*	*0.9616*	*14.3442*	*9.0746*	*0.2797*	*1.2077*	*4.653*	*4.7351*	*1.5558*	*96.6283*
std dev	*1.63382*	*0.188855*	*0.349946*	*1.062752*	*0.037868*	*0.243433*	*0.275582*	*0.237117*	*0.140084*	*0.976289*
Brun C-7										
a	72.973	0.1	12.753	1.975	0.051	0.035	1.296	4.614	2.811	96.654
b	63.065	0.532	15.039	5.728	0.261	0.531	3.837	4.624	1.667	95.466
b	62.787	0.762	14.831	8.035	0.377	0.986	4.234	4.578	1.662	98.558
b	62.777	0.79	14.876	8.283	0.317	0.997	4.351	4.633	1.726	99.028
b	61.822	0.847	14.835	9.401	0.204	1.002	4.574	4.184	1.796	99.042
b	61.269	0.925	15.127	9.222	0.189	1.109	4.752	4.647	1.58	99.289
b	61.156	0.84	14.519	8.863	0.135	1.053	4.514	4.422	1.651	97.53
b	61.049	1.037	15.214	9.792	0.257	1.325	4.792	3.26	1.877	99.093
b	60.339	0.858	14.935	10.082	0.185	1.038	4.837	3.71	1.687	97.969
b	60.078	1.066	14.895	8.953	0.336	1.392	5.082	4.079	1.522	97.886
b	59.928	0.689	13.941	7.308	0.242	0.816	4.071	4.407	1.473	93.119
average	*61.427*	*0.8346*	*14.8212*	*8.5667*	*0.2503*	*1.0249*	*4.5044*	*4.2544*	*1.6641*	*97.698*
std dev	*1.095582*	*0.149479*	*0.343948*	*1.231492*	*0.071787*	*0.228746*	*0.363745*	*0.437161*	*0.114477*	*1.867571*
Brun C-8										
a	74.401	0.096	13.091	1.967	0.07	0.046	1.362	4.798	2.764	98.631
a	73.277	0.091	12.926	1.962	0.025	0.022	1.323	4.822	2.7	97.149
a	73.112	0.104	12.94	2.019	0.152	0.041	1.381	4.8	2.93	97.483
a	72.868	0.107	12.737	1.801	0.137	0.016	1.335	4.61	2.914	96.534
a	72.844	0.085	12.651	2.019	0.098	0.031	1.338	4.936	2.887	96.914
a	72.668	0.1	12.638	2.072	0.038	0.054	1.346	4.913	3.033	96.934
a	71.937	0.093	12.711	1.72	0.133	0.022	1.235	4.916	2.674	95.444
a	70.692	0.174	14.058	3.383	0.209	0.029	2.037	5.063	2.431	98.079
a	69.411	0.202	13.809	3.739	0.193	0.079	2.225	5.308	2.291	97.276

average	*72.35667*	*0.116889*	*13.06233*	*2.298*	*0.117222*	*0.037778*	*1.509111*	*4.907333*	*2.736*	*97.16044*
std dev	*1.407003*	*0.039085*	*0.490098*	*0.688316*	*0.060915*	*0.018665*	*0.337506*	*0.184046*	*0.230291*	*0.854688*
b	64.105	0.659	14.582	7.475	0.198	0.815	3.936	5.032	1.773	98.795
b	62.024	0.735	13.793	8.598	0.226	0.679	4.154	4.652	1.976	97.119
b	61.293	0.858	14.684	8.88	0.21	1.046	4.638	4.352	1.591	97.913
b	59.559	0.98	14.49	9.738	0.328	1.353	4.934	3.576	1.617	97.027
average	*61.74525*	*0.808*	*14.38725*	*8.67275*	*0.2405*	*0.97325*	*4.4155*	*4.403*	*1.73925*	*97.7135*
std dev	*1.63021*	*0.12208*	*0.349885*	*0.808997*	*0.051485*	*0.255504*	*0.392636*	*0.53483*	*0.153389*	*0.713119*
Brun C-9										
a	73.575	0.134	12.536	2.046	0.108	0.013	1.271	4.805	2.888	97.376
a	73.248	0.068	12.412	1.942	0.14	0.013	1.303	4.951	2.819	96.913
a	72.433	0.049	12.648	1.909	0.137	0.043	1.296	4.771	2.792	96.078
a	71.678	0.108	12.296	1.979	0.092	0.063	1.321	4.988	2.826	95.352
a	71.261	0.085	12.271	1.753	0.092	0.041	1.302	5.057	2.795	94.706
a	68.25	0.07	11.709	1.772	0.038	0.037	1.217	4.347	2.685	90.125
average	*71.74083*	*0.085667*	*12.312*	*1.900167*	*0.101167*	*0.035*	*1.285*	*4.819833*	*2.800833*	*95.09167*
std dev	*1.757599*	*0.028099*	*0.299616*	*0.105983*	*0.034149*	*0.017588*	*0.033789*	*0.233777*	*0.060678*	*2.39418*
b	60.682	0.771	14.245	8.417	0.191	0.92	4.254	4.642	1.804	96.257
b	60.118	0.872	14.863	8.6	0.226	1.037	4.758	4.709	1.48	97.062
b	59.273	1.154	14.997	9.738	0.175	1.431	5.027	3.894	1.424	97.623
b	58.401	0.952	14.303	9.124	0.207	1.242	4.772	4.651	1.59	95.692
b	58.319	0.954	15.103	9.128	0.276	1.404	5.098	4.243	1.19	96.187
b	57.139	1.055	14.327	9.256	0.392	1.632	5.201	4.259	1.327	95.106
average	*58.98867*	*0.959667*	*14.63967*	*9.043833*	*0.2445*	*1.277667*	*4.851667*	*4.399667*	*1.469167*	*96.32117*
std dev	*1.185938*	*0.122628*	*0.355694*	*0.434032*	*0.073246*	*0.242261*	*0.312458*	*0.293715*	*0.194515*	*0.830482*
Vik D-10										
a	73.225	0.088	12.81	1.977	0.096	0.036	1.309	4.72	2.834	97.105
a	74.073	0.093	12.99	1.996	0.097	0.036	1.334	4.734	2.742	98.119
a	73.286	0.096	12.929	1.982	0.052	0.03	1.299	4.767	2.841	97.283
a	73.476	0.093	12.851	1.955	0.073	0.025	1.293	4.798	2.775	97.364

a	73.243	0.096	12.733	2.026	0.115	0.052	1.345	4.709	2.861	97.204
a	73.398	0.082	12.733	2.037	0.086	0.02	1.336	4.887	2.697	97.291
a	72.479	0.151	12.908	2.199	0.11	0.119	1.478	4.46	2.826	96.754
a	72.894	0.077	12.7	1.965	0.121	0.035	1.322	4.673	2.728	96.542
a	73.937	0.091	12.946	1.899	0.132	0.037	1.32	4.778	2.768	97.943
a	73.805	0.084	12.928	2.045	0.096	0.017	1.371	4.824	2.821	98.023
average	*73.3816*	*0.0951*	*12.8528*	*2.0081*	*0.0978*	*0.0407*	*1.3407*	*4.735*	*2.7893*	*97.3628*
std dev	*0.456099*	*0.019557*	*0.097931*	*0.07572*	*0.022387*	*0.027749*	*0.050648*	*0.108737*	*0.052284*	*0.499188*
b	61.733	0.851	14.792	9.142	0.299	1.139	5.031	4.947	1.491	99.814
b	61.018	1.157	13.369	10.237	0.291	1.907	4.538	4.177	1.643	98.913
b	59.674	1.052	15.206	8.57	0.269	1.632	6.057	4.829	1.148	98.991
b	58.891	1.107	14.899	9.243	0.249	1.618	5.134	4.378	1.408	97.473
average	*60.329*	*1.04175*	*14.5665*	*9.298*	*0.277*	*1.574*	*5.19*	*4.58275*	*1.4225*	*98.79775*
std dev	*1.111621*	*0.116223*	*0.707879*	*0.599805*	*0.019545*	*0.276321*	*0.54891*	*0.316177*	*0.179494*	*0.842371*
Vik D-11										
a	74.2	0.094	13.069	1.991	0.111	0.026	1.319	4.626	2.822	98.277
b	63.728	0.726	14.37	7.582	0.224	0.846	3.999	4.146	1.822	97.741
b	62.815	0.798	14.751	8.365	0.232	1.028	4.455	3.845	1.666	98.265
b	61.244	0.822	14.488	9.617	0.299	1.031	4.776	4.556	1.62	98.823
b	60.905	1.057	15.205	9.41	0.218	1.234	5.195	4.721	0.853	99.347
b	60.452	0.871	14.268	9.275	0.346	1.079	4.568	4.185	1.509	96.937
b	60.272	1.138	12.729	8.441	0.283	1.553	3.856	4.172	2.056	95.061
b	59.994	0.967	15.41	8.531	0.242	1.26	5.152	4.626	1.171	97.819
b	59.927	1.186	14.704	10.467	0.242	1.53	4.969	4.429	1.412	99.431
b	59.104	0.801	13.751	9.123	0.309	0.872	4.34	4.758	1.509	94.885
b	58.937	0.86	14.299	8.568	0.221	1.082	4.368	3.907	1.471	94.107
b	58.85	1.044	14.667	8.682	0.228	1.385	4.829	4.428	1.465	96.087
b	58.611	1.186	14.474	9.84	0.302	1.777	5.338	4.581	1.393	98.15
b	58.359	1.123	14.103	9.712	0.262	1.592	4.716	3.553	1.478	95.452

b	58.036	1.134	14.406	9.08	0.244	1.372	4.945	4.538	1.544	95.916
average	*60.08814*	*0.9795*	*14.40179*	*9.0495*	*0.260857*	*1.260071*	*4.679*	*4.3175*	*1.497786*	*97.0015*
std dev	*1.605758*	*0.157007*	*0.61519*	*0.717655*	*0.038635*	*0.274871*	*0.424791*	*0.348052*	*0.267982*	*1.688095*
Vik K-5										
a	75.307	0.061	12.637	1.267	0.054	0.038	1.161	4.285	3.335	98.144
a	72.709	0.088	12.711	2.034	0.094	0.048	1.322	4.574	2.768	96.348
a	72.37	0.082	12.986	2.102	0.067	0.037	1.318	4.548	2.896	96.409
a	71.792	0.036	15.388	0.491	0.042	0.026	1.084	5.094	4.783	98.736
a	71.436	0.098	12.443	1.943	0.089	0.023	1.298	4.531	2.9	94.791
average	*72.7228*	*0.073*	*13.233*	*1.5674*	*0.0692*	*0.0344*	*1.2366*	*4.6064*	*3.3364*	*96.8856*
std dev	*1.365649*	*0.022109*	*1.091498*	*0.61538*	*0.019914*	*0.009002*	*0.096635*	*0.265027*	*0.748349*	*1.407911*
b	63.006	0.684	15.12	6.674	0.211	0.739	4.597	5.136	1.457	97.873
b	59.076	1.187	15.099	9.151	0.255	1.632	4.996	4.175	1.633	97.782
b	58.946	1.156	13.066	10.064	0.306	1.965	4.795	4.404	1.678	96.899
b	58.576	1.182	14.236	10.263	0.276	1.723	4.995	4.068	1.624	97.562
b	58.155	1.022	14.262	9.656	0.292	1.338	4.751	4.308	1.531	95.824
b	58.148	1.18	14.492	10.421	0.35	1.671	5.118	2.298	1.595	95.854
b	58.055	1.151	14.507	10.607	0.277	1.688	5.142	3.833	1.516	97.351
average	*59.13743*	*1.080286*	*14.39743*	*9.548*	*0.281*	*1.536571*	*4.913429*	*4.031714*	*1.576286*	*97.02071*
std dev	*1.622927*	*0.170231*	*0.638342*	*1.258698*	*0.039864*	*0.367222*	*0.188263*	*0.801915*	*0.071817*	*0.803225*
c	49.249	1.553	2.349	13.895	0.332	13.447	18.07	0.371	0.004	99.472
c	45.348	2.513	15.363	12.698	0.193	7.374	10.622	2.827	0.43	97.705
Vik H-9										
a	75.378	0.078	12.794	1.413	0.07	0.046	1.228	4.808	2.84	98.657
a	73.277	0.07	12.209	1.417	0.061	0.045	1.189	4.592	2.883	95.79
a	72.909	0.045	12.88	2.038	0.113	0.01	1.37	4.911	2.919	97.25
a	68.135	0.011	18.293	0.727	0.013	0.017	0.05	8.185	5.398	100.829
average	*72.42475*	*0.051*	*14.044*	*1.39875*	*0.06425*	*0.0295*	*0.95925*	*5.624*	*3.51*	*98.1315*

std dev	*2.649739*	*0.026106*	*2.466709*	*0.463795*	*0.03552*	*0.016194*	*0.52926*	*1.483069*	*1.090396*	*1.858247*
b	63.015	0.798	16.664	5.678	0.201	0.529	5.321	5.281	1.381	99.129
b	60.878	0.962	14.705	10.089	0.257	1.306	5.011	4.64	1.594	99.805
b	60.085	0.814	14.039	9.429	0.244	0.977	4.54	4.842	1.543	96.917
b	57.375	1.476	14.532	11.705	0.262	1.611	4.886	4.093	1.489	98.002
average	*60.33825*	*1.0125*	*14.985*	*9.22525*	*0.241*	*1.10575*	*4.9395*	*4.714*	*1.50175*	*98.46325*
std dev	*2.018744*	*0.275134*	*0.999696*	*2.209056*	*0.02401*	*0.401433*	*0.279784*	*0.426905*	*0.078985*	*1.100813*
c	46.683	2.339	14.152	11.416	0.231	8.108	12.298	2.556	0.409	98.49
Brun D-15										
a	76.532	0.024	11.712	0.727	0.035	0.03	0.101	5.725	3.238	98.124
a	71.784	0.086	14.951	1.956	0.073	0.024	0.555	7.463	3.358	100.254
a	71.435	0.231	13.189	2.617	0.089	0.043	0.602	5.965	3.314	97.486
a	71.012	0.234	12.857	3.552	0.161	0.039	0.842	5.277	3.526	97.527
a	70.588	0.251	12.957	3.408	0.114	0.109	1.12	5.474	3.71	97.742
a	70.07	0.245	12.73	3.832	0.18	0.021	0.971	5.15	3.873	97.086
a	70.062	0.183	12.757	3.524	0.095	0	0.874	5.87	3.705	97.069
a	68.96	0.041	17.359	0.701	0.139	0.015	0.117	7.975	4.965	100.273
average	*71.30538*	*0.161875*	*13.564*	*2.539625*	*0.11075*	*0.035125*	*0.64775*	*6.112375*	*3.711125*	*98.19513*
std dev	*2.142927*	*0.089901*	*1.662507*	*1.195354*	*0.04474*	*0.030665*	*0.354922*	*0.97183*	*0.517079*	*1.235641*
c	48.95	2.253	13.816	12.214	0.165	6.953	11.391	2.614	0.338	99.027
c	48.096	4.377	12.91	14.636	0.295	4.639	9.179	3.505	0.837	99.285
c	47.469	4.192	12.269	14.303	0.285	4.837	9.029	3.556	0.862	97.417

Vik D-9/Vik K-7

	SiO2	*TiO2*	*Al2O3*	*FeO*	*MnO*	*MgO*	*CaO*	*Na2O*	*K2O*	*Total*
Vik D-9	49.089	3.16	13.104	13.66	0.238	5.508	9.946	2.824	0.582	98.628
	49.495	3.079	13.033	14.426	0.234	4.956	9.12	3.022	0.585	98.422
	49.399	2.966	12.875	14.306	0.274	4.932	9.093	3.086	0.659	98.042

	49.143	3.02	13.009	14.399	0.249	5.066	9.156	3.028	0.645	98.17
	49.469	3.15	12.936	14.166	0.252	4.919	9.263	3.115	0.738	98.487
	49.657	2.993	13.054	14.535	0.284	4.925	9.163	3.12	0.61	98.837
	49.709	2.994	12.937	14.388	0.224	5.013	9.096	3.046	0.621	98.472
	49.065	3.396	12.703	14.541	0.266	4.705	8.895	3.138	0.723	97.96
	49.432	3.026	13.115	14.604	0.315	5.018	9.246	3.101	0.643	98.966
average	*49.5564*	*3.1457*	*12.8928*	*14.3245*	*0.2623*	*4.9043*	*9.0896*	*3.0745*	*0.6731*	*98.4325*
std dev	*0.558316*	*0.2131*	*0.269695*	*0.258289*	*0.02674*	*0.357085*	*0.470025*	*0.106465*	*0.097369*	*0.307267*
Vik K-7										
	46.51	4.095	12.432	15.07	0.273	5.14	9.164	2.979	0.562	96.765
	48.032	3.327	12.272	14.575	0.277	4.728	9.2	3.069	0.716	96.795
	48.107	3.376	12.463	14.618	0.28	4.776	8.992	3.205	0.695	97.045
	47.736	2.967	12.664	14.377	0.283	5.218	9.192	3.204	0.605	96.702
	48.608	3.019	12.841	14.443	0.286	4.964	9.051	3.214	0.635	97.502
	47.754	3.373	12.745	14.615	0.228	4.62	8.931	3.145	0.798	96.78
	48.575	2.911	12.977	14.584	0.23	4.99	9.171	3.044	0.657	97.601
	48.11	3.058	12.942	14.514	0.236	4.754	9.1	3.165	0.611	96.958
	47.091	2.642	13.283	12.497	0.199	6.501	11.048	2.768	0.489	96.959
	48.627	3.011	12.996	14.507	0.268	5.023	9.071	3.168	0.608	97.705
average	*47.915*	*3.1779*	*12.7615*	*14.38*	*0.256*	*5.0714*	*9.292*	*3.0961*	*0.6376*	*97.0812*
std dev	*0.649795*	*0.375632*	*0.293147*	*0.652025*	*0.028615*	*0.509916*	*0.591366*	*0.132106*	*0.081238*	*0.35836*

Vik D-8

	SiO2	*TiO2*	*Al2O3*	*FeO*	*MnO*	*MgO*	*CaO*	*Na2O*	*K2O*	*Total*
Vik D-8	49.522	1.492	13.792	10.916	0.179	7.786	12.614	2.173	0.184	98.961
	50.155	1.38	14.486	9.642	0.194	8.713	13.804	2.041	0.116	100.804
	50.171	1.379	14.508	8.653	0.199	9.175	13.989	1.991	0.064	100.378
	49.647	1.393	14.196	10.876	0.199	8.104	13.274	2.105	0.108	100.155

	50.455	1.319	14.51	8.97	0.205	9.148	13.511	1.968	0.057	100.435
	49.81	1.488	14.089	11.127	0.22	7.843	12.519	2.235	0.135	99.721
	49.775	1.367	14.162	10.517	0.199	8.369	13.42	2.074	0.146	100.308
	49.348	1.356	13.919	10.314	0.181	8.44	12.959	2.118	0.132	99.027
	49.762	1.351	13.794	9.839	0.176	9.403	13.956	1.861	0.099	100.496
average	*49.84944*	*1.391667*	*14.16178*	*10.09489*	*0.194667*	*8.553444*	*13.33844*	*2.062889*	*0.115667*	*100.0317*
std dev	*0.329622*	*0.056234*	*0.275611*	*0.829378*	*0.013275*	*0.560716*	*0.516635*	*0.106506*	*0.037532*	*0.618106*
	49.224	2.946	12.611	13.899	0.249	5.855	10.262	2.834	0.399	98.648
	49.252	2.655	12.905	13.067	0.256	6.2	10.626	2.774	0.379	98.528
	49.734	2.836	12.982	13.626	0.297	6.061	10.464	2.868	0.384	99.657
average	*49.40333*	*2.812333*	*12.83267*	*13.53067*	*0.267333*	*6.038667*	*10.45067*	*2.825333*	*0.387333*	*98.94433*
std dev	*0.234096*	*0.119973*	*0.159863*	*0.346287*	*0.021171*	*0.141728*	*0.148901*	*0.038862*	*0.008498*	*0.506307*

Vik D-7

	SiO2	*TiO2*	*Al2O3*	*FeO*	*MnO*	*MgO*	*CaO*	*Na2O*	*K2O*	*Total*
Vik D-7	74.252	0.048	11.877	1.129	0	0.014	0.517	2.48	3.09	93.408
	50.116	2.735	13.018	14.543	0.27	4.852	9.191	3.093	0.404	98.58
	49.394	2.927	12.707	15.381	0.253	4.825	9.135	2.921	0.355	98.297
	49.322	2.606	13.065	13.943	0.262	5.657	10.274	2.865	0.321	98.689
	48.901	2.745	12.916	13.526	0.215	6.008	10.502	2.834	0.382	98.407
	48.939	2.051	13.763	11.915	0.25	7.304	11.882	2.395	0.203	99.022
	49.407	1.892	13.728	11.837	0.193	7.132	11.833	2.438	0.241	98.985
	49.053	1.464	14.058	10.963	0.203	8.025	13.032	2.197	0.185	99.455
	49.272	1.455	14.108	10.775	0.237	7.93	12.901	2.214	0.157	99.336
	49.59	1.449	14.391	10.851	0.216	7.981	13.203	2.129	0.099	100.206

Vik D-6

	SiO2	TiO2	Al2O3	FeO	MnO	MgO	CaO	Na2O	K2O	Total
Vik D-6	51.448	2.72	12.73	12.771	0.257	4.798	8.913	3.181	0.616	97.882
	50.248	2.429	13.302	13.185	0.158	5.957	10.095	2.813	0.428	99.017
	49.557	2.117	13.165	12.235	0.185	6.362	10.69	2.573	0.273	97.484
	48.773	2.14	13.337	12.516	0.232	6.267	10.862	2.648	0.341	97.502
	49.77	2.333	13.052	12.813	0.257	6.154	10.682	2.569	0.312	98.353
	49.146	2.065	13.31	12.834	0.224	6.427	11.29	2.443	0.32	98.411
	49.739	2.324	12.742	13.523	0.184	6.324	11.054	2.674	0.32	99.231
average	*49.81157*	*2.304*	*13.09114*	*12.83957*	*0.213857*	*6.041286*	*10.51229*	*2.700143*	*0.372857*	*98.26857*
std dev	*0.798372*	*0.210071*	*0.242639*	*0.389512*	*0.035855*	*0.527538*	*0.73803*	*0.222598*	*0.10852*	*0.639916*
	49.338	1.772	13.654	12.118	0.191	7.418	11.961	2.429	0.219	99.471
	49.68	1.78	13.784	11.61	0.214	7.291	11.754	2.367	0.213	98.954

Vik K-8

	SiO2	TiO2	Al2O3	FeO	MnO	MgO	CaO	Na2O	K2O	Total
Vik K-8	49.535	2.087	12.594	13.97	0.253	5.981	10.126	2.893	0.364	98.085
	48.544	1.645	13.404	11.652	0.223	7.262	11.923	2.386	0.285	97.611
	48.349	1.682	13.516	11.793	0.154	7.225	11.854	2.406	0.307	97.598
	48.047	1.655	13.346	12.182	0.211	7.269	11.866	2.468	0.247	97.607
	47.726	2.144	13.345	11.671	0.175	7.076	11.282	2.647	0.33	96.733
	47.54	2.549	13.297	12.76	0.233	6.499	10.865	2.703	0.386	97.235
average	*48.29017*	*1.960333*	*13.25033*	*12.338*	*0.208167*	*6.885333*	*11.31933*	*2.583833*	*0.319833*	*97.47817*
std dev	*0.6529*	*0.333276*	*0.301457*	*0.824455*	*0.033884*	*0.484403*	*0.655869*	*0.181638*	*0.046753*	*0.414579*
	73.021	0.022	11.751	1.165	0.093	0.017	0.525	3.961	4.273	94.828
	73.005	0.038	11.858	1.175	0.053	0.026	0.53	3.704	4.119	94.508

Vik D-5

	SiO2	TiO2	Al2O3	FeO	MnO	MgO	CaO	Na2O	K2O	Total
Vik D-5										
a	74.027	0.045	11.585	1.095	0	0.018	0.435	3.446	4.312	94.964
a	73.616	0.038	11.972	1.118	0.03	0.015	0.486	3.841	4.29	95.406
a	73.922	0.013	11.944	1.245	0.078	0.01	0.615	3.551	4.268	95.645
a	73.944	0.038	11.672	1.136	0.042	0.034	0.532	4.004	4.445	95.848
a	73.611	0.245	11.016	3.394	0.09	0.022	0.946	3.956	3.068	96.356
a	73.001	0.034	11.857	0.995	0.011	0.019	0.524	3.456	4.699	94.605
a	73.84	0.124	11.727	2.622	0.089	0.01	0.393	1.728	4.795	95.328
average	*73.70871*	*0.076714*	*11.68186*	*1.657857*	*0.048571*	*0.018286*	*0.561571*	*3.426*	*4.268143*	*95.45029*
std dev	*0.324785*	*0.076011*	*0.302007*	*0.881086*	*0.034591*	*0.007648*	*0.170325*	*0.725784*	*0.526069*	*0.532421*
b	49.637	1.168	14.655	10.186	0.203	8.373	13.554	1.736	0.11	99.877
b	49.797	2.158	13.712	12.242	0.234	6.392	10.599	2.503	0.339	98.422
b	49.909	2.498	13.499	12.548	0.221	6.784	11.077	2.686	0.323	99.911
b	50.274	2.416	14.055	12.46	0.202	5.925	10.324	2.75	0.482	99.245
b	49.607	2.342	12.828	12.964	0.26	6.174	10.378	2.802	0.361	98.094
b	49.528	2.529	13.468	13.2	0.25	6.074	10.248	2.61	0.399	98.682
b	50.859	2.431	12.988	13.797	0.233	4.588	8.655	3.064	0.52	97.622
b	49.088	2.082	11.292	11.851	0.224	5.131	8.573	2.636	0.316	91.495
average	*49.83738*	*2.203*	*13.31213*	*12.406*	*0.228375*	*6.180125*	*10.426*	*2.598375*	*0.35625*	*97.9185*
std dev	*0.498951*	*0.418011*	*0.935056*	*1.010141*	*0.01915*	*1.056537*	*1.451403*	*0.361123*	*0.116265*	*2.544157*

Vik D-4

	SiO2	TiO2	Al2O3	FeO	MnO	MgO	CaO	Na2O	K2O	Total
Vik D-4	49.799	2.514	13.377	12.364	0.213	7.041	11.141	2.815	0.294	99.93
	49.163	2.453	13.184	12.65	0.237	6.399	10.637	2.873	0.329	98.211

	49.151	2.413	13.485	13.917	0.254	6.12	10.131	2.701	0.355	98.886
	49.439	2.528	13.193	13.086	0.235	6.141	10.545	2.783	0.356	98.699
	49.437	2.432	13.363	13.197	0.217	6.333	10.61	2.791	0.355	99.061
	48.998	2.367	13.391	13.014	0.208	6.498	10.792	2.804	0.336	98.738
	49.35	2.496	13.388	13.103	0.265	6.287	10.515	2.75	0.358	98.84
	49.339	2.546	13.486	13.495	0.222	5.837	10.447	2.763	0.375	98.864
	48.972	2.513	12.991	13.261	0.221	6.273	10.536	2.871	0.317	98.306
average	*49.29422*	*2.473556*	*13.31756*	*13.12078*	*0.230222*	*6.325444*	*10.59489*	*2.794556*	*0.341667*	*98.83722*
std dev	*0.242801*	*0.056841*	*0.153607*	*0.422526*	*0.01814*	*0.31025*	*0.255711*	*0.052051*	*0.023598*	*0.465552*
	47.886	4.15	12.993	14.245	0.236	4.769	9.123	3.322	0.854	98.246

Vik D-2 & 3

	SiO2	*TiO2*	*Al2O3*	*FeO*	*MnO*	*MgO*	*CaO*	*Na2O*	*K2O*	*Total*
Vik D-3	74.667	0.036	11.764	1.066	0.036	0.004	0.421	2.993	4.365	95.352
	75.363	0.027	12.432	1.06	0.03	0.036	0.607	4.015	4.027	97.596
	73.779	0.062	11.482	1.085	0.042	0.01	0.444	2.63	4.523	94.057
	73.519	0.022	11.522	1.296	0.019	0	0.551	3.487	3.854	94.279
	74.631	0.043	12.029	1.101	0.019	0.031	0.527	4.117	4.219	96.749
	77.388	0.181	11.758	2.685	0.093	0.042	1.464	3.087	1.983	98.681
	71.525	0.131	12.899	1.925	0.123	0.081	0.702	3.905	3.943	95.279
average	*74.41029*	*0.071714*	*11.98371*	*1.459714*	*0.051714*	*0.029143*	*0.673714*	*3.462*	*3.844857*	*95.999*
std dev	*1.665055*	*0.056218*	*0.47882*	*0.57675*	*0.037301*	*0.026057*	*0.334455*	*0.53245*	*0.791004*	*1.602356*
	49.111	2.711	12.697	14.005	0.239	4.67	8.741	3.162	0.386	96.104
	49.174	1.881	13.557	11.986	0.238	6.762	11.505	2.484	0.257	98.128
Vik D-2	75.11	0.039	12.05	1.187	0.023	0.023	0.481	1.875	4.512	95.299
	75.382	0.048	11.853	1.195	0.017	0	0.47	1.792	4.412	95.168
	74.157	0.04	11.839	1.108	0.036	0.042	0.532	4.272	3.801	95.85

	74.735	0.006	12.165	1.105	0.042	0.064	0.519	4.248	4.064	96.948
	74.514	0.032	11.708	1.149	0.036	0.009	0.436	3.572	4.177	95.643
	74.737	0.033	11.828	1.096	0.102	0.027	0.484	4.149	4.109	96.578
	73.934	0.088	11.572	1.141	0.017	0.032	0.513	3.566	4.271	95.152
	74.877	0.051	12.31	1.08	0.019	0.046	0.568	3.71	4.609	97.271
	76.267	0.033	12.281	1.057	0.036	0.042	0.528	2.215	3.748	96.208
	76.74	0.032	12.51	1.155	0.055	0	0.513	2.345	3.424	96.775
average	*75.0453*	*0.0402*	*12.0116*	*1.1273*	*0.0383*	*0.0285*	*0.5044*	*3.1744*	*4.1127*	*96.0892*
std dev	*0.837145*	*0.019676*	*0.284447*	*0.04313*	*0.024249*	*0.019951*	*0.035427*	*0.954637*	*0.350911*	*0.739272*
	49.006	1.805	13.898	10.907	0.196	7.644	12.256	2.273	0.232	98.527

Vik D-1

	SiO2	*TiO2*	*Al2O3*	*FeO*	*MnO*	*MgO*	*CaO*	*Na2O*	*K2O*	*Total*
Vik D-1	49.57	3.47	12.56	14.70	0.26	4.79	9.02	3.15	0.55	98.57
	49.50	3.26	13.05	14.09	0.22	4.65	8.61	3.32	0.74	97.92
	50.17	3.45	12.83	14.20	0.26	4.76	8.84	2.99	0.54	98.49
	49.92	2.83	13.02	13.39	0.20	5.65	9.74	3.02	0.51	98.66
	49.55	2.97	12.67	13.81	0.26	5.64	9.96	3.06	0.49	98.81
	49.59	2.76	12.97	13.43	0.20	5.71	9.87	2.92	0.48	98.32
	49.69	2.85	13.08	13.59	0.23	5.62	9.66	2.94	0.48	98.58
	49.82	2.71	13.07	13.35	0.21	5.92	9.974	2.96	0.42	98.88
average	*49.727*	*3.037*	*12.905*	*13.819*	*0.229*	*5.343*	*9.460*	*3.044*	*0.527*	*98.528*
std dev	*0.214*	*0.291*	*0.187*	*0.449*	*0.023*	*0.481*	*0.514*	*0.124*	*0.091*	*0.281*
	48.47	1.88	13.76	11.15	0.19	7.59	12.24	2.40	0.22	98.14
	49.18	1.82	14.00	10.90	0.16	7.86	12.38	2.44	0.22	99.26
	48.94	1.87	13.94	11.15	0.22	7.85	12.25	2.39	0.19	99.08
	48.56	1.87	14.04	11.16	0.18	7.72	12.33	2.48	0.26	98.88
	49.06	1.82	14.08	10.85	0.18	7.98	12.35	2.32	0.20	99.11
	48.60	1.81	14.04	10.91	0.22	7.78	12.26	2.38	0.21	98.46
	48.66	1.81	14.08	10.76	0.20	7.99	12.36	2.35	0.24	98.70

	48.44	1.80	13.86	10.93	0.20	8.00	12.29	2.39	0.19	98.36
	48.89	1.84	14.18	11.03	0.19	7.98	12.37	2.45	0.25	99.42
	48.32	1.88	13.62	10.96	0.21	7.57	12.38	2.50	0.26	97.96
	48.82	1.80	13.97	10.63	0.19	7.85	12.29	2.37	0.21	98.44
average	*48.72*	*1.84*	*13.96*	*10.95*	*0.19*	*7.83*	*12.32*	*2.41*	*0.22*	*98.71*
std dev	*0.26*	*0.03*	*0.15*	*0.16*	*0.02*	*0.15*	*0.05*	*0.05*	*0.03*	*0.46*
	55.59	2.31	13.54	10.46	0.20	3.32	6.98	3.10	1.18	97.48

APPENDIX III: Radiocarbon Dating Procedures

Samples for radiocarbon dating were analysed at the Scottish Universities Environmental Research Centre (SUERC) in East Kilbride, using the 5 MV National Electrostatic Corporation Accelerated Mass Spectrometer Facility. The main steps in the dating procedure are outlined below.

Sample Dating Procedure

All samples consist of well-humified peat, which is separated into humic acid, fulvic acid and humin, of which humic acid or humin are usually dated (Cook et al. 1998). In this case the humic acid fraction of the sample is dated because it is deemed to be the most stable.

1. Separation of dateable fracton

The peat sample is broken up and any rootlets that are visible are carefully removed. The sample is placed in 1M hydrochloric acid and heated for 2-3 hrs at approximately 80EC. The acid washing solubilises the acid-soluble fulvic acid fraction, which is regarded as being mobile within the peat profile. The sample is filtered through glass fibre paper (GF/A) and the solution discarded. The extraction of the humic acid fraction is accomplished by adding 2% w/v NaOH solution to the acid washed peat, heating for 2-3 hrs at approx. 80EC and leaving to cool. The peat sample is then centrifuged and the humic acid solution transferred into a clean beaker and acidified with 5M HCl to precipitate out the humic acid. This is heated for 2-3 hrs to coagulate the precipitate, cooled and then centrifuged. The solution is decanted leaving the solid humic acid, which is then freeze dried and weighed.

2. Combustion

The sample is combusted for conversion to graphite for AMS measurement. The equation for the combustion of organic material to CO_2 is shown below.

$$CH_2O + O_2\ 6\ CO_2 + H_2O$$

The combustion is carried out in quartz combustion tubes. These are 12 mm o.d open-ended tubes with 6 mm o.d. open-ended stems. A quartz wool plug is placed in the 6 mm stem before adding copper oxide as the oxidant (0.5 g) and silver wire (5-10 mm) (to remove halide contaminants) to the 12 mm end of the tube. The tubes are heated to 500EC for 8 hours to remove all carbon contamination before they are used for combusting samples.

The humic acid samples are weighed into pre-combusted small lengths (approx. 15 mm) of 8 mm quartz tube with a quartz wool plug in one end for the sample to rest on. Once the weight is noted, the other end of the tube is packed with pre-combusted quartz wool. A number (tube number) is scratched on the outside of the quartz combustion tube for identification and the same number is logged on the laboratory sheet. The short 8 mm diameter sample tube is placed into the open end of the combustion tube and taken to a vacuum line housed in a fume cupboard for sealing the open 12 mm end. The combustion tube is attached to the vacuum line at the open 6 mm end and pumped to 10^{-3} mbar. At this point the stem is sealed with a hand-held gas torch.

The tube is placed in a muffle furnace and heated overnight to a temperature of 850EC for 8 hours. The tube is allowed to cool before it is scratched with a glass-cutting knife and put into a breaker unit, which in turn is attached to a vacuum line used for CO_2 recovery and purification. The entire vacuum line is pumped to approx. 10^{-3} mbar. The breaker unit is also evacuated at this stage. The combustion tube is cracked open by closing the breaker stopcock so that it snaps the combustion tube where it has been scored with the glass-cutting knife. The CO_2 is cryogenically trapped using liquid nitrogen and pumped on for several minutes. The CO_2 is then expanded and the yield measured. Sub-samples of CO_2 are removed for (i) graphitisation (2 ml) and subsequent AMS ^{14}C analysis and (ii) ^{13}C analysis (1-2 ml). Any remaining gas is archived in a glass-sealed pyrex tube.

3. AMS dating

The sub-samples of CO_2 are converted to graphite according to the method of (Slota et al. 1987), and then pressed into aluminium sample holders for subsequent ^{14}C analysis. $\delta^{13}C$ analysis (for correcting the sample activity for fractionation) is undertaken on the second sub-sample of CO_2 using a VG Isotech Sira 10 isotope ratio mass spectrometer. The graphite samples for unknowns, together with graphite prepared from modern reference standards (SRM-4990C – oxalic acid II), background standards and known age standards are analysed at the SUERC AMS facility (NEC 5 MV terminal voltage instrument). The AMS is operated at 4.5MV with carbon in the 4+ charge state.

4. Calibration

The errors on ^{14}C ages are expressed at the one sigma level of confidence and include components from the counting statistics on the sample, modern reference standard and background standard, random machine error and are subject to a minimum error defined by analysis of a series of replicate samples. Currently, the minimum error is 35 years. Radiocarbon ages were calibrated to the calendar timescale using OxCal v3.9

Slota, P. J. J., Jull, A. T., Linick, T. W. and Toolin, L. J. 1987. Preparation of small samples for 14C accelerator targetsby catalytic reduction of CO. *Radiocarbon* **29**: 303-306.

APPENDIX IV

GPS points for profile locations

The GPS references for the profile locations are recorded in the WGS84 co-ordinate system, except where marked with *, where they use standard latitude/longitude values.

Profile Name	Easting	Northing	Alt (m)
Víkurá A	558525	7259813	127
Víkurá B	557570	7259205	222
Víkurá C	557601	7259175	238
Víkurá D	556821	7259379	264
Víkurá E	557712	7259195	260
Víkurá F	557712	7259195	260
Víkurá H	557957	7258618	378
Víkurá I	557863	7259113	235
Víkurá J	557632	7259208	230
Víkurá K	557646	7259358	226
Víkurá L	558478	7260449	85
Víkurá M	558631	7260463	48
Víkurá N	557475	7259486	217
Víkurá O	557059	7259608	222
Víkurá P	557719	7259842	220
Víkurá Q	557943	7259373	185
Víkurá R	556683	7257940	290
Afrett A	556452	7257887	291
Brúnavík B	560338	7264981	340
Brúnavík C	560010	7264728	240
Brúnavík D	559143	7264897	168
Brúnavík E	559190	7264848	160
Brúnavík F*	*65° 29' 59" N*	*013° 43' 16" W*	-
Brúnavík G*	*65° 29' 38" N*	*013° 42' 58" W*	164
Brúnavík H*	*65° 29' 58" N*	*013° 42' 55" W*	159
Brúnavík I*	*65° 30' 02" N*	*013° 44' 04" W*	243
Brúnavík J*	*65° 30' 08" N*	*013° 44' 08" W*	241
Brúnavík K	558507	7264868	240
Brúnavík L	558807	7204550	233
Brúnavík M	558837	7364522	242
Brúnavík P	559880	7265113	217
Brúnavík V	559242	7266018	205
Brúnavík W	559847	7266087	113
Kjólsvík B	562481	7264052	253
Kjólsvík C	562230	7263520	157
Kjólsvík D	562284	7263463	155
Kjólsvík E	562689	7263236	124
Kjólsvík F	562689	7263236	165
Kjólsvík G	561991	7263688	179
Kjólsvík H	561634	7263642	245
Svínavík B	503678	7261768	181
Borgarfjörður B	557914	7265724	146

Borgarfjörður C	557987	7265225	275
Borgarfjörður D	557885	7265596	231
Borgarfjörður E	557116	7265942	112
Borgarfjörður F	557116	7265937	85
Borgarfjörður G	556959	7265517	105
Borgarfjörður H	556881	7266697	35
Borgarfjörður I	556832	7266339	33
Borgarfjörður J	556626	7266281	35
Borgarfjörður K	556663	7266167	43
Borgarfjörður L	556935	7265840	95
Borgarfjörður M	557037	7265749	97
Borgarfjörður N	556678	7265812	90
Borgarfjörður O	556626	7265537	66
Bakka A	556461	7266190	25
Bakka B	556464	7266191	22
Bakka C	557177	7264692	99
Bakka D	557283	7264460	99
Lagarfljót A	531409	7252040	62
Lagarfljót C	532150	7267820	51
Lagarfljót D	532041	7238842	293
Loðmundarfjörður A	553491	7250370	146
Loðmundarfjörður D	553502	7249979	109
Loðmundarfjörður G	555225	7249388	59
Loðmundarfjörður H	555495	7249925	80
Húsavík B	558565	7253852	198
Húsavík C	558260	7254815	255
Húsavík D	558903	7255005	326
Breiðavík D	561535	7261245	64
Breiðavík I	562943	7261810	254
Breiðavík J	562762	7261645	204
Breiðavík K	556798	7258900	264
Breiðavík L	555591	7259177	233
Breiðavík M	555425	7259053	230
Breiðavík N	555441	7259025	207
Breiðavík P	555025	7258998	193
Breiðavík Q	650054	7261488	162
Breiðavík R	558947	7261135	186
Jökulsá B	553194	7265081	98
Jökulsá C	552982	7264771	99